Oklahoma Geological Survey
Charles J. Mankin, *Director*

Circular 105
ISSN 0078-4397

Silurian, Devonian, and Mississippian Geology and Petroleum in the Southern Midcontinent, 1999 Symposium

KENNETH S. JOHNSON, *Editor*

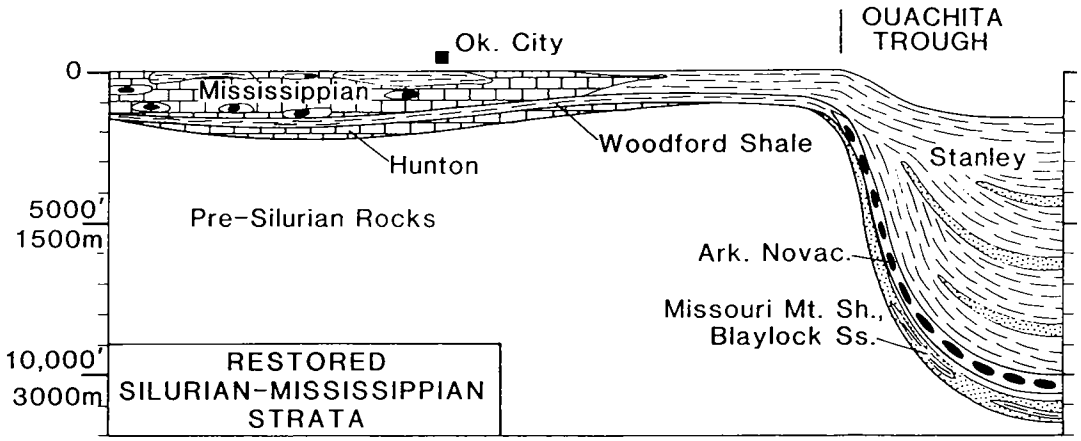

Proceedings of a symposium held March 23–24, 1999, in Norman, Oklahoma.

Co-sponsored by:

Oklahoma Geological Survey

and

National Petroleum Technology Office,
U.S. Department of Energy

The University of Oklahoma
Norman

2001

OKLAHOMA GEOLOGICAL SURVEY

CHARLES J. MANKIN, *Director*

SURVEY STAFF

JAMES H. ANDERSON, *Cartographic Technician III*
RICHARD D. ANDREWS, *Geologist IV*
LARRY T. AUSTIN, *Core and Sample Library Assistant*
BETTY D. BELLIS, *Word-Processing Operator II/Technical Typist*
MITZI G. BLACKMON, *Clerk-Typist I*
DAN T. BOYD, *Geologist III*
JERLENE A. BRIGHT, *Technical Project Specialist*
RAYMON L. BROWN, *Geophysicist III*
RUTH E. BROWN, *Assistant to the Director*
JOCK A. CAMPBELL, *Geologist IV*
BRIAN J. CARDOTT, *Geologist IV*
JAMES R. CHAPLIN, *Geologist IV*
JANISE L. COLEMAN, *Office Assistant IV*
CHRISTIE L. COOPER, *Managing Editor*
TAMMIE K. CREEL-WILLIAMS, *Secretary II*
CHARLES R. DYER III, *Drilling Technician*
WALTER C. ESRY, *Manager, Core and Sample Library*
ROBERT O. FAY, *Geologist IV*
AMIE R. FRIEND, *Research Specialist I*
T. WAYNE FURR, *Manager of Cartography*
PATRONALIA M. HANLEY-BROWN, *Chemist*
PRISCILLA A. JOHNSON, *Office Assistant IV*
JAMES W. KING, *Research Specialist I*
JAMES E. LAWSON, JR., *Chief Geophysicist*
LAURIE A. LOLLIS, *Cartographic Technician II*
KENNETH V. LUZA, *Geologist IV*
MICHAEL J. MERCER, *Manager, Log Library*
GALEN W. MILLER, *Research Associate*
RICHARD G. MURRAY, *Copy Center Operator*
SUE M. PALMER, *Office Assistant II*
DAVID O. PENNINGTON, *Operations Assistant II*
CONNIE G. SMITH, *Promotion and Information Specialist*
PAUL E. SMITH, *Supervisor, Offset Press Copy Center*
THOMAS M. STANLEY, *Geologist III*
LLOYD N. START, *Assistant Drilling Technician*
JOYCE A. STIEHLER, *Chief Clerk*
MICHELLE J. SUMMERS, *Technical Project Coordinator*
NEIL H. SUNESON, *Assistant Director, Geological Programs*
JANE L. WEBER, *Publication and Database Coordinator*
STEPHEN J. WEBER, *Chief Chemist*

Cover Picture

Schematic cross section showing restored thickness of Silurian, Devonian, and Mississippian strata in Oklahoma at the end of Mississippian time (from p. 3 of this volume).

This publication, printed by the Oklahoma Geological Survey, is issued by the Oklahoma Geological Survey as authorized by Title 70, Oklahoma Statutes, 1981, Sections 231–238. 1,050 copies have been prepared for distribution at a cost of $8,494 to the taxpayers of the State of Oklahoma. Copies have been deposited with the Publications Clearinghouse of the Oklahoma Department of Libraries.

PREFACE

The transfer of technical information will aid in the search for, and production of, our oil and gas resources. To facilitate this technology transfer, the Oklahoma Geological Survey (OGS) and the U.S. Department of Energy, National Petroleum Technology Office (DOE–NPTO), in Tulsa, cosponsored a symposium dealing with the search for, and production of, oil and gas resources from reservoirs of Silurian, Devonian, and Mississippian age in the southern Midcontinent. The symposium was held on March 23–24, 1999, in Norman, Oklahoma. This volume contains the proceedings of that symposium.

Research reported upon at the symposium focused on the reservoirs, geologic events, and petroleum of rocks deposited during the Silurian, Devonian, and Mississippian Periods. Clastic and carbonate reservoirs of this age are major sources of oil and gas in the southern Midcontinent, and they have great potential for additional recovery using advanced technologies. The research reports on geology, depositional settings, diagenetic history, sequence stratigraphy, reservoir characterization, exploration, petroleum production, and enhanced oil recovery. In describing these petroleum reservoirs, the researchers have increased our understanding of how the geologic history of an area can affect reservoir heterogeneity and our ability to efficiently recover the hydrocarbons they contain. We hope that the symposium and these proceedings will bring such research to the attention of the geoscience and energy-research community, and will help foster exchange of information and increased research interest by industry, university, and government workers.

Fifteen talks and posters presented at the symposium are printed here as full papers or extended abstracts. An additional eleven talks and posters are presented as abstracts at the end of the volume. About 200 persons attended the symposium. Stratigraphic nomenclature and age determinations used by the various authors in this volume do not necessarily agree with those of the OGS.

This is the twelfth symposium in as many years dealing with topics of major interest to geologists and others involved in petroleum-resource development in Oklahoma and adjacent states. These symposia are intended to foster the exchange of information that will improve our ability to find and recover our nation's oil and gas resources. Earlier symposia covered: Anadarko Basin (published as OGS Circular 90); Late Cambrian–Ordovician Geology of the Southern Midcontinent (OGS Circular 92); Source Rocks in the Southern Midcontinent (OGS Circular 93); Petroleum-Reservoir Geology in the Southern Midcontinent (OGS Circular 95); Structural Styles in the Southern Midcontinent (OGS Circular 97); Fluvial-Dominated Deltaic Reservoirs in the Southern Midcontinent (OGS Circular 98); Simpson and Viola Groups in the Southern Midcontinent (OGS Circular 99); Ames Structure in Northwest Oklahoma and Similar Features—Origin and Petroleum Production (OGS Circular 100); Platform Carbonates in the Southern Midcontinent (OGS Circular 101); Marine Clastics in the Southern Midcontinent (OGS Circular 103); and Pennsylvanian and Permian Geology and Petroleum in the Southern Midcontinent (OGS Circular 104).

Persons involved in the organization and planning of this symposium include: Kenneth Johnson and Charles Mankin of the OGS; and Bill Lawson and Herb Tiedemann of DOE–NPTO. Other personnel who contributed include Michelle Summers and Tammie Creel, registration co-chairs; LeRoy Hemish, poster-session chair; Connie Smith, publicity chair; and Judy Schmidt, exhibits coordinator. Technical editing of this volume was done by William Rose, Frederick, Maryland; layout and production was done by Virginia Rose, Frederick, Maryland. Appreciation is expressed to each of them and to the many authors who worked toward a highly successful symposium.

KENNETH S. JOHNSON
General Chairman

CONTENTS

169 **Conodont Biofacies and Biostratigraphy of Silurian Strata of the Hunton Group in Oklahoma, and Equivalent Units in West Texas and Eastern New Mexico**
James E. Barrick

170 **Thermal Maturation of the Woodford Shale in South-Central Oklahoma**
Brian J. Cardott

171 **Sequence Stratigraphy of Chesterian Sandstones in the Black Warrior Basin, Northeastern Mississippi**
Arthur W. Cleaves

172 **Mississippian 3-D Case History—Porosity Prediction Using Seismic-Trace Conversion—a Prospector's Perspective**
Jasha Cultreri

173 **Depositional Environment and Sequence Stratigraphy of Silurian through Mississippian Strata in the Midcontinent**
Richard D. Fritz and Edward A. Beaumont

174 **Exploration Potential of the Lower Mississippian Sycamore Limestone**
Richard D. Fritz and Larry Gerken

175 **3-D Seismic and Hydrocarbon-Microseepage Surveys: Exploration Adventures in Osage County, Oklahoma**
Daniel C. Hitzman

176 **Advanced Reservoir Characterization of a Hunton Field, Kingfisher County, Oklahoma**
Daniel C. Hitzman, Brooks A. Rountree, and Charles O'Donnell

177 **Discovery of Economic Fractured Source-Rock Reservoirs in the Devonian and Mississippian of Oklahoma**
Fred S. Jensen, Thomas L. Thompson, and James R. Howe

178 **Mississippi Lime: Chert Occurrence Related to Productive Reservoirs, Blaine County, Oklahoma**
Dan J. Towns

179 **Reservoir Characterization and Comparison of the Hunton in the Texas–Oklahoma Anadarko Basin to Equivalent Devonian and Silurian (Fusselman) Rocks of the Texas Permian Basin**
Ronald J. Woods, Charles E. Willey, Paul W. Smith, Walter J. Hendrickson, and John V. Hogan

Geology and Petroleum Reservoirs in Silurian, Devonian, and Mississippian Rocks in Oklahoma

Robert A. Northcutt
Independent Geologist
Oklahoma City, Oklahoma

Kenneth S. Johnson
Oklahoma Geological Survey
Norman, Oklahoma

G. Carlyle Hinshaw
Independent Geologist
Norman, Oklahoma

ABSTRACT.—Silurian, Devonian, and Mississippian (SDM) rocks in Oklahoma comprise a moderately thick to thick sequence of marine strata that underlie most parts of the State, and they are important sources of oil and gas throughout most of their distribution. Silurian and Devonian strata in the Oklahoma basin (i.e., all areas outside the Ouachita basin) are mainly shallow-marine carbonates of the Hunton Group; they are clean-washed skeletal limestones in the lower part (Chimneyhill Subgroup), argillaceous and silty carbonates in the middle (Henryhouse and Haragan–Bois d'Arc Formations), and clean-washed limestones at the top (Frisco Formation). Most of the Hunton carbonates are dolomitized in the northern shelf. Unconformably above the Hunton in the Oklahoma basin is the Late Devonian–Early Mississippian Woodford (Chattanooga) Shale, with the Misener sandstone at its base. The Woodford is a dark gray to black fissile shale that contains chert and siliceous shale; although best known as a source rock, fractured Woodford Shale locally is also a good reservoir. The other Mississippian strata in the Oklahoma basin are marine limestones and shales in most areas, but thick, dark gray fissile shales predominate in south-central Oklahoma. Springeran (latest Mississippian and earliest Pennsylvanian) strata are restricted to the Anadarko and Ardmore basins and adjacent areas; they are mostly dark gray marine shales with interbeds of marine sandstone. The total thickness of SDM strata in the Oklahoma basin is typically 1,000–2,000 ft in the shelf areas but increases to 2,000–5,000 ft in depocenters in the south. The Ouachita trough of southeastern Oklahoma received a thick marine sequence of black shale, novaculite, and sandstones during the SDM; these strata, including the Arkansas Novaculite and the Stanley Shale, aggregate about 8,000–15,000 ft in thickness.

Production data for leases producing from SDM reservoirs have been used to prepare a series of six maps to show the distribution of production for different increments of geologic time, regardless of reservoir lithology. The six maps and related production data are for the following geologic intervals: Silurian–Devonian (Hunton), Upper Devonian (Woodford and Misener), Lower Mississippian (Osagean), middle Mississippian (Meramecian), Upper Mississippian (Chesterian), and Springeran. Cumulative production from all six intervals from 1969 through July 31, 1998, was about 1.3 billion barrels of oil and condensate, and 24.1 trillion cubic feet of natural gas.

INTRODUCTION

Oklahoma is one of the leading petroleum-producing states in the nation, and a significant part of its production is from reservoirs of Silurian, Devonian, and Mississippian age. In 1999, Oklahoma ranked fifth in crude-oil production, third in natural-gas production, and second in number of wells drilled for petroleum. Unfortunately, production from Silurian, Devonian, and Mississippian reservoirs commonly is commingled with production from other reservoirs in many major oil and gas fields, so precise data on yields of individual reservoirs are not available.

This paper discusses the general geology of Silurian, Devonian, and Mississippian strata in Oklahoma, and

Northcutt, R. A.; Johnson, K. S.; and Hinshaw, G. C., 2001, Geology and petroleum reservoirs in Silurian, Devonian, and Mississippian rocks in Oklahoma, *in* Johnson, K. S. (ed.), Silurian, Devonian, and Mississippian geology and petroleum in the southern Midcontinent, 1999 symposium: Oklahoma Geological Survey Circular 105, p. 1–15.

then discusses the plays (types of traps) that have yielded the greatest amounts of oil and gas from these strata. An understanding of these major petroleum-producing plays should improve our search for new oil and gas fields or reservoirs, and should also improve our techniques of recovery from established fields.

Production data for leases were retrieved from the Natural Resources Information System (NRIS) by Geo Information Systems (GIS), a research department of the University of Oklahoma, by the geological names of the producing intervals. Oklahoma petroleum production is recorded by lease, *not by well,* by the Oklahoma Tax Commission. These data are public records and are marketed in several forms by commercial and governmental organizations. GIS provides the data 6 months in arrears, updated each 6 months. The database begins in 1979, with oil, condensate, associated gas, and nonassociated gas, recorded monthly. It is possible, through the mapping capabilities of SAS (an integrated system of software), to post a location map at almost any scale for one or several (or all) producing intervals by product or products. Also, individuals or companies can acquire the raw data and construct their own analyses.

GEOLOGIC FRAMEWORK

The geology of Oklahoma is complex, but it is remarkably well understood as a result of the extensive amount of drilling and seismic exploration in search of oil and gas. Great thicknesses of sedimentary rock are preserved in a series of major depositional and structural basins separated by orogenic uplifts that formed mainly during Pennsylvanian time (Fig. 1). The major sedimentary basins contain as much as 20,000–40,000 ft of sediments, most of which are Paleozoic and marine, resting upon a basement complex of Precambrian and Lower and Middle Cambrian igneous rocks and some low-rank metasedimentary rocks (Denison and others, 1984; Johnson and others, 1988).

By early Paleozoic time (Cambrian and Ordovician Periods), Oklahoma had three major tectonic/depositional provinces: the Oklahoma basin, the southern Oklahoma aulacogen, and the Ouachita trough (Fig. 2). The Oklahoma basin was a broad, shelflike area that received a sequence of remarkably thick and extensive shallow-marine carbonates interbedded with thinner marine shales and sandstones (Johnson and others, 1988). The southern Oklahoma aulacogen was the depocenter for the Oklahoma basin (Fig. 3). It was a west–northwest-trending trough where sediments are generally similar to those elsewhere in the basin, but they are two to three times as thick. The aulacogen embraced the Anadarko, Ardmore, and Marietta protobasins, along with the Arbuckle anticline and the Wichita Mountain uplift. The Ouachita trough was the site of deep-water sedimentation along a rift at the southern margin of the North American craton. These sediments later were thrust some 50 mi northward to their present position in the Ouachita Mountain uplift.

Middle Paleozoic strata (Silurian, Devonian, and Mississippian) range from about 3,000–6,000 ft thick in the aulacogen to about 1,000–3,000 ft thick in most other parts of the Oklahoma basin (Fig. 3). The aulacogen, which subsided rapidly and accumulated a thick column of sediments during the Cambrian and Ordovician, subsided at a much slower rate during the Silurian and Devonian. Rapid subsidence was then renewed during the Mississippian, chiefly in the eastern part of the aulacogen. At the same time, as much as 10,000 ft of black shale, novaculite, and flysch sediments was dumped into the Ouachita trough, mainly during the Mississippian Period (Fig. 3). Recent reports on middle Paleozoic strata include those by Ham (1969), Ham and Wilson (1967), Amsden (1975, 1980), Craig and others (1979), Johnson and others (1988),

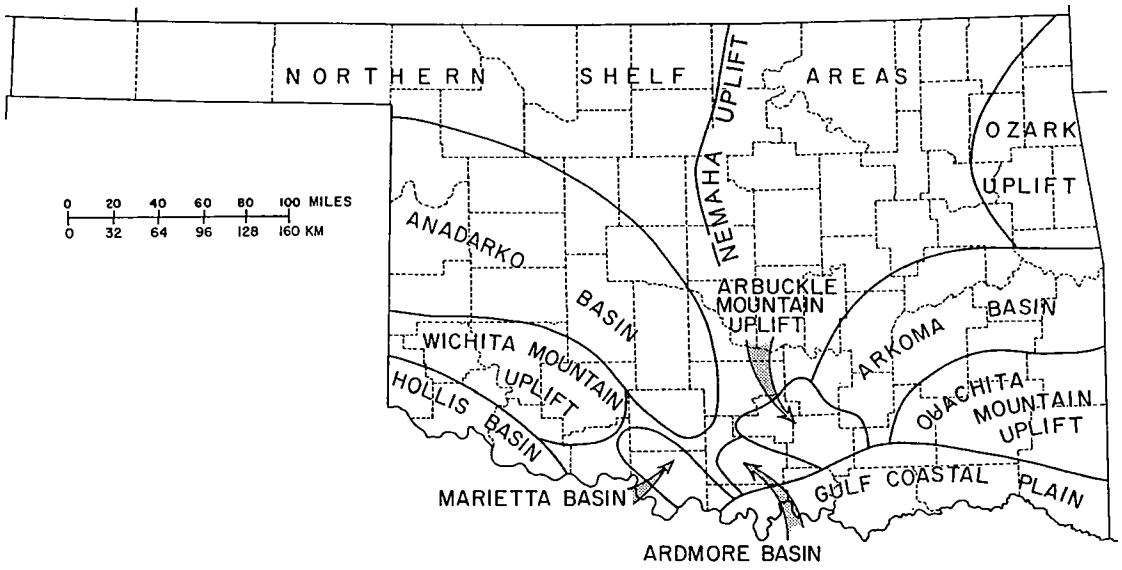

Figure 1. Map showing major geologic provinces of Oklahoma (Johnson and Cardott, 1992).

Fay (1989), Johnson (1993), Al-Shaieb and Puckette (2000), Rottmann (2000), Rottmann and others (2000), Smith and others (2000a, 2000b), and Rogers and others (2000).

These three major tectonic/depositional provinces persisted through the middle Paleozoic until Pennsylvanian time, when the Oklahoma basin and the aulacogen were divided into a series of well-defined marine basins by sharply uplifted crustal blocks. The Ouachita trough was destroyed by Pennsylvanian uplift and northward thrusting. Orogenic activity throughout the State was limited to folding, faulting, and uplift, and was not accompanied by igneous or high-grade-metamorphic activity.

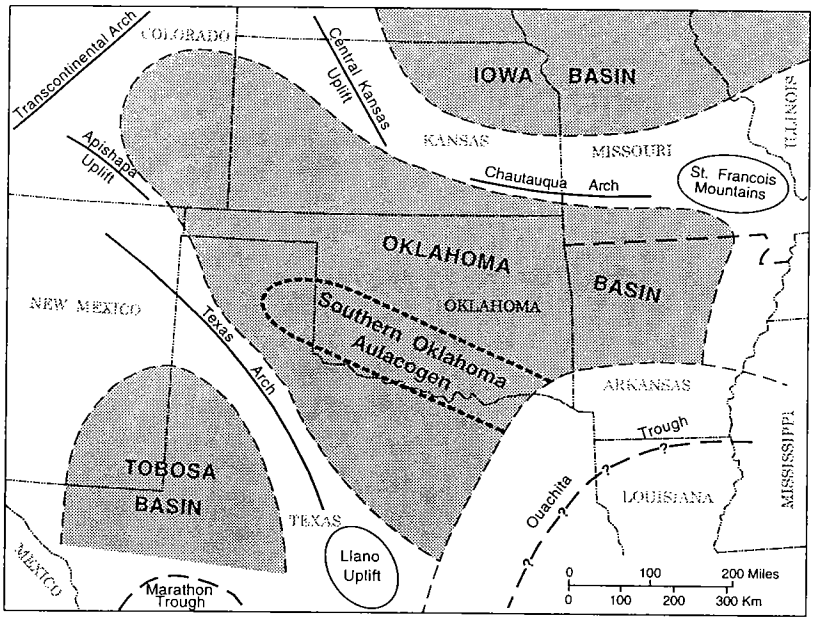

Figure 2. Map of southwestern United States, showing approximate boundary of the Oklahoma basin and other major features that existed in early and middle Paleozoic time. Modified from Johnson and others (1988).

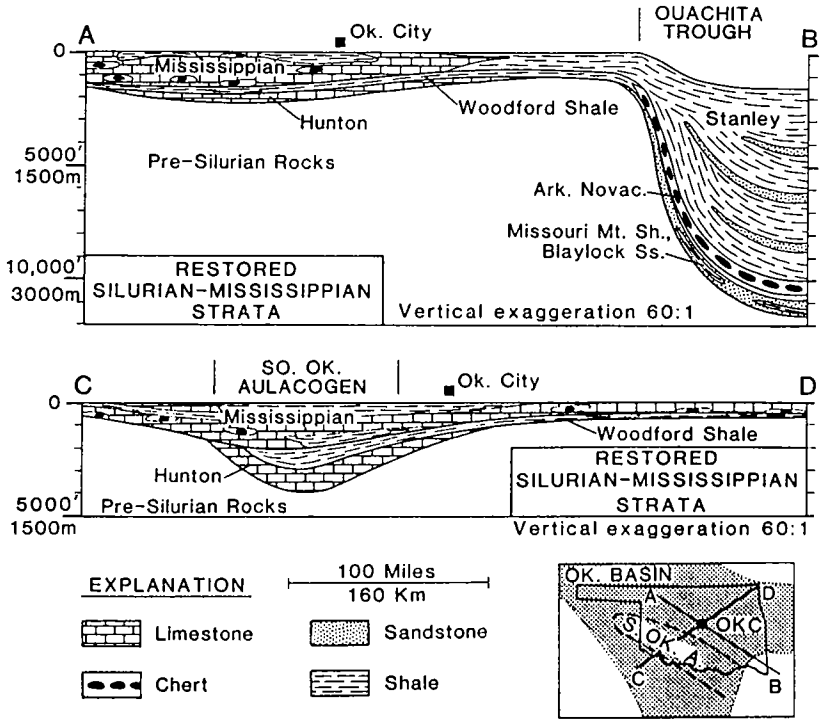

Figure 3. Schematic cross sections showing restored thickness of Silurian, Devonian, and Mississippian strata in Oklahoma. Modified from Johnson and Cardott (1992).

SILURIAN AND LOWER DEVONIAN GEOLOGY AND RESERVOIRS

Silurian and Devonian strata in Oklahoma commonly are referred to the Hunton Group. The Hunton has been studied extensively by T. W. Amsden and other geologists, mainly because it is a prolific petroleum reservoir in various parts of the State. Hunton strata are widely distributed in the Anadarko basin, Arkoma basin, and central and southern Oklahoma (Figs. 4, 5), and the nomenclature for these strata was summarized by Amsden *in* Johnson and others (1988). Hunton strata typically are 100–400 ft thick in most parts of southern, central, and western Oklahoma, although they are up to 800 ft thick in the deep Anadarko basin (Amsden and Rowland, 1967). Hunton strata are commonly 30–250 ft thick in the Arkoma basin. The following geologic discussion is largely modified from Amsden's description *in* Johnson and others (1988), and from the more recent data released by Amsden and Barrick (1993) and Johnson (1993).

The base of the Hunton Group is the Late Ordovician Keel oolite, which represents a shoaling of the water probably related to the eustatic lowering of sea level during North African glaciation. The Keel is overlain by the generally clean-washed skeletal limestones of the Chimneyhill Subgroup. Some silt- and clay-size detritus was introduced during Chimneyhill time and was largely restricted to the southeastern areas bordering the Ouachita province. The volume of detritus increased sharply in the Late Silurian (Henryhouse) and Early Devonian (Haragan–Bois d'Arc) and extended much farther west into the Anadarko basin. Late Ordovician (Keel), Silurian (Chimneyhill, Henryhouse), and Early Devonian (Haragan–Bois d'Arc) strata in the northern and western parts of this region are moderately to heavily dolomitized and are a part of the North American Silurian dolomite province,

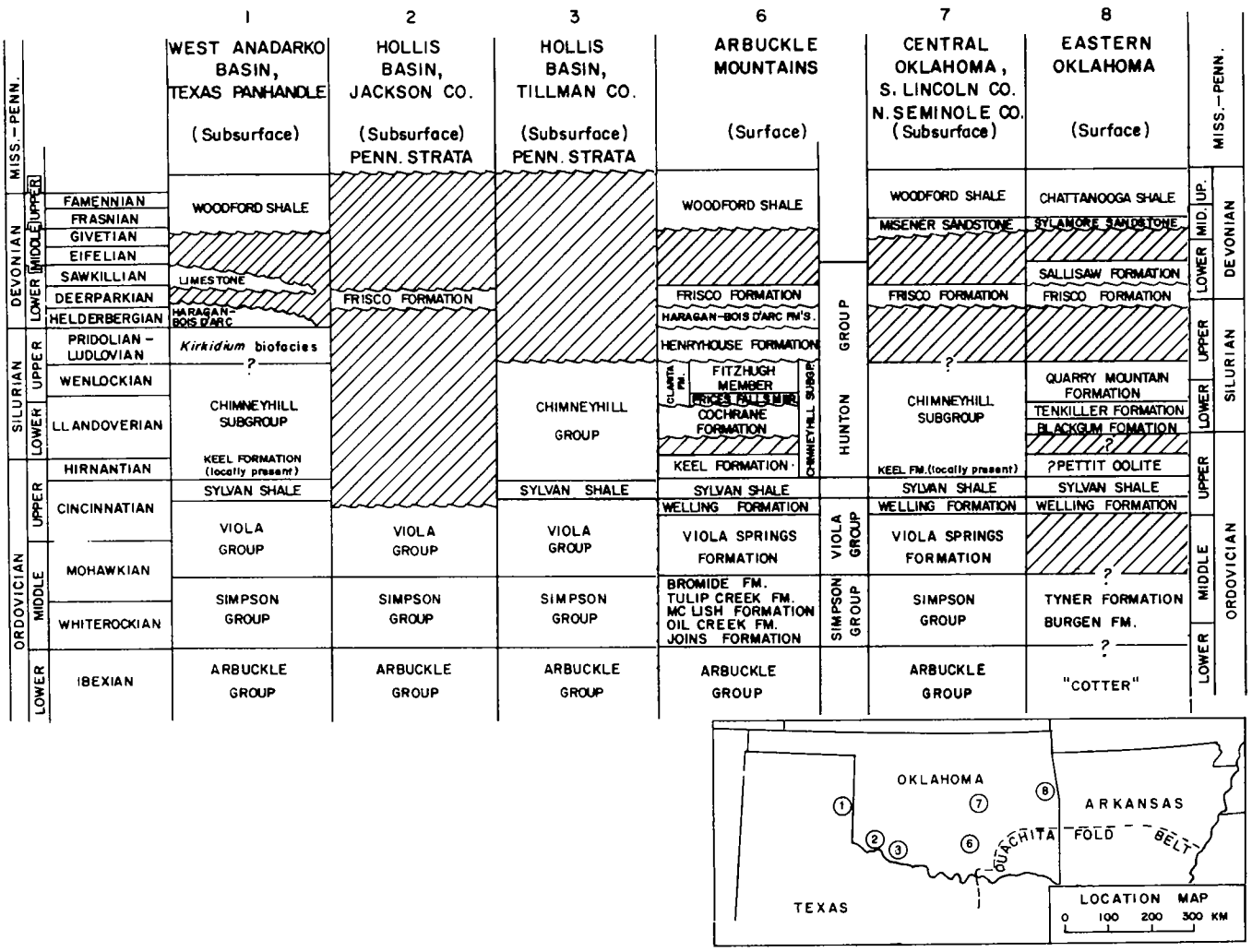

Figure 4. Correlation chart for Ordovician, Silurian, and Devonian strata in Oklahoma. Modified from Johnson and others (1988).

which occupied the continental interior (Amsden, 1975, 1980; Berry and Boucot, 1970). Following deposition of earliest Devonian strata, the entire area was uplifted and eroded (pre-Frisco–Sallisaw erosion, Fig. 5A). When deposition resumed, the flood of detritus had ceased, and the Frisco Formation is everywhere a clean-washed, low-magnesium limestone.

Latest Early Devonian strata are represented by cherts and cherty limestones (Penters and Sallisaw) in the east, grading into clean-washed skeletal limestones in the west. The only Middle Devonian strata currently recognized in this region are the Clifty Sandstone, present in a small area in northwestern Arkansas, and locally the Misener sandstone in north-central Oklahoma.

Sedimentation in the Ouachita trough during the Silurian and Devonian Periods produced a thick sequence of black shale, novaculite, and sandstones (Fig. 3). Silurian and Devonian strata are nearly 1,000 ft of shale and sandstone in the Blaylock and Missouri Mountain Formations, overlain by at least 600 ft of Arkansas Novaculite, the upper part of which is Mississippian in age. These strata reflect continued deposition in slope to deep-water (abyssal) environments.

Names used for Hunton producing intervals are shown in Table 1. Most of the names applied in subsurface nomenclature are the same formal names used in Hunton Group outcrops. A list of the significant oil and gas fields in Oklahoma that produce from each of the six geologic intervals is given in Table 2.

A production map for the Silurian–Devonian (Hunton) (Fig. 6) shows oil and gas production from leases with Silurian–Devonian (Hunton) platform-carbonate reservoirs. In the Anadarko, Ardmore, and Arkoma basins, and in the frontal fault belt of the Wichita uplift, producible Hunton oil and gas are generally found in structural traps where porosity and permeability were enhanced by fracturing and dolomitization. Hydrocarbons are also found in stratigraphic traps at and near the erosional limit of the Hunton Group, or its members, on the northern shelf area of the Anadarko and Arkoma basins. A classic example of a stratigraphic trap in the Hunton is the

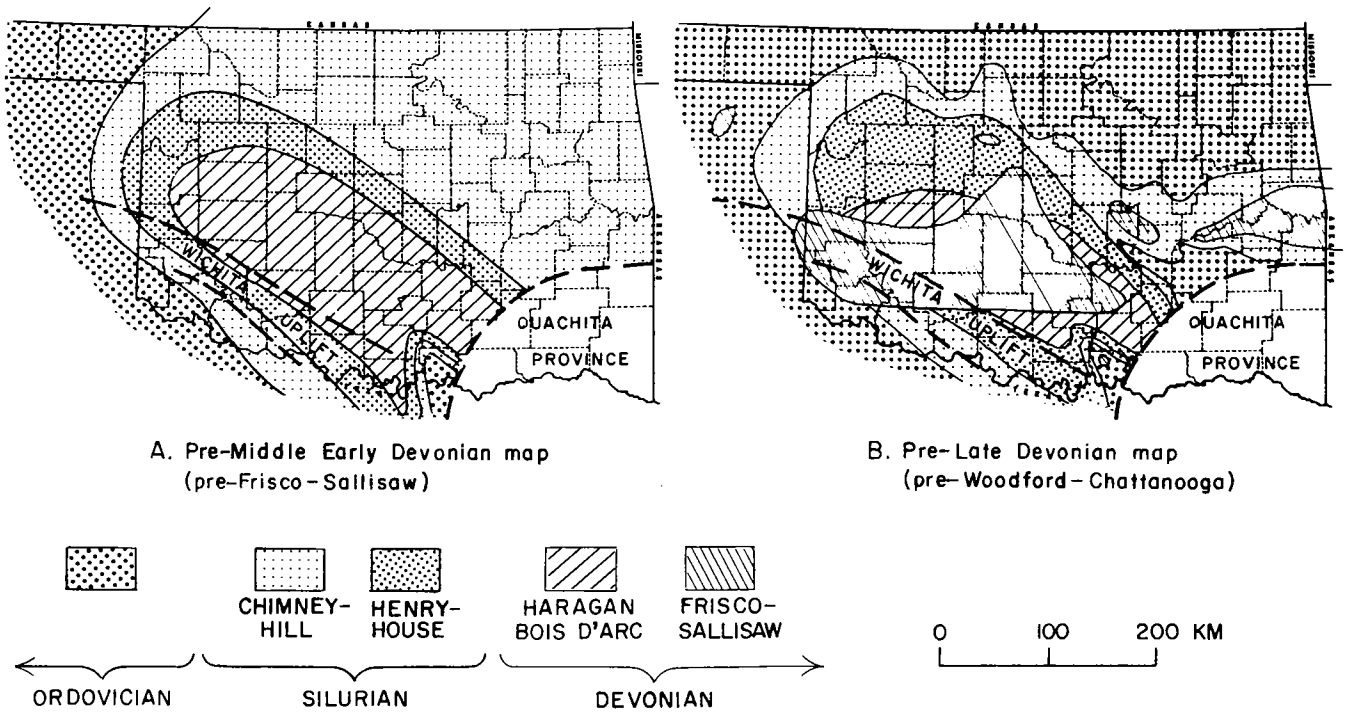

Figure 5. Paleogeologic maps showing inferred distribution of strata in the Oklahoma basin following two major epeirogenic uplifts. Map A shows pre–middle Early Devonian strata (pre-Frisco–Sallisaw subcrop map); map B shows pre–Late Devonian strata (pre-Woodford–Chattanooga subcrop map). From Johnson and others (1988).

West Edmond field in Oklahoma County, on the west flank of the Anadarko shelf. Significant accumulations of Hunton oil were produced from the many structural fields of the Seminole area in central Oklahoma, where reservoir rocks were subjected to karstification.

Graphs of annual production for the period 1979 through 1998 from Silurian–Devonian (Hunton) reservoirs for pure and commingled leases show liquid production (crude oil and condensate) in Figure 7 and gas production (associated and nonassociated) in Figure 8. Cumulative lease production from Silurian–Devonian (Hunton) reservoirs (pure and commingled) for the period 1979–1998 was 256,649,306 bbl of oil and 4,913,608,907 MCF of gas as of July 31, 1998.

UPPER DEVONIAN GEOLOGY AND RESERVOIRS

Following Early Devonian sedimentation, the area was uplifted and exposed to erosion (pre-Woodford–Chattanooga unconformity, Fig. 5B), during which time extensive dissolution and channeling occurred. In late Middle Devonian to early Late Devonian time the Woodford–Chattanooga sea advanced from the east, burying the old erosion surface under a blanket of dark gray to black fine silt and clay. Where the advancing sea encountered weathered clastic debris on the underlying eroded surface, this material was incorporated into the basal sediments (Sylamore–Misener formations). Conditions on the sea floor during deposition inhibited almost all benthic organisms, probably the result of anaerobic conditions and/or a high rate of siltation.

Woodford–Chattanooga sediments covered most of the Oklahoma basin. The Woodford–Chattanooga ranges from 200 to 900 ft thick in the Anadarko basin area and is 50–100 ft thick in most of the shelf areas (Amsden, 1975).

Names used for Upper Devonian producing intervals are shown in Table 1. Some of the names applied in subsurface nomenclature are the same formal names given to outcropping Upper Devonian formations and members. However, the Misener sandstone, a significant producing interval in northern Oklahoma, is an informal subsurface name.

The production map for the Upper Devonian (Fig. 9) shows the area of Misener sandstone production in northern Oklahoma, and the areas of production from the fractured and cherty Woodford Shale along the Wichita Mountain frontal fold belt and in the Ardmore basin. A limited area of production from the Arkansas Novaculite is shown in southernmost Oklahoma, on the east flank of the Ardmore basin. Upper Devonian production from fractured shale is mostly limited to structural traps, whereas Misener sandstone production is from stratigraphic traps, in some cases associated with local structures.

Graphs of annual production for the period 1979 through 1998 from Upper Devonian reservoirs for pure and commingled leases show liquid production (crude oil and condensate) in Figure 10 and gas production (associated and nonassociated) in Figure 11. Cumulative lease production from Upper Devonian reservoirs (pure and commingled) for the period 1979–1998 was

Table 1.—Names Used for Silurian, Devonian, and Mississippian Reservoir Rocks That Produce Petroleum in Oklahoma

Springeran	
Springer	Parks
Overbrook	Britt
Woods	Flattop
Rod Club	Hutson
Velma	Sims
Cunningham	Goodwin
Markham	Spiers
Aldridge	Inscore
Humphreys	Boatwright
Horton	Anderson
Upper Mississippian	
Chester	Pitkin
Goddard	Hindsville
Kimball	Caney
Okeene	Wedington
Parvin	Stanley
Manning	
Middle Mississippian	
Meramec	Spergen
Mississippi lime	Warsaw
Ste. Genevieve	Mayes
St. Louis	Chappel
Salem	
Lower Mississippian	
Mississippi chat	Welden
Osage	Keokuk
Boone	Reeds Spring
Sycamore	St. Joe
Upper Devonian	
Woodford	Chattanooga
Arkansas Novaculite	Sylamore
Misener	Clifty
Hunton	
Hunton	Sallisaw
Bois d'Arc	Penters
Haragan	Frisco
Henryhouse	St. Clair
Chimneyhill	Brassfield
Keel	

106,233,257 bbl of oil and 594,300,798 MCF of gas as of July 31, 1998.

LOWER MISSISSIPPIAN GEOLOGY AND RESERVOIRS

During the Mississippian Period, broad epeirogenic movements continued throughout the southern Midcontinent. Deposition of shallow-marine limestones and shales was predominant, and in middle Mississippian time, cherty-limestone deposition was widespread. Major tectonic features that influenced Mississippian sedimentation include the Oklahoma

Table 2.—Significant Oil and Gas Fields in Oklahoma That Produce Petroleum from Silurian, Devonian, and Mississippian Rocks

Springeran Reservoirs
- Cement (gas)
- Chitwood (oil & gas)
- Eakly-Weatherford Trend (gas)
- Elk City (gas)
- Golden Trend (oil & gas)
- Knox (oil & gas)
- Sho-Vel-Tum (oil & gas)
- Watonga-Chickasha Trend (gas)
- Weatherford (gas)

Upper Mississippian Reservoirs
- Altona (gas)
- Chester, W (gas)
- Mocane-Laverne (gas)
- Okarche, N (gas)
- Okeene, NW (oil & gas)
- Ringwood (oil & gas)
- Sho-Vel-Tum (oil & gas)
- Sooner Trend (oil & gas)

Middle Mississippian Reservoirs
- Caddo (oil)
- Cheyenne Valley (oil & gas)
- Enid, NE (oil & gas)
- Okeene, NW (oil & gas)
- Ringwood (oil & gas)
- Sho-Vel-Tum (oil & gas)
- Sooner Trend (oil & gas)

Lower Mississippian Reservoirs
- Caddo (oil)
- Eola-Robberson (oil & gas)
- Garber (oil & gas)
- Golden Trend (oil & gas)
- Ringwood (oil)
- Sho-Vel-Tum (oil & gas)
- Sooner Trend (oil)
- Tonkawa (oil)
- Webb (gas)

Upper Devonian Reservoirs
- Alden, NE (oil)
- Caddo (oil)
- Cumberland (oil)
- Kremlin, W (oil & gas)
- Sho-Vel-Tum (oil)
- Sooner Trend (oil)

Hunton Reservoirs
- Aledo (gas)
- Custer City, N (gas)
- Edmond, W (oil)
- Fitts (oil)
- Golden Trend (oil & gas)
- Mayfield, W (gas)
- Moore, W (oil)
- Putnam (gas)
- Ringwood (oil & gas)
- Sooner Trend (oil & gas)

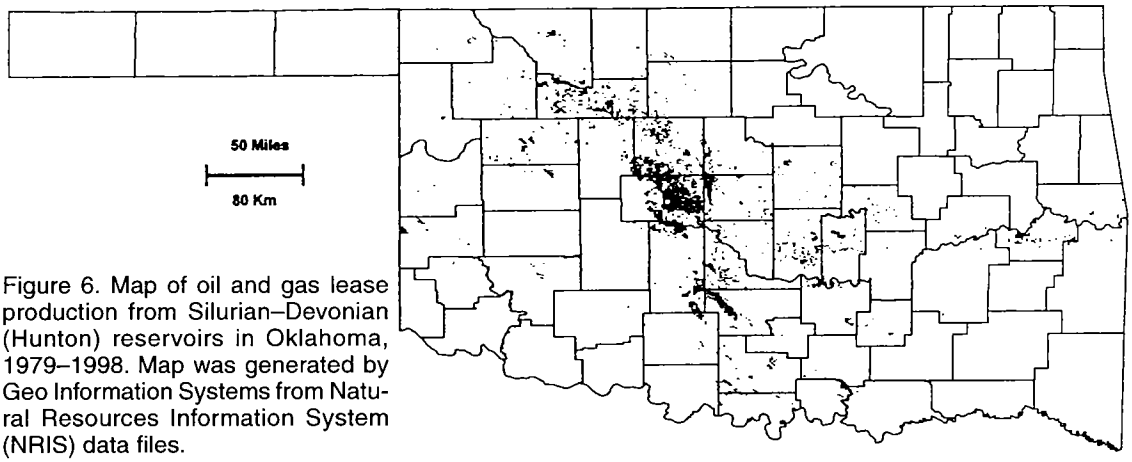

Figure 6. Map of oil and gas lease production from Silurian–Devonian (Hunton) reservoirs in Oklahoma, 1979–1998. Map was generated by Geo Information Systems from Natural Resources Information System (NRIS) data files.

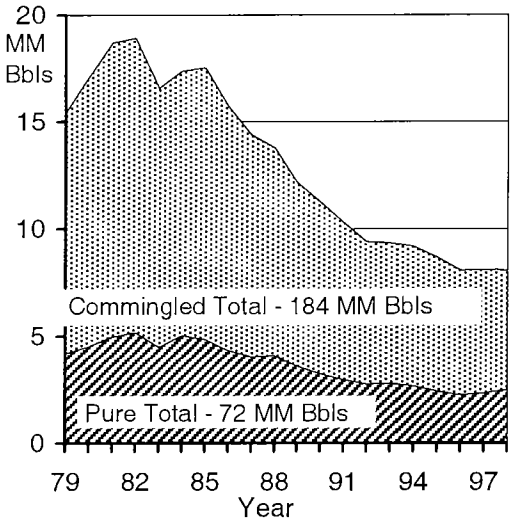

Figure 7. Graph of annual pure and commingled liquid (oil and condensate) production from leases producing from Silurian–Devonian (Hunton) reservoirs in Oklahoma, 1979–1998 (*MM Bbls* = million barrels). Total 1979–1998 liquid production was 256,649,306 bbl as of July 31, 1998.

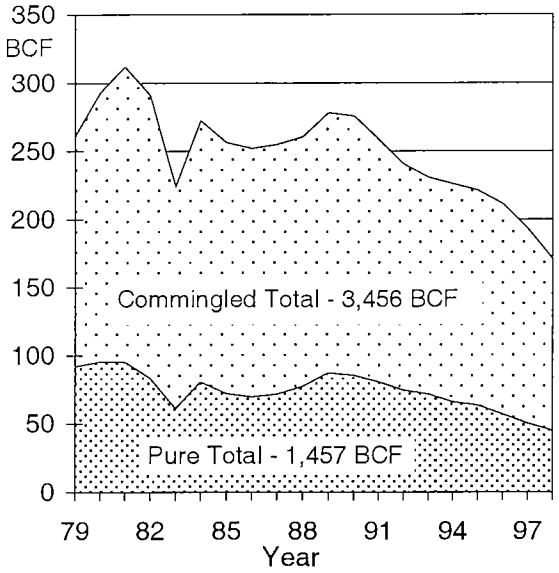

Figure 8. Graph of annual pure and commingled gas (associated and nonassociated) production from leases producing from Silurian–Devonian (Hunton) reservoirs in Oklahoma, 1979–1998 (*BCF* = billion cubic feet). Total 1979–1998 gas production was 4,913,608,907 MCF as of July 31, 1998.

basin, the Texas arch, and the Ozark uplift; most other regions of the southern Midcontinent were low-energy shelves or platforms. The correlation of Mississippian stratigraphic units in various parts of the southern Midcontinent is shown in Figure 12. Principal sources of data for the Mississippian System are by Craig and others (1979), Frezon and Jordan (1979), Mapel and others (1979), and Fay and others (1979). The following geologic discussion is modified from Johnson and others (1988).

Although most of the Woodford–Chattanooga Shale is Late Devonian in age, Mississippian conodonts occur in the top few meters at several localities (Frezon and Jordan, 1979). Commonly, however, the base of the lowest Mississippian (Kinderhookian Series) is placed arbitrarily at the top of the Woodford–Chattanooga Shale. This easily recognized rock-stratigraphic boundary is more indicative of paleotectonic change than is the time-stratigraphic boundary within the upper part of the Woodford–Chattanooga Shale (Frezon and Jordan, 1979).

After withdrawal of the euxinic seas in which the organic-rich black shales of the Woodford–Chattanooga were deposited, the region was inundated in Kinderhookian time by shallow, well-oxygenated marine waters that originally covered almost all parts of the State. The limestone–shale sequence is less than 100 ft thick in the northeast, is typically 50–225 ft thick in the northwest, and was largely removed from the central and southern parts of Oklahoma by post-Kinderhookian erosion.

The Osagean sea occupied most of the continental interior, and sedimentation in the southern Midcontinent occurred in aerated, warm, shallow seas that were stirred by currents or waves that gently affected the sea floor. Limestone and cherty limestone were the dominant sediments. A rich marine fauna, princi-

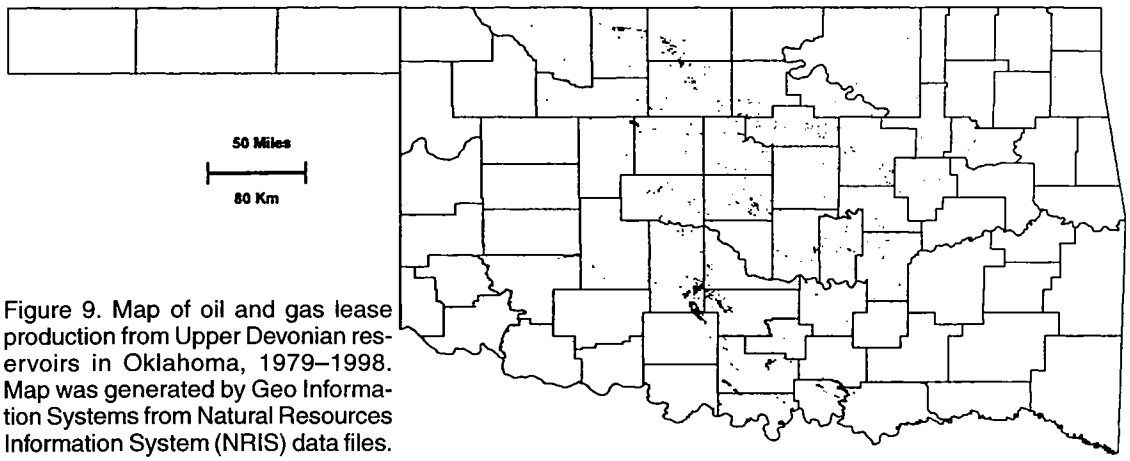

Figure 9. Map of oil and gas lease production from Upper Devonian reservoirs in Oklahoma, 1979–1998. Map was generated by Geo Information Systems from Natural Resources Information System (NRIS) data files.

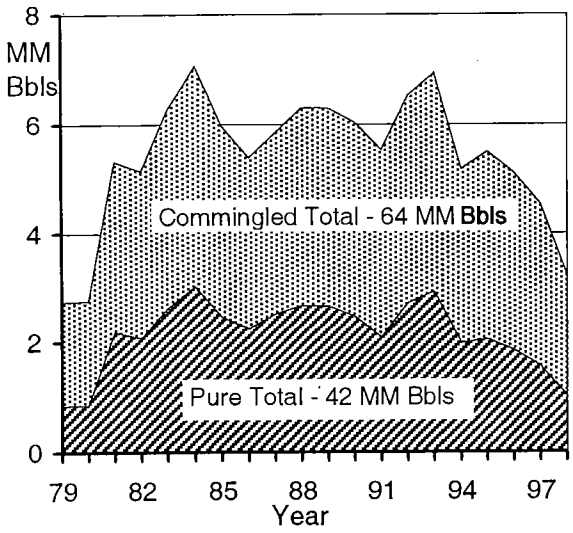

Figure 10. Graph of annual pure and commingled liquid (oil and condensate) production from leases producing from Upper Devonian reservoirs in Oklahoma, 1979–1998 (*MM Bbls* = million barrels). Total 1979–1998 liquid production was 106,233,257 bbl as of July 31, 1998.

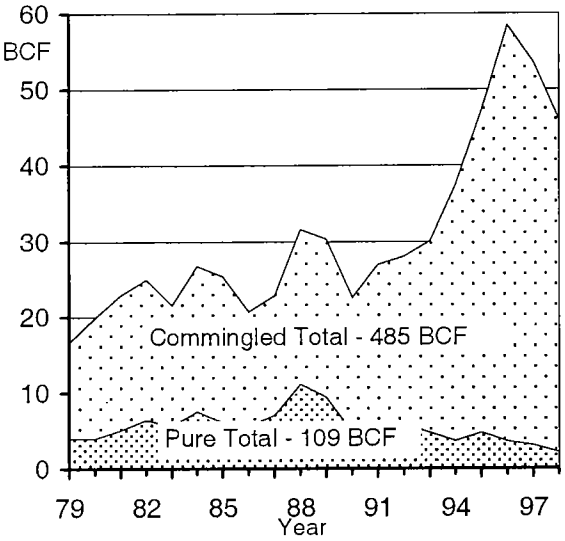

Figure 11. Graph of annual pure and commingled gas (associated and nonassociated) production from leases producing from Upper Devonian reservoirs in Oklahoma, 1979–1998 (*BCF* = billion cubic feet). Total 1979–1998 gas production was 594,300,798 MCF as of July 31, 1998.

pally crinoids, flourished in the Osagean sea. The region was affected only by slight epeirogenic movements during the Osagean Epoch. Gentle subsidence or uplift of 300 ft or less was enough to cause large areas to be submerged by, or emergent from, the shallow sea.

Chert, which occurs in most Osagean rocks, is a replacement of carbonate by silica. Chert generally makes up 10–30% of the rocks in much of the area. Terrigenous clastic sediments are present in many of the Osagean units, but they occur mainly as disseminated clays and silts, and only locally as discrete shales. Carbonates grade southward into shale toward the Ouachita trough (Fig. 3).

The maximum thickness of Osagean strata is in the western part of the Oklahoma basin, where 700 ft of cherty limestone is preserved. In other areas, Osagean strata typically range from 150 to 300 ft thick. Thickness variations in Osagean strata resulted mainly from post-Osagean erosion. Epeirogenic uplift during Meramecian time caused erosion of Osagean strata deposited in central and southern Oklahoma.

Names used for Lower Mississippian producing intervals are shown in Table 1. Some of the names applied to the subsurface nomenclature are the same formal names used for outcropping Lower Mississippian formations and members. However, Lower Mississippian reservoirs in northern Oklahoma are mostly called the *Mississippi "chat,"* an informal subsurface name for a significant producing interval in the shelf areas of northern Oklahoma.

The production map for the Lower Mississippian reservoirs (Fig. 13) shows the areas of northern Oklahoma where hydrocarbons are produced from Mississippian carbonates and Mississippi chat in stratigraphic traps associated with local structures. In the Ardmore basin of southern Oklahoma, Lower Mississippian production is generally from Sycamore reservoirs in faulted structural traps.

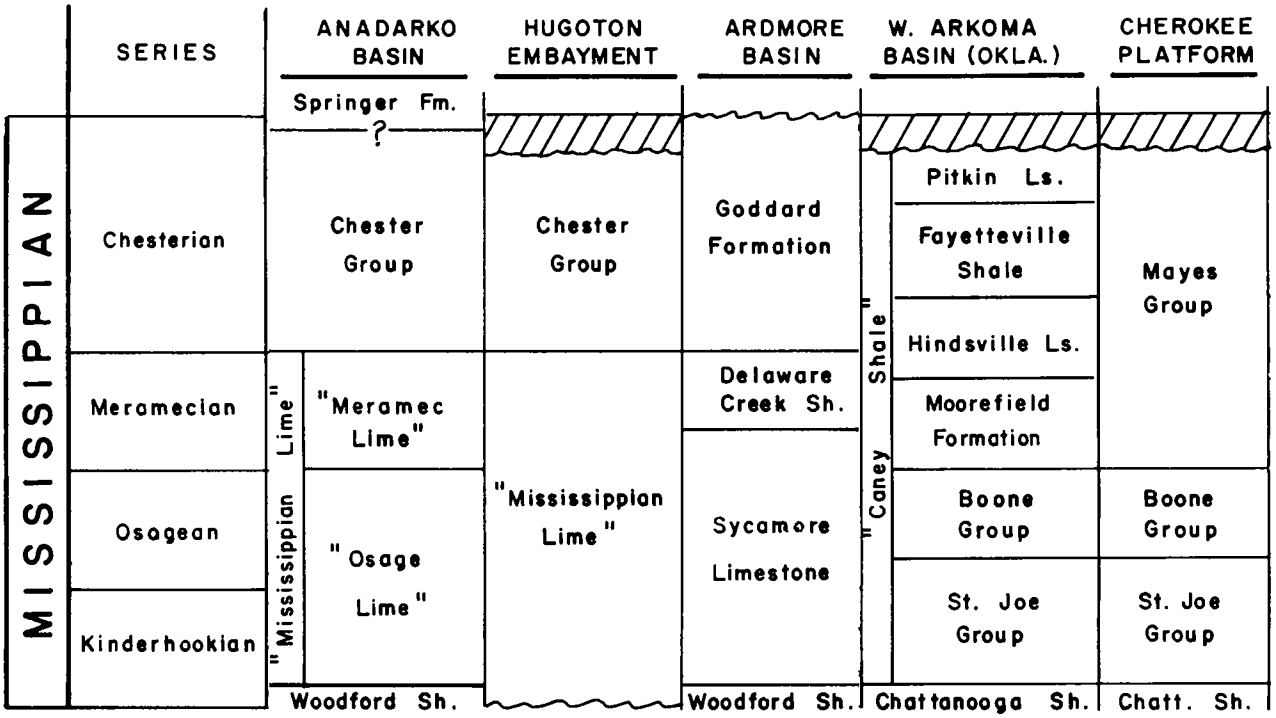

Figure 12. Correlation of Mississippian stratigraphic units in the southern Midcontinent, based upon COSUNA charts (published by the American Association of Petroleum Geologists). Modified from Johnson and others (1988).

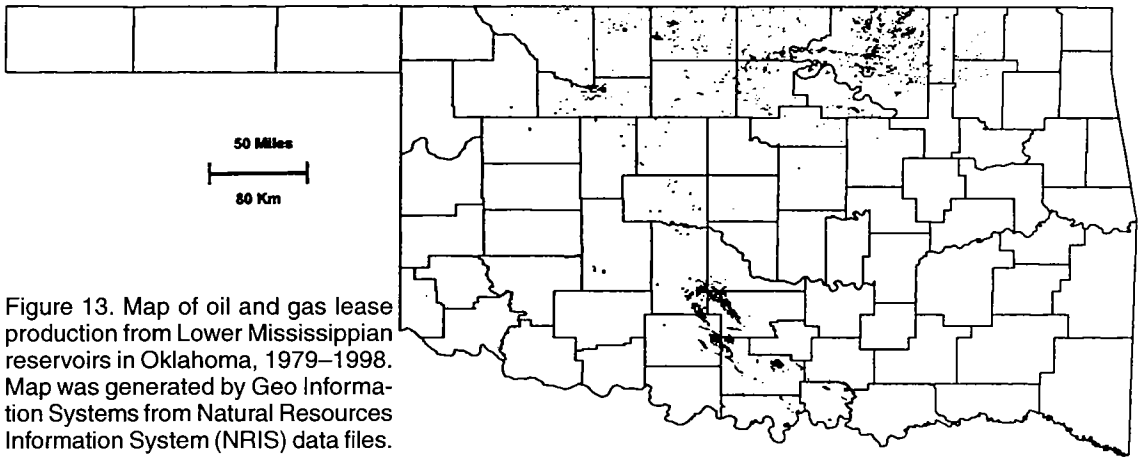

Figure 13. Map of oil and gas lease production from Lower Mississippian reservoirs in Oklahoma, 1979–1998. Map was generated by Geo Information Systems from Natural Resources Information System (NRIS) data files.

Graphs of annual production for the period 1979 through 1998 from Lower Mississippian reservoirs for pure and commingled leases show liquid production (crude oil and condensate) in Figure 14 and gas production (associated and nonassociated) in Figure 15. Cumulative lease production from Lower Mississippian reservoirs (pure and commingled) for the period 1979–1998 was 196,553,280 bbl of oil and 1,782,113,553 MCF of gas as of July 31, 1998.

MIDDLE MISSISSIPPIAN GEOLOGY AND RESERVOIRS

Meramecian marine environments in the southern Midcontinent resembled those of the Osagean Epoch. Shallow, well-aerated, warm seas were widespread and favored deposition of fossiliferous (commonly crinoidal) and oolitic limestones with some interbeds of claystone, shale, and siltstone. Most of the region was a carbonate shelf, and chert formation, similar to the Osagean occurrences, was largely restricted to the northern half of Oklahoma. The presence of oolitic limestone in many parts of Arkansas, Oklahoma, and Texas indicates that the shallow sea bottom was more agitated by wave and current action during the Meramecian than at other times during the Mississippian.

In the Arkoma basin area the Meramecian carbonates grade southward into calcareous shales deposited in, and adjacent to, the Ouachita trough (Fig. 3). According to Frezon and Jordan (1979), a depression extended to the west and northwest of the Ouachita trough across a shoal area and into the Oklahoma

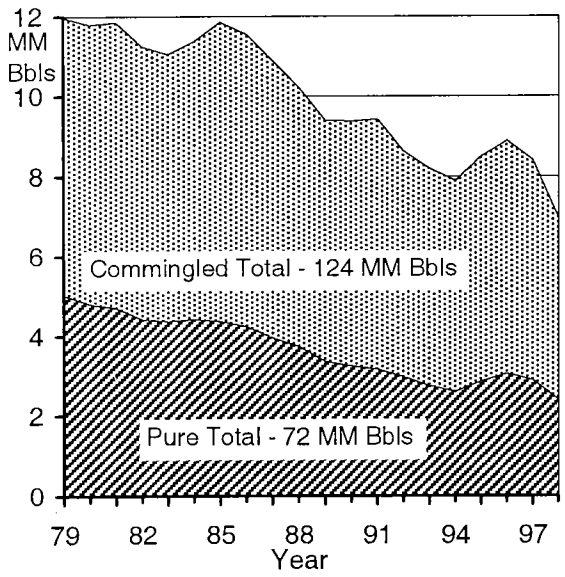

Figure 14. Graph of annual pure and commingled liquid (oil and condensate) production from leases producing from Lower Mississippian reservoirs in Oklahoma, 1979–1998 (*MM Bbls* = million barrels). Total 1979–1998 liquid production was 196,553,280 bbl as of July 31, 1998.

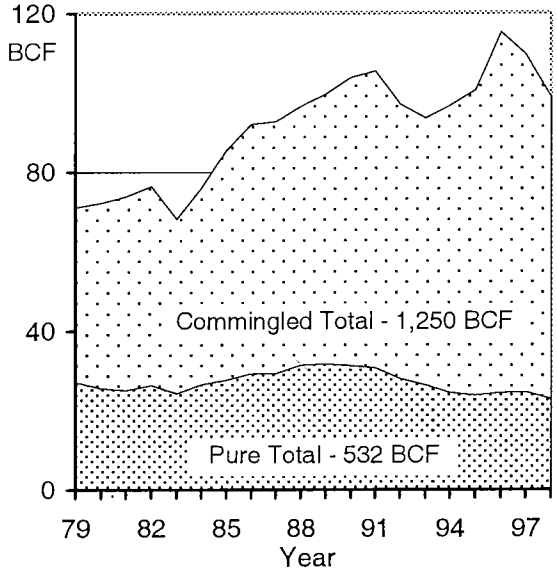

Figure 15. Graph of annual pure and commingled gas (associated and nonassociated) production from leases producing from Lower Mississippian reservoirs in Oklahoma, 1979–1998 (*BCF* = billion cubic feet). Total 1979–1998 gas production was 1,782,113,553 MCF as of July 31, 1998.

basin. The shoal area, which apparently was in the vicinity of the future Arbuckle Mountains, was a high-energy environment where fine-grained clastics were winnowed and transported westward to a low-energy environment in the central part of what would become the Anadarko basin.

There was little or no tectonic activity in Oklahoma during the Meramecian Epoch. Epeirogenic movements in mid-Meramecian time raised the Ozark region slightly above sea level. Thickness variations in the Meramecian resulted mainly from post-Meramecian erosion. In most areas the thickness now ranges from 150 to 500 ft; the maximum preserved thickness is nearly 1,300 ft in the western part of the Anadarko basin.

Sedimentation probably was continuous from Meramecian into Chesterian time in the Anadarko basin. Small areas where Meramecian strata are missing—in southern and central Oklahoma, and along the Nemaha uplift in northern Oklahoma—resulted from post-Mississippian tectonic uplift and erosion.

Names used for middle Mississippian producing intervals are shown in Table 1. Most of the names applied to the subsurface nomenclature are the formal names of middle Mississippian formations and members from outcrop sections. However, middle Mississippian reservoirs in northern Oklahoma are mostly called *Mississippi lime* and *Mississippi "solid,"* which are informal subsurface names.

The production map for the middle Mississippian (Fig. 16) shows the extensive area in northern Oklahoma where producible hydrocarbons from Mississippian carbonates and Mississippi chat are usually found in stratigraphic traps associated with local structures. In the Ardmore basin of southern Oklahoma, middle Mississippian production is generally from reservoirs in the Mayes in structural traps.

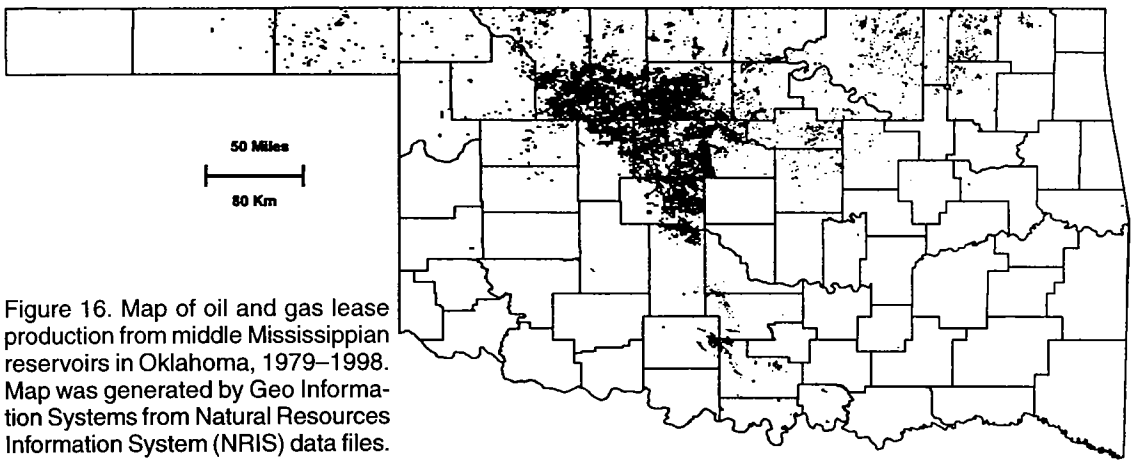

Figure 16. Map of oil and gas lease production from middle Mississippian reservoirs in Oklahoma, 1979–1998. Map was generated by Geo Information Systems from Natural Resources Information System (NRIS) data files.

Graphs of annual production for the period 1979 through 1998 from middle Mississippian reservoirs for pure and commingled leases show liquid production (crude oil and condensate) in Figure 17 and gas production (associated and nonassociated) in Figure 18. Cumulative lease production from middle Mississippian reservoirs (pure and commingled) for the period 1979–1998 was 304,784,193 bbl of oil and 5,481,870,857 MCF of gas as of July 31, 1998.

UPPER MISSISSIPPIAN GEOLOGY AND RESERVOIRS

Chesterian seas covered all parts of Oklahoma, although epeirogenic movements and eustatic changes of sea level caused intermittent emergence of many areas. In much of the region the Chesterian sequence consists of shale with some limestone and marginal sandstones in the lower part, and limestone with some shales in the upper part. These strata were deposited in normal-marine waters, although the shales were generally laid down in somewhat deeper and more turbid waters than were the limestones.

The Ouachita trough became an increasingly important factor, affecting sedimentation in eastern Oklahoma during Chesterian time. By now the trough was subsiding sharply along the arcuate trace of the present-day Ouachita fold belt. Shales, which reach a thickness of 5,000 ft within the Ouachita trough, extend to the north and west into the area of the future Arkoma and Ardmore basins, where they interfinger with overlying shelf limestones (Fig. 3).

Lithologic changes in Chesterian rocks commonly reflect the amount of post-Mississippian uplift and the depth of erosion around the margins of some of the basins; the upper limestone units have been removed, leaving only the lower shaly units at the basin margins. Post-Mississippian uplift and erosion along the Nemaha uplift also account for the absence of Chesterian strata, which were originally deposited across a large area in central and northern Oklahoma.

The thickest Chesterian rocks in the region are the 2,000 ft of shales in the eastern part of the Arkoma basin, where these strata thicken sharply into the Ouachita basinal facies. Also, about 1,500 ft of shales and limestones is present in the deep Anadarko basin area.

The total thickness of the Mississippian (excluding Springeran strata) is greatest in the western part of the Anadarko basin (~3,000 ft) and in the southern part of the Arkoma basin of Arkansas (>2,500 ft). The Mississippian is ~1,300 ft thick in the northern part of the Hollis basin. Elsewhere, the Mississippian is commonly 300–600 ft thick. The thickening of the pre-Springeran Mississippian into the several major basins resulted partly from depositional thickening toward centers of ancestral basins that were to become dominant in Pennsylvanian time and partly from intermittent Mississippian and Pennsylvanian uplift and truncation along the margins of these basins.

The names used for Upper Mississippian producing intervals are shown in Table 1. Most of the names used in subsurface nomenclature are informal.

The production map for the Upper Mississippian (Fig. 19) shows the extensive area in northern Oklahoma where production has been obtained from Upper Mississippian carbonates in stratigraphic traps associated with local structures. Porosity development in differing environments controls the areas of production from these carbonates.

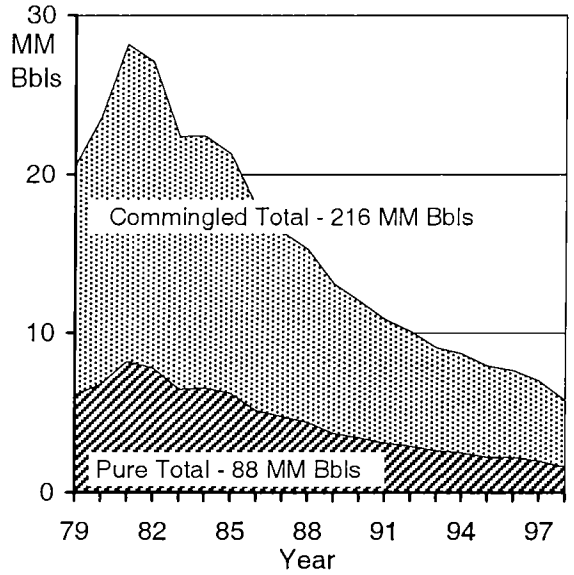

Figure 17. Graph of annual pure and commingled liquid (oil and condensate) production from leases producing from middle Mississippian reservoirs in Oklahoma, 1979–1998 (*MM Bbls* = million barrels). Total 1979–1998 liquid production was 304,784,193 bbl as of July 31, 1998.

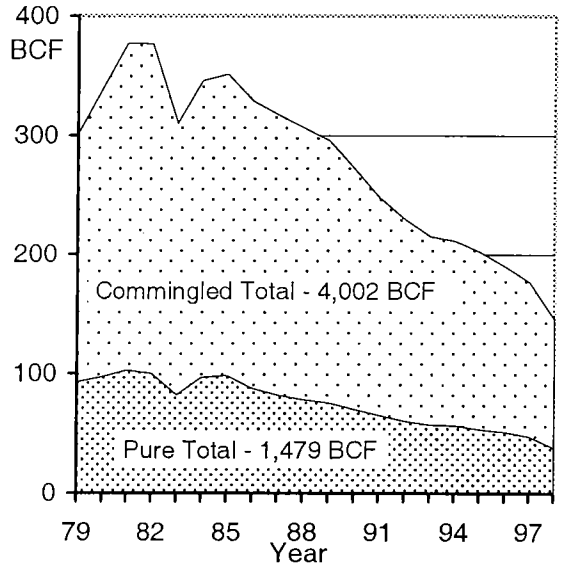

Figure 18. Graph of annual pure and commingled gas (associated and nonassociated) production from leases producing from middle Mississippian reservoirs in Oklahoma, 1979–1998 (*BCF* = billion cubic feet). Total 1979–1998 gas production was 5,481,870,857 MCF as of July 31, 1998.

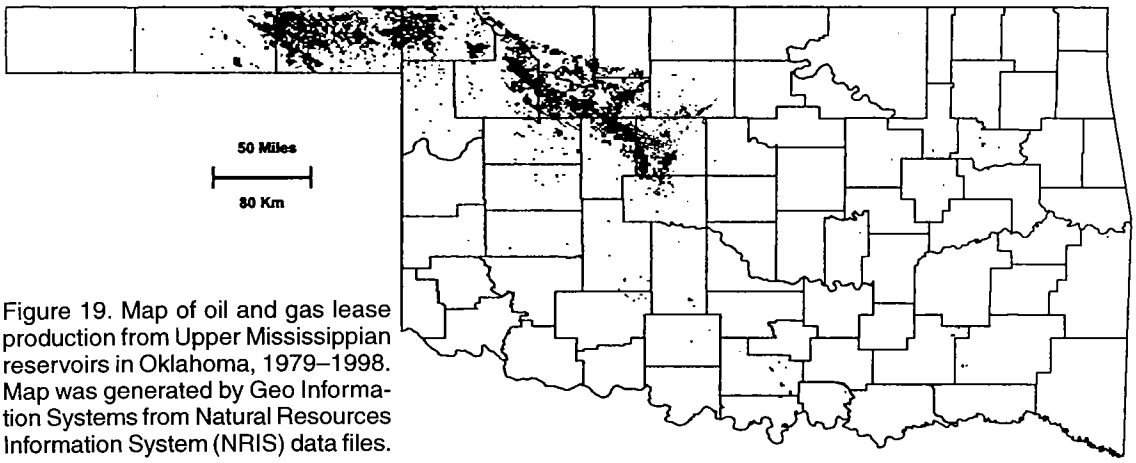

Figure 19. Map of oil and gas lease production from Upper Mississippian reservoirs in Oklahoma, 1979–1998. Map was generated by Geo Information Systems from Natural Resources Information System (NRIS) data files.

Graphs of annual production for the period 1979 through 1998 from Upper Mississippian reservoirs for pure and commingled leases show liquid production (crude oil and condensate) in Figure 20 and gas production (associated and nonassociated) in Figure 21. Cumulative lease production from Upper Mississippian reservoirs (pure and commingled) for the period 1979–1998 was 106,152,509 bbl of oil and 4,786,155,427 MCF of gas as of July 31, 1998.

SPRINGERAN GEOLOGY AND RESERVOIRS

Although the top of the Mississippian System is well marked by a pre-Pennsylvanian unconformity in most parts of the southern Midcontinent, the Mississippian–Pennsylvanian boundary occurs within the thick sequence of shales and sands of the Springer Group and equivalent strata, where sedimentation was uninterrupted in the deep parts of the Anadarko and Ardmore basins (Johnson and others, 2001). These Springer clastic rocks in Oklahoma commonly are assigned a "Springeran" age—an age that spans a period between the Late Mississippian Chesterian Epoch and the Early Pennsylvanian Morrowan Epoch. We follow that concept here because we cannot separate out the Pennsylvanian part of the Springeran. Thus we present data on all Springeran production as though it is Mississippian in age.

Deposition of Springeran strata was restricted to the deeper parts of the Anadarko–Ardmore basins. Springeran strata marked a change from the dominantly carbonate and shale deposition of the Late Mississippian to the clastic environments of the Early Pennsylvanian. Rapid subsidence of the Anadarko–Ardmore basins and the adjacent shelf areas in Late Mississippian and Early Pennsylvanian time caused transgression of the Springeran seas over the shelf

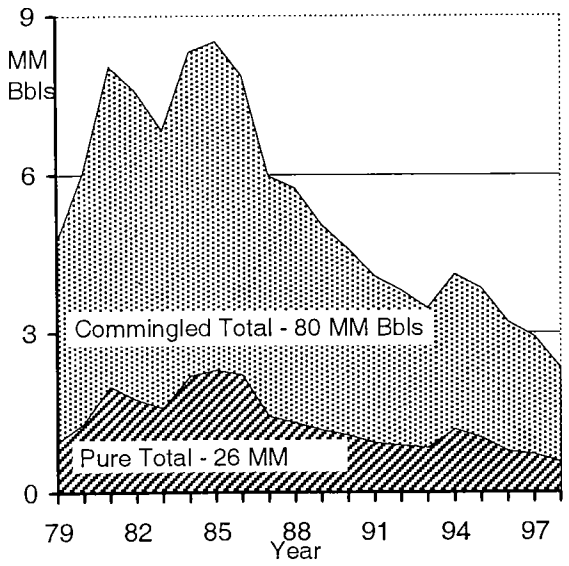

Figure 20. Graph of annual pure and commingled liquid (oil and condensate) production from leases producing from Upper Mississippian reservoirs in Oklahoma, 1979–1998 (*MM Bbls* = million barrels). Total 1979–1998 liquid production was 106,152,509 bbl as of July 31, 1998.

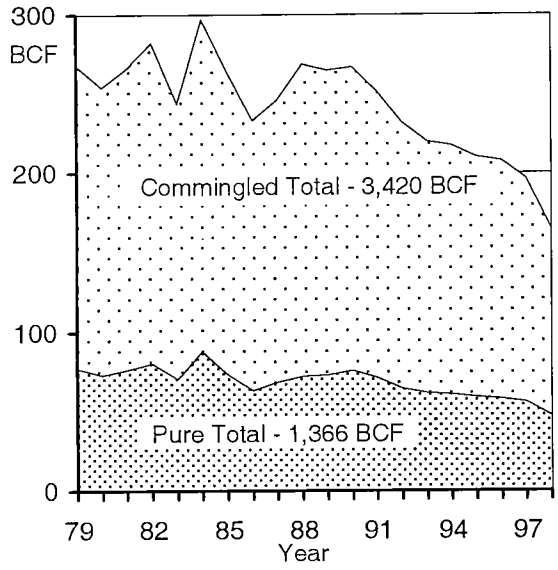

Figure 21. Graph of annual pure and commingled gas (associated and nonassociated) production from leases producing from Upper Mississippian reservoirs in Oklahoma, 1979–1998 (*BCF* = billion cubic feet). Total 1979–1998 gas production was 4,786,155,427 MCF as of July 31, 1998.

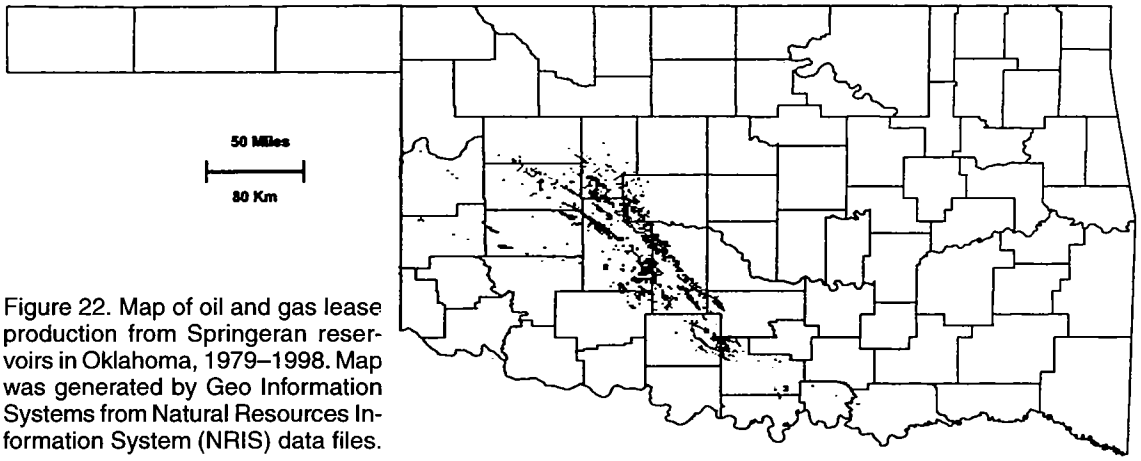

Figure 22. Map of oil and gas lease production from Springeran reservoirs in Oklahoma, 1979–1998. Map was generated by Geo Information Systems from Natural Resources Information System (NRIS) data files.

areas of Chester carbonates and deposition of shallow-marine and shoreline sands of the Springer. Intervals of Springer sands in the Anadarko and Ardmore basins are as thick as 250 ft in some areas, with discrete marine sand bars attaining a thickness of 50 ft or more for several miles (Brown and Northcutt, 1993).

Springer sands were first named after leases in the fields of southern Oklahoma where they produced oil and/or gas. Correlation of the individual sands was not attempted between fields, so some of the names of the Springeran producing intervals shown in Table 1 may, in fact, be equivalent to other names.

The production map for the Springeran (Fig. 22) shows oil and gas production from Springeran reservoirs, mainly marine sands, in the Anadarko and Ardmore basins and in the frontal fault belt of the Wichita uplift. Springeran production comes from both stratigraphic and structural traps. Stratigraphic traps dominate in the Anadarko and Ardmore basins, and structural traps are prevalent in the faulted and folded belts in southern Oklahoma and the faulted frontal area of the Wichita uplift.

Graphs of annual production for the period 1979 through 1998 from Springeran reservoirs for pure and commingled leases show liquid production (crude oil and condensate) in Figure 23 and gas production (associated and nonassociated) in Figure 24. Cumulative lease production from Springeran reservoirs (pure and commingled) for the period 1979–1998 was 352,117,687 bbl of oil and 6,523,657,609 MCF of gas as of July 31, 1998.

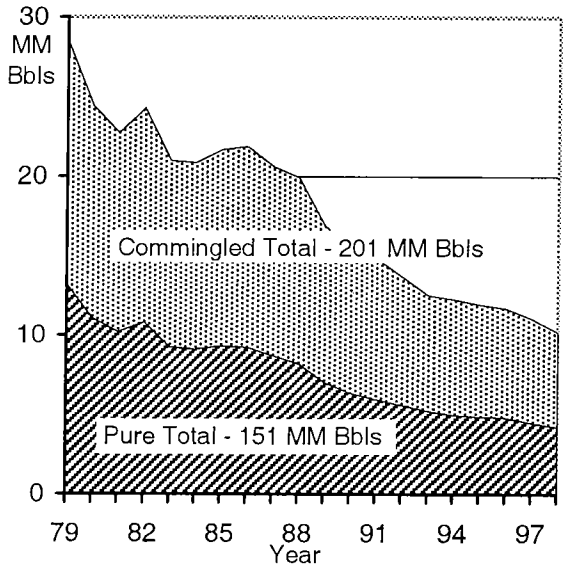

Figure 23. Graph of annual pure and commingled liquid (oil and condensate) production from leases producing from Springeran reservoirs in Oklahoma, 1979–1998 (*MM Bbls* = million barrels). Total 1979–1998 liquid production was 352,117,687 bbl as of July 31, 1998.

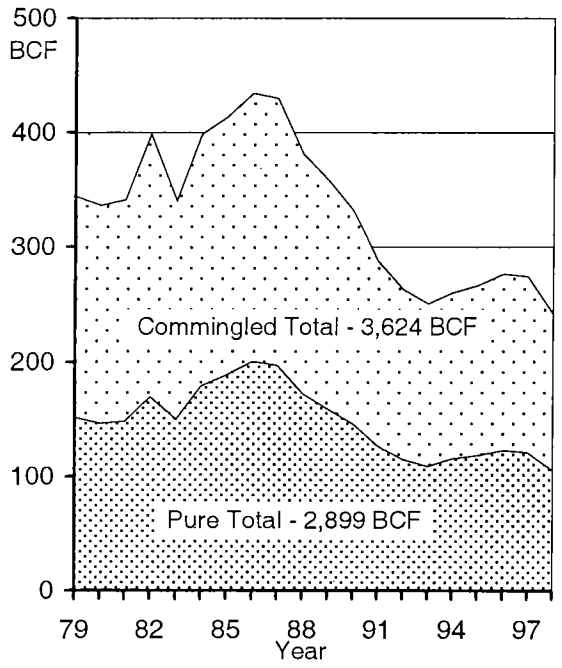

Figure 24. Graph of annual pure and commingled gas (associated and nonassociated) production from leases producing from Springeran reservoirs in Oklahoma, 1979–1998 (*BCF* = billion cubic feet). Total 1979–1998 gas production was 6,523,657,609 MCF as of July 31, 1998.

SUMMARY AND CONCLUSIONS

Petroleum reservoirs of Silurian, Devonian, and Mississippian age have yielded significant amounts of oil and gas in Oklahoma. The geologic history of reservoir development and petroleum entrapment in these rocks encompasses many depositional, diagenetic, orogenic, and tectonic environments. The discovery of new reservoirs and the application of new methods to develop old reservoirs in all these rock units continue today.

Some of the significant oil and gas fields that produce from these rocks are shown in Table 2. Many of these fields yield significant amounts of petroleum, and although several are in the mature stage of development, new reserves are still being developed from Silurian, Devonian, and Mississippian reservoirs.

Graphs of liquid and gas production for the six geologic intervals under investigation show the comparative amounts of annual lease production for only pure liquids (Fig. 25) and pure gas (Fig. 26) for the period from 1979 through 1998. The total production of liquids (crude oil and condensate) from all Silurian, Devonian, and Mississippian reservoirs for both pure and commingled leases for 1979–1998 was 1,322,490,232 barrels (about 1.3 billion barrels). The total production of gas (associated and nonassociated) from all Silurian, Devonian, and Mississippian reservoirs for both pure and commingled leases for 1979–1998 was 24,084,707,151,000 cubic feet (about 24.1 trillion cubic feet).

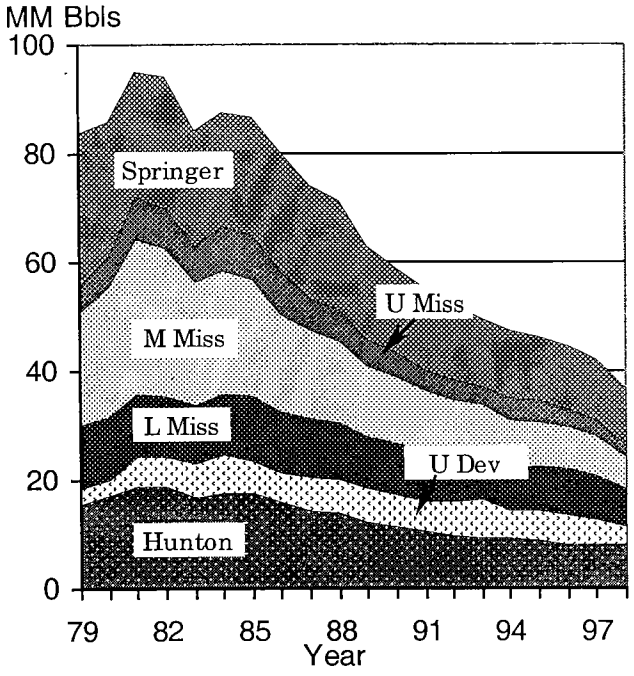

Figure 25. Graph of annual pure and commingled liquid (oil and condensate) production from leases producing from all Silurian, Devonian, and Mississippian reservoirs in Oklahoma, 1979–1998 (*MM Bbls* = million barrels). Total 1979–1998 liquid production was 1,322,490,232 barrels as of July 31, 1998.

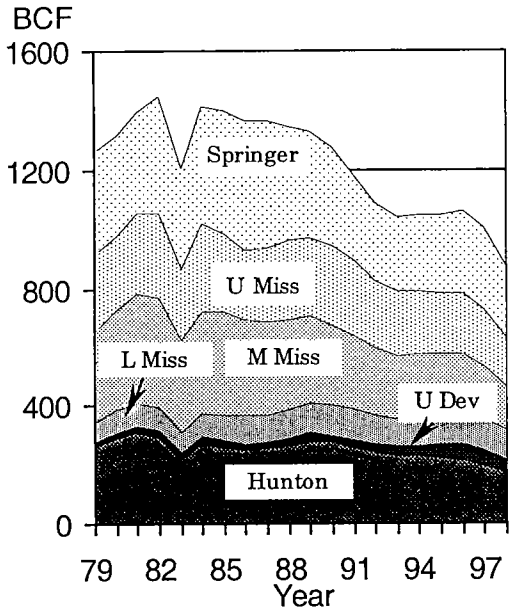

Figure 26. Graph of annual pure and commingled gas (associated and nonassociated) production from leases producing from all Silurian, Devonian, and Mississippian reservoirs in Oklahoma, 1979–1998 (*BCF* = billion cubic feet). Total 1979–1998 gas production was 24,084,707,151,000 cubic feet as of July 31, 1998.

A summary showing liquid and gas production, by interval, from the Silurian, Devonian, and Mississippian reservoirs is shown in Table 3.

REFERENCES CITED

Al-Shaieb, Zuhair; and Puckette, Jim, 2000, Sequence stratigraphy of Hunton Group ramp facies, Arbuckle Mountains and Anadarko basin, Oklahoma, *in* Johnson, K. S. (ed.), Platform carbonates in the southern Midcontinent, 1996 symposium: Oklahoma Geological Survey Circular 101, p. 131–137.

Amsden, T. W., 1975, Hunton Group (Late Ordovician, Silurian, and Early Devonian) in the Anadarko basin of Oklahoma: Oklahoma Geological Survey Bulletin 121, 214 p.

_____1980, Hunton Group (Late Ordovician, Silurian, and Early Devonian) in the Arkoma basin of Oklahoma: Oklahoma Geological Survey Bulletin 129, 136 p.

Amsden, T. W.; and Barrick, J. E., 1993, Pre-Woodford subcrop map of the Anadarko basin, western Oklahoma and Texas Panhandle: Oklahoma Geological Survey Map GM-34, scale 1:500,000.

Amsden, T. W.; and Rowland, T. L., 1967, Geologic maps and stratigraphic cross sections of Silurian strata and Lower Devonian formations in Oklahoma: Oklahoma Geological Survey Map GM-14.

Berry, W. B. N.; and Boucot, A. J., 1970, Correlation of North American Silurian rocks: Geological Society of America Special Paper 102, 289 p.

Brown, R. W.; and Northcutt, R. A., 1993, Springer marine sandstone—Anadarko basin, *in* Bebout, D. C.; White, W. A.; Hentz, T. F.; and Grasmick, M. K. (eds.), Atlas of major Midcontinent gas reservoirs: Texas Bureau of Economic Geology, Austin, p. 53–54.

Craig, L. C.; and 24 others, 1979, Paleotectonic investigations of the Mississippian System in the United States:

Table 3.—Silurian, Devonian, and Mississippian Petroleum Production in Oklahoma, 1979–1998[a]

Geologic interval	Liquid production Million barrels (MM bbl)			Gas production Billion cubic feet (BCF)		
	Pure	Commingled	Total	Pure	Commingled	Total
Springeran	151	201	352	2,899	3,624	6,523
Upper Mississippian	26	80	106	1,366	3,420	4,786
Middle Mississippian	88	216	304	1,479	4,002	5,481
Lower Mississippian	72	124	196	532	1,250	1,782
Upper Devonian	42	64	106	109	485	594
Hunton	72	184	256	1,457	3,456	4,913
Totals	451	869	1,320	7,842	16,237	24,079

[a]1998 production only through 7/31/98. Annual production for 1998 was estimated for graphs.

U.S. Geological Survey Professional Paper 1010, part I, p. 1–369; part II, p. 371–559; part III, 15 pls.

Denison, R. E.; Lidiak, E. G.; Bickford, M. E.; and Kisvarsanyi, E. B., 1984, Geology and geochronology of Precambrian rocks in the central interior region of the United States: U.S. Geological Survey Professional Paper 1241-C, 20 p.

Fay, R. O., 1989, Geology of the Arbuckle Mountains along Interstate 35, Carter and Murray Counties, Oklahoma [revised edition]: Oklahoma Geological Survey Guidebook 26, 50 p.

Fay, R. O.; Friedman, S. A.; Johnson, K. S.; Roberts, J. F.; Rose, W. D.; and Sutherland, P. K., 1979, Oklahoma, *in* The Mississippian and Pennsylvanian (Carboniferous) Systems in the United States: U.S. Geological Survey Professional Paper 1110-R, 35 p.

Frezon, S. E.; and Jordan, Louise, 1979, Oklahoma, *in* Craig, L. C.; and 24 others, Paleotectonic investigations of the Mississippian System in the United States: Part I, Introduction and regional analysis of the Mississippian System: U.S. Geological Survey Professional Paper 1010-I, p. 147–159.

Ham, W. E., 1969, Regional geology of the Arbuckle Mountains, Oklahoma: Oklahoma Geological Survey Guidebook 17, 52 p.

Ham, W. E.; and Wilson, J. L., 1967, Paleozoic epeirogeny and orogeny in the central United States: American Journal of Science, v. 265, p. 332–407.

Johnson, K. S. (ed.), 1993, Hunton Group core workshop and field trip: Oklahoma Geological Survey Special Publication 93-4, 212 p.

Johnson, K. S.; and Cardott, B. J., 1992, Geologic framework and hydrocarbon source rocks of Oklahoma, *in* Johnson, K. S.; and Cardott, B. J. (eds.), Source rocks in the southern Midcontinent, 1990 symposium: Oklahoma Geological Survey Circular 93, p. 21–37.

Johnson, K. S.; Amsden, T. W.; Denison, R. E.; Dutton, S. P.; Goldstein, A. G.; Rascoe, Bailey, Jr.; Sutherland, P. K.; and Thompson, C. M., 1988, Southern Midcontinent region, *in* Sloss, L. L. (ed.), Sedimentary cover—North American craton, U.S.: Geological Society of America, The Geology of North America, v. D-2, p. 307–359. [Reprinted in 1989 as Oklahoma Geological Survey Special Publication 89-2, 53 p.]

Johnson, K. S.; Northcutt, R. A.; Hinshaw, G. C.; and Hines, K. E., 2001, Geology and petroleum reservoirs in Pennsylvanian and Permian rocks of Oklahoma, *in* Johnson, K. S. (ed.), Pennsylvanian and Permian geology and petroleum in the southern Midcontinent, 1998 symposium: Oklahoma Geological Survey Circular 104, p. 1–19.

Mapel, W. J.; Johnson, R. B.; Bachman, G. O.; and Varnes, K. L., 1979, Southern Midcontinent and Southern Rocky Mountains region, *in* Craig, L. C.; and 24 others, Paleotectonic investigations of the Mississippian System in the United States: Part I, Introduction and regional analysis of the Mississippian System: U.S. Geological Survey Professional Paper 1010-J, p. 161–187.

Rogers, S. M.; Forgotson, J. M., Jr.; and Dewers, T. A., 2000, Depositional and diagenetic history of Mississippian chat reservoirs, northern Oklahoma, *in* Johnson, K. S. (ed.), Platform carbonates in the southern Midcontinent, 1996 symposium: Oklahoma Geological Survey Circular 101, p. 157–161.

Rottmann, Kurt, 2000, Defining the role of Woodford–Hunton depositional relationships in Hunton stratigraphic traps of western Oklahoma, *in* Johnson, K. S. (ed.), Platform carbonates in the southern Midcontinent, 1996 symposium: Oklahoma Geological Survey Circular 101, p. 139–146.

Rottmann, Kurt; Beaumont, E. A.; Northcutt, R. A.; Al-Shaieb, Zuhair; Puckette, Jim; and Blubaugh, Paul, 2000, Hunton play in Oklahoma (including northeast Texas Panhandle): Oklahoma Geological Survey Special Publication 2000-2, 131 p.

Smith, P. W.; Hendrickson, W. J.; and Williams, C. M., 2000a, Production and reservoir characteristics of selected Hunton fields in the Anadarko basin, *in* Johnson, K. S. (ed.), Platform carbonates in the southern Midcontinent, 1996 symposium: Oklahoma Geological Survey Circular 101, p. 147–156.

Smith, P. W.; Hendrickson, W. J.; Williams, C. M.; and Woods, R. J., 2000b, Stratigraphic relationships of Springer and Chester Groups within the Oklahoma portion of the Anadarko basin and shelf: a clarification, *in* Johnson, K. S. (ed.), Platform carbonates in the southern Midcontinent, 1996 symposium: Oklahoma Geological Survey Circular 101, p. 197–207.

The Hunton Group: Sequence Stratigraphy, Facies, Dolomitization, and Karstification

Zuhair Al-Shaieb, Jim Puckette, and Paul Blubaugh
Oklahoma State University
Stillwater, Oklahoma

ABSTRACT.—The Hunton Group consists of shallow-water carbonates that were deposited on a gently inclined ramp. In this setting, facies belts developed subparallel to bathymetric contours. Sea-level changes caused extensive migration of facies and generated multiple disconformities that are used to define major stratigraphic divisions within the Hunton. The Henryhouse and Haragan/Bois d'Arc (HHB) section represents a type 1 carbonate sequence. The lower boundary is the unconformity that separates the Henryhouse from the underlying Chimneyhill Subgroup. The upper boundary is the pre-Woodford (or pre-Frisco) unconformity. The Henryhouse–Haragan/Bois d'Arc sequence is a major oil and gas reservoir in the Anadarko basin.

Henryhouse–Haragan/Bois d'Arc facies in the Arbuckle Mountain section are notably different from those examined in cores from the Anadarko basin. Outcrop parasequences consist only of subtidal facies, whereas time-equivalent rocks in the western Anadarko basin include intertidal and supratidal facies. The thickening of these additional facies indicates a northwestward shallowing of the basin during the Late Silurian–Early Devonian. Sedimentary structures, lithology, fossil content, and fabric relationships were used as criteria to recognize various depositional-facies bands that parallel the paleoshoreline. Supratidal (I), intertidal (II), and subtidal (III) facies are readily recognized, and their spatial relationships consistently indicate shallowing-upward sequences.

Three stages of dolomitization are documented in the Henryhouse Formation: (1) penecontemporaneous hypersaline dolomite, (2) marine and freshwater mixed dolomite, and (3) deep-burial or thermal dolomite. Four types of porosity that developed are moldic, vuggy, intercrystalline, and fracture. Moldic and intercrystalline porosity are fabric selective, whereas vuggy and fracture porosity are nonfabric selective.

Cores from the Hunton exhibit a variety of paleokarstic and other diagenetic features. Vuggy porosity, solution-enlarged fractures, breccias, and infill sediments are common. Paleokarstic reservoirs were classified into two types. Type 1 are focused-flow reservoirs with solution-enlarged conduits, collapse breccias, and cavern-fill parabreccia. Type 2, which are diffuse-flow reservoirs with interparticle and vuggy porosity, are the major hydrocarbon-producing reservoirs.

INTRODUCTION

The general stratigraphic divisions of the Hunton are the Chimneyhill Subgroup (Keel, Cochrane, and Clarita Formations); the Henryhouse, Haragan, and Bois d'Arc Formations (HHB type 1 carbonate sequence); and the Frisco Formation (Amsden, 1980, 1989) (Fig. 1). The Frisco is genetically different from earlier Hunton rocks because it was deposited mainly as bryozoan–crinoid carbonate bioherms (Medlock, 1984) on a post-epeirogenic unconformity surface. Henryhouse–Haragan/Bois d'Arc depositional facies are different from those of the underlying Clarita Formation and the overlying Woodford or Frisco Formation. The vertical juxtaposition of Chimneyhill, Frisco, or Woodford facies against distinctly different Henryhouse–Haragan/Bois d'Arc facies identifies depositional breaks or disconformities in the section. A significant disconformity separates the Chimneyhill Subgroup from the overlying Henryhouse–Haragan/Bois d'Arc sequence. Two major epeirogenies interrupted deposition during the Devonian (Amsden, 1975). The Early Devonian (pre-Frisco) and pre-Woodford uplifts (declines in sea level) generated unconformities that affected the entire region. Erosion associated with this later episode truncated the Hunton and removed it from much of the northeastern Oklahoma platform.

Reprinted with minor modifications from Rottmann, Kurt, and others, 2000, Hunton play in Oklahoma (including northeast Texas Panhandle: Oklahoma Geological Survey Special Publication 2000-2, p. 39–50.

Al-Shaieb, Zuhair; Puckette, Jim; and Blubaugh, Paul, 2001,The Hunton Group: sequence stratigraphy, facies, dolomitization, and karstification, *in* Johnson, K. S., (ed.), Silurian, Devonian, and Mississippian geology and petroleum in the southern Midcontinent, 1999 symposium: Oklahoma Geological Survey Circular 105, p. 17–29.

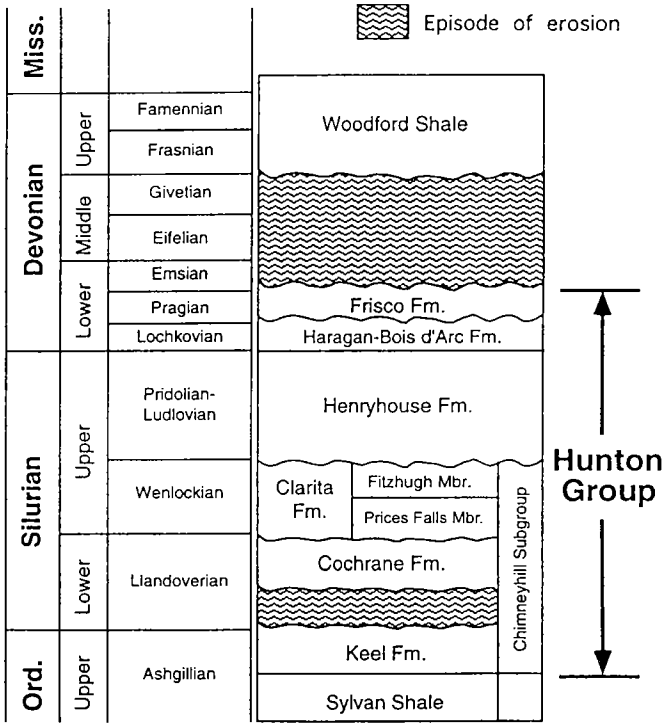

Figure 1. General stratigraphic nomenclature of the Hunton Group in Oklahoma. Modified from Barrick and others (1990) and Amsden (1989).

As a result of its economic importance, the Hunton has been the focus of numerous studies. Many researchers have presented evidence regarding the subject of unconformities and their use in establishing stratigraphic divisions. Reeds (1911) refers to "times of no deposition as well as eroded sediments" before and after Chimneyhill deposition, as well as for the Henryhouse and Haragan/Bois d'Arc. Others who discussed possible unconformities include Maxwell (1936), Anderson (1939), Tarr (1955), Bowles (1959), Maxwell (1959), Amsden (1960, 1975, 1980), Withrow (1971), Manni (1985), and Morgan (1985). Fritz and Medlock (1995) showed the impact of regional unconformities on Hunton reservoirs. Matthews (1992) and Matthews and Al-Shaieb (1993) presented the first systematic classification of Hunton paleokarst and indicated its importance to oil and gas productivity.

Investigations conducted by Beardall (1983), Medlock (1984), Manni (1985), and Menke (1986) addressed specific Hunton stratigraphic units and established depositional models for reservoir facies. Morgan (1985) showed the importance of oolitic facies and certain aspects of reservoir development. Al-Shaieb and Puckette (2000) showed the Henryhouse–Haragan/Bois d'Arc interval to be a type 1 carbonate sequence defined by bounding unconformities (Fig. 2).

Other important studies addressing various aspects of Hunton geology include Morgan (1922), Ballard (1930), Posey (1932), Decker (1935), Swesnick (1948), Tarr (1955), Oxley (1958), England (1965), Kunsman (1967), Harvey (1969), Isom (1973), Hollrah (1977), Borak (1978), and Throckmorton and Al-Shaieb (1986).

DEPOSITIONAL FACIES AND ENVIRONMENTS

Pre-Woodford erosion removed much of the Henryhouse–Haragan/Bois d'Arc sequence in Oklahoma. The absence of the Haragan/Bois d'Arc in the subsurface prevents the interpretation of its depositional facies. However, similar bathymetric conditions prevailed throughout deposition of the Henryhouse–Haragan/Bois d'Arc sequence, and the processes that affected the Henryhouse can be applied uniformly across the sequence. As a result, the Henryhouse is used to illustrate facies and reservoir characteristics that are analogous to all pre-Frisco units.

During the Silurian, the Midcontinent region remained a stable province (Adler and others, 1971; Feinstein, 1981). Under these tectonic conditions, the Henryhouse Formation was deposited over much of Oklahoma without any major unconformities (Shannon, 1962). The distribution of depositional facies for the Henryhouse is shown in Figure 3. These facies and reservoir characteristics are generally analogous to all pre-Frisco Hunton units.

HENRYHOUSE–HARAGAN/BOIS D'ARC FORMATIONS

The Henryhouse–Haragan/Bois d'Arc (HHB) Formations are genetically related strata. This is evident in outcrop where the HHB interval is bounded by unconformities; rock types above and below the unconformities are distinctly different. Erosion associated with the upper unconformity truncated the Hunton across northern Oklahoma, and the Woodford Shale is disconformable on the eroded surface. Erosion below the lower bounding unconformity thinned the Clarita Formation. Subaerial exposure and erosion are characteristic of type 1 carbonate-sequence boundaries (Sarg, 1988). These enclosing unconformities, as well as the genetically related strata, define the HHB carbonates as a type 1 sequence.

The HHB sequence contains shallowing-upward shale–carbonate cycles (parasequences). Although subtidal facies is the only one present in the Arbuckle Mountains, equivalent rocks in the western and northern parts of the Anadarko basin contain additional intertidal and supratidal facies. Parasequences to the north and west of the Arbuckle Mountains are thicker and composed mainly of carbonate (Fig. 2). A general absence of shale and marly carbonates is evident in comparison to the outcrops. These additional facies and cycle thickening indicate a northwestward shallowing of the basin during the Late Silurian–Early Devonian. An interpretation of the HHB sequence lithofacies in the context of sequence stratigraphy is discussed in Al-Shaieb and Puckette (2000).

The shallow, low-energy sea developed facies belts (Fig. 4) subparallel to bathymetric contours (Al-Shaieb

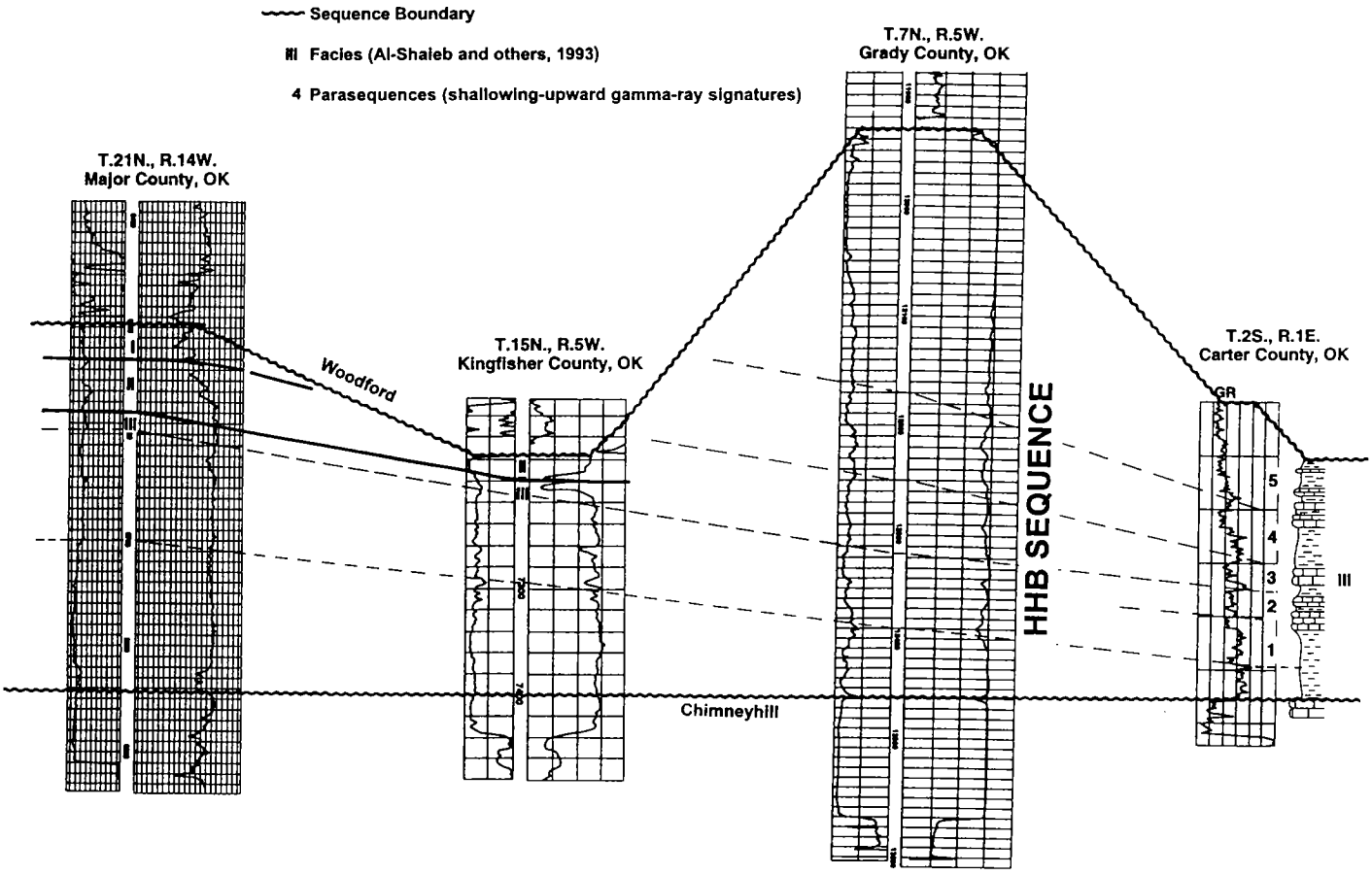

Figure 2. Cross section showing the Henryhouse–Haragan/Bois d'Arc (HHB) type 1 carbonate sequence, bounding unconformities, and correlation of outcrop and subsurface facies. North and west of the Arbuckle Mountains, parasequences are thicker and contain additional intertidal and supratidal facies. Line of section shown in Figure 3. Five parasequences (shallowing-upward gamma-ray signatures) are indicated by Arabic numerals; facies are indicated by Roman numerals. Modified from Al-Shaieb and Puckette (2000, fig. 8).

and others, 1993). Facies classification is based on vertical successions of facies or aggradational sequences. Transgression and regression apparently caused extensive migration of facies, thereby producing similarity of log signatures across large areas of the basin. Environmental interpretations of facies were determined by using the criteria established by Wilson (1975) and Al-Shaieb and others (1993).

Facies I

Facies I sediments were deposited on the supratidal tidal flat very near, or above, mean high tide. Cryptal algal fabrics, fenestral fabrics (Fig. 5), an absence of fossils, and a scarcity of burrowing are prominent features of this facies. Silica nodules, silt-sized quartz, intraclasts, and peloids may be present in the low-porosity dolo-mudstones that characterize this facies. A shallow, restricted environment (Fig. 4) is indicated for facies I.

Facies II

The sediments of this facies were deposited in a shallow, restricted subtidal to upper intertidal environment. Burrow-mottling features are a distinct characteristic. Rocks of the facies are dominantly dolowackestones. They are completely dolomitized, with significant porosity. Fossil percentages and types are estimated as a result of the dissolution of original grains. Molds and scattered remaining grains indicate that crinoids were the most common bioclasts (Fig. 5). Vertical burrows and crinoid fragments suggest shallowing, with increasing energy (Fig. 4).

Oolitic grainstones and peloid-rich mudstone occur in this facies in central Oklahoma and are used to subdivide facies II into subfacies: intertidal lagoonal (IIa) and oolitic (IIb).

The lagoonal subfacies (IIa) likely represents restricted marine conditions, as fossils are rare but burrows are present. The rock is typically massive peloidal dolo-mudstone. The original texture in facies IIa is commonly masked by dolomitization. The facies represents deposition in quiet water, landward of oolitic shoals (Fig. 4).

The oolitic subfacies (IIb) contains abundant ooids (Fig. 6) and locally bioclastic debris and peloids. Cross-bedding and horizontal laminations are common. Do-

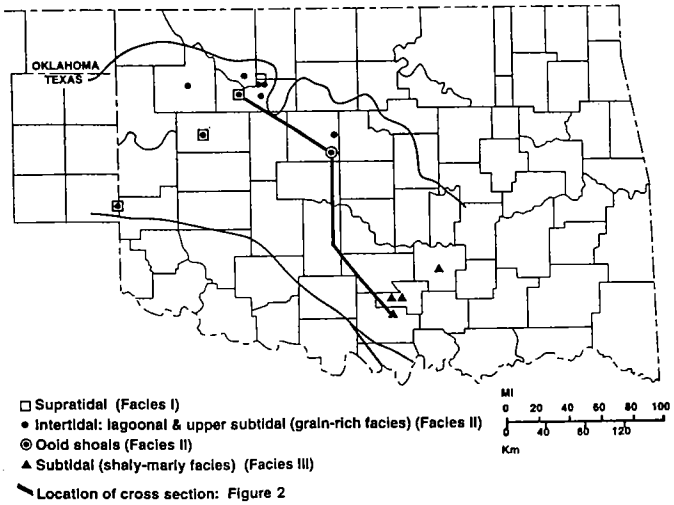

Figure 3. Distribution of subtidal, intertidal, and supratidal facies in the Henryhouse Formation. Cross section shown in Figure 2. Modified from Al-Shaieb and Puckette (2000, fig. 9).

lomitization obliterates original textures in some of these grainstones. Facies IIb developed in the lower intertidal–upper subtidal environment (Fig. 4) (Al-Shaieb and others, 1993). Morgan (1985) mapped the distribution of the calcitic-oolite subfacies in Oklahoma County. He attributed the thinning and absence of the facies to removal by a tidal channel, post-Henryhouse erosion, or nondeposition.

Facies III

This facies developed in a subtidal environment and is typically a medium-dark, silty, dolomitic mudstone (Fig. 5). Fossils include brachiopods, trilobites, ostracodes, bryozoans, and echinoderms. This facies may be featureless or contain burrows, nodular bedding, or storm-type deposits. The more diverse, better preserved fossils indicate a lower energy, shallow, open-water environment (Fig. 4) below normal wave base (Al-Shaieb and others, 1993).

DOLOMITIZATION

Reservoir rocks of the Hunton Group, specifically the Chimneyhill Subgroup and Henryhouse Formation, are mostly dolomitized. Howery (1993) tied the location of Hunton fields to a regional dolomite trend in the Anadarko basin that coincides with the Henryhouse and Chimneyhill subcrop (Fig. 7). Amsden (1975) interpreted dolomite in the Silurian Hunton rocks as being the penecontemporaneous-replacement type, formed seaward of the tidal zone. Beardall and Al-Shaieb (1984) recognized three distinct types of dolomite: hypersaline, mixed water, and deep burial (Fig. 8).

Hypersaline dolomite (Fig. 8) formed in the supratidal area of the restricted inner-ramp–shelf areas. Anhydrite in the Henryhouse suggests that evaporation of the supratidal area was of sufficient intensity and duration to form hypersaline brines. Seaward of

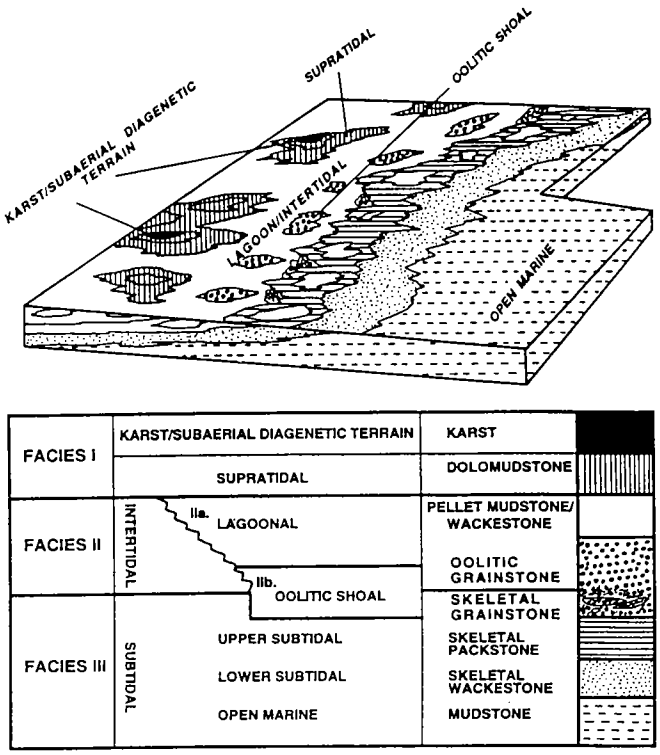

Figure 4. Schematic diagram showing generalized model of depositional environments and facies of the Henryhouse Formation. From Al-Shaieb and others (1993, fig. 5).

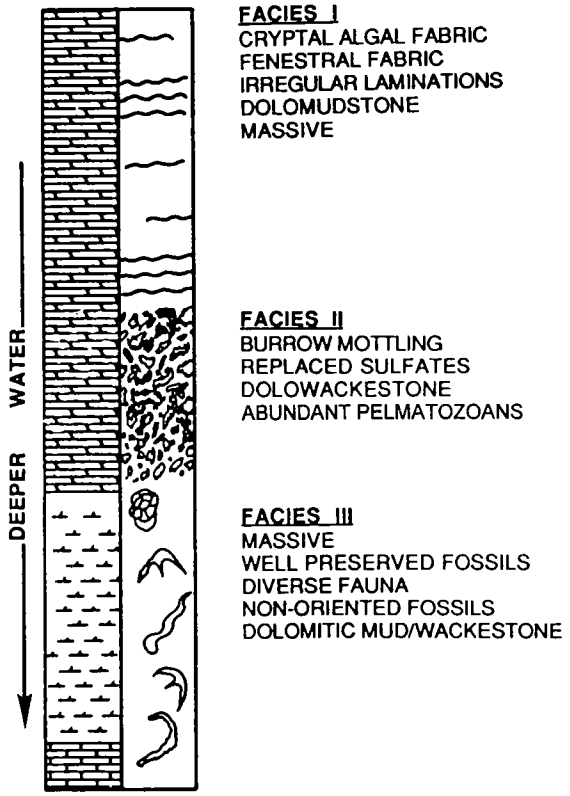

Figure 5. Typical vertical facies sequence, showing sedimentological, faunal, and mineralogical features from cores and thin sections of the Henryhouse Formation. From Al-Shaieb and others (1993, fig. 6).

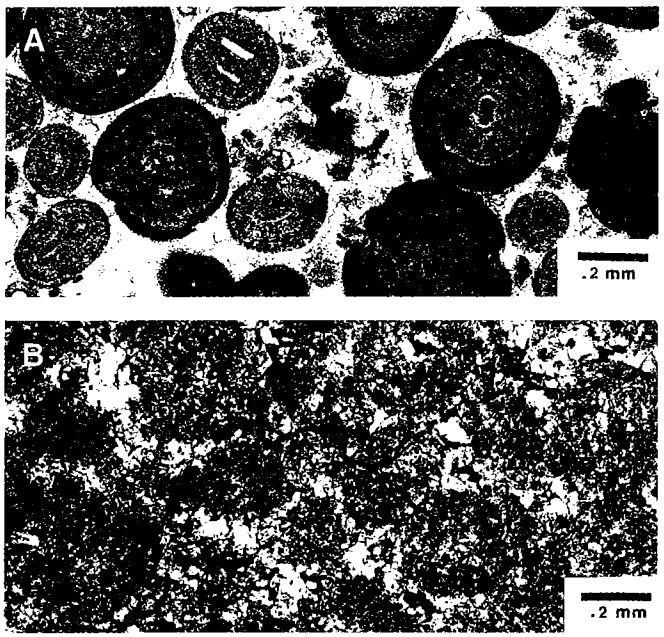

Figure 6. Photomicrographs of oolitic subfacies (IIb). (A) Ooids with isopachous calcite cement that fills interooidal space (Kirkpatrick Cronkite well, 7,119 ft). (B) Dolomitized ooid ghosts with clear rims (Duncan Garrett well, 8,751 ft; Medlock,1984).

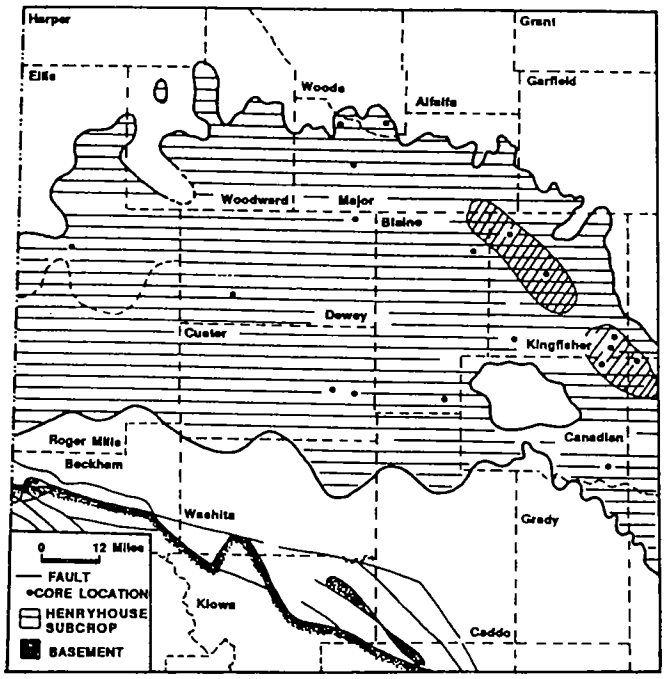

Figure 7. Pre-Woodford subcrop map of the Hunton Group, Anadarko basin, showing lagoonal and shoal subfacies (cross-hatched).

the supratidal area, normal-marine conditions were hospitable to organisms that thoroughly burrowed sediments in the intertidal–shallow-subtidal area. A consequence of the precipitation of calcium sulfate ($CaSO_4$) is an increase in the Mg^{2+}/Ca^{2+} ratio, which is of major importance to the formation of dolomite. Fluids with high Mg^{2+}/Ca^{2+} ratios probably enhanced dolomitization of the intertidal–shallow-subtidal facies (Fig. 9).

Mixed-water dolomites (Fig. 8) formed where migrating meteoric water mixed with ocean-derived brines. A sea-level drop and the resulting basinward shift of the shoreline during deposition of the Hunton carbonates would have allowed meteoric water to migrate through the sediments. As the shoreline advanced basinward across the newly deposited carbonate, a wide zone of dolomitization would have formed. A mixed-water mechanism is supported by exceedingly clean overgrowths of dolomite and their near-uniform distribution across facies. Cathodoluminescence of dolomite from the Henryhouse is regionally similar, which suggests a common diagenetic history (Choquette and Steinen, 1980).

During the hiatuses that occurred within and after Hunton deposition, a system of recharge and hydrodynamics may have developed that was sufficient to generate additional mixing dolomite in the Hunton. Lenses of fresh water, developed under exposed terrains of carbonate rock, could have migrated basinward and mixed with interstitial seawater that is richer in Mg^{2+}. The mixing of fresh water and connate seawater is considered the most likely mechanism for paleotopographic dolomitization of the Chimneyhill and Henryhouse.

Deep-burial dolomite or saddle dolomite (Fig. 8) is evident in voids or vugs in the Hunton. The distorted crystal lattice and curved crystal faces of saddle dolomite are found only in dolomitized zones. These crystals usually fill secondary vugs and fractures, and rarely molds of fossils. Fracture- and vug-filling saddle dolomite is a relatively deep-burial, late-diagenetic mineral. Radke and Mathis (1980) postulated that it forms at temperatures >80°C, thus implying a deep-burial or hydrothermal origin at shallower depths (Al-Shaieb and others, 1993).

POROSITY

Four types of porosity are recognized in Hunton rocks (Fig. 10). These porosity types belong to both general porosity classes (fabric selective and nonfabric selective) described by Choquette and Pray (1970). Two fabric-selective porosity types are (1) moldic and (2) intercrystalline. These types are responsible for most high-porosity zones in cores.

Moldic porosity is generated by dissolution of fossil grains, predominantly crinoid and mollusk fragments. Occasionally, partially dissolved faunal remnants are found within the molds. Late saddle dolomite or calcite subsequently filled molds.

Intercrystalline pore space evolved primarily as a consequence of the dissolution of nondolomitized cryptocrystalline calcite matrix. Important solution enlargement of this porosity is common. Intercrystalline porosity is likely to have developed between larger rhombs in mixed-water dolomite (Fig. 10). Late cal-

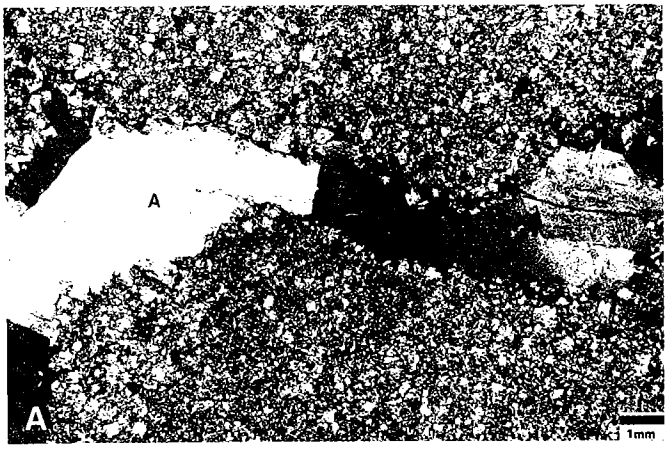

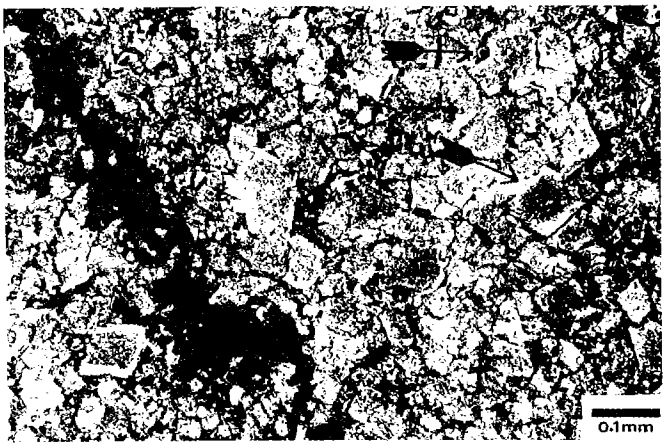

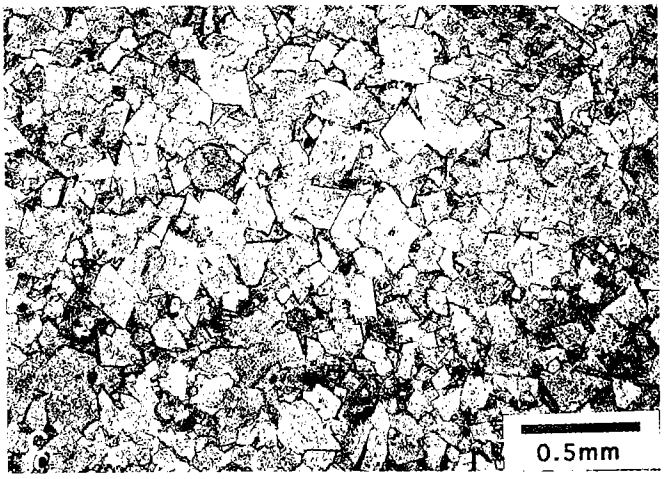

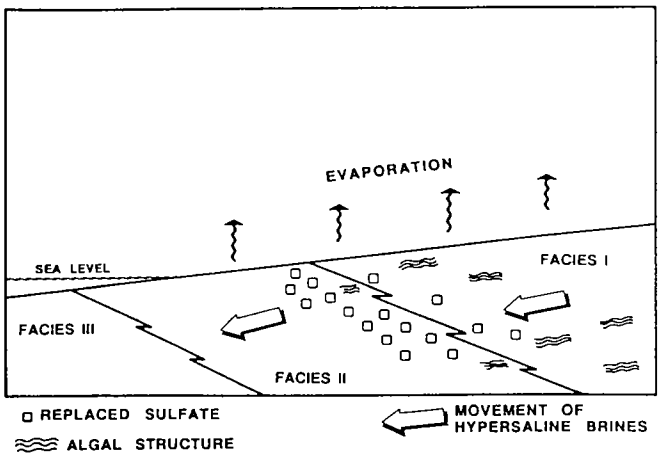

Figure 9. Schematic diagram illustrating movement of hypersaline brines and their role in dolomitizing Hunton carbonate during regression. From Al-Shaieb and others (1993, fig. 18).

cite cement may occlude some intercrystalline porosity.

Porosity is better developed in intertidal facies (facies II), especially in the bioturbated and burrowed wackestone. A positive relationship between dolomitization and porosity is clearly evident (Al-Shaieb and others, 1993), but depositional facies has a strong influence. If both facies I and II are completely dolomitized, only facies II would have significant porosity.

The characteristics of facies II that cause it to be preferentially porous are burrowing and common pelmatozoan debris. Burrowing is important because it redistributes finer particles, allowing low-pH fluids to move through the rock and dissolve nondolomitized matrix. The resultant patchy, irregular porosity distribution is clearly evident in cores and thin sections (Al-Shaieb and others, 1993).

Moldic porosity is important in grain-rich rocks (Fig. 10). Both facies II and III are fossiliferous, but the highly dolomitized facies II develops much higher moldic porosity. Porosity in oolitic grainstones is predominantly interooid (Fig. 10). This type of porosity shows a strong correlation with the degree of dolomitization, and porosity in nondolomitized oolitic rocks is commonly poorly developed because of early cementation by sparry calcite.

The most important nonfabric-selective porosity is dissolution porosity. Commonly, vuggy pores are solution-enlarged molds (Fig. 10) in which the original fossil outlines have been destroyed. The coincidence

Figure 8 *(left)*. Dolomite types in the Hunton Group. (A) Hypersaline dolomite characterized by poorly formed rhombohedra and cloudy appearance. Porosity is filled with anhydrite cement (*A*). (B) Mixed-water dolomite with euhedral rhombohedra formed around dark centers. (C) Mixed-water euhedral dolomite rhombohedra. (D) Thermal or saddle-type dolomite with large size and curved morphology.

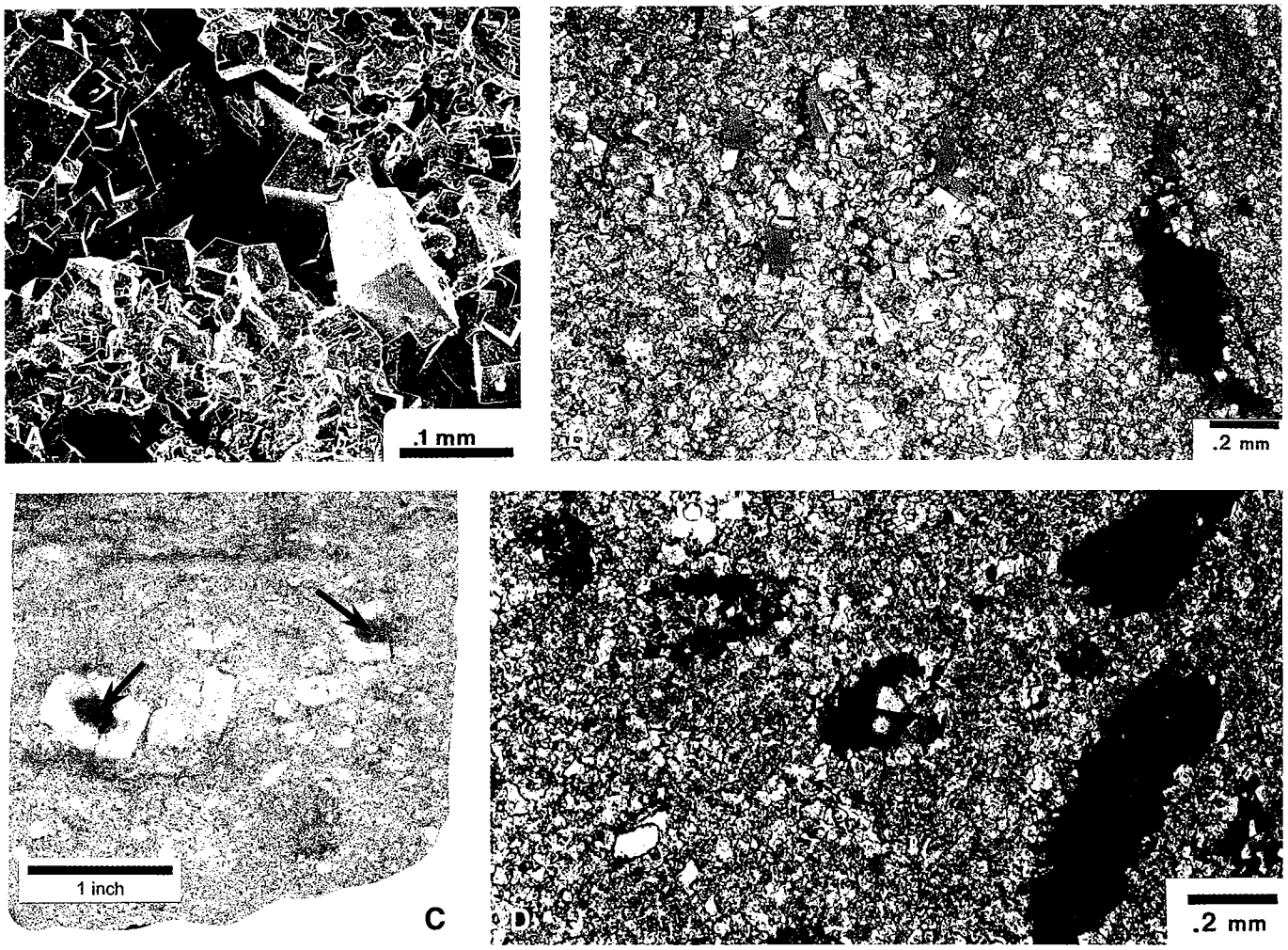

Figure 10. Porosity types in the Hunton Group. (A) Interooid porosity in oolitic subfacies, Henryhouse Formation. (B) Intercrystalline and moldic porosity, Chimneyhill Subgroup (Apexco Green well, 17,000 ft). (C) Intrabioclastic porosity (arrows), Frisco Formation (Mobil East Fitts Unit well, 3,450 ft). (D) Moldic porosity, Henryhouse Formation.

of vuggy porosity with fossiliferous, moldic zones supports this interpretation. The dissolution of fragmented fossils within the less densely burrowed zones was the most important mechanism in development of moldic or vuggy karstic porosity.

KARSTIC FEATURES

Subaerial exposure during regression resulted in extensive meteoric diagenesis and the development of paleokarstic features. Many of these features are found below the pre-Woodford and pre-Henryhouse unconformities (Manni, 1985; Matthews, 1992). An extensive description of Hunton paleokarst genesis, features, and textures is provided by Matthews and Al-Shaieb (1993); furthermore, they classified Hunton Group reservoirs into two types: type 1 and type 2.

Type 1 Reservoirs

Type 1 paleokarstic reservoirs consist of massive limestone with low interparticle or matrix porosity. These tightly cemented rocks forced water to flow along bedding planes or fractures. As dissolution progressed, solution-widened joints and caves formed. Kerans (1989) called this type *conduit-flow karst*, and White (1969) used the term *free-flow karst hydrologic regime* to characterize fluid movement.

Breccia is the most distinctive feature of large-scale conduit-flow paleokarst. Collapse breccia, an aggregate of pieces derived from the conduit (cave) roof, is common in Hunton type 1 reservoirs (Fig. 11). Collapse breccia is a main indicator of subaerial exposure (Esteban and Klappa, 1983) and is a result of the structural collapse of a cave roof into a previously open cavern. A diversity of clasts, poor sorting, and angularity of grains characterizes collapse breccia (Matthews and Al-Shaieb, 1993). If the clasts are supported by matrix, it is called a *cavern-fill parabreccia* (Lynch, 1990).

Other breccias associated with cavern-roof foundering are crackle and mosaic (Fig. 11). They represent in-place brecciation of the cave roof (Kerans, 1989). Both are evident in the Hunton and tend to grade into one another (Matthews, 1992).

Pores in type 1 reservoirs are typically sparse. Porosity in collapse breccias can occur between the clasts. However, type 1 reservoirs are often low in porosity because the fractures, solution-widened joints, and vugs were filled with cave sediments and cements. Many type 1 Hunton paleokarstic reservoirs are not major producers of oil or gas (Matthews and Al-Shaieb, 1993). Some are characterized by high initial flow rates but exhibit a sharp decline in fluid production as solution-enlarged fractures are drained.

Type 2 Reservoirs

Type 2 reservoirs are porous grain-rich rocks that allow fluid to flow through the rock. This flow is called *interparticle* (Kerans, 1989) or *diffuse* (White, 1969). Rocks with diffuse-flow characteristics are believed to represent intertidal deposits (facies II) that underwent extensive burrowing and dolomitization. Karstic dissolution enhanced porosity and permeability in facies II rocks by enlarging existing pores (Fig. 12). Type 2 porosity is common in the Hunton and is characterized by high-volume fluid flow. Reservoirs not capable of producing oil or gas deliver high volumes of salt water to the wellbore. This reflects the interconnected pore network inherent in type 2 paleokarstic reservoirs.

The differences in composition and fabric of type 1 conduit-flow and type 2 diffuse-flow lithologies are noticeably apparent in cores. In type 1 lithologies, meteoric fluids moved through the rock in solution-enlarged channels or along bedding planes and formed cavern-sized pores. In type 2 lithologies, water passed through the interparticle pores with little or no additional dissolution of carbonate. Consequently, collapse and cavern-filling parabreccias are rare in type 2 reservoirs. Cores with multiple karst episodes commonly contain both type 1 and type 2 lithologies. In some cores, type 1 features associated with the pre-Woodford unconformity are superposed on carbonate with type 2 reservoirs.

PALEOTOPOGRAPHY AND PRODUCTION

Hunton rocks are believed to have been subaerially exposed and weathered at various times in their history (Amsden, 1975, 1980; Fritz and Medlock, 1995). Amsden (1975) asserts that the Hunton represents an incomplete depositional sequence with significant time-stratigraphic gaps. Local unconformities probably existed during pre-Cochrane, pre-Clarita, pre-Henryhouse, pre-Haragan/Bois d'Arc, and pre-Frisco times (Amsden, 1980). The pre-Woodford unconformity in Oklahoma resulted in a fairly uniform regional beveling of the Hunton toward the north and its complete removal across the north-central and northeastern parts of the State. Within the Hunton outcrop area of the Arbuckle Mountains, pre-Woodford erosion locally truncates the Hunton, allowing the Woodford to rest unconformably on the Sylvan Shale (Amsden, 1975).

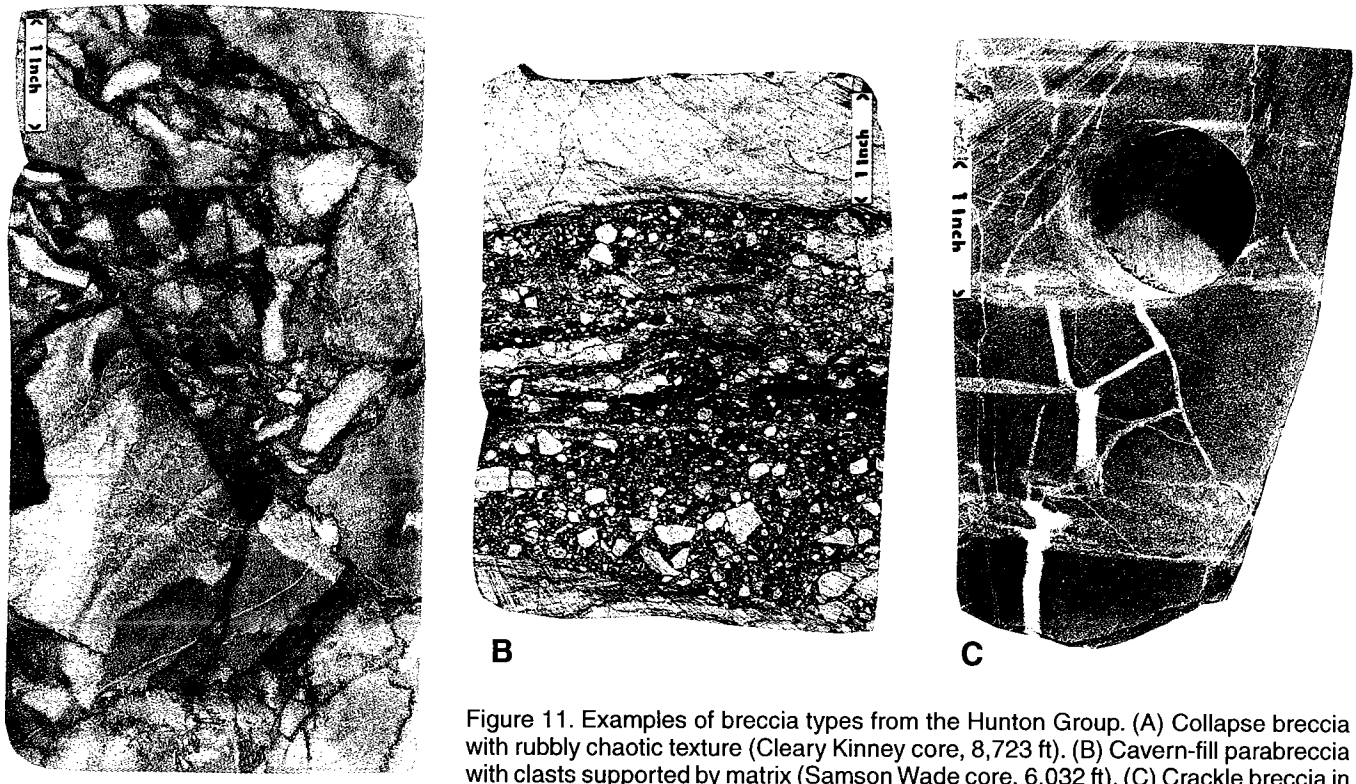

Figure 11. Examples of breccia types from the Hunton Group. (A) Collapse breccia with rubbly chaotic texture (Cleary Kinney core, 8,723 ft). (B) Cavern-fill parabreccia with clasts supported by matrix (Samson Wade core, 6,032 ft). (C) Crackle breccia in gray crystalline dolomite. Fractures are filled with white saddle dolomite (MacKellar Ferguson core, 9,754 ft).

Drainage patterns developed during the pre-Woodford depositional hiatus are evident on the eroded Hunton topography. Subaerial exposure and erosion may have impacted reservoir evolution through additional meteoric diagenesis (grain cementation or dissolution), dolomitization (Sarg, 1988), dedolomitization (Manni, 1985), or karstification (Matthews, 1992; Fritz and Medlock, 1995). The relationship between paleodrainage patterns and production is evident when the pre-Woodford topography is compared to the distribution of Hunton oil and gas fields (Fig. 13).

Pre-Woodford paleotopography and drainage patterns were analyzed on regional to local scales. Woodford-thickness maps of the Anadarko basin define major north–south-trending drainages (Fig. 14). Many Hunton fields in the central and western parts of the basin (Custer, Dewey, and Ellis Counties, Oklahoma) are adjacent to these drainages. These fields all lie in a fairway (Fig. 15) where intertidal facies in the Henryhouse Formation were dolomitized (Al-Shaieb and others, 1993). Many of these dolomitic reservoirs were subjected to additional dissolution to form type 2 reservoirs (Matthews and Al-Shaieb, 1993). Blubaugh (1999) compared flowing and shut-in pressures from drillstem tests to evaluate permeability by using a gauge called the *permeability index*. Many high-permeability reservoirs (index values approaching 1.0) lie within the dolomite fairway in the Henryhouse and Chimneyhill (Fig. 15). Comparing the permeability index, dolomite fairway, and field locations summarizes the importance of dolomitization to reservoir evolution. On the northern shelf (Blaine and Major Counties, Oklahoma) production is concentrated along a northwest–southeast trend where pre-Woodford erosion thinned the Hunton (Fig. 16) but did not remove dolomitic type 2 reservoirs in the Henryhouse. North of this trend, type 2 reservoirs are generally absent, and production is sparse.

Type 2 reservoirs in the Chimneyhill Subgroup are responsible for the production trend in Harper and Woods Counties, Oklahoma (Figs. 13, 14). Type 2 reservoirs are also found in the deep Hunton fields in Beckham County, Oklahoma, and Wheeler and Hemphill Counties, Texas. Here, vuggy and intercrystalline dolomitic porosity in the Chimneyhill are preserved below 20,000 ft.

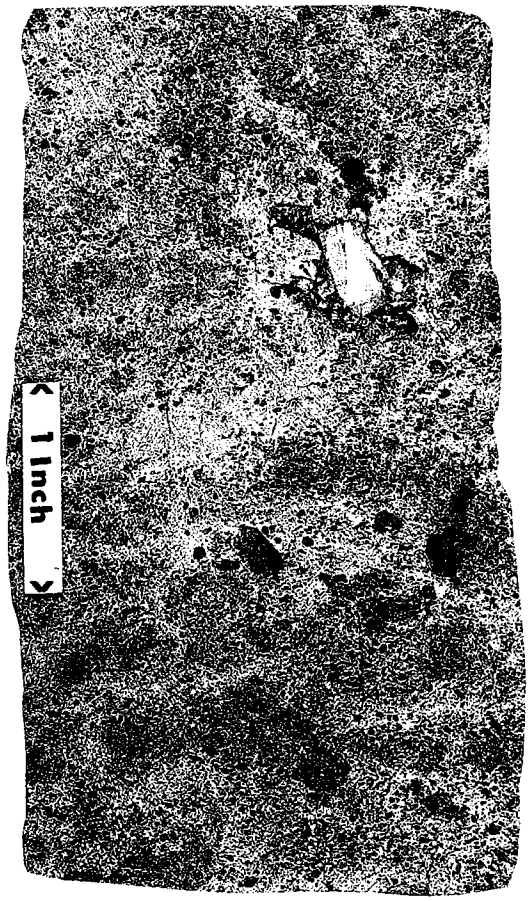

Figure 12. Enlarged moldic porosity in dolo-wackestone with vugs that are greater than twice the average grain size. Vugs are partially filled with calcite (Amax Hickman core, 13,525 ft).

IMPLICATIONS

The identification of depositional facies and postdepositional diagenesis in the Hunton Group is an essential parameter in determining potential reservoir rocks. It is most evident that the intertidal facies (facies II) is the major reservoir rock in the Henryhouse–Haragan/Bois d'Arc Formations. In this facies, grain-rich zones provided a fabric that was susceptible to dissolution. Dolomitization preserved pathways for corrosive fluids to move through the carbonate. Therefore, exploration programs for the Hunton in the Anadarko basin should consider the location of the prospect with respect to the position of facies trends and the dolomite fairway. Subaerial exposure associated with hiatuses (sequence boundaries) impacted reservoir evolution through meteoric diagenesis, dolomitization, and karstification. Consequently, the spatial relationship of the target reservoir to unconformities can be critical. Paleotopography may be useful in predicting areas of increased meteoric flow and porosity enhancement below the pre-Woodford unconformity. Therefore, any exploration strategy should include a precise understanding of stratigraphy, facies analysis and distribution, dolomitization and other diagenetic overprints (karst), and the position of unconformities with respect to the proposed reservoir.

REFERENCES CITED

Adler, F. J.; Caplan, W. M.; Carlson, M. P.; Goebel, E. D.; Henslee, H. T.; Hicks, I. C.; Larson, T. G.; McCracken, M. H.; Parker, M. C.; Rascoe, Bailey, Jr.; Schramm, M. W., Jr.; and Wells, J. S., 1971, Future petroleum provinces of the Mid-Continent, region 7, *in* Cram, I. H. (ed.), Future petroleum provinces of the United States—their geology and poten-

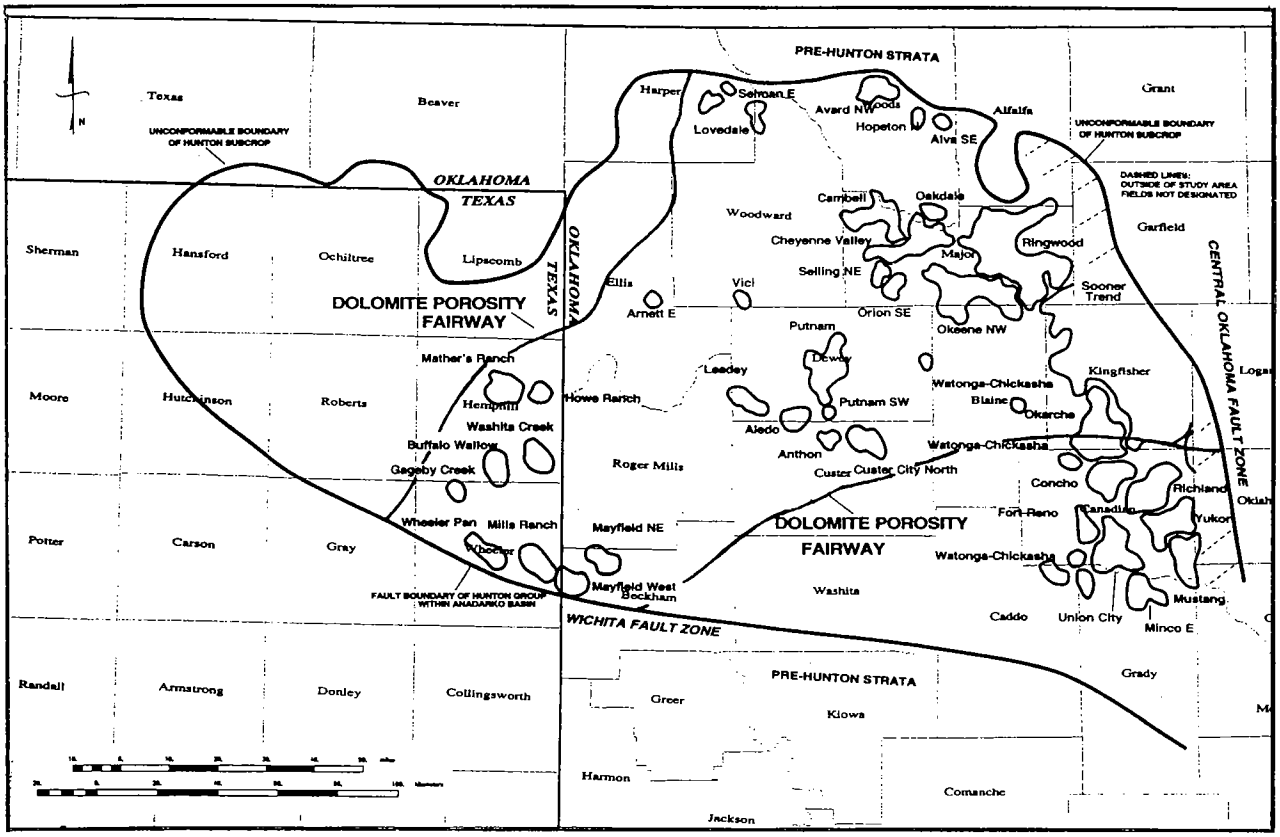

Figure 13. Map showing Hunton oil and gas fields in the Anadarko basin, and the dolomite porosity fairway.

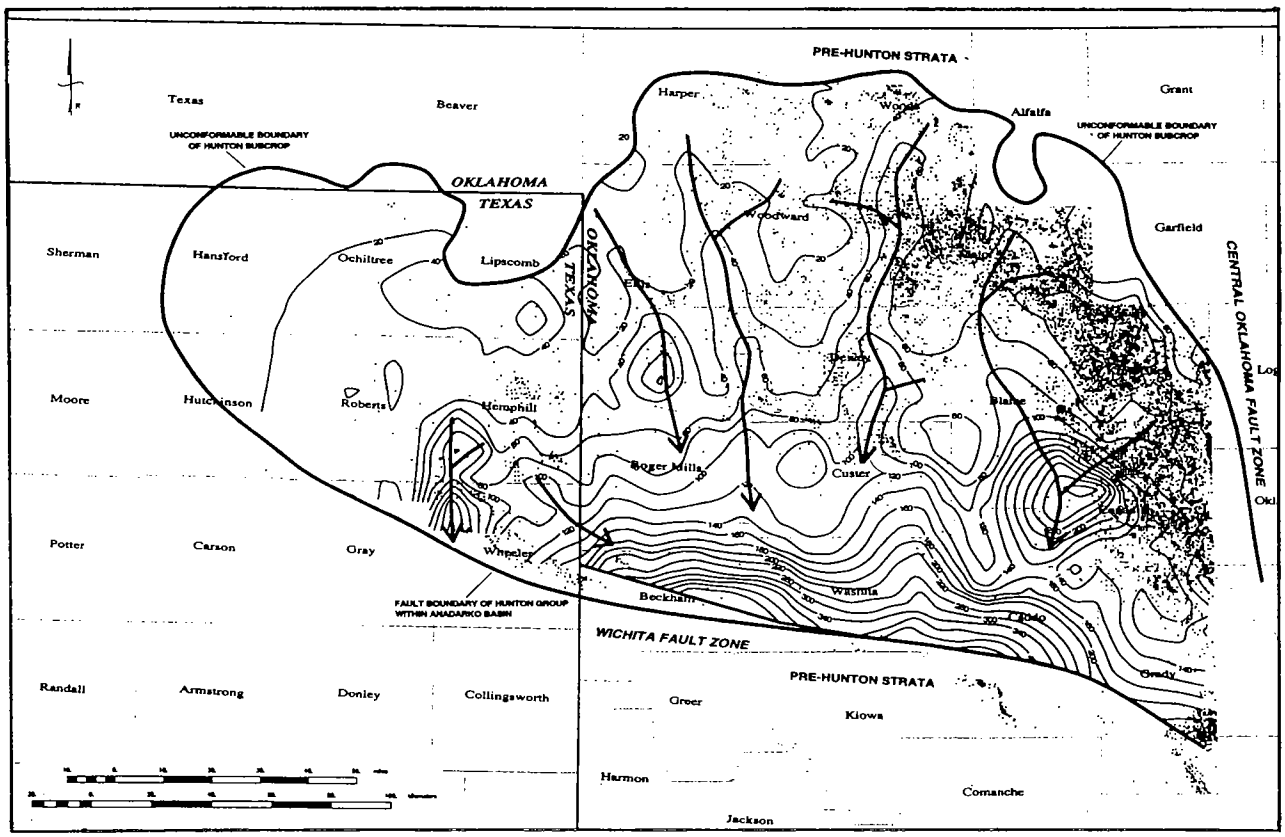

Figure 14. Map showing Woodford Shale thickness in the Anadarko basin, major paleodrainage patterns, and Hunton penetrations.

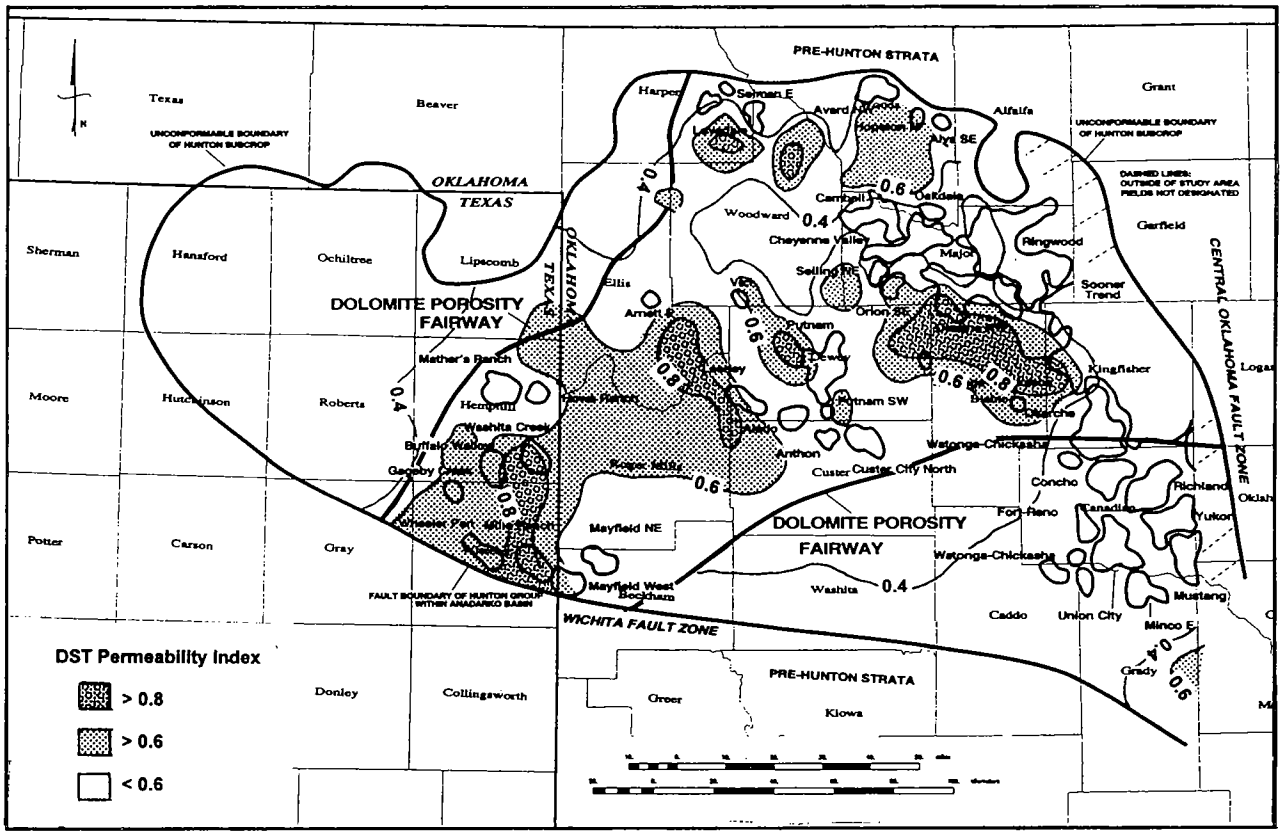

Figure 15. Map showing Hunton dolomite porosity fairway in the Anadarko basin, with drillstem-test (DST) permeability indexes.

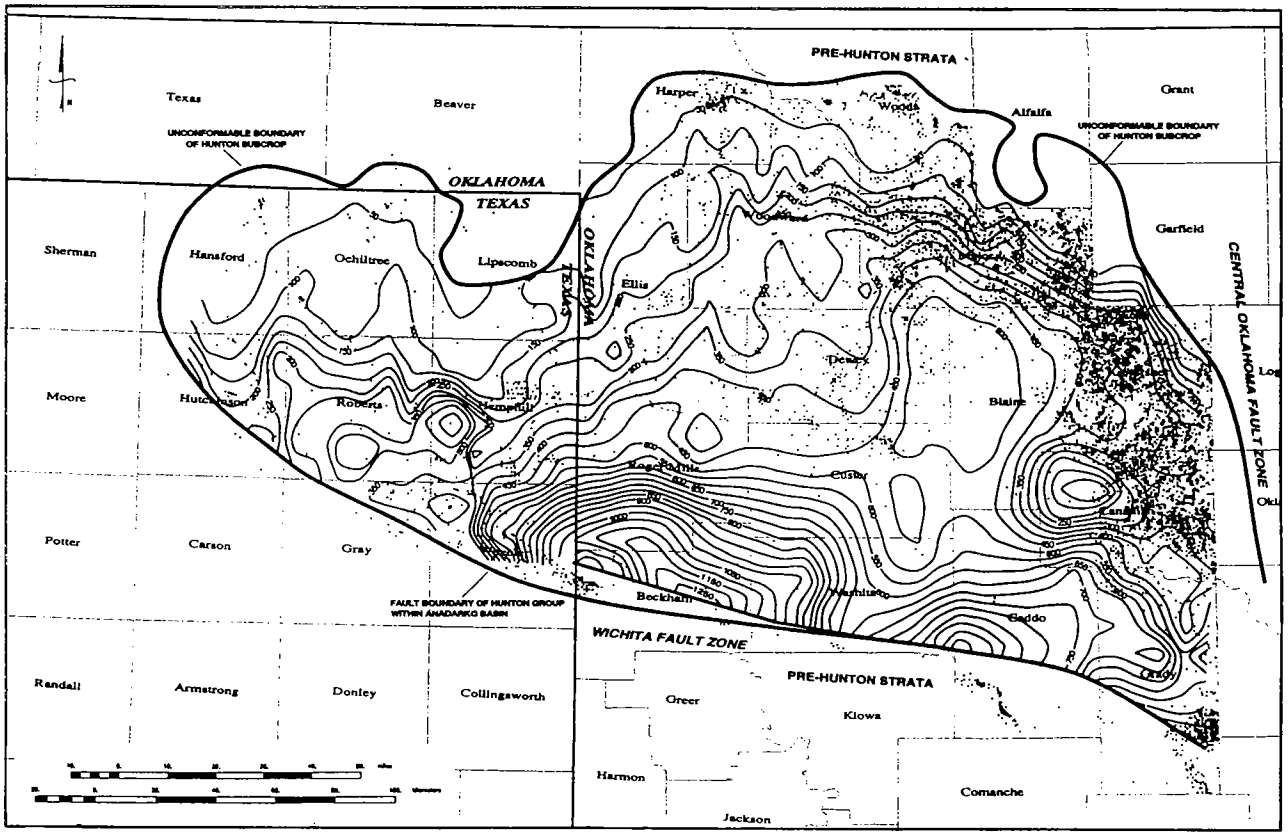

Figure 16. Map of Hunton Group thickness in the Anadarko basin, showing relationship between thinning or truncation of the Hunton and productive trends.

tial: American Association of Petroleum Geologists Memoir 15, v. 2, p. 985–1120.

Al-Shaieb, Zuhair; and Puckette, Jim, 2000, Sequence stratigraphy of Hunton Group ramp facies, Arbuckle Mountains and Anadarko basin, Oklahoma, *in* Johnson, K. S. (ed.), Platform carbonates in the southern Midcontinent, 1996 symposium: Oklahoma Geological Survey Circular 101, p. 131–137.

Al-Shaieb, Z.; Beardall, G.; Medlock, P.; Lippert, K.; Matthews, F.; and Manni, F., 1993, Overview of Hunton facies and reservoirs in the Anadarko basin, *in* Johnson, K. S. (ed.), Hunton Group core workshop and field trip: Oklahoma Geological Survey Special Publication 93-4, p. 3–39.

Amsden, T. W., 1960, Stratigraphy, *part 6 of* Stratigraphy and paleontology of the Hunton Group in the Arbuckle Mountain region: Oklahoma Geological Survey Bulletin 84, 311 p., 17 pls.

_____1975, Hunton Group (Late Ordovician, Silurian, and Early Devonian) in the Anadarko basin of Oklahoma: Oklahoma Geological Survey Bulletin 121, 214 p., 15 pls.

_____1980, Hunton Group (Late Ordovician, Silurian, and Early Devonian) in the Arkoma basin of Oklahoma: Oklahoma Geological Survey Bulletin 129, 136 p., 12 pls.

_____1989, Depositional and post-depositional history of middle Paleozoic (Late Ordovician through Early Devonian) strata in the ancestral Anadarko basin, *in* Johnson, K. S. (ed.), Anadarko basin symposium, 1988: Oklahoma Geological Survey Circular 90, p. 143–146.

Anderson, R. F., 1939, A subsurface study of the Hunton Formation in central Oklahoma: University of Oklahoma unpublished M.S. thesis, 30 p., 2 pls.

Ballard, W. N., 1930, An isopachous map of the Hunton Formation in the Seminole district: University of Oklahoma unpublished M.S. thesis, 33 p., 4 pls.

Barrick, J. E.; Klapper, Gilbert; and Amsden, T. W., 1990, Late Ordovician–Early Devonian conodont succession in the Hunton Group, Arbuckle Mountains and Anadarko basin, Oklahoma, *in* Ritter, S. M. (ed.), Early to middle Paleozoic conodont biostratigraphy of the Arbuckle Mountains, southern Oklahoma: Oklahoma Geological Survey Guidebook 27, p. 55–62.

Beardall, G. B.; and Al-Shaieb, Zuhair, 1984, Dolomitization stages in a regressive sequence of the Hunton Group, Anadarko basin, Oklahoma: American Association of Petroleum Geologists Bulletin, v. 68, p. 452.

Blubaugh, Paul, 1999, Hydrodynamics of the Hunton Group, Anadarko basin, Oklahoma and Texas Panhandle: Oklahoma State University unpublished M.S. thesis, 170 p.

Borak, B., 1978, Progressive and deep burial diagenesis in the Hunton (Late Ordovician to Early Devonian) and Simpson (Early to Middle Ordovician) Groups of the deep Anadarko basin in southwestern Oklahoma: Rensselaer Polytechnic Institute unpublished M.S. thesis.

Bowles, J. P., 1959, Subsurface geology of Woods County, Oklahoma: Shale Shaker Digest, v. 3, p. 202.

Choquette, P. W.; and Pray, L. C., 1970, Geologic nomenclature and classification of porosity in sedimentary carbonates: American Association of Petroleum Geologists Bulletin, v. 54, p. 207–250.

Choquette, P. W.; and Steinen, R. P., 1980, Mississippian nonsupratidal dolomite, Ste. Genevieve Limestone, Illinois basin: evidence for mixed-water dolomitization, *in* Concepts and models of dolomitization by ground water: Society for Sedimentary Geology (SEPM) Special Publication 28, p. 163–196.

Decker, C. E., 1935, Graptolites from the Silurian of Oklahoma: Journal of Paleontology, v. 9, p. 434–446.

England, R. L., 1965, Subsurface study of the Hunton Group (Silurian–Devonian) in the Oklahoma portion of the Arkoma basin: Shale Shaker Digest, v. 4, p. 19–35.

Esteban, M.; and Klappa, C. F., 1983, Subaerial exposure environment, *in* Scholle, P. A.; Bebout, D. G.; and Moore, C. H. (eds.), Carbonate depositional environments: Springer-Verlag, New York, p. 2–72.

Feinstein, S., 1981, Subsidence and thermal history of southern Oklahoma aulacogen: implications for petroleum exploration: American Association of Petroleum Geologists Bulletin, v. 65, p. 2521–2533.

Fritz, R. D.; and Medlock, P. L., 1995, Recognition of unconformities and sequences in Mid-Continent carbonates, *in* Hyne, N. J. (ed.), Sequence stratigraphy of the Mid-Continent: Tulsa Geological Society Special Publication 4, p. 49–80.

Harvey, R. L., 1969, West Campbell field—key to unlock Hunton: Shale Shaker Digest, v. 6, p. 176–188.

Hollrah, T. L., 1977, Subsurface lithostratigraphy of the Hunton Group in parts of Payne, Lincoln, and Logan Counties, Oklahoma: Shale Shaker Digest, v. 9, p. 76–91.

Howery, S. D., 1993, A regional look at Hunton production in the Anadarko basin, *in* Johnson, K. S. (ed.), Hunton Group core workshop and field trip: Oklahoma Geological Survey Special Publication 93-4, p. 77–81.

Isom, J. W., 1973, Subsurface stratigraphic analysis, Late Ordovician to Early Mississippian, Oakdale–Campbell trend, Woods, Major and Woodward Counties, Oklahoma: Shale Shaker Digest, v. 8, p, 116–132.

Kerans, C., 1989, Karst-controlled reservoir heterogeneity and an example from the Ellenburger Group (Lower Ordovician) of West Texas: Texas Bureau of Economic Geology, 234 p.

Kunsman, H. S., 1967, Hunton oil and gas fields, Arkansas, Oklahoma, and Panhandle of Texas, *in* Toomey, D. F. (ed.), Symposium—Silurian–Devonian rocks of Oklahoma and environs: Tulsa Geological Society Digest, v. 35, p. 165–197.

Manni, F. M., 1985, Depositional environment, diagenesis, and unconformity identification of the Chimneyhill Subgroup in the western Anadarko basin and northern shelf, Oklahoma: Oklahhoma State University unpublished M.S. thesis, 133 p.

Matthews, F. D., 1992, Paleokarstic features and reservoir characteristics of the Hunton Group in the Anadarko basin, Oklahoma: Oklahoma State University unpublished M.S. thesis, 174 p.

Matthews, F. D.; and Al-Shaieb, Zuhair, 1993, Paleokarstic features and reservoir characteristics of the Hunton Group in central and western Oklahoma, *in* Johnson, K. S.; and Campbell, J. A. (eds.), Petroleum-reservoir geology in the southern Midcontinent, 1991 symposium: Oklahoma Geological Survey Circular 95, p. 140–162.

Maxwell, R. A., 1931, The stratigraphy and areal distribution of the "Hunton formation," Oklahoma: Northwestern University unpublished Ph.D. dissertation, 120 p. [A summary of this dissertation was published in 1936 in Northwestern University Summaries of Ph.D. Dissertations, v. 4, p. 131–136.]

Maxwell, R. W., 1959, Post-Hunton, pre-Woodford unconformity in southern Oklahoma: Ardmore Geological Society, v. 11, p. 101–125.

Medlock, P. L., 1984, Depositional environment and diagenetic history of the Frisco and Henryhouse Formations in central Oklahoma: Oklahoma State University unpublished M.S. thesis.

Menke, K. P., 1986, Subsurface study of the Hunton Group in the Cheyenne Valley field, Major County, Oklahoma:

Oklahoma State University unpublished M.S. thesis.
Morgan, G. D., 1922, A Siluro–Devonian oil horizon in southern Oklahoma: Oklahoma Geological Survey Circular 10, 13 p.
Morgan, W. A., 1985, Silurian reservoirs in upward-shoaling cycles of the Hunton Group, Mount Everette and Southwest Reeding fields, Kingfisher County, Oklahoma, *in* Roehl, P. O.; and Choquette, P. W. (eds.), Carbonate petroleum reservoirs: Springer-Verlag, New York, p. 109–120.
Oxley, M. L., 1958, A subsurface study of the Hunton in northwestern Oklahoma: University of Oklahoma unpublished M.S. thesis, 67 p.
Posey, Ellen, 1932, The Hunton of Kansas: University of Oklahoma unpublished M.S. thesis, 25 p.
Radke, B. M.; and Mathis, R. L., 1980, On the formation and occurrence of saddle dolomite: Journal of Sedimentary Petrology, v. 50, p. 1149–1168.
Reeds, C. A., 1911, The Hunton Formation of Oklahoma: American Journal of Science, v. 182, p. 256–262.
Sarg. J. F., 1988, Carbonate sequence stratigraphy, *in* Sea level changes: an integrated approach: Society for Sedimentary Geology (SEPM) Special Publication 42, p. 155–182.
Shannon, J. P., Jr., 1962, Hunton Group (Silurian–Devonian) and related strata in Oklahoma: American Association of Petroleum Geologists Bulletin, v. 46, p. 1–29.
Swesnick, R. M., 1948, Geology of the West Edmond oil field and related strata in Oklahoma, *in* Howell, J. V. (ed.), Structure of typical American oil fields: American Association of Petroleum Geologists, Tulsa, v. 3, p. 359–398.
Tarr, R. S., 1955, Paleogeologic map at base of Woodford and Hunton isopachous map of Oklahoma: American Association of Petroleum Geologists Bulletin, v. 39, p. 1851–1858.
Throckmorton, H. C.; and Al-Shaieb, Zuhair, 1986, Core-calibrated log utilization in recognition of depositional facies and reservoir rock of the Henryhouse Formation (Silurian), Anadarko basin: Society of Professional Well Log Analysts, 27th Annual Logging Symposium, p. 1–18.
White, W. B., 1969, Conceptual models for carbonate aquifers: Groundwater, v. 7, p. 15–21.
Wilson, J. L., 1975, Carbonate facies in geologic history: Springer-Verlag, New York, 471 p.
Withrow, P. C., 1971, Hunton geology of the Star–Lacey field: Shale Shaker Digest, v. 19, p. 78–88.

Utilization of Dipmeter Techniques in the Exploration for Lower Paleozoic Reservoirs in Southern Oklahoma

Robert F. Ehinger
Consulting Geologist
Oklahoma City, Oklahoma

INTRODUCTION

This paper evolved from a long-term consulting project with Helmerich & Payne in which we were given the task of exploring for new reserves along the Mountain View fault trend in southern Oklahoma. I was teamed up with Donald V. Jones, a consulting geophysicist, who provided the interpretation of >1,500 mi of two-dimensional (2-D) seismic lines. Because of the complex structures and very high dips, it became apparent that dipmeter data were essential to the overall interpretation. After our involvement with the project was phased out, Helmerich & Payne subsequently drilled a wildcat discovery well, the Buddy No. 1-32, in sec. 32, T. 8 N., R. 17 W. That well penetrated a very thick sequence of steeply dipping overturned Springer sand, which resulted in the Rocky East field discovery.

DEVELOPMENT OF THE DIPMETER

Dipmeters were first developed in the 1920s and were used first in the Gulf Coast region. These early dipmeters measured the differences in the spontaneous-potential (SP) response among three sensors across the borehole where dipping beds were penetrated. The results were correlated optically to get a dip and azimuth at a specific depth. Essentially, all dipmeters solve a three-point problem at each depth. This is the same method that is taught in most structural-geology courses, except the scale has been reduced to the size of the borehole. A number of proprietary tools were invented by various companies to mechanically or electrically record the attitude of dipping beds within the borehole. Unfortunately, many of these early devices were never described in the geological literature.

The SP-type dipmeters generally produced unsatisfactory results in the lithified Midcontinent rocks and were not widely used. With the advent of the resistivity-based three-arm dipmeter, it became possible to obtain reliable dip data from specific intervals in Midcontinent wells.

The oldest dipmeter I have seen in Oklahoma was run in a 1949 survey. Dipmeters have become more sophisticated through the decades, with modern dipmeters consisting of six or more arms and multiple sensors on each pad. This enables accurate readings at high dip angles (80°+) and also solves a number of earlier problems with borehole conditions and lithologies.

Two generations of dipmeter logs are presented at the end of this paper.

MAPPING COMPLEX STRUCTURES WITH SUBSURFACE DATA

When you map complex subsurface structures, you can draw from four primary sources of data: (1) detailed stratigraphic determinations from both measured sections and subsurface logs, (2) various types of electric logs, (3) seismic and other geophysical data, and (4) dipmeter data.

In mapping complex subsurface structures, it is important to remember how you map surface structures, and then modify those skills for subsurface mapping, using different tools. In subsurface mapping, the dipmeter replaces the Brunton compass, but the dipmeter can provide most of the same data—strike, dip, plunge, etc.

Table 1 is a comparison of subsurface and surface mapping methods. Although one might initially think that surface mapping has all the advantages, this table shows this presumption not to be necessarily true. In general, stratigraphic control is better with electric-log data, which have a greater degree of precision, eliminating human biases in measuring sections and overcoming the problem of covered intervals. Electric-log data also enhance the reliability of formation identification and correlation.

Figure 1 defines some of the measurements that can be generated during the drilling of a well through steeply dipping beds. This figure also shows how most wellbores tend to deviate updip, which complicates the data interpretation on electric logs from wells in which no dipmeter was run.

There seems to be a myth among many geologists concerning the relationship of dipping beds to usual logging data. This myth is usually expressed by the phrase, "If there is much dip, I can detect it by the expansion of the formation thickness."

Ehinger, R. F., 2001, Utilization of dipmeter techniques in the exploration for lower Paleozoic reservoirs in southern Oklahoma, *in* Johnson, K. S. (ed.), Silurian, Devonian, and Mississippian geology and petroleum in the southern Midcontinent, 1999 symposium: Oklahoma Geological Survey Circular 105, p. 31–36.

Table 1.—Comparison of Geological Methods Used for Subsurface and Surface Mapping in Structurally Complex Areas

Subsurface	Surface
Measurement tools	
Dipmeter (strike, dip, plunge, cores, inclined beds)	**Brunton compass** (strike, dip, plunge)
Subcrop mapping	Outcrop mapping
Seismic	Seismic
Stratigraphy	
Less detailed but more standardized (electric logs, etc.)	More detailed but less standardized (fossils, sedimentary features)
Complete stratigraphic section	Problems with covered intervals
Structural features	
Better 3-D data—large vertical range	Better 2-D data—500–1,000 ft relief
Measures internal elements of folds	Three-point problem
Difficult to tell local structure from regional structure	Easier to get true measurements

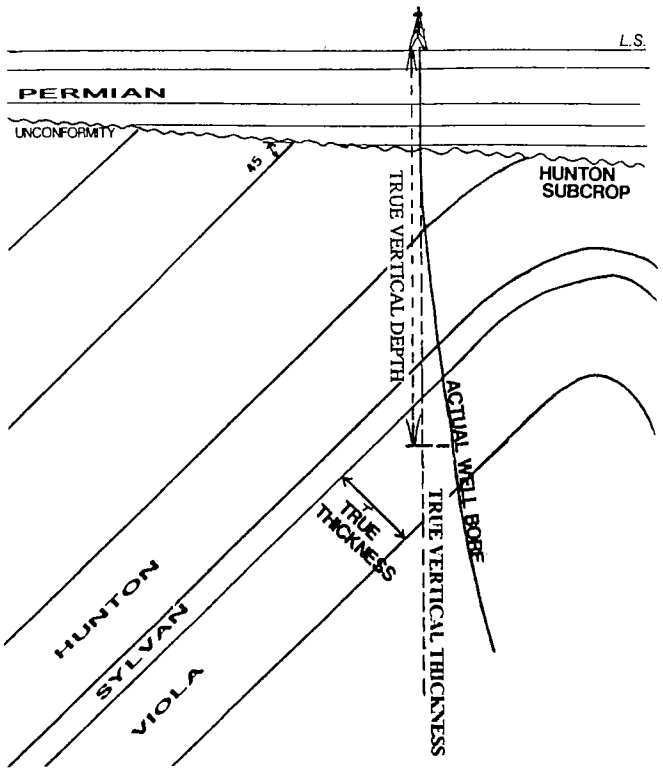

Figure 1. Sketch showing some of the parameters needed to define the attitude of a steeply dipping bed during drilling. *L.S.*, land surface.

Table 2 is a recalculation in stratigraphic terms of the trigonometric functions that control formation thickness and subcrop (or outcrop) widths. The table uses a hypothetical formation thickness of 100 ft and shows the effects of various dip angles on the apparent formation thickness and the subcrop width. From Table 2, it becomes obvious that bedding dips have to exceed 20° before there is any observable change in formation thickness in a vertical borehole. Referring back to Figure 1, a modest amount of borehole deviation in the updip direction would mean that the formation dips could approach 30° before they would become apparent. A dip of 20° can produce a closure of approximately 1,800 ft per mi. One wonders how many traps have been missed below an unconformity or thrust fault because a dipmeter survey was not run!

Figure 2 illustrates how steep dips can complicate log correlation between wells where the Springer sequence is not very distinctive. The situation becomes more challenging when one or more of the wells contains an overturned sequence.

Table 3 summarizes some of the applications of dipmeter data to geological problems within a structurally complex well. With the emphasis on 2-D and 3-D seismic data, it is important to remember that 2-D seismic lines start to degrade with dips >35° and that 3-D seismic lines probably degrade with dips >50°. By contrast, a modern dipmeter or formation-imaging tool can provide reliable dip information up to 80°+ dips. Other data obtained from the dipmeter can provide the borehole location with respect to the surface at any depth. Values for true vertical depth, true vertical thickness, and other parameters can be obtained from the dipmeter data. These parameters aid in the preparation of balanced cross sections and are required for the Wharton (1948) method for calculating reserves in steeply dipping reservoirs.

PARAMETERS THAT AFFECT DIPMETERS

As with most other logging tools, dipmeters can be adversely affected by various borehole conditions. Some of these factors are summarized in Table 4. Many of the problems become less bothersome with the newer logging tools, but one has to be cognizant of these factors when using different generations of dipmeter data.

Dipmeter data are also sensitive to various lithologies. Some of the effects of lithology on the reliability of dipmeter data are presented in Table 5. The more modern, sophisticated dipmeter tools and improved data processing tend to minimize these problems. However, in many of the structurally complex areas in Oklahoma, the key wells were drilled during 1960–1970. Here, the interpreter has to consider the effects of different lithologies, especially data derived from dolomitic sequences such as those of the Arbuckle Group. Dipmeter data should *always* be cross-checked against the known formation thickness, using an ap-

Table 2.—Calculation of Apparent Bed Thickness and Subcrop Widths for Various Dip Angles[a]

Dip (°)	Observed bed thickness (feet)	Observed subcrop width (feet)
5	100.4	1,147.0
10	101.5	575.8
15	103.5	386.3
20	106.4	292.3
25	110.3	236.6
30	115.5	200.0
40	130.5	155.5
50	155.6	130.5
60	200.0	115.4
65	236.6	110.3
70	292.3	106.4
75	386.3	103.5
80	575.8	101.5

[a]Calculations assume a vertical borehole and a true bed thickness of 100 ft.

Table 3.—Some of the Benefits of Using a Dipmeter Tool in a Structurally Complex Well

Only method that gives true strike and dip
Locates the true crestal position of a fold
Quantifies the internal geometry within a fold
Aids in stratigraphic correlations
Assists in seismic interpretations
Identifies subtle unconformities
Identifies the plunge of a fold
Combines effectively with other subsurface methods
Improves vertical and balanced cross sections
Defines structural and stratigraphic data in deviated wells
May point to missed hydrocarbon traps

proach similar to that shown in Table 2. Nondistinctive sequences corrected for dip and borehole deviation may show subtle repeated beds or missing beds from faulting. If dipmeter data are available, the typical logs (induction, porosity, etc.) can be corrected to a horizontal interval by using the dipmeter data to reduce the logs on a copy machine. With the advent of digital copying machines, one can independently adjust the x and y scales to produce a log with a nearly normal appearance instead of a narrow strip log. This procedure facilitates the comparison of the structurally disturbed interval with a "type log" from a "normal" well. In complex areas, much of the faulting and folding are found in shaly intervals, where they can be disguised by moderately steep dips.

EXPLORATION APPLICATIONS

As I have shown by the preceding tables and illustrations, the dipmeter provides a lot of unique information that is not obtainable by the normal logging suites. The primary reasons that this paper has focused on the dipmeter instead of the newer generation of formation-imaging tools are because much of the data for complex structural areas involve older generations of dipmeter tools, and because newer imaging data are not as accessible. Because the imaging-data output is color-based and commonly involves the use of computer workstations, the data are far less available to subsequent exploration companies. It should be remembered that if a formation-imaging tool is run, it is a relatively simple procedure for the logging company to generate the conventional "tadpole plot" from the imaging data stored in the computer. The tadpole-plot data are easier to use and to integrate with typical logging suites and seismic data.

In many areas in Oklahoma, folds tend to be asymmetric so that crestal positions within folds are not vertically aligned. This makes it very difficult to test all of the potential traps on an asymmetric anticline with a single vertical well. Dipmeter data, combined with seismic and other data, make possible the construction of true-scale cross sections through such a fold so that potential multiple traps can be tested with a single directional well.

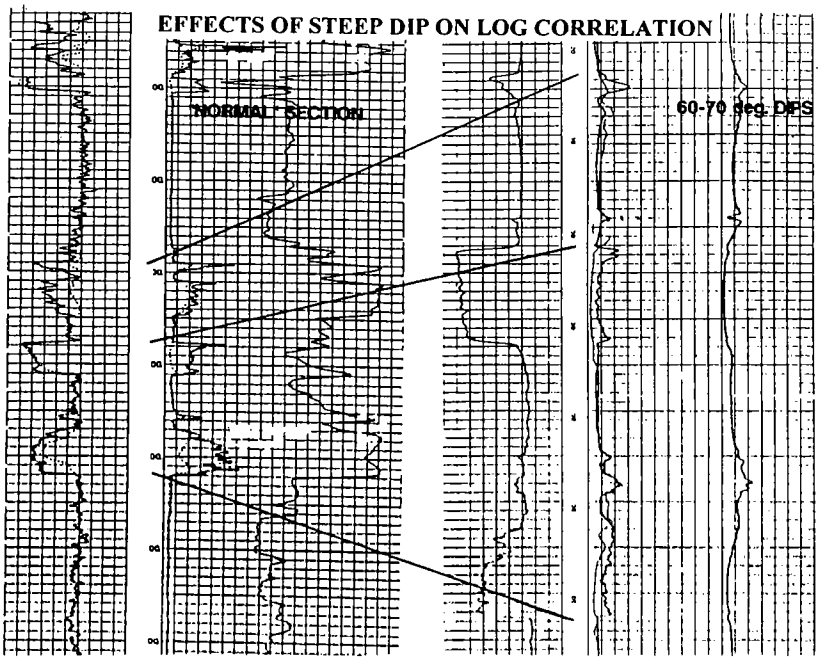

Figure 2. Hypothetical cross section of two well logs, showing the effects of steep dip on several Springer sands between the nearly horizontal section to the left and the ~60° dipping interval to the right. Three correlation "tie lines" are shown for the three sands.

Table 4.—Factors That Adversely Affect the Reliability of Dipmeter Data

Rugose or enlarged hole
Abnormal mud resistivities <0.1 ohm or >3.0 ohms
Chemical- or oil-based muds
Threaded boreholes
Cored intervals
Excessive tool rotation
Old wellbores (OWWO)[a]

[a] OWWO = old well workover.

Table 5.—Effects of Lithology on the Reliability of Dipmeter Data—Especially Applicable to the Older Generations of Dipmeter Tools

Best ↑	Interbedded shales and siltstones or limestones (2–8 ft thick)
	Laminated sandstones
	Limestones
	Dolomites
	Secondary dolomites
Worst ↓	Salt
	Intrusive igneous rocks

In a faulted area, the dipmeter gives the strike and dip values for each fault slice within the borehole. It can also define the updip direction of the trap and identify the type of faulting and the relative displacement of the blocks. Dipmeter data can help with stratigraphic correlations in stretched or overturned sections, as shown by Table 2.

Dipmeter data can also help to identify angular unconformities or previously unrecognized fault slices. Abrupt changes in dip angle, dip azimuth, and/or borehole orientation indicate that the well has crossed into a different structural environment. Another important use for dipmeter data is in providing an independent check on seismic interpretation, especially for 2-D data.

SUMMARY AND CONCLUSIONS

As I have attempted to point out in this paper, dipmeter-type logging tools provide unique data on the three-dimensional aspects of an exploration prospect. There is a tendency for companies not to run a dipmeter on lower amplitude features (<20°). However, Table 2 shows that it is very difficult to detect these lower angle dips by any other subsurface method. Usually, some companies are reluctant to run dipmeter-type tools because of the additional logging costs plus the rig time. This can prove to be a costly mistake! The cost for a minimum dipmeter run (20–25% of total drilling depth) is usually negotiable but may equate with shooting 1–2 mi of a 2-D seismic survey. With the information derived from the initial logging suite, it should be possible to interpret the structures adequately with a minimum dipmeter run. It should be remembered that the dipmeter run can be divided into different segments.

Data from dipmeter tools should not be interpreted in isolation. Maximum benefits are obtained by integrating the dipmeter data with other stratigraphic, structural, and seismic data. Often, an iterative approach to data processing is required to arrive at *the* correct interpretation of the record of structural events penetrated by the borehole. In making structural interpretations, older dipmeter data can usually be found with some geo-detective work. Although this may require some staff time, the minuscule cost is much smaller than the cost of a single dry hole.

SELECTED REFERENCES

Atlas Wireline Services, 1987, Fundamentals of dipmeter analysis: Western Atlas International, Inc., Houston, 216 p.

Pennebaker, P. E., 1972, Vertical net sandstone determination for isopach mapping of hydrocarbon reservoirs: American Association of Petroleum Geologists Bulletin, v. 56, p. 1520–1529.

Rider, Malcolm, 1996, The geological interpretation of well logs (2nd edition): Gulf Publishing Co., Houston, 280 p.

Wharton, J. B., 1948, Isopachous maps of sand reservoirs: American Association of Petroleum Geologists Bulletin, v. 32, p. 1331–1339.

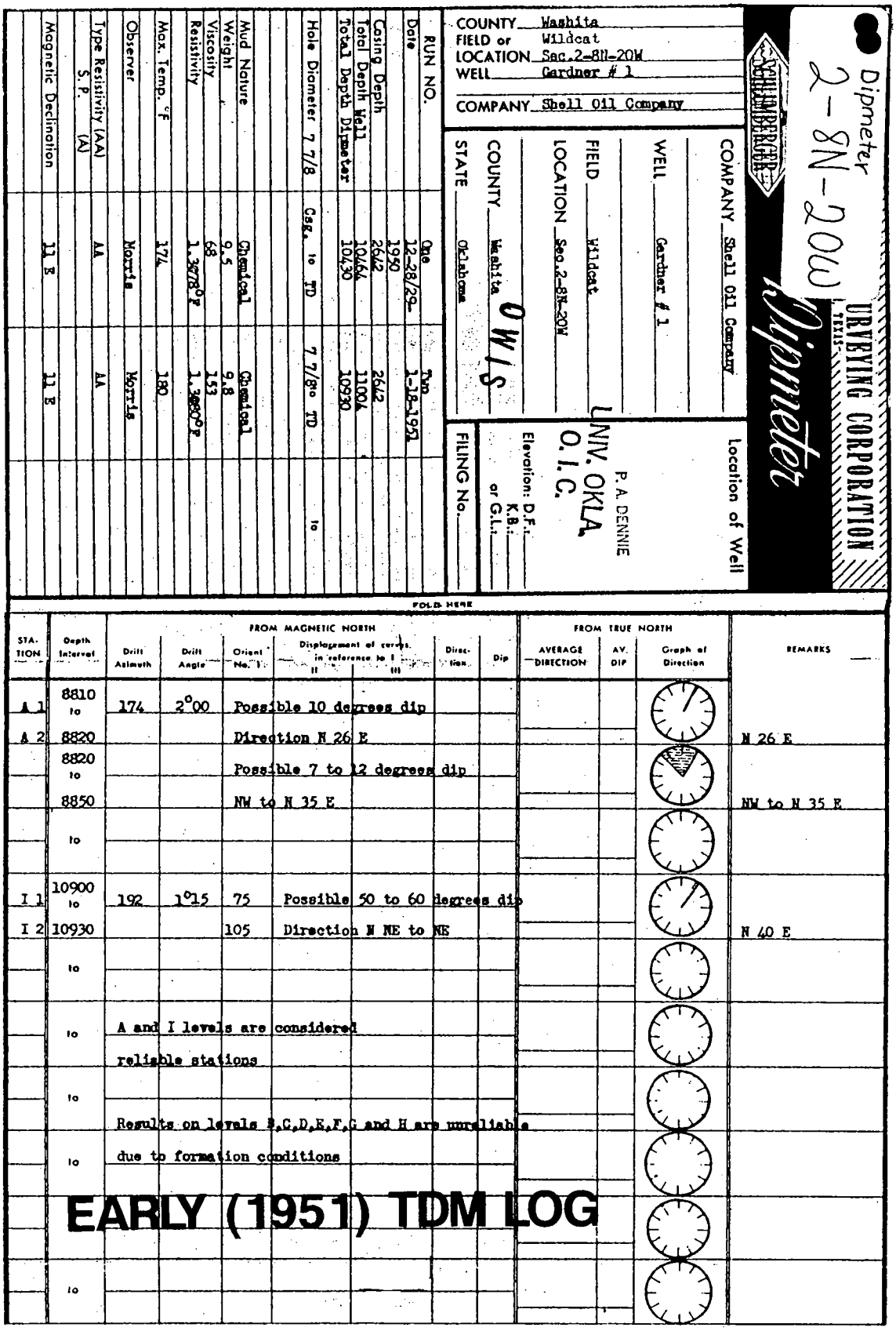

Two examples of early dipmeter surveys *(above and page 36)*.

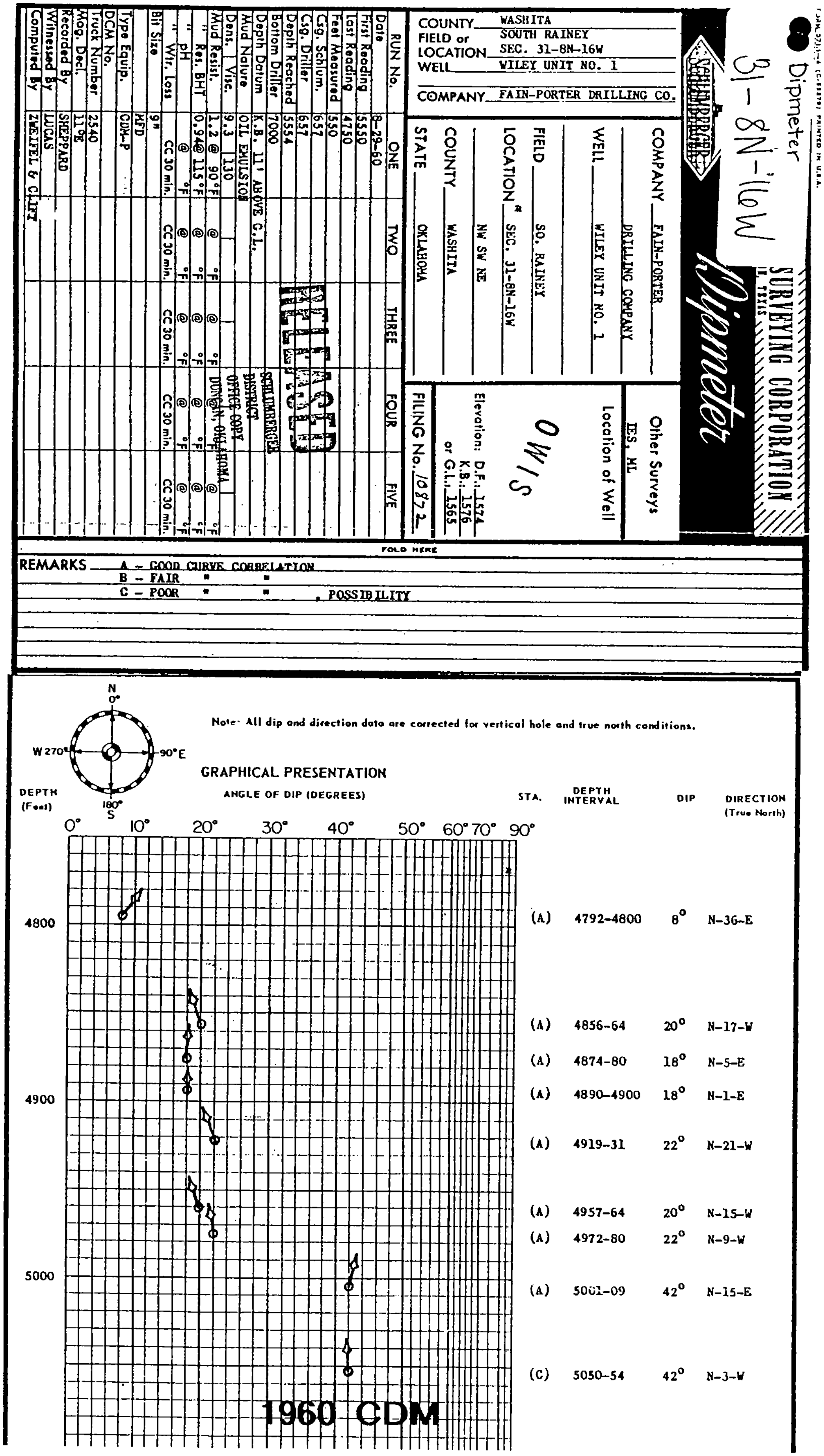
Dipmeter
31-8N-16W
SCHLUMBERGER SURVEYING CORPORATION
Dipmeter
COUNTY WASHITA
FIELD or SOUTH RAINEY
LOCATION SEC. 31-8N-16W
WELL WILEY UNIT NO. 1
COMPANY FAIN-PORTER DRILLING CO.
COMPANY FAIN-PORTER DRILLING COMPANY
WELL WILEY UNIT NO. 1
FIELD SO. RAINEY
LOCATION SEC. 31-8N-16W NW SW NE
COUNTY WASHITA
STATE OKLAHOMA
Other Surveys IES, ML
Location of Well
Elevation: D.F. 1574 K.B. 1576 or G.L. 1565
FILING No. 10872
RUN No. ONE TWO THREE FOUR FIVE
Date 8-29-60
First Reading 5550
Last Reading 4750
Feet Measured 550
Csg. Schlum. 657
Csg. Driller 657
Depth Reached 5554
Bottom Driller 7000
Depth Datum K.B. 11' ABOVE G.L.
Mud Nature OIL EMULSION
Dens. 9.3 Visc. 130
Mud Resist. 1.2 @ 90°F
Res. BHT 0.94 @ 115°F
pH
Wtr. Loss CC 30 min.
Bit Size 9"
Type Equip. CDM-P
Truck Number 2540
Mag. Decl. 11°E
Recorded By SHEPPARD
Witnessed By LUCAS
Computed By ZWEIFEL & CLIFF
RELEASED
SCHLUMBERGER DISTRICT OFFICE COPY DUNCAN, OKLAHOMA
FOLD HERE
REMARKS A - GOOD CURVE CORRELATION
B - FAIR " "
C - POOR " " POSSIBILITY
N 0°
W 270°
90° E
180° S
Note: All dip and direction data are corrected for vertical hole and true north conditions.
GRAPHICAL PRESENTATION
ANGLE OF DIP (DEGREES)
DEPTH (Feet)
0° 10° 20° 30° 40° 50° 60° 70° 90°
STA. DEPTH INTERVAL DIP DIRECTION (True North)
4800
4900
5000
(A) 4792-4800 8° N-36-E
(A) 4856-64 20° N-17-W
(A) 4874-80 18° N-5-E
(A) 4890-4900 18° N-1-E
(A) 4919-31 22° N-21-W
(A) 4957-64 20° N-15-W
(A) 4972-80 22° N-9-W
(A) 5001-09 42° N-15-E
(C) 5050-54 42° N-3-W
1960 CDM

Geologic Setting Provides Keys to Locating the Elusive Devonian Misener Sandstone in Central Northern Oklahoma

William F. Ripley
Consulting Geologist
Oklahoma City, Oklahoma

ABSTRACT.—The Upper Devonian Misener sandstone has been a prolific oil and gas producer in Garfield, Grant, and Alfalfa Counties in central northern Oklahoma. The sandstone has been an attractive target because of its shallow depth of about 6,000 ft and its secondary-recovery potential. The sandstone has produced well over 19 million barrels of oil and 19 billion cubic feet of gas in 10 producing units, not counting non-unitized wells. Without an understanding of the geologic setting, exploring for new fields and developing existing fields can be both frustrating and expensive.

In the area of study, the Misener sandstone was deposited on the post-Hunton unconformity in a marine environment. The sandstone accumulated within preexisting fluvial channels cut in the Ordovician Sylvan Shale. Evidence provided by thickness variations of the overlying Woodford Shale members shows that the area was part of a depocenter during the Late Devonian Epoch. Streams on the post-Hunton unconformity flowed to the northeast, stripping away the resistant Hunton Group and eroding channels in the underlying Sylvan Shale. Locally, the channels eroded through the Sylvan into the underlying Viola Limestone and Simpson Group. The early Woodford sea transgressed across the eroded Ozark uplift to the east and transported Simpson sands, eroded from the uplift, that were deposited as the Misener sandstone in the preexisting fluvial channels. The Misener sandstone thus overlies the Sylvan, Viola, or Simpson.

The keys to exploring for Misener sandstone deposits include mapping the subcrop pattern of the post-Hunton unconformity, mapping the thickness of the Sylvan Shale, isopaching the Misener sandstone thickness with careful attention given to thin sandstone occurrences, and observing the relationship between all three maps. Geologic mapping must be used as the foundation for seismic interpretation and modeling.

INTRODUCTION

In any play, an understanding of the present geologic setting and past geologic history provides the keys to exploring for the pay zones. In the past, there have been several theories to explain the distribution of the Upper Devonian Misener sandstone along the producing trend. The theories include eolian, fluvial, and shallow-marine depositional environments. With the increase in the number of wells drilled in the expanding Misener play, enough data have accumulated to construct the geologic setting and reconstruct the geologic history. A number of published and unpublished works provide an excellent base of information from which to draw while mapping the play.

The purpose of this discussion is to show the findings of a subsurface investigation, using well logs almost exclusively, and drawing on the data collected and reported by other researchers. This is an example of how the transfer of technical information aids the geologist in developing a working geologic model to find drilling prospects.

LOCATION

The subsurface investigation extends from northern Garfield County, across Grant and Alfalfa Counties, and north to the Oklahoma–Kansas border (Fig. 1). The study includes the area from east of Kremlin, Oklahoma, in T. 24 N., R. 5 W., to near Capron, Oklahoma, in T. 29 N., R. 12 W. In the study area, the producing trend is about 50 mi long. The trend of the play varies from southeast–northwest in Garfield County and across Grant County, nearly east–west across Alfalfa County, and then north to the Kansas border. The fields appear as disconnected pods delineated by 1 to 25 wells scattered along the trend. Producing areas are separated by numerous dry holes.

REGIONAL GEOLOGY

The study area lies on the northern shelf of the Anadarko basin, west of the Nemaha ridge (Fig. 2). The Sedgwick basin lies to the north in central southern Kansas. The Chautauqua uplift, to the north and northeast, and the Ozark uplift, to the east, played an

Ripley, W. F., 2001, Geologic setting provides keys to locating the elusive Devonian Misener sandstone in central northern Oklahoma, *in* Johnson, K. S. (ed.), Silurian, Devonian, and Mississippian geology and petroleum in the southern Midcontinent, 1999 symposium: Oklahoma Geological Survey Circular 105, p. 37–46.

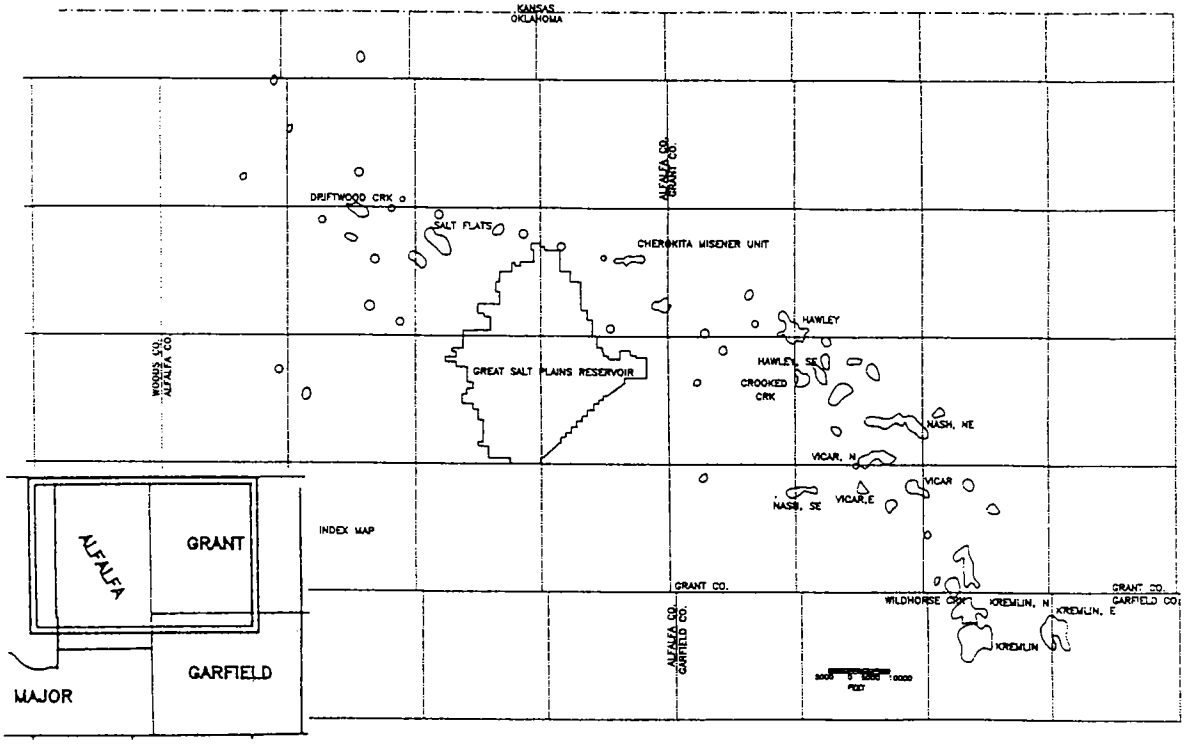

Figure 1. Location of study area and Misener sandstone producing trend.

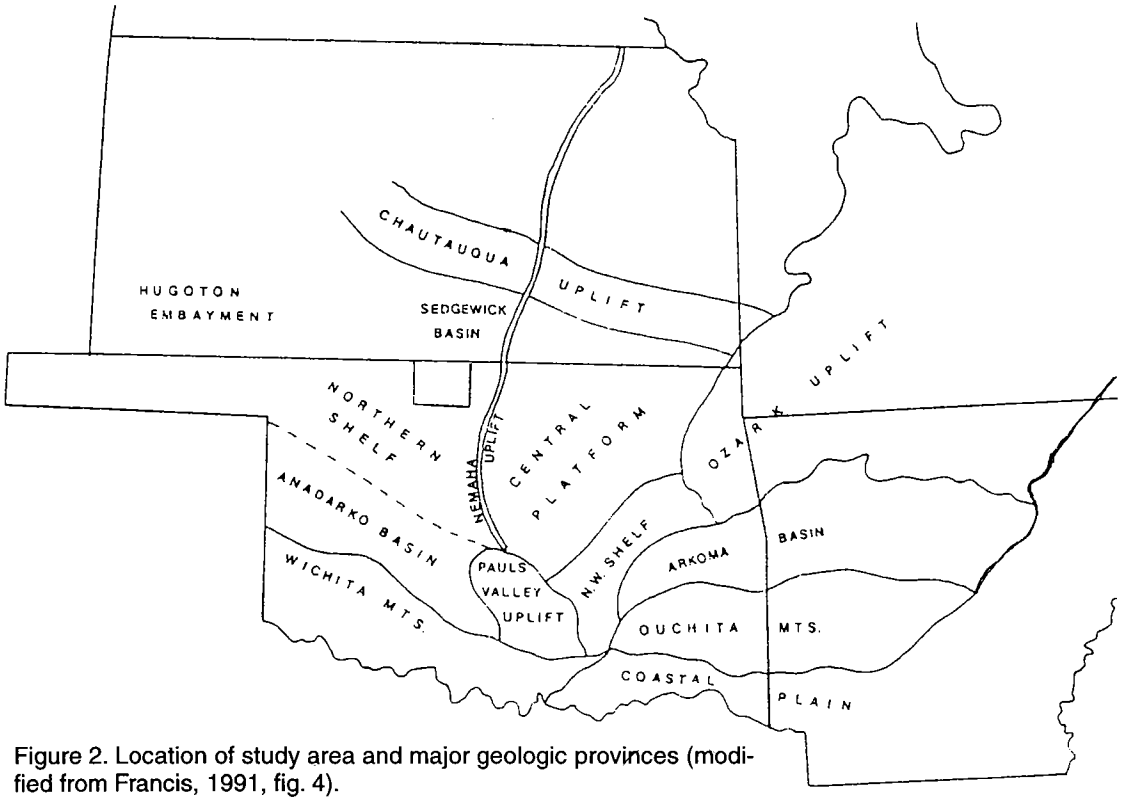

Figure 2. Location of study area and major geologic provinces (modified from Francis, 1991, fig. 4).

important part in the depositional history of the Misener sandstone.

A stratigraphic column (Fig. 3) shows that the Misener is associated with the post-Hunton unconformity and is overlain by the Late Devonian and Early Mississippian Woodford Shale. In the study area, the complete Hunton section is not preserved. Only the basal Chimneyhill Formation has survived, if the Hunton is present at all. Erosion on the post-Hunton unconformity has locally removed the normal strati-

graphic section, including the entire Silurian–Devonian Hunton Group, the Ordovician Sylvan Shale, the Viola Limestone, and the upper few feet of the Simpson Group.

Figure 4 shows a generalized pre–Woodford Shale (post-Hunton unconformity) subcrop map. From southwest to northeast, the subcropping units consist of the Devonian–Silurian Hunton Group, the Ordovician Sylvan Shale, the Ordovician Viola Limestone, the Ordovician Simpson Group, and the Cambrian–Ordovician Arbuckle sequence. Thus, the formations exposed at the unconformity are progressively older to the northeast. The Misener sandstone was deposited on the post-Hunton unconformity and, therefore, may overlie any of the above rock units. The Misener producing fields on the northern shelf of the Anadarko basin are primarily associated with the Sylvan subcrop, and with the contact of the subcropping Sylvan Shale and Viola Limestone.

The Misener sandstone is found where "something happens" to the log correlations. That "something" is not only an unconformity but a point source of evidence about the erosional pattern, which has important implications. Recording and mapping key parameters above and below the unconformity are part of the exploration technique.

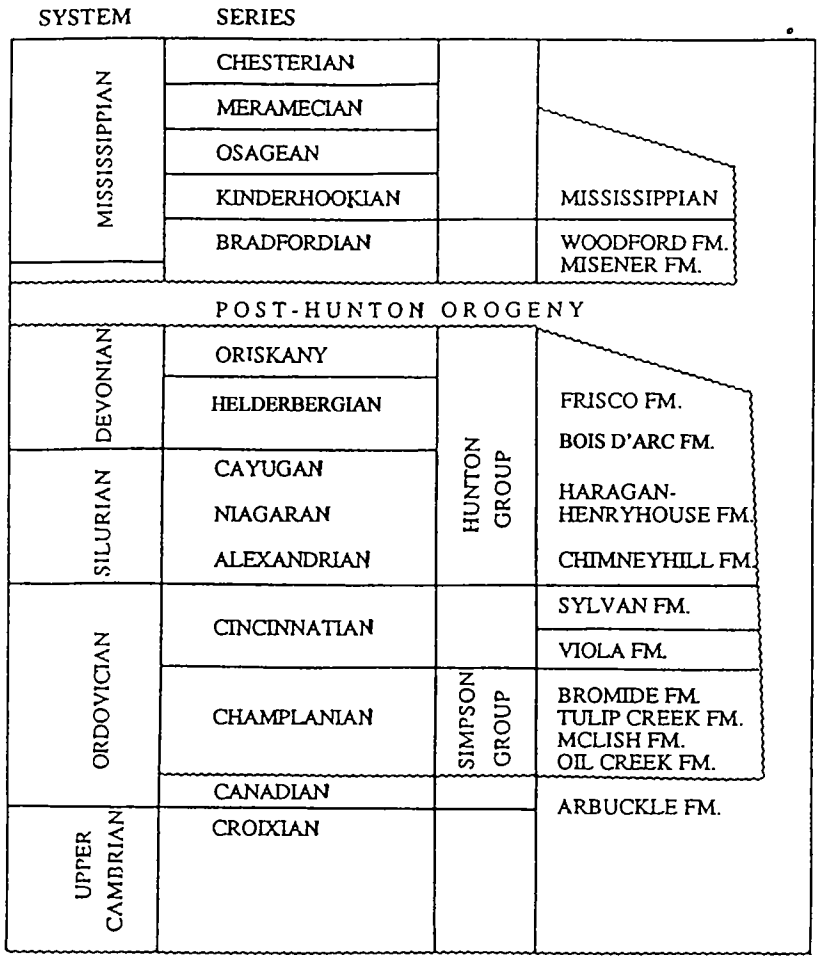

Figure 3. Stratigraphic column (from Francis, 1991, fig. 2).

LOCAL STRATIGRAPHY

Misener Sandstone

The Misener is generally composed of very fine to fine, subrounded to rounded quartz-sand grains. Cross-bedding is not common. Some sand grains are scattered in a matrix of crystalline dolomite, and some dolomite overgrowths are present. Various amounts of glauconite, phosphate, pyrite, and chert also occur. Conodonts are also present and were used by Amsden and Klapper (1972) to interpret the age of the Misener as Middle to Late Devonian. Bioturbation is evident. Locally, the Misener is interbedded with Woodford-like shale.

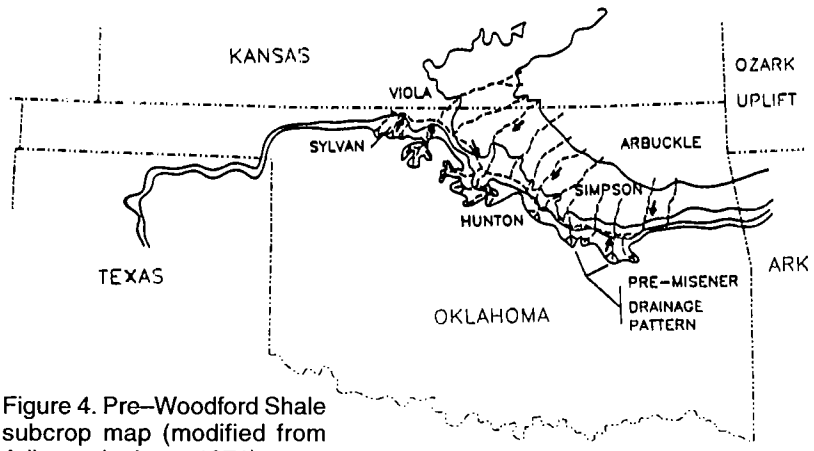

Figure 4. Pre–Woodford Shale subcrop map (modified from Adler and others, 1971).

Thicknesses of Misener greater than 50 ft were encountered in the study area. Figure 5 is a log tracing of a pay sand in Southeast Hawley field, Grant County. The sandstone shows a good crossover of the neutron–density curves, and a well-developed gamma-ray profile. Here, the Misener contains 38 ft of gross sandstone and 30 ft of net porosity >10% on the density curve, and it overlies 30 ft of Sylvan Shale. This well had an initial potential of 1,572 barrels of oil per day (BOPD) and 2.5 million cubic ft of gas per day (MMCFGPD), with no water.

Not all Misener sandstone developments are as spectacular. Figure 6 is a log tracing of one of several key wells that indicate an east–west channel in the Sylvan Shale and thus that thicker Misener sandstone can be anticipated. The well log shows 3 ft of gross

sandstone and 2 ft of porosity for the Misener, which overlies 20 ft of Sylvan Shale. The well was completed for 8 BOPD, 86 MCFGPD, and 102 barrels of water per day (BWPD). In a nearby well in Northeast Nash gas field, the Misener contains 49 ft of gross and net porous sandstone and had an initial potential of 2.4 MMCFGPD and 19 BOPD. In this well, the Misener overlies the Viola Limestone.

Constituents associated with the quartz-sand grains can affect the log response. The presence of highly conductive pyrite can suppress the resistivity. The gamma-ray log is also affected by the presence of phosphate. The combination of lithologies produces a log character that makes the sandstone appear shaly and wet, whereas in reality the zone is capable of producing 100% oil. Care must be taken to evaluate the cuttings, cores, and different combinations of logs during the initial well completion, and to examine key wells on a prospective lead. For a regional study, standard resistivity logs and compensated neutron–density logs are adequate.

Woodford Shale

The Misener sandstone is overlain everywhere by the Woodford Shale. The Woodford is a typical organic-rich, black, radioactive shale that can be divided into three mappable units (upper, middle, and lower) on the basis of log character. Figure 7 is a typical log through the Woodford, showing the three units. The variation in thickness of the Woodford members is significant to piecing together the geologic history of the Misener sandstone. In the absence of the Misener, the Woodford can overlie any of the formations that subcrop at the post-Hunton unconformity.

Sylvan Shale

The Sylvan Shale is normally overlain by the Hunton Group. Over most of the study area the Hunton has been eroded away, leaving the Sylvan unprotected and subjected to erosion. Most of the Misener sandstone development and production is associated with the Sylvan subcrop. The uneroded Sylvan Shale is 100 or more ft thick. Such thicknesses occur in wells near the Hunton subcrop or where the overlying Hunton is present.

In western Alfalfa County and in Woods County, the Sylvan is more dolomitic and more resistant to erosion. This change in lithology is why the Sylvan subcrop broadens to the west and turns northward into Kansas. (Note that Figure 4 does not incorporate more recent well control.) The silty-dolomite facies of the Sylvan is called the Maquoketa and produces hydrocarbons in the Capron area in northwestern Alfalfa County.

The Sylvan Shale formed the shoreline for the transgressing Woodford sea. Most of the Misener sandstone development and production is associated with the Sylvan subcrop.

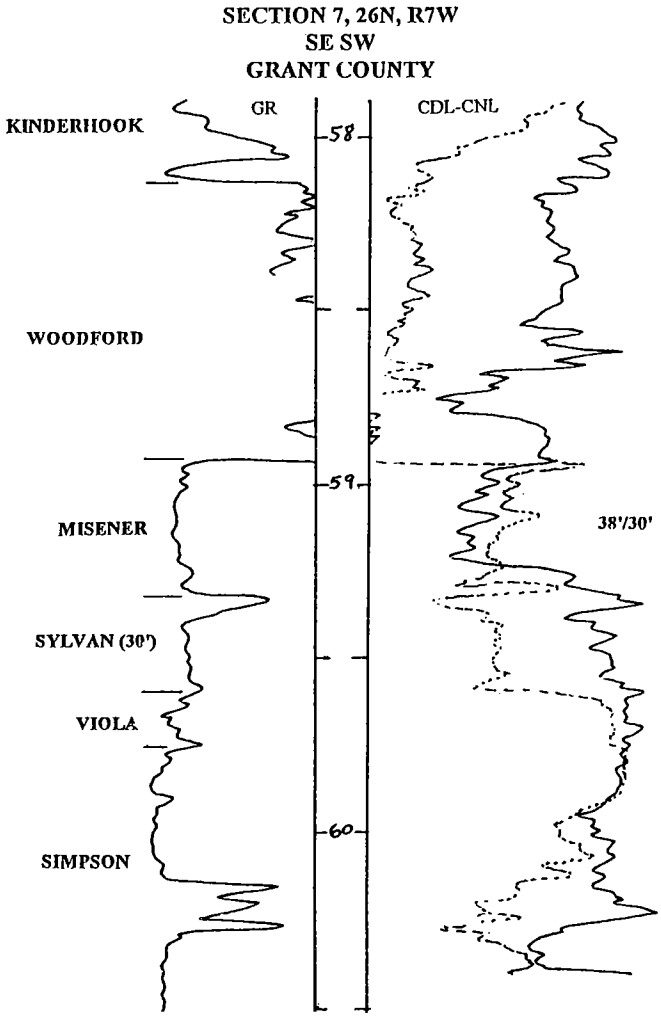

Figure 5. Log tracing showing a well-developed Misener sandstone zone. Depths are in hundreds of feet.

Viola Limestone

The Viola Limestone normally underlies the Sylvan Shale, but it commonly underlies the Misener sandstone just beyond the Sylvan subcrop or in channels within the Sylvan subcrop. On the basis of log correlations, the Viola varies in thickness even where not exposed at the unconformity.

Simpson Group

The Simpson Group underlies the Viola Limestone, or the Misener sandstone where the Viola has been eroded. The Bromide dense limestone overlies the thick Tulip Creek Sandstone, which is usually porous and wet. The Bromide is rarely eroded away in the study area.

PRODUCTION

Published information on 10 Misener producing units in the study area indicates that more than 19 million barrels of oil and 19 billion cubic ft of gas have been produced. Some of the reservoir parameters of the existing fields are listed as follows:

1. Depth: 5,700–6,500 ft;
2. Maximum gross-sandstone thickness: 60 ft; average, <20 ft;
3. Average porosity: 13–14%;
4. Minimum salt-water saturation: <20%;
5. R_w: 0.035–0.045 ohms;
6. Typical producing zone: S_w, <50%; R_t, ≥14 ohms; density porosity, >10%;
7. Initial potentials: often >1,000 BOPD;
8. Typical original gas/oil ratio: 550:1 to 1,060:1;
9. Reservoir drive: solution-gas with some water drive;
10. Typical reservoir extent: <640 acres; maximum, 1,200 acres;
11. Typical completions require no stimulation.

The hydrocarbons are found in combination structure and stratigraphic traps. The Misener sandstone reservoir rock abruptly pinches out against the Sylvan Shale, which forms the channel walls. Individual channels in the shale are separated by shale divides.

GEOLOGIC SETTING

The Misener sandstone was obviously deposited on the post-Hunton unconformity and is invariably overlain by the Woodford Shale. A marine environment of deposition is indicated for the sandstone by the presence of conodonts, glauconite, pyrite, dolomite, and phosphate. The rounded quartz-sand grains closely resemble the sand grains in the older Ordovician Simpson Group. Locally, the Misener is interbedded with thin Woodford-like shale.

The Misener sandstone occurs in discontinuous pods or in elongate, channel-like deposits. Most of the sandstone is found on the Sylvan subcrop or in close proximity to the Sylvan–Viola subcrop. The structural dip of the Viola is generally to the south toward the Anadarko basin. The structure is not homoclinal

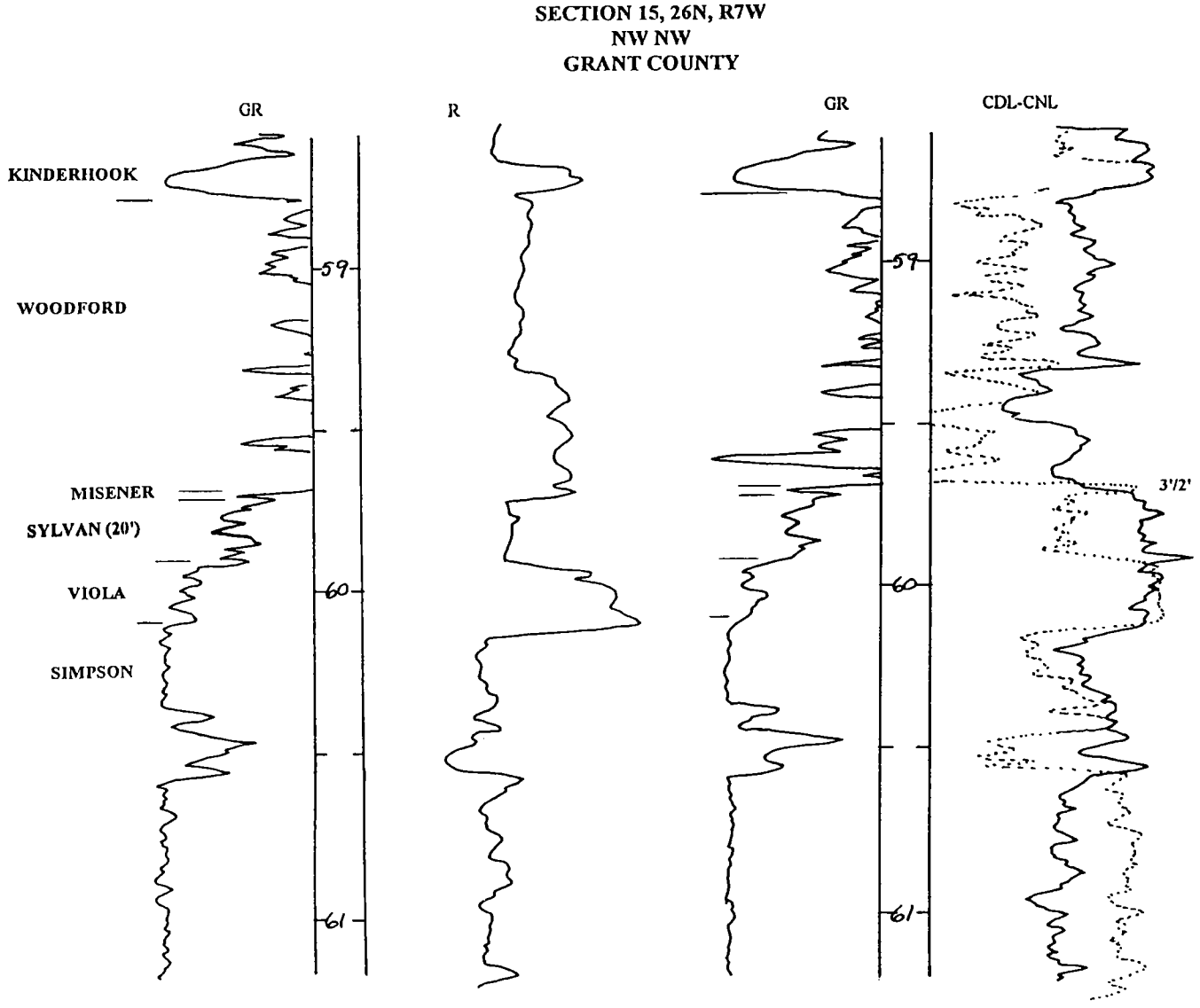

Figure 6. Log tracing showing a thin Misener sandstone zone. Depths are in hundreds of feet.

but is characterized by structural noses and abrupt changes in strike.

GEOLOGIC HISTORY

During the post-Hunton erosional cycle, the northern shelf of the Anadarko basin was being stripped of Hunton through Viola stratigraphic units. To the north and east, on the Chautauqua and Ozark uplifts, the erosion had reached the Simpson Group sandstones. Sand was being carried by streams to the south and southwest.

To determine what was happening in the Kremlin-to-Capron area, let's examine the overlying Woodford Shale. Hester and others (1990) divided the Woodford into the three members (Fig. 7) and constructed maps and profiles to show the regional variations in thickness. On the basis of the total thickness of the Woodford (Fig. 8), a paleotopographic high was indicated that extended from southwestern Major County into northeastern Blaine County and northern Kingfisher County. This high was interpreted to be a basin-margin forebulge that developed as the southern Oklahoma aulacogen was subsiding. The paleo-high separated a depocenter on the northern shelf from the aulacogen to the south.

Profiles (Fig. 9) showing the thicknesses of the individual Woodford members indicate that the depocenter was present during deposition of the lower and upper members. The lower member is missing in local areas. In the study area, the lower member is missing at the eroded edge of the Hunton, indicating that the Hunton formed an escarpment overlooking the Sylvan Shale valley to the north.

The pre-Woodford subcrop pattern (Fig. 4) includes the Hunton, Sylvan, Viola, Simpson, and Arbuckle units, from southwest to northeast. The pre-Misener drainage pattern is superimposed on the subcrop map diagrammatically. Eroding streams from the north and east cut into the Simpson sandstones and carried the eroded sand toward the northern shelf area. At the same time, streams were eroding the Hunton outcrop; these streams flowed to the north and northeast into a subbasin, indicated by the Woodford thickening. The streams created a pattern of eroded valleys in the soft Sylvan Shale and flowed in the opposite direction to the streams that brought the sediments for the Misener sand deposits.

During the early deposition of the Woodford Shale, the sea transgressed from east to west and redeposited the fluvial sands eroded from the Simpson outcrops. The Sylvan Shale formed the coastline of valleys and divides. The sand was deposited near the mouths of these valleys, usually on the Sylvan Shale and Viola Limestone, and locally on the Simpson Group. In the Kremlin area, storms may have carried the sand through narrow channels, creating thick sand buildups upstream.

There is evidence of multiple sea-level stillstands. The thickest Misener sandstone deposits occur in the

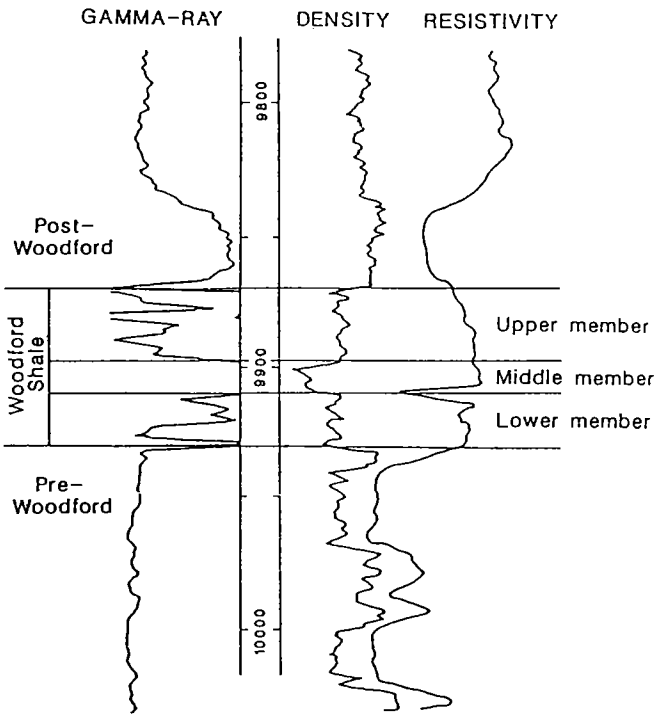

Figure 7. Typical log showing the three mappable members of the Woodford Shale (from Hester and others, 1990, fig. 2).

channels where the Sylvan is very thin or absent. This is true throughout the Misener play in the study area and indicates that sea level remained at this level long enough to deposit the sand along the 50-mi shoreline.

Lesser amounts of Misener sandstone occur in association with 30–40 ft of Sylvan Shale and 50–60 ft of shale. This sand distribution indicates at least two more stillstands. A cross section (Fig. 10) illustrates the occurrence of Misener sandstone at three different levels in relation to the underlying Sylvan Shale: (1) Sylvan Shale removed, (2) 30–40 ft of shale, and (3) 50–60 ft of shale. Thus, the Misener sandstone was deposited at three different levels within the same preexisting channel system. A knowledge of these depositional trends is important in exploring for additional Misener sandstone development.

KEYS TO EXPLORING FOR THE MISENER SANDSTONE

Collecting Well-Log Data

Before picking up the first log to begin studying the Misener play, a list of parameters to collect from each log should be made. The Misener was deposited on a major unconformity, and key parameters should be recorded concerning the stratigraphic section above and below the erosional surface. Suggested data items include:

1. Misener top, base, lithology, gross and net porous sandstone (>10% porosity) or absence of sandstone;
2. Pre-Woodford subcropping formation;

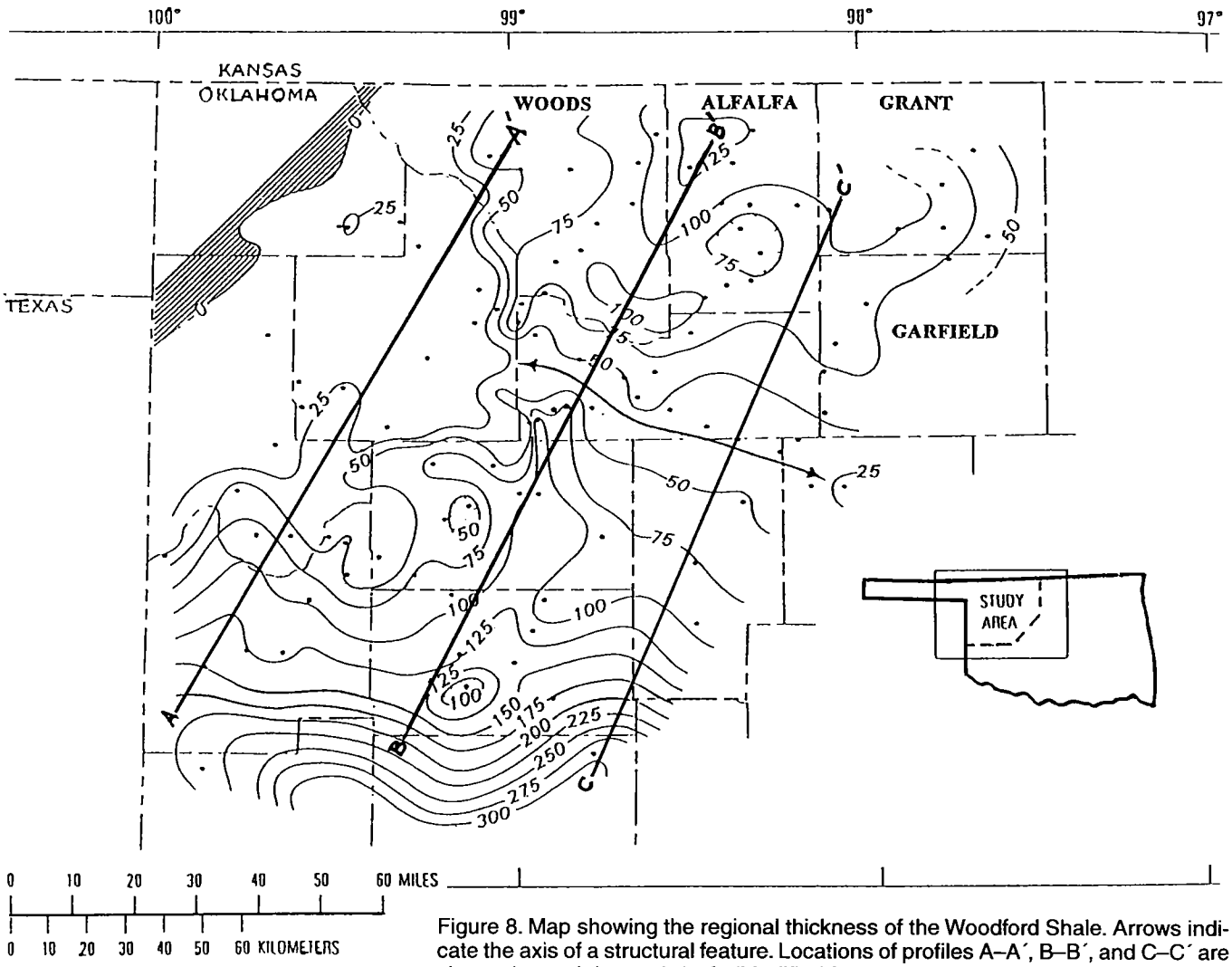

Figure 8. Map showing the regional thickness of the Woodford Shale. Arrows indicate the axis of a structural feature. Locations of profiles A–A′, B–B′, and C–C′ are shown. Isopach interval, 25 ft. (Modified from Hester and others, 1990, fig. 6.)

3. Sylvan Shale top, base, thickness, lithology (dolomitic or clean);
4. Viola Limestone top, base, thickness;
5. Simpson Group top;
6. Woodford Shale, top and base of each member;
7. Producing formation, perforations, shows, tests, initial-potential tests, etc.

Map Preparation

The first map to be constructed is the preliminary pre-Woodford subcrop map. Next, the Sylvan interval isopach map is prepared, using the subcrop map as a general guide. The two maps are refined by comparing one to the other, and they should be compatible when overlaid. The Sylvan isopach "thin" is the "cradle" in which the Misener sand was deposited. Third, the Misener gross-sandstone isopach map is prepared while overlaying the Sylvan interval isopach map. Finally, a Viola Limestone structure map is drawn. This map is prepared carefully, while keeping in mind that the top of the Viola has been locally eroded and that post-Woodford orogenic activity has altered the smooth surface normally expected with a map of this type.

All of these maps should be compatible, and helpful in guiding the explorationist to areas of Misener sandstone development and potential traps. An area in Grant County illustrates the method: Figure 11 is a Misener gross-sandstone isopach map, with the producing wells circled. One would be hard pressed to explain the field distribution from this map alone.

A pre-Woodford subcrop map (not shown) indicates a channel in the Sylvan Shale. A Sylvan Shale interval isopach map (Fig. 12) was constructed, with the pre-Woodford subcrop information posted for each well. The erosion cut down into the Viola and the Simpson. The channel flowed from west to east, cutting deeper into the stratigraphic section. This assumes that the bedrock is nearly horizontal or is dipping from east to west with a minimum of folding or faulting (which is reasonable in this area).

Now we can see an interpretation of the drainage pattern developed on the Sylvan (arrows in Fig. 12). The channel, indicated on the subcrop map, has dis-

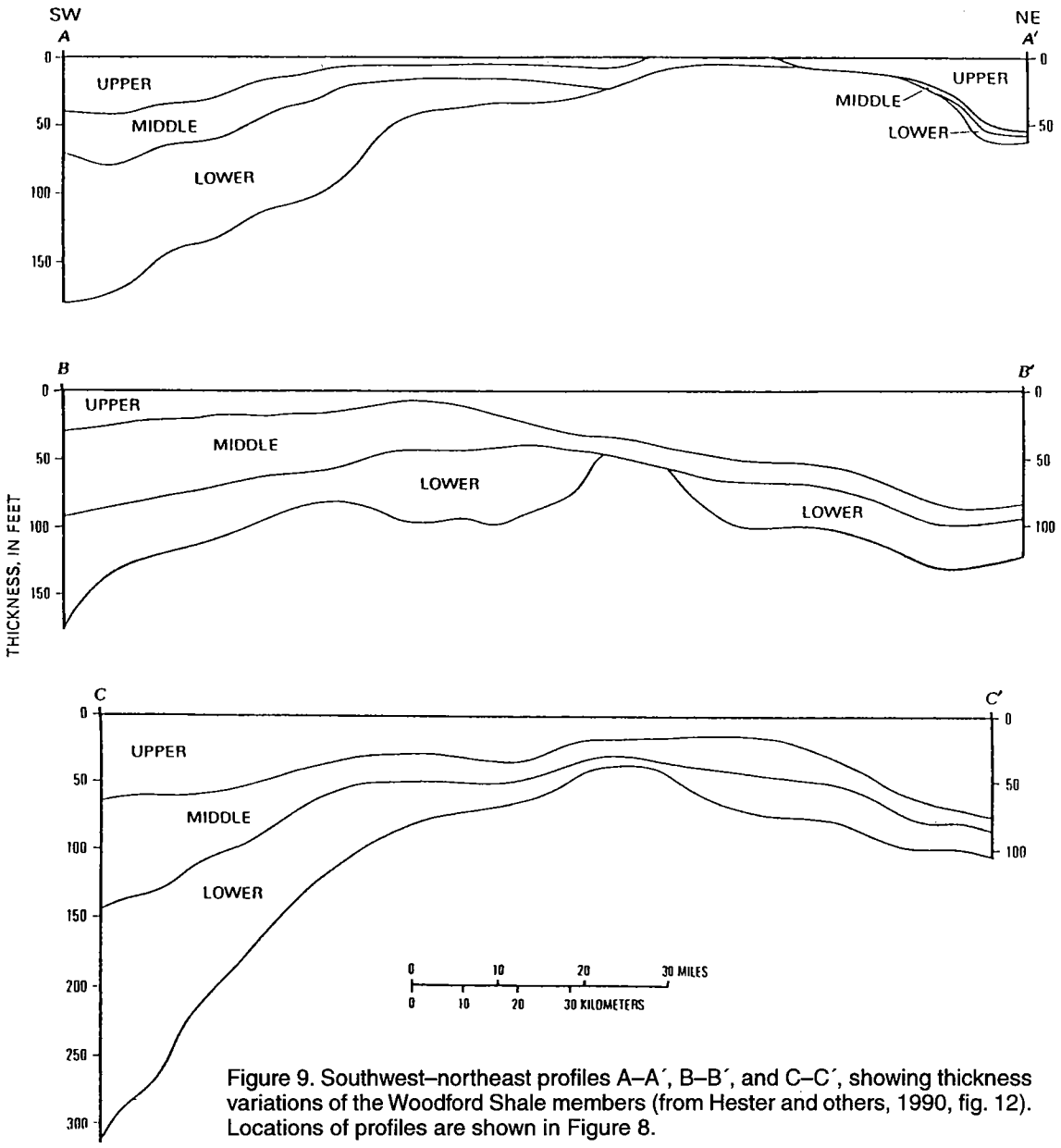

Figure 9. Southwest–northeast profiles A–A′, B–B′, and C–C′, showing thickness variations of the Woodford Shale members (from Hester and others, 1990, fig. 12). Locations of profiles are shown in Figure 8.

tributaries to the west and south. The subaerial channel flowed north and then east to the shoreline.

Note that Northeast Nash field has been developed where the Sylvan is 0–25 ft thick—that is, in the deepest part of the channel. The sand was deposited during the first stillstand of the Woodford sea. North Vicar field is in the same drainage system, but where the Sylvan is 30–50 ft thick. This is the level for the second stillstand. The small field to the south in the same drainage system overlies about 60 ft of Sylvan Shale, or the level of the third stillstand. The thickness of the Misener (Fig. 11) is 0–45 ft in Northeast Nash field, 0–20 ft in North Vicar field, and 0–8 ft in the small field to the south. The Misener in the small field to the southeast also overlies 30–50 ft of Sylvan Shale but appears to be in a separate drainage system, which flowed from west to east. The Hunton is present southwest of the Misener production, and the complete Sylvan Shale section is 115 ft thick (Fig. 12). The structure at the top of the Viola Limestone (not shown) depicts a general dip to the south at an average of 30–80 ft per mile.

Now by using the pre-Woodford subcrop map, the Sylvan Shale interval isopach map, the Misener gross-sandstone isopach map, and the Viola Limestone structure map, the geologist can identify the areas that hold the most potential for additional Misener sandstone development and production. A thin remnant of Misener sandstone near a channel in the Sylvan Shale, associated with one of the stillstands of the early Woodford sea, could develop into a significant discovery.

SUMMARY AND CONCLUSIONS

The Misener sandstone producing trend in central northern Oklahoma is like any other play from the

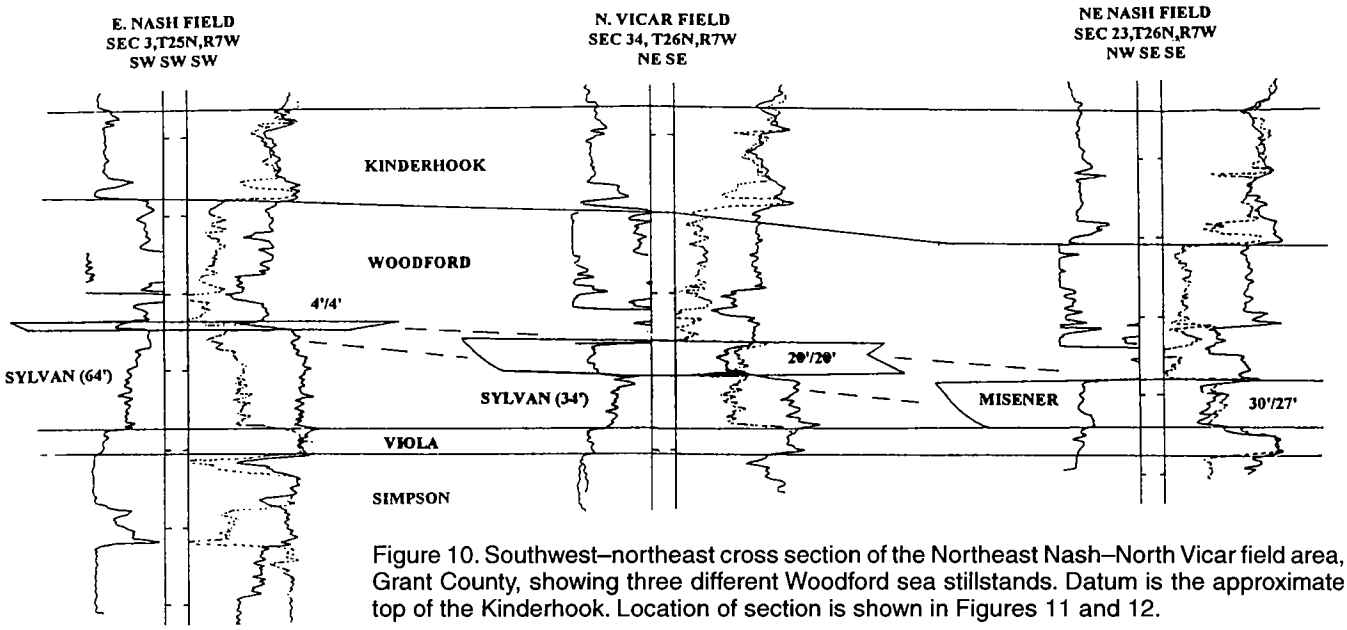

Figure 10. Southwest–northeast cross section of the Northeast Nash–North Vicar field area, Grant County, showing three different Woodford sea stillstands. Datum is the approximate top of the Kinderhook. Location of section is shown in Figures 11 and 12.

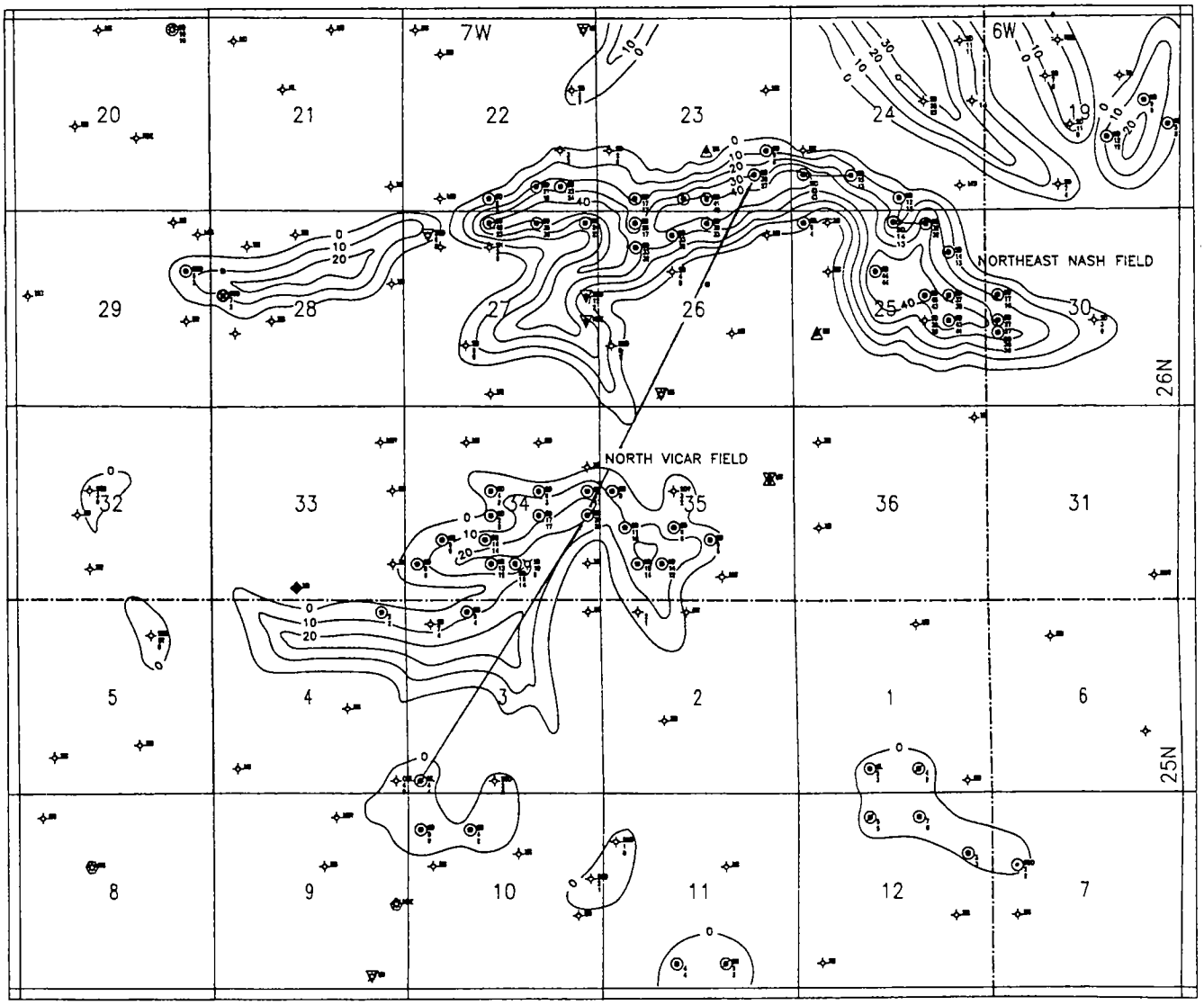

Figure 11. Misener gross-sandstone isopach map of the Northeast Nash–North Vicar field area, Grant County, showing the line of the cross section in Figure 10. Isopach interval, 10 ft.

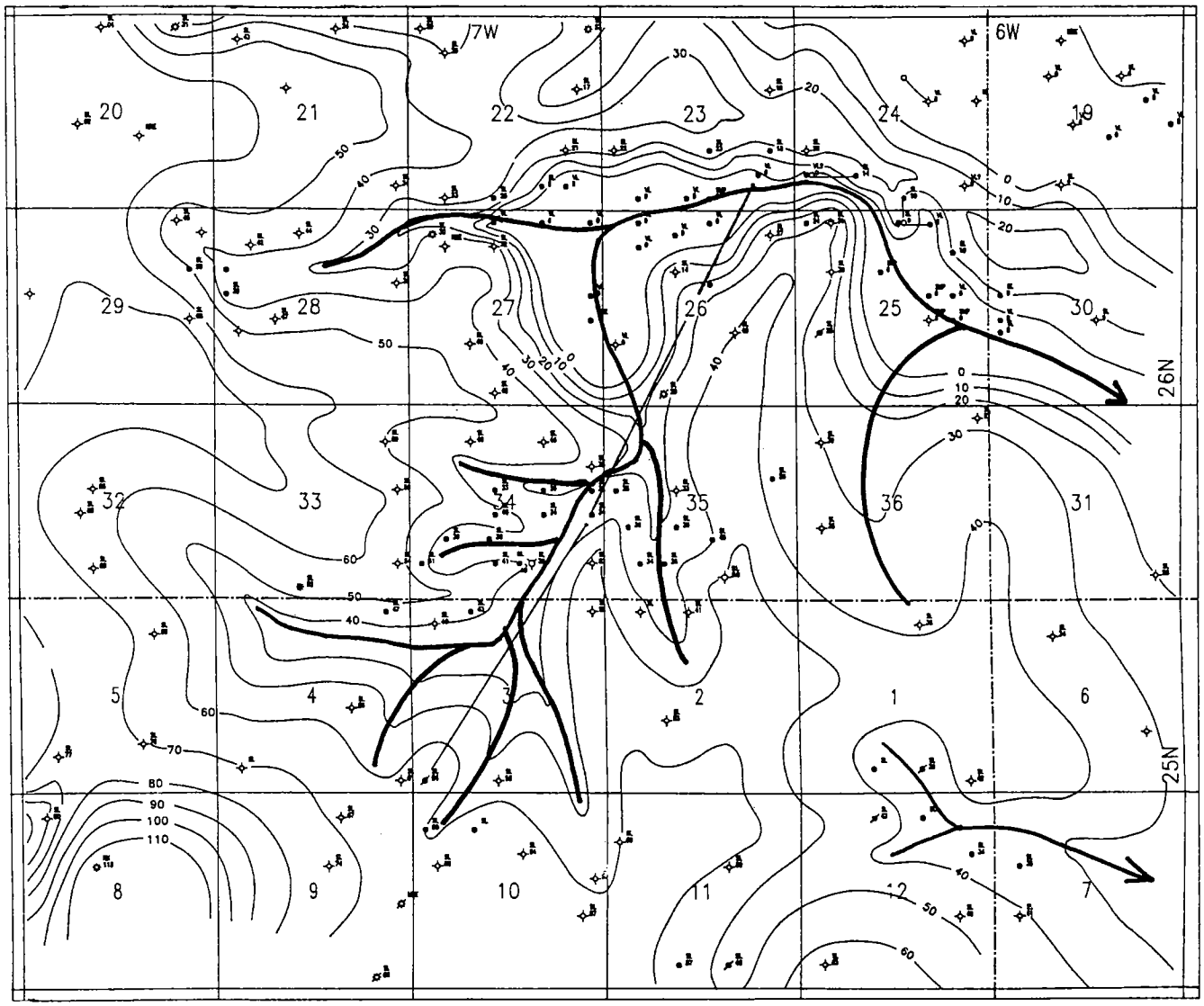

Figure 12. Sylvan Shale interval isopach map of the Northeast Nash–North Vicar field area, Grant County, showing the line of the cross section in Figure 10. Isopach interval, 10 ft.

standpoint of requiring a working knowledge of the present geologic setting and past geologic history. This knowledge is obtained by researching the works of others and applying their theories, concepts, and hard data to your own area of interest. An exploration model is built and tested repeatedly with log correlations and maps. Then the model is applied to the area of exploration interest until it must be modified or becomes invalid.

REFERENCES CITED

Adler, F. J.; Caplan, W. M.; Carlson, M. P.; Goebel, E. D.; Henslee, H. T.; Hicks, I. C.; Larson, T. G.; McCracken, M. H.; Parker, M. C.; Rascoe, Bailey, Jr.; Schramm, M. W., Jr.; and Wells, J. S., 1971, Sub-Woodford paleogeologic map, *in* Future petroleum provinces of the Mid-Continent, region 7, *in* Cram, I. H. (ed.), Future petroleum provinces of the United States—their geology and potential: American Association of Petroleum Geologists Memoir 15, p. 985–1120. (Reprinted in Rascoe, Bailey, Jr.; and Hyne, N. J., eds., 1988, Petroleum geology of the Mid-Continent: Tulsa Geological Society Special Publication 3, pl. 13, p. 58.)

Amsden, T. W.; and Klapper, Gilbert, 1972, Misener Sandstone (Middle–Upper Devonian), north-central Oklahoma: American Association of Petroleum Geologists Bulletin, v. 56, p. 2323–2334.

Francis, B. M., II, 1991, Petrology and sedimentology of the Devonian Misener Formation, northcentral Oklahoma, part I: Oklahoma City Geological Society, Shale Shaker, v. 42, no. 3, p. 48–68.

Hester, T. C.; Schmoker, J. W.; and Sahl, H. L., 1990, Log-derived regional source-rock characteristics of the Woodford Shale, Anadarko basin, Oklahoma: U.S. Geological Survey Bulletin 1866-D, 38 p.

Geometry of the Devonian Misener Sandstones in Northeastern Oklahoma

George W. Krumme
Krumme Oil Company
Bristow, Oklahoma

ABSTRACT.—In northeastern Oklahoma, from the Ozark dome southwestward, the Woodford Shale progressively covers beveled edges of the Arbuckle, Simpson, Viola, Sylvan, and Hunton stratigraphic units. The Devonian Misener sands that were buried by the Woodford Shale on these peneplaned wedges were deposited in channels, pods, and extensive thin patches. Most of the sands lie in incised valleys cut into the Sylvan Shale, although the sands also invaded the Viola and Hunton outcrops. Other contemporaneously deposited detritus is minimal.

The Misener is composed of reworked Middle Ordovician Simpson sands deposited on a generally southeastern slope. The channels do not merge into typical shoreline sand bodies but rather seem to have wasted away. Post-Misener erosion may have occurred, but the geometry of the sands suggests that the erosive capacity of the subaerial streams may have dissipated before a shoreline was reached.

These sands represent only the final stage of the prolonged erosion of a regional uplift. The Misener appears to be a fluvial deposit reworked by the transgressive Woodford sea.

GEOLOGIC SETTING

Eighty years ago, as the early cable-tool wildcatters moved westward from the oil fields south of Tulsa, they were continually forced to drill deeper holes, because the formations in northeastern Oklahoma generally dip to the west. In 1920, in Creek County, just west of the Okmulgee County line, Fred Misener found prolific oil production in a sand that looked like the "Wilcox" sand, at about the same level as the "Wilcox" but above the Viola Limestone rather than below it. The sand was distributed erratically, but it was highly productive. At first, it was considered to be a "Wilcox" sand. It was called "Wilcox" in the well records of the area until late in the 1920s and occasionally even into the 1930s. In some of the wells that were drilled deeper, this upper sand was called the "first Wilcox," and the true "Wilcox" was called the "second Wilcox."

In 1926, Luther White, a pioneer oil geologist, explained that the so-called "first Wilcox" was much younger than the "second Wilcox" and was genetically unrelated. To disseminate his insight, the Oklahoma Geological Survey published a short monograph in which White (1926) presented a first analysis of the major unconformity at the base of the Woodford Shale, generally called the pre-Woodford unconformity.

White (1926) noted that by some time in the Late Devonian Epoch, Hunton carbonates had covered virtually the entire Midcontinent area. Toward the close of the Devonian, White said, the Midcontinent experienced an uplift of state-sized dimensions that was centered in eastern Kansas. All of the beds in northeastern Oklahoma were tilted slightly to the south and west. A long period of erosion followed, an erosion that beveled the older formations and exposed the Ordovician Arbuckle limestones to the northeast. This period of erosion did not close until the land area over northeastern Oklahoma was practically reduced to base level.

A modified version of White's paleogeologic map of the subcrop below the Woodford is shown in Figure 1. The truncation required the removal of an enormous amount of material and must have required a long period of time, during which eroded detritus was washed downstream and deposited, then cannibalized and redeposited, over and over until the entire dome was reduced to a peneplain. The surprisingly small amount of debris left on this old eroded surface represents only the last stage of this long process of denudation.

This debris—almost all of it Misener sand—was covered by the waters of an advancing sea and preserved by deposition of the Woodford Shale. Wherever they appear, these Misener sands are universally recognized to be reworked Simpson sands.

THEORIES OF ORIGIN

White (1926) noted that the Misener sands were irregularly distributed. He believed erroneously that "the patterns of these sand bodies are generally subcircular in outline," and he proposed that they were

Krumme, G. W., 2001, Geometry of the Devonian Misener sandstones in northeastern Oklahoma, *in* Johnson, K. S. (ed.), Silurian, Devonian, and Mississippian geology and petroleum in the southern Midcontinent, 1999 symposium: Oklahoma Geological Survey Circular 105, p. 47–55.

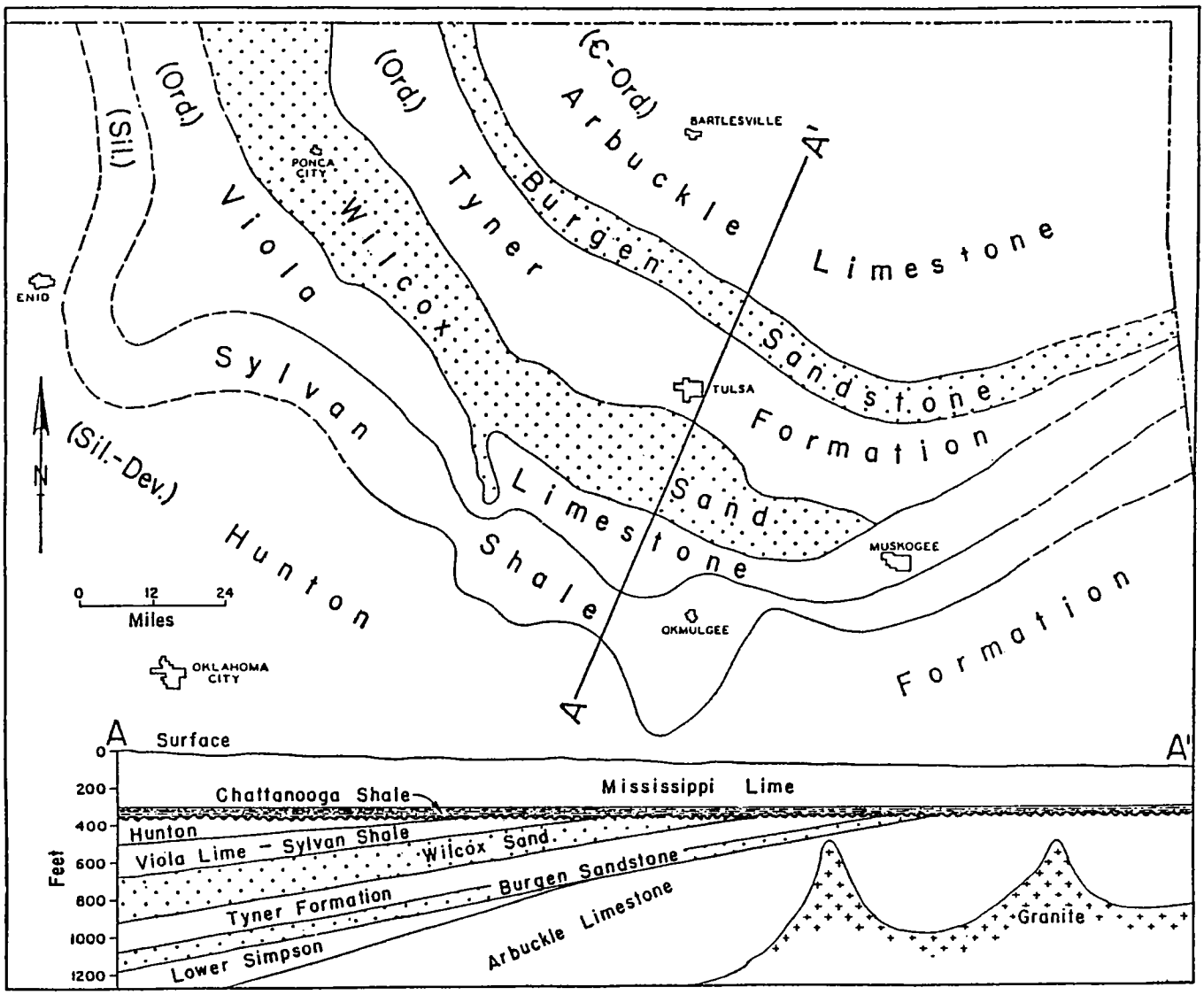

Figure 1. Paleogeologic map of the subcrop below the Woodford Shale (Chattanooga Shale) of northeastern Oklahoma. From Levorsen (1960, fig. 5-7, used with permission, modified from White, 1926).

windblown dunes. This belief and this opinion have both proven to be incorrect.

Since White's time, geologists have abandoned the dune theory, and later proposals for the origin of the Misener have varied widely. Students of the sand have variously interpreted the environment of deposition as shallow marine, estuarine, tidal channel, tidal flat, fluvial, and fluvial reworked in a shallow-marine environment. I am an advocate of the latter interpretation—that the Misener was a fluvial deposit in an incised-valley system mostly cut into the Sylvan, which was subsequently reworked by the transgressive Woodford sea.

MISENER AS REWORKED ALLUVIUM IN INCISED VALLEYS

I first became acquainted with the Misener sand in an area south of Slick in southeastern Creek County, where our company had drilled a few wells to the Misener. Many cable-tool wells had tested the Misener in the Slick area, but only a few rotary holes had been drilled and not many electric logs were available. Even so, it was apparent that the sand was not deposited on top of the Sylvan Shale as White had presumed but was instead deposited as depositional fill in an incised valley (Fig. 2). Note that in the No. 1 Kimble well the Misener completely displaces some 55 or 60 ft of Sylvan Shale. Figure 3 is a cross section across a different channel east of Slick, near the well that, in the 1920s, Fred Misener had chanced upon and given his name to the sandstone under discussion. This cross section looks similar to the one in the previous figure. One unusual feature is the relative steepness of the east bank of the channel, where the Misener thickens from zero to almost 50 ft in a horizontal distance of less than 1,000 ft.

In 1969, while doing graduate work at the University of Tulsa, I wrote a paper on the Misener covering

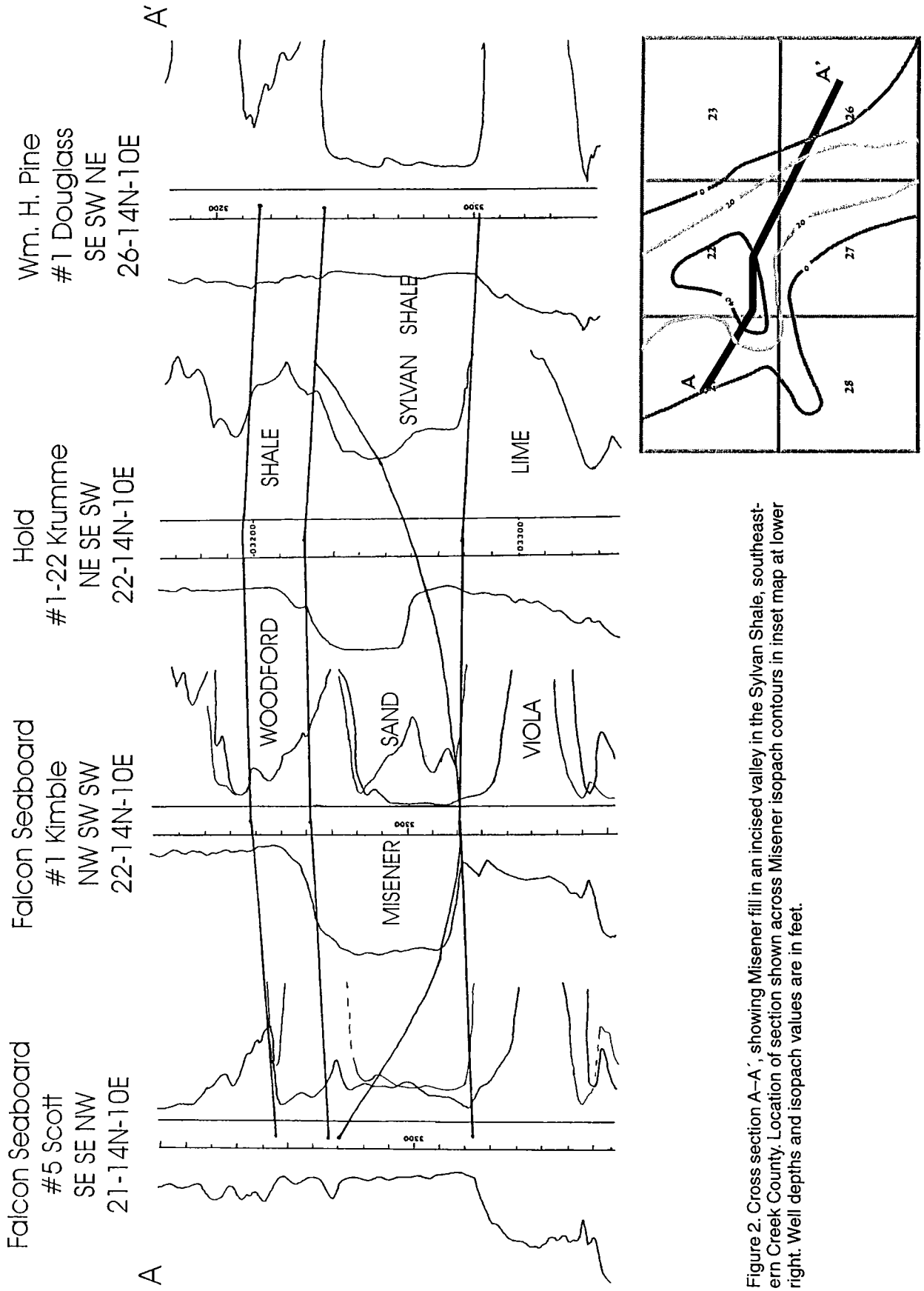

Figure 2. Cross section A–A′, showing Misener fill in an incised valley in the Sylvan Shale, southeastern Creek County. Location of section shown across Misener isopach contours in inset map at lower right. Well depths and isopach values are in feet.

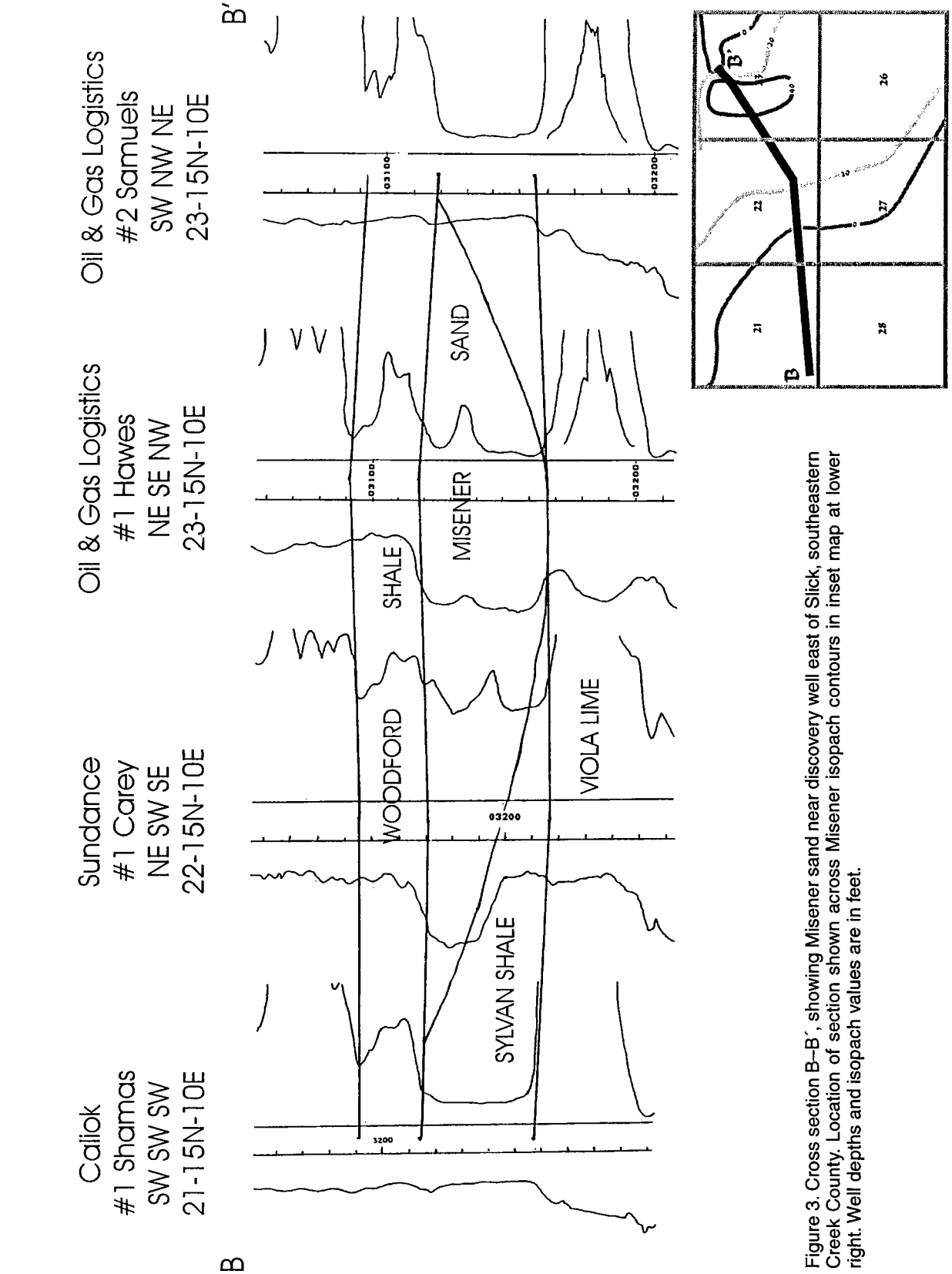

Figure 3. Cross section B–B′, showing Misener sand near discovery well east of Slick, southeastern Creek County. Location of section shown across Misener isopach contours in inset map at lower right. Well depths and isopach values are in feet.

Ts. 14–15 N., R. 10 E., and adjacent areas. As far as I know, my paper was the first to observe that the Misener occupies channels cut into the Sylvan Shale, a reflection of the fact that no real study of the Misener had been published in the five decades after it was discovered. Figure 4 shows the distribution of the Misener sands in the southeastern Creek County area covered by my paper.

Several observations may be made regarding this distribution. First, it is noteworthy that the channels appear only where they cross the Sylvan Shale subcrop. To the north, where the channels presumably crossed the Viola, the channels are not found. To the south, the channels disappear before they reach the Hunton subcrop. There are other patches and pods of Misener to the south of the channels, but they are independent of the channels.

Whether the absence of channels across the limestone subcrops is due to nondeposition or to subsequent removal is not clear. Certainly, the clays that later formed the Sylvan Shale would have been much more easily eroded. The Sylvan deposits would have been buried previously only under the Hunton and were probably stiff mud, only somewhat compacted. The Viola Limestone and the Hunton Limestone would have been more firmly indurated and more resistant to erosion. Patches of Misener sand do appear on the Hunton subcrop, but the streams that carried the sand over the Hunton subcrop apparently lacked the power to incise. Perhaps the resistivity of the Hunton to erosion created a temporary base level, which, in the absence of further tilting, the streams could not overcome. The streams that cut the channels seem to have run out of sand or out of energy. It is also possible that subsequent erosion shaved the sands at the ends of the channels, but such a process is hard to visualize.

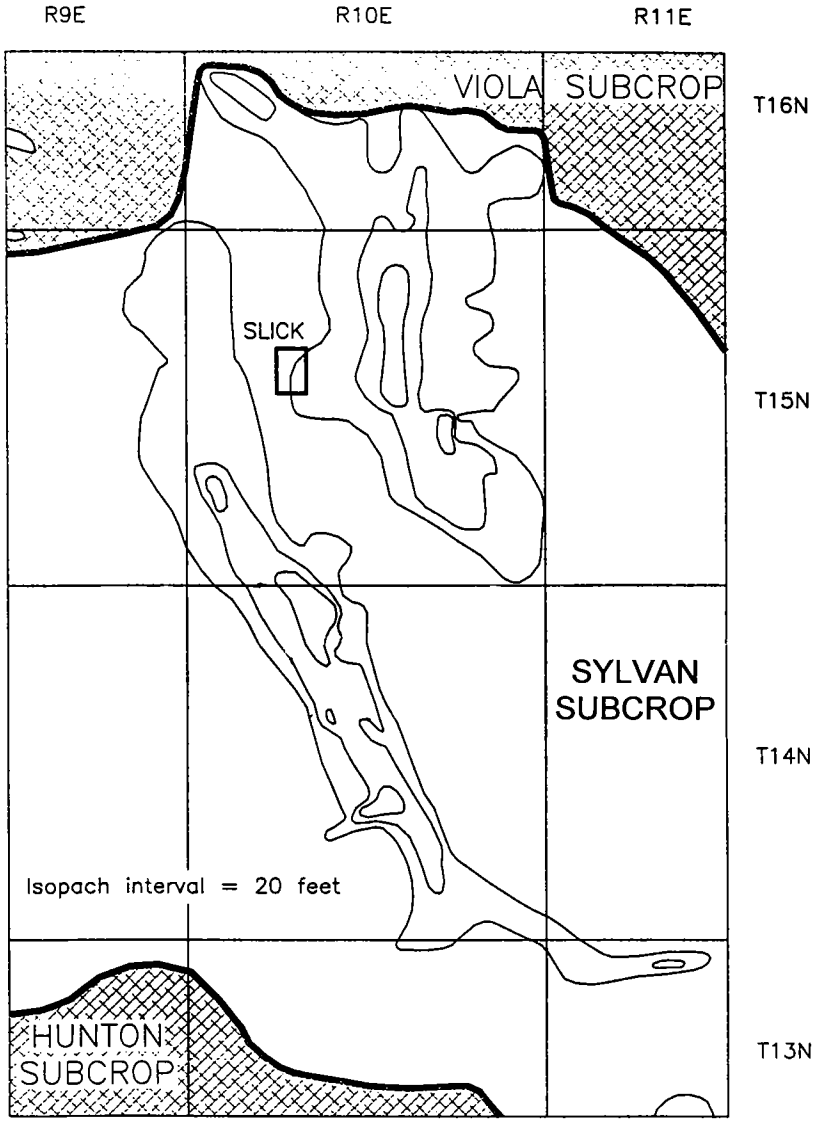

Figure 4. Map showing distribution of Misener sands in southeastern Creek County.

PAPERS INCORPORATED INTO REGIONAL STUDY

Even though unpublished, the paper I prepared became available to the geology schools at Oklahoma State University and the University of Oklahoma. Subsequently, a master's thesis at each of the geology schools covered Misener channels in other parts of northeastern Oklahoma. In 1978, James Kochick, in a thesis for Oklahoma State University, studied thick and prolific Misener sands in a six-township area north of Cushing—Ts. 17–19 N., Rs. 4–5 E. In 1980, Paul Bauernfeind at the University of Oklahoma prepared a thesis covering scarcer Misener sands in a four-township area northeast of Stroud —Ts. 15–16 N., Rs. 6–7 E.

Both Kochick and Bauernfeind found that the Misener sands in the areas they studied appear to be incised valley fill. Kochick in particular, however, emphasized that petrographic evidence and common sense convinced him that the sands were reworked by the transgressive Woodford sea that covered the Midcontinent in the Late Devonian, a finding with which I agree.

In this paper, I have integrated the work of Kochick and Bauernfeind and my previous work into a regional map that covers much of the Misener sand in northeastern Oklahoma (Fig. 5). To fill in the gaps between the three works, I used mostly well records and scout tickets.

There is much less sand in the areas between the three studies, and, furthermore, the pattern at the end of the channels is unusual. One would expect the channels to lead to a complex of shore-

line sands. On the contrary, these sands seem just to have wasted away. At the ends of some of the channels the sand becomes thin and spreads out into a thin veneer, commonly from 1–2 ft to perhaps 10 ft thick. There is no evidence of marine bars perpendicular to these channels, probably for two reasons. Long erosion had left the area so close to base level that there was a paucity of sand. Secondly, the margin of the basin during Misener time was so far south that no shoreline may have been close to the ends of the channels.

The channels north and east of Cushing extend onto the Viola subcrop before they terminate. Where the ends of the channels terminate on the Viola, the sands become thin and spread over a wide area. Patches and pods of Misener sand appear at places on the Sylvan terrane, but in northeastern Oklahoma, as previously noted, thin, widespread sandstones appear mostly where the channels terminate on the Viola Limestone. Perhaps this phenomenon is due to the resistance of the Viola to erosion, which would have prevented the streams from cutting deep channels. As the shoreline of the advancing Woodford sea passed over the area, the shallow depth of incisement allowed the marine currents to spread the sand outside the valleys onto the adjacent terrain.

The reason that Misener channels in northeastern Oklahoma did not reach the Hunton, but did invade the Viola subcrop, must lie in the local topography at the time. Both the Viola and the Hunton would have been resistant to erosion, but water insists on flowing downhill; and apparently in the area north and east of Cushing, the gradient lay eastward strongly enough to allow the streams to flow out over the Viola subcrop.

Since both limestones, particularly the Hunton, were subject to dissolution by vadose waters, some sands carried across the limestone surface would surely have been lost into underground channels and vugs.

As at Slick, cross sections of Misener sand in the

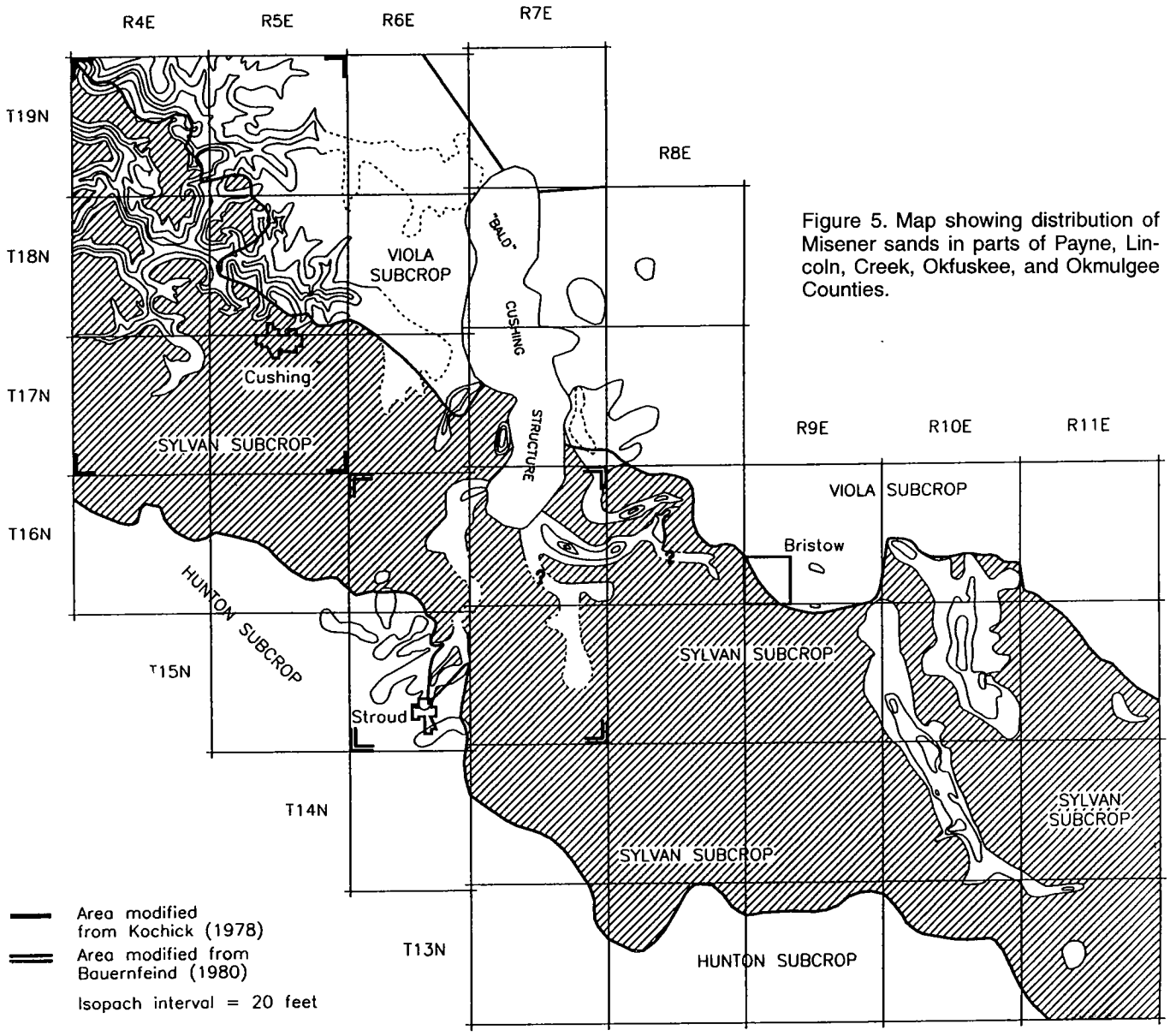

Figure 5. Map showing distribution of Misener sands in parts of Payne, Lincoln, Creek, Okfuskee, and Okmulgee Counties.

Sylvan Shale farther to the west also clearly show channel fill in an incised valley. Figure 6 is a cross section of a channel southeast of the Cushing pool. The entire Sylvan section has been eroded, as well as most of the Viola. In a cross section across a channel northwest of Cushing (Fig. 7), the Sylvan is relatively thin. The sandstone is noticeably thicker than the Sylvan Shale on each side, presumably owing to differential compaction.

TIME OF COMPACTION

Regarding time of compaction, Figure 7 is an exception to the general relationship of the Misener–Sylvan interval. The other cross sections show no effect of differential compaction, nor does an isochore map of the Misener–Sylvan interval reflect the presence of a channel. Busch (1974) contrasts a channel-fill profile that is formed after the substrata have been compacted with one created before or during compaction (Fig. 8). The cross sections in this paper resemble more closely his post-compaction profile, even though the Sylvan should never have been buried deeply enough to have been thoroughly compacted before the Misener sands were deposited.

It is possible that the channels were not completely filled, and that the compacted sand approximated the thickness of the compacted shale, because the shale, though initially thicker, was subject to greater shrinkage. If that circumstance had been true, however, and the channel had not been full of sand at the time the beds were being covered by the Woodford shale, the Woodford should be thicker above the Misener channel, and no such relationship is evident.

Whether or not the incised valley was totally filled

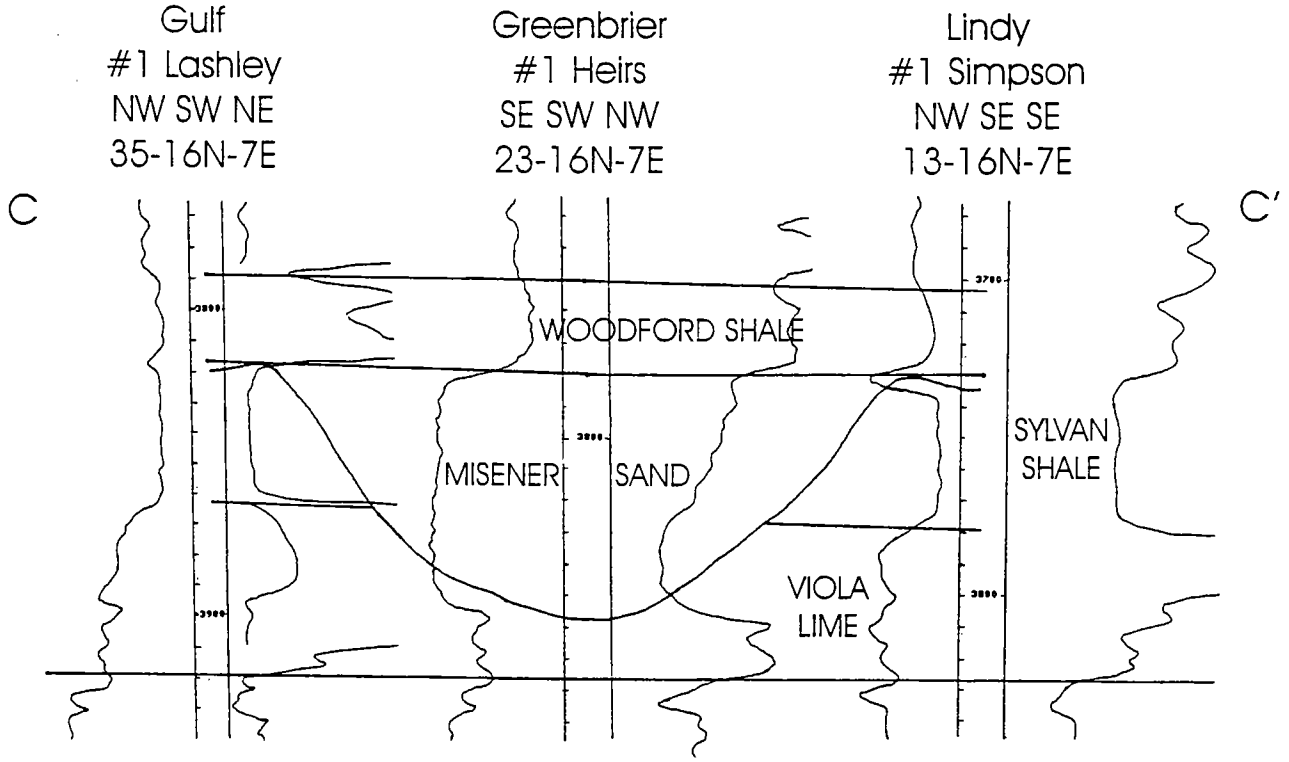

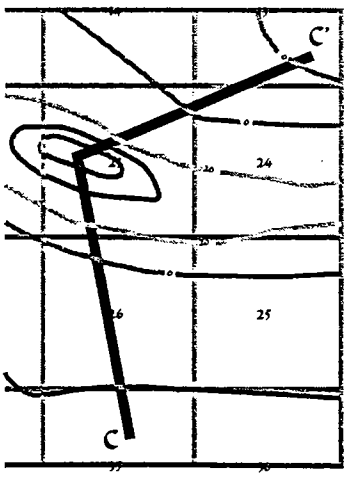

Figure 6. Cross section C–C′ of an incised valley in western Creek County filled with sand eroded from the bald-headed Cushing high. The channel cut deeply into the Viola Limestone. Location of section shown across Misener isopach contours in inset map at lower right. Well depths and isopach values are in feet.

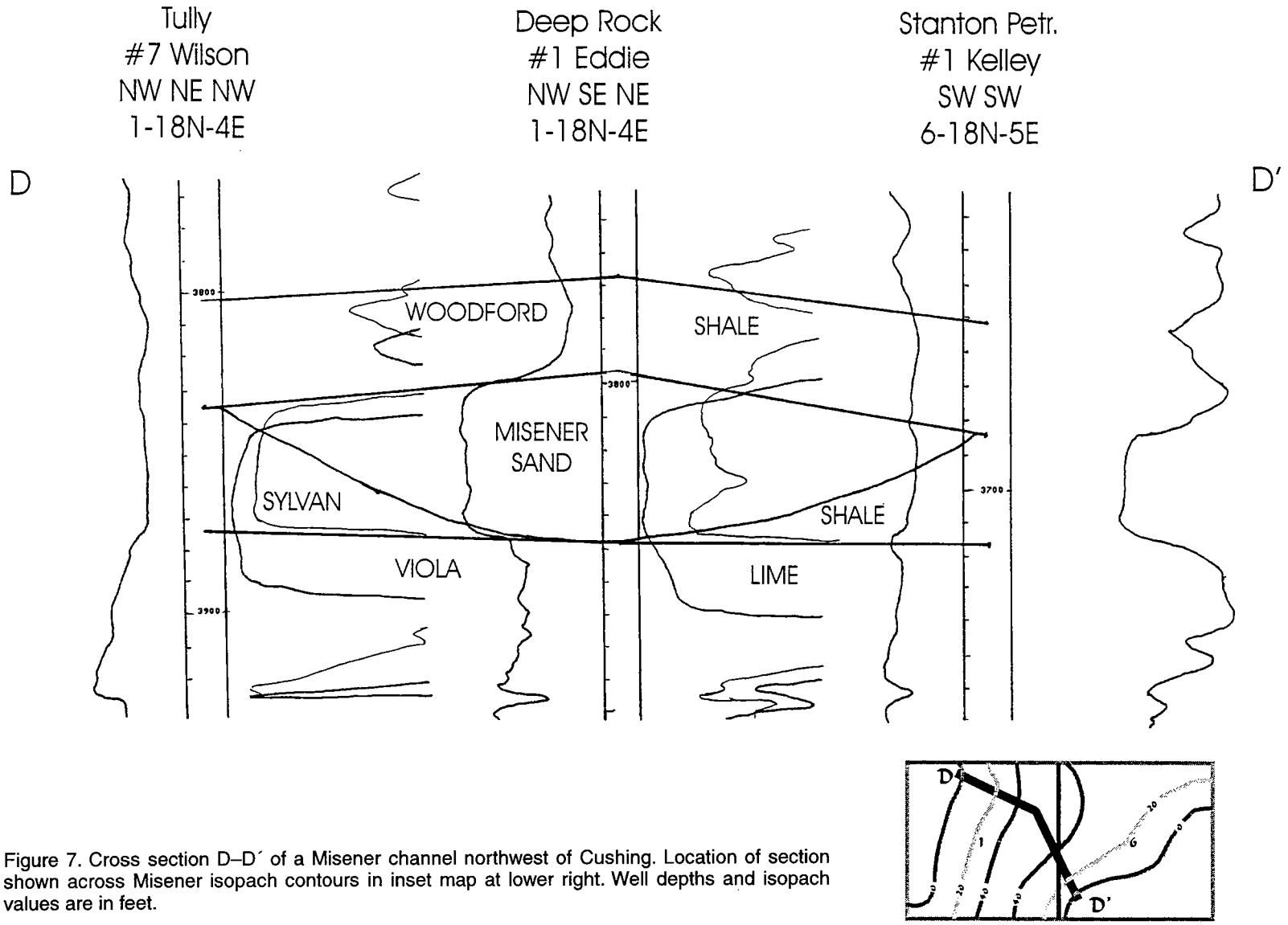

Figure 7. Cross section D–D´ of a Misener channel northwest of Cushing. Location of section shown across Misener isopach contours in inset map at lower right. Well depths and isopach values are in feet.

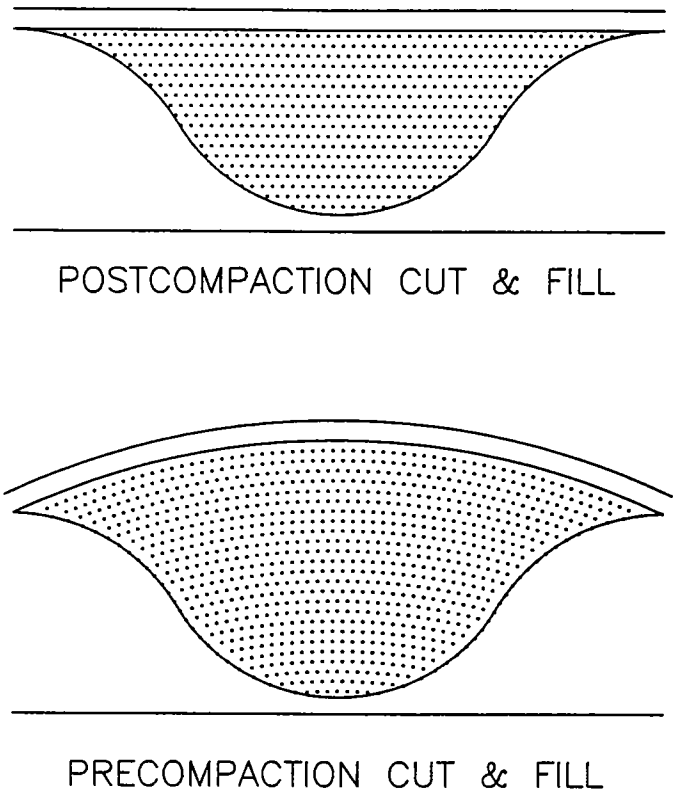

Figure 8. Schematic diagrams of two types of compacted channel fill in a shale valley (modified from Busch, 1974, fig. 57).

with sand, the approach of the Woodford sea shoreline would have converted the incised valley into an estuary. For a time thereafter, fluvial and marine forces competed in shaping the final form of the channel sands. Tidal currents reworked the sands far into the estuary. As sea level rose, the lower reaches of the estuary became truly marine, the tidal zone crept up the estuary, and the river continued to deliver sand down the valley. This process continued until the advancing sea covered all the land, and eventually the muds of the Woodford began to accumulate. Subsequently, compaction and lithification of the sediments shaped the beds into the form in which we find them today.

REFERENCES CITED

Bauernfeind, P. E., 1980, The Misener sandstone in portions of Lincoln and Creek Counties, Oklahoma: Shale Shaker, v. 3, no. 8, p. 173–185; no. 9, p. 188–197; no. 10, p. 204–210.

Busch, D. A., 1974, Stratigraphic traps in sandstones—exploration techniques: American Association of Petroleum Geologists Memoir 21, 174 p.

Kochick, J. P., 1978, Petroleum geology of the Misener sandstone in parts of Payne and Lincoln Counties, Oklahoma: Oklahoma State University unpublished M.S. thesis, 63 p.

Levorsen, A. I., 1960, Paleogeologic maps: W. H. Freeman, San Francisco, 174 p.

White, L. H., 1926, Subsurface distribution and correlation of the pre-Chattanooga ("Wilcox" sand) series of northeastern Oklahoma: Oklahoma Geological Survey Bulletin 40-B, 23 p. (Also Oil and Gas Journal, April 1, 1926.)

Facies and Petrophysical Characteristics of the Chattanooga Shale and Misener Sandstone in Central Kansas

K. David Newell and John H. Doveton
Kansas Geological Survey
Lawrence, Kansas

Michael W. Lambert
Kansas State University
Manhattan, Kansas

ABSTRACT.—The Upper Devonian–Lower Mississippian Chattanooga Shale in Kansas has an angular unconformity at its base that truncates Silurian and Devonian carbonate rocks and older Ordovician strata. Isopach maps and subcrop maps define a broad paleovalley in Marion, McPherson, and Reno Counties that is approximately 120 mi long, 20 mi wide, and 100 ft deep. This paleovalley, named the *McPherson valley*, is developed on the Central Kansas arch, a broad uplift that separates the North Kansas basin from the Southwest Kansas basin. The Chattanooga Shale within the McPherson valley has elevated gamma-ray readings, which may be associated with potential petroleum source rocks. Limestone beds covering several townships also are present in the upper part of the Chattanooga and seem to have their depositional limits confined to near the axis of the paleovalley. Locally in the Zenith field in Stafford County, one of these limestones is chertified and is a viable reservoir rock.

The Misener Sandstone, a transgressive sandstone at the base of the Chattanooga Shale, is locally important for petroleum production. It is erratically developed, being several feet thick in some wells but absent in nearby wells. Nevertheless, depositional trends of the Misener can be detected by regional mapping. In central Kansas, these trends are parallel and lie along the flanks of the McPherson valley, whereas the axis of the paleovalley is relatively free of Misener deposits. The Misener therefore probably is a series of paralic and estuarine-fluvial sand bodies developed during successive stillstands during the sea-level rise associated with Chattanooga deposition. On the western flank of the McPherson valley the Misener can be up to 50 ft thick owing to clastic material that was shed off the nearby Ancestral Central Kansas uplift from eroding Precambrian basement and Ordovician siliciclastics such as the St. Peter and Reagan Sandstones.

The Misener is a medium- to fine-grained quartzose sandstone, locally conglomeratic near its base. It seems to have been deposited in bathymetric depressions and erosional cuts that are characteristic of fluvial and estuarine sands, but marine depositional conditions also are indicated by thin planar cross-bedding, abundant burrowing, marine fossils such as crinoid stems, and thin limestone beds interstratified with the sandstone. Black phosphatic grains, fine to coarse, also are present, which contain elevated concentrations of uranium that can be detected with spectral gamma-ray logs. Log-derived porosities for the sandstone average 11% but can be as great as 15%.

INTRODUCTION

The Upper Devonian–Lower Mississippian Chattanooga Shale is colloquially known by drillers in Kansas as "Kinderhook shale" (Goebel, 1968). It is a silty, pyritiferous, black shale in southern Kansas, but it is dark gray and varicolored farther north (Goebel, 1968; Lambert, 1992a). The Chattanooga of Kansas is lithologically contiguous with the Woodford Shale in Oklahoma (Lambert, 1992b, 1994). The Chattanooga Shale is present over much of central and eastern Kansas, reaching a maximum thickness of 250 ft in northeastern Kansas in the Forest City basin near the Nebraska state line (Goebel, 1968).

The basal sandstone of the Chattanooga is known as the Misener Sandstone in the subsurface of Kansas and Oklahoma (Fig. 1), and the Sylamore Sandstone at the surface in eastern Oklahoma, Arkansas, and Missouri. It is a time-transgressive unit that gen-

Newell, K. D.; Doveton, J. H.; and Lambert, M. W., 2001, Facies and petrophysical characteristics of the Chattanooga Shale and Misener Sandstone in central Kansas, *in* Johnson, K. S. (ed.), Silurian, Devonian, and Mississippian geology and petroleum in the southern Midcontinent, 1999 symposium: Oklahoma Geological Survey Circular 105, p. 57–70.

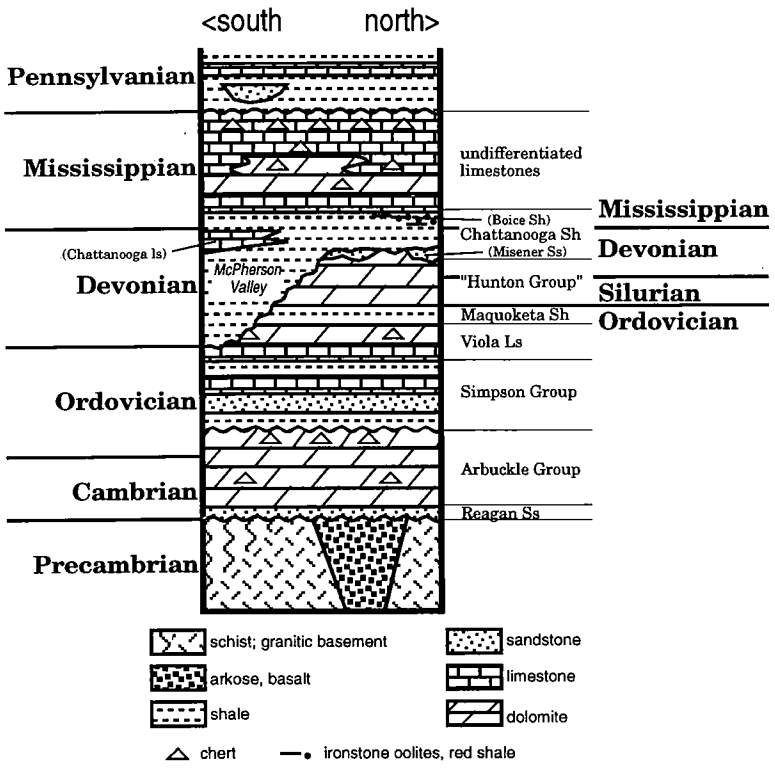

Figure 1. Local stratigraphic column for the Paleozoic in central Kansas.

erally is older to the south and younger to the north (Freeman and Schumaker, 1969; Amsden and Klapper, 1972).

Examination of some of the facies and petrophysical features of the Chattanooga and Misener can supply information on the transition from the early Paleozoic structural regime to that of the late Paleozoic (Fig. 2), as well as yield data that aid in predicting depositional facies and diagenetic properties upon which petroleum-reservoir characteristics depend. This paper thus concentrates on the spatial and stratigraphic distribution of some key facies of the Chattanooga in central Kansas, including limestone bodies present within it and also the Misener Sandstone at its base. Petrophysical aspects of the Chattanooga, as revealed by wireline logs and cuttings samples, give additional lithologic characteristics that bear on the interpretation of its depositional and diagenetic history.

THE CHATTANOOGA IN KANSAS

Deposition During a Tectonic Transition

The Chattanooga Shale and its equivalents form the base of the Kaskaskia sequence in the Midcontinent (Sloss, 1963). Regional exposure and erosion by major stream channels occurred before the deposition of these rocks, followed by a marine transgression that advanced onto the craton from the south (Bunker and others, 1988). Subtle early Paleozoic cratonic features (i.e., the Chautauqua arch and the adjacent North and Southwest Kansas basins) (Merriam, 1963) (Fig. 2A) can be defined by paleogeologic maps of the rock units truncated by the angular unconformity at the base of the Chattanooga. These early Paleozoic features may have been active during Chattanooga deposition, but they are not readily evident on an isopach map of this unit (Fig. 2B). The effects of a markedly different tectonic pattern, however, are evident on isopach maps of Mississippian carbonate strata, which directly overlie the Chattanooga. Isopach "thins" and "thicks" of Mississippian strata generally correspond respectively to structural highs and lows that were active in Late Mississippian–Early Pennsylvanian time (Merriam, 1963). Most of this structural movement expressed in Mississippian isopach maps is attributable to the Ouachita orogeny, which initiated between Late Mississippian and Middle Pennsylvanian time (Merriam, 1963; Newell and others, 1987).

In contrast to the angular unconformity at its base, the Chattanooga may be separated by a disconformity from the overlying Mississippian carbonates (Goebel, 1968). Weathering along this surface is suggested by red and purple shale that overlies the normally gray to black shale of the Chattanooga. Ironstone oolites composed of goethite and hematite also are present at the top of this unit in the vicinity of the Nemaha uplift and northern parts of the Salina basin (Lambert, 1992a). A map (Fig. 3) showing the presence of red shales and ironstone oolites at the top of the Chattanooga (versus gray or black shale) implies that at the end of Chattanooga time regions of north-central Kansas were subject to oxidizing conditions, possibly associated with subaerial exposure or reworking in shallow water. Conversely, areas in south-central Kansas are characterized by shales that are mostly gray to black, implying anoxic depositional conditions and nearly continuous deposition without reworking. Basin conditions are implied for this area and farther south toward Oklahoma. Lambert (1992a,b) also noted that gamma-ray levels of the Chattanooga Shale correspondingly increase southward in Kansas. Total-organic-carbon values and the amount of marine organic matter also increase southward as well (Lambert, 1993), indicating increasingly anoxic conditions and possibly deeper water toward the Anadarko basin in Oklahoma.

There is no significant southward bowing of the zone of oxidized Chattanooga over the trace of the south–southwesterly-plunging Nemaha uplift (Fig. 3); thus, oxidizing conditions apparently did not develop over this structural feature during or immediately after Chattanooga deposition. The Nemaha uplift evidently was not yet active during or immediately after Chattanooga deposition.

Although minor amounts of red shales are present

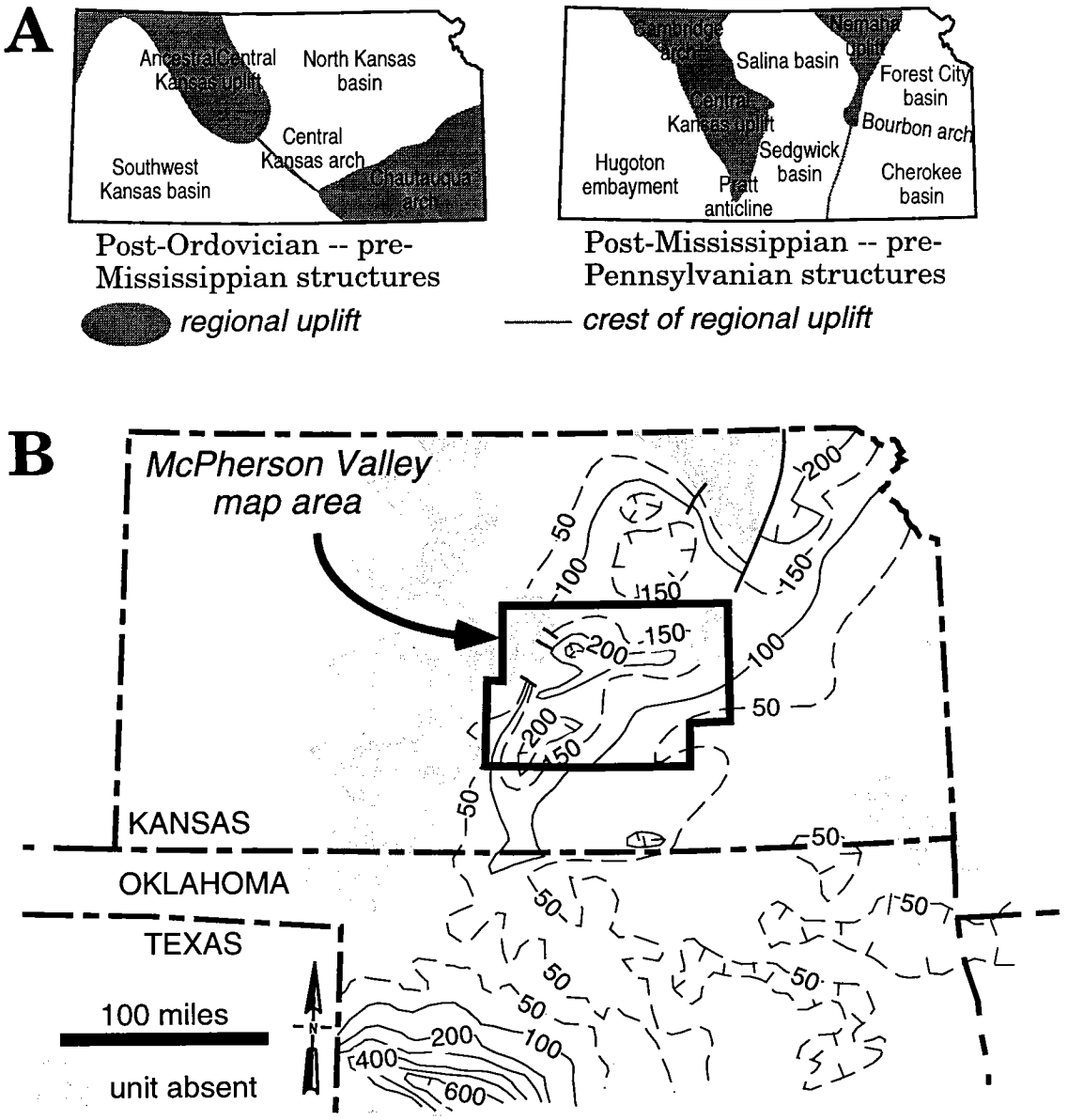

Figure 2. (A) Early and late Paleozoic structural features of Kansas (from Merriam, 1963). (B) Isopach map of Chattanooga Shale in Kansas and northern Oklahoma (from Hester and others, 1990; Lambert, 1992b; Comer, 1992), with location of McPherson valley area. Contours are in feet.

over the area of the Central Kansas arch (Fig. 3), it is unclear if the arch was active near the end of deposition of the Chattanooga Shale. Early Paleozoic structural features such as the Central Kansas arch also were thus not well expressed at the end of Chattanooga time. The Chattanooga therefore appears to have been deposited during a time in which neither early nor late Paleozoic tectonic features were dominant.

Lithologic Characteristics Revealed by Spectral Gamma-Ray Logs

Spectral gamma-ray logs are considerably less abundant than conventional gamma-ray logs, but they provide valuable additional information for geological interpretation. A conventional gamma-ray tool records natural gamma radiation pooled from all radioactive sources, scaled in API units. The spectral tool subdivides the gamma radiation by energy level into the three major contributors of potassium-40 and isotopes in the uranium and thorium series (Doveton, 1994). The subdivision allows potassium, uranium, and thorium to be displayed as quantitative logs scaled in percentages (K) and ppm (U and Th). Alternatively, the total gamma-ray log can be partitioned into its potassium, thorium, and uranium components, as shown for the seven spectral gamma-ray logs in the Chattanooga in Kansas examined here (Fig. 4).

The potassium content is linked primarily with illite within the Chattanooga Shale. Most of the tho-

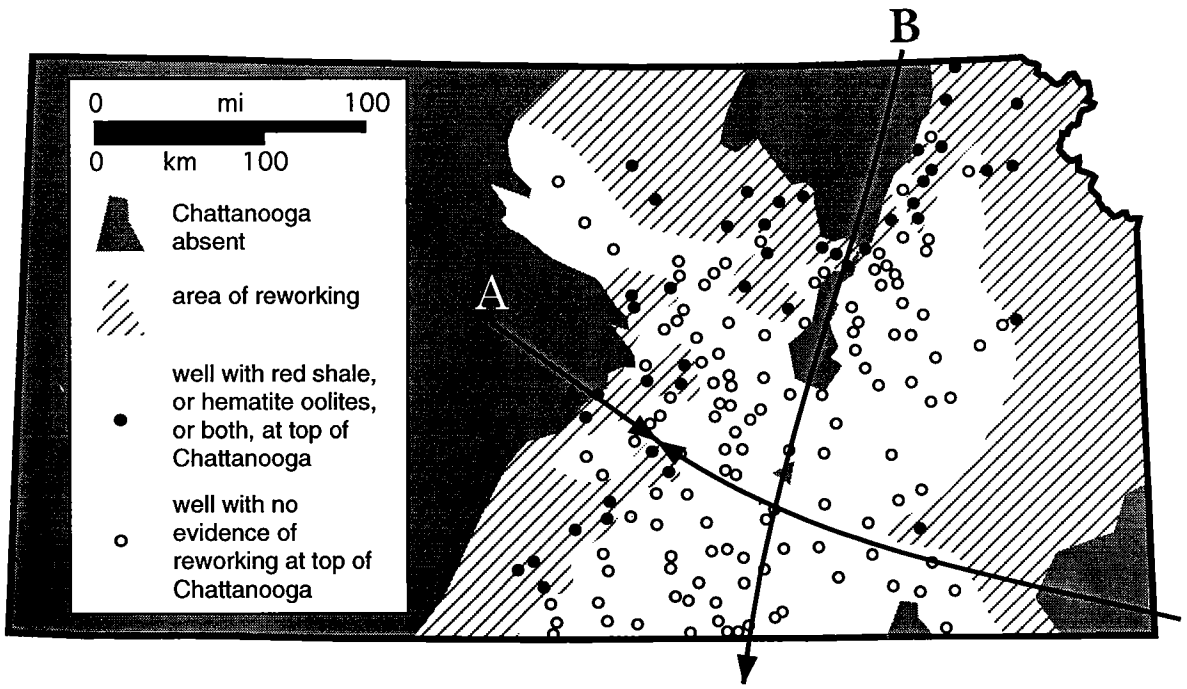

A. crestal trace of Ancestral Central Kansas uplift - Central Kansas arch - Chautauqua arch
B. crestal trace of Nemaha uplift

Figure 3. Map showing the presence or absence of red shales and ironstone oolites at the top of the Chattanooga (from Lambert, 1992a). Lithologic descriptions from sample logs by J. D. Davies filed at the Kansas Geological Survey were utilized for construction of this map. Increasing exposure and attendant oxidation at the top of the Chattanooga are indicated for northern and eastern Kansas, whereas less oxidation and exposure characterize the top of the Chattanooga in central Kansas. An embayment, with seaward being to the south, is defined.

rium in these sections probably is adsorbed on clay-mineral surfaces, although a zone of extremely high thorium content at the top of the Chattanooga occurs locally in northeastern Kansas. An example is shown on the *fund* (Petro-Lewis No. 7-1 Richards-Fund well) spectral gamma-ray profile in Nemaha County (Fig. 4). This stratigraphic interval is present throughout northeastern Kansas and southeastern Nebraska, and is a light-colored shale that has sometimes been called the Boice Shale (Reed, 1946; Moore and others, 1951; Goebel, 1968) (Fig. 1). This shale is considered to be the stratigraphic equivalent of the Hannibal Shale that crops out in Missouri (Goebel, 1968). The Boice Shale locally contains iron (goethite) oolites, and analyzed oolite samples have thorium contents as high as 71 ppm.

Thorium is concentrated usually in residual weathered deposits such as bauxites. Doveton and others (1994) observed that the geographic distribution of the iron oolite zone at the top of the Chattanooga formed shoal-like accumulations peripheral to the Nemaha uplift and suggested derivation of both iron and thorium from a bauxite–laterite precursor on nearby granitic islands, possibly on the Nemaha uplift, that underwent intense weathering.

The relatively lower levels of uranium in wells in the north are contrasted with increasing contents in the south, with high uranium anomalies shown most strongly at the base of the Chattanooga Shale (Fig. 4). The calculation of the thorium-to-uranium ratio (Th/U) is a useful measure of relative uranium enrichment or depletion, which can be linked with geological processes of reduction or oxidation (Adams and Weaver, 1958). Average Th/U ratios for the Chattanooga Shale in the seven wells show a regional pattern (Fig. 5) of relative increase in uranium content to the south. The contours depict a quadratic trend surface fitted to all the points. The seven data points are consistent with the southward-opening embayment defined by the oxidizing characteristics at the top of the Chattanooga (Fig. 3).

If uranium content is subtracted from the total gamma-ray reading, then the remainder is contributed by potassium and thorium sources, which reflect clay content. A map of this average "corrected" gamma-ray (CGR) reading in the Chattanooga Shale (Fig. 6) shows a feature reminiscent of a basin flank, with increasing clay contents to the southeast. Inspection of the average CGR at individual wells shows similar values in the five eastern wells that contrast with the markedly lower values in the two western wells. The simplest and most likely interpretation of this pattern is that the Chattanooga in the two western wells contains a higher proportion of nonradioactive coarse material weathered from the nearby Ancestral Central Kansas uplift. Shales in these wells probably have

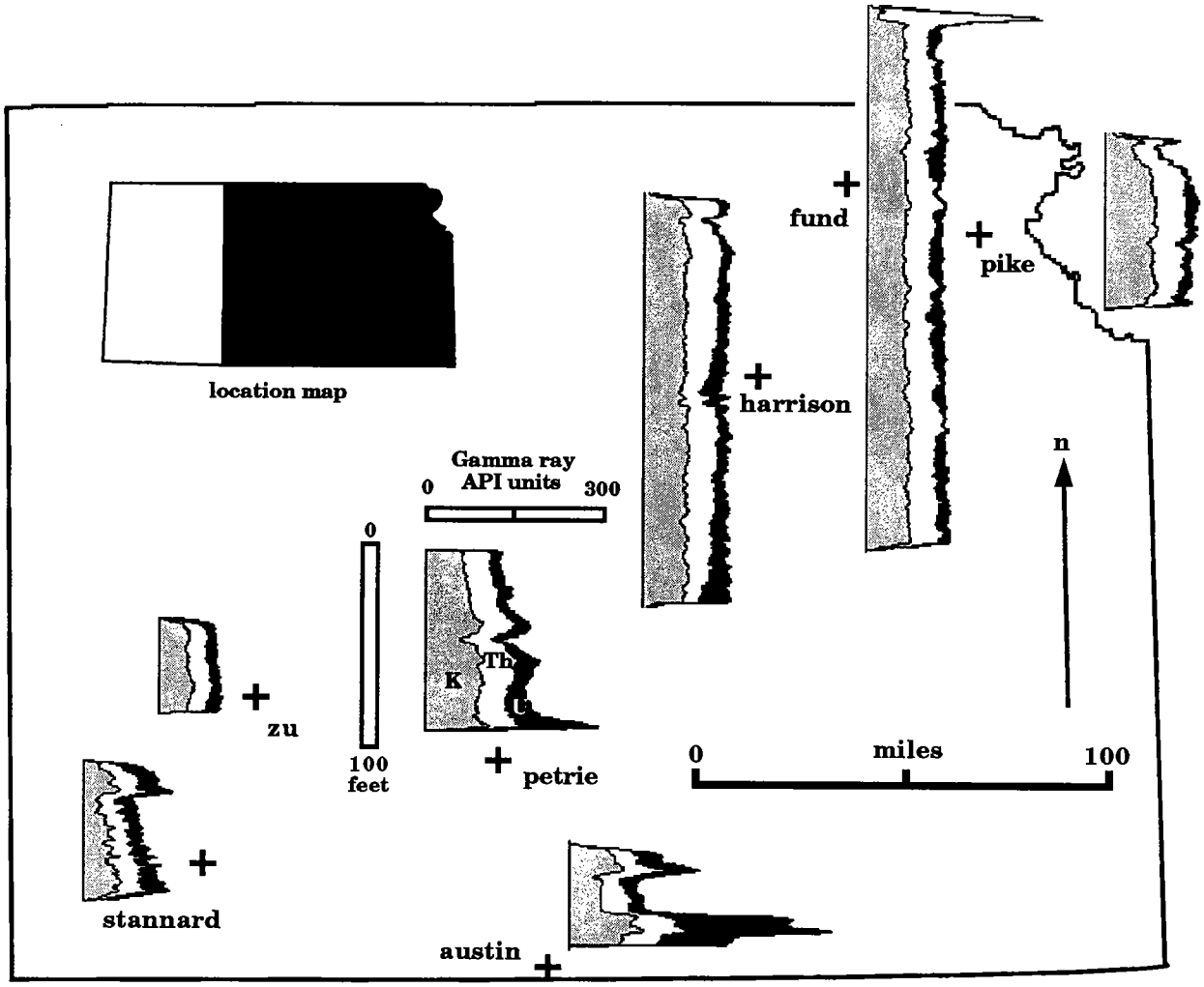

Figure 4. Spectral gamma-ray-log profiles of the Chattanooga Shale in seven wells in eastern Kansas. These wells are noted on the map as *fund* (Petro-Lewis No. 7-1 Richards-Fund, NW¼SE¼ sec. 7, T. 4 S., R. 10 E.), *pike* (Lear Petroleum No. 1-14 Pike, NE¼NW¼ sec. 14, T. 6 S., R. 19 E.), *harrison* (Conoco No. 1 Harrison, SW¼NW¼ sec. 33, T. 11 S., R. 10 E.), *zu* (Quinoco ZU-swd1, N½SW¼ sec. 12, T. 24 S., R. 11 W.), *petrie* (Pioneer Exploration No. 4 Petrie, SE¼NW¼SW¼ sec. 36, T. 26 S., R. 1 W.), *stannard* (F. G. Holl, SE¼NW¼SE¼ sec. 15, T. 30 S., R. 13 W.), and *austin* (Source Petroleum No. 4 Austin, S½SE¼NW¼ sec. 3, T. 35 S., R. 1 E.).

a higher silt content in comparison with sections to the east, where the shales are more proportionately rich in clay minerals. The average thorium-to-potassium ratio (Th/K) in the Chattanooga Shale is 2.88 ppm/percent, with a standard deviation of 0.40. This measure of relative potassium richness is a close match with expectations for a composition dominated by illite (2.0–3.5 ppm/percent; Schlumberger, 1998) with probably only minor clay-mineral compositional variability, as suggested by the small standard deviation. Laboratory analyses suggest that the thorium enrichment in the Boice Shale of northern Kansas is associated with the goethite oolites in this zone.

McPHERSON VALLEY

Internal Depositional Geometry

Isopach maps of the Chattanooga Shale (Figs. 2, 7) show thickening over the Central Kansas arch—precisely where one would expect regional thinning to occur if the early Paleozoic structures in the Midcontinent were active during deposition of this unit. The anomalous thickening of the Chattanooga was identified by Lee (1956) as a paleovalley that was erosionally carved into the Central Kansas arch prior to deposition of the Chattanooga. The valley trends east–west across the Central Kansas arch, and then just east of the more recent Central Kansas uplift it turns southward. This valley also is expressed on a paleogeologic map drawn at the angular unconformity at the base of the Chattanooga Shale (Fig. 7). The oldest rock units subcrop along the axis of the valley, where the deepest erosion took place.

Lambert (1992b) extended an internal stratigraphy for the Woodford Shale (stratigraphically equivalent to the Chattanooga) that was first developed by Ellison (1950) in west Texas and southeast New Mexico and

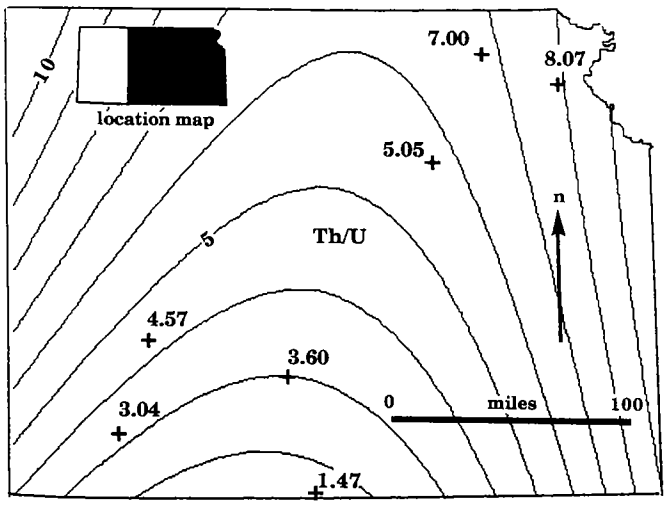

Figure 5. Quadratic trend-surface map of average Th/U ratios in the Chattanooga Shale from spectral gamma-ray logs in seven Kansas wells. Higher values indicate a relatively oxidizing depositional environment; lower values suggest more reducing conditions. Contour interval = 1 ppm Th/ppm U.

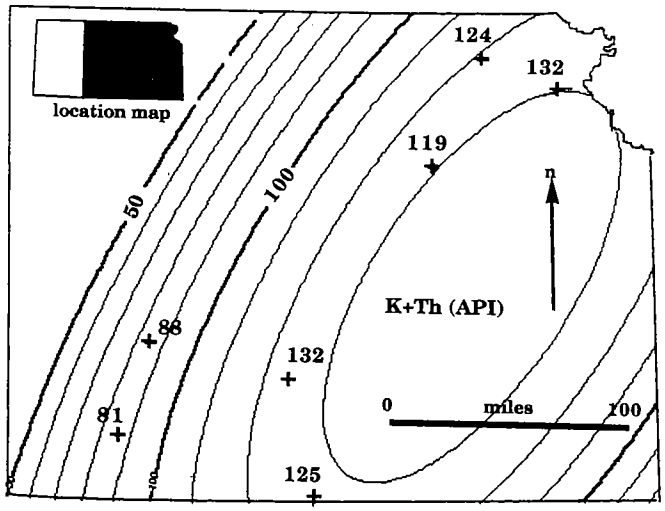

Figure 6. Quadratic trend-surface map of average corrected gamma-ray (CGR) values in the Chattanooga Shale from spectral gamma-ray logs in seven Kansas wells. The corrected gamma-ray value is calculated from the total gamma-ray reading by subtracting uranium. The remaining radioactive sources of potassium and thorium are a good aggregate indicator of total clay-mineral content. Contour interval = 10 API gamma-ray units.

extended by Hester and others (1990) into Oklahoma. Three informal members are distinguished principally on their gamma-ray characteristics, with the middle member having the highest gamma-ray readings. Only the middle and upper members are present in the McPherson valley because the lower member is present only in southernmost Kansas (Lambert, 1992b). The middle member is the most widespread of the three units.

A stratigraphic cross section along the axis of the McPherson valley (Fig. 8) shows that the middle member of the Chattanooga accounts for most of the valley fill. The relative thickness and high gamma-ray readings of the middle member perhaps indicate that its role as a potential petroleum source rock may be enhanced locally where it is abnormally thick within the McPherson valley. A westward and southward thickening of the upper member, and a corresponding thinning of the middle member, also are evident (Fig. 8). If this downlapping contact between the two units represents a time line, then water depth could have been 60–80 ft deeper in the western end of the valley. The contact between the upper and middle units of the Chattanooga in the eastern part of the valley is unclear, but most of the shale in this area probably correlates with the middle member of the Chattanooga.

Misener Sandstone

A thin sandstone termed the Misener Sandstone is developed erratically at the base of the Chattanooga Shale. It is a medium- to fine-grained quartzose sandstone that locally is an important petroleum reservoir in both Kansas and Oklahoma (Adler and others, 1971; Newell and others, 1987; Kuykendall and Fritz, 1993).

The Misener is difficult to isopach on a basinwide scale because of its erratic distribution. It can be several feet thick in some wells, but adjacent wells may have none. In most of eastern Kansas it may be represented only by rounded quartzose sand grains disseminated at or near the base of the Chattanooga Shale (Goebel, 1968).

In order to construct a map that could define Misener depositional trends effectively, map sections (nominally 1 mi^2) were utilized as basic blocks of information. Scout cards, lithologic logs, and geophysical logs available at the Kansas Geological Survey were inspected, and the presence (or absence) of Misener Sandstone for a section was noted. If no wells in a particular section recorded the presence of Misener Sandstone, the section was assigned a certain color. If one or more wells in the section noted the presence of Misener (even though other wells may not have noted its presence), the section was designated with a different color, depending on the maximum thickness noted in any well in the section. On the basis of mapping experience, two thickness categories were designated: one if the sandstone was <10 ft thick, and a second level (color) if any well discovered sandstone

When color-coded, the mapping sections basically play the role of pixels in a computer-generated image. As more territory is mapped, the pixels eventually define a larger picture in which depositional trends can be discerned. The results for the McPherson valley study area (Fig. 9) show two parallel trends of Misener deposition along the flanks of the valley. The axis of the valley, which separates the two trends, is relatively free of the Misener.

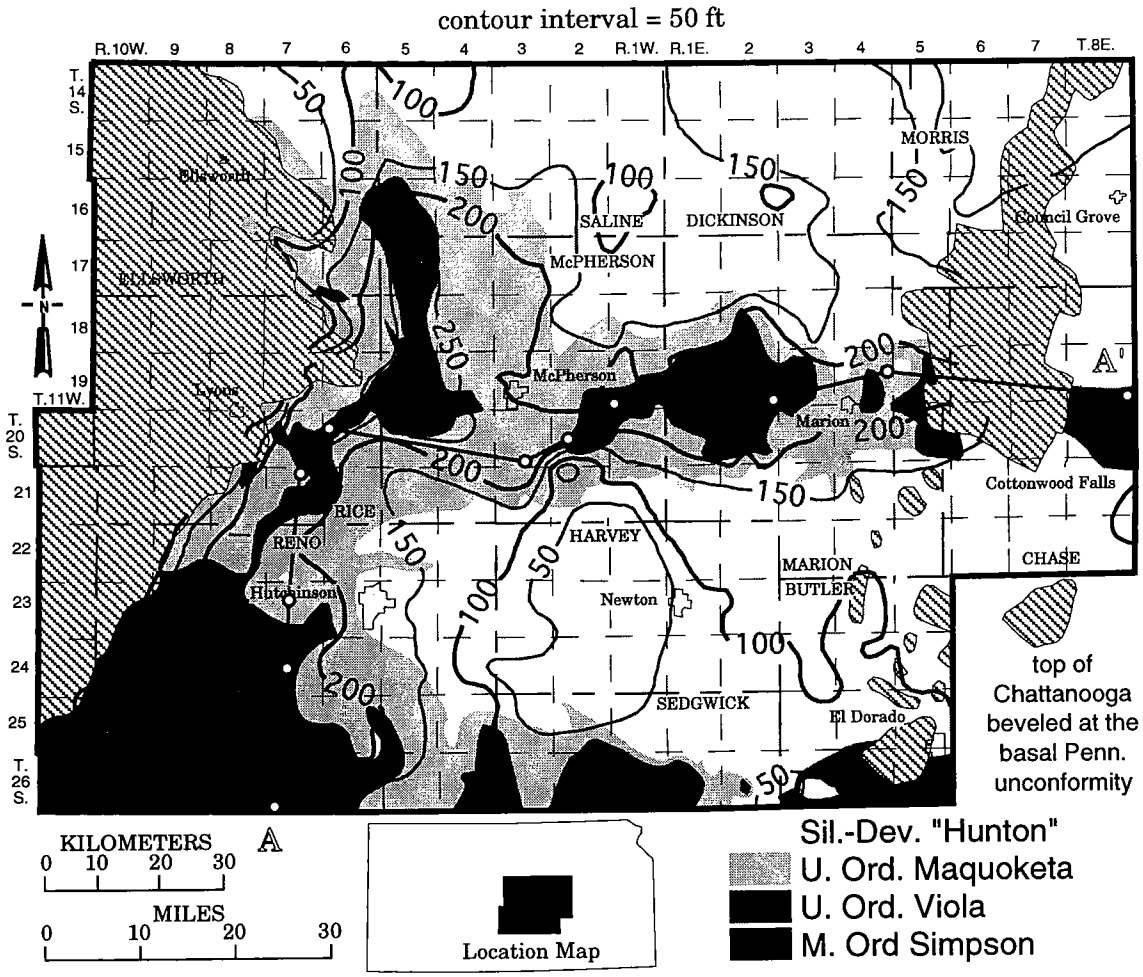

Figure 7. Paleogeologic map of rock units that subcrop beneath the angular unconformity at the base of the Chattanooga Shale (from Newell, 1987), with Chattanooga isopachs (from Lee, 1956) superimposed. The McPherson valley is largely defined by the area encompassed by the 200-ft contour line, which trends east–west across Marion and McPherson Counties, then south in western McPherson County. Wells used in cross section A–A′ are shown in Figure 8. Note that the pattern with diagonal lines defines the area where the Chattanooga is either partly or completely eroded. In these areas the original thicknesses of the Chattanooga can only be projected. Areas where the Chattanooga is completely eroded are presented in Figure 9.

The parallel nature of the sand trends suggests that a regional process such as sea-level rise, or rate of sea-level rise, may in part control the presence of the Misener. Perhaps the sands are a series of paralic sand bodies developed during successive stillstands during the sea-level rise associated with Chattanooga deposition. The axis of the McPherson valley is notably free of sand; therefore, fluvial-type sand bodies, which would most likely be preserved within the axis of the valley before the marine transgression, evidently are not preserved.

Relatively thick sands along the western side of the McPherson valley (Fig. 9) indicate proximity of a source area. In this situation, the Misener provenance is probably siliciclastics derived from the Middle Ordovician Simpson Group, the Cambrian Reagan Sandstone, and Precambrian granitic basement exposed on the Ancestral Central Kansas uplift. On the opposite side of the McPherson valley a separate source area may be indicated, possibly the Ozark uplift and outcrops of older Paleozoic sandstones on the Chautauqua arch in southeastern Kansas. Because of its textural and mineralogical maturity, much of the sand in the Misener over much of the Midcontinent is likely reworked from Simpson and older clastics (Lee, 1956; Amsden and Klapper, 1972; Kuykendall and Fritz, 1993).

The petroleum fields that produce from the Misener Sandstone are represented in depositional trends on both flanks of the McPherson valley. The Misener Sandstone at the Zenith–Peace Creek field in eastern Stafford County is in a north–south-trending channel-like body (Fig. 10), but sheet sands also are a common depositional geometry elsewhere (Ehm, 1965; Wright, 1965; Kuykendall and Fritz, 1993).

Eighty-seven fields in Kansas have a component of

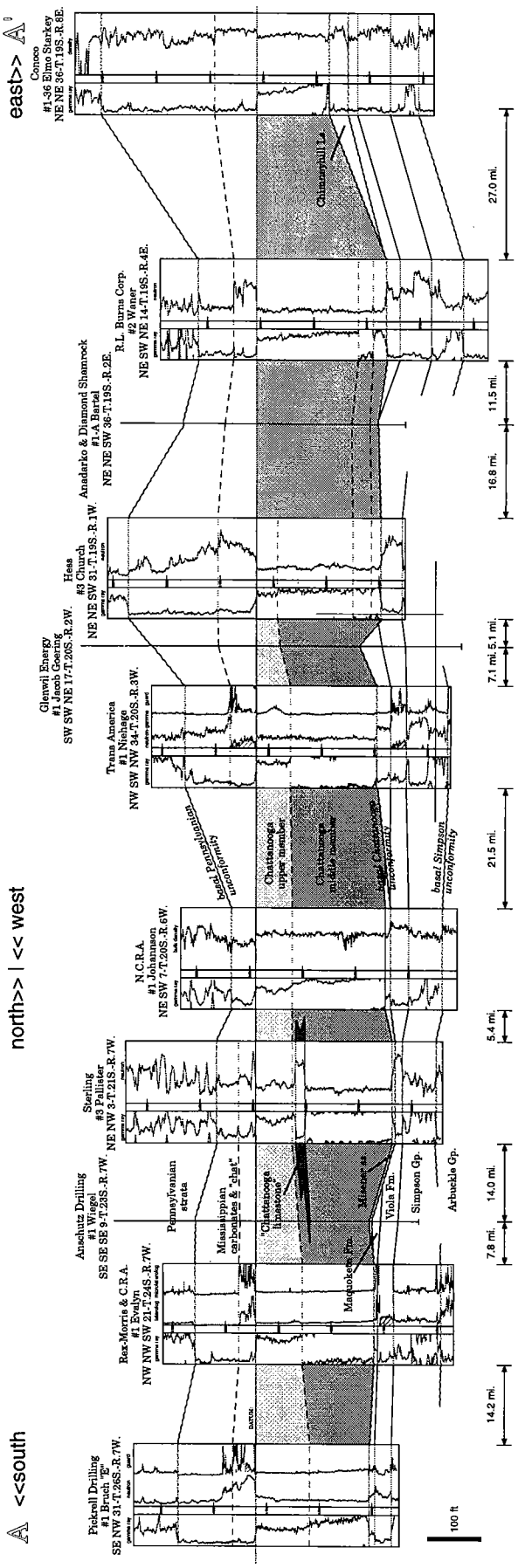

Figure 8. Cross section along the axis of the McPherson valley. Correlations in Lambert (1992b) identify the relatively high gamma-ray-intensity section in the lower part of the Chattanooga as the middle member, whereas the section with the lower gamma-ray levels is the upper member. The lower member is not present in the McPherson valley. Westward and southward (downvalley?) thickening of the upper member of the Chattanooga is evident. Chattanooga limestone is present just below the contact between the middle and upper members. Misener Sandstone, shed off the Ancestral Central Kansas uplift, is locally present near the base of the Chattanooga. See Figure 7 for the location of this cross section. Some electric logs are not shown for space considerations.

their production attributable to the Misener (Kansas Geological Survey and Tertiary Oil Recovery Project, 1991). The Misener at the Zenith–Peace Creek field in Stafford and Reno Counties (Fig. 9), one of the largest of these fields, contained 27–33 million barrels of original oil in place (Newell and others, 1990).

A more detailed look at the Zenith–Peace Creek field affords a perspective by which other Misener fields can be compared. The Misener Sandstone at that locality is up to 32 ft thick (Figs. 9, 10) (Newell and others, 1991). The sandstone is quartzose, well sorted, and locally cross-bedded. Shaly intervals can be intensely burrowed. A shale 2–5 ft thick, which separates the Misener into an upper and a lower bed, is present in some wells. Both sandstone beds produce oil, but the lower bed, which is coarser grained and locally conglomeratic, tends to have better permeability (Fig. 11A). Crinoid and bryozoan fragments near the base of the sandstone and thin planar cross-bedding and burrowing indicate that it is partly marine (Fig. 12). The presence of marine limestones directly above the Misener at the Zenith–Peace Creek field also indicates the establishment of marine conditions soon after sandstone deposition. Hence, the sandstone also may be marine.

The average porosity of the Misener Sandstone at the Zenith–Peace Creek field is 11.5% (Fig. 11C). V_{shale} (the ratio of the gamma-ray measurement of the sandstone to that of 100% shale) indicates that most of the sandstone contains very little shale. In Misener intervals with elevated gamma-ray readings, spectral gamma-ray logs indicate that a significant part of the elevated response is from uranium (Fig. 13). Petrography and laboratory analyses indicate that the uranium is contained in phosphatic grains. Sedimentary phosphates commonly contain elevated levels of uranium. This uranium is typically in insoluble tetravalent form, fixed in phosphatic complexes that formed under reducing conditions (Adams and Weaver, 1958).

Chattanooga Limestone

In the western part of the McPherson valley at least three geographically separate limestone bodies are present in the Chattanooga Shale (Fig. 14). The limestone typically is nonporous and micritic (Lee, 1956; Hilpman, 1967), but oil staining and fluorescence have been noted in cuttings descriptions. The thickest and most extensive limestone body reaches 100 ft in thickness in

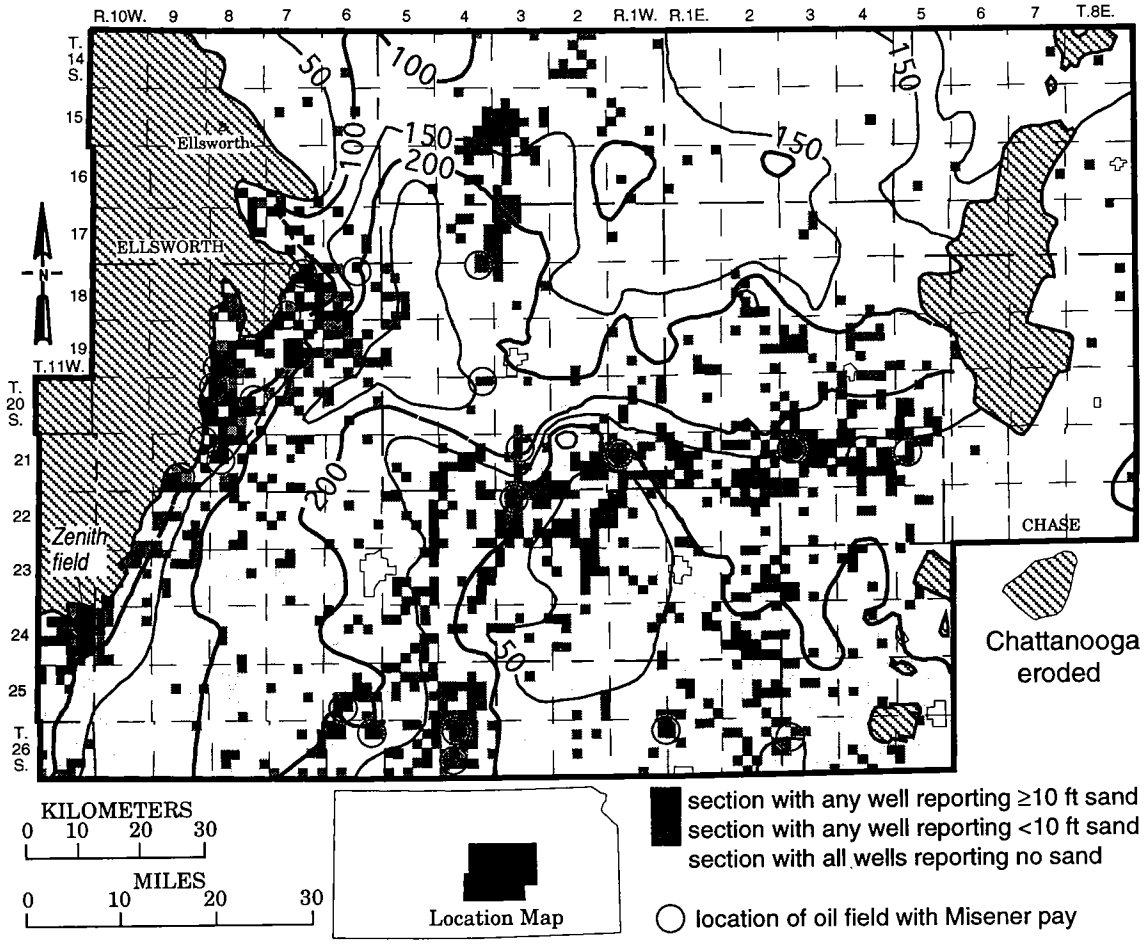

Figure 9. Distribution of Misener Sandstone in the McPherson valley (from Newell, 1989), with the Chattanooga isopachs from Figure 7 superimposed. Locations of 22 oil fields that produce from Misener Sandstone are from the Kansas Geological Survey internet website (Kansas Geological Survey, 1999). Contour interval = 50 ft.

southern Rice County, but it is commonly about 25 ft thick elsewhere. Correlations indicate that deposition of the thickest limestone body preceded that of the northern and southern limestone bodies, but all terminated at approximately the same stratigraphic level—directly below the contact between the middle and upper units of the Chattanooga (Fig. 8).

The deeper water in the western part of the McPherson valley (see Fig. 8) and the micritic nature of the Chattanooga limestone argue that the limestone may be a quiet-water, subtidal type. However, farther west at the Zenith–Peace Creek field (see Fig. 9) on the western flank of the McPherson valley, the "Misener limestone," as the Chattanooga limestone is known there, is coarser grained. On the eastern side of the field, the Chattanooga limestone is mostly a gray, nonporous, fine- to coarse-grained lime packstone, with minor wackestone (Newell and others, 1991). Crossbedding is abundant, and constituent grains are a diversity of skeletal fragments (bryozoans, mollusk fragments, ostracodes, crinoids), pellets, and intraclasts. Subtidal, moderate- to high-energy marine conditions are inferred.

On the western side of the Zenith–Peace Creek field the Chattanooga limestone is a laminated skeletal wackestone (Fig. 15). The presence of fine-grained pelleted carbonate, restricted fauna, very light-gray color, fenestral fabric, mud cracks, and autobrecciation indicates a restricted intertidal to supratidal environment (Newell and others, 1991).

The Zenith–Peace Creek field is possibly the only place where limestones in the Chattanooga produce oil. The best reservoir characteristics in the Chattanooga limestone are present only in the western part of the field, where this unit contains the largest amounts of chert (Fig. 10). Vugular and moldic porosity associated with the chert replacement of the original limestone fabric improves porosity and permeability (Fig. 11A,B), but the coarse-grained bioclastic texture at that locality also is likely a factor in porosity development. Fracture porosity caused by brecciation of the chert also augments total permeability (Newell and others, 1991).

The shallowing of the depositional environment of the Chattanooga limestone at the Zenith–Peace Creek field may have to do with that locality being on an

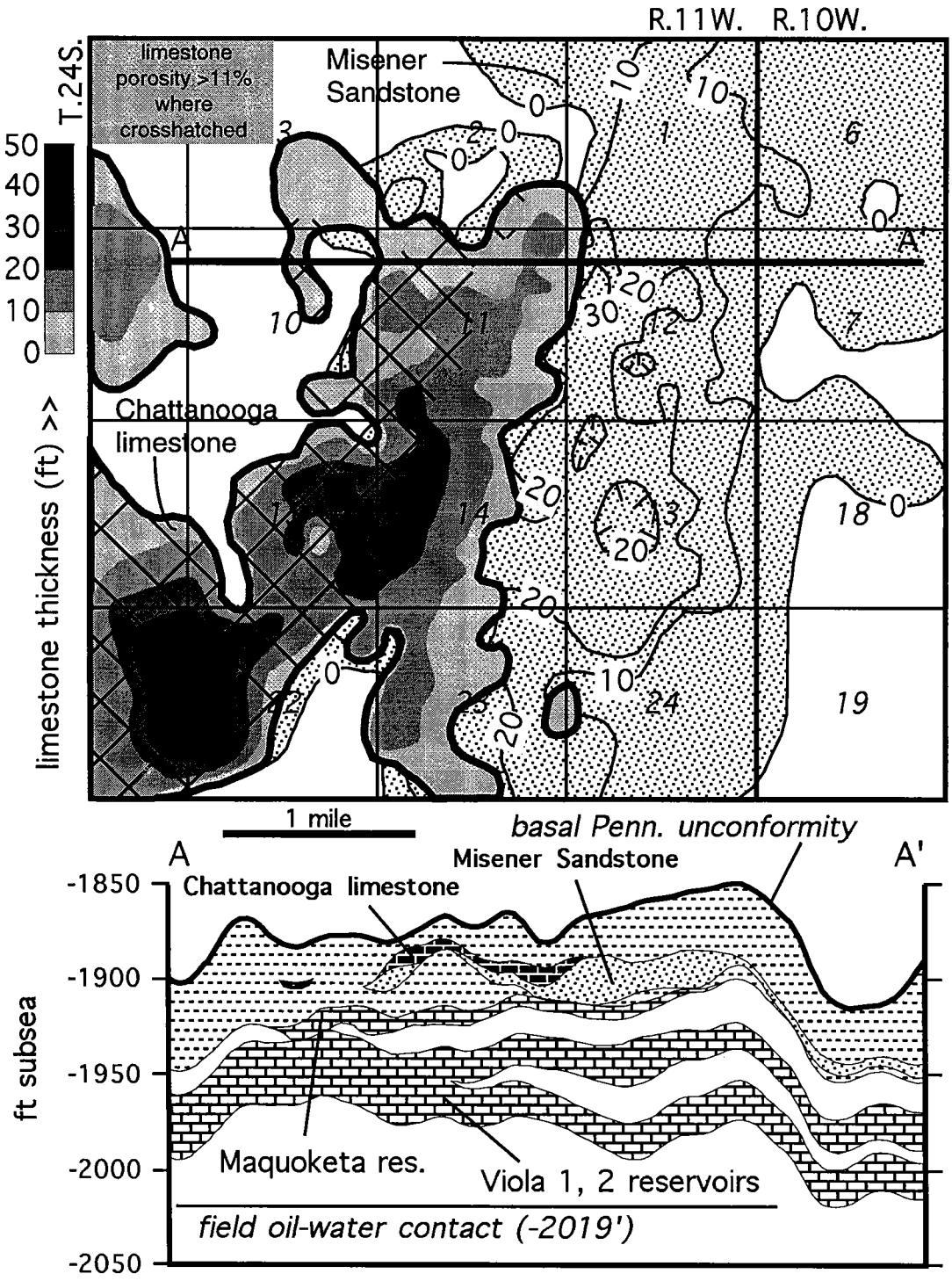

Figure 10. Top diagram shows isopach maps of Misener Sandstone and Chattanooga limestone reservoirs at Zenith–Peace Creek field in central Kansas. Chattanooga limestone is shaded and overlies the Misener Sandstone. Both reservoirs are in north–south-trending geometries. Porosity development in the western side of the Chattanooga limestone is spatially associated with chertification. Location of Zenith–Peace Creek field is shown in Figure 9. Contour interval for both Misener Sandstone and Chattanooga limestone = 10 ft. Bottom diagram is a west–east cross section (see line of section A–A′ on map above).

uplifted block that corresponds to the eastern margin of the present-day Central Kansas uplift. The eastern margin of the uplift also roughly corresponds to where the Chattanooga is eroded in the western part of Ellsworth and Rice Counties, and in northwestern Reno and northern Stafford Counties (see Fig. 7). The margin is relatively linear, owing to the presence of a north-northeast–south-southwest-trending fault zone. The Zenith–Peace Creek area is west of this fault zone, but a thin interval of Chattanooga Shale is preserved

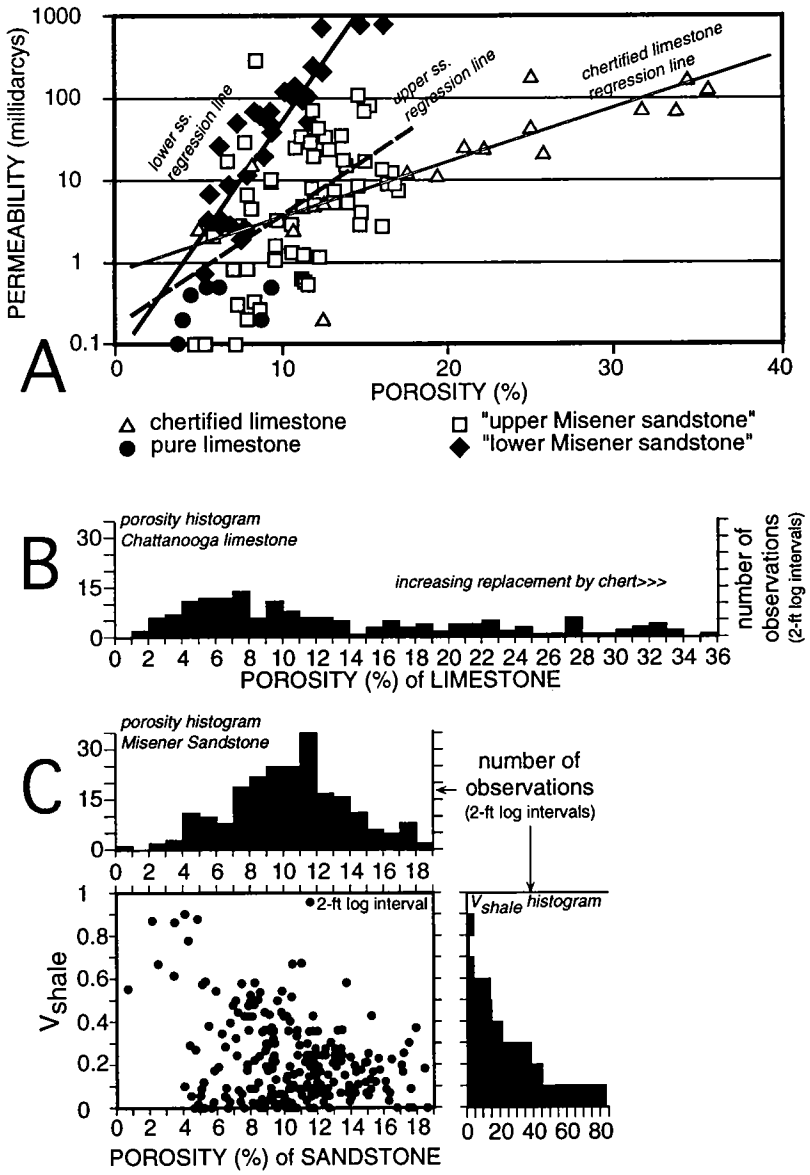

Figure 11. Reservoir characteristics of the Misener Sandstone and Chattanooga limestone at Zenith–Peace Creek field. (A) Core-plug porosity–permeability crossplot (from Newell and others, 1991). (B) Calculated log porosity of the Chattanooga limestone from 23 wells, with porosity data calculated over 2-ft log intervals. (C) V_{shale}-porosity crossplot for the Misener Sandstone. V_{shale} is the ratio of the gamma-ray response of the sandstone to that of the pure Chattanooga Shale. Porosity measurements were over 2-ft log intervals from 49 wells. Density–neutron crossplot porosity calculations, with shale correction, were determined according to equations in Asquith (1982, p. 103). The lower bed of Misener Sandstone generally has better permeability than the upper bed. Perhaps this is attributable to larger pores associated with coarser grain size, and differing cementation. Chattanooga limestone is a poor reservoir, with a modal porosity of 7–8%. Chertification significantly enhances its porosity, but even then its permeability is less than that of sandstones with similar porosity.

at this locality because Zenith–Peace Creek is slightly down the southern flank of the Central Kansas uplift. Nevertheless, because of the shallow-water facies of the Chattanooga limestone at Zenith–Peace Creek, slight up-to-the-west movement at this locality is suggested to have occurred during Chattanooga deposition.

Even though the Chattanooga is no longer present on the Central Kansas uplift, the presence of quiet-water Chattanooga limestones in the McPherson valley parallel to this uplift margin suggests that perhaps shallow-water limestones such as those at the Zenith–Peace Creek field once were present in a trend atop the uplifted block. We speculate that subsequent erosion of the uplift removed these shallow-water carbonates, but the finer grained carbonate muds that were swept off the uplift into the deeper waters of the McPherson valley were preserved.

SUMMARY

1. The McPherson valley developed by erosion over the uplifted Central Kansas arch. The valley is filled with Devonian–Mississippian Chattanooga Shale.

2. The Misener Sandstone, which is the basal sandstone of the Chattanooga, is erratically distributed along two broad, parallel trends along the flanks of the McPherson valley.

3. The Misener Sandstone is thickest where it occurs directly off the Ancestral Central Kansas uplift into the western part of the McPherson valley. Lower Paleozoic siliciclastic strata and Precambrian granitic basement may be the source terranes for quartzose Misener sands.

4. The Misener Sandstone produces from several traps with a stratigraphic component along the flanks of the McPherson valley. Its porosity averages 11.5%.

5. Limestone in the Chattanooga, which occurs in at least three separate stratigraphically correlative bodies at the western end of the McPherson valley, is mostly a nonporous micrite. It probably was deposited in relatively deep water at the western end of the McPherson valley.

6. "Chattanooga limestone" produces at the Zenith–Peace Creek field at the western end of the McPherson valley. Unlike the Chattanooga limestone within the McPherson valley, it seems to be a shallow-water limestone.

7. Chertification improves the reservoir qualities of the Chattanooga limestone at Zenith–Peace Creek field.

8. Spectral gamma-ray logs can aid in determining

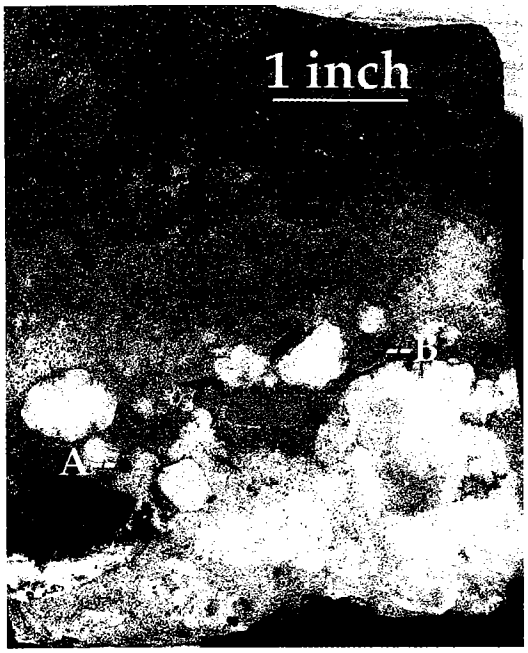

Figure 12. Photograph of core from near the base of the Misener Sandstone in Zenith–Peace field (Braden-Zenith ZU-2, 3,749 ft, NW¼ sec. 7, T. 24 S., R. 10 W.). This sandstone is conglomeratic, containing large clasts of chert that probably are derived from cherty Viola Limestone that subcrops beneath the Chattanooga Shale in this vicinity. Dark grains (*A*) are phosphatic material, which contains uranium that affects the overall gamma-ray response of the Misener. A bryozoan fragment (*B*) indicates a marine depositional environment.

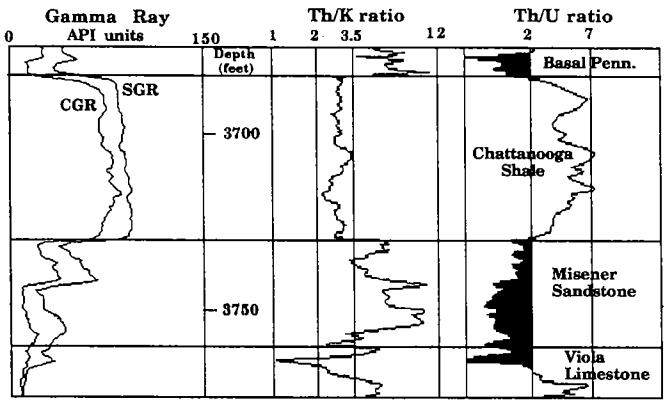

Figure 13. Spectral gamma-ray ratio logs of the Chattanooga section at Zenith–Peace Creek field, from Quinoco ZU-swd1, N½SW¼ sec. 12, T. 24 S., R. 11 W. The uranium within the Misener Sandstone is linked with apatite that occurs in phosphatic grains (see Fig. 12). The shaly nature of the upper sandstone bed is indicated by a slightly higher gamma-ray reading than the lower sandstone bed. Radioactive potassium mostly in the chemical structure of clays contributes to this response. *SGR* = spectral gamma ray; *CGR* = corrected gamma ray.

lithologic and diagenetic influences in the Chattanooga Shale and Misener Sandstone.

9. Distinct spectral gamma-ray signatures are associated with high uranium levels in phosphatic grains in the Misener Sandstone at Zenith–Peace Creek field.

10. A high thorium content at the top of the Chattanooga Shale indicates that intense weathering and exposure occurred before deposition of overlying Mississippian limestones.

ACKNOWLEDGMENTS

The authors would like to thank Daniel Merriam (Kansas Geological Survey), James Schmoker (U.S. Geological Survey), and Brian Cardott (Oklahoma Geological Survey) for reviewing early drafts of this paper. John Charlton at the Kansas Geological Survey is thanked for his help with reproducing photographic illustrations.

REFERENCES CITED

Adams, J. A. S.; and Weaver, C. E., 1958, Thorium to uranium ratios as indications of sedimentary processes—example of concept of geochemical facies: American Association of Petroleum Geologists Bulletin, v. 42, p. 387–430.

Adler, F. J.; Caplan, W. M.; Carlson, M. P.; Goebel, E. D.; Henslee, H. T.; Hicks, I. C.; Larson, T. G.; McCracken, M. H.; Parker, M. C.; Rascoe, Bailey, Jr.; Schramm, M. W., Jr.; and Wells, J. S., 1971, Future petroleum provinces of the Mid-Continent, region 7, *in* Cram, I. H. (ed.), Future petroleum provinces of the United States—their geology and potential: American Association of Petroleum Geologists Memoir 15, p. 985–1120.

Amsden, T. W.; and Klapper, Gilbert, 1972, Misener Sandstone (Middle–Upper Devonian), north-central Oklahoma: American Association of Petroleum Geologists Bulletin, v. 56, p. 2323–2334.

Asquith, G. B.; with Gibson, C. R., 1982, Basic well log analysis for geologists: American Association of Petroleum Geologists, Tulsa, 216 p.

Bunker, B. J.; Witzke, B. J.; Watney, W. L.; and Ludvigson, G. A., 1988, Phanerozoic history of the Midcontinent, United States, *in* Sloss, L. L. (ed.), Sedimentary cover—North American craton, U.S.: Geological Society of America, The Geology of North America, v. D-2, p. 243–260.

Comer, J. B., 1992, Organic geochemistry and paleogeography of Upper Devonian formations in Oklahoma and northwestern Arkansas, *in* Johnson, K. S.; and Cardott, B. J. (eds.), Source rocks in the southern Midcontinent, 1990 symposium: Oklahoma Geological Survey Circular 93, p. 70–93.

Doveton, J. H., 1994, Geologic log interpretation: SEPM (Society for Sedimentary Geology) Short Course 29, 169 p.

Doveton, J. H.; Berendsen, P.; Hoth, P.; and Haug, D., 1994, Log analysis of Paleozoic ironstones in the U.S. Midcontinent—a key to paleogeographic mapping: Transactions of Society of Professional Well Log Analysts, 35th Annual Logging Symposium, Paper ZZ, 17 p.

Ehm, A. E., 1965, Lyons West field, *in* Kansas oil and gas fields, v. 4: Kansas Geological Society, p. 146–156.

Ellison, S. P., Jr., 1950, Subsurface Woodford black shale, West Texas and southeast New Mexico: Texas Bureau of Economic Geology Report of Investigations 7, 17 p.

Freeman, T.; and Schumaker, D., 1969, Qualitative pre-Sylamore (Devonian–Mississippian) physiography delineated by onlapping conodont zones, northern Arkansas: Geological Society of America Bulletin, v. 80, p. 2327–2334.

Goebel, E. D., 1968, Undifferentiated Silurian and Devonian, *in* Zeller, D. E. (ed.), The stratigraphic succession in

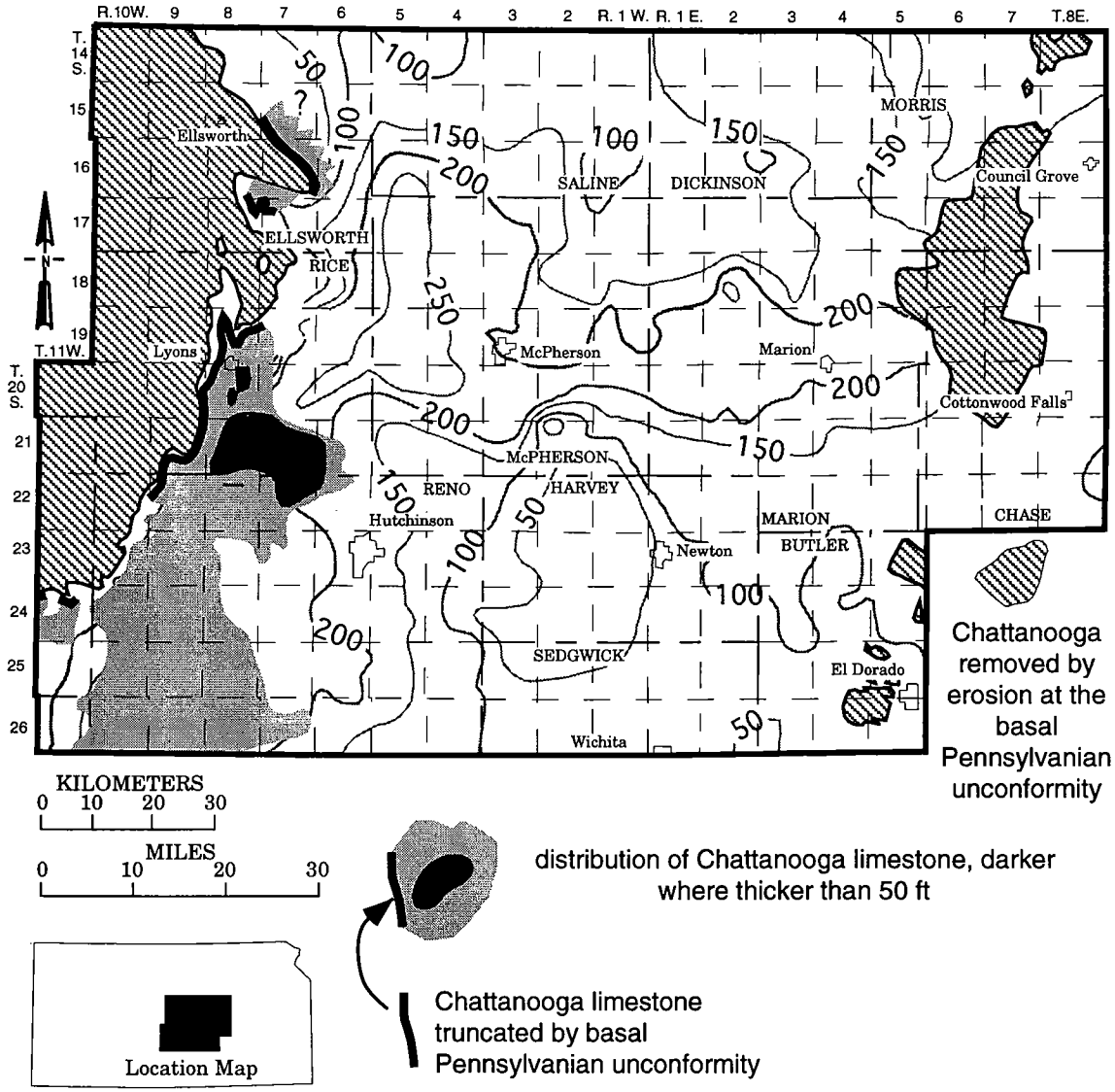

Figure 14. Distribution and thickness of limestone bodies in the Chattanooga Shale. The central and northern limestones are dominantly micritic and are at the western end of the McPherson valley. This part of the McPherson valley may have been characterized by relatively deeper water (see Fig. 8). The southern body, which is productive in Zenith–Peace Creek field, has characteristics of relatively shallow-water deposition. Contour interval for entire Chattanooga Shale = 50 ft. Contour interval for Chattanooga limestone = 50 ft.

Kansas: Kansas Geological Survey Bulletin 189, p. 15–17.

Hester, T.; Schmoker, J.; and Sahl, H., 1990, Log-derived regional source-rock characteristics of the Woodford Shale, Anadarko basin, Oklahoma: U.S. Geological Survey Bulletin 1866-D, 38 p.

Hilpman, P. L., 1967, Devonian stratigraphy in Kansas; a progress report: Tulsa Geological Society Digest, v. 35, p. 88–98.

Kansas Geological Survey, 1999, Production from Kansas oil and gas fields: http://magellan.kgs.ukans.edu/Field/index.html

Kansas Geological Survey and Tertiary Oil Recovery Project, 1991, Zenith field—a field demonstration project for improved efficiency for oil and gas recovery in Kansas: Report submitted to Kansas Corporation Commission, Topeka, 92 p., with appendices.

Kuykendall, M. D.; and Fritz, R. D., 1993, Misener Sandstone—distribution and relationship to late/post-Hunton unconformities, northern shelf, Anadarko basin, *in* Johnson, K. S. (ed.), Hunton Group core workshop and field trip: Oklahoma Geological Survey Special Publication 93-4, p. 117–134.

Lambert, M. W., 1992a, Lithology and geochemistry of shale members within the Devonian–Mississippian Chattanooga (Woodford) Shale, Midcontinent, USA: University of Kansas, Lawrence, unpublished Ph.D. dissertation, 163 p.

_____1992b, Internal stratigraphy of the Chattanooga Shale in Kansas and Oklahoma, *in* Johnson, K. S.; and Cardott, B. J. (eds.), Source rocks in the southern Midcontinent, 1990 symposium: Oklahoma Geological Survey Circular 93, p. 94–105.

_____1993, Internal stratigraphy and organic facies of the Devonian–Mississippian Chattanooga (Woodford) Shale in Oklahoma and Kansas, *in* Katz, B.; and Pratt, L. (eds.), Source rocks in a stratigraphic framework: American

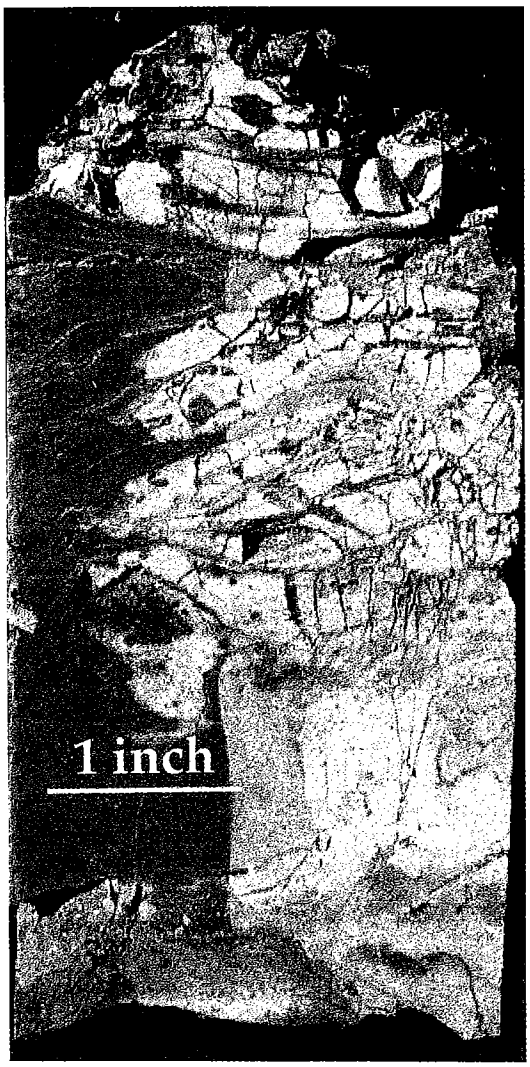

Figure 15. Photograph of core of partly chertified Chattanooga limestone from Zenith–Peace Creek field (Braden-Zenith ZU-1, 3,766 ft, SW¼ sec. 11, T. 24 S., R. 11 W.). Alizarin Red S stain (appearing as gray) on the left side of the core delineates a fine-grained lime wackestone. Fracture porosity in the chertified (white) portion of the core is partly stained by oil.

Association of Petroleum Geologists Studies in Geology 37, p. 163–176.

_____1994, Revised Upper Devonian and Lower Mississippian nomenclature in Kansas, *in* Baars, D. L. (compiler), Revision of stratigraphic nomenclature in Kansas: Kansas Geological Survey Bulletin 230, p. 75–77.

Lee, W., 1956, Stratigraphy and structural development of the Salina basin area: Kansas Geological Survey Bulletin 121, 167 p.

Merriam, D. F., 1963, The geologic history of Kansas: Kansas Geological Survey Bulletin 162, 317 p.

Moore, R. C.; Frye, J. C.; Jewitt, J. M.; Lee, W.; and O'Connor, H. G., 1951, The Kansas rock column: Kansas Geological Survey Bulletin 89, 132 p.

Newell, K. D., 1987, Pre-Chattanooga subcrop map of Salina basin, Kansas: Kansas Geological Survey Open-File Report 87-4 [map], scale 1:500,000.

_____1989, Distribution of Upper Devonian–Lower Mississippian Misener Sandstone in Salina basin, Kansas: Kansas Geological Survey Open-File Report 89-18 [map], scale 1:500,000, with discussion.

Newell, K. D.; Watney, W. L.; Cheng, S. W. L.; and Brownrigg, R. L., 1987, Stratigraphic and spatial distribution of oil and gas production in Kansas: Kansas Geological Survey Subsurface Geology Series 9, 86 p.

Newell, K. D.; Schoeling, L. G.; and Wong, J. C., 1990, PC and mainframe computer-graphics techniques applied to volumetric evaluation of a mature oil field: Society of Petroleum Engineers Computer Applications, November–December, p. 8–14.

Newell, K. D.; Cunningham, K. J.; Wong, J. C.; Watney, W. L.; and Weatherbie, W. J., 1991, Large- and small-scale geological features of the Zenith field and their bearing on planning for enhanced oil recovery operations: Proceedings of 9th Tertiary Oil Recovery Conference, Wichita, Kansas; Tertiary Oil Recovery Project, University of Kansas, p. 99–130.

Reed, E. C., 1946, Boice Shale; new Mississippian subsurface formation in southeastern Nebraska: American Association of Petroleum Geologists Bulletin, v. 30, p. 348–352.

Schlumberger, 1998, Log interpretation charts: Sugar Land, Texas, 87 p.

Sloss, L. L., 1963, Sequences in the cratonic interior of North America: Geological Society of America Bulletin, v. 74, p. 93–114.

Wright, B. J., 1965, Lyons West field, Rice County, Kansas: American Association of Petroleum Geologists Bulletin, v. 49, p. 1562.

Magnetostratigraphic Susceptibility of the Frasnian–Famennian Boundary (Upper Devonian) in Southern Oklahoma and Its Relationship to the Type Area in Southern France

Rex E. Crick
The University of Texas at Arlington
Arlington, Texas

Brooks B. Ellwood
Louisiana State University
Baton Rouge, Louisiana

D. Jeffrey Over
SUNY College at Geneseo
Geneseo, New York

Raimund Feist
Université de Montpellier II
Montpellier Cedex, France

Catherine Girard
Université Claude Bernard-Lyon I
Villeurbanne Cedex, France

ABSTRACT.—A magnetosusceptibility event and cyclostratigraphy (MSEC) method is used to establish a nonpolarity-based magnetostratigraphic susceptibility (MSS) between the stratotype region for the Frasnian–Famennian (F–F) boundary sequence in the Montagne Noire of southern France and two F–F sequences in the Arbuckle Mountains and Criner Hills of southern Oklahoma. Despite differences in depositional environment, the MSS is remarkably consistent and can be described in the context of a hierarchy of magnetozones that allow extension of correlation away from the Montagne Noire reference section. The nature of the controls on the influx of iron into the marine system produces a natural hierarchy of at least seven orders or magnetozones designated MSZ1, MSZ2, MSZ3, MSZ4, MSZ5, MSZ6, and MSZ7. These are characterized in terms of the magnitude of their duration.

The MSS reference section of choice for the F–F boundary is the well-known Trench C at La Serre (LSC) in the northeastern Montagne Noire of southern France. The F–F boundary lies at the base of MSZ La Serre $I\alpha 3_b$ at La Serre, and magnetozones MSZ4 and MSZ5 at LSC are used to establish correlation between France and Oklahoma and to establish the position of the F–F boundary in the Oklahoma sections.

INTRODUCTION

The purpose of this paper is to present the magnetostratigraphic-susceptibility (MSS) record for three Frasnian-Famennian (F–F) boundary sequences deposited on the Devonian landmasses of Gondwana and Euramerica (Fig. 1). We have chosen the boundary sequence of Trench C at La Serre (LSC) in the northeastern Montagne Noire (Fig. 2A) as the reference section for comparison with the Oklahoma sections (Fig. 2B). In establishing a magnetic-susceptibility (MS) record indicative of a global boundary stratotype section and point (GSSP), the sequence at LSC has the advantages of having been deposited in a basinal setting where the chance of major interruptions in sediment accumulation are less, having been a candidate for the F–F GSSP and thus an agreed-upon stable biostratigraphy, and having been close to the GSSP. Probably the best candidate for a reference section on the basis of the extent of sediment deposited per unit of time from the latest Frasnian through the earliest

Crick, R. E.; Ellwood, B. B.; Over, D. J.; Feist, Raimund; and Girard, Catherine, 2001, Magnetostratigraphic susceptibility of the Frasnian–Famennian boundary (Upper Devonian) in southern Oklahoma and its relationship to the type area in southern France, *in* Johnson, K. S. (ed.), Silurian, Devonian, and Mississippian geology and petroleum in the southern Midcontinent, 1999 symposium: Oklahoma Geological Survey Circular 105, p. 71–82.

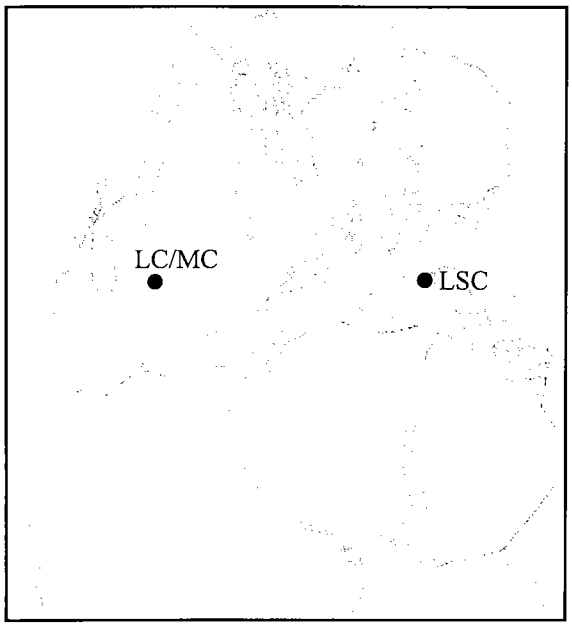

Figure 1. Paleogeographic map at the time of the Frasnian–Famennian boundary (~376.5 Ma). *LC,* Lake Classen spillway, northern Arbuckle Mountains, southern Oklahoma; *MC,* McAlister Cemetery, Criner Hills, southern Oklahoma; *LSC,* Cabrières area of the Montagne Noire, southern France. Reconstruction from the PaleoMap Program, courtesy of C. Scotese, University of Texas at Arlington.

Famennian is the Lake Classen spillway exposure of the Woodford Shale in the Arbuckle Mountains of southern Oklahoma. Unfortunately, the absence of carbonate throughout the sequence makes the extraction and identification of pelagic fossils difficult for some groups and impossible for others. For reasons of uncertainty regarding the future choice of an MSS magnetostratotype for the F–F boundary, we offer the named and defined magnetozones at LSC as a convenient method for demonstrating the correlative power of MSS among sequences of various paleogeographic, tectonic, and environmental settings.

MSEC

We have been using MS data in developing a method for high-resolution, global correlation of sedimentary strata, and call the method MSEC, which stands for magnetosusceptibility event and cyclostratigraphy (Crick and others, 1997; Crick and others, 2000a,b; Ellwood and others, 1999, 2000). MSEC is not affected adversely by the drawbacks of magnetostratigraphic-polarity (MSP) methods, such as remagnetization, required orientation of samples, corrections for structural complexity, field tests for a stable remanence (such as fold or reversal tests), or relatively large sample sizes. When high-density data sets are used, MSEC typically provides better resolution than the associated biostratigraphy upon which it is dependent for temporal control. MS also has the important advantage of being measurable in the field, helping geologists to resolve ambiguities while at the outcrop. Besides its many other qualities, MS has the additional advantage of being quickly and easily measured on small samples using a device such as a balanced coil induction system—a susceptibility bridge. Mass rather than volume MS makes it possible to quickly, and with high precision, measure small, irregular lithic fragments and highly friable material, and to sample downhole cores, cuttings, and assorted field collections. Thus the wealth of lithic material in university and industrial collections that has been utilized for biostratigraphic studies is amenable to MS measurement. This makes it possible to rapidly and efficiently develop MSEC data that can be tied directly to existing mature biozonations.

It has been demonstrated that the MS signature in marine rocks resides mainly in paramagnetic and/or other detrital constituents contained in these rocks (Ellwood and others, 2000). The MSEC record that these detrital grains exhibit is found in two forms. The first is a short-term, low-magnitude, high-frequency "cyclic" climate signature linked to orbital forcing cycles, which is often used for regional correlation (Crick and others, 1997, 2000a; Ellwood and others, 2000; Shackleton, 1999). The second form is a longer term, higher magnitude, low-frequency "event" signature resulting from global transgression and regression or from special circumstances such as extraterrestrial impacts. It is these events that can be used for global correlation when applying the MSEC method. In all sections that we have examined, the short-term cyclic MSEC component is superimposed on the longer term events (Ellwood and others, 2000). When comparisons are made between stratigraphic sections for which MS and biostratigraphic measurements have been compiled, MSEC events can be correlated between sections, while local, within-basin effects are also easily identified (Crick and others, 1997; Ellwood and others, 1999).

In order to effectively use MSEC data for between-section comparisons, several sampling constraints must be placed on data sets. First, only well-exposed and stratigraphically continuous sections should be used. Here, the reference or standard sections we have sampled are not "covered" but either are exposed naturally or the interval of interest is excavated and cleaned by us. Therefore, for development of MSEC standards, we choose sections that have segments that are only slightly covered over short intervals, and these can then be easily cleaned with a pick, shovel, and brush. Second, sections must be chosen that have adequate biostratigraphic control. Third, the method requires high-density sample sets. In the sections presented here, we have collected samples at intervals of 1.0, 2.5, and 5 cm, depending on perceived rates of sediment accumulation. This sampling density largely reduces the effect of minor hiatuses, while it also serves to expose their presence through documentation of large and unexpected shifts in MS magnitude.

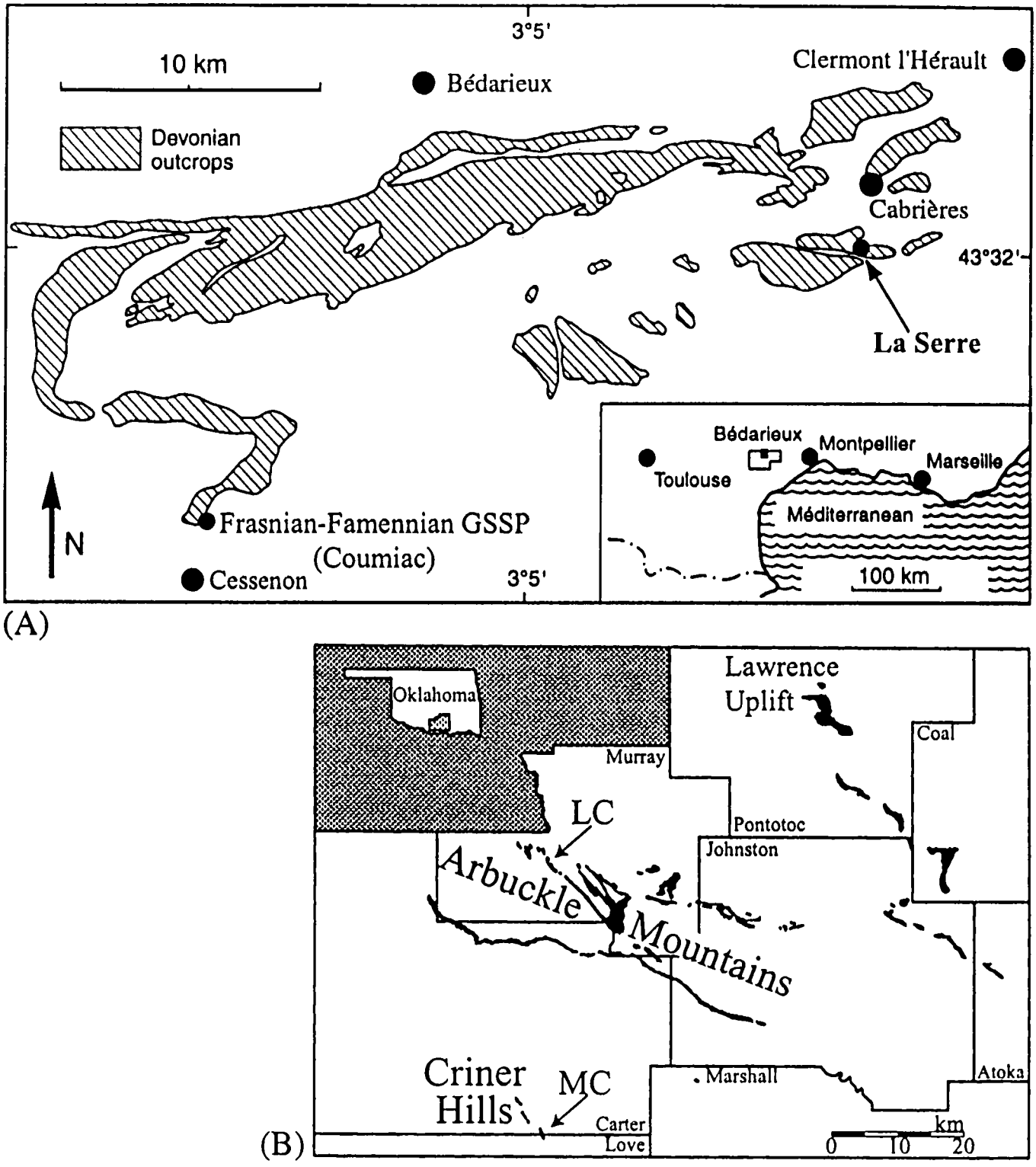

Figure 2. Location maps. (A) Montagne Noire, southern France, with major areas labeled. La Serre is the location of the LSC reference sequence. Frasnian–Famennian GSSP is the location of the official boundary stratotype. (B) Devonian outcrop map of southern Oklahoma, including Arbuckle Mountains and Criner Hills. *LC,* Lake Classen spillway; *MC,* McAlister Cemetery. Modified from Over (1992).

The primary controls on MSEC signatures in marine rocks are sea-level (base-level) changes and climate. These MSEC signatures can result from (1) global sea-level fluctuations that cause base-level changes and therefore corresponding changes in detrital influx into the world oceans from erosion, (2) changes in global climate and rainfall/erosion rates, (3) local small-scale tectonic effects, or (4) impact-related ef-

fects. During times of sea-level regression, base level is lowered, and increased erosion brings an increased detrital component into the marine system, primarily from rivers. This material is then dispersed by bottom currents throughout ocean basins (Sachs and Ellwood, 1988), with the result that MS magnitudes rise. Locally, sections sampled that were deposited near the mouths of ancient river systems will have elevated MS values from sections far removed from rivers, but while the MS magnitudes may be different, the variations (trends) resulting from erosional events will be identifiable in all sections. If the event is global, then the MS effects will be global. In the case of transgression, MS magnitudes are reduced as a result of the rise in base level.

Climate has two effects on MSEC data sets. First, changes in rainfall associated with variations in climate result in high MS magnitudes during periods of high rainfall and therefore increased continental erosion, whereas lower rainfall results in lower erosion rates and reduced MS magnitudes. Second, glacial advances and associated base-level changes, resulting from larger amounts of water being tied up in ice, produce increased erosion and higher MS magnitudes. A third effect, erosion by glaciers, also produces an increase in detrital input into the marine system. Erosion by glaciers causing elevated MS values from detrital input into the South Atlantic Ocean can be seen today coming from glacial erosion of Antarctica and dispersal of this material northward into ocean basins by bottom currents (Sachs and Ellwood, 1988).

High-density data sets provide a large number of samples whereby overall MSEC trends can be identified. Such data sets allow long-term trends or events to dominate over single, essentially instantaneous sediment influxes, like those associated with storms. MSEC trends must be characterized by multiple data points to define MS data that result from long-term geological processes. Because these data are the result of long-term trends, this yields low-frequency, as opposed to high-frequency, variability in MS data sets.

Correlation between sections on a global basis is extremely difficult, and few robust methods exist to solve the problem. MSEC in the form of MSS is one of these. We argue that, like its polarity counterpart MSP (Remane and others, 1996), MSS should be given equal standing alongside MSP and biostratigraphy as a factor in the definition or redefinition of GSSPs.

Shackelton (1999) recently argued that in order for non-biostratigraphic, geochemical stratigraphic methods, primarily oxygen isotopic data, to be useful for global-correlation purposes, such data sets should be formally tied to GSSPs. We agree and for 10 years have been developing the MSEC method and an MSEC data set that is tied to Devonian stage-boundary GSSPs. It has become clear from this work that high-resolution, high-density data sets are required to identify adequately the MSEC character of the marine sections we have examined. Therefore, our data set now includes more than 50 continuously sampled sections collected at 1.0-, 2.5-, 5-, and 10-cm intervals. One section is ~270 m long and has yielded >2,700 samples.

MAGNETIC SUSCEPTIBILITY (MS)

All materials are susceptible to becoming magnetized when placed in a magnetic field, and MS is an indicator of the strength of this induced magnetism within a sample. This characteristic is very different from remanent magnetism, the intrinsic permanent magnetization that accounts for the magnetic polarity of materials. MS can be quickly and easily measured on small samples and is largely a function of the concentration of the magnetizable material they contain. Magnetizable materials in marine sedimentary sequences include not only the ferrimagnetic minerals that may acquire a remanence (required for MSP) but also any other mineral containing an odd number of electrons. These less magnetic, or paramagnetic, substances include clay minerals, ferromagnesian silicates such as biotite, iron sulfides such as pyrite, and other materials. Even though these paramagnetic constituents exhibit a very low MS, when relatively abundant they dominate the measured MS in limestones, marls, and shales (Ellwood and others, 2000). In addition, although magnetite grains are present in small amounts in the samples studied here, we have demonstrated by our work in Morocco that they do not dominate the MS in most samples (Ellwood and others, 2000). Calcite and/or quartz may also be abundant in marine limestones and shales. However, the MS of paramagnetic minerals is much greater than the MS of diamagnetic minerals, and therefore a small amount of a paramagnetic mineral can significantly outweigh the MS of volumetrically more abundant diamagnetic minerals. See Crick and others (2000a, b) and Ellwood and others (2000) for additional details.

MAGNETOSTRATIGRAPHIC SUSCEPTIBILITY (MSS)

MSS is the integration of MS and the biostratigraphy of marine sedimentary sequences into magnetozones. Like the better known MSP units, MSS units are rock units unified by similar magnetic characteristics (exclusive of magnetic polarity) that allow them to be differentiated from adjacent rock bodies (Salvador, 1994). The unifying characteristic of MSS units is the detrital grains, such as biotite or tourmaline, contained within the lithogenic component of marine sediments that are susceptible to acquiring an induced magnetization. Most of the MS variations are due to the influx of weathered terrigenous paramagnetic grains. Magnetite is usually responsible for a component of the signal as either detrital grains or in some instances as very fine grained biomagnetite.

The basic formal unit in MSS classification is the MSZ. On the basis of our studies of Silurian and De-

vonian sequences, Pleistocene and Holocene sequences (Ellwood and others, 2001), an excellent Devonian chronology (Tucker and others, 1998), and work in progress with sequence stratigraphers, magnetozones can be classified in a hierarchical arrangement of magnetozones of the first through seventh orders (Fig. 3). The first- through third-order magnetozones (MSZ1, MSZ2, and MSZ3) represent MSEC event-scale effects driven by base-level changes and are somewhat analogous to those observed by sequence stratigraphers, whereas the fourth- through seventh-order magnetozones (MSZ4, MSZ5, MSZ6, and MSZ7) were controlled by climate (where the scale is as follows: first order >100 Ma, second order >10 Ma, third order >1 Ma, fourth order >100,000 years, fifth order >10,000 years, sixth order >1,000 years, and seventh order >100 years). The lettering and numbering system used to identify the magnetozones is given in Figure 3.

The definition and recognition of an MSS unit should be based on a designated stratotype of the type used in the definition of a GSSP. This criterion provides a definite relationship between a known stratigraphic section and a mature biostratigraphic record as well as a reference section from which MSS units can be extended geographically. A standard requirement for defining the stratotype of an MSS unit is the inclusion of a *lower-boundary stratotype* and an *upper-boundary stratotype*. In the likely event of a gradual transition between two MSZs of the same rank, it is necessary to select an arbitrary boundary within the transition (Salvador, 1994). Because a transition commonly occurs within a lithologic unit, it is helpful to identify MSS boundary stratotypes at the time of unit definition. Magnetozones defined in this paper have boundaries picked at midpoints along such transition trends. Following the practice of defining biostratigraphic zones, the base (lower-boundary stratotype) of an MSZ defines the top (upper-boundary stratotype) of the preceding MSZ.

The naming of MSS units follows the general rules for naming stratigraphic units (Salvador, 1994, section 3.B.3). In the context of MSS, we have designated formal names for MSZ1s inclusive of bodies of rock with characteristics of either high or low magnitudes of MS that permit the units to be differentiated from adjacent rocks. The formal names for MSZ1 magnetozones introduced here are taken from local geographic features. We estimate that the ~3-m sequence represented here from the La Serre Trench C locality accumulated in less than 1 million years. Therefore, the magnetozones represented in the MSEC data are probably fourth- and fifth-order magnetozones (MSZ4 and MSZ5, respectively).

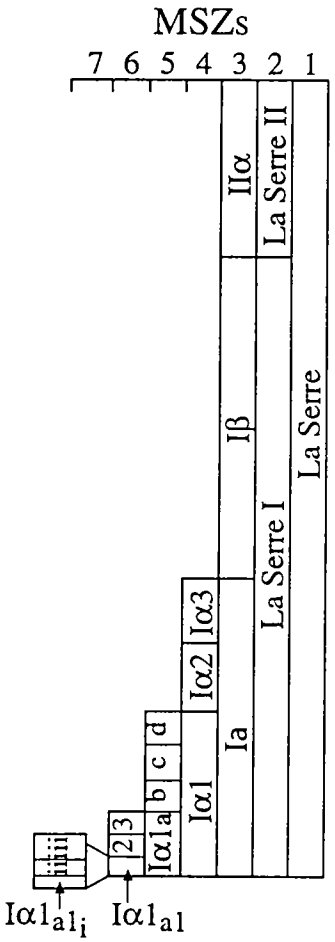

Figure 3. Hierarchy of MSS magnetozones. The seven orders of magnetozones (MSZs) are arranged from right to left and numbered accordingly at the top of the diagram.

MSS OF THE FRASNIAN–FAMENNIAN BOUNDARY

La Serre Trench C (Southern France)

Unmetamorphosed, highly fossiliferous Upper Devonian strata crop out for 40 km in a northeast–southwest trend across the southeastern part of the Montagne Noire of southern France (Fig. 2A). Excellent outcrop exposure and stratigraphic control have permitted the definition of three GSSPs in the Montagne Noire: Givetian–Frasnian (Middle–Upper Devonian) boundary (Klapper and others, 1987), F–F boundary (Klapper and others, 1993), and Famennian–Tournaisian (Devonian–Carboniferous) boundary (Paproth and others, 1991). The Upper Devonian succession consists, almost exclusively, of pelagic to hemipelagic facies deposited either on well-oxygenated submarine rises or in small intervening basins during the period when the region was part of the northern margin of Gondwana (Feist and others, 1994). The submarine rises are characterized by calcilutite sedimentation, and the basins are characterized by mudstones developed under reducing conditions (Feist and Klapper, 1985).

Early Late Devonian sequences in the Cabrières area, approximately 30 km northeast of the F–F GSSP at Coumiac, are characteristic of an oxygen-deficient offshore basinal environment. The well-known Trench C section at La Serre (LSC) was chosen to represent the MSEC signature for the region and to serve as the

MSS reference section for the F–F boundary (Fig. 4). Like other sections in this facies, the LSC sequence is considered to represent a distal and basinal time equivalent of the submarine-rise sections. LSC strata begin with Upper Frasnian light gray pyritic wacke- and mudstones rich in pelagic biota. These strata are succeeded by a latest Frasnian sequence consisting of alternating dark brown to black, fissile bituminous argillites and platy, thinly bedded bituminous limestones lacking benthic biota. Unlike the submarine-rise sections, the LSC sequence shows no physical evidence of condensed sedimentation, gaps, or discontinuities. The rate of sediment accumulation at LSC appears to have been constant, as evidenced by the undisturbed and finely laminated character of sediments throughout the section. The LSC sequence was fully described in several publications (Becker and House, 1994; Feist and others, 1990; Girard and Feist, 1996; Paris and others, 1996).

The MSS at La Serre is based on 83 samples over 2.35 m of section, beginning with the upper *Pa. rhenana* Zone and continuing into the middle *Pa. triangularis* Zone (Fig. 4). The stratigraphic position of samples is shown on the curve by black dots. We interpret the data to indicate the presence of six MSZ4 magnetozones. These are well defined in the upper part of the data set. From the base of the sequence to a height of approximately 0.8 m, the data are somewhat "noisy," and here we provisionally identify two MSZ5 magnetozones that make up the basal MSZ4

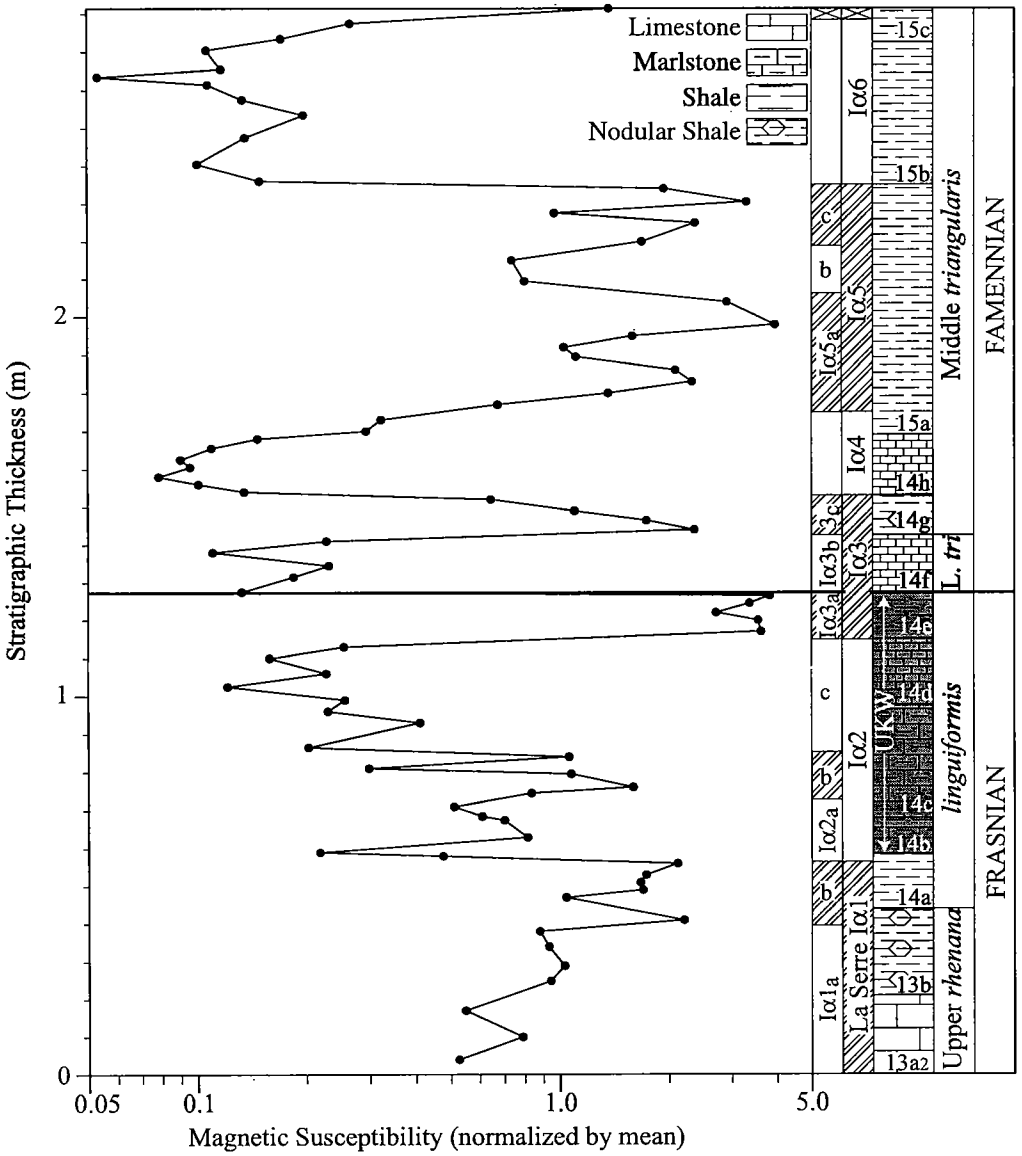

Figure 4. MSS for the F–F-boundary reference sequence at Trench C at La Serre (LSC) in the eastern Montagne Noire of southern France. Magnetozones MSZ4 and MSZ5 are illustrated. Descriptions of the MSZs are given in the text. Unit designations and biozone boundaries are those of Feist and others (1990) and of Girard and Feist (1996). The ordinate is stratigraphic thickness in meters, and the abscissa represents units of MS magnitude normalized by the mean 2.59×10^{-8}. Data were splined slightly to reduce high-frequency variations. Interval for Upper Kellwasser event (UKW) is shaded.

magnetozone. La Serre Iα2, Iα3, and Iα5 can be subdivided into MSZ5s, whereas La Serre Iα4 and Iα6 cannot. We suspect that additional sampling at closer intervals will result in further subdivision of these latter magnetozones. The La Serre boundary sequence is too brief to allow documentation of magnetozones MSZ1, MSZ2, and MSZ3. The presence of these magnetozones is evident in the hierarchy of magnetozones.

The MSS record begins in the *Pa. rhenana* Zone and continues for 2.35 m into the middle *Pa. triangularis* Zone (Fig. 4). Variations in lithology impart a degree of variability to the MSS, but, for the most part, changes in the pattern of high and low magnitudes occur independently of lithology. It is this fact that makes the MSS record diagnostic of the boundary sequence and predictable among coeval boundary sequences. Details relating to the use of MSS in this context are given in Crick and others (2000a,b).

La Serre Iα1

The base of La Serre Iα1 may not be exposed at LSC. La Serre Iα1 is fully documented in the Lake Classen (LC) section, where the base of the MSZ is designated at the midpoint of the transition from the zone of low susceptibility of the preceding MSZ4, which we have elected not to name at this time. The details of the MS are such that we can only describe two MSZ5 magnetozones, although we suspect that the five MSZ5 magnetozones documented in the LC and McAlister Cemetery (MC) sections are present in the LSC sequence. Etymology: the name of the hill 2.4 km south of Cabrières (Fig. 2A). Biostratigraphic equivalent: upper *Pa. rhenana* through lowermost *Pa. linguiformis* Zones.

La Serre Iα1 represents a stratigraphic interval during which MS magnitudes were moderately high for the sequence. Superimposed on the MS record are at least two MSZ5s.

La Serre Iα1$_a$.—This MSZ5 begins somewhere below that part of exposed bed 13a$_2$ available to us. The MSZ extends into the upper part of bed 13b, and the extent of this MSZ should be treated as provisional until we can increase the sampling density over this interval. Biostratigraphic equivalent: upper *Pa. rhenana* Zone.

La Serre Iα1$_b$.—La Serre Iα1$_b$ begins in upper bed 13b and extends to upper bed 14a. The magnetozone contains the highest magnitude peak in the MSZ4. Biostratigraphic equivalent: latest *Pa. rhenana* Zone and early *Pa. linguiformis* Zone.

La Serre Iα2

The base of La Serre Iα2 is designated at the midpoint of the transition from the interval of high susceptibility defined by La Serre Iα1 to the interval of low susceptibility that characterizes this magnetozone (Fig. 4). The transition is within the upper part of bed 14a, and La Serre Iα2 extends to the base of bed 14e. The magnetozone represents a stratigraphic interval during which MS magnitudes were some of the lowest for the LSC sequence. La Serre Iα2 contains three MSZ5s. Biostratigraphic equivalent: early to late *Pa. linguiformis* Zone.

La Serre Iα2$_a$.—The initial MSZ5 describes a sharp decrease in MS magnitude that begins in uppermost bed 14a and continues into lower bed 14c. The base of the Upper Kellwasser event (UKW) is recorded in lower La Serre Iα2$_a$. Biostratigraphic equivalent: lower *Pa. linguiformis* Zone.

La Serre Iα2$_b$.—The base of La Serre Iα2$_b$ is in lower bed 14c, and this MSZ5 extends to the middle of bed 14c. The MSZ represents an interval of high magnitude. Biostratigraphic equivalent: lower *Pa. linguiformis* Zone.

La Serre Iα2$_c$.—The final MSZ5 for La Serre Iα2 has its base near the middle of bed 14c, and it extends to the base of bed 14e. La Serre Iα2$_c$ defines a low-magnitude peak of the longest duration for the Frasnian portion of the boundary sequence. Biostratigraphic equivalent: middle to late *Pa. linguiformis* Zone.

La Serre Iα3

La Serre Iα3 is the boundary magnetozone (Fig. 4). It includes all of bed 14e, the last Frasnian unit, and beds 14f and 14g of the earliest Famennian. The transition from La Serre Iα2 to La Serre Iα3 is represented by more than an order-of-magnitude increase in MS between the last sample in 14d and the first sample in 14e. The change represents either the need for higher density sampling over the interval because of an increase in condensation or a hiatus in sediment accumulation. The magnetozone represents a stratigraphic interval during which MS magnitudes were some of the highest and most variable for the boundary sequence at LSC. The variability in MS defines three MSZ5s for La Serre Iα3. Biostratigraphic equivalent: upper *Pa. linguiformis* Zone, lower *Pa. triangularis* Zone, and earliest middle *Pa. triangularis* Zone.

La Serre Iα3$_a$.—The base of La Serre Iα3$_a$ coincides with the base of 14e, where it is defined by more than an order-of-magnitude increase in MS between the last sample in 14d and the first sample in 14e. The magnetozone represents an interval of sustained high MS magnitude that extends to the base of bed 14f and the base of the Famennian. Biostratigraphic equivalent: latest *Pa. linguiformis* Zone.

La Serre Iα3$_b$.—The base of La Serre Iα3$_b$ defines the base of the Famennian in the Montagne Noire region. The transition between La Serre Iα3$_a$ and Iα3$_b$ includes more than an order-of-magnitude decrease in MS between the last sample in 14e and the first sample in 14f. The magnetozone extends to the base of bed 14g, represents the low-magnitude interval for La Serre Iα3, and contains the entire lower *Pa. triangularis* Zone. Biostratigraphic equivalent: lower *Pa. triangularis* Zone.

La Serre Iα3$_c$.—The high-magnitude interval defined as La Serre Iα3$_c$ begins at the base of 14g with nearly an order-of-magnitude increase in MS between the last sample in 14f and the first sample in 14g and extends to the base of bed 14h. Biostratigraphic equivalent: early middle *Pa. triangularis* Zone.

La Serre Iα4

La Serre Iα4 is an interval of very low MS magnitudes with essentially no variability at our scale of sampling (Fig. 4). It includes all of bed 14h and the lowermost part of bed 15a. The transition from La Serre Iα3 to La Serre Iα4 is part of an orderly and continual decrease in MS magnitudes that begin in the middle of bed 14g and end in the middle of bed 14h. The magnetozone represents a stratigraphic interval during which MS magnitudes were some of the lowest and least variable for the boundary sequence. The lack of MS variability precludes the definition of MSZ5 magnetozones. Biostratigraphic equivalent: early middle *Pa. triangularis* Zone.

La Serre Iα5

The base of La Serre Iα5 is designated at the midpoint of the transition that begins in the upper part of limestone bed 14h and ends in the lower part of shale bed 15a. The midpoint along the transition occurs between the second and third samples above the base of 15a. La Serre Iα5 extends to the base of bed 15b and represents a sustained interval of high MS magnitude with sufficient variability to allow the definition of three MSZ5 magnetozones. Biostratigraphic equivalent: lower middle *Pa. triangularis* Zone.

La Serre Iα5$_a$.—The high-magnitude interval defined as La Serre Iα5$_a$ begins in the lowermost part of bed 15a and extends to the middle of that bed. This MSZ5 accounts for roughly half of La Serre Iα5 and is characterized by containing the peak of highest magnitude for the LSC boundary sequence. Biostratigraphic equivalent: middle *Pa. triangularis* Zone.

La Serre Iα5$_b$.—The base of La Serre Iα5$_b$ is near the middle of bed 15a, and the magnetozone extends into the upper one-third of bed 15a. La Serre Iα5$_b$ represents an interval of low MS magnitudes superimposed on the general high magnitudes of La Serre Iα5. Biostratigraphic equivalent: middle *Pa. triangularis* Zone.

La Serre Iα5$_c$.—La Serre Iα5$_c$ begins in the upper one-third of bed 15a and extends to the base of bed 15b, also a shale unit. The magnetozone represents an interval of high MS magnitudes. Biostratigraphic equivalent: middle *Pa. triangularis* Zone.

La Serre Iα6

The base of La Serre Iα6 is designated at the midpoint of the transition from the interval of high MS defined by La Serre Iα5 to the interval of low MS defined here as the Iα6 (Fig. 4). The transition begins near the top of bed 15a and ends in lowermost bed 15b. The midpoint along the transition occurs between the last sample in bed 15a and the first sample in bed 15b. The transition zone for the base is marked by more than an order-of-magnitude decrease in MS between the last samples in 15a and the first samples in 15b. La Serre Iα6 extends into bed 15c and represents a sustained interval of low-MS magnitudes for the GSSP sequence. The MS record suggests that the whole of the magnetozone is represented, but this cannot be determined without additional sampling. The MS variability is not sufficient to attempt to document MSZ5s. Biostratigraphic equivalent: middle *Pa. triangularis* Zone.

U.S.A. (Arbuckle Mountains, Southern Oklahoma)

The gently overturned anticline that makes up the Arbuckle Mountains offers the best and most continuous exposures of marine Devonian rocks in the southern Midcontinent of the United States. It is, however, far from complete, with unconformities of at least regional extent between Pridolian–Lochkovian carbonates, between Lochkovian–Pragian carbonates, and the most pronounced between various formations of the Early Devonian Hunton Group and the Late Devonian Woodford Shale, where there is no evidence of the Emsian, Eifelian, Givetian, and various parts of the Lower Frasnian. The remaining Frasnian, all of the Famennian, and the lower part of the Tournaisian (up to and including the upper *Si. duplicata* Zone) are represented by roughly 90 m of the Woodford Shale. The Woodford is part of the widespread Upper Devonian and Lower Carboniferous black-shale deposition in the United States and is the western equivalent of the widespread Chattanooga Shale. The early conodont zonation established by Hass and Huddle (1965) was modernized and very much expanded by Over (1990, 1992) and Over and Barrick (1990). Notwithstanding these efforts, the position of the F–F boundary could not be placed with certainty within a 2-m interval. As part of this study, Over and his students undertook a bed-by-bed search for the base of the *Pa. triangularis* Zone and found the lowest occurrence to be 16.15 m above the base of the Woodford in the spillway at Lake Classen (LC); but they were unable to recover *Pa. triangularis* from the McAlister Cemetery (MC) locality. Neither the Lower Kellwasser event (LKW) nor the Upper Kellwasser event (UKW) has been identified in the Woodford. The greater rate of sediment accumulation at both LC and MC allows for a much higher sample to sediment-thickness ratio than could be obtained at the LSC reference section. The increase in resolution resulting from the greater density of sampling, particularly at LC, allowed the recognition of magnetozones of the MSZ6 level.

Lake Classen Spillway

We chose the Woodford where it crops out in the spillway at Lake Classen because it offers a continuous 55-m exposure, beginning with its unconformable

contact on weathered Pridolian–Lochkovian limestones of the Henryhouse Formation. The 17.5-m portion of the sequence illustrated in Figure 5 represents 533 samples, or roughly one sample per 3 cm, although sample intervals varied between 1 and 5 cm, depending on conditions. The section above and below this interval is too poorly known biostratigraphically to permit further definition of magnetozones. The sequence begins 7.5 m above the base in what we believe is the equivalent of Klapper's MN 12 Zone

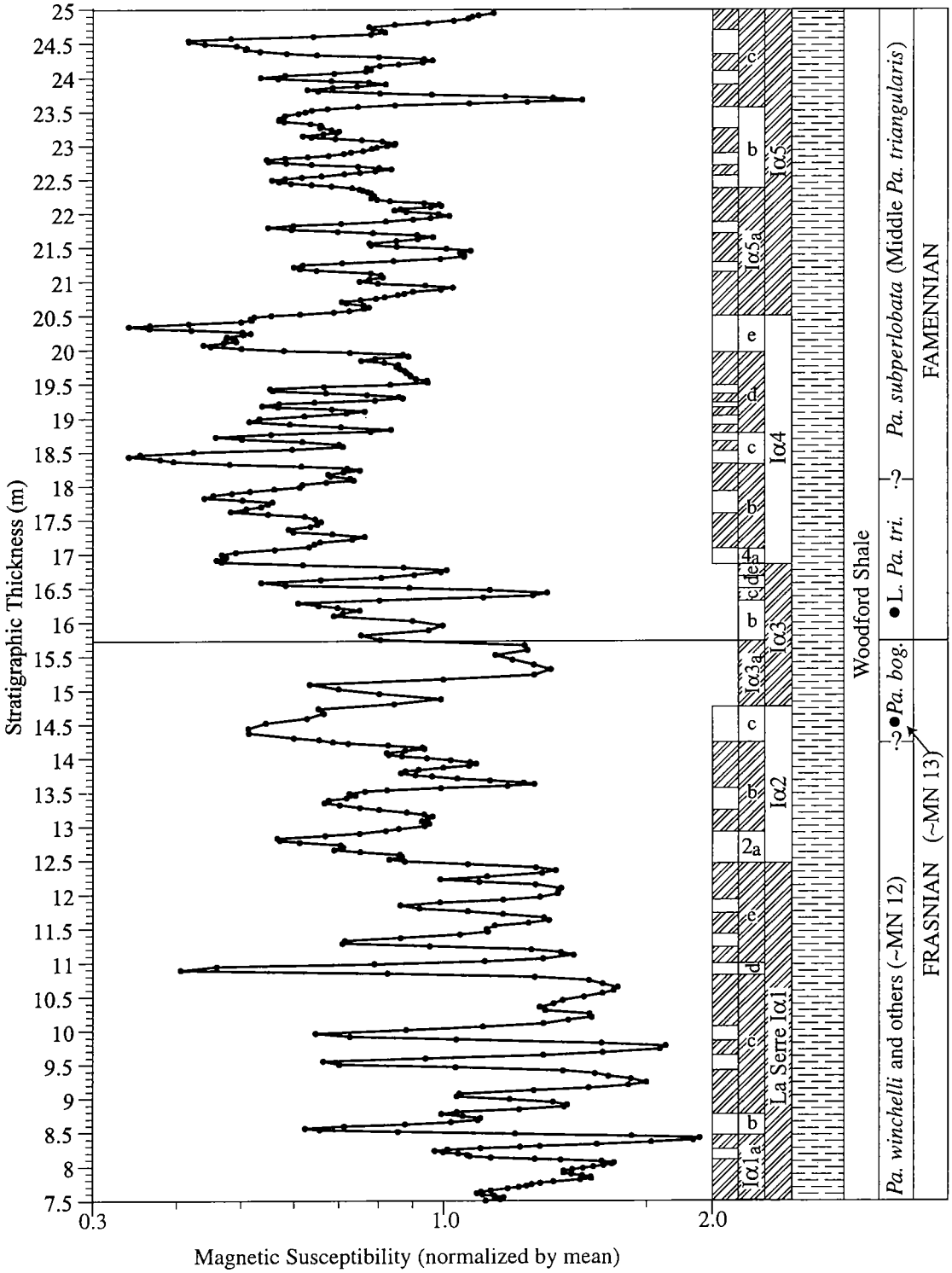

Figure 5. MSS for the F–F boundary sequence at Lake Classen spillway (LC) in the Arbuckle Mountains of southern Oklahoma. Magnetozones MSZ4, MSZ5, and MSZ6 are illustrated. Descriptions of the MSZs are given in the text. Biozone boundaries are based on those of Over (1990) with modifications introduced in this study. The original data were normalized by the mean MS magnitude 2.24×10^{-8} and splined slightly to reduce high-frequency variations.

(Klapper, 1988; Johnson and Klapper, 1992) (upper *Pa. rhenana* Zone) and continues into the equivalent of the middle *Pa. triangularis* Zone.

The MSS begins with the base of La Serre Iα1. Five MSZ5s are recognized in the Iα1 at LC, and these are provisionally correlated with the two MSZ5s recognized in the LSC reference section. Additionally, 15 MSZ6s are documented for Iα1. The character of the MSS at the base of La Serre Iα2 at 12.6 m above the base of the Woodford is similar to that of LSC, where there is a sharp decrease in MS magnitude. There is no change in facies or any obvious hiatuses in this Woodford interval. Three MSZ5s and five MSZ6s occur in the Iα2 interval. The base of La Serre Iα3 occurs, as it does in the LSC reference section, at the onset of high, sustained MS magnitudes (Fig. 5). Five MSZ5s are present in the Iα3 interval. We feel that La Serre $I\alpha3_{c,d,e}$ correlate with $I\alpha3_c$ of the reference section. The Frasnian portion of Iα3 corresponds to what we believe to be the equivalent of the MN 13 Zone. The MS pattern through the Iα3 at LC is virtually identical with that observed in the LSC reference section for the same interval. The base of $I\alpha3_b$ occurs slightly below the first record of *Pa. triangularis* and defines the position of the F–F boundary at 15.7 m above the base of the Woodford at LC. $I\alpha3_{b,c,d,e}$ and $I\alpha4_{a,b}$ fall within what we believe to be the lower *Pa. triangularis* Zone. As it does in the reference section, Iα4 represents an interval of low MS magnitudes subdivided by five MSZ5s and 15 MSZ6s (Fig. 5). The base of Iα5 defines a return to elevated MS magnitudes, which continue through the remainder of the LC sequence illustrated in Figure 5. Like the Iα5 of the reference section, the LC Iα5 interval contains three MSZ5s as well as 15 MSZ6s.

McAlister Cemetery (MC)

This locality was chosen for its exposure and because it offers a test of the regional correlative value of MSS within the Woodford Shale. The MC, also commonly referred to as the McAlister Cemetery Pit, is part of a largely inactive shale quarry in the southern Criner Hills. The entire thickness of the Woodford Shale is exposed in the quarry floor and face. Like most Woodford exposures, the lack of fauna makes correlation difficult to impossible. The base of the Woodford is represented by a green, glauconitic, sandy shale similar to that at LC and rests unconformably on the weathered Pragian-age Haragan Formation (Over, 1990). Over's earlier work (1990) suggested that the F–F boundary is ~12 m above the base of the Woodford but that the first proven occurrence of *Pa. triangularis* is some 4 m above the provisional F–F boundary. As part of this study, Over and his students decreased the sampling interval from the original 1 m to ~10 cm, whereas MSEC samples were collected at ~1-cm intervals. The increased sampling for conodonts did not improve the conodont biostratigraphy. The MSEC sampling produced 361 samples over the 5.4 m of the boundary sequence shown in Figure 6. A comparison of the stratigraphic reach of MSZ4 magnetozones La Serre Iα2, Iα3, and Iα4 represented at LC and MC indicates that the rate of sediment accumulation at LC was ~2.5 times higher than that of MC. For this reason, the sample density at MC was not sufficient to define MSZ6 magnetozones adequately and consistently.

With only the benefit of a limited biostratigraphic zonation, we have recognized MSZ4 magnetozones La Serre Iα1, Iα2, Iα3, Iα4, and a part of Iα5 in the MC sequence as well as all of the MSZ5 magnetozones of the LC sequence for the same MSS interval. The F–F boundary is placed at the base of $I\alpha3_b$ at 12.5 m above the base of the Woodford at MC.

Correlation Summary

Figure 7 summarizes the MSS relationship among the MSS F–F reference sequence in southern France and the two boundary sequences chosen in the Arbuckle Mountains of southern Oklahoma. Despite differences in paleogeography, environments of deposition, rates of sediment accumulation, and sample spacing, the MSS is consistent at the MSZ4 level and all of the MSZ5 level except for parts of the lower La Serre Iα1 and upper Iα3 magnetozones, where the Oklahoma sections show greater detail. While these differences may be regional in nature, we suspect that they may also reflect a need for more closely spaced sampling in the condensed LSC sequence. There is reasonably close agreement between the magnetozone–biostratigraphic relationship of LC and the similar relationship at LSC—perhaps more than expected, given the differences in controlling factors.

Comparing the MSS of LC with MC strongly suggests that rates of sediment accumulation at LC were much more variable relative to MC than expected. Given the character of the Woodford, the duration of magnetozones is the only objective means of gaining insight into this aspect of variability, which is completely obscured by the monotony of the lithology.

The correlation demonstrated here, and based on very different lithologies and paleogeographies, expresses the relevance of MSS magnetozones in long-range as well as inter- and intra-basinal correlation. The recognition of the F–F boundary was possible only because the reference sequence was developed in conjunction with a mature biostratigraphy, and thus the MSZs were given a relative time frame. Correlation between the LC and MC sequences would have been possible without comparison with the LSC reference sequence, given only the limited biostratigraphic knowledge available before this study. Although bereft of time, these local magnetozones would still possess the same correlative power.

ACKNOWLEDGMENTS

The participation of Crick and Ellwood was made possible by grants from the Petroleum Research Fund

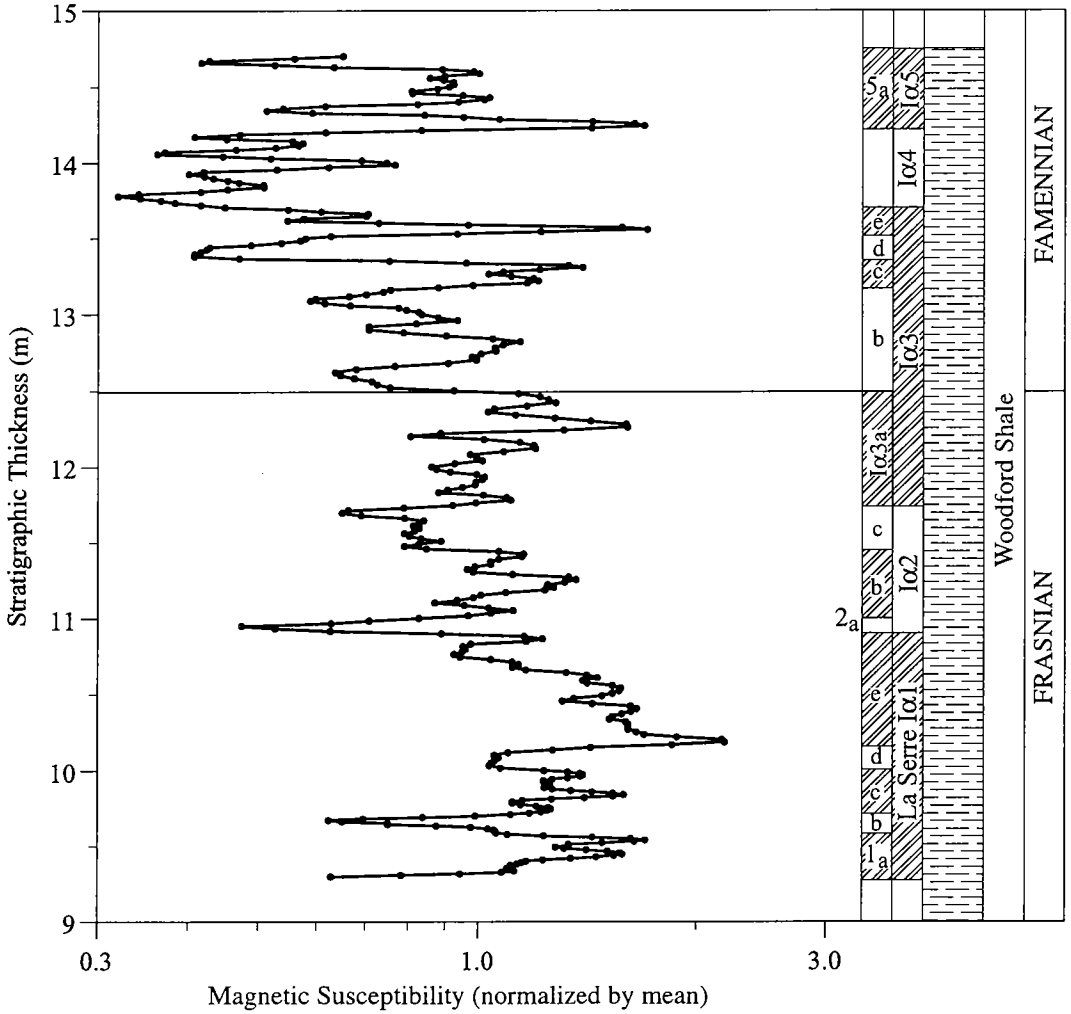

Figure 6. MSS for the F–F boundary sequence at McAlister Cemetery (MC) in the Criner Hills of southern Oklahoma. Magnetozones MSZ4 and MSZ5 are illustrated. Descriptions of the MSZs are given in the text. The original data were normalized by the mean MS magnitude 1.81×10^{-8} and splined slightly to reduce high-frequency variations.

of the American Chemical Society (no. 30845-AC8) and the National Science Foundation (EAR-9628202). Feist and Girard were supported by the French Centre National de la Recherche scientifique (UMR 5554, contribution ISEM 99/000, and UMR 5565).

REFERENCES CITED

Becker, R. T.; and House, M. R., 1994, Kellwasser events and goniatite successions in the Devonian of the Montagne Noire with comments on possible causations: Courier Forschungsinstitut Senckenberg, v. 169, p. 45–77.

Crick, R. E.; Ellwood, B. B.; Hassani, A. E.; Feist, R.; and Hladil, J., 1997, MagnetoSusceptibility Event and Cyclostratigraphy (MSEC) of the Eifelian–Givetian GSSP and associated boundary sequences in North Africa and Europe: Episodes, v. 20, p. 167–175.

Crick, R. E.; Ellwood, B. B.; Hassani, A. E.; and Feist, R., 2000a, Proposed Magnetostratigraphy Susceptibility Magnetostratotype for the Eifelian–Givetian GSSP (Anti-Atlas, Morocco): Episodes, v. 23, p. 93–101.

Crick, R. E.; Ellwood, B. B.; Hladil, J.; El Hassani, A.; Hrouda, F.; and Chlupác, I., 2000b, Magnetostratigraphy susceptibility of the Prídolian–Lochkovian (Silurian–Devonian) GSSP (Klonk, Czech Republic) and a coeval sequence in Anti-Atlas Morocco: Palaeogeography, Palaeoclimatology, Palaeoecology, v. 167, p. 73–100.

Ellwood, B. B.; Crick, R. E.; and El Hassani, A., 1999, The MagnetoSusceptibility Event and Cyclostratigraphy (MSEC) method used in geological correlation of Devonian rocks from Anti-Atlas Morocco: American Association of Petroleum Geologists Bulletin, v. 83, p. 1119–1134.

Ellwood, B. B.; Crick, R. E.; El Hassani, A.; Benoist, S.; and Young, R., 2000, MagnetoSusceptibility Event and Cyclostratigraphy (MSEC) in marine rocks and the question of detrital input versus carbonate productivity: Geology, v. 28, p. 1135–1138.

Ellwood, B. B.; Harrold, F. B.; Benoist, S. L.; Straus, L. G.; Gonzalez-Morales, M.; Petruso, K.; Bicho, N. F.; Zilhão, Z.; and Soler, N., 2001, Paleoclimate and intersite correlations from late Pleistocene/Holocene cave sites: results from southern Europe: Geoarchaeology, v. 16, in press.

Feist, R.; and Klapper, G., 1985, Stratigraphy and conodonts in pelagic sequences across the Middle–Upper Devonian boundary, Montagne Noire, France: Palaeontographica. Abteilung A: Palaeozoologie Stratigraphie, v. 188, p. 1–18.

Feist, R.; Becker, R. T.; House, M. R.; Babin, C.; Flaja, G.; Klapper, G.; Lethiers, F.; Pedder, A.; Racheboeuf, P.; and

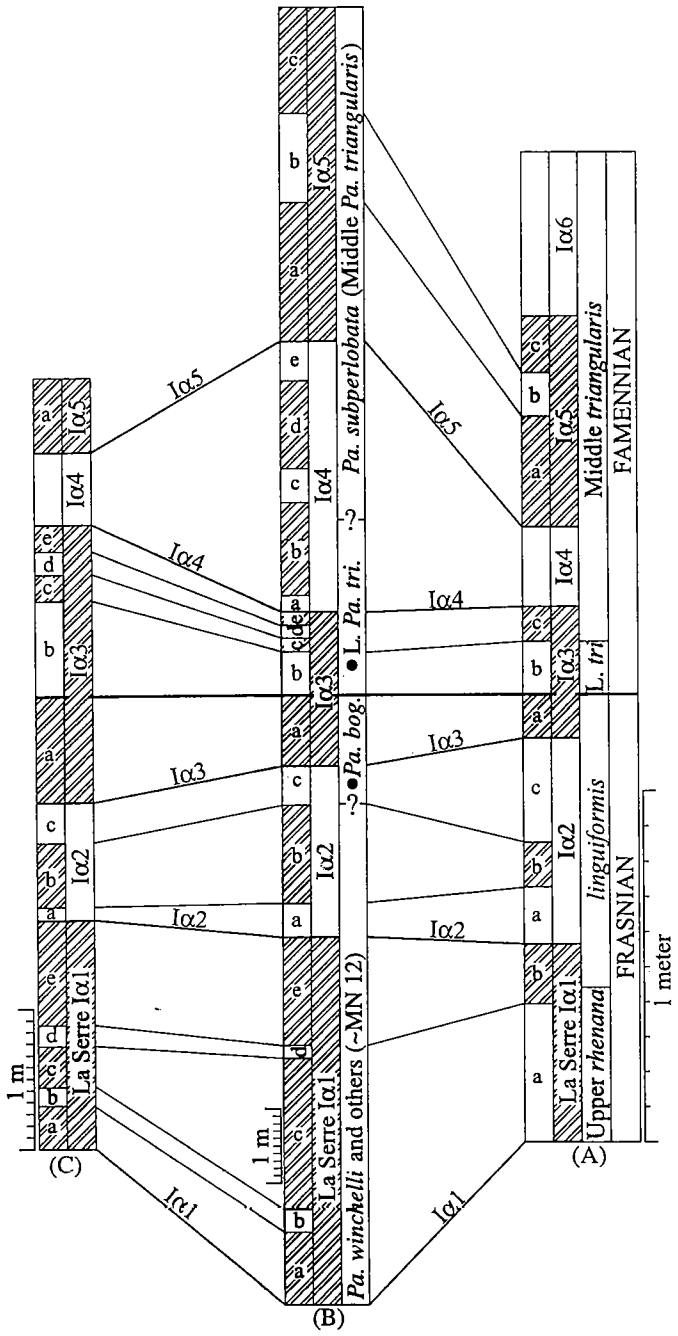

Figure 7. Correlation by MSS. Regional and extra-regional correlation of F–F boundary sequences, using magneto-zones MSZ4 and MSZ5. (A) LSC reference sequence at La Serre, Montagne Noire, southern France. (B) Lake Classen, Arbuckle Mountains, southern Oklahoma. (C) McAlister Cemetery, Criner Hills, southern Oklahoma. Sections are at different scales, as shown. See figures of individual sequences for additional details.

Truyols-Massoni, M., 1990, The Frasnian–Famennian boundary and adjacent strata of the eastern Montagne Noire, France: International Subcommission on Devonian Stratigraphy, Montpellier, France, 69 p.

Feist, R.; Echtler, H.; Galtier, J.; and Mouthier, B., 1994, Biostratigraphy and dynamics of the nonmetamorphic sedimentary record, *in* Keppie, J. D. (ed.), Pre-Mesozoic geology in France and related areas: Springer-Verlag, Heidelberg, p. 289–304.

Girard, C.; and Feist, R., 1996, Eustatic trends in conodont diversity across the Frasnian/Famennian boundary in the stratotype area, Montagne Noire, Southern France: Lethaia, v. 29, p. 329–337.

Hass, W. H.; and Huddle, J. W., 1965, Late Devonian and Early Mississippian age of the Woodford Shale in Oklahoma, as determined from conodonts: U.S. Geological Survey Professional Paper 525-D, p. 125–132.

Johnson, J. G.; and Klapper, G., 1992, North American Midcontinent Devonian T–R cycles, *in* Chaplin, J. R.; and Barrick, J. E. (eds.), Special papers in paleontology and stratigraphy: a tribute to Thomas W. Amsden: Oklahoma Geological Survey Bulletin 145, p. 127–135.

Klapper, G., 1988, The Montagne Noire Frasnian (Upper Devonian) conodont succession, *in* McMillan, N. J.; Embry, A. F.; and Glass, D. J. (eds.), Devonian of the world, vol. 3: Canadian Society of Petroleum Geologists, Calgary, p. 449–468.

Klapper, G.; Feist, R.; and House, M. R., 1987, Decision on the boundary stratotype for the Middle/Upper Devonian Series boundary: Episodes, v. 10, p. 97–101.

_____1993, Definition of the Frasnian/Famennian Stage boundary: Episodes, v. 16, p. 433–441.

Over, D. J., 1990, Conodont biostratigraphy of the Woodford Shale (Late Devonian–Early Carboniferous) in the Arbuckle Mountains, south-central Oklahoma: Texas Tech University, Lubbock, unpublished Ph.D. thesis, 174 p.

_____1992, Conodonts and the Devonian–Carboniferous boundary in the upper Woodford Shale, Arbuckle Mountains, south-central Oklahoma: Journal of Paleontology, v. 66, p. 293–311.

Over, D. J.; and Barrick, J. E., 1990, The Devonian/Carboniferous boundary in the Woodford Shale, Lawrence uplift, south-central Oklahoma, *in* Ritter, S. M. (ed.), Early to middle Paleozoic conodont biostratigraphy of the Arbuckle Mountains, southern Oklahoma: Oklahoma Geological Survey Guidebook 27, p. 63–74.

Paproth, E.; Feist, R.; and Flajs, G., 1991, Decision on the Devonian–Carboniferous boundary stratotype: Episodes, v. 14, p. 331–336.

Paris, F.; Girard, C.; Feist, R.; and Winchester-Seeto, T., 1996, Chitinozoan bioevent in the Frasnian/Famennian boundary beds at La Serre (Montagne Noire, southern France): Palaeogeography, Palaeoclimatology, Palaeoecology, v. 121, p. 131–145.

Remane, J.; Bassett, M. G.; Cowie, J. W.; Gohrbrandt, K. H.; Lane, H. R.; Michelsen, O.; and Naiwen, W., 1996, Revised guidelines for the establishment of global chronostratigraphic standards by the International Commission on Stratigraphy (ICS): Episodes, v. 19, p. 77–81.

Sachs, S. D.; and Ellwood, B. B., 1988, Controls on magnetic grain-size variations and concentrations in the Argentine basin, South Atlantic Ocean: Deep Sea Research, v. 35, p. 929–942.

Salvador, A., 1994, The International Stratigraphic Guide: a guide to stratigraphic classification, terminology, and procedure (2nd edition): Geological Society of America, Boulder, Colorado, 214 p.

Shackleton, N. J., 1999, Will oxygen isotope stratigraphy survive to the next millennium? [abstract]: Eos Transactions, American Geophysical Union, Abstracts of Annual Meeting (San Francisco), v. 80, p. F505.

Tucker, R. D.; Bradley, D. C.; Ver Straeten, C. A.; Harris, A. G.; Ebert, J. R.; and McCutcheon, S. R., 1998, New U-Pb zircon ages and the duration and division of Devonian time: Earth and Planetary Science Letters, v. 158, p. 175–186.

Mississippian Springer Sands as Conduits for Emplacement of Hydrocarbons in Prolific Ordovician Reservoirs in Southern Oklahoma

Harry W. Todd
Certified Petroleum Geologist
Highland Village, Texas

ABSTRACT.—Millions of barrels of oil have been produced from Simpson and Arbuckle reservoirs in southern Oklahoma. Production patterns and regional geology outline a probable hydrocarbon system to explain the migration and emplacement of hydrocarbons in those prolific Ordovician reservoirs.

Hydrocarbons were generated along the axis of the Anadarko basin as the Woodford Shale (Devonian–Mississippian) was buried below 10,000 ft. During dewatering, the buoyant multiphase fluids migrated vertically upward through fissures in the shales and collected in the overlying porous network of Mississippian Springer paralic and distributary sandstones. Moving laterally southeastward along the Springer subcrop toward the rising mountain system, the geopressured fluids were injected through major transpressive faults into uplifted Ordovician reservoirs. Preceded by carbonic and organic acids that enhanced existing porosity, hydrocarbons filled the first traps upstream from the faults. These migrating fluids moved onward to expulsion at Ordovician subcrop/outcrop seeps in the Arbuckle and Wichita Mountains and in the Criner Hills.

This hydrocarbon system is proposed as a major route of basin dewatering accompanied by periodic release of geopressures along the fault boundaries. In this scenario the Springer was neither source nor reservoir; it was a conduit. The Springer sandstone was a hydrocarbon-gathering system, a pipeline, and a hydrocarbon injector. The migration routes can be mapped and thus are predictable, and the process is a technology transferable to other basins. For the explorationist, "*X* marks the spot" where a major fault crosses the Springer sand.

INTRODUCTION

In 1987 during an economic slump, CNG drilled through a reverse fault at their Cottonwood Creek prospect in Carter County, Oklahoma, and the drill bit dropped into cavernous Arbuckle limestone. Their 4,000-BOPD completion through drill pipe inspired the oil industry into a burst of Arbuckle exploration. Popular geologic theories favored anticlines along the faulted boundaries of karsted Ordovician subcrops (Gao and others, 1992). While prospecting these boundaries, the writer observed what seems to be a significant geologic relationship. The Arbuckle oil deposits at Healdton, Cottonwood Creek, and Southeast Hoover fields occur where the subcrops of the Springer sands intersect the faulted boundaries of the Ordovician subcrops along the northeastern flanks of the Arbuckle and Wichita Mountains (Fig. 1). Possible injection of hydrocarbons into an Arbuckle carbonate along a fault by a Springer sand conduit is illustrated at Southeast Hoover Arbuckle oil field in Figures 2 and 3. The Reagan fault exhibits both reverse and left-lateral movement; the Springer conduit may have injected the Southwest Davis Oil Creek sand at –3,000 ft prior to injection of the Southeast Hoover Arbuckle at –6,000 ft. A similar relationship between the Springer and the Simpson sands may exist at the Golden Trend in Caddo County. A hypothetical scenario for the full hydrocarbon system is outlined in succeeding maps.

PROBABLE HYDROCARBON SYSTEM

Source

The Devonian–Mississippian Woodford Shale has been recognized as the primary source rock for Oklahoma crudes. Low permeability within the Woodford black shales impairs long-distance lateral movement of fluids. The water, carbonic and organic acids, and hydrocarbons generated by burial of the source rock below 10,000 ft are assumed to have been expelled through vertical fractures, moving toward areas of lower pressure. A vitrinite-isoreflectance map of the Woodford Shale (Fig. 4), modified from Cardott and Lambert (1985, fig. 4), has been applied to production maps of surrounding geologic strata to determine the movement of those hydrocarbons.

Todd, H. W., 2001, Mississippian Springer sands as conduits for emplacement of hydrocarbons in prolific Ordovician reservoirs in southern Oklahoma, *in* Johnson, K. S. (ed.), Silurian, Devonian, and Mississippian geology and petroleum in the southern Midcontinent, 1999 symposium: Oklahoma Geological Survey Circular 105, p. 83–88.

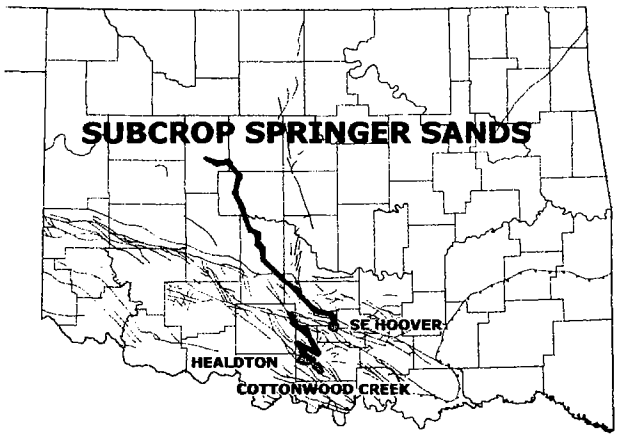

Figure 1. Map indicating subcrops of Springer sandstones intersecting faults near Cottonwood Creek, Healdton, and Southeast Hoover Arbuckle oil fields.

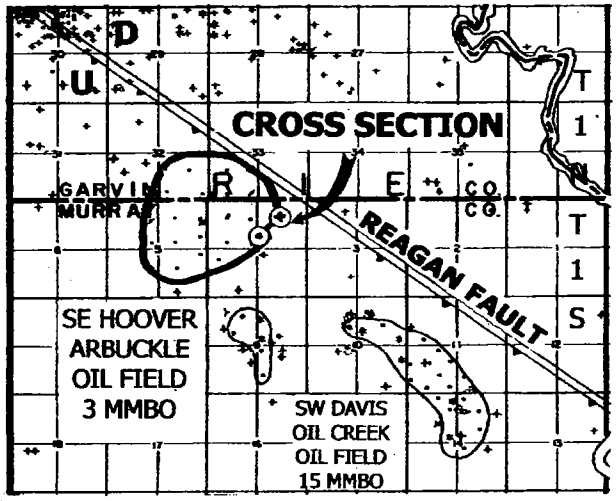

Figure 2. Map showing location of cross section at Southeast Hoover Arbuckle field.

Downward Migration

Dewatering fluids moved from the Woodford Shale and carried hydrocarbons into the porous Hunton carbonates directly below the Woodford (Fig. 5) along the isoreflectance contours for oil generation. Oil traps appear almost as in-situ accumulations, with little overall movement toward the Hunton subcrop.

Upward Migration

Fluids expelled from Woodford and lower Mississippian black shales migrated upward and filled hydrocarbon reservoirs in the Sycamore and Chester carbonates (Fig. 6) directly above the oil-generation band on the isoreflectance contours. The map shows no production from the deeper part of the basin. The Woodford source rock along the basin axis would have passed through the oil-generation window during Early Pennsylvanian deposition, and the hydrocarbons would have migrated vertically toward porous strata.

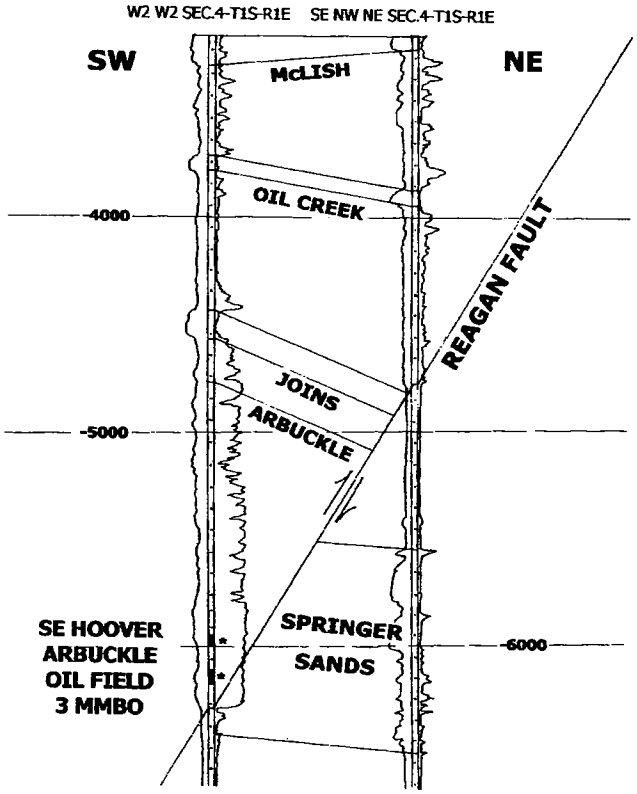

Figure 3. Cross section showing possible injection of Arbuckle hydrocarbons by Springer conduit. See Figure 2 for location of section.

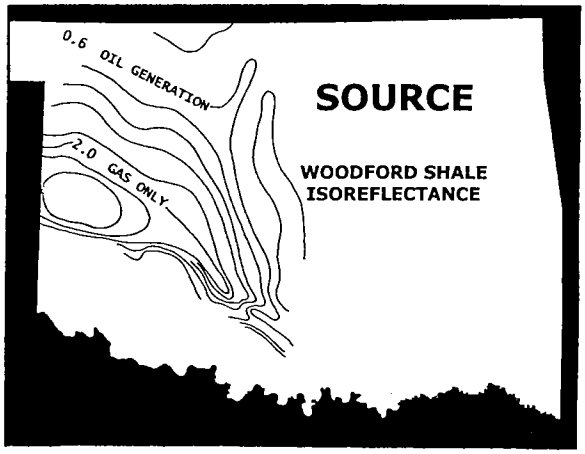

Figure 4. Vitrinite isoreflectance map of Woodford Shale in Anadarko basin (modified from Cardott and Lambert, 1985, fig. 4; reprinted by permission of American Association of Petroleum Geologists, whose permission is required for future use).

Gathering Network

Porous Springer paralic and distributary sands lie above the Mississippian shales near the axis of the southeastern Anadarko basin (Fig. 7). These sands gathered the dewatering fluids migrating from the deep basin and transported them laterally southeastward along the subcrops toward lower pressures in

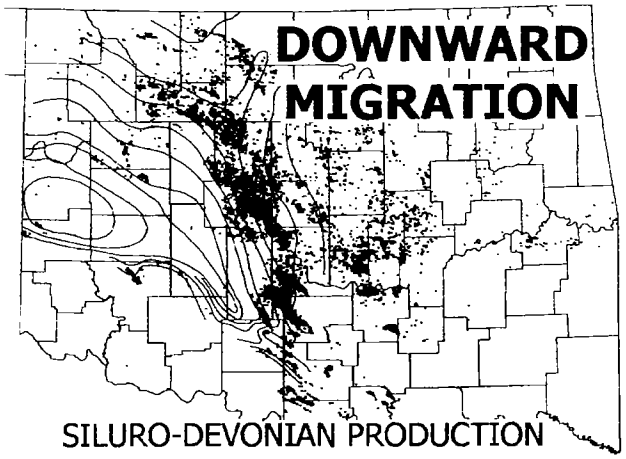

Figure 5. Woodford isoreflectance map with fields producing hydrocarbons from Silurian–Devonian carbonate reservoirs, 1979–1998. Data from Natural Resources Information System (NRIS), University of Oklahoma.

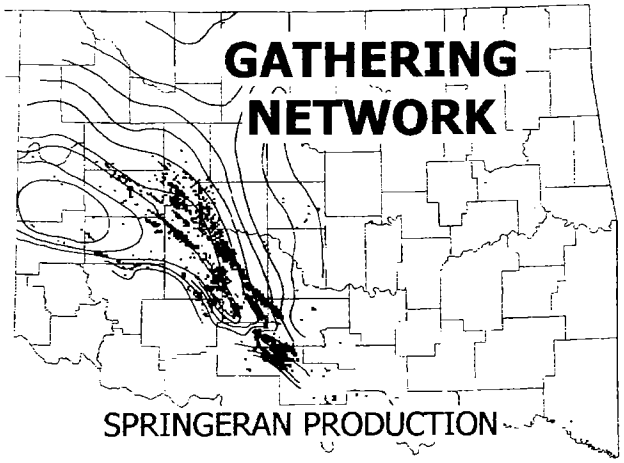

Figure 7. Woodford isoreflectance map with fields producing from Springer sandstone reservoirs, 1979–1998. Data from Natural Resources Information System (NRIS), University of Oklahoma.

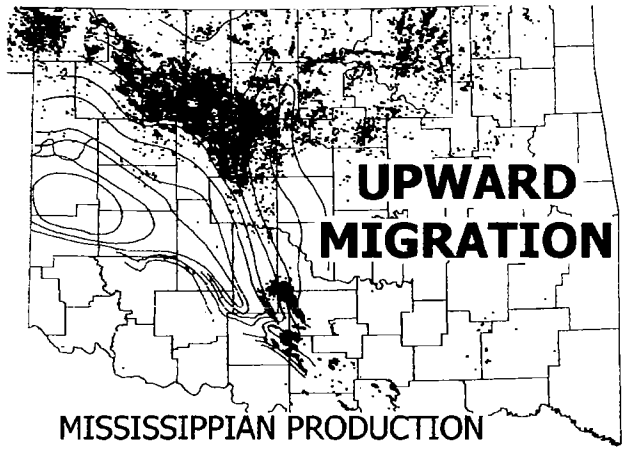

Figure 6. Woodford isoreflectance map with fields producing from Mississippian carbonate reservoirs, 1979–1998. Data from Natural Resources Information System (NRIS), University of Oklahoma.

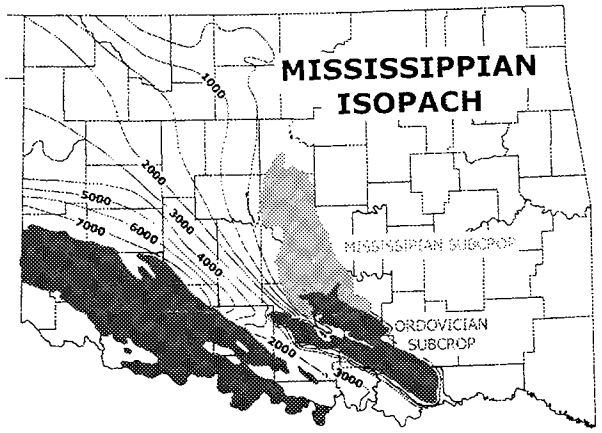

Figure 8. Map showing Mississippian isopach and subcrop, plus Ordovician subcrop. Contours in feet. Data from Geomap Co., Plano, Texas.

uplifted strata. The Mississippian isopach thins southeastward toward the rising mountains (Fig. 8). The Springer trend conduit system, however, remained generally closed and geopressured most of the time.

Faulted Conduit

Major transpressive faults cut the Springer conduits periodically during Pennsylvanian time (Fig. 9), releasing geopressures. Pressurized fluids were injected across the faults into low-pressure porous strata in the Springer and uplifted older formations. Pressurized fluid movement along faults can defy our normal expectations of gravity flow across juxtaposed reservoirs; hydrocarbons may move up, down, or laterally along the faults toward a low-pressure reservoir. Early-moving fluids entrapped oil deposits southeast of the faults. After the faults sealed by lack of movement, later fluids gener-

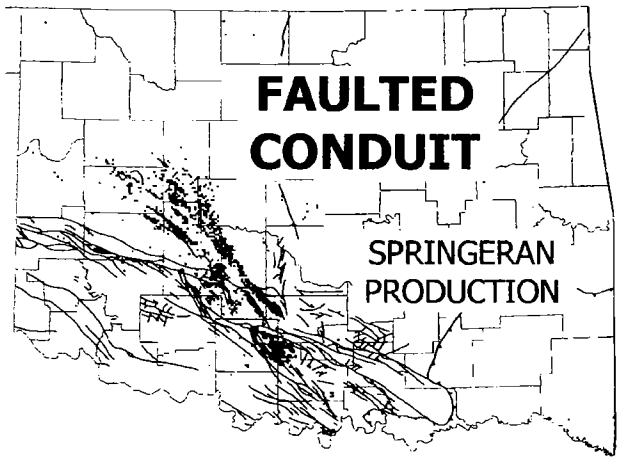

Figure 9. Map showing major transpressive fault system intersecting Springer production trend. Data from Geomap Co., Plano, Texas.

ated by the deepening basin axis filled the northwestern Springer reservoirs with gas.

Ordovician Production

A comparison of the Ordovician production pattern with the isoreflectance contours shows little relationship with the hydrocarbon-generation band in the Anadarko basin (Fig. 10). What is striking about the map is a wide prong of oil production jutting westward into Caddo County—the Golden Trend. Running perpendicular to the isoreflectance contours, the Golden Trend looks like a huge funnel extending to the area where the Springer trend encounters the major fault system.

Springeran Conduits Emplacing Ordovician Reserves

"*X*s mark the spots" (Fig. 11) where the Springer trend sandstone conduits are crossed by major transpressive faults and where hydrocarbons were injected into the upthrown Ordovician reservoirs south of the faults. This *X* signature is a trademark for the proposed hydrocarbon system: a geopressured conduit crossing a fault-enhanced reservoir.

Hydrocarbon-System Details

The relationships between Springer production, major faults, Ordovician production, seeps, and Ordovician subcrops are shown on a more detailed map

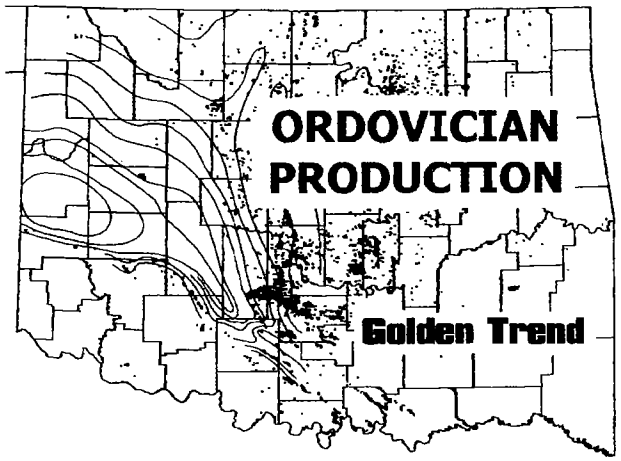

Figure 10. Woodford isoreflectance map with fields producing hydrocarbons from Ordovician reservoirs, 1979–1998. Data from Natural Resources Information System (NRIS), University of Oklahoma.

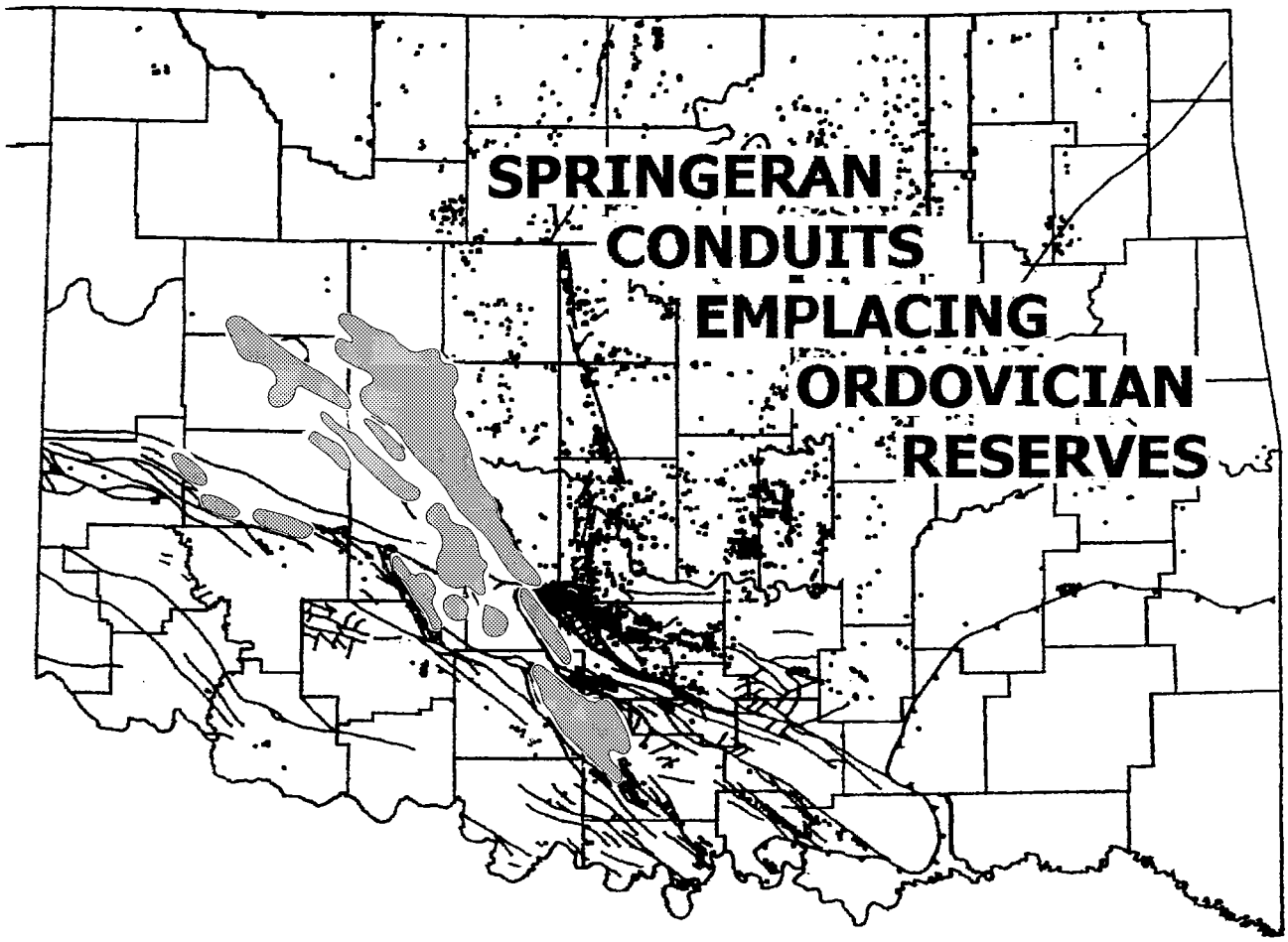

Figure 11. Map showing relationship of Springer production trend, major fault systems, and Ordovician production. "*X*s mark the spots" where Springer sandstone conduits are crossed by major transpressive faults.

of the Ardmore basin (Fig. 12). Geopressured fluids gathered by the Springer conduits were released across major faults, which opened periodically, injecting fluids along the faults into low-pressure porous formations. Carbonic and organic acids enhanced the Simpson and Arbuckle porosity by mesogenetic dissolution (Mazzullo and Harris, 1992). Hydrocarbons then filled the enhanced reservoirs in the first anticlinal traps on the uplifted south sides of the faults. The fluids continued migrating toward areas of lower pressure and were expelled from the system at seeps on the Ordovician subcrop/outcrop. Productive Arbuckle carbonates are confined generally to the southern part of the Ardmore basin where porous Simpson sandstones were not deposited and therefore could not act as fluid thief zones as the fault blocks moved upward.

Traps and Production

Fields in this hydrocarbon system are shown in Figure 13. Cumulative oil and gas production from the Simpson and Arbuckle traps is shown in Table 1. This entire sequence has produced 350 million bbl of oil and 1.2 trillion cubic ft of gas—prolific by Midcontinent standards.

Table 1.—Cumulative Production from Ordovician Traps "Marked by *X*s"

Ordovician production	(MMBO)	(BCFG)
Simpson fields		
Apache	67	11
Carter–Knox	18	181
Chitwood	11	69
Davis, S.W.	15	3
Eola	95	102
Golden Trend	116	864
Arbuckle fields		
Cottonwood Creek	8	6
Healdton	17	4
Hoover, S.E.	3	
Cumulative production	350	1,240

Data from Geomap Co., Plano, Texas.

SUMMARY AND CONCLUSIONS

A prospector's geologic map can be made depicting with "*X* marks the spot" the localities where major faults cross Springer conduits. At these localities, hydrocarbons may have been injected into enhanced uplifted reservoirs. Here, major treasures of "black gold" have been discovered in Ordovician rocks of southern Oklahoma, and this is where a complete hydrocarbon system can be described and further ex-

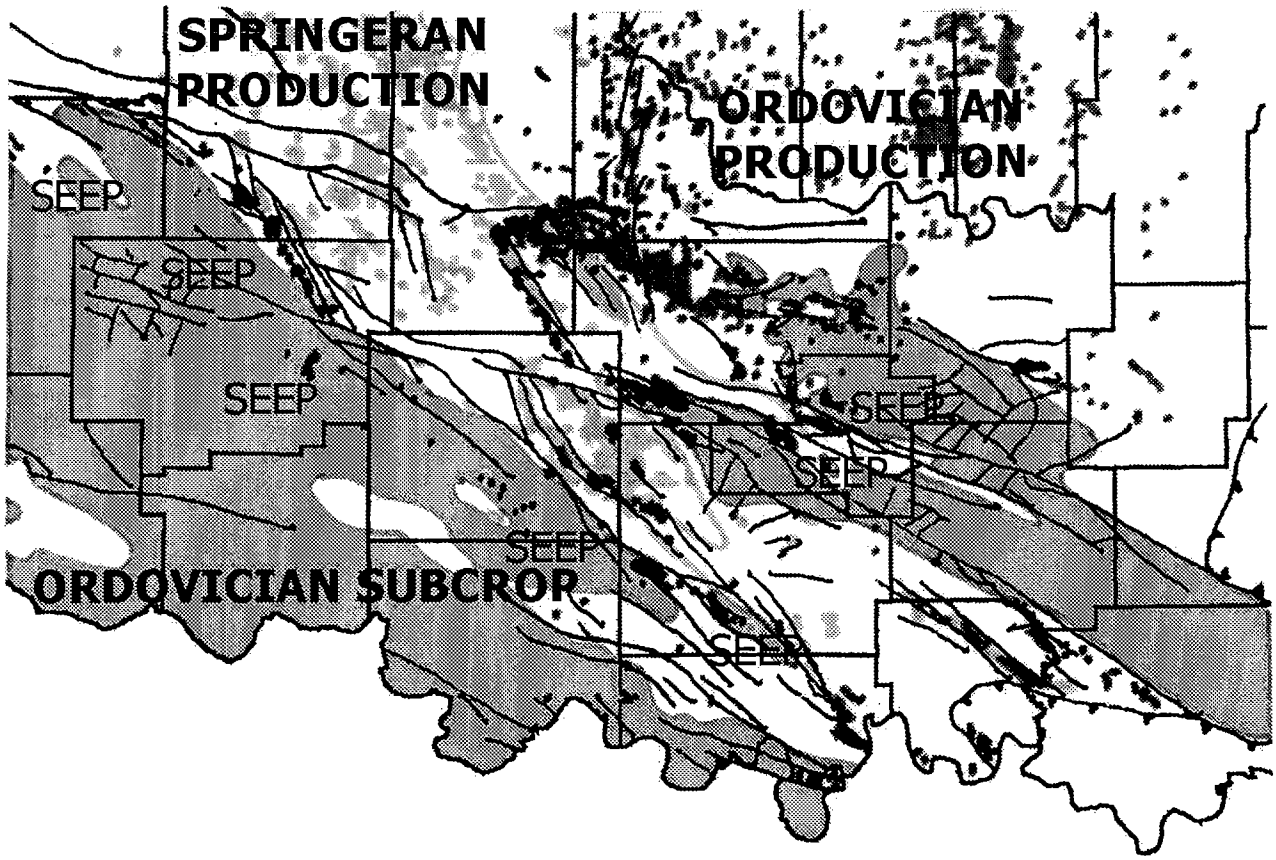

Figure 12. Detailed composite map of hydrocarbon system in Anadarko–Ardmore basin.

ploited. Similar conduit migration systems might be found in other geologic basins. Early recognition would improve our exploration efforts.

ACKNOWLEDGMENTS

The author is grateful to Joseph K. Campbell for his encouragement with the original concept and to William F. Sinclair for his thoughtful suggestions and critical review of the manuscript. Thanks also are extended to Geomap Co., to the Natural Resources Information System at the University of Oklahoma, and to the Tulsa Geological Society for their assistance.

REFERENCES CITED

Cardott, B. J.; and Lambert, M. W., 1985, Thermal maturation by vitrinite reflectance of Woodford Shale, Anadarko basin, Oklahoma: American Association of Petroleum Geologists Bulletin, v. 69, p. 1982–1998.

Gao, Guoqiu; Land, L. S.; and Folk, R. L., 1992, Meteoric modification of early dolomite and late dolomitization by basinal fluids, upper Arbuckle Group, Slick Hills, southwestern Oklahoma: American Association of Petroleum Geologists Bulletin, v. 76, p. 1649–1664.

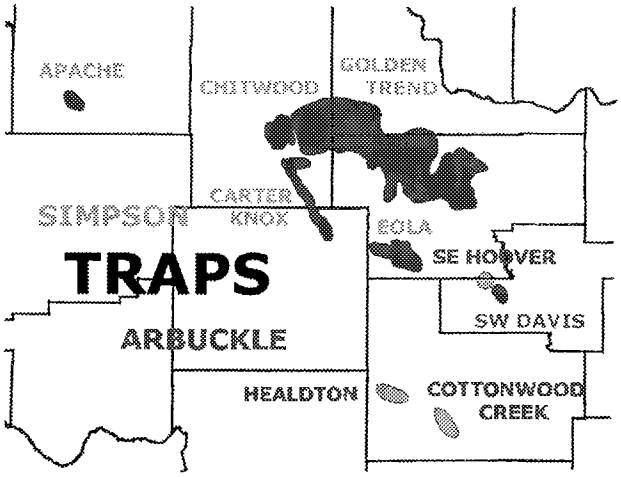

Figure 13. Map showing Ordovician traps in hydrocarbon system presented in this paper.

Mazzullo, S. J.; and Harris, P. M., 1992, Mesogenetic dissolution: its role in porosity development in carbonate reservoirs: American Association of Petroleum Geologists Bulletin, v. 76, p. 607–620.

Example of a Carbonate Platform and Slope System and Its Stratigraphically Equivalent Basinal Clastic System: Springeran–Chesterian Relationships in the Anadarko Basin and Shelf of Northwestern Oklahoma and Texas Panhandle

Walter J. Hendrickson, Paul W. Smith, Ronald J. Woods, John V. Hogan, and Charles E. Willey
IHS Energy Group[1]
Oklahoma City, Oklahoma

ABSTRACT.—An extensive regional study covering the Anadarko basin and shelf of Oklahoma and Texas has been conducted that included the generation of regional cross sections, production allocation, and reservoir characterization. It has long been apparent to those working this area of Oklahoma and Texas that the nomenclature used is typically erratic and the resulting production allocation less than precise. A correlative and equivalent formation may be called various names, and there are too many instances of nomenclature being vague, too broad, or incorrect altogether. As part of a regional study, the logs from every producing well within the majority of the Anadarko basin and shelf were reviewed to verify the actual producing reservoirs. Approximately 35,000 wells in an area of northwestern Oklahoma and the panhandles of Oklahoma and Texas were examined. Regional cross sections were constructed and used to determine the stratigraphic relationships and to develop a stratigraphic-nomenclature system that could be used across the area with accuracy, detail, and consistency. Although the entire stratigraphic section has been studied, the Springer Group and the Upper Mississippian and Lower Pennsylvanian sequences demonstrate most clearly a carbonate platform and slope system and its stratigraphically equivalent basinal clastic system.

The Springer Group is often misidentified as the overlying Pennsylvanian Morrow sandstone or the underlying Mississippian Chester limestone. Historically, the first carbonate encountered below the Morrow–Springer clastic section has been called Chester limestone by convention. Generally, the Springer Group consists of the Boatwright, Britt, and Cunningham units, in ascending order. Whereas in Oklahoma the Cunningham was always found to be a sandstone, extensive correlations indicated that the Boatwright and/or Britt in certain areas developed a carbonate facies that was almost always referred to as Chester limestone. Regional correlations in both Oklahoma and Texas, from the deep Anadarko basin through the slope and onto the shelf, indicate that the Springer clastics of the deep basin are stratigraphically equivalent to Springer carbonate facies on the slope and shelf. As a result of these correlations, Britt and Boatwright carbonates have been identified, which heretofore have generally been considered to be the Chester limestone. A highly conductive Boatwright shale directly above the true Chester limestone provides a reliable regional marker as the base of the Springer Group. In Texas, the Cunningham also was observed to develop a carbonate facies, but it was rare and nonproductive.

Regional cross sections show these facies changes and indicate trapping mechanisms. Production and lithofacies maps delineate trends.

PURPOSE

It was the purpose of this study to ensure that the production within the study area was accurately allocated to a common and consistent stratigraphic nomenclature. This nomenclature was developed through regional correlations and substantiated by a dense framework of contiguous and detailed cross sections.

Hendrickson and others (1996a,b), Williams and others (1996), and Smith and others (1996) previously discussed correlation and allocation projects with specific results. Smith and others (2000) reported that certain Springer sandstones were observed to undergo facies changes to carbonates. In the areas of Springer carbonate deposition, these carbonates had been iden-

[1]See Addendum on page 93.

Hendrickson, W. J.; Smith, P. W.; Woods, R. J.; Hogan, J. V.; and Willey, C. E., 2001, Example of a carbonate platform and slope system and its stratigraphically equivalent basinal clastic system: Springeran–Chesterian relationships in the Anadarko basin and shelf of northwestern Oklahoma and Texas Panhandle, *in* Johnson, K. S. (ed.), Silurian, Devonian, and Mississippian geology and petroleum in the southern Midcontinent, 1999 symposium: Oklahoma Geological Survey Circular 105, p. 89–98.

tified as Mississippian Chester carbonates. This paper provides condensed cross sections of those that were presented as a poster session at a workshop held in Oklahoma City in March 1999 on Silurian, Devonian, and Mississippian geology and petroleum resources in the southern Midcontinent—the subject of this volume. These cross sections demonstrate the relationships of the Springer sandstones, the Springer carbonates, and Mississippian Chester rocks. The correlations have resulted in notable reserves being reallocated from what was originally indicated as Mississippian Chester into what more specifically is herein identified as Boatwright and Britt carbonates of the Springer Group. The production maps indicate the areas of Boatwright and Britt production (specific as to sandstone and carbonate areas) as well as the areas of true Chester production.

STUDY AREA

Figure 1 is a map of the study area, which encompasses most of the Anadarko basin and shelf area of Oklahoma and Texas.

METHODOLOGY

A producing well is originally defined by the completion report (Form 1002A), filed with the Oklahoma Corporation Commission, on which both the perforated interval(s) and the producing formation(s) are listed. It is the operator's responsibility to identify the producing formation as fully and correctly as possible, but there are no exacting standards in this process nor are there any mechanisms to ensure that the producing formation has been correctly and fully defined. As a result, the nomenclature in the basin and shelf area is erratic and less than precise.

During a recent effort at IHS Energy Group to standardize reservoir nomenclature, the authors generated >15,000 mi of geologic cross sections to demonstrate the stratigraphic sequences and relationships throughout the Anadarko basin and shelf area. Figure 2 shows the stratigraphic section used in this study to designate reservoir and formation names. Figure 3 is a base map of the approximate study area, indicating the network of nearly 3,000 mi of drafted cross sections, which are a small part of the total used in this project. Also indicated are the traces of the cross sections included in this paper (A–A′, B–B′, C–C′, and D–D′) that demonstrate the facies changes that have resulted in certain formations within the Springer Group, as herein defined, being identified as Mississippian Chester. To ensure nomenclatural consistency and accuracy, the electric logs of approximately 35,000 wells were reviewed for this study.

Regarding the perforated interval(s) for a well (as defined by the operator on the completion card and/or Form 1002A), a comparison was made between the formation as indicated by the IHS regional cross sections and the operator-defined producing formation. Where there was a difference between the two, the nomenclature as indicated by the regional cross sections was used. Almost 40% of the producing formations as originally defined on completion cards were too vague, too broad, or incorrect and were consequently reassigned a reservoir name to conform with the cross-section correlations. Furthermore, about 15% of the perforated intervals required correction because of reporting errors, typographical errors, or the absence of information.

RESULTS

The overall results of this study have been twofold. First has been the development of a dense framework of regional cross sections that demonstrate the stratigraphic sequences and relationships found within the Anadarko basin and shelf area. Second has been a great improvement in the accuracy, detail, and consistency in the allocation of production as reflected in the IHS Production Database, which should be of great and varied benefit to anyone using production data within the study area.

Additionally, and discussed in some detail herein, the relationships and facies of the Springer and Chester Groups have been clarified. Regional correlations from the deep part of the Anadarko basin northwestward demonstrate that the Boatwright and Britt undergo a facies change from sandstone to carbonate. Previously, these carbonates have been identified as Mississippian Chester by convention. However, they are distinct from the true Chester in that the intervening Boatwright shale is everywhere present and correlative, lying above the true Chester and separating it from the overlying Boatwright and Britt carbonates. Thus, the Boatwright shale is present independently of the facies (sandstone or carbonate) of the Boatwright and Britt. The overlying Cunningham sandstone was deposited over the south half of the study area, and no carbonate facies has yet been observed for this unit.

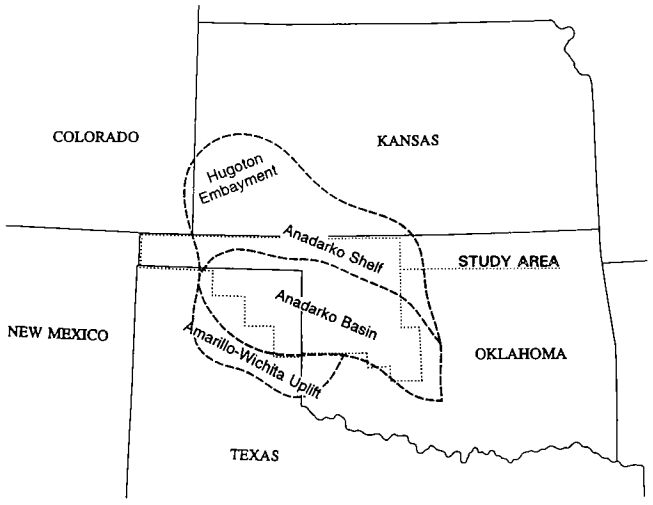

Figure 1. Index map of a part of the Midcontinent region, showing the study area in the Anadarko basin and shelf of Oklahoma and Texas.

Cross section A–A′ (Fig. 4) is an approximate strike section over the southeastern two-thirds of its extent. The northwestern one-third of the section is a dip section, showing the beds rising from the Anadarko basin at its westernmost extent. The southeasternmost well of the section, the Arkla No. 1-21 Clancey Estate, was drilled in the Eakley–Weatherford trend (an area of notable Boatwright and Britt sandstone production) and produces from Boatwright sandstone between 16,115 and 16,220 ft. The massive Boatwright shale

SYS	SERIES	GROUP	UNIT	SANDSTONE	CARBONATE	EQUIVALENT
PENNSYLVANIAN	VIRGILIAN	Shawnee/Cisco	Topeka Ls Pawhuska Ls Hoover Ss Elgin Sd Oread Ls Heebner Sh Endicott Ss	Hoover Endicott	Pawhuska Oread Ls	
		Douglas/Cisco	Lovell Ls Haskell Ls Tonkawa Ss	Tonkawa	Douglas Group	
	MISSOURIAN	Lansing/Hoxbar	Avant Ls Cottage Grove Ss	Cottage Grove	Lansing Group	
		Kansas City/Hoxbar	Dewey Ls Hogshooter Ls Layton Ss Checkerboard Ls Cleveland Ss	Layton Cleveland Culp	Kansas City Group Melton	Marchand Upper Marchand Lower
	DES MOINESIAN	Marmaton	Big Lime Oswego		Big Lime Oswego	Marmaton Wash
		Cherokee	Cherokee Marker Prue Ss Verdigris Ls Skinner Ss Pink Ls Red Fork Ss Inola Ls Mona	Prue Skinner Red Fork Cherokee Wash Middle Cherokee Wash Lower/ Mona	Verdigris Inola	Prue Wash Skinner Wash Red Fork Wash Bartlesville, Tussy
	ATOKAN	Atoka	Atoka 13 Finger Ls	Atoka	Atoka 13 Finger	
	MORROWAN	Morrow	Morrow Primrose	Upper Morrow Morrow Lower Morrow Primrose		
MISSISSIPPIAN	SPRINGERAN	Springer	Cunningham Britt Boatwright	Cunningham Britt Boatwright	Britt Boatwright	
	CHESTERIAN	Chester	Chester Ls		Chester	
		Manning	Manning Ls		Manning	
	MERAMECIAN	Meramec	Meramec Chat Meramec Ls		Meramec Chat Meramec	
	OSAGEAN	Osage	Osage Ls			
	KINDERHOOKIAN	Kinderhook	Kinderhook Sh			
SIL./DEV.	CHATTANOOGIAN		Woodford Sh Misener Ss	Misener		
	ULSTERIAN	Hunton	Hunton Group		Hunton (Frisco) Hunton (Bois d'Arc) Hunton (Haragan) Hunton (Henryhouse) Hunton (Chimney Hill)	
	NIAGARAN ALEXANDRIAN					
ORDOVICIAN	CINCINNATIAN	Sylvan	Sylvan Sh Maquoketa		Maquoketa	
	CHAMPLAINIAN	Viola	Viola Group		Viola (Fernvale) Viola (Trenton)	
		Simpson	Simpson Dense Bromide Ss Tulip Creek Ss McLish Ss Oil Creek Ss Joins	Bromide Tulip Creek McLish Oil Creek Joins		
	CANADIAN	Arbuckle	Arbuckle Group		Arbuckle	
CAMB.	CROIXAN					

6/96

Figure 2. Stratigraphic section for the study area.

in this well occurs from 16,220 to 16,550 ft, at which depth the true Chester was encountered. Over the extent of cross section A–A′, the Boatwright shale thins from 330 ft in the southeast to 225 ft in the northwest, but it is everywhere present and lies above the true Chester. From the No. 1-21 Clancey well, the cross section progresses northwestward, where the Boatwright sandstone first thins and then undergoes a facies change to thin carbonates. Northwestward, these thin carbonates coalesce into a massive carbonate section of more than 200 ft (T. 15 N., R. 21 W.), which in turn thins to a regionally persistent Boatwright carbonate bed ~40 ft thick at the northwestern end of the section. Similarly, the Britt sandstone, present in the southeastern part of the section, undergoes a facies change to a massive carbonate section (T. 16 N., R. 21 W.). This lithologic change takes place farther to the northwest than was observed for the Boatwright. The Boatwright and Britt carbonates are shown to be continuous through northwestern Oklahoma and across the northeastern part of the Texas Panhandle to the point at which they are truncated, as shown on this cross section.

Cross section B–B′ (Fig. 5) is a dip section, which intersects strike section A–A′ (Fig. 4) in T. 16 N., R. 21 W. From the southwestern end of cross section B–B′, the Boatwright and Britt carbonates can be correlated to their truncation points—first the Britt, and then the Boatwright. These units are carbonates throughout the area of this cross section, as its trace lies to the northwest of the point at which both units undergo a facies change from sandstone to carbonate. The Boatwright shale thins from 215 ft in the southwest to 60 ft toward the northeast, where an intervening limestone member that developed within the Boatwright shale unit accounts for 20 ft of the 60-ft gross thickness. As with the overlying Boatwright, Britt, and Cunningham members, the Boatwright shale is ultimately truncated just before the last log of the cross section. However, in the absence of truncation, the Boatwright shale is a regionally continuous and correlative marker unit between the underlying true Chester and the overlying Boatwright and Britt, being carbonates and/or sandstones.

Cross section C–C′ (Fig. 6) is another dip section, which intersects cross section A–A′ (Fig. 4) in Section 163, Blk. 43, H&TC Survey, Hemphill County, Texas, and traces the Boatwright shale, Boatwright carbonate, Britt carbonate, and Cunningham sandstone to the northeast to the point at which they are successively truncated in a manner identical to that observed on cross sections A–A′ (Fig. 4) and B–B′ (Fig. 5).

Cross section D–D′ (Fig. 7) is another dip section and ties to cross section A–A′ (Fig. 4) in Section 475, Blk. 43, H&TC Survey, Ochiltree County, Texas. The cross section's southwesternmost log is from Roberts County, Texas, and shows the Cunningham sandstone and Britt carbonate truncated and the Boatwright carbonate rising from the Anadarko basin toward its southwestern extent. The tie log to cross section A–A′

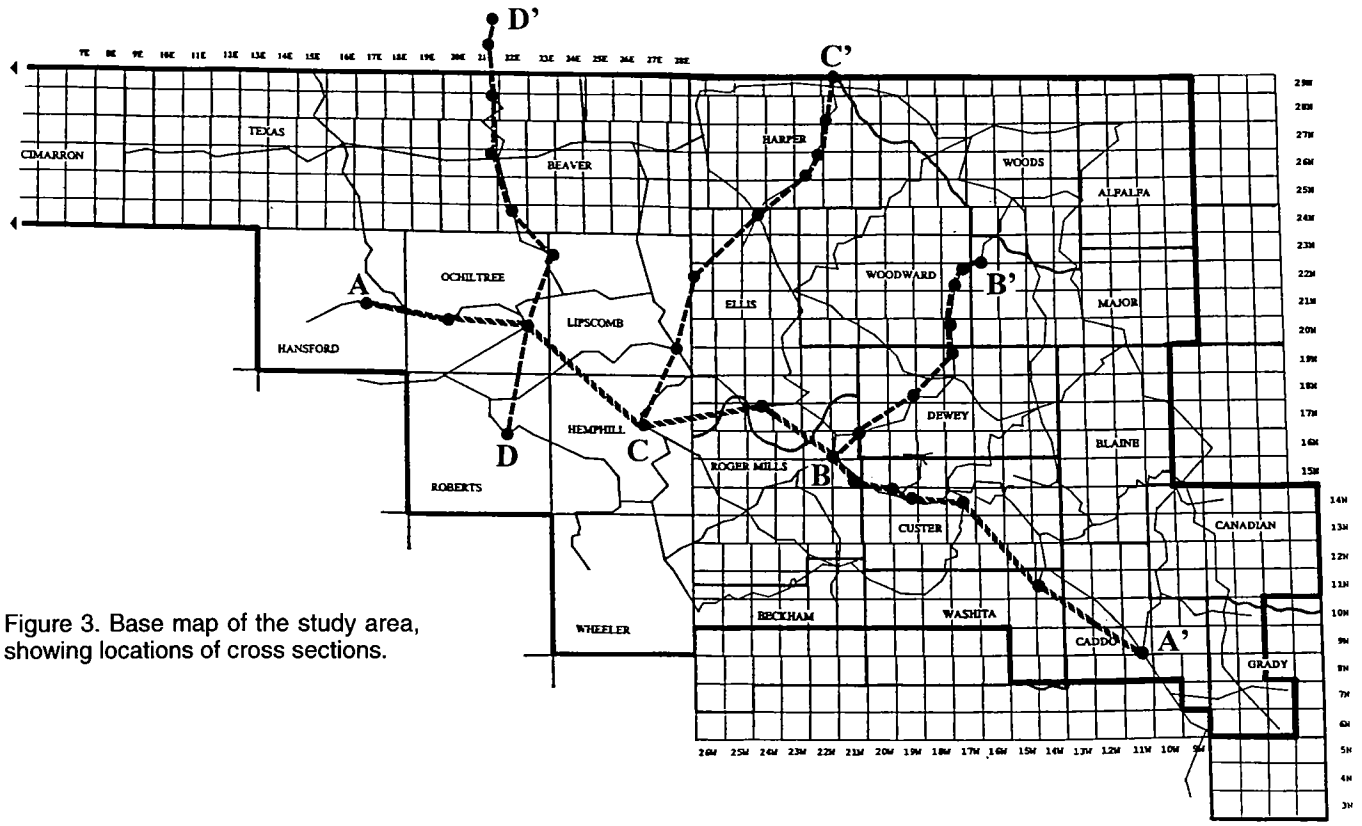

Figure 3. Base map of the study area, showing locations of cross sections.

(Fig. 4) shows the Cunningham sandstone truncated but also shows a full sequence of Boatwright and Britt carbonates near the thickest part of the Anadarko basin represented on this cross section. Cross section D–D′ progresses northward into Lipscomb County, Texas, and into the panhandle of Oklahoma and ultimately ends in Seward County, Kansas, where the Boatwright and Britt carbonates, as well as the Boatwright shale, are successively truncated.

Owing to the constraints of space, the cross sections presented here have no horizontal scale, and the wells are widely spaced. These sections are a distillation of literally thousands of miles of cross sections that have been constructed at IHS Energy Group. The logs included on the sections were chosen to clearly demonstrate specific points. Although, in certain aspects, correlations may not appear irrefutable, many additional logs between any two logs represented in the sections were used in the correlation process. Thus the well-to-well correlation of individual sandstone members is not intended to be taken literally but is only graphic in nature and intended to illustrate lithology.

A reallocated-production database has been completed for the northwestern part of Oklahoma, excluding the Oklahoma Panhandle. The Oklahoma Panhandle and Texas Panhandle portions of the database will be completed shortly but not in time for this publication. Therefore, Figure 8 is a map of northwestern Oklahoma, indicating wells that have produced from the Springer Group as herein defined. In general, Springer sandstone production, being from the Boatwright, Britt, and Cunningham, is limited to the southeastern quarter of the study area, with the exception of the Cunningham, which produces over the south half, having never developed a carbonate facies. Two northeast–southwest trend lines delineate the approximate facies changes from sandstone to carbonate for both the Boatwright and the Britt, with sand deposition to the southeast and carbonate deposition to the northwest. As the Britt and Boatwright carbonates are successively truncated, the productive trends of these two units are indicated as they are found in subcrop.

Figure 9, covering the same area as Figure 4, is a map showing true Mississippian Chester production. In the southeastern part of indicated Chester production, a full section of Chester rocks is approximately 300 ft thick just before the beginning of its subcrop, whereas, near the northwestern limit of the study area, a full section is usually 150 ft thick. The Chester is productive predominantly downdip from its ultimate truncation. Hydrocarbon trapping has occurred where the Chester first subcrops and/or slightly downdip of that point. Such hydrocarbon trapping is generally limited to the upper part of the Chester sequence. At a point where a well encounters the Chester near its ultimate truncation, the upper, potentially productive part has been truncated, and the remaining lower part typically is not productive.

SUMMARY AND CONCLUSIONS

Production within the study area has been allocated by IHS Energy Group to conform to a standardized nomenclature system in the study area, and this information has been used to generate a new database called Intelligent Reservoirs. For this effort, an extensive network of cross sections was generated to enhance the accuracy, detail, and consistency of the allocation process, resulting in nearly 3,000 mi of cross sections in support of this database.

The stratigraphic and facies relationships of the Springer and Chester Groups have been demonstrated. In the case of the Boatwright and Britt carbonates, the definition of these individual units and their separation from true Mississippian Chester limestone give additional, and heretofore unavailable, detail and insight into the reservoir production data, as shown in Figure 10. Additionally, an understanding of these relationships is necessary for the proper mapping of these units within the study area.

It is anticipated that the increased accuracy, detail, and consistency of the allocated production, as well as the stratigraphic and facies relationships developed by this study, will aid in future exploration/exploitation endeavors.

ADDENDUM

When this paper was written, the authors were employees of IHS Energy Group in the Reservoir Geology Division. Prior to publication of this paper, Geological Data Services (GDS), Addison, Texas, purchased the Reservoir Geology Division, including all referenced cross sections and databases. Currently, Hendrickson, Smith, and Woods are consultants to GDS; Hogan and Willey are independent consultants.

Reservoir ID® is a database with geologically defined producing reservoirs plus State-reported producing reservoirs, accompanied by current production data.

A Reservoir Characterization database contains more than 120 parameters, including values for multiple thickness and porosity, water saturation, pressure, cumulative production, ultimate recovery, current and ultimate drainage, and other geological and engineering data.

REFERENCES CITED

Hendrickson, W. J.; Smith, P. W.; and Williams, C. M., 1996a, Regional correlations and reservoir characterization studies of the Pennsylvanian System in the Anadarko basin area of western Oklahoma and the panhandle of Texas: Transactions of the 1995 American Association of Petroleum Geologists, Mid-Continent Section Meeting, Tulsa Geological Society, p. 100–108.

Hendrickson, W. J.; Smith, P. W.; Williams, C. M.; and Woods, R. J., 1996b, A regional correlation and production allocation project within the Oklahoma portion of the Anadarko basin and shelf with a specific discussion of the Springer and Chester Groups: Shale Shaker, September/October, v. 47, no. 2, p. 31–41.

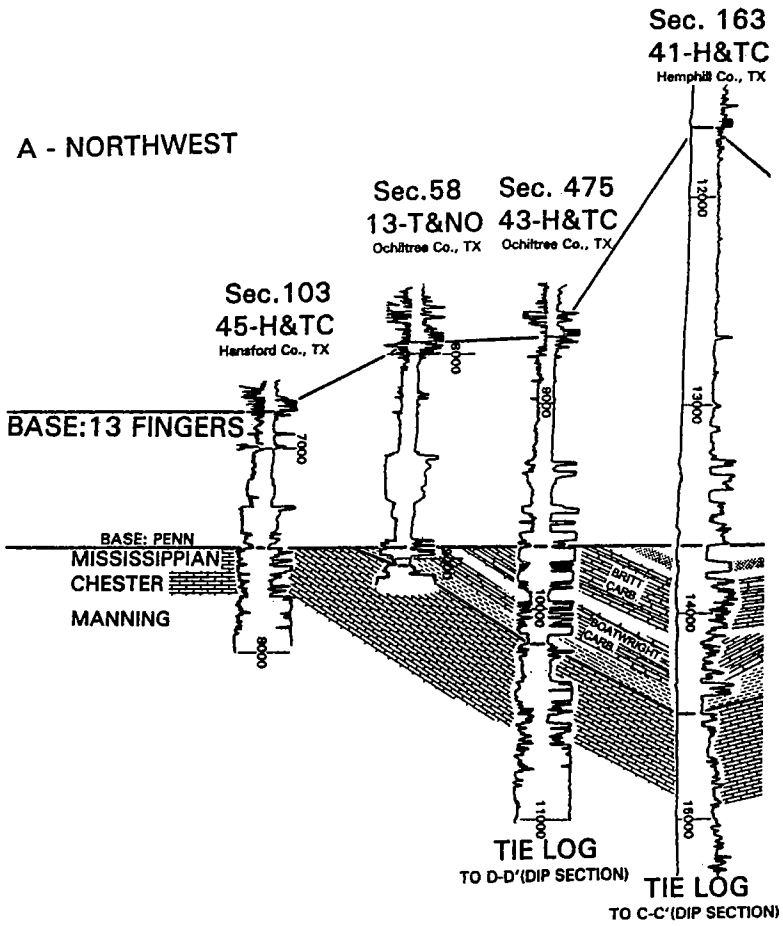

Figure 4. Cross section A–A′ *(continued on facing page)*, from northwest to southeast, is a dip section in its northwesternmost part and then becomes an approximate strike section. Line of section shown in Figure 3. See text for further explanation.

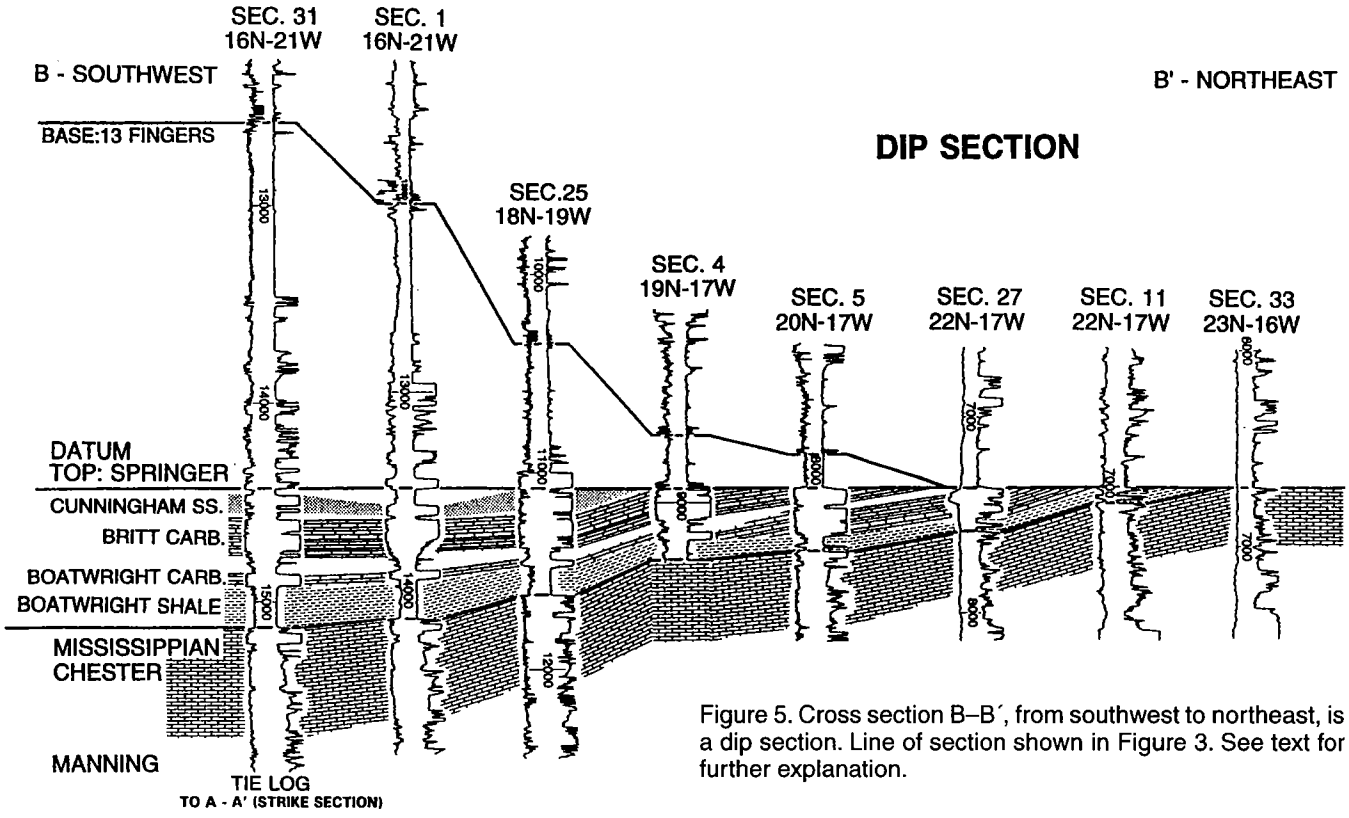

Figure 5. Cross section B–B′, from southwest to northeast, is a dip section. Line of section shown in Figure 3. See text for further explanation.

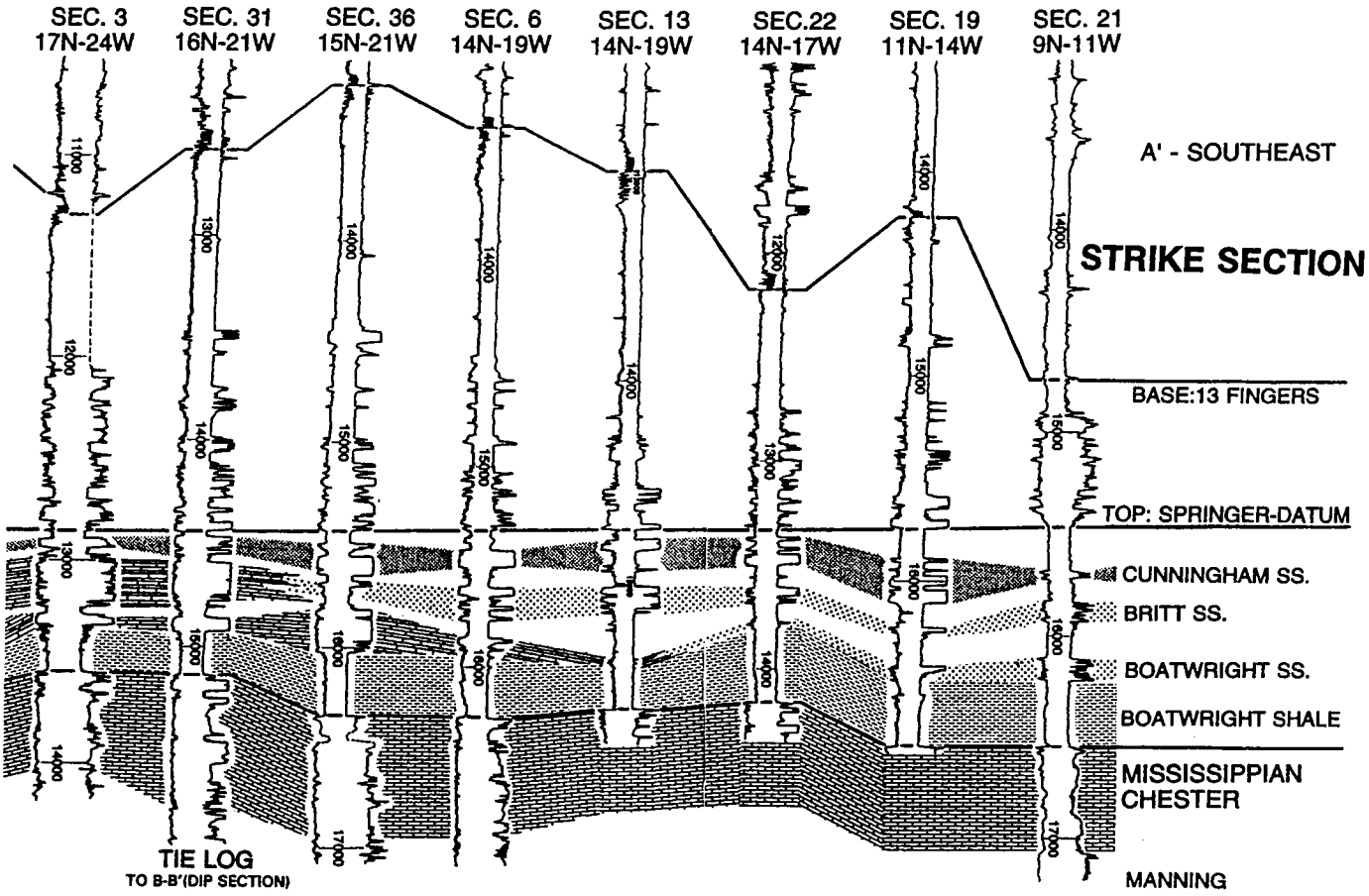

Figure 4 *(continued)*.

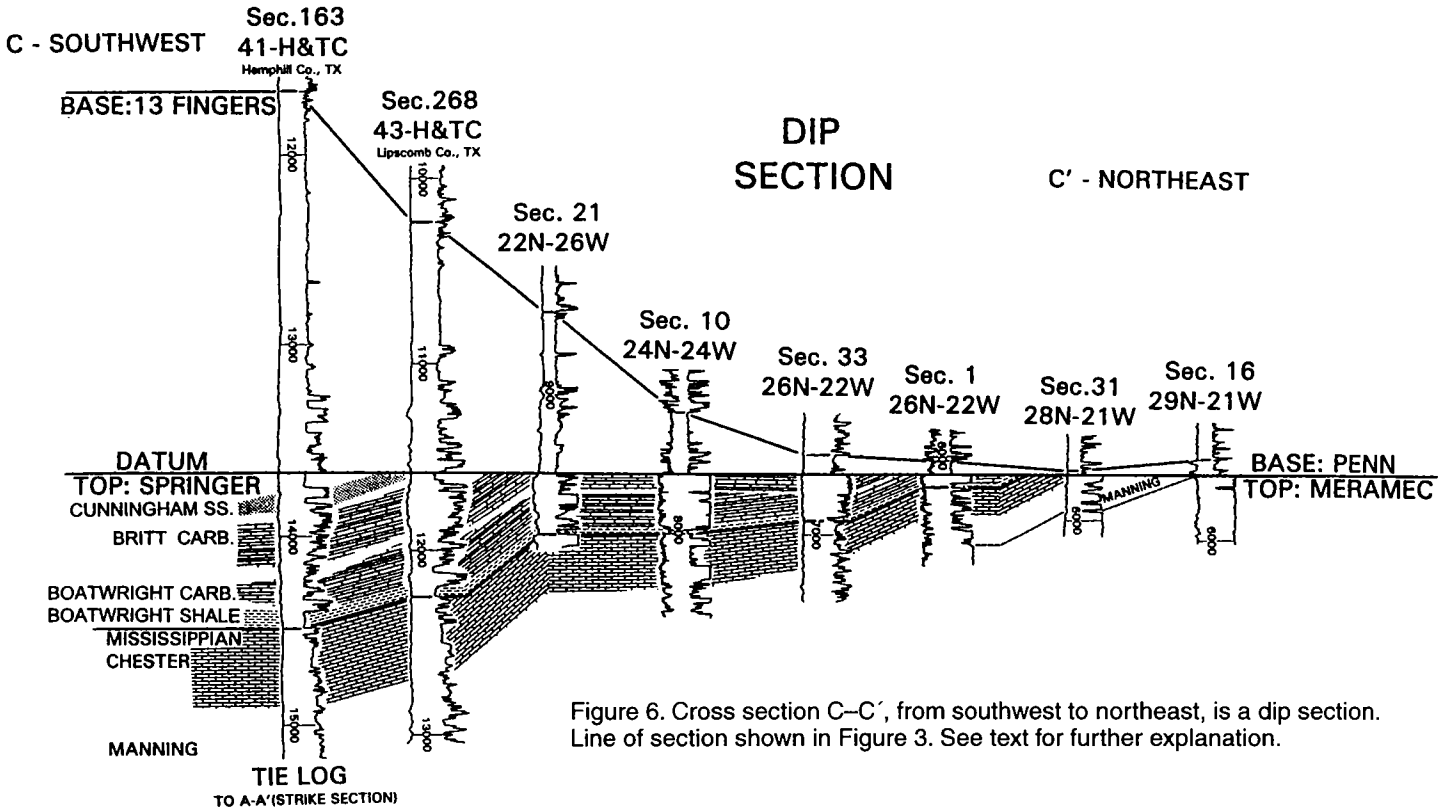

Figure 6. Cross section C–C′, from southwest to northeast, is a dip section. Line of section shown in Figure 3. See text for further explanation.

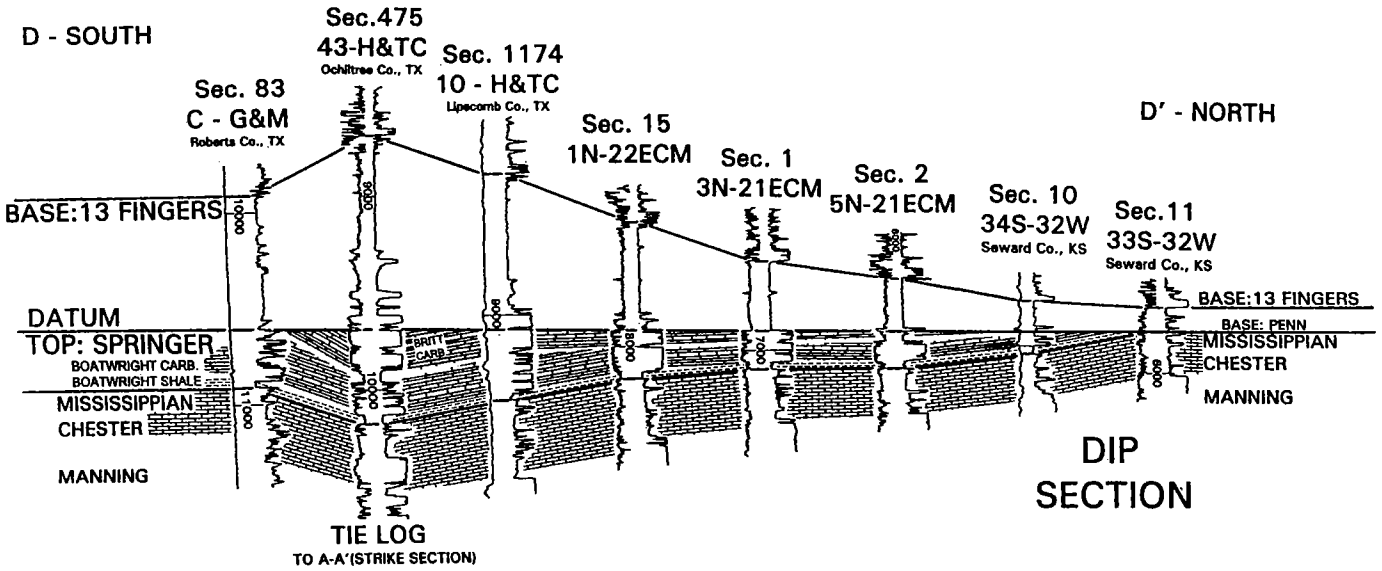

Figure 7. Cross section D–D′, from south to north, is a dip section. Line of section shown in Figure 3. See text for further explanation.

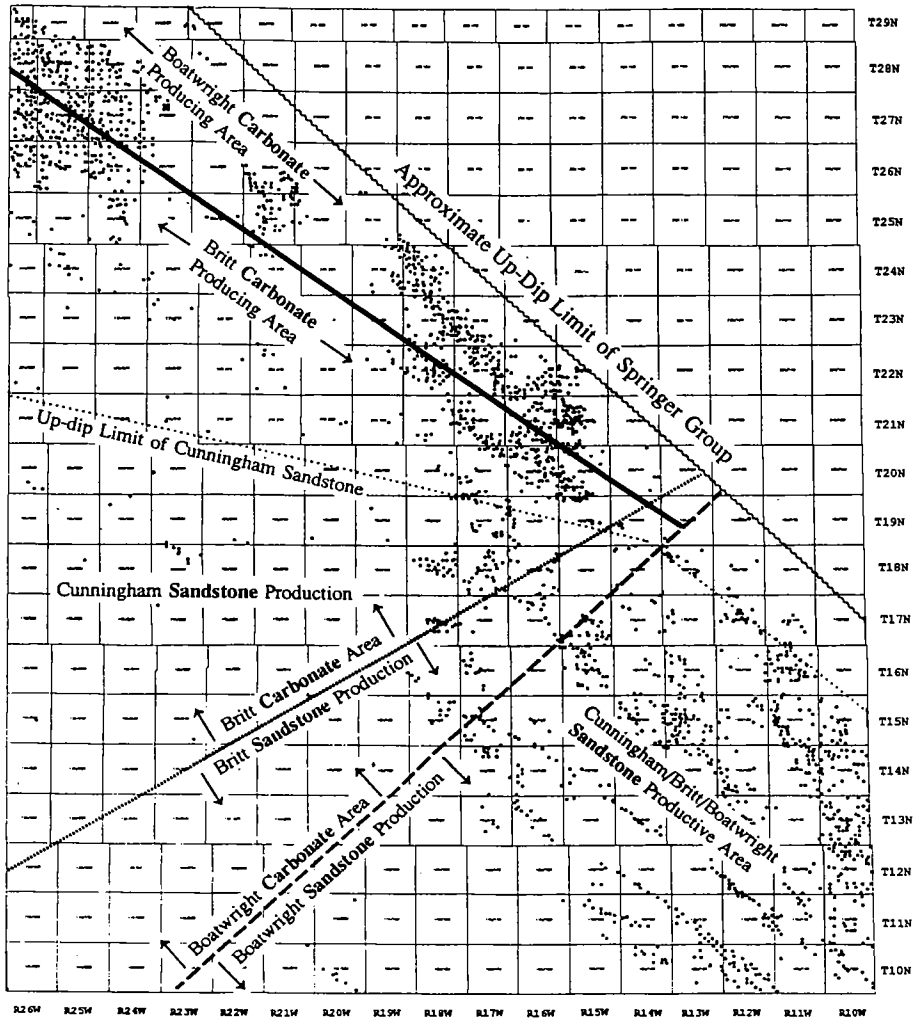

Figure 8. Generalized Springer production map of northwestern Oklahoma, showing areas where Boatwright, Britt, and Cunningham sandstones are productive and where Boatwright and Britt carbonates are productive. Northeast–southwest trend lines delineate approximate facies changes of the Boatwright and Britt from sandstone to carbonate.

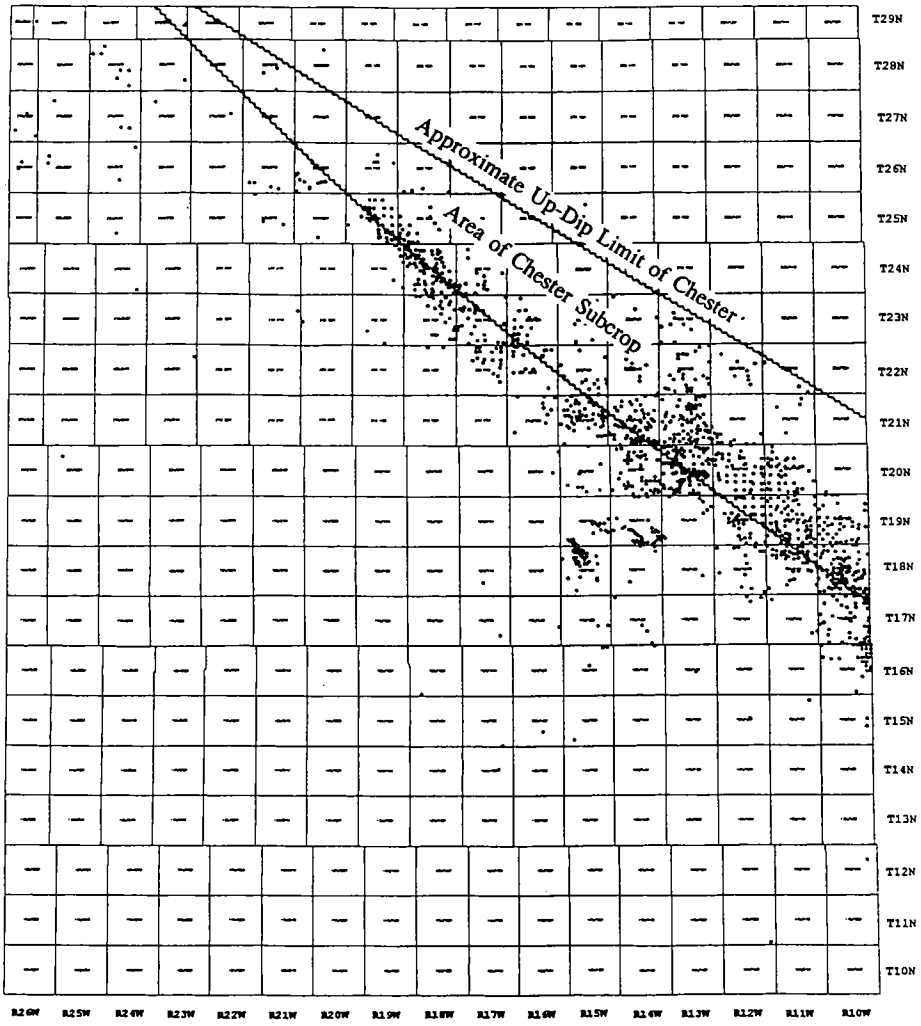

Figure 9. Map of northwestern Oklahoma showing wells producing from true Chester reservoirs.

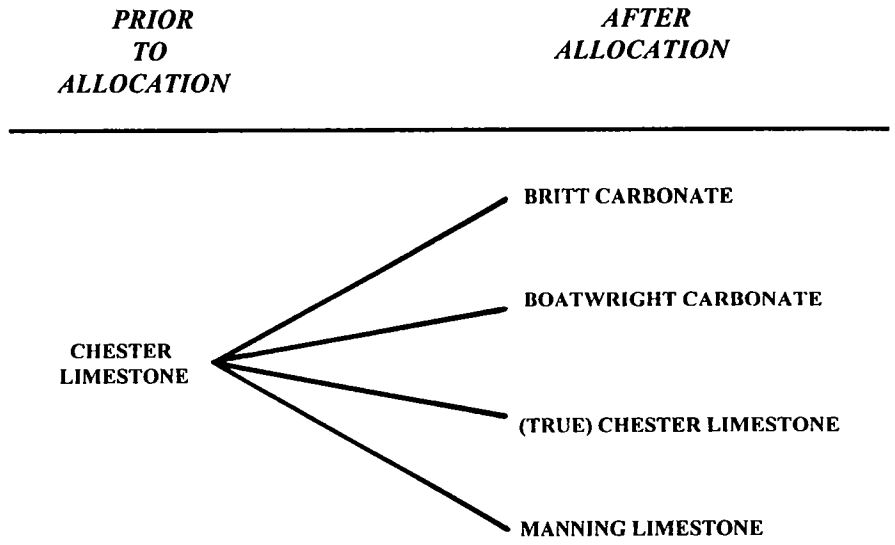

Figure 10. Diagram illustrating corrections in nomenclature of stratigraphic units whose production was formerly allocated to Chester limestone.

Smith, P. W., 1996, Anadarko basin statistical study: gas well recovery -vs- depth in the Anadarko basin of western Oklahoma: Gas Research Institute, Chicago, GRI Report no. GRI-96/0196, 65 p.

Smith, P. W.; Hendrickson, W. J.; and Williams, C. M., 1996, Regional correlations and reservoir characterization studies of the Springer Group in the Anadarko basin area of western Oklahoma: Transactions of the 1995 American Association of Petroleum Geologists, Mid-Continent Section Meeting, Tulsa Geological Society, p. 116–126.

Smith, P. W.; Hendrickson, W. J.; Williams, C. M.; and Woods, R. J., 2000, Stratigraphic relationships of Springer and Chester Groups within the Oklahoma portion of the Anadarko basin and shelf: a clarification, *in* Johnson, K. S. (ed.), Platform carbonates in the southern Midcontinent, 1996 symposium: Oklahoma Geological Survey Circular 101, p. 197–207.

Williams, C. M.; Hendrickson, W. J.; and Smith, P. W., 1996, Regional correlation and reservoir characterization studies of the Morrow Group in the Anadarko basin area of western Oklahoma: Transactions of the 1995 American Association of Petroleum Geologists, Mid-Continent Section Meeting, Tulsa Geological Society, p. 109–115.

Significance of Accurate Carbonate-Reservoir Definition and Delineation: Chester and Springer Carbonates

Paul W. Smith, Walter J. Hendrickson, and Ronald J. Woods
IHS Energy Group[1]
Oklahoma City, Oklahoma

ABSTRACT.—Reservoir definition is often vague or poor even in mature areas, owing to misidentified angular unconformities, facies changes, or a poor understanding of the relationships in deep parts of a basin that were undrilled until late in its development history. Typically, no mechanism exists to correct misnamed reservoirs, as such an effort is often dismissed as being purely academic, insignificant, or unnecessary.

As the result of a recent Gas Research Institute project (GRI96/0196), a classic example of the significance of accurate reservoir definition and delineation was identified. A total of 1,232 wells were reported as having been completed in Chester (Upper Mississippian) reservoirs. After detailed correlations were made, it was demonstrated that only 221 completions could be attributed to the Chester. Consequently, the ultimate recovery of the Chester diminished from 1,781 to 277 billion cubic feet of gas. Most of the gas was being produced from carbonate reservoirs belonging to the overlying Springer Group and could be identified as such through regional stratigraphic correlations. Although found at comparable depths, the carbonate reservoirs belonging to the Springer Group typically produce 50–80% more gas per completion than those of the Chester.

This paper presents findings that explain the significance of the disparity between the misidentified reservoirs. Opportunities exist for significant infield development, trend extensions, and further development of newly recognized trends.

PURPOSES AND METHODOLOGY

The purposes of this study were to (1) confirm the distinction between Upper Mississippian carbonates and overlying Springer carbonates (uppermost Mississippian–lowermost Pennsylvanian), (2) identify any significance of that distinction and its impact on continued operation and development of these reservoirs, and (3) examine the cause(s) of productivity disparities between the different reservoirs. For a detailed discussion on the methodology and the results of the geologic differentiation of the Britt and Boatwright (Springeran carbonates) from the underlying Chester and Manning carbonates, refer to Hendrickson and others (2001, this volume). This paper examines the significance of differentiating oil and gas production from these two carbonate groups and its impact on present and future production.

A database containing reservoir characteristics was generated through detailed well-log analysis. In using the database, we examined the relationships and influences on ultimate recovery derived from the following reservoir parameters: thickness, porosity, water saturation, initial pressure, and drill-pattern spacing. By examining the reservoir characteristics of the Britt, Boatwright, Chester, and Manning units, the cause(s) of increased productivity from the Springer carbonates as opposed to the underlying Mississippian carbonates could be established. For this study, we distinguished the difference between "perforated" thickness and "saturated" thickness. Figure 1 illustrates the difference in thickness definitions. Corresponding values for perforated porosity and saturated porosity were recorded to determine reservoir volumes.

STUDY AREA

The study area covers parts of the Anadarko basin and shelf area (Fig. 2). Although most of the Anadarko basin in Oklahoma and Texas has been examined, this paper deals with an area specifically defined as containing Ts. 10–29 N., Rs. 10–26 W. Identical nomenclature problems were noted for the Oklahoma Panhandle and Texas Panhandle areas.

Figure 3 shows the stratigraphic section and demonstrates the vague and incorrect nomenclature observed. For detailed correlations and a complete description, see the paper by Hendrickson and others (2001, this volume).

[1]See Addendum on page 106.

Smith, P. W.; Hendrickson, W. J.; and Woods, R. J., 2001, Significance of accurate carbonate-reservoir definition and delineation: Chester and Springer carbonates, *in* Johnson, K. S. (ed.), Silurian, Devonian, and Mississippian geology and petroleum in the southern Midcontinent, 1999 symposium: Oklahoma Geological Survey Circular 105, p. 99–107.

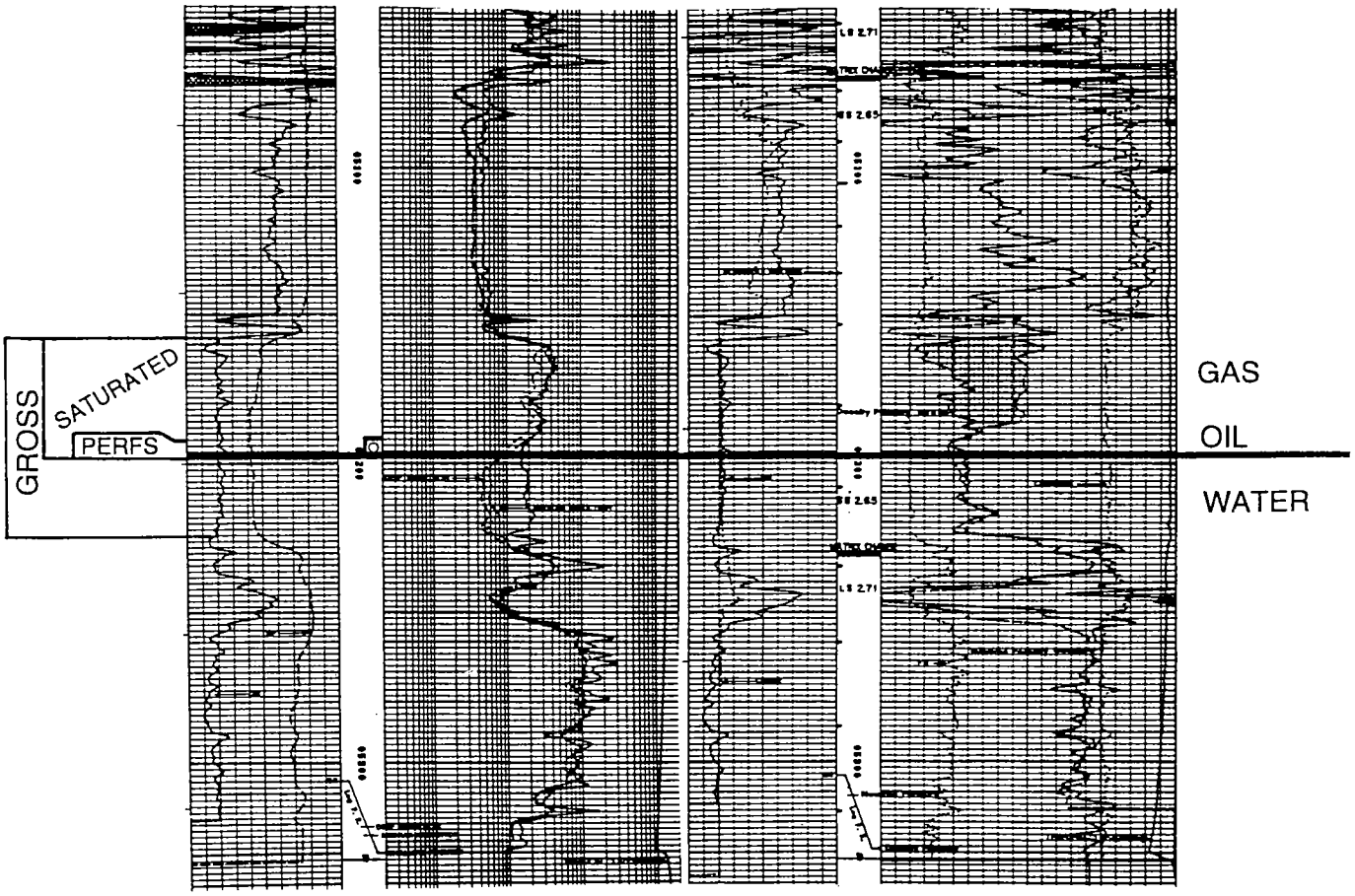

Figure 1. Well log illustrating an Anadarko basin carbonate reservoir. Saturated reservoir thickness and perforated reservoir thickness are indicated, as are the gas- and oil-productive portions and the oil–water contact.

PREVIOUS WORK

Papers published by Smith and others (1996), Hendrickson, Smith, and Williams (1996a), Hendrickson, Smith, Williams, and Woods (1996b), and Williams and others (1996) identify significant nomenclature problems in productive reservoirs in the Anadarko basin (Springeran, granite wash, and Morrowan). The magnitude and significance of these nomenclature problems are quantified by Smith (1996) in a final report prepared for the Gas Research Institute (GRI-96/0196). As reported by Smith (1996), 1,232 wells were reported as having been completed in the Chester (Mississippian), whereas, after detailed correlations, it was demonstrated that only 221 completions could be attributed to the Chester. Consequently, the ultimate recovery from the Chester diminished from 1,781 to 277 billion cubic feet of gas (BCFG). Most of the gas was being produced from carbonate reservoirs belonging to the overlying Springer Group and could be identified as such through regional stratigraphic correlations. A significant difference in ultimate recovery was identified (see Fig. 4). Smith (1996) suggested that reservoir volume, not differences in reservoir pressure, likely caused the difference in ultimate recovery between the Springer

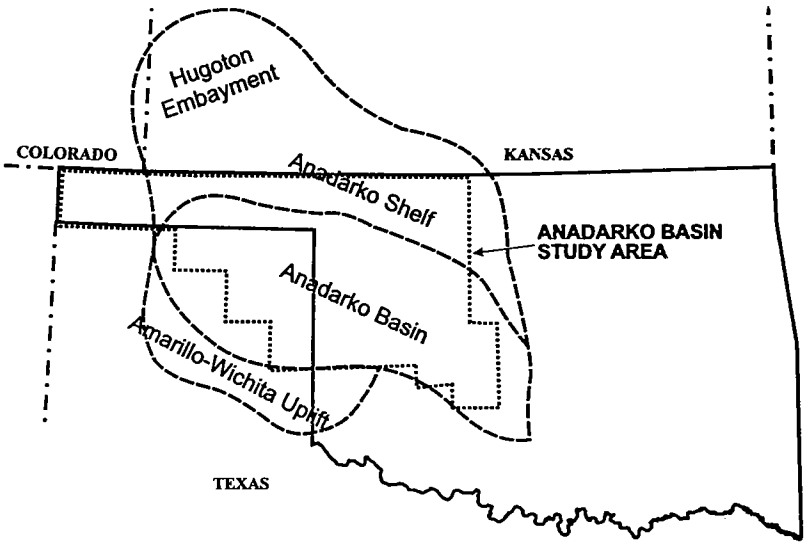

Figure 2. Index map of Oklahoma and the Texas Panhandle, showing the Anadarko basin study area (dotted outline).

carbonates and the underlying Mississippian carbonates (see Fig. 5).

PRODUCTION MAP—BEFORE

A production map showing the geographic relationships of five reservoirs (Cunningham, Britt, Boatwright, Chester, and Manning) prior to evaluation is shown in Figure 6. The top of the Chester section is commonly considered to be the first carbonate section below the clastic Morrow interval. Because this area was developed from the shelf toward the basin, early recognition and separation of the four carbonate reservoirs was difficult. This difficulty arose from not correctly recognizing that *four* carbonate reservoirs were truncated in the productive trend—not just one. Correlations from the deep basin enabled recognition of the true relationships for this trend, which contained some 2 trillion cubic feet of gas.

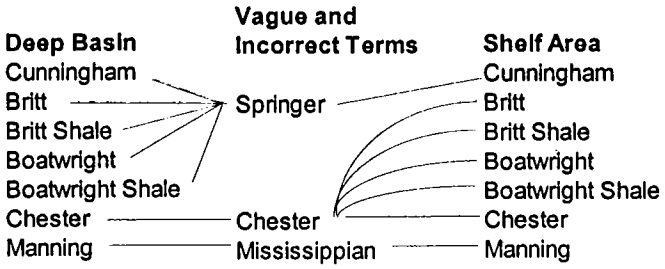

Figure 3. Stratigraphic sequence of Upper Mississippian (Chester) and overlying Springer units in the Anadarko basin and shelf areas of northwestern Oklahoma, showing vague, confusing, and incorrect nomenclature observed.

As shown on this "before" map, the Boatwright and Britt completions north of Dewey County were misidentified as Chester. Most of the completions from the Manning in Woods County were also misidentified as Chester. Even in the clastic section of the Springer Group (south half of map), improper reservoir identification masks producing trends or identifies trends that do not exist. The "Springer" trend straddling the Custer–Roger Mills county line actually produces from the Skinner sand (Pennsylvanian, Cherokee Group).

PRODUCTION MAP—AFTER

Accurate reservoir definition and delineation make useful production maps. Producing trends of the same five reservoirs shown on the map of Figure 6 are shown on the corrected map of Figure 7. The Boatwright shale can be mapped throughout the basin, and separates the Chester limestone from the overlying Boatwright carbonates of the Springer Group. Typically, the Springer Group consists of a clastic section. It has been demonstrated, however, that each of the three members has developed a carbonate facies within the basin. The Britt and Boatwright exhibit this change in the western and northern parts of the basin. Although not found productive, the Cunningham (Springer) has become a carbonate section in the western part of the basin. In northwestern Oklahoma, the Britt, Boatwright, Chester, and Manning carbonate reservoirs

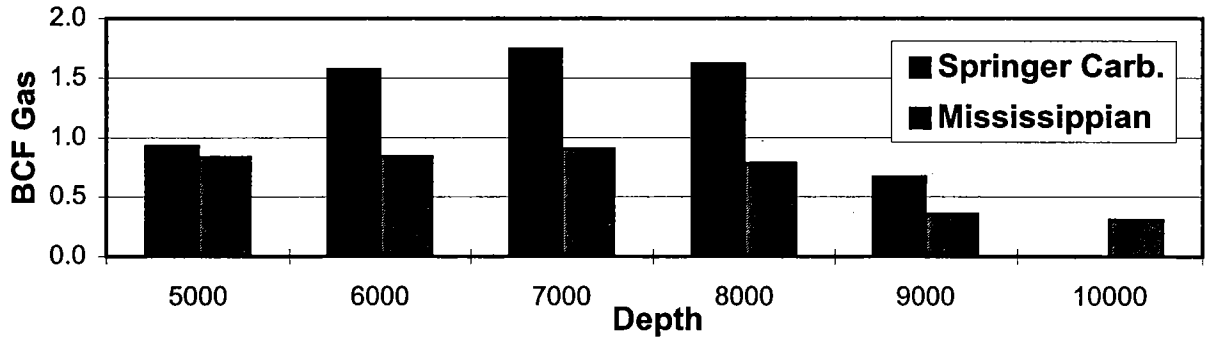

Figure 4. Average ultimate gas recovery versus depth for Springer carbonates and underlying Mississippian carbonates.

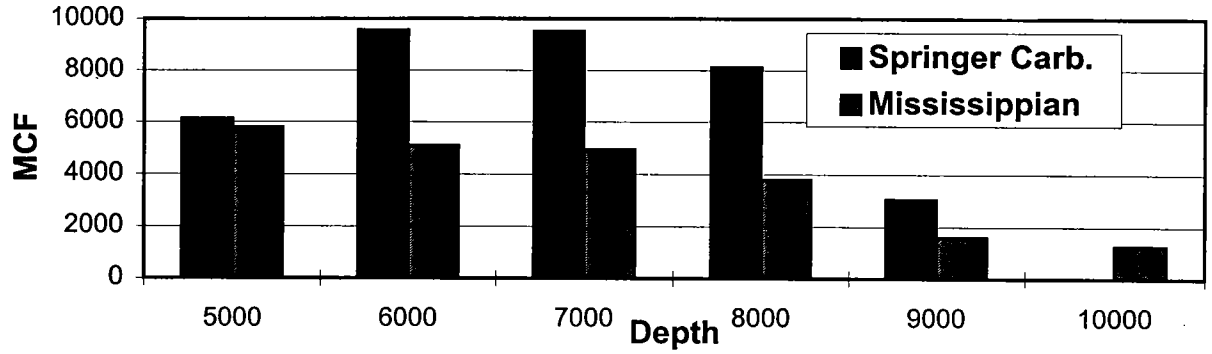

Figure 5. Average required reservoir volume versus depth for Springer carbonates and underlying Mississippian carbonates.

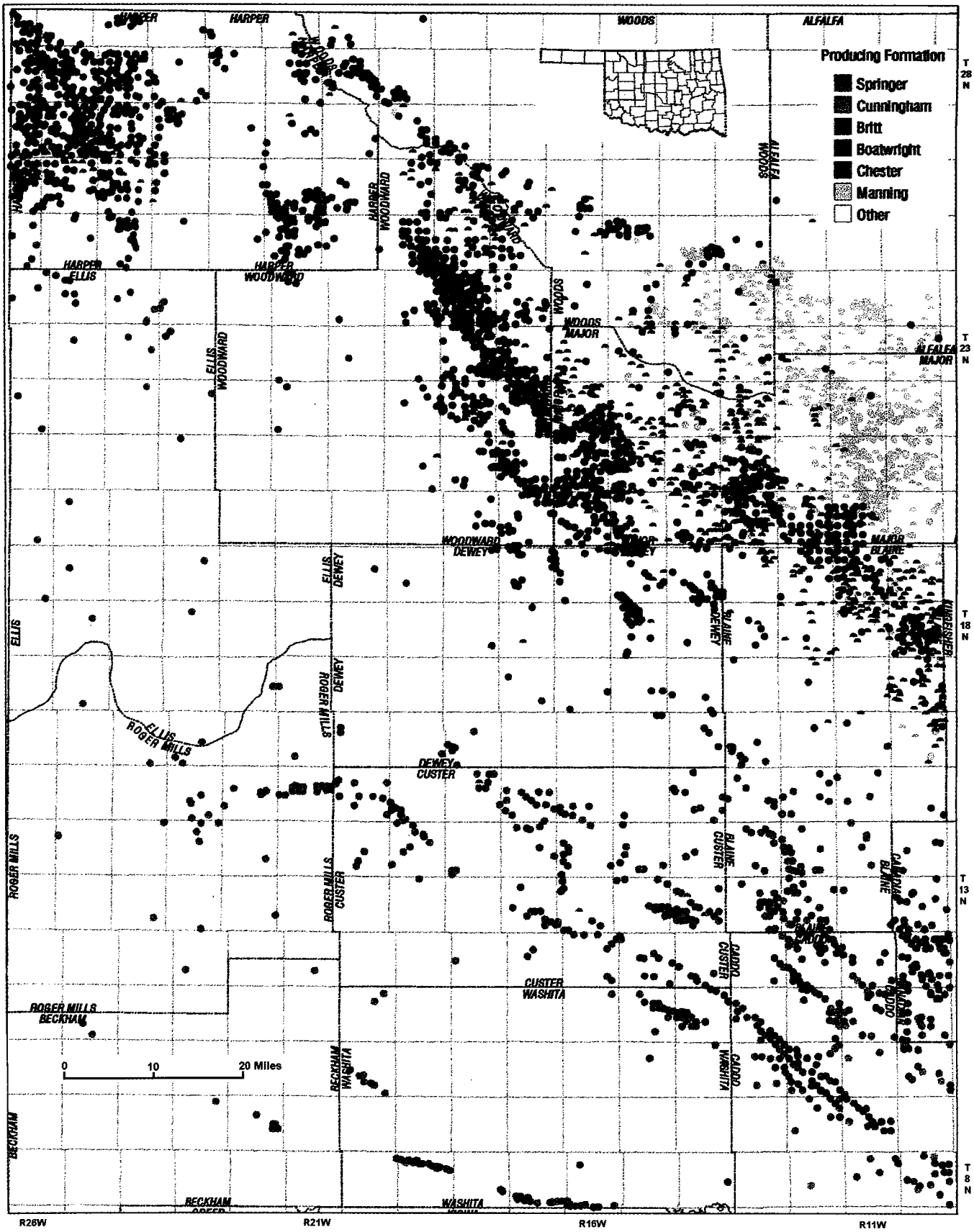

Figure 6. Petroleum production from Springer/Chester reservoirs in northwestern Oklahoma. Producing reservoirs on this map show information reported to the Oklahoma Corporation Commission. Map prepared by IHS Energy Group.

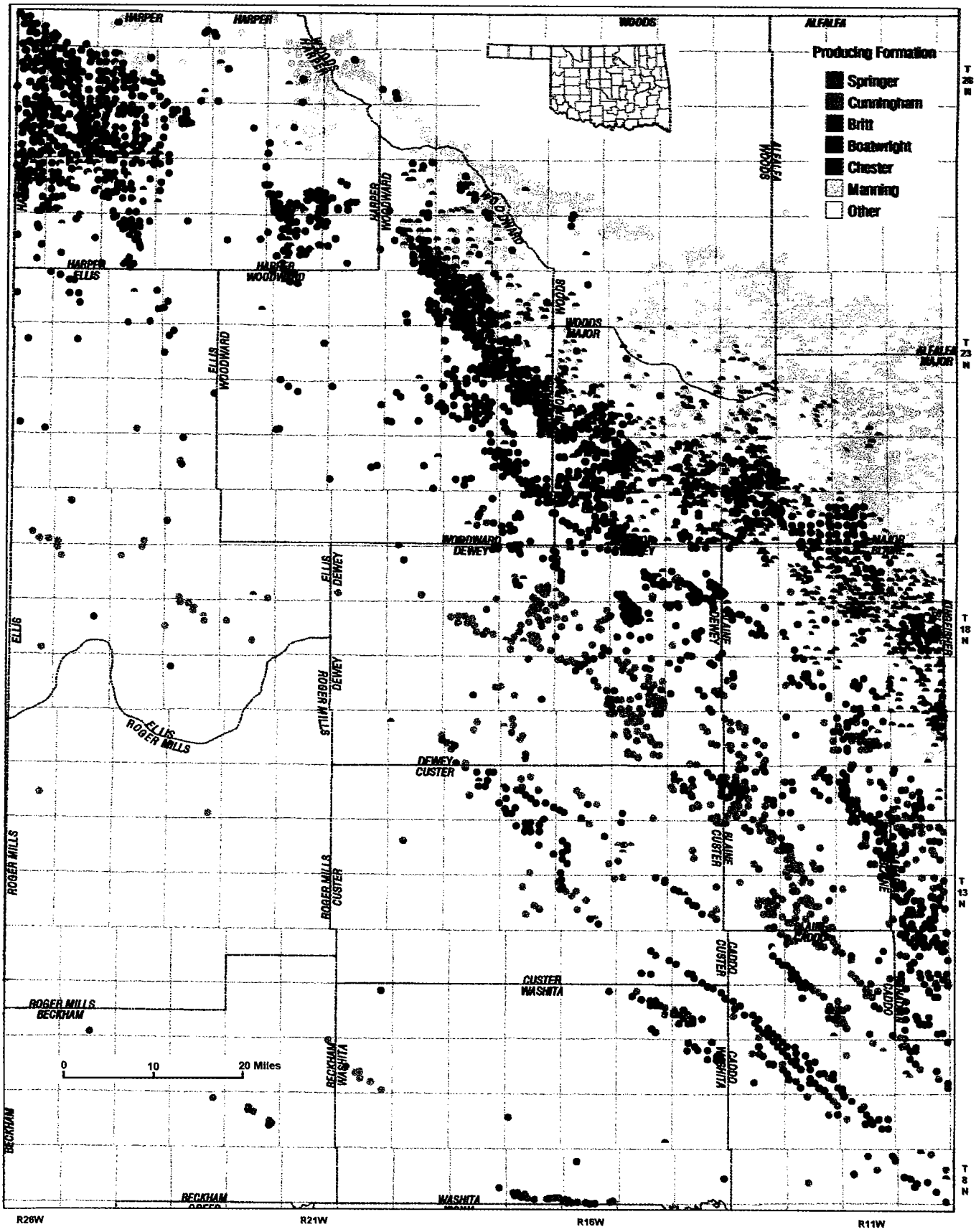

Figure 7. Petroleum production from Springer/Chester reservoirs in northwestern Oklahoma. Producing reservoirs on this map show revised data resulting from accurate definition and delineation of the reservoirs. Map prepared by IHS Energy Group.

produce as the result of a large stratigraphic trap. In the area shown by the map (Fig. 7), the northern and northeastern edges of production correspond with the truncated edge of each reservoir. Accurate production maps suggest areas with possible exploration and development opportunities. Because the true Chester is the poorest producing reservoir in this sequence, it is important to identify which reservoir is actually productive. Many wells may not have been drilled deep enough to evaluate all four reservoirs thoroughly. Some of the more obvious exploration and development trends are listed as follows:

Exploration trends:

Southeast corner of Harper County: Boatwright and Britt;

South-central Harper County: Boatwright and Britt;

Downdip from the Boatwright "island" in northern Woodward County: Britt.

Development trends:

Corner of Woods, Major, and Woodward Counties: Chester and Manning;

Gaps in Manning truncation trend: Woods County;

Northwestern Harper County: Chester and Manning.

RESULTS

Figure 8 compares the average thicknesses of the four reservoirs studied. The four reservoirs typically have about 20–30 ft of interval perforated. However, ~20% more of the reservoir is perforated in the Springer carbonates than in the underlying Mississippian carbonates. Additionally, the Springer carbonates have ~60% greater saturated thickness from which to produce oil and gas. Surprisingly, about half the saturated interval of the reservoirs in the Springer carbonates is not perforated.

From examination of the relationships between the saturated thickness and the perforated thickness, the first question that might come to mind is, Does the non-perforated section have sufficient porosity to warrant perforations?

The perforated porosities range from about 7.5% to 9% within the four reservoirs (Fig. 9). The average perforated porosity of the Mississippian carbonates is ~13% better than in the Springer carbonates. Interestingly, most of the non-perforated (but hydrocarbon-saturated) Springer section does have sufficient porosity to be productive. This observation raises the question, Does the non-perforated porosity contribute to overall production, or do any hydrocarbons it may contain remain in the ground?

Water saturation (S_w) was determined for each well evaluated in this study. Springer carbonates have a higher water saturation than do Mississippian carbonates. Wells producing from the Britt, Boatwright, and Chester had nearly equivalent water saturation: 28%, 29%, and 32%, respectively. The average water saturation in the Manning was substantially higher—38%. Figure 10 illustrates the average water saturation for each reservoir.

A majority of the wells in this study are productive as a result of a regional truncation trap of the Britt, Boatwright, Chester, and Manning (in succession). Wells producing from the Manning reservoir are shallower than those producing from the other reservoirs. This explains the observation that the Manning has the lowest average initial pressure. However, some fields produce from the Chester in structural traps that are deeper than the Britt truncation edge. This skews the initial pressure data into showing that the Chester has the highest initial pressure. Most of the Chester completions have initial pressures lower than those of the Boatwright and higher than those of the Manning. Figure 11 compares the initial pressures observed in the study area.

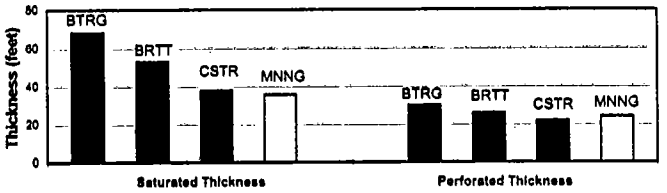

Figure 8. Comparison of average thicknesses of Springer/Chester reservoirs. *BTRG* = Boatwright; *BRTT* = Britt; *CSTR* = Chester; *MNNG* = Manning.

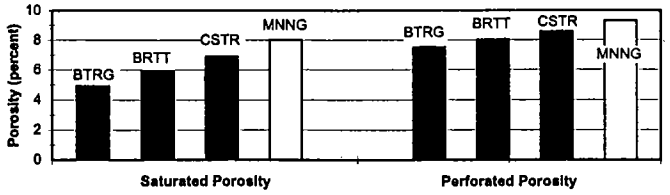

Figure 9. Comparison of average porosity of Springer/Chester reservoirs. See Figure 8 caption for explanation of abbreviations.

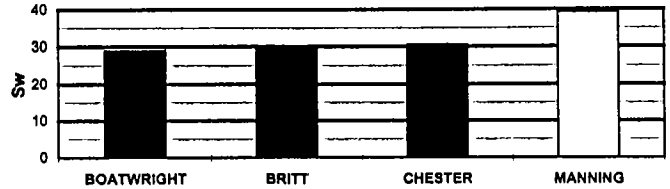

Figure 10. Comparison of average water saturation (S_w) of Springer/Chester reservoirs.

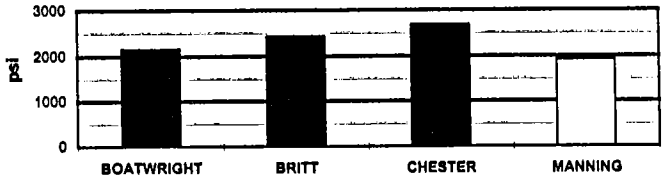

Figure 11. Comparison of average initial pressure (psi) of Springer/Chester reservoirs.

Hydrocarbon saturation per acre was calculated using the following formulas: thickness × porosity × (1.00 – water saturation). As shown in Figure 12, the Springer carbonates have considerably more saturated-reservoir volume. The Springer Britt and Boatwright carbonates contain ~50% more hydrocarbons per acre than the underlying Mississippian carbonates. This observation confirms the hypothesis provided by Smith (1996) that the disparity in production must be due to differences in reservoir volume. The Britt and Boatwright carbonates also contain more hydrocarbons per acre of perforated interval. A quick confirmation of these observations is provided by comparing average ultimate recovery and gas recovered per pound of pressure drawdown (Figs. 13, 14). The data indicate that Springer carbonates produce about 70% more gas, primarily because they have significantly greater reservoir capacity. Increased average reservoir pressures over those observed for the underlying Mississippian reservoirs (excluding deep Chester wells) increase the separation in reservoir capacity.

The gas recovery per pound of pressure drawdown was examined by two methods—pressure decline and MCF/psi (see Fig. 14). Using the pressure-decline method, the first- and last-reported pressure tests were compared, and the amount of gas produced per pound of pressure depletion was calculated (gas production divided by change in pressure). The MCF/psi was calculated using a calculated ultimate recovery divided by initial pressure. There exists a large degree of similarity between the trend in saturated hydrocarbon capacity (Fig. 12) and pressure decline (Fig. 14). There is ~18% more hydrocarbon capacity in the Boatwright than in the Britt. Similarly, the Boatwright yields ~18% more gas per pound of pressure depletion. Similarly, a difference slightly more than 50% can be observed between the Chester and Britt in both graphs.

About the same amount of reservoir is perforated, and fairly similar porosity is perforated; yet the Springer carbonates produce significantly more gas per completion. One might expect the relative recoveries to mimic the perforated reservoir capacity, or mimic perforated reservoir capacity multiplied by initial pressure. Interestingly, the best average production is found in the Britt reservoirs; yet the Boatwright has the most capacity (see Figs. 12, 13). The data suggest that Boatwright completions may not be optimized. The relationships in average ultimate recovery do not mimic hydrocarbon capacity; however, once initial pressure is considered, the disparity is partially explained. Even considering initial pressure, though, the average ultimate recovery from the Boatwright does not conform to these observations, lacking an average of 0.75 BCFG per completion. There exists a noticeable similarity between MCF/psi in Figure 14 and average ultimate recovery (Fig. 13). The recovery per pound of pressure depletion suggests that many Boatwright wells may have been prematurely abandoned. Because of reduced pressures in the Manning, Manning completions yield only 10% more gas than Chester completions, even though the Chester contains 25% more reservoir volume.

The disparity in ultimate recovery should also be considered in economic terms. Although the average Manning well yields only 10% more gas than the average Chester completion, the Manning is nearly two times more profitable to exploit than the Chester. Figure 15 shows a comparison of economic viability through a return on investment in exploiting these four reservoirs. These calculations are based on increased drilling and completion costs with depth, $2.00/MCF gas, 81.25% NRI leases, and 7% severance tax. Operational costs were not factored into the return on investment.

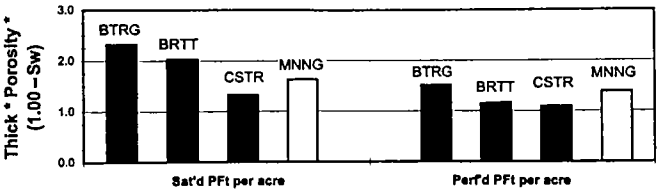

Figure 12. Comparison of hydrocarbon capacity per acre of Springer/Chester reservoirs. See Figure 8 caption for explanation of abbreviations.

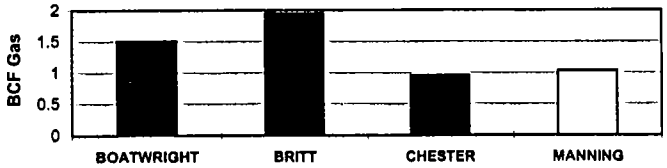

Figure 13. Comparison of average ultimate recovery from Springer/Chester reservoirs.

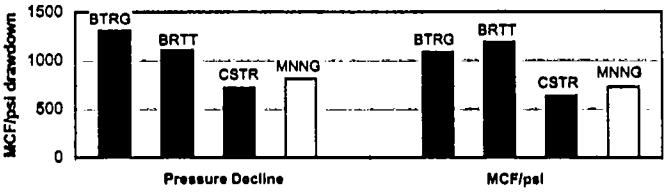

Figure 14. Gas recovery per pound of pressure drawdown from Springer/Chester reservoirs. See Figure 8 caption for explanation of abbreviations.

Figure 15. Comparison of economic viability of Springer/Chester reservoirs.

CONCLUSIONS

Although considerable effort is required to accurately delineate and define the various oil- and gas-producing reservoirs at the Mississippian–Springeran contact, accurate reservoir definition and delineation are important. These accurate divisions provide better methods for comparing expectations and results. Maps showing accurate production trends can identify gaps in exploration fairways, possibly identifying areas where field extensions are possible. On a smaller scale, gaps in field development emerge, indicating areas for possible infield well locations. In contrast to the use of accurate data for reservoir definition, the use of data reported to the Oklahoma Corporation Commission can be seriously misleading.

Springer carbonates produce ~70% more gas per completion at equivalent depths. In addition to accurate reservoir definition, detailed well-log analysis of the four reservoirs identified causes of the differences in productivity. Springer carbonates have greater reservoir volumes saturated with hydrocarbons, which cause them to be more productive than underlying Mississippian carbonates.

Accurate reservoir definition allows correct comparisons of well populations. Originally reported as "Chester," Britt carbonate completions yield nearly 2 BCFG per completion, twice that of the true Chester. Such accuracy permits underachieving, normal, or overachieving completions to be identified. A 1-BCF well might be identified as producing from the Britt, not the Chester. A 1-BCF completion in the Chester is average, but well below average for the Britt. Thus, such a well may be a candidate for stimulation to bring it up to Britt standards (rather than Chester standards). Conversely, money can be wasted in an attempt to stimulate a 1.5-BCF Chester well when it is incorrectly compared to other 2-BCF "Chester" wells that are actually producing from the Britt.

The data resulting from detailed log analysis demonstrate that ultimate recovery and gas recovery per pound of pressure depletion both mimic the observed relationships in saturated volume, not perforated volume. Therefore, non-perforated intervals adjacent to perforated intervals are likely being drained. However, non-perforated intervals separated by shale or tight sequences may not be drained. Good wells may not be optimized as previously believed. The data suggest that the Boatwright carbonate may not be optimally developed and that many completions may have been prematurely abandoned. Without accurate reservoir definition and detailed log analysis, critical porosity assumptions for completions may be overstated. Thus, recompletion opportunities may exist. Productive intervals may have been overlooked.

Accurate carbonate-reservoir definition and delineation can lead to improved strategies for exploration, exploitation, acquisitions, and divestitures. In addition, a basinwide database containing reservoir parameters can be used to identify numerous underdeveloped opportunities. Our work has shown that numerous opportunities exist primarily because of nomenclature problems. A review of an area using incorrect data might suggest complete development, whereas the area might have been incompletely developed. By using accurate reservoir nomenclature, combined with detailed reservoir analysis, a radius of drainage can be determined for each well completion. A map with the drainage area of each well plotted to actual map scale is much more informative than a simple production-bubble map. Potentially undrained areas become obvious. Numerous opportunities were identified during evaluation of the data resulting from this study.

ADDENDUM

When this paper was written, the authors were employees of IHS Energy Group in the Reservoir Geology Division. Prior to publication of this paper, Geological Data Services (GDS), Addison, Texas, purchased the Reservoir Geology Division, including all referenced cross sections and databases.

Reservoir ID® is a database with geologically defined producing reservoirs plus State-reported producing reservoirs, accompanied by current production data.

A Reservoir Characterization database contains more than 120 parameters, including values for multiple thickness and porosity, water saturation, pressure, cumulative production, ultimate recovery, current and ultimate drainage, and other geological and engineering data.

REFERENCES CITED

Hendrickson, W. J.; Smith, P. W.; Williams, C. M., 1996a, Regional correlations and reservoir characterization studies of the Pennsylvanian System in the Anadarko basin area of western Oklahoma and the panhandle of Texas, *in* Swindler, D. L.; and Williams, K. P. (eds.), Transactions of the 1995 American Association of Petroleum Geologists, Mid-Continent Section Meeting: Tulsa Geological Society, p. 100–108.

Hendrickson, W. J.; Smith, P. W.; Williams, C. M.; and Woods, R. J., 1996b, A regional correlation and production allocation project within the Oklahoma portion of the Anadarko basin and shelf with a specific discussion of the Springer and Chester Groups: Shale Shaker, v. 47, no. 2, p. 31–41.

Hendrickson, W. J.; Hogan, J. V.; Smith, P. W.; Willey, C. E.; and Woods, R. J., 2001, An example of a carbonate platform and slope system and its stratigraphically equivalent basinal clastic system: Springeran–Chesterian relationships in the Anadarko basin and shelf of northwestern Oklahoma and Texas Panhandle, *in* Johnson, K. S. (ed.), Silurian, Devonian, and Mississippian geology and petroleum in the southern Midcontinent, 1999 symposium: Oklahoma Geological Circular 105 [this volume], p. 91–99.

Smith, P. W., 1996, Anadarko basin statistical study: gas well recovery -vs- depth in the Anadarko basin of western Oklahoma: Gas Research Institute, Chicago, Final Report GRI-96/0196, 65 p.

Smith, P. W.; Hendrickson, W. J.; Williams, C. M., 1996, Regional correlations and reservoir characterization studies of the Springer Group in the Anadarko basin area of western Oklahoma, *in* Swindler, D. L.; and Williams, K. P. (eds.), Transactions of the 1995 American Association of Petroleum Geologists, Mid-Continent Section Meeting: Tulsa Geological Society, p. 116–126.

Williams, C. M.; Hendrickson, W. J.; and Smith, P. W., 1996, Regional correlations and reservoir characterization studies of the Morrow Group in the Anadarko basin area of western Oklahoma, *in* Swindler, D. L.; and Williams, K. P. (eds.), Transactions of the 1995 American Association of Petroleum Geologists, Mid-Continent Section Meeting: Tulsa Geological Society, p. 109–115.

Extended Tricyclic Terpanes in Mississippian Rocks from the Anadarko Basin, Oklahoma

Dongwon Kim and R. Paul Philp
University of Oklahoma
Norman, Oklahoma

ABSTRACT.—Tricyclic terpanes extending to at least C_{45} have been identified in the m/z 191 chromatograms of saturate fractions from extracts of Mississippian carbonate rocks of the Anadarko basin, Oklahoma.

The Anadarko basin was a shallow-marine depositional environment during the Mississippian Period. Four lithologic facies have been recognized in Mississippian rocks deposited in the northeastern part of the basin: (1) intramicrudite, dominated by marine algae and terrigenous detritus; (2) bio-oosparite; (3) biomicrudite; and (4) micrite. The algal-dominated intramicrudite facies is characterized by extended tricyclic terpanes in relatively high concentrations. In contrast, the extended tricyclic terpanes are below the limit of detection in the biomicrudite facies. The presence of extended tricyclic terpanes is thought to be source-dependent, and it is proposed that they were probably derived from marine calcareous algae living in the shallow carbonate environment. Rock-Eval and kerogen analyses revealed the organic matter of the Mississippian rocks to be types II and III amorphous kerogen without typical structured plant debris.

Concentrations of tricyclic terpanes relative to hopanes vary with organic source and lithology but appear to be related primarily to source materials. In rocks of similar lithology and source, relative tricyclic terpane concentration increases with increases of total organic carbon and hydrogen index. Hence, an event such as an algal bloom could have been a possible cause for the increase in tricyclic terpane production. Large amounts of terrigenous detritus are observed under the microscope in rocks with an abundance of tricyclic terpanes. The strong relationship between the tricyclic terpane content and terrigenous detritus may indicate that post-depositional processes have had a possible influence on the preservation of tricyclic terpanes.

INTRODUCTION

Geochemical studies of organic-rich Paleozoic rocks and crude oils from the Anadarko basin, Oklahoma, have revealed that variations in biomarker distribution appear to be related to organic-source material, environmental conditions, and thermal maturity (Jones and Philp, 1990; Wang and Philp, 1997). Among the Paleozoic samples previously studied, Mississippian rocks and Pennsylvanian crude oils have been found to exhibit a number of characteristic geochemical features—namely, the occurrence of an extended series of tricyclic terpanes up to C_{45}, and enhanced concentrations of tricyclic terpanes relative to pentacyclic hopanes (Philp and others, 1991; Alam and others, 1993). Philp and others (1991) proposed that specific environmental conditions and/or organic-source materials are most likely responsible for the characteristic biomarker distributions of the Mississippian rocks and Pennsylvanian oils in the Anadarko basin.

Tricyclic terpanes ranging from C_{19} to C_{30} are common constituents of ancient sedimentary rocks and crude oils and have been reported in samples from a large number of sedimentary basins worldwide (Seifert and Moldowan, 1978; Aquino Neto and others, 1982; Ekweozor and Strausz, 1983; Aquino Neto and others, 1986; Chicarelli and others, 1988; Wang and Simoneit, 1995). Moldowan and others (1983) presented evidence, using metastable-ion-monitoring mass-spectrometric analysis, that the series extended to at least C_{45} in a concentrate of tricyclic terpanes isolated from a California crude-oil sample. Subsequent studies noted the occurrence of extended tricyclic terpanes over various carbon-number ranges (about C_{41}–C_{54}) in geologic samples from saline, lacustrine, and marine carbonate environments (Kruge and others, 1990; de Grande and others, 1993) and Permian tasmanites (Simoneit and Leif, 1990; Aquino Neto and others, 1992; Simoneit and others, 1993; McCaffrey and others, 1994). The tricyclic terpane hydrocarbons appear to be absent in Holocene sediments but are ubiquitous in ancient sediments and

Kim, Dongwon; and Philp, R. P., 2001, Extended tricyclic terpanes in Mississippian rocks from the Anadarko basin, Oklahoma, *in* Johnson, K. S. (ed.), Silurian, Devonian, and Mississippian geology and petroleum in the southern Midcontinent, 1999 symposium: Oklahoma Geological Survey Circular 105, p. 109–127.

crude oils, implying their formation during maturation from a microbial or algal source (Aquino Neto and others, 1983). Prokaryotic-bacteria-membrane lipids (Ourisson and others, 1982; Ekweozor and Strausz, 1983) were suggested as sources for the tricyclic terpanes. Higher homologues of the tricyclic terpane series (>C_{30}) have been reported only in geologic samples from specific environments with normal salinity, which may be favorable for production and preservation of the extended tricyclic terpanes (de Grande and others, 1993). Biochemical cyclization of polyprenols of varying chain lengths from specific marine organisms was proposed as a possible source for the extended tricyclic terpanes (McCaffrey and others, 1994).

In the present study, core samples from the Mississippian carbonate rocks in the northeastern margin of the Anadarko basin (Fig. 1) have been investigated on the basis of their biomarker distributions and depositional-facies types. Effects such as organic source, depositional environment, and thermal maturity have been examined in an effort to establish possible precursor-product relationships associated with the occurrence of the extended tricyclic terpanes and the enhanced abundance of tricyclic terpanes relative to pentacyclic terpanes in the Mississippian rocks.

EXPERIMENTAL METHODS

Twenty-nine core samples of Mississippian rocks from seven wells in the Anadarko basin (Fig. 2; Table 1) have been analyzed by a variety of geochemical and petrographic techniques (Fig. 3). The initial step involved pulverization of about 400 g of each sample to 100–200-mesh size (45–90 μm). Prior to the pulverization, core slabs were described petrographically, and thin sections (3 × 5 cm square) were prepared and examined under the microscope. A simple optical technique under a transmitted-light microscope (Nikon LABOPHOT2-POL) was used to identify the carbonate-framework components and matrix compositions. Kerogen isolation involved treating the crushed rocks with hydrochloric acid (HCl) to dissolve carbonates, and hydrofluoric acid (HF) to dissolve silicates. Following preparation of strew-mount slides, isolated organic matter was examined under a Leitz MPV compact microscope (Leitz Ortholux II POL-BK) with a 100-watt mercury lamp as an ultraviolet (UV) light source.

The total organic carbon (TOC) content was measured by a LECO CR-12 carbon determinator and a Rock-Eval apparatus (Oil Show Analyzer, Vinci Instrument). Rock-Eval pyrolysis values such as S_0, S_1, S_2, S_4, and T_{max} were also obtained with the Oil Show Analyzer. Crushed rock samples (~100 g) were extracted for 48 hours using a Soxhlet extractor with a 1:1 mixture of methylene chloride and methanol. Asphaltenes were precipitated from the extract by addition of excess *n*-pentane to the extracts. This procedure was repeated three times with *n*-pentane to collect pure non-asphaltene fractions. The maltene fractions (non-asphaltene fractions) were separated into saturate, aromatic, and polar (NSO) fractions by high-performance liquid chromatography (HPLC, Eldex Model 9600). The solvent program described in McDonald and Kennicutt (1992) was adapted for this separation procedure.

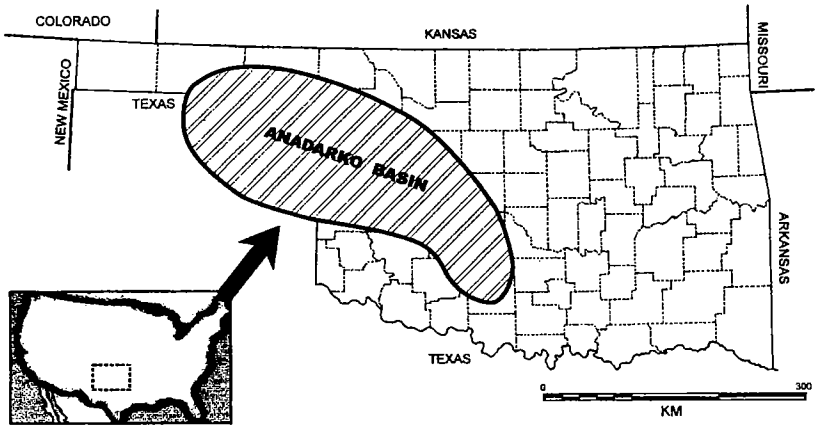

Figure 1. Location map for the Anadarko basin.

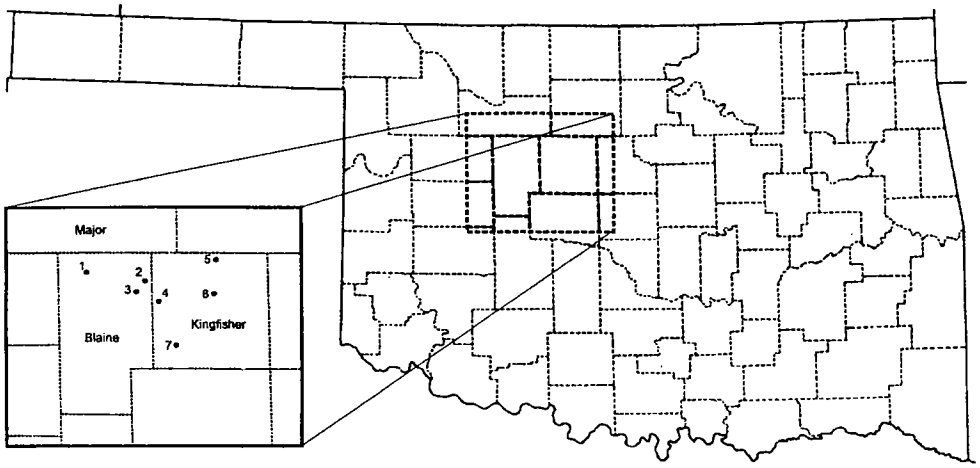

Figure 2. Well-location map for Mississippian rock samples from Oklahoma. (1) Flint 1-34; (2) Alvin Weigand 1; (3) Capps Unit 1; (4) Jacob Betz 1; (5) Huntsberger 1; (6) Stewart-Cronkite 1; (7) Conley Unit 1.

Table 1.—Well Locations and Sampling Information

Well name	County	Township, range, sec.	Depth of Miss. (feet)	Sampling depth (feet)	Sample ID
Conley Unit 1	Kingfisher	16N-9W-36	8,654–8,796	8,562	CU-8562
				8,564	CU-8564
				8,564	CU-8564B
				8,656	CU-8656
Jacob Betz 1	Kingfisher	18N-9W-31	7,790–8,030	7,877	JB-7877
				7,902	JB-7902
				7,914	JB-7914
Capps Unit 1	Blaine	18N-10W-27	7,870–9,150	8,722	C-8722
				8,724	C-8724
				8,730	C-8730
				8,857	C-8857
				8,862	C-8862
				8,869	C-8869
				8,873	C-8873
				8,877	C-8877
				8,880	C-8880
				8,888	C-8888
				8,892	C-8892
				8,897	C-8897
				8,892 & 8,897	CM-9297
				8,903	C-8903
				8,904	C-8904
AW 1[a]	Blaine	18N-10W-13	7,630–8,663	8,325	AW-8325
Flint 1-34	Blaine	19N-12W-34	8,220–9,660	8,298	F-8298
				8,298	F-8298B
				8,310	F-8310
S-C 1[b]	Kingfisher	18N-7W-26	6,990–7,100	6,992	SC-6992
Huntsberger 1	Kingfisher	19N-7W-11	6,721–7,552	7,012	H-7012
				7,022	H-7022

[a]Alvin Weigand 1.
[b]Stewart-Cronkite 1.

The saturate fractions from the rock extracts were analyzed by gas chromatography (GC) with a Hewlett Packard 5890 gas chromatograph equipped with a 30-m × 0.32-mm (i.d.) DB-1HT fused silica capillary column (film thickness = 0.1 μm). The initial temperature was 40°C, with 1.5-minute holding time, and with the temperature programmed at a rate of 4°C/minute to 360°C and held for 31 minutes. The injector temperature was 300°C, and the detector temperature was 310°C. Helium was used as a carrier gas. Prior to analysis by gas chromatography–mass spectrometry (GCMS), branched/cyclic fractions were isolated by molecular sieving with a silicalite column (West and others, 1990). The GCMS analysis of the branched/cyclic compounds was carried out with a Varian 3400 gas chromatograph interfaced with a TSQ 70 (Finnigan MAT) mass spectrometer operated at 70eV. The gas chromatograph was equipped with a 60-m × 0.32-mm (i.d.) J&W Scientific DB-5 fused silica capillary column with a 0.25-μm film thickness. The GC oven was programmed from 40° to 310°C at a temperature rate of 4°C/minute.

Quantitative biomarker analysis was used to obtain relative and absolute amounts of certain biomarkers and biomarker groups. The relative ratios were obtained from peak areas in GC and GCMS chromatograms by manual calculation. The amount of each compound was measured in parts per million per g/TOC on the basis of the following equations using the quantitative GC and GCMS data with an internal standard.

The GCMS procedure is:

$$(1)\ \frac{\text{(component peak area)}}{\text{(int. std. peak area)}} \times \text{(conc. of int. std.)} = \text{(conc. of component) [mg/mL in B/C].}$$

(2) $\text{(conc. of component)} \times \frac{\text{(mg of B/C)}}{\text{(conc. of B/C injected)}}$
= total mg of component in B/C or saturate fraction [mg].

(3) $\frac{\text{(total mg of component in B/C)} \times 1{,}000 \times \text{(total mg of bitumen)}}{\text{(mg of bitumen injected into HPLC)} \times \text{(recoverable factor of HPLC)}}$
= total μg of component in bitumen [μg].

(4) $\frac{\text{(total μg of component in bitumen)} \times 100}{\text{(g rock weight used)} \times \text{(\%TOC)}}$
= μg component/g TOC [μg/g].

The GC procedure is:

(1) $\frac{\text{(component peak area)}}{\text{(int. std. peak area)}} \times \text{(conc. of int. std.)}$
= (conc. of component) [mg/mL].

(2) $\text{(conc. of component)} \times \frac{\text{(mg of saturate fraction)}}{\text{(conc. of saturate fraction)}}$
= total mg of component in saturate fraction [mg].

(3) $\frac{\text{(total mg of component in saturate fraction)} \times 1{,}000 \times \text{(total mg of bitumen)}}{\text{(mg of bitumen injected into HPLC)} \times \text{(recoverable factor of HPLC)}}$
= total μg component in bitumen [μg].

(4) $\frac{\text{(total μg of component in bitumen)} \times 100}{\text{(g rock weight used)} \times \text{(\%TOC)}}$
= μg component/g TOC [μg/g].

RESULTS AND DISCUSSION

Geochemical and petrographic investigations of Mississippian carbonate-rock samples from the Anadarko basin showed significant variations in the tricyclic terpane distributions and concentrations, relative to the hopanes, in the m/z 191 chromatograms within various lithologic facies. A typical distribution of tricyclic terpanes and hopanes in the m/z 191 chromatogram is shown in Figure 4, and peak identifications are listed in Table 2. The Mississippian rocks characterized in this study can be divided into four lithologic types, each of which represents its geological characteristic feature and depositional environment (Table 3). Biomarker characteristics for each type of carbonate facies are discussed in the following sections, and the discussion is focused particularly on variations in the tricyclic terpane distributions.

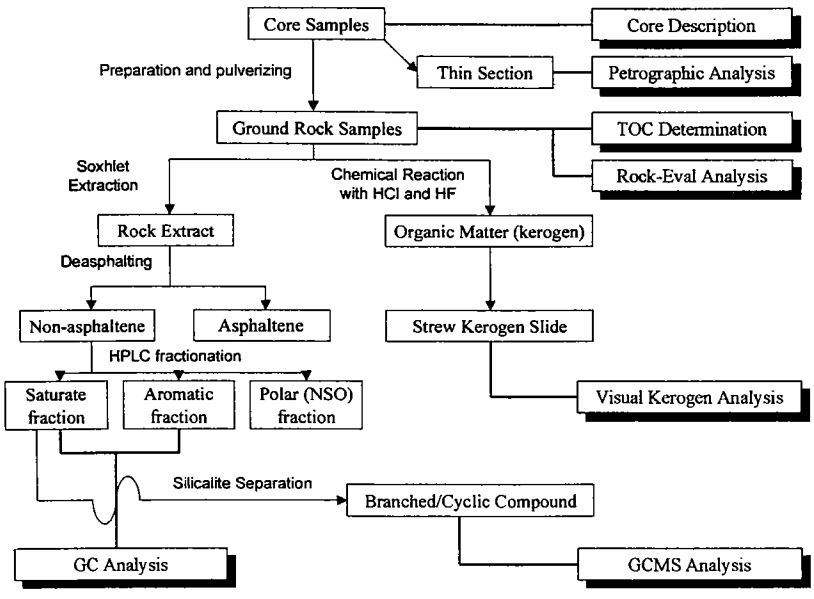

Figure 3. Flow chart for the general analytical procedures used in this study.

Facies I: Intramicrudite Facies

The rock samples that characterize this facies contain large amounts of terrigenous clastic sediments such as quartz, feldspars, mica, and clay minerals (Fig. 5). This facies is referred to as "dirty limestone," consisting of 50–70 weight% carbonate minerals and randomly scattered siliciclastic sediments. No calcareous marine invertebrate fossils are seen under the microscope; instead, needle-like spicules and algal remains are present. This type of facies is interpreted to have been deposited in a carbonate peritidal environment restricted to the nearshore region, where stromatolites produced by cyanobacteria ("blue-green algae") and other resistant types of marine organisms are most common.

The major characteristic biomarker features of this facies in the Anadarko basin are (1) the predominance of *n*-alkanes in the range of nC_{17} to nC_{19} (Fig. 6); (2) a pristane/phytane ratio ≅ 1.0; (3) the presence of higher molecular-weight acyclic isoprenoids (>C_{28}) in relatively high concentration (Fig. 7); (4) the high concentration of tricyclic terpanes relative to hopanes (Fig. 8); (5) a Ts/(Ts + Tm) ratio >0.85; and (6) the high concentration of 17α(H)-diahopane relative to C_{30}-17α(H) hopane (>0.30). The greatest abundance of tricyclic terpanes is observed over a relatively narrow interval in the stratigraphic column from the Capps Unit No. 1 well (Fig. 9). In this interval, values for TOC and hydrogen index (HI) are high, whereas hopanes are present in low concentrations relative to the tricyclic terpanes.

Facies II: Bio-oosparite or Intrasparite Facies (Oolitic Grainstone)

The major rock-forming components in this facies are ooids, bioclasts, and terrigenous clastic grains (Fig. 10). Terrigenous clastic sediments consisting mostly of subrounded quartz grains are fine to medium sand size. The presence of quartz/bioclast-bearing ooids in this facies indicates that the depositional environment was a shallow nearshore shelf but

Table 2.— Identification of Chromatographic Peaks at Ion m/z 191

Peak	Structure assignment
1	C_{23} tricyclic terpane
2	C_{24} tricyclic terpane
3	C_{25} tricyclic terpane
4	C_{26} tricyclic terpane (22S)
5	C_{26} tricyclic terpane (22R) + C_{24} tetracyclic terpane
6	C_{28} tricyclic terpane (22S and 22R)
7	C_{29} tricyclic terpane (22S and 22R)
8	C_{27} 18α(H)-22,29,30-trisnorhopane (Ts)
9	C_{27} 17α(H)-22,29,30-trisnorhopane (Tm)
10	C_{30} tricyclic terpane (22S and 22R)
11	C_{31} tricyclic terpane (22S and 22R)
12	C_{29} 17α(H),21β(H)-norhopane
13	C_{29} 18α(H)-norneohopane (C_{29}-Ts)
14	C_{30} 17α(H)-diahopane
15	C_{30} 17α(H),21(β)-hopane
16	C_{33} tricyclic terpane (22S and 22R)
17	C_{31} 17α(H),21β(H)-homohopane (22S and 22R)
18	C_{30} gammacerane[a]
19	C_{32} 17α(H),21β(H)-homohopane (22S and 22R)
20	C_{35} tricyclic terpane (22S and 22R)
21	C_{33} 17α(H),21β(H)-homohopane (22S and 22R)
22	C_{34} 17α(H),21β(H)-homohopane (22S and 22R)

[a] C_{30} gammacerane co-elutes with C_{34}-22R-tricyclic terpane under the GC condition used in this study.

was moderately agitated by current and wave action.

The main biomarker features that characterize this facies are (1) the predominance of *n*-alkanes in the nC_{21} to nC_{23} range (Fig. 11); (2) a pristane/phytane ratio less than 0.5; (3) the relatively high concentration of higher molecular-weight acyclic isoprenoids compared to lower molecular-weight homologues (C_{18} to C_{27}); (4) the moderate concentration of tricyclic terpanes compared to hopanes (Fig. 12); and (5) a Ts/(Ts + Tm) ratio of 0.45–0.60. Compared to the other samples in this study, this facies has unique features in that the concentration of *n*-alkanes maximizes in the nC_{21} to nC_{23} range, and gammacerane is present in moderate abundance in the m/z 191 chromatogram.

Facies III: Biomicrudite or Biosparudite Facies (Packstone to Wackestone)

This facies is dominated by a large number of marine invertebrate bioclasts such as bryozoan, crinoid, echinoderm, trilobite, brachiopod, and molluscan debris without any terrigenous sediment (Fig. 13). The shallow carbonate shelf supports the greatest diversity of marine fauna by far, which is much more diverse than the peritidal fauna.

The m/z 191 chromatogram in Figure 14 shows the typical biomarker distribution of samples from this environment, dominated by pentacyclic hopanes in comparison to tricyclic terpanes. Extended tricyclic terpanes cannot be detected, whereas pentacyclic hopanes to C_{35} are present in high concentrations. A lack of the higher molecular-weight compounds is observed not only in the terpane distribution but also in the *n*-alkane and acyclic isoprenoid distributions.

Facies IV: Micrite Facies (Mudstone)

This rock is poorly bedded. It shows no evidence of bioturbation and appears in a stratigraphic position just above the oolitic grainstone (facies II). Thus, the rocks are interpreted as having been deposited in a lagoonal carbonate shelf under low-energy conditions, where the lime mud is usually composed of aragonite needles precipitated as the skeletons of certain types of calcareous algae (Prothero and Schwab, 1996).

The main biomarker features of this facies are similar to those of facies II (bio-oosparite facies), especially in the m/z 191 chromatograms (Fig. 15), except that gammacerane is undetectable, and the concentration

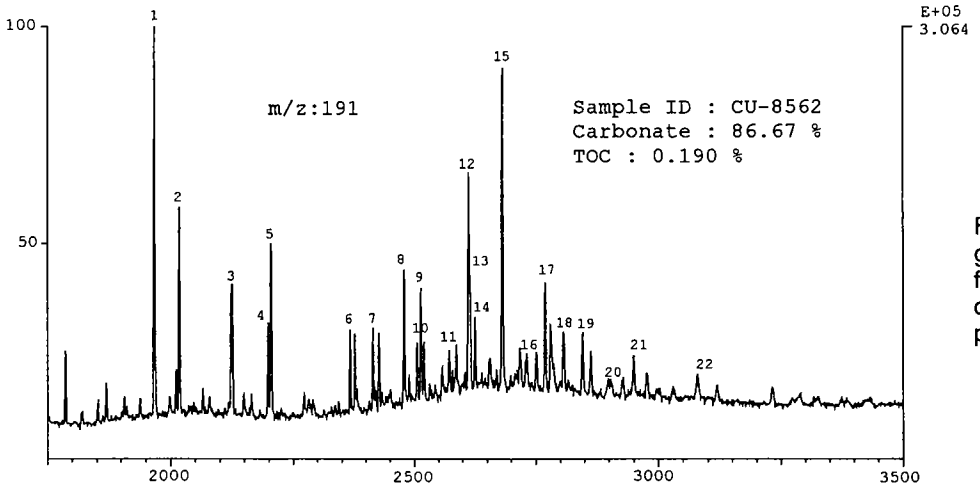

Figure 4. M/z 191 mass chromatogram for the branched/cyclic fraction from sample CU-8562. Peak identifications of tricyclic terpanes and hopanes are given in Table 2.

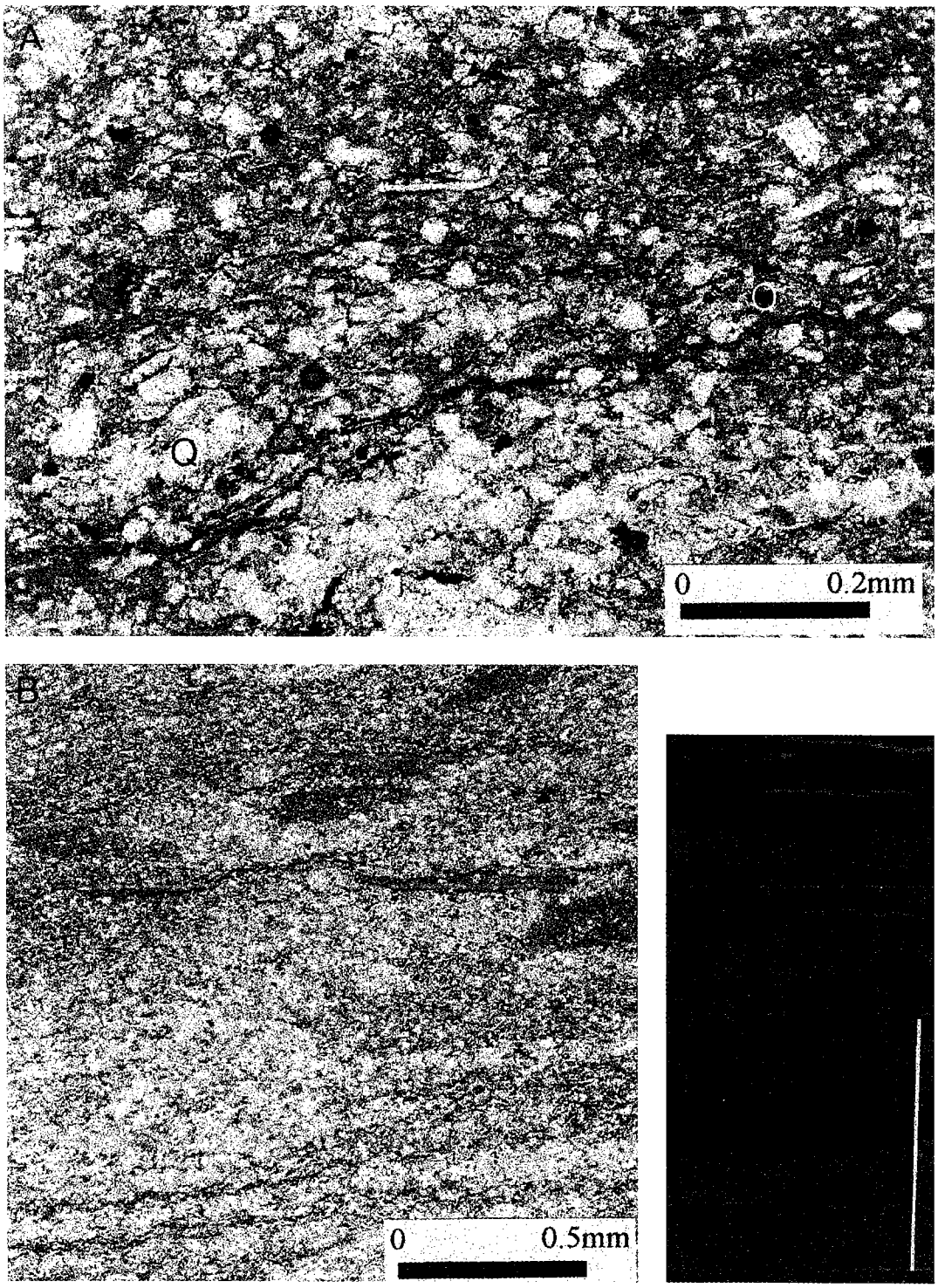

Figure 5. (A) Magnified view of intramicrudite facies (C-8857), showing a typical dirty limestone with terrigenous clastic sediments. Spicules (arrow) and quartz grains (*Q*) are seen, with a void (*O*) formed by leaching evaporitic minerals. Organic-rich layers have been squeezed horizontally by compaction. (B) Thin section (left) and rock slab (right) of the upper part of the Capps Unit 1 core (C-8724), showing well laminae with mud flats. Detrital grains are sparsely scattered but are much denser in organic-poor layers. Vertical bar scale in rock slab represents 5 cm.

Table 3.—Characteristics of Four Lithologic Facies Based on Petrographic Investigation

Type	Facies I	Facies II	Facies III	Facies IV
Facies (Folk, 1962)	Intramicrudite	Oosparite/ biosparite	Biomicrudite/ bio-intrasparite	Micrite
Caronate-rock classification (Dunham, 1962)	Packstone to wackestone	Grainstone	Packstone to wackestone	Mudstone
Major rock-forming components	Algal remains, terrigenous sediments	Ooids, quartz grains	Marine bioclasts (bryozoans, echinoderms, etc.)	--
Minor Components	Spicules	Bioclasts	--	--
Matrix	Partially dolomitized micrite and clays	Sparry calite cements	Sparry calcite/ microcrystalline ooze	Microcrystalline ooze
Depositional environment	Peritidal carbonate	High-energy shallow shelf	Shallow shelf	Lagoonal carbonate
Sample ID	All Capps Unit 1 AW-8325 H-7012 & 7022	CU-8564 SC-6992	All Flint 1-34 All Jacob Betz 1	CU-8562

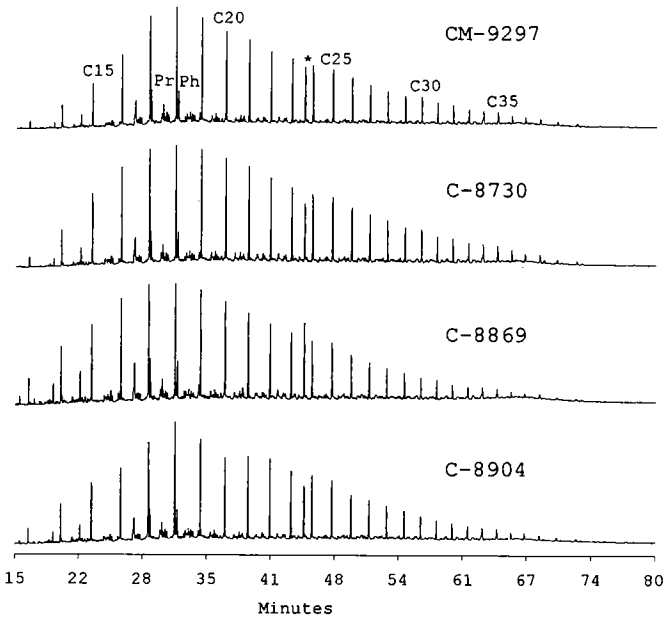

Figure 6. Gas chromatograph (GC) fingerprints for various saturate fractions, illustrating the *n*-alkane distributions maximizing in the nC_{17} to nC_{19} range. Asterisk (*) represents C_{24} internal standard (*n*-tetracosane-d_{50}).

of higher molecular-weight acyclic isoprenoids is relatively low.

Although each facies is characterized by its own biological features as described above, the four facies have something in common, especially in kerogen type and *n*-alkane distributions. Type II or III amorphous kerogens, without typical structured plant debris but with organic matter derived initially from phytoplankton or bacteria (Lewan, 1986), are dominant in all of the samples. GC fingerprints of saturate fractions from the Mississippian rocks do not show any significant differences in their *n*-alkane distributions except those for facies II and IV. The predominance of *n*-alkanes in the range of nC_{15} to nC_{19} is indicative of a contribution of marine algae or a bacterial organic source (Gelpi and others, 1970; Volkman, 1988). On the basis of kerogen type and *n*-alkane distribution, marine organisms and bacteria generally appear to have been the source of organic matter in the Mississippian rocks. The m/z 217/218 chromatograms shown in Figure 16, with peak identifications in Table 4, represent a typical sterane distribution for the Mississippian rocks. The sterane distributions do not appear to have any relationship with the other biomarker characteristics in the m/z 191 chromatogram and facies determined by petrographic observation. The sterane distributions, when plotted in a ternary diagram, are scattered but fall into the general area for marine carbonates (Fig. 17).

Variations in the Ts/(Ts + Tm) ratio determined from the m/z 191 chromatogram show a direct relationship to variations in the ratio of tricyclic terpanes to regular hopanes (Fig. 18). It was shown in many studies that the Ts/(Ts + Tm) ratio is a reliable maturity parameter under constant source conditions (Seifert and Moldowan, 1978), but it is more likely to be changed by facies variations and diagenetic conditions rather than just by thermal maturity (Moldowan and others, 1986; Peters and Moldowan, 1993). In addition, a predominance of 17α(H)-diahopane over

Table 4.—Identification of Chromatographic Peaks at Ion m/z 217

Peak	Structure assignment	Peak	Structure assignment
1	13β,17α-diacholestane (20S)	11	24-ethyl-13β,17α-diacholestane (20R)
2	13β,17α-diacholestane (20R)	12	24-ethyl-13α,17β-diacholestane (20S)
3	13α,17β-diacholestane (20S)	13	24-methyl-14α,17α-cholestane (20S)
4	13α,17β-diacholestane (20R)	14	24-ethyl-13α,17β-diacholestane (20R) + 24-methyl-14β,17β-cholestane (20R)
5	24-methyl-13β,17α-diacholestane (20S)	15	24-methyl-14β,17β-cholestane (20S)
6	24-methyl-13β,17α-diacholestane (20R)	16	24-methyl-14α,17α-cholestane (20R)
7	24-methyl-13α,17β-diacholestane (20S) + 14α,17α-cholestane (20S)	17	24-ethyl-14α,17α-cholestane (20S)
8	24-ethyl-13β,17α-diacholestane (20S) + 14β,17β-cholestane (20R)	18	24-ethyl-14β,17β-cholestane (20R)
9	14β,17β-cholestane (20S) + 24-methyl-13α,17β-diacholestane (20R)	19	24-ethyl-14β,17β-cholestane (20S)
10	14α,17α-cholestane (20R)	20	24-ethyl-14α,17α-cholestane (20R)
		21	C_{30} steranes (24-*n*-propylcholestanes)

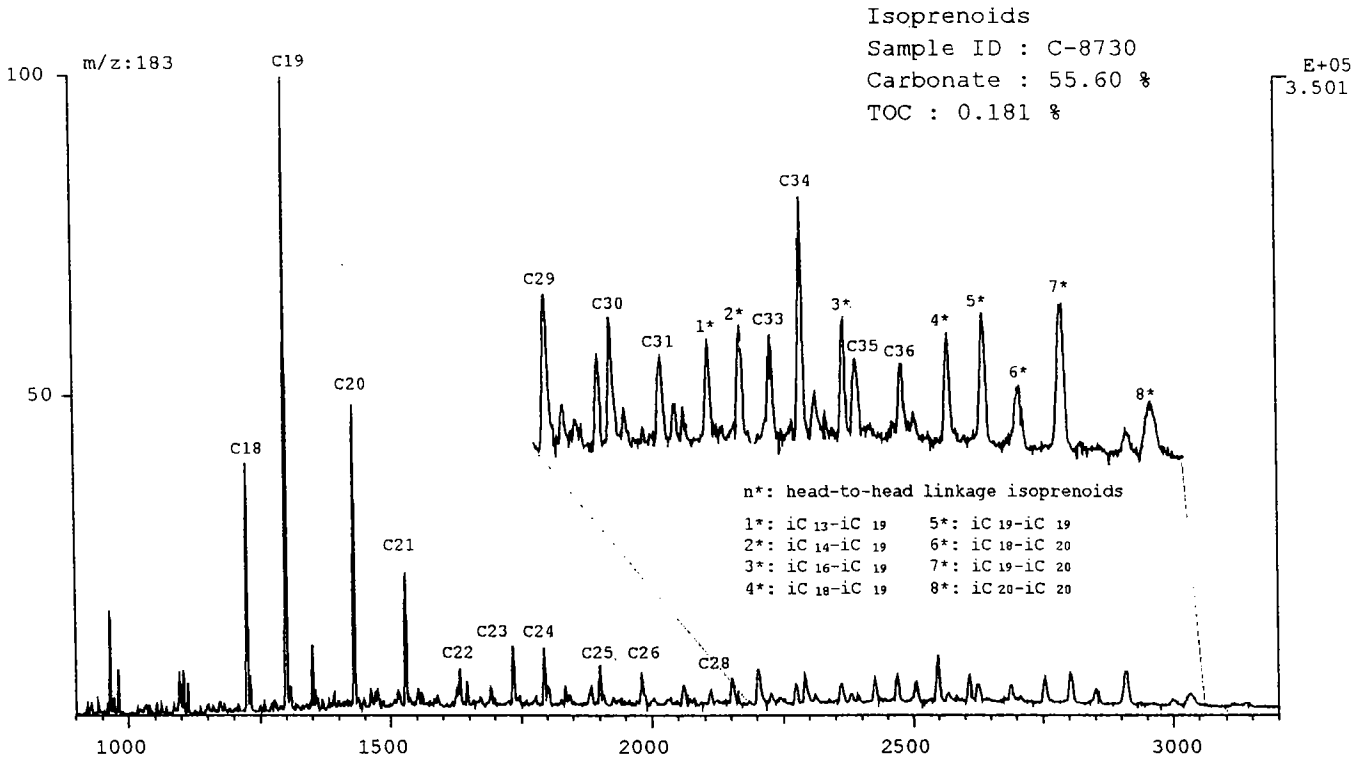

Figure 7. Typical distribution of acyclic isoprenoids found in branched/cyclic fractions of Mississippian rock extracts (facies I). Tentative identification of regular and head-to-head linkage isoprenoids was based on a comparison of distributions with those described in Moldowan and Seifert (1979) and Petrov and others (1990).

C_{30}-17α(H) hopane is observed in the samples that are characterized by a high relative concentration of tricyclic terpanes (Fig. 19). The enhanced concentration of 17α(H)-diahopane to other hopane homologues is observed in sediments deposited under oxic or suboxic conditions, which may be favorable for its formation via rearrangement by clay-mediated acid catalysis (Chen, 1992; Peters and Moldowan, 1993). Therefore, it appears that the abundance of tricyclic terpanes is related not only to specific source organisms but also to the supply of terrigenous detritus in a nearshore environment.

Kruge and others (1990) and Philp and others (1991) previously discussed the relative abundance of tricyclic terpanes in comparison to pentacyclic terpanes in geologic samples. The relative concentration of tricyclic terpanes within the terpane distribution may be affected by thermal maturity (Aquino Neto and oth-

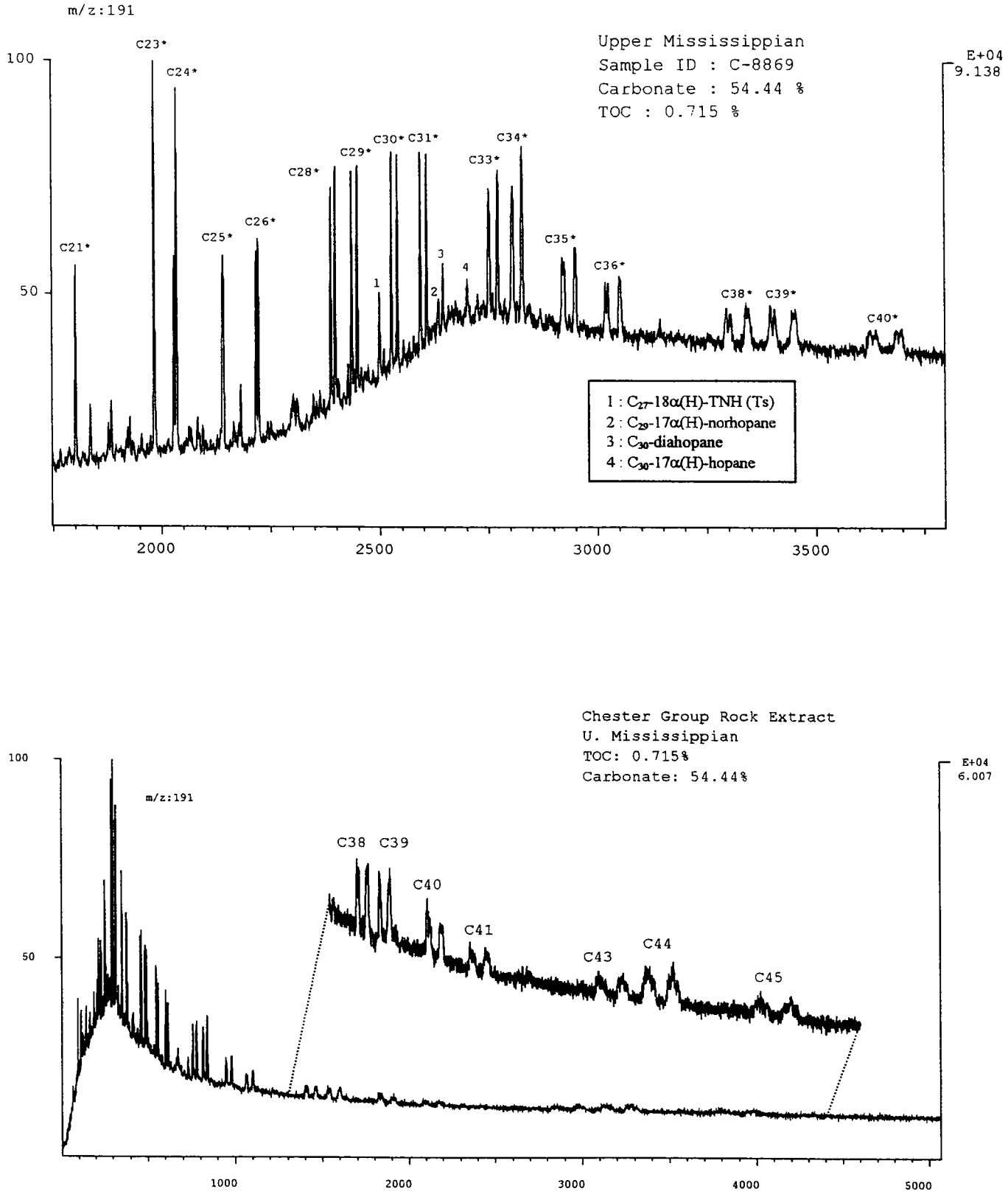

Figure 8. The m/z 191 chromatograms for the Mississippian rock extract (facies I) show an abundance of tricyclic terpanes relative to pentacyclic hopanes and the presence of tricyclic terpanes extending to C_{45}. GC temperature program for the lower chromatogram is 40°–325°C @ 25°C/minute with 88-minute final holding time. Asterisk (*) represents tricyclic terpanes.

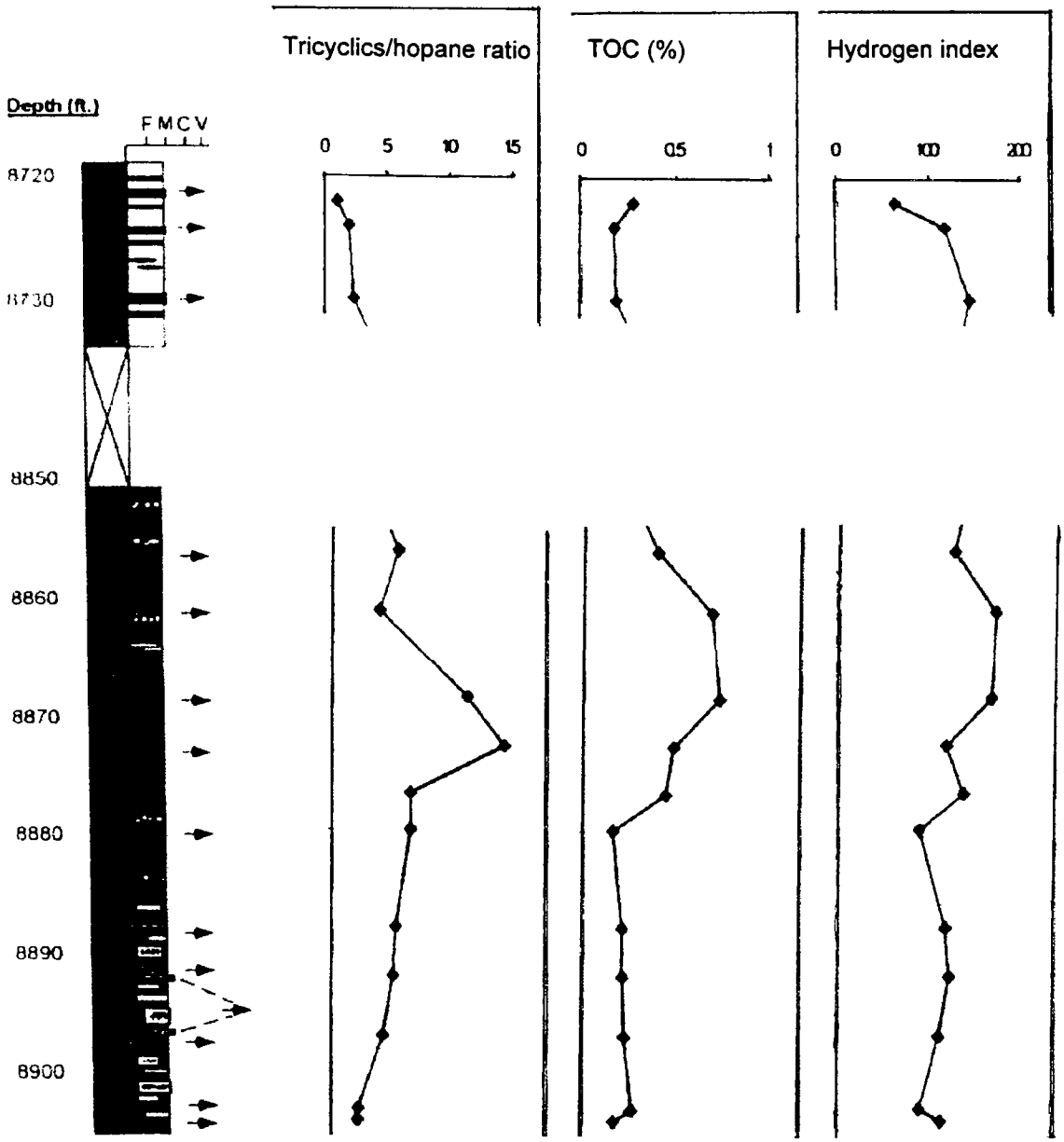

Figure 9. Stratigraphic position of samples in Capps Unit No. 1 well and variations in the tricyclics/hopane ratio, TOC, and HI with depth.

ers, 1983) or preferential migration (Fan and Philp, 1987; Jiang and others, 1988). A burial-history model for Paleozoic rocks in the Anadarko basin (Carter and others, 1998), and vitrinite-reflectance (R_o) values for the underlying Woodford Shale (Cardott, 1989), indicate that the Mississippian rocks were thermally mature in late Paleozoic time and are in the zone of hydrocarbon generation. T_{max} values between 435° and 450°C for the Mississippian rocks, analyzed by Rock-Eval pyrolysis in this study, indicate mature organic matter, mainly in the oil window. Sterane-maturity parameters for the Mississippian rock samples suggest that they are in the maturity range between early and peak stages of oil generation. Therefore, it is proposed that thermal maturation has played only a minor role in controlling the relative concentration of tricyclic terpanes to hopanes in the Mississippian rocks of the Anadarko basin.

It is also possible that the relatively high concentration of tricyclic terpanes is strongly dependent on organic-source material and depositional environment. It has been previously noted that the extended series of tricyclic terpanes (C_{19}–C_{54}) is particularly abundant in organic-rich rocks and crude oils from marine carbonate environments (Palacas and others, 1984; Kruge and others, 1990; de Grande and others, 1993). However, in the present study, some of the samples from the Mississippian rocks of the marine carbonate environments lack the extended tricyclic terpanes (C_{31}–C_{45}). The relative concentration of tricyclic terpanes

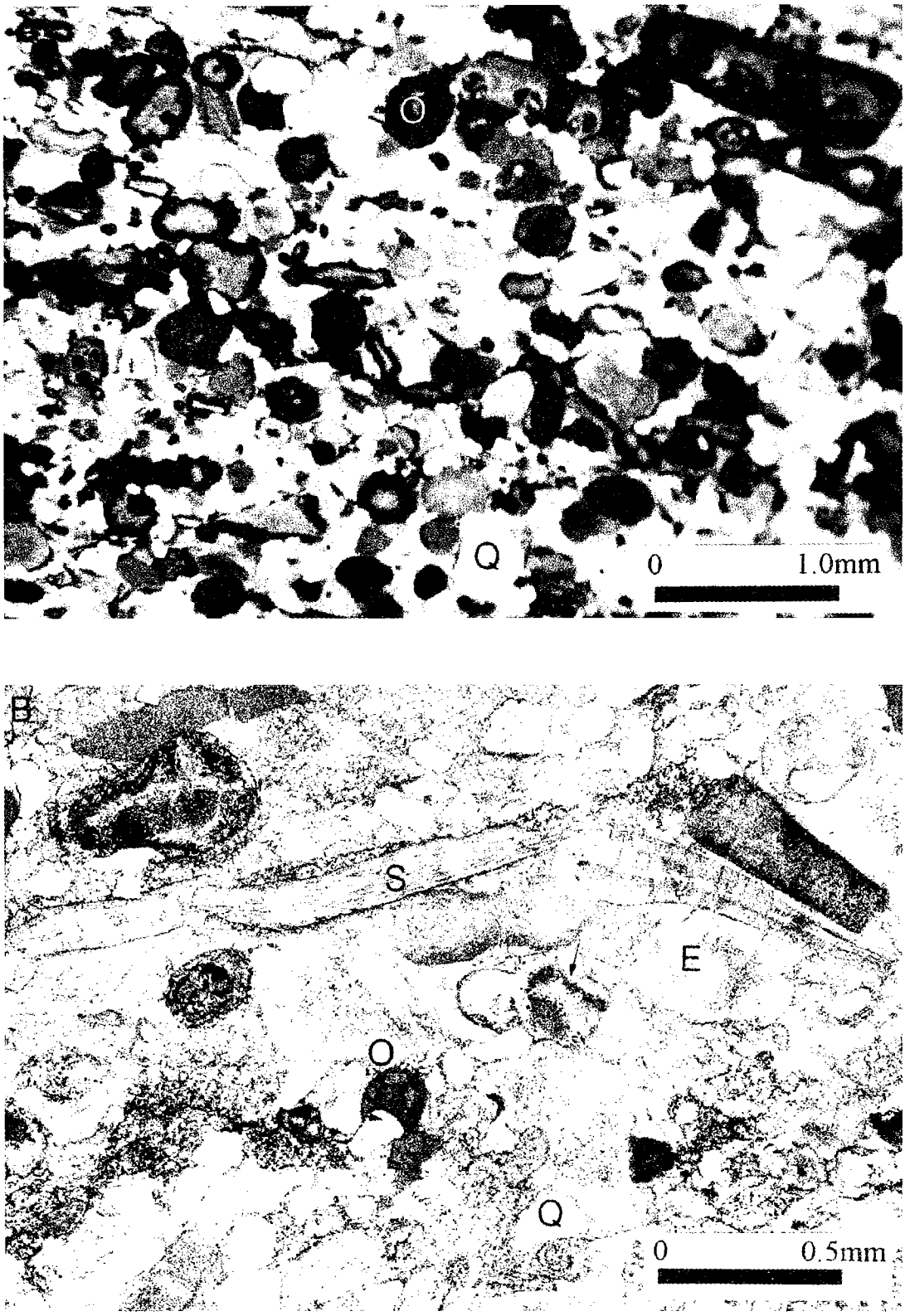

Figure 10. (A) Photomicrograph of oolitic grainstone (facies II), containing coarse quartz grains and bioclast debris. Ooids (*O*) with various types of nuclei are dominant species in this facies, and the quartz grains (*Q*) are poorly sorted and subrounded. (B) Bio-skeletal-dominated oolitic grainstone (SC-6992) with poorly sorted quartz grains (*Q*). Bioclasts consist predominantly of echinoderms (*E*), brachiopods (*S*), and trilobite and molluscan shell fragments.

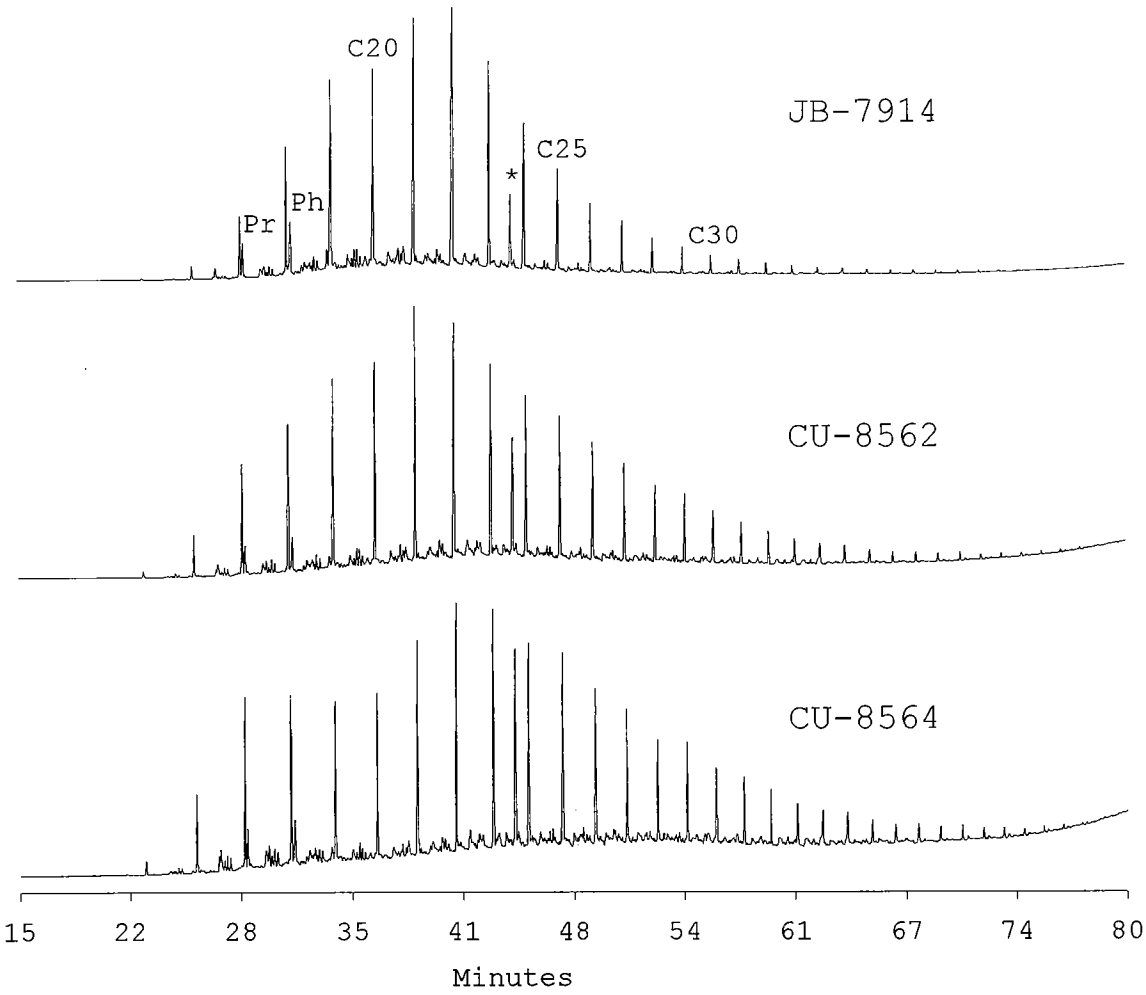

Figure 11. GC fingerprints of saturate fractions from facies II and IV showing maxima of *n*-alkane distribution in the range of nC_{21} to nC_{23}. Asterisk (*) represents C_{24} internal standard.

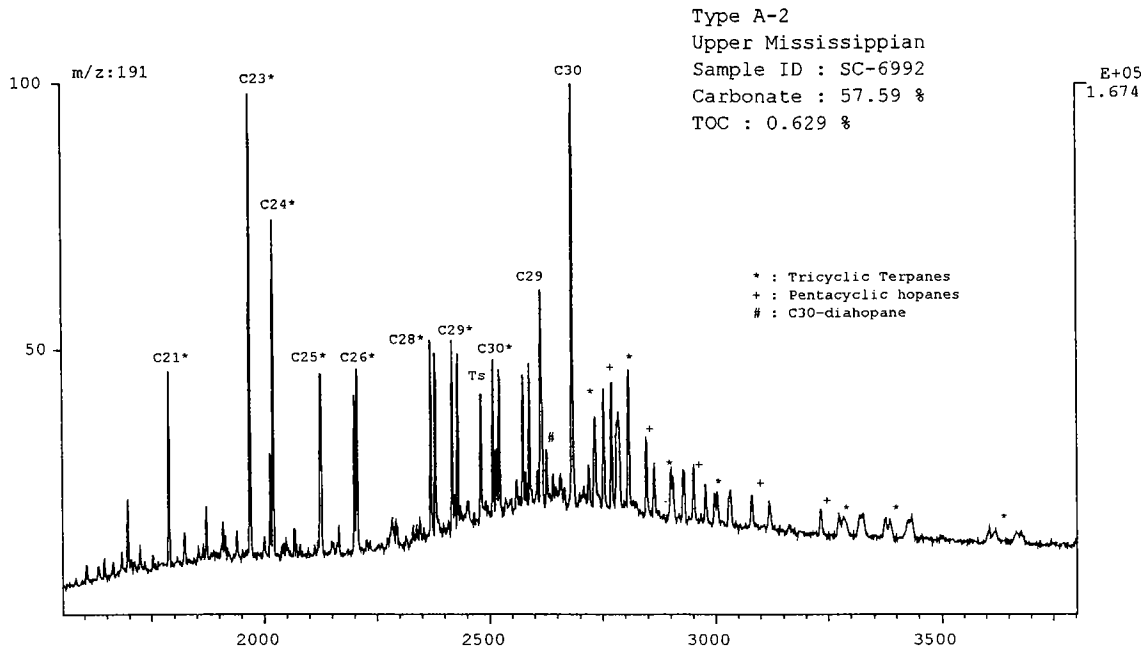

Figure 12. M/z 191 chromatogram showing terpane distribution in an extract from a sample of facies II.

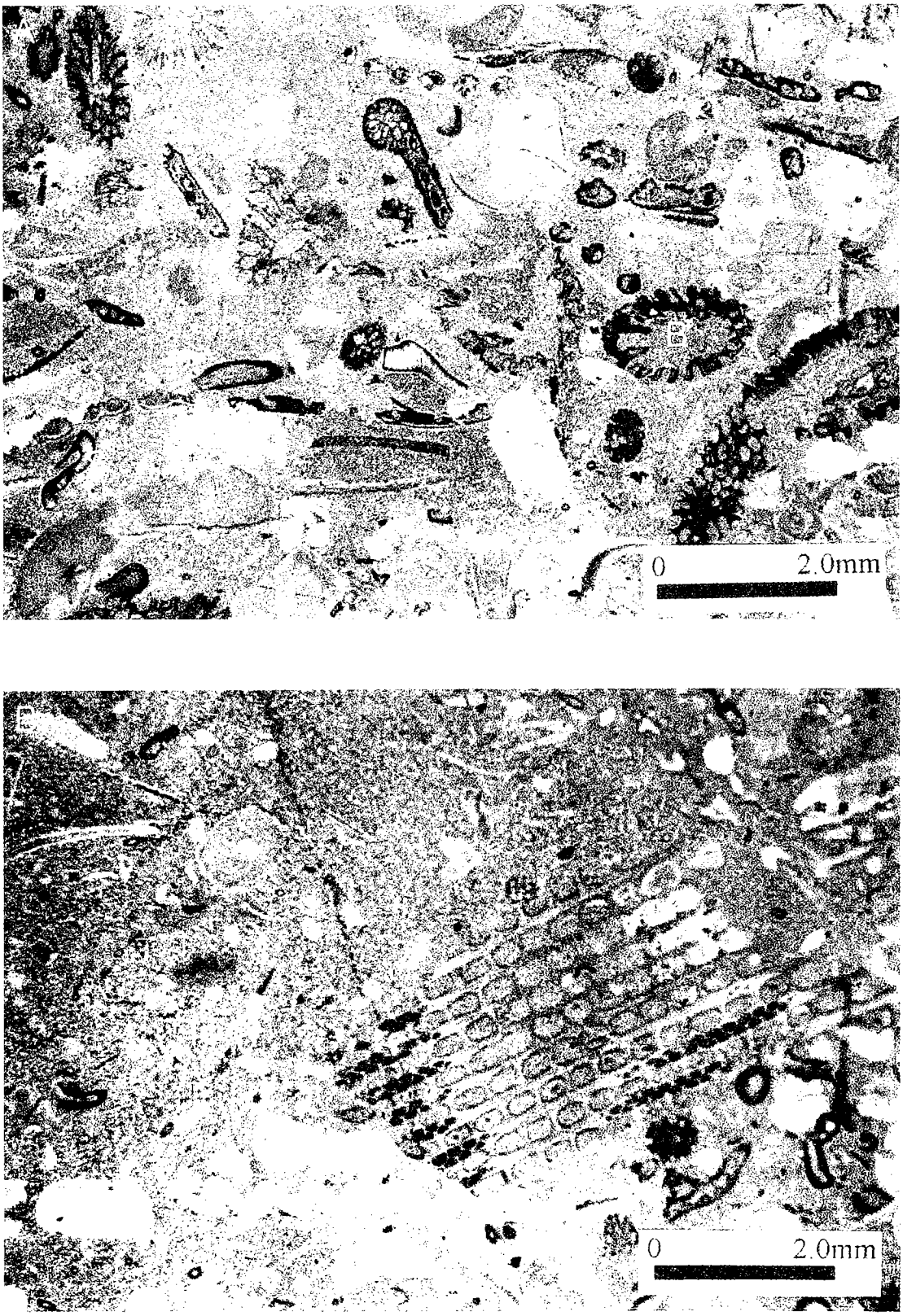

Figure 13. (A) Bioclast-rich rock, thin sections (F-8298). All carbonate allochems are composed of a variety of invertebrate fossils such as bryozoan (*B*), echinoderm (*E*), and trilobite shell fragments (*S*). (B) Cross section of a fenestrated bryozoan.

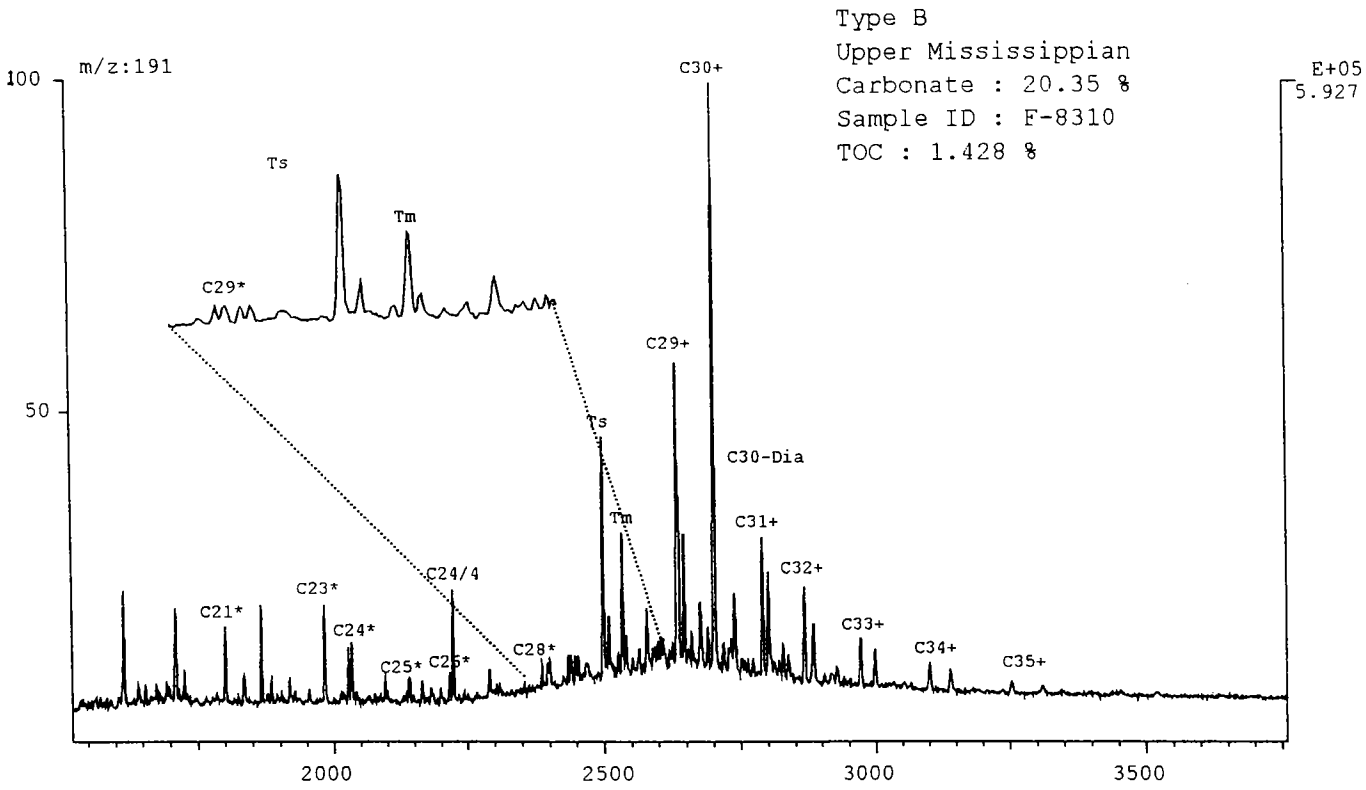

Figure 14. M/z 191 chromatogram showing a terpane distribution dominated by pentacyclic hopanes in comparison with tricyclic terpanes. Tricyclic terpanes are identified up to C_{30} in relatively low concentrations. The C_{24} tetracyclic terpane co-elutes with the C_{26} tricyclic terpane (22R epimer) under this GC condition. Asterisk (*) represents tricyclic terpanes, and plus symbol (+) represents pentacyclic regular 17α(H)-hopanes.

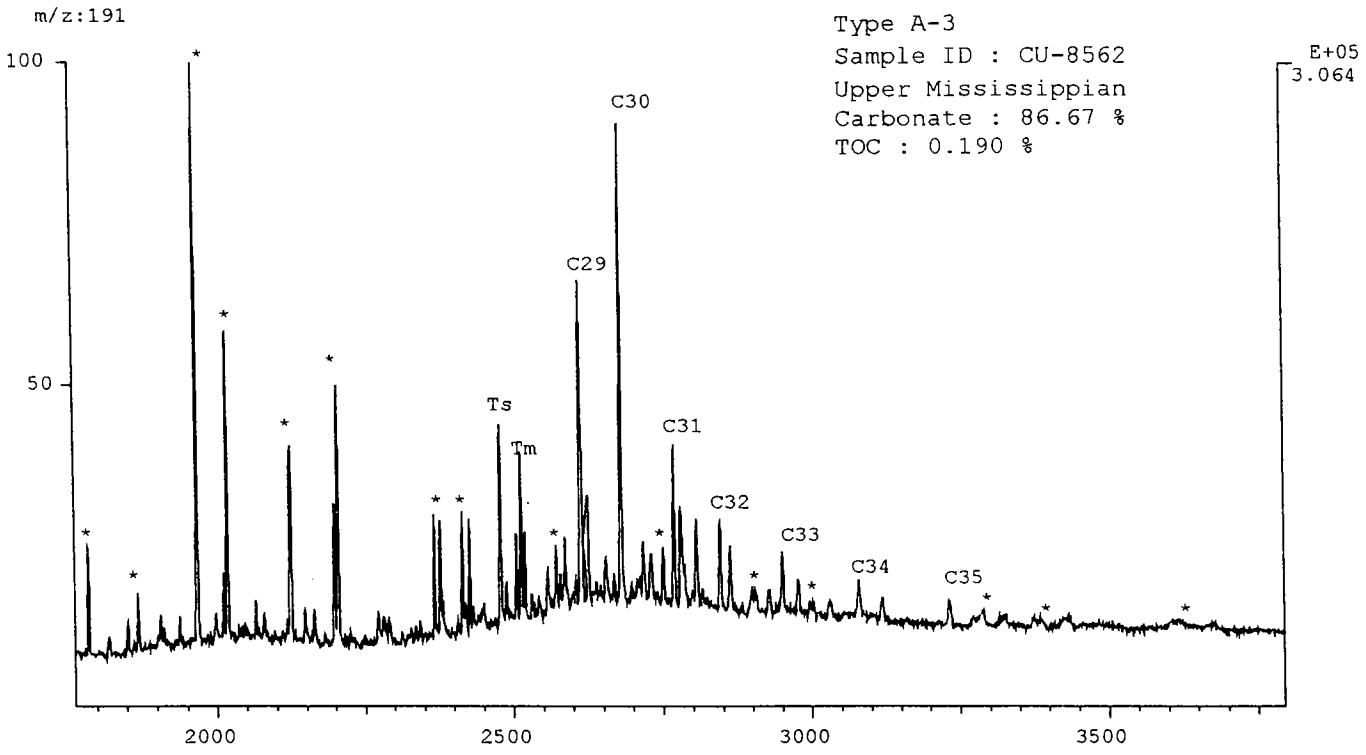

Figure 15. M/z 191 chromatogram of a Mississippian rock extract (facies IV) from the Anadarko basin, showing a terpane distribution of mixed tricyclic and pentacyclic type. The tricyclic terpanes extend to C_{45} in extremely low concentrations, with pentacyclic terpanes up to C_{35}. Asterisk (*) represents tricyclic terpanes.

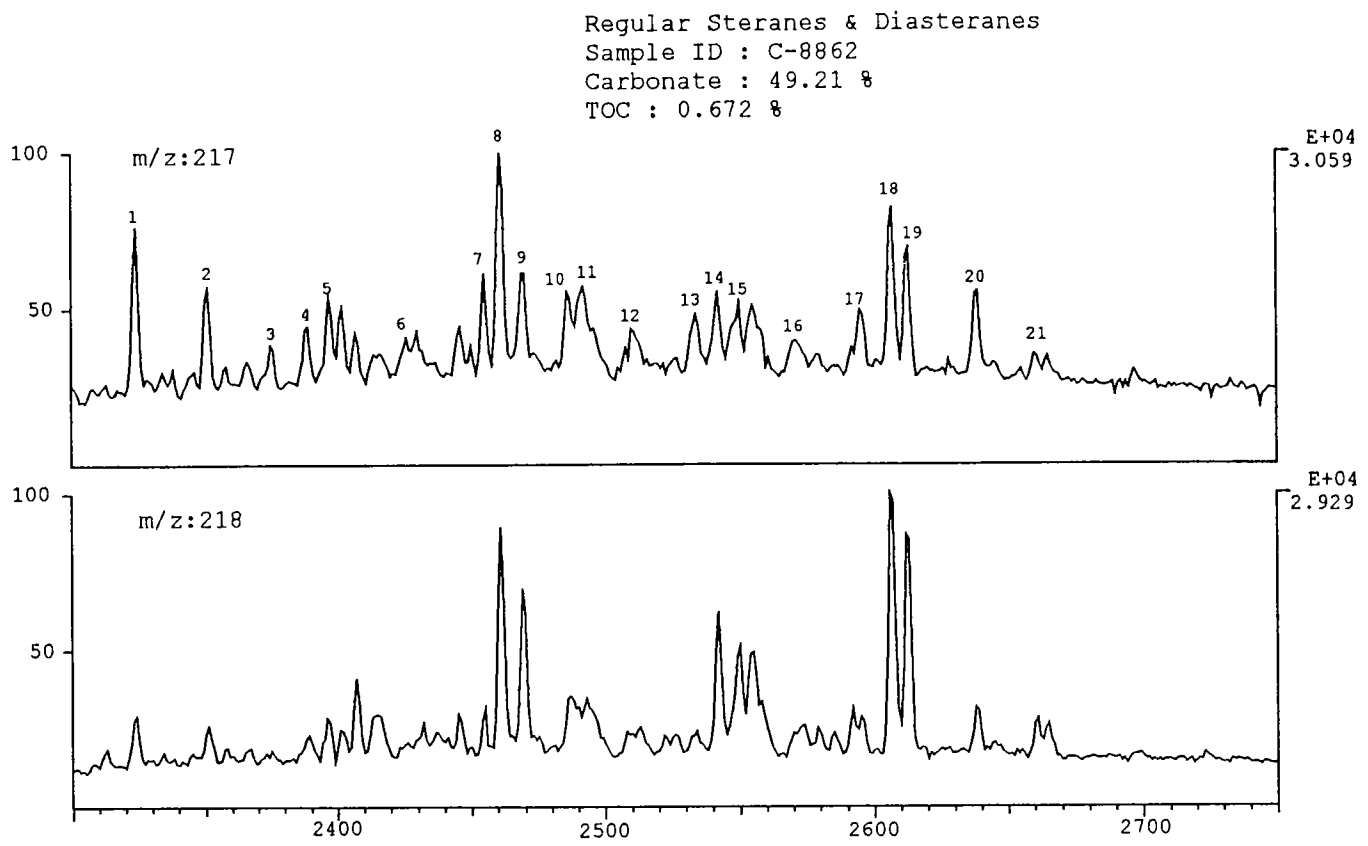

Figure 16. M/z 217 and 218 chromatograms for the branched/cyclic hydrocarbon fraction from sample C-8862. Peak identifications of regular steranes and diasteranes are given in Table 4.

to hopanes appears to vary even in similar facies. Therefore, it is proposed that the prevailing environmental conditions and specific organic sources in marine carbonate environments control the tricyclic terpane composition in the Mississippian rocks in the Anadarko basin. The presence of extended tricyclic terpanes is highly related to the fossil biota in shallow-marine carbonate settings. The large amounts of tricyclic terpanes relative to other compounds, and more specifically relative to the hopanes, are observed in the algae-dominated rocks (facies I). The extended tricyclic terpanes have been reported in Permian tasmanites, but *Tasmanites* was not seen under transmitted light or fluorescent light in either thin section or kerogen slides. Thus, other types of marine algae living in nearshore environments could have been additional and significant sources for the extended tricyclic terpanes in the Mississippian rocks of the Anadarko basin. Moreover, the absolute amounts of tricyclic terpanes (μg/g TOC) show a tendency to increase with TOC and HI at specific intervals in the Capps Unit No. 1 well, but hopanes decrease slightly in absolute amounts at the same intervals. Hence, the main driving force for the increase in the tricyclic to hopane ratio is an increase in the absolute concentration of the tricyclics rather than a significant decrease in the hopanes (Fig. 20). This again supports the idea that an event such as an algal bloom led to an increase in the tricyclic terpane production in these intervals.

SUMMARY

The organic-geochemical analysis of the Mississippian rocks from the Anadarko basin reveals that some of the source-rock extracts contain a series of tricyclic terpanes that extend at least to C_{45} and show an abundance of tricyclic terpanes relative to pentacyclic hopanes in the m/z 191 chromatogram. The present geochemical and petrographic studies indicate that biomarker patterns in the Mississippian rock extracts from the Anadarko basin were primarily controlled by biological organic-source and depositional conditions rather than by thermal maturity. The effects on biomarker distributions from differential thermal maturation were taken into consideration but were excluded in this study because the Mississippian rock samples cover a narrow range of thermal-maturity values.

Four facies were found in the Mississippian carbonate rocks deposited in a shallow-marine environment. The biomarker characteristics, including the relative concentration of tricyclic terpanes to hopanes, are closely related to the facies patterns (Table 5). Extended tricyclic terpanes above C_{30} were not observed in the m/z 191 chromatograms of the extracts from

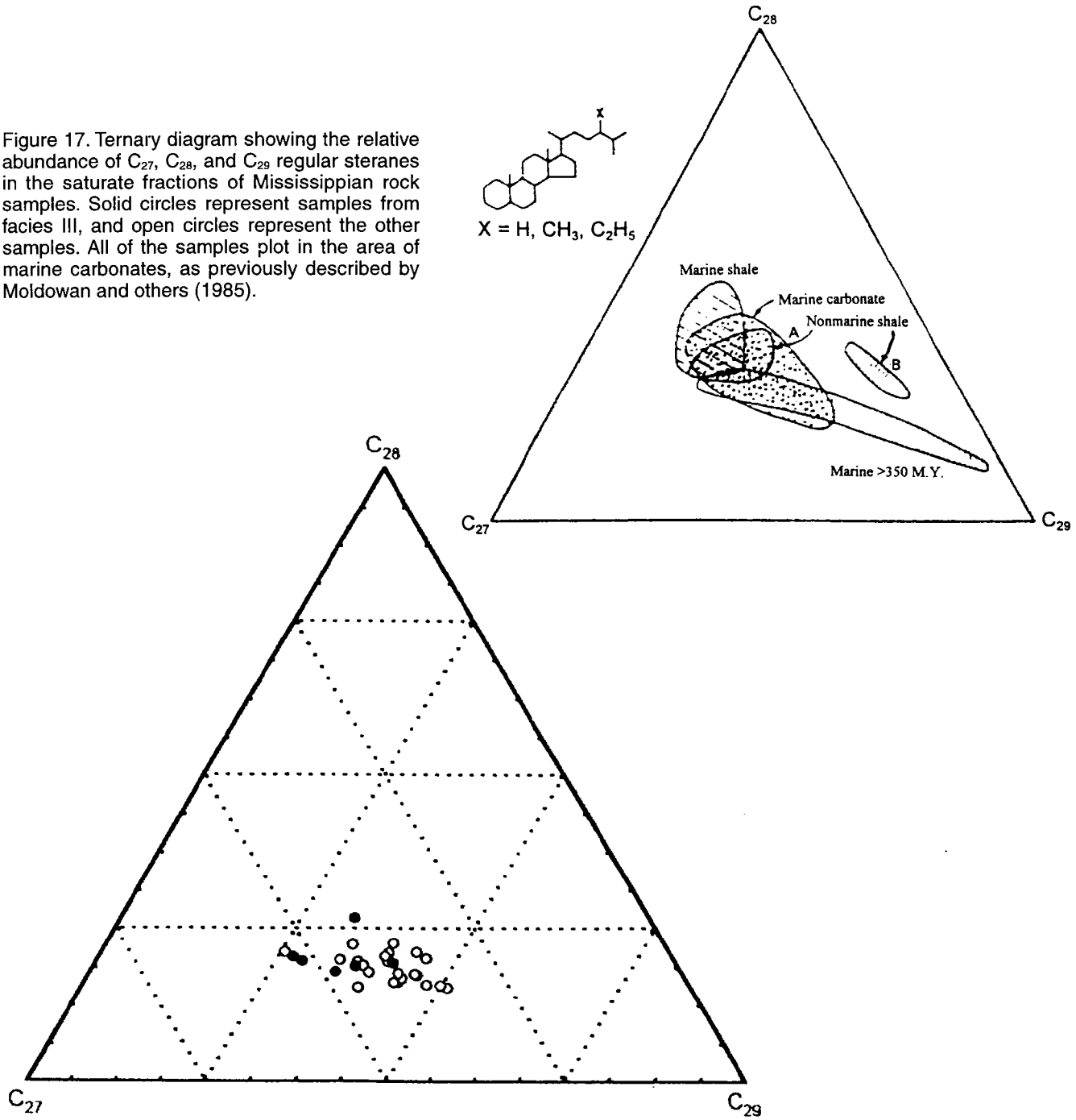

Figure 17. Ternary diagram showing the relative abundance of C_{27}, C_{28}, and C_{29} regular steranes in the saturate fractions of Mississippian rock samples. Solid circles represent samples from facies III, and open circles represent the other samples. All of the samples plot in the area of marine carbonates, as previously described by Moldowan and others (1985).

facies III, in which large amounts of invertebrate bioclasts could be observed under the microscope. On the other hand, the extended tricyclic terpanes up to C_{45} were readily observable in the m/z 191 chromatograms of the extracts from the other facies of the Mississippian carbonate rocks. Therefore, it is proposed that the presence of extended tricyclic terpanes is closely related to the fossil biota (organic source) in marine carbonate settings. Tricyclic terpanes dominate over hopanes in facies I samples, whose major components are algal remains and terrigenous detrital grains on the basis of sedimentary petrography. In addition, the relative concentrations of tricyclic terpanes to hopanes increase with a corresponding increase in TOC and HI at certain depths in the Capps Unit No. 1 well (Fig. 21), although the organic-source materials thoughout the entire section appear to be identical on the basis of petrographic and kerogen studies. It is suggested that a marine algal bloom was the major source of organic material responsible for the abundance of tricyclic terpanes in the Mississippian rocks of the Anadarko basin.

Table 5.—Geological and Geochemical Data for Four Lithologic Facies

Type	Facies I	Facies II	Facies III	Facies IV
Depositional environment	Supratial to intertidal	High-energy shallow shelf	Shallow shelf	Lagoon
Major components	Algal remains	Ooids, bioclasts	Invertebrate bioclasts	Micrite
Terrigenous clastic sediments	High	High	Rare	--
Tricyclic terpanes up to	C_{45}	C_{45}	C_{30}	C_{45}
TT/hopane ratio (average value)	>1.0 (4.44)	≅1.0 (0.94)	<0.5 (0.21)	0.59
Ts/(Ts + Tm)	> 0.70 (0.85)	0.55–0.70	0.53–0.62	0.58
17α(H)-diahopane/ C_{30}17α(H)-hopane	0.32	0.20	0.13	0.18
C_{29}-Ts/ C_{29}-17α(H)-norhopane	> 0.40 (0.59)	0.44–0.64	0.35–0.55 (0.44)	0.49
Pr/Ph	≅1.0	< 1,0	>1.0	0.89

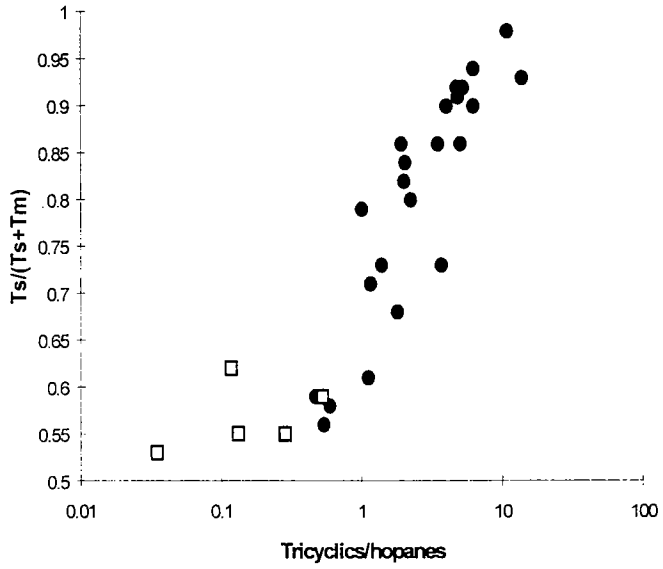

Figure 18. Ratio of tricyclic terpanes to hopanes plotted against the Ts/(Ts + Tm) ratio for extracts examined in this study. The amounts of tricyclic terpanes and hopanes were determined from the m/z 191 chromatograms. Solid circles indicate samples that contain extended tricyclic terpanes, whereas open squares indicate samples in which the extended tricyclic terpanes are absent (facies III).

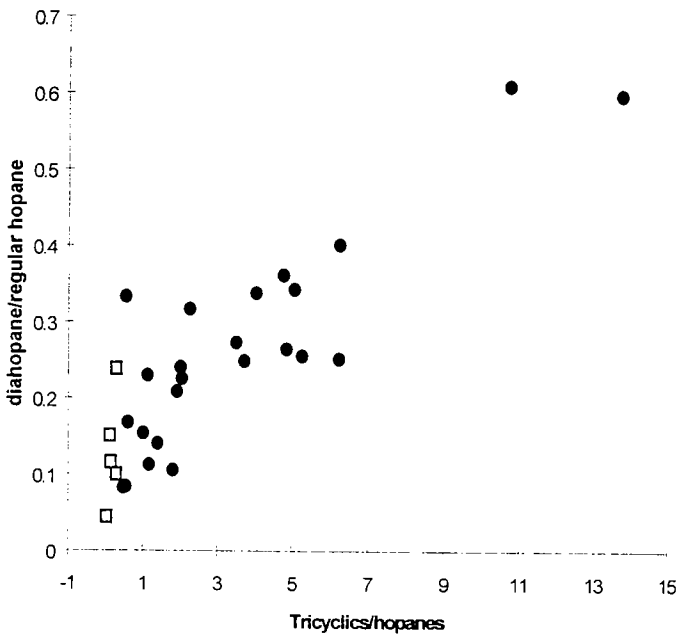

Figure 19. Plot of the ratio of 17α(H)-diahopane/C_{30}-17α(H)-hopane against the ratio of tricyclic terpanes/hopanes in samples that contain extended tricyclic terpanes. Open squares indicate samples in which the extended tricyclic terpanes are in extremely low concentrations in the m/z 191 chromatograms.

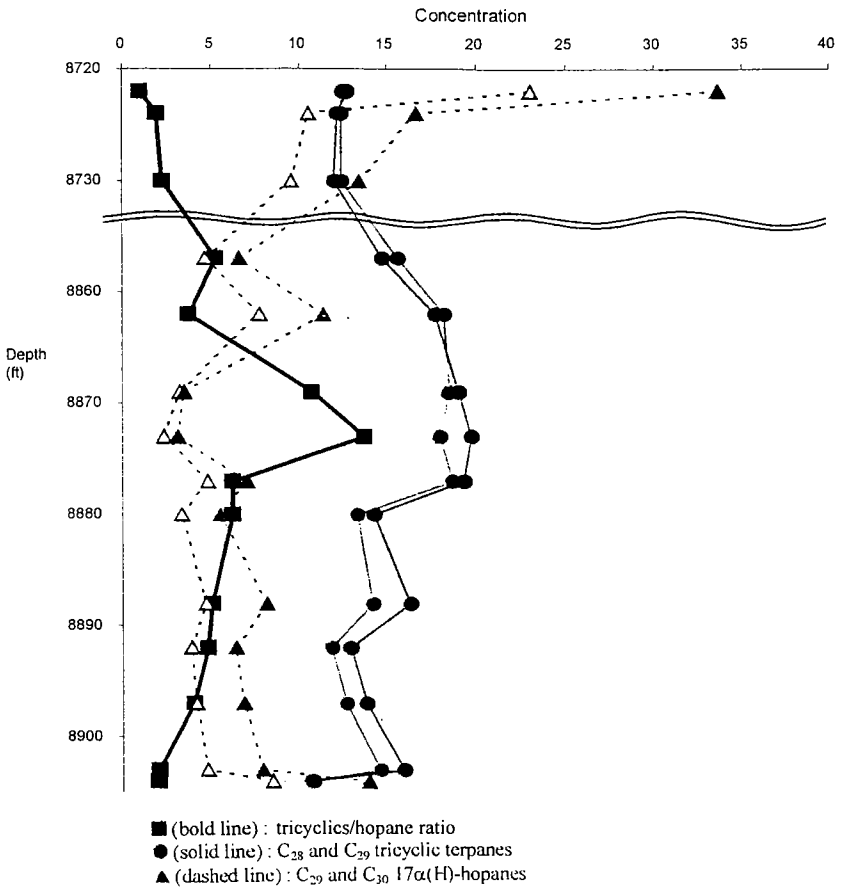

Figure 20. Plots of relative concentrations (ratio of tricyclic terpanes to 17α(H)-hopanes) versus absolute concentrations (μg/g TOC) of tricyclic terpanes (C_{28}-22S and C_{29}-22R), C_{29}-17α(H)-norhopane, and C_{30}-17α(H)-hopane with stratigraphic depth in the Capps Unit No. 1 well.

REFERENCES CITED

Alam, M.; Wang, H. D.; and Philp, R. P., 1993, Extended tricyclic terpanes in sediments from the Anadarko basin [abstract]: Proceedings of 16th International Meeting of European Association of Organic Geochemists, Stavanger, Norway.

Aquino Neto, F. R.; Restle, A.; Connan, J.; Albrecht, P.; and Ourisson, G., 1982, Novel tricyclic terpanes in sediments and petroleums: Tetrahedron Letters, v. 23, p. 2027–2030.

Aquino Neto, F. R.; Trendel, J. M.; Restle, A.; Connan, J.; and Albrecht, P. A., 1983, Occurrence and formation of tricyclic and tetracyclic terpanes in sediments and petroleum, *in* Bjorøy, M.; and others (eds.), Advances in organic geochemistry, 1981: Wiley, New York, p. 659–676.

Aquino Neto, F. R.; Cardoso, J. N.; Rodrigues, R.; and Trindade, L A. F., 1986, Evolution of tricyclic alkanes in the Espirito Santo Basin, Brazil: Geochimica et Cosmochimica Acta, v. 50, p. 2069–2072.

Aquino Neto, F. R.; Triguis, J.; Azevedo, D. A.; Rodrigues, R.; and Simoneit, B. R. T., 1992, Organic geochemistry of geographically unrelated tasmanites: Organic Geochemistry, v. 18, p. 791–803.

Cardott, B. J., 1989, Thermal maturation of the Woodford Shale in the Anadarko basin, *in* Johnson, K. S. (ed.), Anadarko basin symposium, 1988: Oklahoma Geological Survey Circular 90, p. 32–46.

Carter, L. S.; Kelley, S. A.; Blackwell, D. D.; and Naeser, N. D., 1998, Heat flow and thermal history of the Anadarko basin, Oklahoma: American Association of Petro-

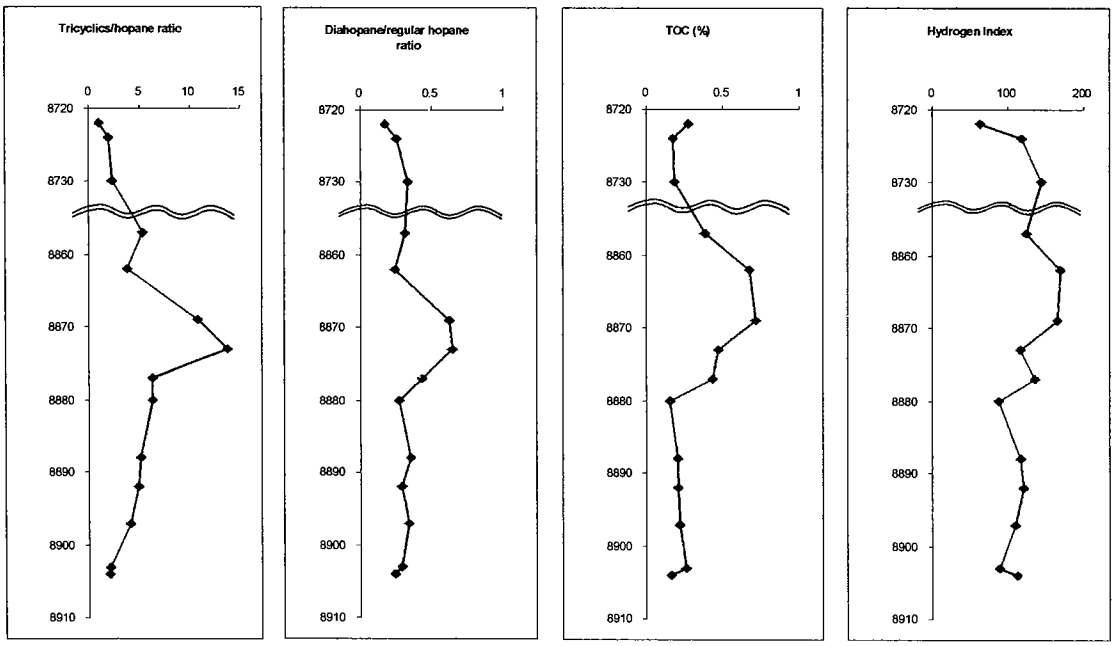

Figure 21. Four diagrams showing tricyclic/hopane ratio, 17α(H)-diahopane/C_{30}-17α(H)-hopane ratio, TOC, and HI with depth in Mississippian rock samples from the Capps Unit No. 1 well. *Y* axis represents depth in feet.

leum Geologists Bulletin, v. 82, p. 291–316.
Chen, Gongquan, 1992, Organic geochemical investigation of the evaporitic cycles in the Paradox basin of southeastern Utah and southwestern Colorado, USA: University of Oklahoma unpublished M.S. thesis, 195 p.
Chicarelli, M. I.; Aquino Neto, F. R.; and Albrecht, P., 1988, Occurrence of four stereoisomeric tricyclic terpane series in immature Brazilian shales: Geochimica et Cosmochimica Acta, v. 52, p. 1955–1959.
de Grande, S. M. B.; Aquino Neto, F. R.; and Mello, M. R., 1993, Extended tricyclic triterpanes in sediments and petroleum: Organic Geochemistry, v. 20, p. 1039–1047.
Dunham, R. J., 1962, Classification of carbonate rocks according to depositional texture, *in* Ham, W. E. (ed.), Classification of carbonate rocks: American Association of Petroleum Geologists Memoir 1, p. 108–121.
Ekweozor, C. M.; and Strausz, O. P., 1983, Tricyclic terpanes in the Athabasca oil sands: their geochemistry, *in* Bjorøy, M.; and others (eds.), Advances in organic geochemistry, 1981: Wiley, New York, p. 746–766.
Fan, Z.; and Philp, R. P., 1987, Laboratory biomarker fractionations and implications for migration studies: Organic Geochemistry, v. 11, p. 169–175.
Folk, R. L., 1962, Spectral subdivision of limestone types, *in* Ham, W. E. (ed.), Classification of carbonate rocks: American Association of Petroleum Geologists Memoir 1, p. 62–84.
Gelpi, E.; Schneider, H.; Mann, J.; and Oro, J., 1970, Hydrocarbons of geochemical significance in microscopic algae: Phytochemistry, v. 9, p. 603–612.
Jiang, Z.; Philp, R. P.; and Lewis, C. A., 1988, Fractionation of biological markers in crude oils during migration and the effects on correlation and maturation parameters: Organic Geochemistry, v. 13, p. 561–571.
Jones, P. J.; and Philp, R. P., 1990, Oils and source rocks from Pauls Valley, Anadarko Basin, Oklahoma, U.S.A.: Applied Geochemistry, v. 5, p. 429–448.
Kruge, M. A.; Hubert, J. F.; Akes, R. J.; and Meriney, P. E., 1990, Biological markers in Lower Jurassic synrift lacustrine black shales, Hartford basin, Connecticut, U.S.A.: Organic Geochemistry, v. 15, p. 281–289.
Lewan, M. D., 1986, Stable carbon isotopes of amorphous kerogens from Phanerozoic sedimentary rocks: Geochimica et Cosmochimica Acta, v. 50, p. 1583–1591.
McCaffrey, M. A.; Simoneit, B. R. T.; Aquino Neto, F. R.; and Moldowan, J. M., 1994, Functionalized biological precursors of tricyclic terpanes: information from sulfur-bound biomarkers in a Permian tasmanite: Organic Geochemistry, v. 21, p. 481–487.
McDonald, T. J.; and Kennicutt, M. C., II, 1992, Fractionation of crude oils by HPLC and quantitative determination of aliphatic and aromatic biological markers by GCMS with selected ion monitoring: LC · GC, v. 10, p. 935–938.
Moldowan, J. M.; and Seifert, W. K., 1979, Head-to-head linked isoprenoid hydrocarbons in petroleum: Science, v. 204, p. 169–171.
Moldowan, J. M.; Seifert, W. K.; and Gallegos, E. J., 1983, Identification of an extended series of tricyclic terpanes in petroleum: Geochimica et Cosmochimica Acta, v. 47, p. 1431–1434.
_____1985, Relationship between petroleum composition and depositional environment of petroleum source rocks: American Association of Petroleum Geologists Bulletin, v. 69, p. 1255–1268.
Moldowan, J. M.; Sundararaman, P.; and Schoell, M., 1986, Sensitivity of biomarker properties to depositional environment and/or source input in the Lower Toarcian of S.W. Germany: Organic Geochemistry, v. 10, p. 915–926.
Ourisson, G.; Albrecht, P.; and Rohmer, M., 1982, Predictive microbial biochemistry, from molecular fossils to procaryotic membranes: Trends in Biochemical Sciences, v. 7, p. 236–239.
Palacas, J. G.; Anders, D. E.; and King, J. D., 1984, South Florida basin—a prime example of carbonate source rocks of petroleum, *in* Palacas, J. G. (ed.), Petroleum geochemistry and source rock potential of carbonate rocks: American Association of Petroleum Geologists, Studies in Geology 18, p. 71–96.
Peters, K. E.; and Moldowan, J. M., 1993, The biomarker guide, interpreting molecular fossils in petroleum and ancient sediments: Prentice Hall, Englewood Cliffs, New Jersey, 363 p.
Petrov, Al. A.; Vorobyova, N. S.; and Zemskova, Z. K., 1990, Isoprenoid alkanes with irregular "head-to-head" linkage: Organic Geochemistry, v. 16, p. 1001–1005.
Philp, R. P.; Alam, M.; and Wang, H. D., 1991, An organic geochemistry study of crude oils and source rocks in the Anadarko basin, Oklahoma: DOE Sedimentary Basin Workshop Proceedings, University of Oklahoma, p. 42–160.
Prothero, D. R.; and Schwab, F., 1996, Sedimentary geology: an introduction to sedimentary rocks and stratigraphy: W. H. Freeman, New York, 575 p.
Seifert, W. K.; and Moldowan, J. M., 1978, Applications of steranes, terpanes, and monoaromatics to the maturation, migration, and source of crude oils: Geochimica et Cosmochimica Acta, v. 42, p. 77–95.
Simoneit, B. R. T.; and Leif, R. N., 1990, On the presence of tricyclic terpane hydrocarbons in Permian tasmanite algae: Naturwissenschaften, v. 77, p. 380–383.
Simoneit, B. R. T.; Schoell, M.; Dias, R. F.; and Aquino Neto, F. R., 1993, Unusual carbon isotope compositions of biomarker hydrocarbons in a Permian tasmanite: Geochimica et Cosmochimica Acta, v. 57, p. 4205–4211.
Volkman, J. K., 1988, Biological marker compounds as indicators of the depositional environments of petroleum source rocks, *in* Fleet, A. J.; Kelts, K.; and Talbot, M. R. (eds.), Lacustrine petroleum source rocks: Geological Society [London] Special Publication 40, p. 103–122.
Wang, H. D.; and Philp, R. P., 1997, Geochemical study of potential source rocks and crude oils in the Anadarko basin, Oklahoma: American Association of Petroleum Geologists Bulletin, v. 81, p. 249–275.
Wang, T. G.; and Simoneit, B. R. T., 1995, Tricyclic terpanes in Precambrian bituminous sandstone from the eastern Yanshan region, North China: Chemical Geology, v. 120, p. 155–170.
West, N.; Alexander, R.; and Kage, R. I., 1990, The use of silicalite for rapid isolation of branched and cyclic alkane fractions of petroleum: Organic Geochemistry, v. 15, p. 499–501.

The Resource-Full Mississippian of Kansas

Paul Gerlach*[1] *and Daniel F. Merriam
Kansas Geological Survey
Lawrence, Kansas

ABSTRACT.—The Mississippian units of Kansas represent the last of the widely occurring, fairly uniform lower Paleozoic rocks in the Midcontinent Stable Interior. Near the end of the Mississippian Period, the North and South American plates collided, causing a change in the previous, mainly stable structural and sedimentary regimes in the region. All of the major structural features in Kansas, which were formed at this time and which overprinted the older structures, are reflected in the structure at the top of the Mississippian rocks. The influx of upper Paleozoic clastics, alternating rhythmically with carbonates, signaled the onset of the Ouachita orogeny and a major change in conditions. These Mississippian units—including, from oldest to youngest, the Kinderhookian, Osagian, Meramecian, and Chesteran—unconformably overlie Silurian–Devonian or Ordovician units and are unconformably overlain by rocks of Pennsylvanian age, which are, from oldest to youngest, Morrowan, Atokan, or Desmoinesian. At this time, Mississippian rocks were stripped by erosion from the crest of newly formed major structural highs of the central Kansas uplift/Cambridge arch, Nemaha anticline, and Pratt anticline.

The mass of Mississippian carbonates, up to 1,700 ft thick, acted as a rigid unit in the deformation and reacted differentially to the vertical movement of the Precambrian basement fault blocks, which readjusted to the tectonism. As a result, the overlying Pennsylvanian units were draped over the fault blocks, forming the *plains-type folds* that served as structural traps for migrating fluids in the sedimentary package overlying the crystalline basement. Mississippian rocks in Kansas thus are important for the resources they contain, which, in addition to petroleum, include the Tri-State lead and zinc ores.

The discovery well of the Virgil field in Greenwood County in 1916 was one of the first to produce from Mississippian rocks in Kansas. Since that time, petroleum production from Mississippian rocks has accounted for slightly more than 16% of Kansas' total oil production and 10% of its gas production. During the 10-year period from 1987 through 1996, oil discoveries in the Mississippian have accounted for slightly more than 33% of the State's total production. Although, historically, most of the Mississippian oil has been produced from the Salina basin and Sedgwick basin, the increasing contribution of Mississippian oil to total production is primarily the result of exploration in the Hugoton embayment in western Kansas. Separating these new discoveries by formation and comparing their spatial distribution to historical production provide a better understanding of emerging trends and new areas for exploration.

INTRODUCTION

Mississippian rocks of Kansas have been prolific producers of oil and gas since discovery of oil in the Virgil field in Greenwood County (southeastern Kansas) in 1916, although some minor production from the Mississippian may have been obtained slightly earlier in Chautauqua and Montgomery Counties (Goebel and Merriam, 1959). A history of the development of petroleum exploration in Kansas was summarized by Merriam and Goebel in 1959. Not only are Mississippian rocks prolific producers of petroleum, but they are host to the famous Tri-State lead and zinc deposits in southeastern Kansas. Thus, the Mississippian has been of special economic importance to the State for slightly more than a century.

Mississippian rocks, probably Osagian and possibly Meramecian in age, crop out in Cherokee County in extreme southeastern Kansas. These rocks were recognized first as Lower Carboniferous (Mississippian) on the Hitchcock and Blake geologic map of the state in 1872, and later as Mississippian on the 1896 map of Erasmus Haworth (Merriam, 1996). This outcrop forms the extreme southwestern edge of the

[1]Current affiliation: Charter Development Corp., Wichita, Kansas.

Gerlach, Paul; and Merriam, D. F., 2001, The resource-full Mississippian of Kansas, *in* Johnson, K. S. (ed.), Silurian, Devonian, and Mississippian geology and petroleum in the southern Midcontinent, 1999 symposium: Oklahoma Geological Survey Circular 105, p. 129–138.

Ozark Plateau, which has been exposed by the denudation of overlying younger clastic deposits of Pennsylvanian age (Late Carboniferous or "Coal Measures").

The Mississippian sequence, mainly carbonates and predominantly limestone, is up to 1,700 ft thick in the subsurface of southwestern Kansas (Zeller, 1968). The different units in the subsurface were recognized originally by the insoluble residues contained in the carbonates. Subsequent studies revealed that these units could be correlated with units from the adjoining states of Missouri and Oklahoma, and those nomenclatures then were applied in Kansas.

The Mississippian has been stripped from the major structural features of the State and extensively karsted by post-Mississippian–pre-Pennsylvanian erosion. Locally, there is a residuum of chert (or "chat") on this surface. Because of the nature of the structural development and erosion, the older units subcrop below Pennsylvanian clastics subparallel to the major structural features, and the youngest units are present in the center of the adjacent basins.

STRATIGRAPHY

Four series are recognized in the Kansas Mississippian, from oldest to youngest: Kinderhookian, Osagian, Meramecian, and Chesteran (Fig. 1). The lower (older) two can be considered Lower Mississippian, and the upper (younger) two Upper Mississippian. The lower contact of Mississippian rocks is gradational locally with underlying units but is unconformable over much of the State. The end of Mississippian deposition was followed by a major erosional unconformity.

Most of the Mississippian consists of limestone and dolomite with a few thin shales. Some of the limestones and dolomites contain chert, which is abundant in certain units. Thus, where the carbonates were weathered and eroded, the chert (or chat) residuum locally serves as a reservoir for petroleum. In south-central Kansas the carbonate units are replaced laterally by the Cowley facies, which is composed of dark silty and sandy dolomite and limestone with chert.

At the base of the Mississippian is the Hannibal Shale (Boice Shale), which also is known informally as the Kinderhook shale. This clastic unit overlies the dark gray to black Chattanooga Shale, at the base of which is the Misener Sandstone. The Devonian–Mississippian contact lies somewhere within the Chattanooga Shale.

The distribution of the different Mississippian stratigraphic units is shown in Figure 2. The pre-Pennsylvanian–post-Mississippian unconformity is probably the most important in Kansas, because the subcrop pattern defines the main structural and petroliferous provinces.

The present distribution of the Mississippian units beneath the Pennsylvanian indicates that they once covered the entire State and since were eroded from the uplifts. The youngest units occur in the deepest parts of the basins, and successively older beds are encountered outward from the basin centers. On the higher parts of the upwarped areas the Mississippian

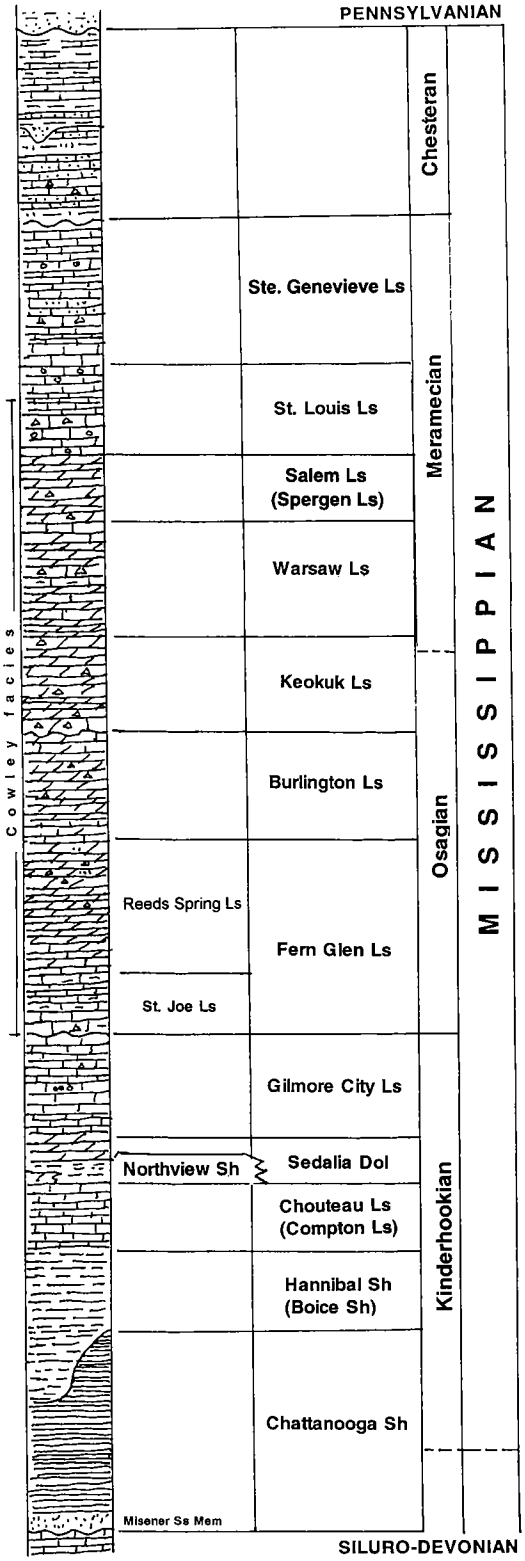

Figure 1. Generalized stratigraphic section of Mississippian rocks in Kansas. From Merriam (2001).

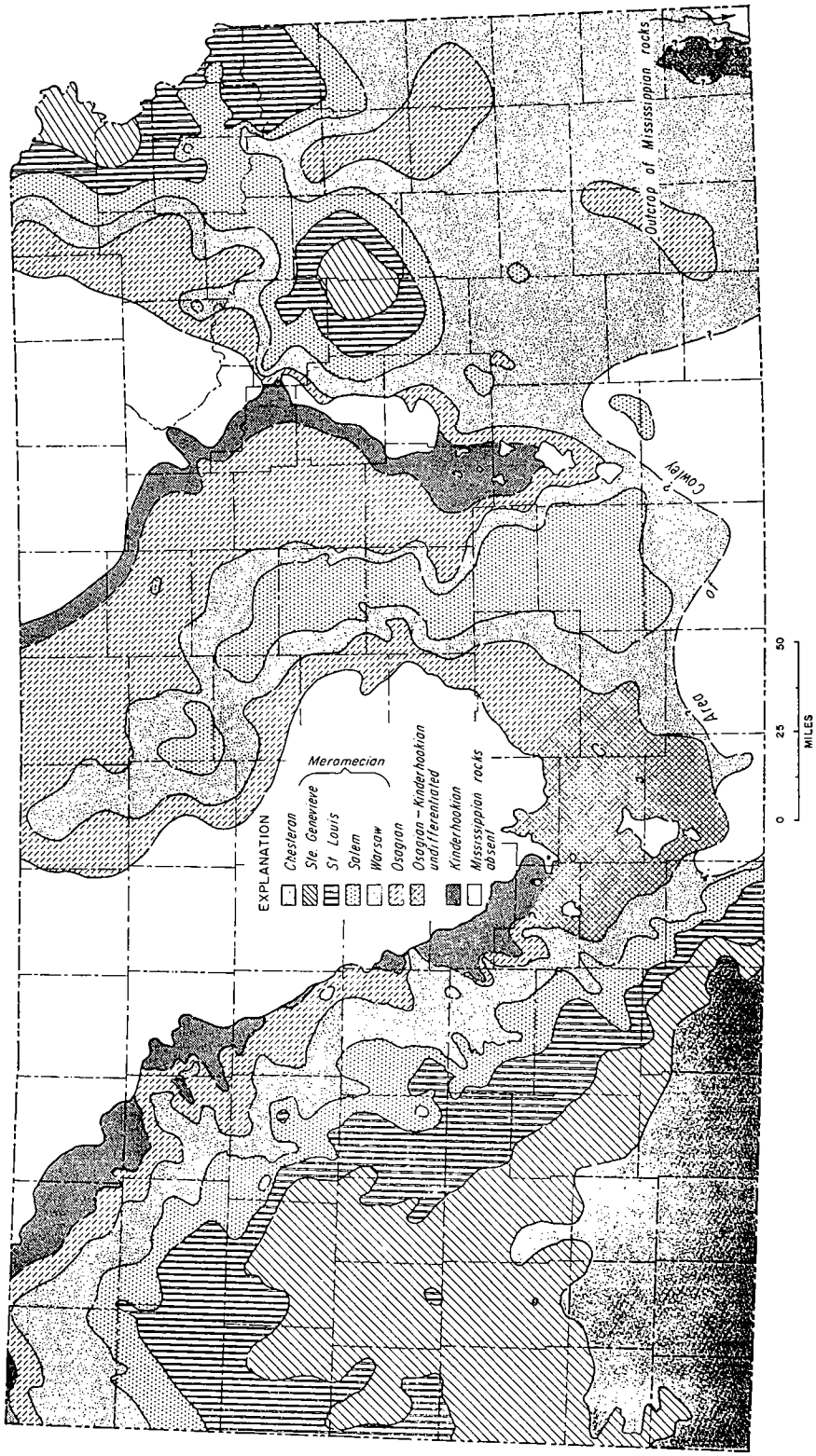

Figure 2. Map of Kansas showing generalized distribution of Mississippian units below Pennsylvanian deposits. From Merriam (1963).

is completely missing. If all the Mississippian units formerly extended across the uplifts, the amount of sediment derived by their removal was voluminous.

STRUCTURE

Although the top of the Mississippian is erosional, it is sufficiently planar to be used as a horizon for contouring structure both on a regional and local scale (Fig. 3). Local petroleum-producing anticlines reflect major structural development that occurred at the end of the Mississippian Period, when the North and South American plates collided. The local anticlines, termed *plains-type folds,* continued to develop after their formation (Merriam and Förster, 1996). The anticlines essentially were formed in sediments, which were draped over differentially tilted Precambrian fault blocks. The porous upper part of the Mississippian carbonates, then, served as conduits and reservoirs for the migrating fluids through this sedimentary package. Plains-type folds in the basins served locally as traps.

1960 Structure Map

The structure at the top of the Mississippian rocks is shown statewide in Figure 4 (Merriam, 1960). Note that the Mississippian is absent from the higher part of the major uparched Nemaha anticline and Cambridge arch/central Kansas uplift. The two prominent features where the Mississippian has been removed on the southern end of the Nemaha anticline are the El Dorado dome (north) and the Augusta dome (south) in Butler County. The structure ranges from outcrop (+900 ft) to the deepest part of the Hugoton embayment at –3,800 ft. This 1960 map was based on about 4,800 control points (Merriam, 1963).

The regional dip of the Mississippian surface in southeastern Kansas is to the west, or slightly north of west. This homoclinal surface is interrupted by numerous minor but economically important structures. Just to the east of the Nemaha anticline is a narrow, sinuous syncline that parallels the structure with a steep dip on the west flank and a gentle dip on the east. This is the axis of the Forest City basin to the north and the Cherokee basin to the south.

West of the Nemaha anticline, the Mississippian surface dips westward into the lower parts of the Salina basin and Sedgwick basin. On this flank are several prominent anticlines. The configuration of the Mississippian is least known in the Salina basin because of the paucity of wells, but local anticlinal oil-producing structures have been outlined by intensive drilling. The Sedgwick basin is reflected as a south-dipping surface having many minor, south-plunging structural noses and reentrants. Many structures, especially on the eastern side of the basin, are semiparallel or parallel to the Nemaha anticline. The west side of the basin is discernible by the south-plunging Pratt anticline.

West of the Cambridge arch/central Kansas uplift complex is the large, shovel-shaped, south-plunging Hugoton embayment. The western side of the Hugoton is bounded by the eastern flank of the Las Animas arch with several subsidiary, north-plunging anticlinal structures. In the embayment are many small, long, narrow, south-plunging anticlines and small domal structures. In the extreme southwestern corner of the State is the prominent Keyes dome in Morton County.

1998 Structure Map

Information from 16,000 qualified wells was used to quality-check formation data from approximately

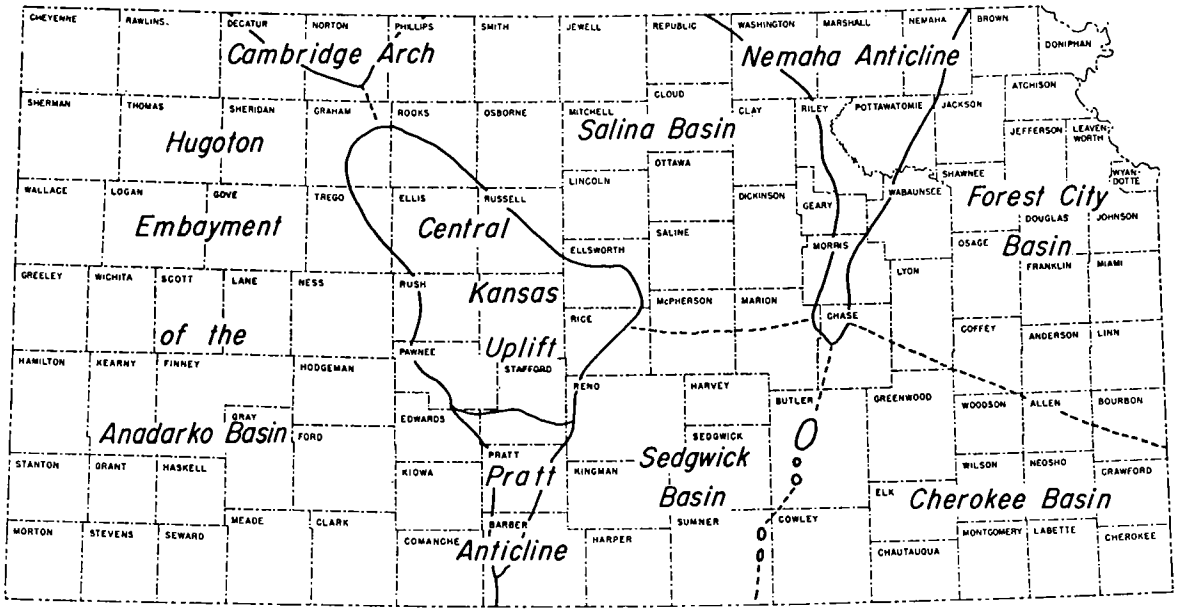

Figure 3. Map showing major structural features of Kansas. From Merriam (1963).

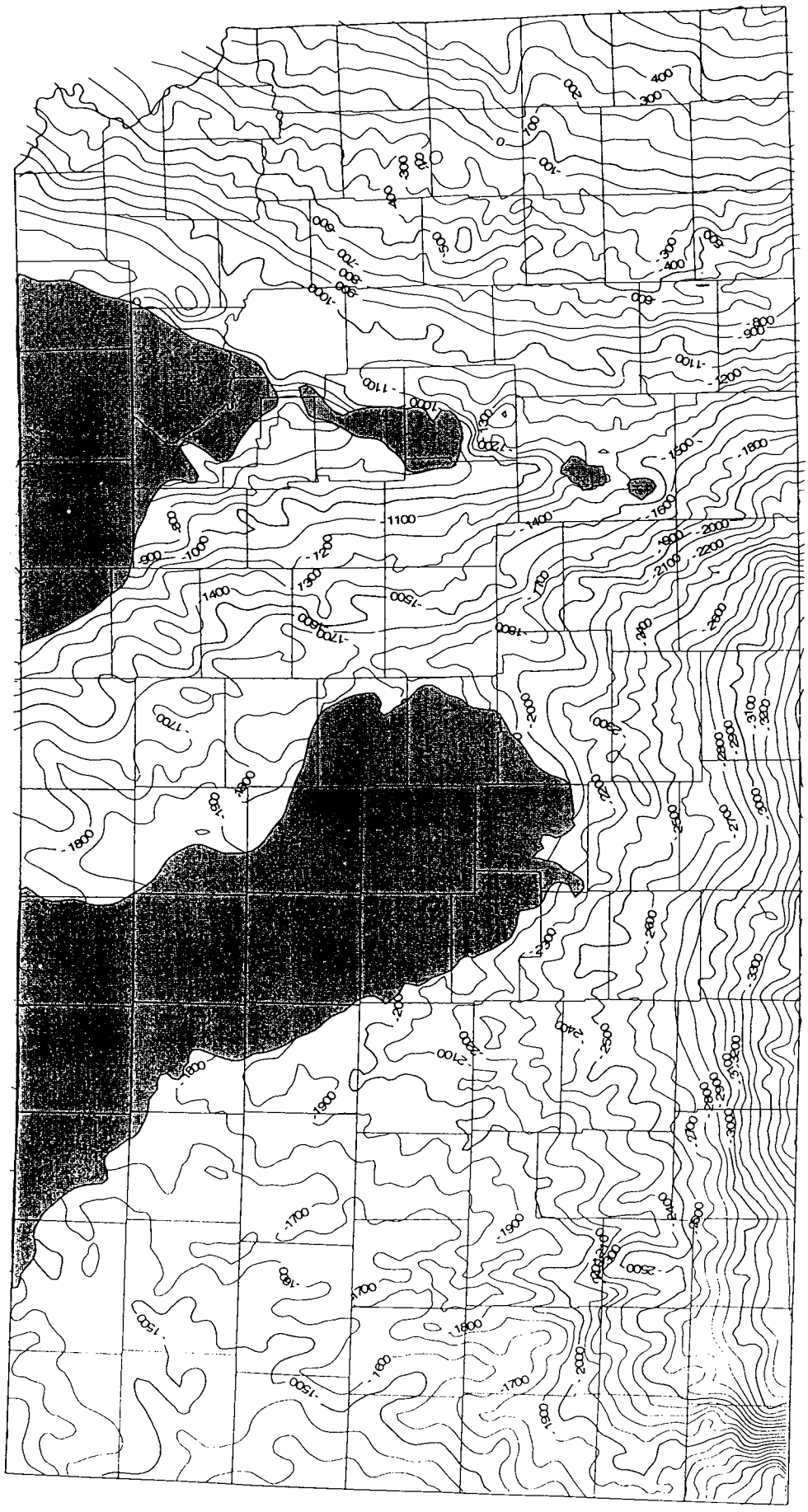

Figure 4. Regional structural map contoured in 1960, showing the top of the Mississippian rocks in Kansas. From Merriam (1960, 1963). Contour interval = 100 ft.

53,000 operator-reported wells. Structure, isopach, subcrop, and worm's-eye-view maps were constructed from this data set. The values for the top of the Mississippian were contoured using a minimum-curvature gridding algorithm with an x, y grid size of 5,280 ft.

Note that the major Mississippian structural features on the 1998 map are essentially the same as on the 1960 map, but the detail is greatly enhanced (Fig. 5). The structural attitude ranges from +800 ft on outcrop to a depth of –3,500 ft in the Hugoton embayment in the extreme southwestern corner of the State. Visually, most changes are seen in the Sedgwick basin and Hugoton embayment. This result was to have been expected because of the focus of exploration in those areas since 1960.

"Difference" Maps

The biggest changes between the 1960 and 1998 maps are in the areas that were intensely drilled, which for the most part were in the Hugoton embayment, Salina basin, and Cherokee basin. These deeper basins had not been the focus of earlier exploration because of their depth, the cost of exploratory drilling, and low expectations. As the price of petroleum increased in the 1970s, these deeper and more speculative targets became economically attractive.

The positive-difference map (Fig. 6) shows the areas where the 1960 map had shown the top of the Mississippian too high and by what amount. The Hugoton embayment is an area where not many wells had been drilled previously. The large changes in the Salina basin and Cherokee basin also were the result of wells drilled in areas that had no previous tests. The 1960 map was hand contoured and subject to subjective interpretation, whereas the 1998 map was constructed using an automated contouring program. This technical difference in the two maps could account for some of the implied difference. All things considered, the 1960 map was a fair representation of the configuration of the top of the Mississippian over most of the State.

Other major differences occur in the Hugoton embayment. In the extreme southwestern corner of the State, new data show that the 1960 surface was too low and by what amount (Fig. 7). A big difference occurs in the area of the Keyes dome, where only meager data were available in earlier days. Numerous other areas in the Hugoton gas field were changed by deeper drilling under the gas reservoir and by infill drilling. Again, only a few wells prior to 1960 had been drilled below the large, shallow Hugoton gas field for reasons other than geological.

MISSISSIPPIAN OIL AND GAS PRODUCTION

Since the discovery of petroleum in Mississippian rocks in the early part of the 20th century, oil from Mississippian rocks has accounted for slightly more than 16% of the State's production—up from about 10% in the 1950s. The total gas production is about 10% of the State's total (see Merriam and Goebel, 1959, 1960, for early statistics). During the 10-year period from 1987 through 1996, however, additional discoveries in the Mississippian increased oil production so that it accounted for slightly more than 33% of the State's total. Although, historically, most of the Mississippian oil has been produced from the Salina and Sedgwick basins, the increasing contribution of Mississippian oil to total production is primarily the result of exploration and development in the Hugoton embayment in western Kansas.

Figure 8 shows the cumulative estimated ultimate recovery of Mississippian oil, which is about 1 billion barrels. The estimated ultimate recovery from new annual discoveries has declined during the years, as is evident in Figure 9. The cumulative estimated ultimate recovery of Mississippian gas is almost 4 trillion cubic feet (Fig. 10). As for oil, the estimated ultimate recovery from annual gas discoveries is declining (Fig. 11).

Although most of the major discoveries probably have been made in Mississippian rocks, much remains to be discovered, and the Mississippian remains a viable target for exploration.

ACKNOWLEDGMENTS

We would like to thank Saibal Bhattacharya and David Newell of the Kansas Geological Survey for reading a preliminary version of this paper and offering helpful comments.

REFERENCES CITED

Goebel, E. D.; and Merriam, D. F., 1959, Mississippian rocks in eastern Kansas, *in* Proceedings of 6th Symposium on Geology: University of Oklahoma, p. 99–121.

Merriam, D. F., 1960, Preliminary regional structural contour map on top of Mississippian rocks in Kansas: Kansas Geological Survey Oil and Gas Investigation 22, map.

_____1963, The geologic history of Kansas: Kansas Geological Survey Bulletin 162, 317 p.

_____1996, Kansas 19th-century geologic maps: Kansas Academy of Science, v. 99, nos. 3/4, p. 95–114.

_____2001, The stratigraphic record in Kansas: Kansas Geological Survey, chart, in preparation.

Merriam, D. F.; and Förster, A., 1996, Precambrian basement control on 'plains-type folds' (compactional features) in the Midcontinent region, USA, *in* Oncken, O.; and Janssen, C. (eds.), Basement tectonics 11: Kluwer Academic Publisher, Dordrecht, Netherlands, p. 149–166.

Merriam, D. F.; and Goebel, E. D., 1956, Kansas' structural provinces offer varied types of traps: Oil and Gas Journal, v. 54, no. 52, p. 141, 143–145, 147–149, 151, 153–154.

_____1959, Alert explorers find Kansas oil: Oil and Gas Journal, v. 57, no. 10, p. 166–168, 171–175; Where's the oil in Kansas?: Oil and Gas Journal, v. 57, no. 11, p. 212–218.

_____1960, Kansas' oil, gas-field discoveries continue to mount: Oil and Gas Journal, v. 58, no. 13, p. 250–253.

Zeller, D. E. (ed.), 1968, The stratigraphic succession in Kansas: Kansas Geological Survey Bulletin 189, 81 p.

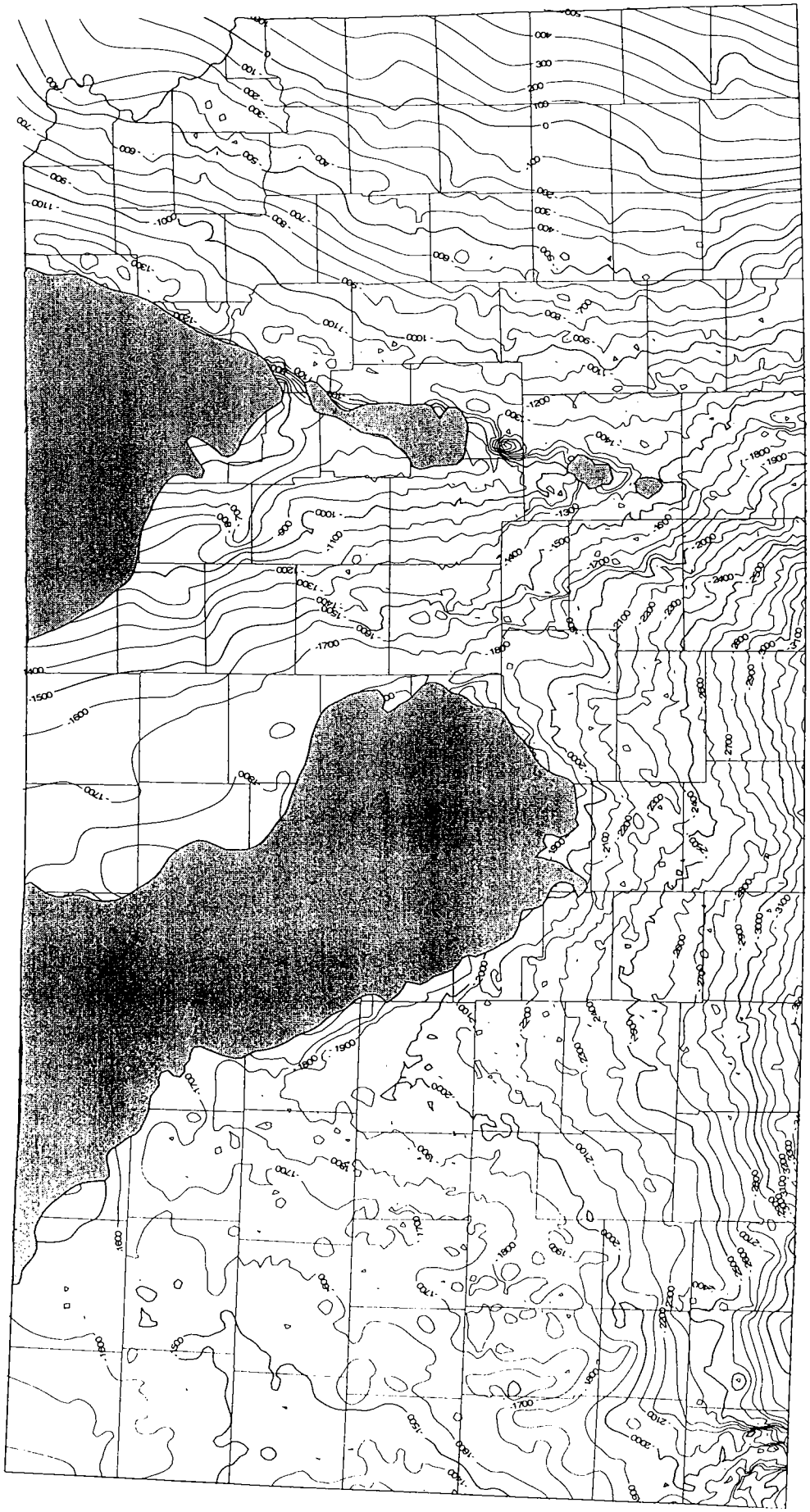

Figure 5. Regional structural map contoured in 1998, showing the top of the Mississippian rocks in Kansas. Contour interval = 100 ft.

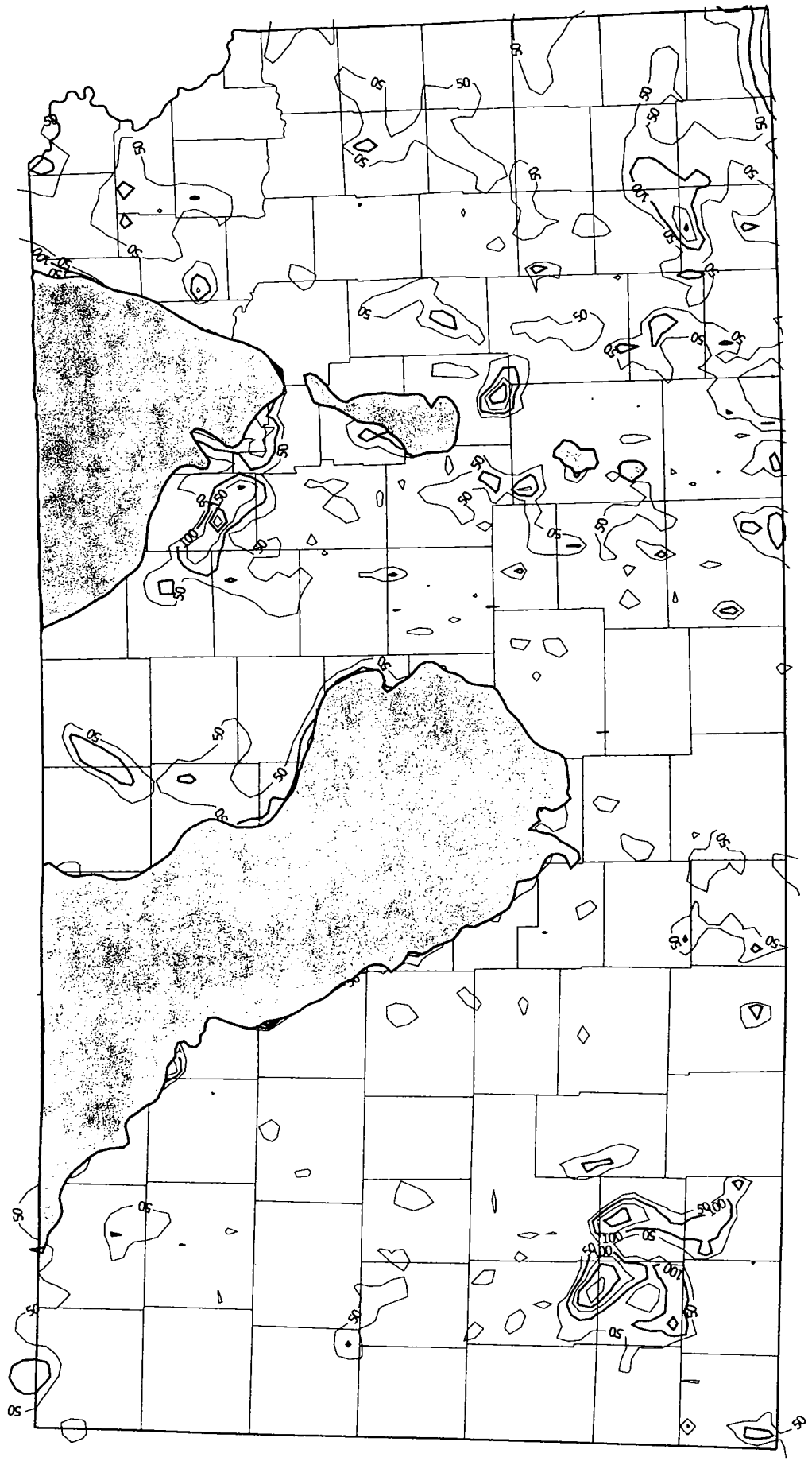

Figure 6. Positive-difference map of the configuration of the top of the Mississippian rocks in Kansas from 1960 to 1998. Map shows where the 1960 map of the Mississippian was too high. Contour interval = 50 ft.

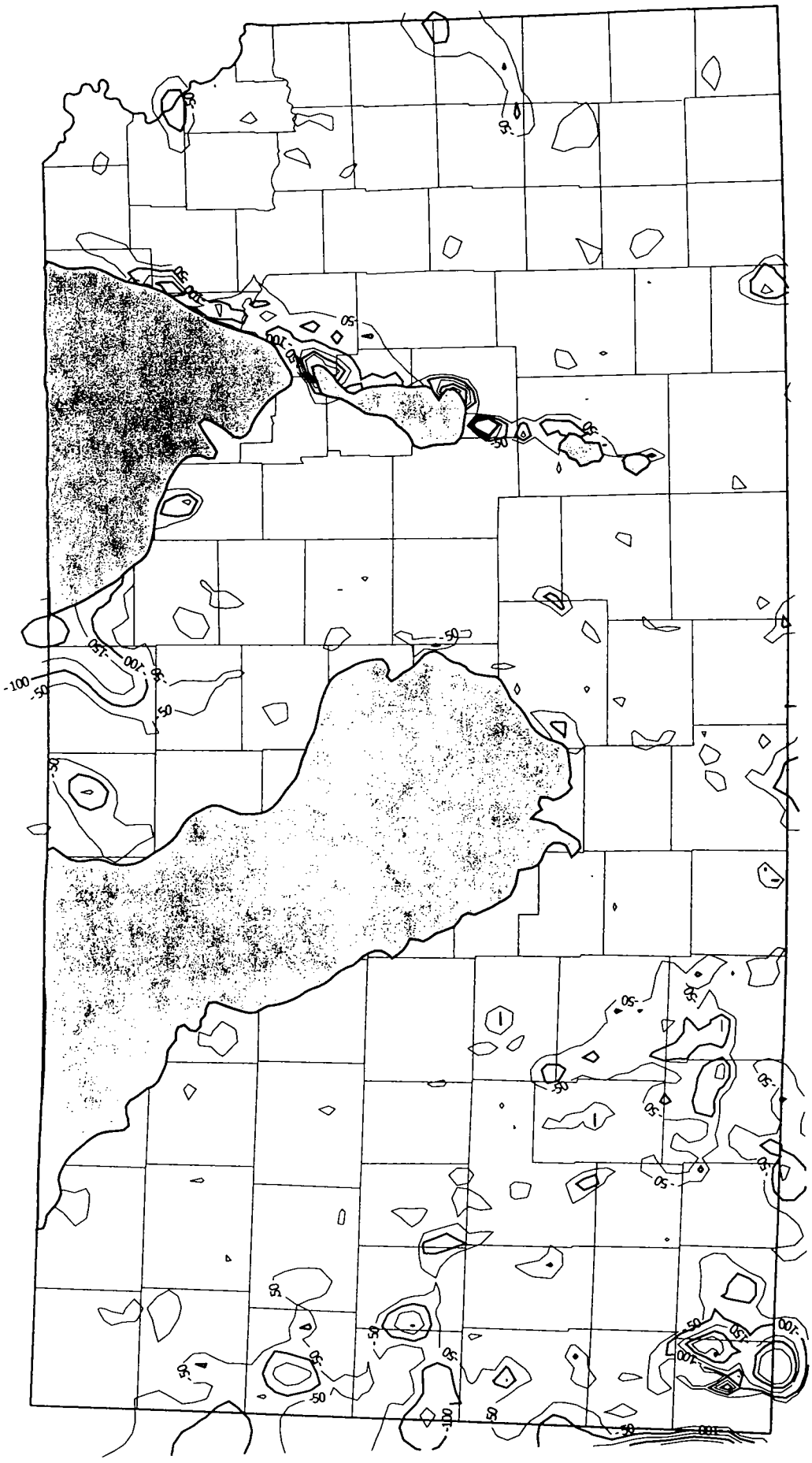

Figure 7. Negative-difference map of the configuration of the top of the Mississippian rocks in Kansas from 1960 to 1998. Map shows where the 1960 map of the Mississippian was too low. Contour interval = 50 ft.

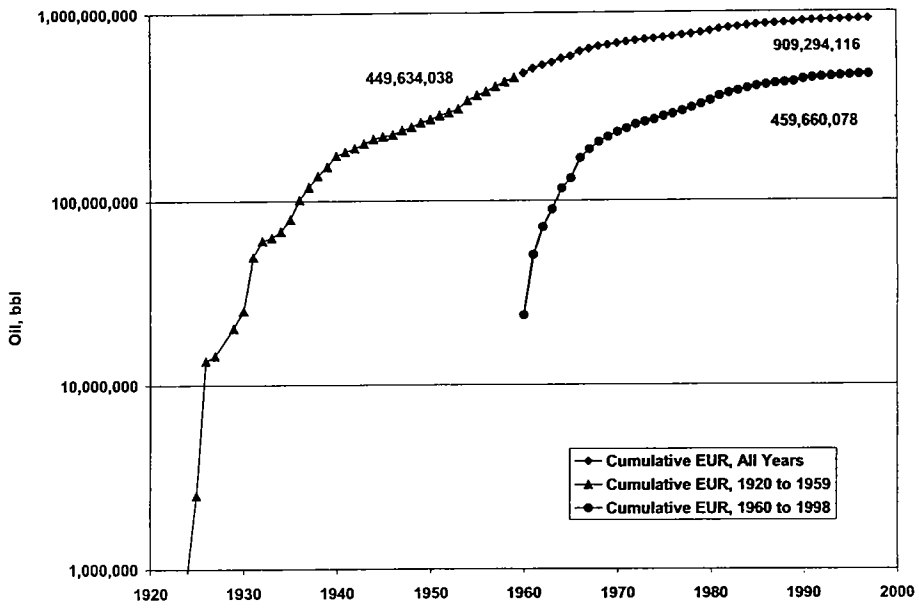

Figure 8. Cumulative estimated ultimate recovery (EUR) of Mississippian oil from Kansas reservoirs.

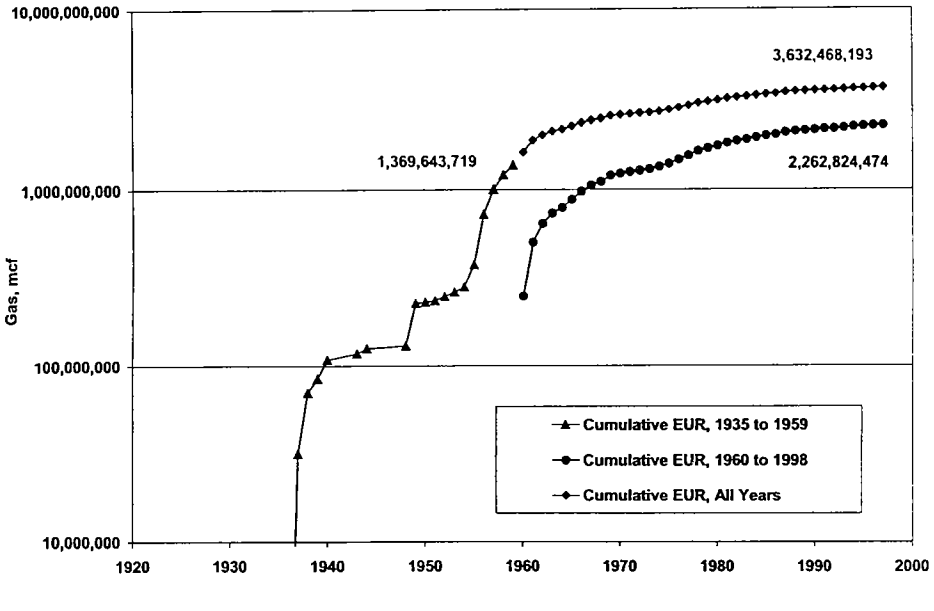

Figure 10. Cumulative estimated ultimate recovery (EUR) of Mississippian gas from Kansas reservoirs.

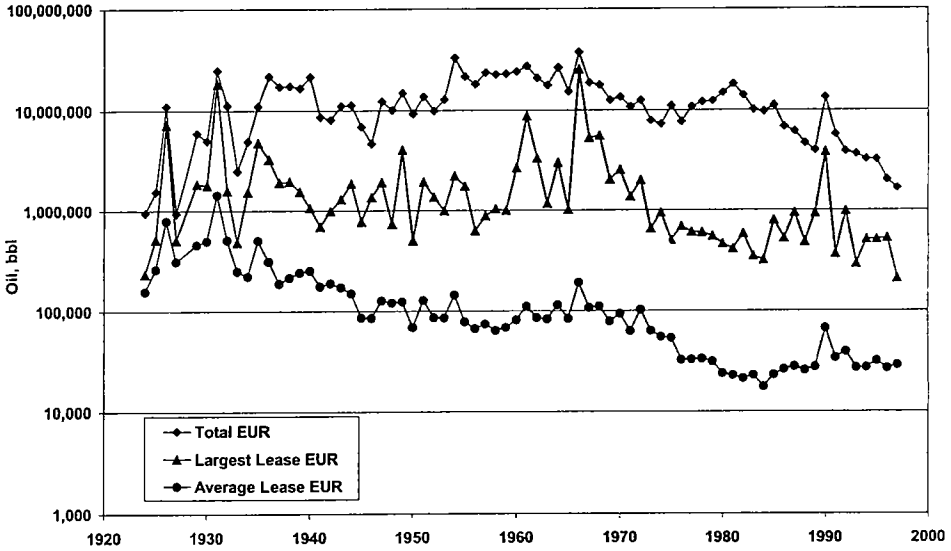

Figure 9. Estimated ultimate recovery (EUR) from annual discoveries of Mississippian oil in Kansas: total, maximum, and average.

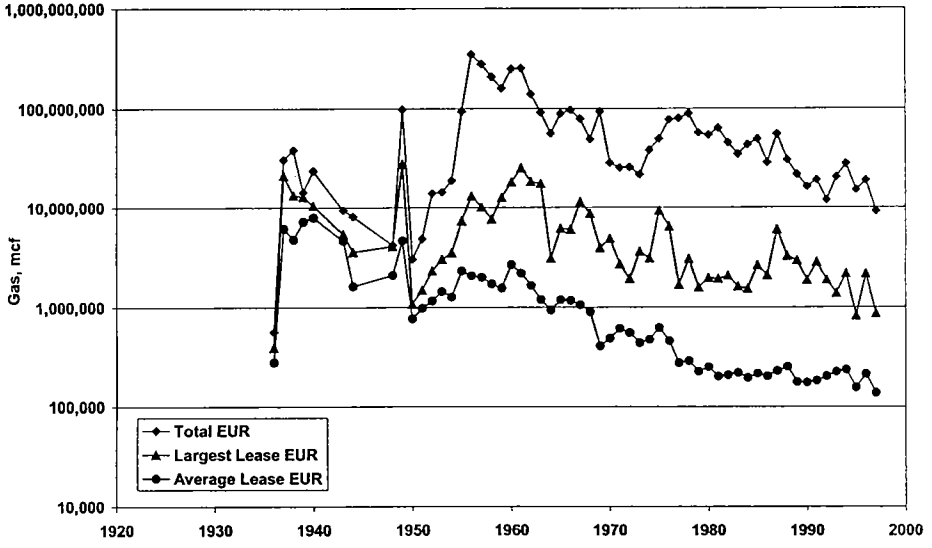

Figure 11. Estimated ultimate recovery (EUR) from annual discoveries of Mississippian gas in Kansas: total, maximum, and average.

Field Study of the Sycamore Formation on Interstate Highway 35 in the Arbuckle Mountains, Oklahoma

R. Nowell Donovan
Texas Christian University
Fort Worth, Texas

ABSTRACT.—The Early Mississippian Sycamore Formation records the beginning of a period of crustal mobility that marked the beginning of the closure of the Laurentian and Gondwana plates. Prior to this time, Laurentian sedimentation took place within a relatively stable tectonic framework. A new tectonic framework, involving localized basin and uplift, developed from the beginning of Sycamore time.

The Sycamore Formation, which is 250–350 ft thick, ranges in age from Kinderhookian to earliest Meramecian. It conformably overlies the Upper Devonian Woodford Formation and unconformably underlies the Mississippian Caney Shale. Stratigraphically, the Sycamore is something of an orphan, disappearing generally to the northeast beneath a regional unconformity at the base of the Caney. Sycamore paleogeography is thus heavily inferential. Two members can be recognized in the Sycamore: the lower "transition" member is composed of gray shales and argillaceous chert-bearing limestones, and the upper member consists of interbedded gray shales and tan-weathering marlstones containing up to 50% silt-sized siliciclastic grains. The shales, which are little disturbed by bioturbation, record slow deposition in a quiet, deep-water setting. Paleontological evidence suggests that the shales are a condensed sequence. Individual marlstone beds display a sharp or slightly erosive base and a massive basal bed from a few inches to 4 ft thick. Other commonly observed features include, in the uppermost parts of some beds, low-amplitude ripple marks and horizontal burrows. A few thin lag deposits of fossil hash occur at the base of some of the beds: detritus in this position includes calcispheres, a little glauconite, some quartz sand, and (rarely) brachiopod valves. These beds are interpreted as turbidites that reworked fine-grained distal shelf material; there is a hierarchical arrangement of the marlstones into deep submarine-fan packages. The near absence of typical Bouma profiles is probably a reflection of the fine-grained nature of the available sediment. Current movement was dominantly to the west.

Well-exposed sections on Interstate Highway 35, 7 mi apart on the north and south limbs of the Arbuckle anticline, display similar but not identical sequences. The northern section displays features that suggest a location closer to source than the southern section. This relationship can be extended to the transition member, where a shelf carbonate—the Welden Limestone—is represented to the south by "deep"-water bedded chert and calcareous shale.

INTRODUCTION

Road cuts along Interstate Highway 35 in the Arbuckle Mountains expose a magnificent cross section through the Arbuckle anticline, a large-scale, much-faulted, highly asymmetric west-northwest–east-southeast-trending structure on the northern flank of the southern Oklahoma aulacogen. The road cuts display an important section of the lower Paleozoic sedimentary sequence (Ham, 1969; Fay, 1989); the topography is bracketed by exposures of the Early Mississippian Sycamore Formation.

The southern section of the Sycamore dips to 165° (i.e., west-southwest) at 45°. The most complete road cut on the west side of the interstate exposes a lengthy unbroken section (370 ft, ~113 m) as measured by Ham (1969), and 358 ft (~109 m) as measured by Fay (1989). The sequence is easy to log but is somewhat monolithic with relatively little three-dimensional undercutting of bed contacts (Fig. 1). In this study the top part of the section was not logged in detail, as it is no longer in pristine condition.

By contrast, the northern section is slightly overturned, dipping to the south-southwest (190°) at angles of about 70° in a lengthy exposure on the east side of the interstate (Fig. 2). The section is substantially less than that seen in the southern exposures; both Ham (1955) and Fay (1989) recorded 221 ft (~67 m). Most of this difference is probably due to genuine

Donovan, R. N., 2001, Field study of the Sycamore Formation on Interstate Highway 35 in the Arbuckle Mountains, Oklahoma, *in* Johnson, K. S. (ed.), Silurian, Devonian, and Mississippian geology and petroleum in the southern Midcontinent, 1999 symposium: Oklahoma Geological Survey Circular 105, p. 139–149.

stratigraphic variation; on the other hand, some may be the result of structural thinning during overturning of the beds on the northern outcrop. The nature of the exposure is such that a reasonable appreciation of the three-dimensional character of the beds can be gained; in particular, bed bases are clearly exposed.

The purpose of this study is to compare and contrast the two sections, placing particular emphasis on facies interpretation. The petrographic character of the beds is also evaluated.

STRATIGRAPHIC POSITION OF THE SYCAMORE FORMATION

The Sycamore Formation was first recognized by Taff in 1903 as the "Sycamore Limestone" at a type locality on Sycamore Creek in western Johnston County. Gould (1925, p. 22–23) described the Sycamore as about 200 ft of "rather hard, tough, slaty, blue limestone, weathering yellow. Often separated into thin beds, usually a foot or two in thickness."

The early workers recognized that the Sycamore is of limited lateral extent, being restricted at outcrop to the southwestern part of the Arbuckle Mountain area (Ham, 1969). This restriction is in part due to erosion that is recorded by an unconformity at the base of the overlying Caney Shale, as a result of which the Caney completely overlaps the Sycamore to rest on the Welden Limestone in the northeastern Arbuckle Mountains.

The limited outcrop area of the Sycamore is of interest in the general Paleozoic history of southern Oklahoma in that it is one of the earliest formations that is so laterally restricted. In general, underlying units can be carried stratigraphically over a wide area, with the earlier Cambrian–Ordovician strata generally thickening into the southern Oklahoma aulacogen but being easily traceable on to the adjacent craton. Overlying Silurian–Devonian units show less thickening into the aulacogen but are similarly widespread. This tectonic template was broken first by epeirogenic movements that preceded craton-wide deposition of the Late Devonian Woodford Formation and its lateral equivalents. As a result, a sub-Woodford unconformity can be traced over much of Oklahoma, in places cutting down into Ordovician strata (Ham, 1955). The Sycamore, which overlies the Woodford, is the earliest of a sequence of units that show marked thickening into the southern Oklahoma aulacogen and have limited, if any, presence on the adjacent craton. The Sycamore apparently records the commencement of a Mississippian redefinition of the aulacogen that was characterized by the deposition of immense volumes of siliciclastics. This redefinition continued until the Pennsylvanian basin inversion event, which led to the formation of the Arbuckle Mountains.

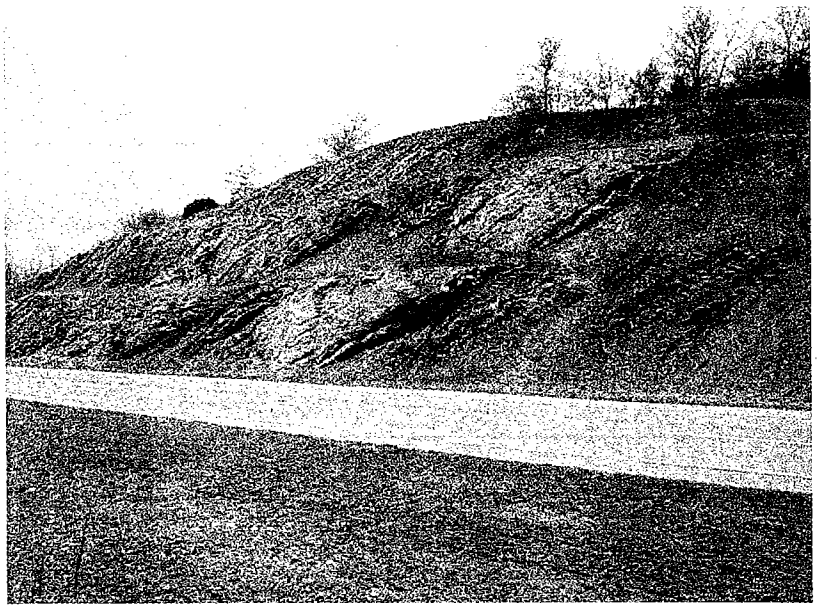

Figure 1. Outcrop of the southern exposure of the Sycamore Formation as exposed on the west side of I-35. View to southwest illustrates the robust weathering profile of the marlstones in the formation.

Figure 2. Outcrop of the northern exposure of the Sycamore Formation as exposed on the east side of I-35. Strata are overturned, clearly displaying the undersides of individual beds.

LITHOLOGIC DIVISION AND AGE OF THE SYCAMORE FORMATION

Lithologic logs of the I-35 sections are presented in Figures 3 and 4. Two lithologies dominate the Sycamore Formation: gray shales (many of which are calcareous), and tan-weathering, light gray impure limestones (marlstones). Fay (1989), in logging these sections during construction of the highway, recognized sequences that are dominated by one or the other of these two lithologies. Thus, in the southern exposure, he defined lower, middle, and upper limestone members, separated by shale-dominated sequences. In the thinner, northern exposure he recognized just two limestone members. In both exposures he erected a "transition zone" of shales, cherts, and limestones between the underlying Woodford Formation and the aforementioned ridge-forming marlstones. In doing this, he followed earlier work by Prestridge (1959), who had recognized a lower Cornell Ranch Member (apparently equivalent to Fay's 1989 transition zone) and an upper Worthey Member (the Sycamore sensu stricto).

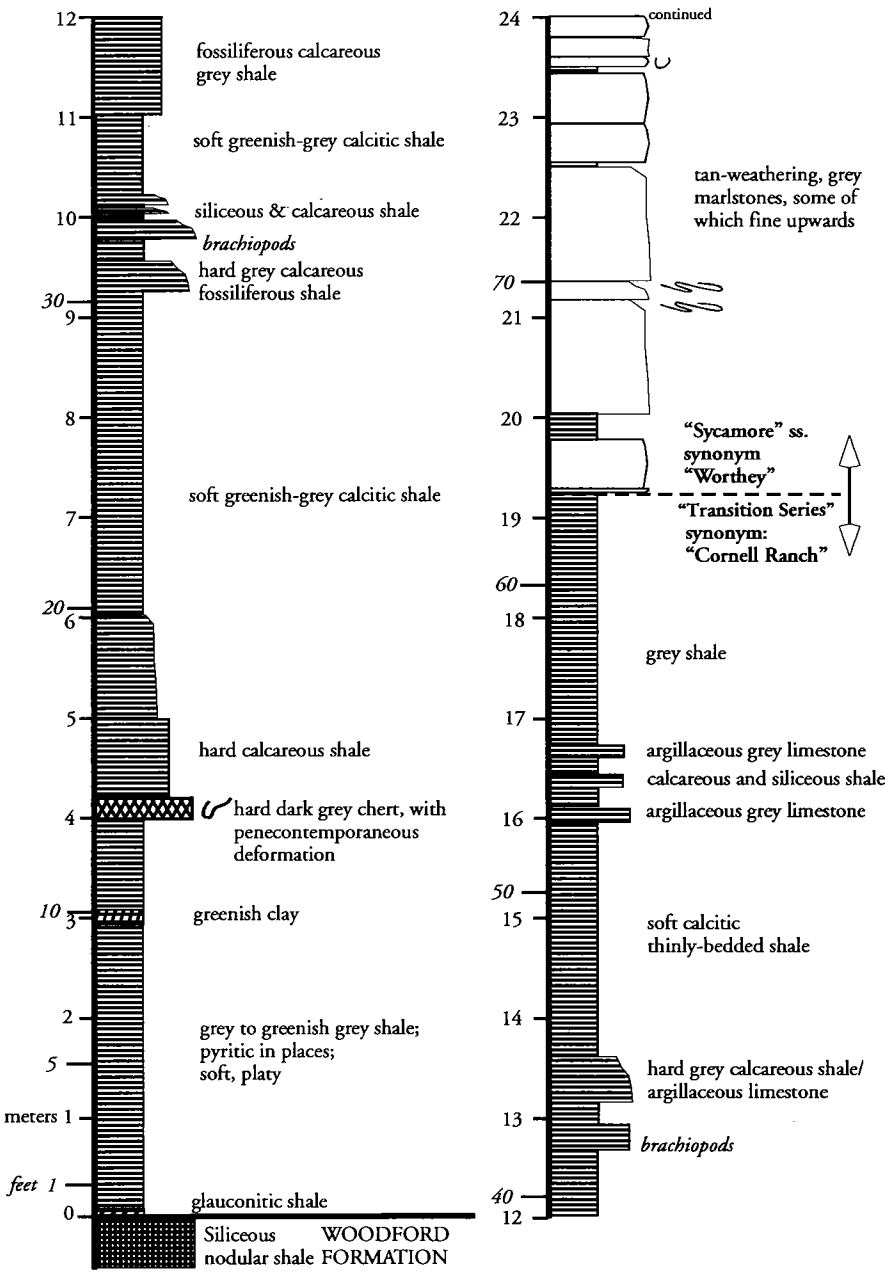

Figure 3 *(continued on pages 142 and 143).* Lithologic log of the Sycamore Formation in the west lane of I-35 on the southern flank of the Arbuckle Mountains. Topmost part (~100 ft, 30 m) of the sequence recorded by Fay (1989) was not logged in detail, as the exposure is partly covered. General key for the logs is given on page 143.

The precise age of the Sycamore has been the subject of some dispute (Gould, 1925; Ormiston and Lane, 1976; Schwartzapfel, 1990; Noble, 1995). Ham (1955, p. 9) concluded that the stratigraphic span of the formation is "principally Kinderhookian and Osagean and possibly earliest Meramecian." In 1976, Ormiston and Lane identified Osagean conodonts in the lower part of the formation. More recently, Noble (1995), following Schwartzapfel (1990), suggested that few or no Osagean strata are present and that the Osagean conodonts identified by Ormiston and Lane are contained in rip-up clasts. These later authors, again basing their conclusions on conodont distributions, considered the Sycamore to be of late Meracamecian to Chesterian age. This diversity of opinion in part may be due to some differences in defining the base of the Sycamore. In particular, the work of Schwartzapfel (1990) and Noble (1995) suggests that the northern I-35 section is considerably condensed in comparison to the southern section. However, Noble's section (1995, fig. 6) seems to indicate that different boundaries have been taken in defining the base of the Sycamore than those chosen by Prestridge (1959) and Fay (1989). This paper focuses on the Sycamore sensu stricto—i.e., the Worthey Member of Prestridge (1959).

LITHOLOGIC DESCRIPTION

Shales

Shales, which, as noted, are more common toward the base of the Sycamore Formation and dominate

the transition zone, are most commonly dark to medium gray, poorly indurated, slightly fissile, and thinly bedded. More rarely they are greenish gray or, exceptionally, green. Many contain carbonate, and some grade into argillaceous limestones in the transition zone. In this zone, some shales are siliceous and contain abundant sponge spicules. However most shales are dominated by siliciclastic grains and detrital clay; most of this clay is illite, although kaolinite is increasingly abundant in the upper part of the formation—i.e., the Sycamore sensu stricto. In both sections a glauconitic zone occurs in the transition zone.

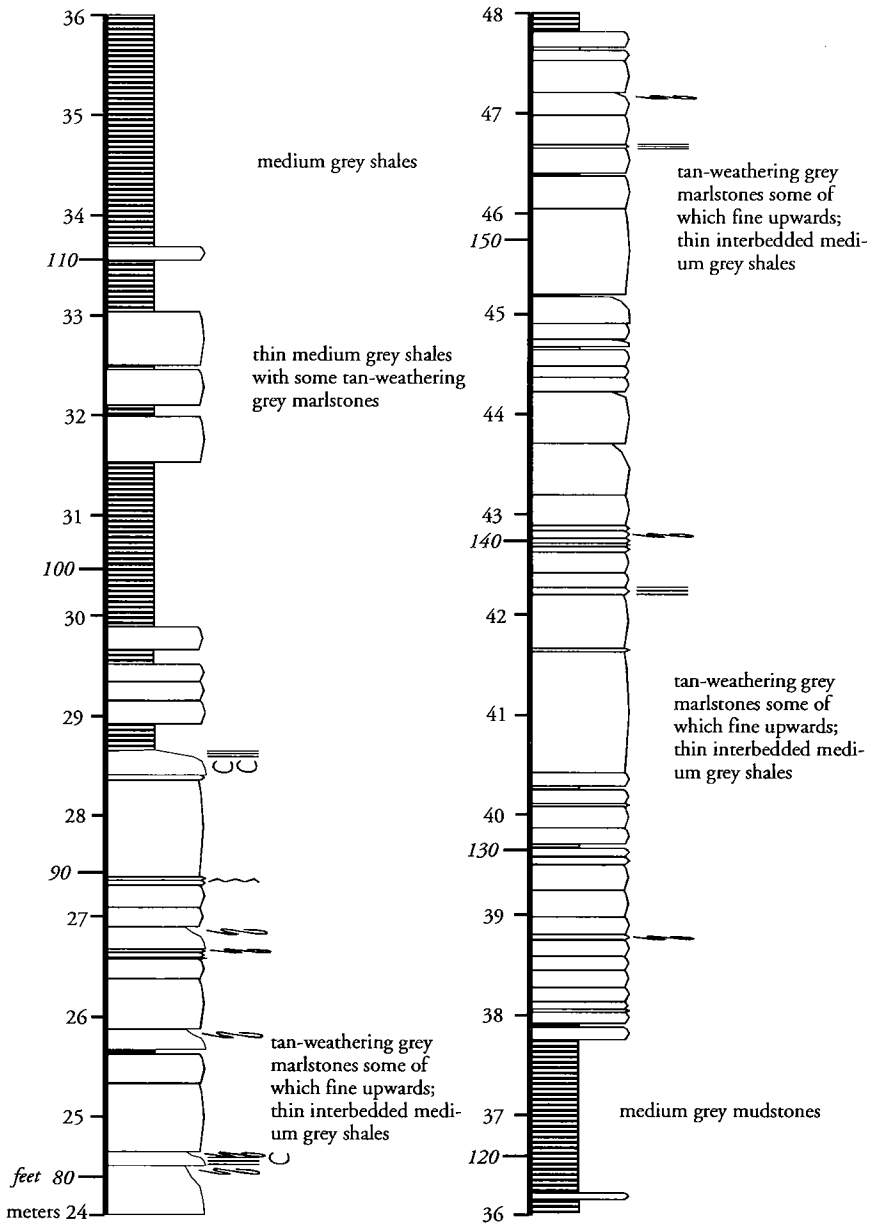

Figure 3 *(continued).*

Sycamore Carbonates

The impure limestones (marlstones) that make up the bulk of the Sycamore, and are responsible for the positive relief of the formation as a whole, are notably homogeneous in character (Fig. 5). These beds conventionally have been referred to as limestones (e.g., Ham, 1973; Fay, 1989; Noble, 1995). However, the acid-insoluble fraction varies from 36% to 57% in 10 samples analyzed during this study; petrographically, therefore, the beds are more properly described as marlstones than limestones. Thin-section studies support this interpretation.

Individual beds of this type show little, if any, variation in thickness throughout the available exposures. Most beds have sharp bases, although evidences of erosive downcutting are uncommon (Fig. 6). Bottom structures, including load features and a variety of grooves, mark the base of some beds; the most spectacular example of this is seen in the northern section, where the base of a single bed is marked by numerous linear bottom structures that suggest a transport vector to the west-northwest (Fig. 7). Small concentrations of shell hash (calcispheres, crinoid ossicles and echinoid fragments, broken brachiopods, etc.) occur at the base of some of the thicker beds, particularly in the northern section. Sedimentary structures are rarely observed in the basal and central parts of the beds, save for a few examples of penecontemporaneous dewatering folds in one or two of the more massive beds. However, the topmost parts of some, but not all, beds show evidence of upward fining and an increase in clay content (Fig. 8). Accompanying this decreasing grain size may be horizontal lamination, low-amplitude small-scale trough cross-bedding, and, at the top of some units, horizontal burrowing (*Chondrites* sp.). In addition, some horizontal crawling traces are present in the interbedded shales.

The bulk of each marlstone bed consists of finely crystalline ferroan calcite and silt-sized angular quartz with subordinate feldspar (Table 1). Identifiable carbonate grains include small fossil fragments (ostracodes, sponge spicules, calcispheres, brachiopod spines, etc.), spherical micritic peloids, and irregularly shaped micrite grains. Accessory minerals include muscovite mica, phosphate grains, glauconite peloids, and secondary pyrite. The beds are tightly cemented by fine-grained calcite, much of which is ferroan.

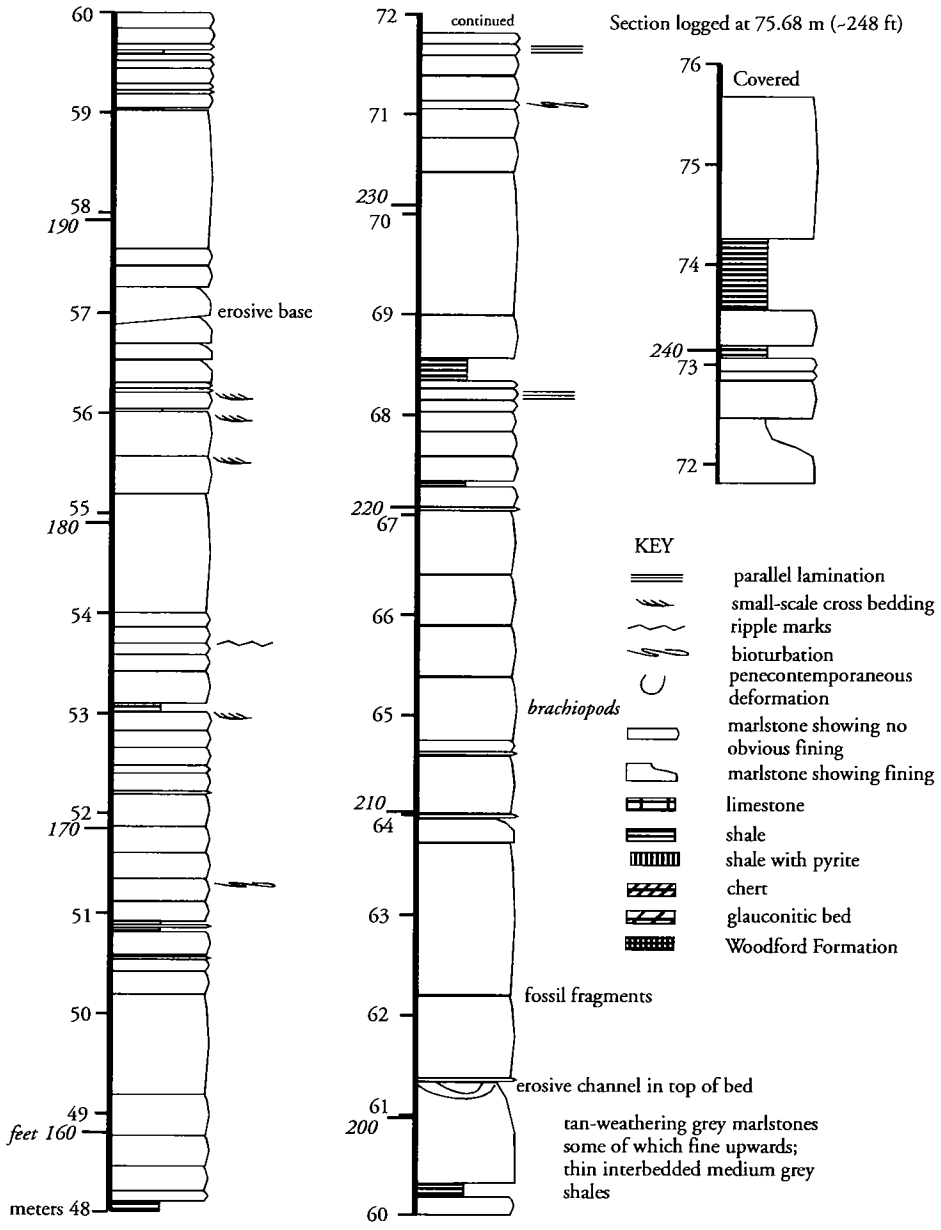

Figure 3 *(continued).*

COMPARISON OF THE NORTHERN AND SOUTHERN SECTIONS

Transition Zone

As noted in a preceding section, paleontological evidence (Schwartzapfel, 1990) suggests that a comparison of the two sections at this level may be the equivalent of comparing apples and oranges. In general, both sections, which are of similar thickness, are dominated by gray shales, within which several zones are notably calcareous and, to a lesser degree, siliceous. The calcite in these zones is generally ferroan, and pyrite is a common minor constituent. In consequence, these units weather to an orange or yellowish hue.

The principal difference between the two sections is that the calcareous zones are more impressive in the northern section. This is particularly so in the case of the lowest calcareous zone, which is a thick, light gray biomicrite (i.e., a fossiliferous packstone/wackestone) with nodular black chert toward the top. On the basis of conodont evidence, Ormiston and Lane (1976) equated this bed with the Welden Limestone, a unit that crops out to the north of the Arbuckles and exhibits characteristics typical of a shallow-water shelf carbonate. Assuming that the calcareous units in the transition zone are stratigraphic correlatives, the presumed Welden Limestone equivalent may be represented in the southern section by calcareous shales that contain a bedded chert ~9 in. (~23 cm) thick. This chert, which under the microscope shows replacement textures, also shows considerable evidence of penecontemporaneous deformation. However, the Welden Limestone is of Osagean age, and Schwartzapfel (1990) was unable to confirm that in-situ sediments of this age exist in the southern I-35 section. Noble (1995) suggested that the presence of glauconite and the absence of Osagean rocks in the area indicate that the cessation of "Woodford-style" deposition was followed by a hiatus associated with a sediment bypass of the area as a result of Laurentian–Gondwanan closure. If this is the case, the limestone near the base of the northern section has no known equivalents.

Sycamore Formation sensu stricto

Although the Sycamore Formation sensu stricto in the southern outcrop is about twice as thick as it is in the northern outcrop, both exposures are dominated by marlstones (as described in the previous section), with shales generally subordinate. There is little difference in the mineralogy and texture of the beds. However, no obvious detailed lithologic correlation appears possible between the members noted in 1989 by Fay (Fig. 9). On average, individual beds are thicker in the northern section than in the southern (Fig. 10). In addition, evidence of erosion and channeling on

the base of the beds is more common in the northern section, and beds in this section are more likely to display basal concentrations of shell hash.

FACIES INTERPRETATION

A synopsis of the features shown by the marlstones that constitute the bulk of the Sycamore is given in Figure 11. Taken individually, the sedimentary features documented are not uniquely diagnostic of any particular environment. Taken as a whole, a case can be made that each bed records rapid deposition from a fluidized (turbidity) flow and that together the beds record the debouchment of small submarine fans into a "deep"-water basin. The case can be buttressed by paleogeographic considerations.

The turbidite interpretation does not depend on the recognition of classic motifs in the section; as previously noted, few complete Bouma profiles were detected during this study (Bouma, 1964). Rather, it can be put together by the coupling of clearly attributable features with some special pleading. Thus, the sharp (and rarely erosional) basal contact that is a ubiquitous characteristic of the marlstones is an indicator of episodic sedimentation. Further, a few examples of penecontemporaneous dewatering structures suggest that this sedimentation was rapid. In addition, some beds show clear evidence of upward fining and a sequence of bed forms that is indicative of declining current power (an indication that is strengthened by a few occurrences of basal shell hash), but even where present this evidence is restricted to the topmost fraction of a bed. Nevertheless, in spite of the aforementioned caveats, most marlstones are apparently featureless beds. Thin sections show settling fabrics with flake-shaped grains (e.g., mica and shell fragments) parallel to bedding; bioturbation, seen in thin section as disruption of the settling fabric, is restricted to the topmost parts of some beds. These observations support the suggestion that the marlstones were deposited rapidly, overwhelming resident bottom-dwelling organisms. The near absence of typical Bouma profiles is probably a reflection of the fine-grained nature of the available sediment; it was too fine to discriminate into the characteristic suite of bed forms.

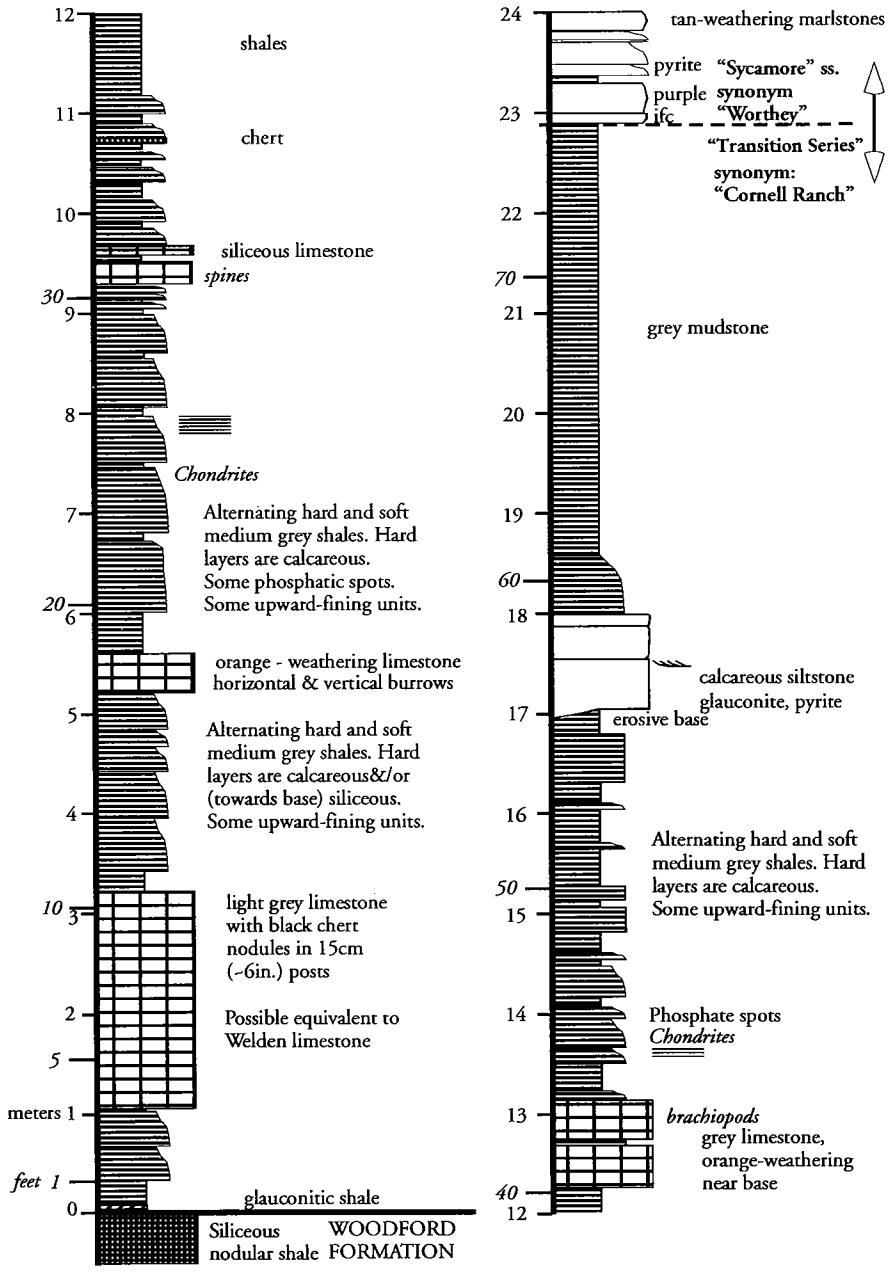

Figure 4 *(continued on pages 145 and 146).* Lithologic log of the Sycamore Formation in the east lane of I-35 on the northern flank of the Arbuckle Mountains. General key for the logs is given on page 143.

The mixed siliciclastic/carbonate composition of the marlstones is compatible with reworking of fine-grained distal shelf material derived from two sources: first, a carbonate shelf that may represent a continuation of the shelf that is inferred to have existed to the north during deposition of the transition rocks (see above); and second, a fluvial system debouching from a highland that developed to the north and/or east. This last inference is based on two lines of evidence: First, the transport directions obtained from bottom structures, lineations, etc., suggest transport to the

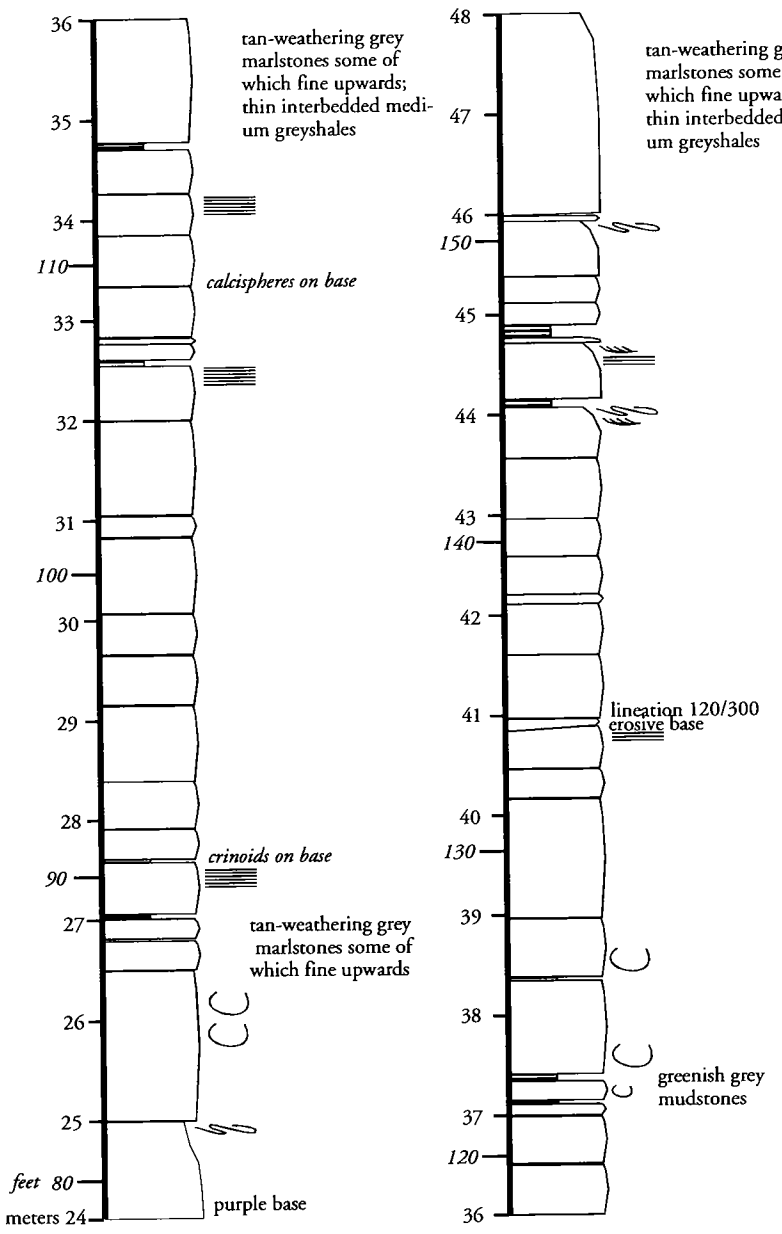

Figure 4 *(continued).*

west. Second, as noted previously, the northern exposure on I-35 appears to have more features that indicate it was proximal (i.e., nearer to source) in comparison to the southern exposure.

Histograms of marlstone-bed thickness suggest that the beds in each section are part of a single population, as might be expected if they accumulated as the result of submarine-fan activity emanating from a common shelf-margin slope. A more detailed appraisal of the measured sections indicates a tendency for beds of similar thickness to have clustered, again as might be expected from minor shifts in the axis of deposition on a submarine fan. Beds in the northern section are, on average, thicker, as might be expected if they were more proximal (as suggested in the preceding paragraph). There is no relationship between bed thickness and grain size in either the siliciclastic- or carbonate-grain populations, suggesting that they all were derived from a similar source.

INFERENCES AS TO BASIN EVOLUTION AND PRINCIPAL CONCLUSIONS

As noted in the Introduction, the Sycamore Formation records a period when the tectonic framework of the Oklahoma area was in a state of flux. In a regional sense, a narrow equatorial ocean lay to the south (in contemporary coordinates). Small cratonic blocks in this ocean were gradually juxtaposed as the Laurentian and Gondwanan blocks assembled (Noble, 1995). In the area of the old early Paleozoic southern Oklahoma aulacogen, a preexisting crustal weakness appears to have facilitated a local tectonic response on the southern edge of the Laurentian craton. The following sequence of events is suggested:

1. A breakdown of the established framework of a thermally stratified epeiric sea occurred in which the Late Devonian–earliest Mississippian Woodford Formation was deposited.

2. During Osagean time the whole area was essentially a bypass region in which little sediment was preserved (following Noble, 1995), except for the Welden Limestone in southern Oklahoma, north of the Arbuckle uplift. If the work of Ormiston and Lane (1976) is accepted, a Welden equivalent may exist near or at the base of the northern I-35 section.

3. Subsequent deposition is recorded by the transition strata that form the base of the Sycamore Formation (Fig. 12). These beds seem to indicate that a carbonate shelf lay to the north, although most of the beds would appear to be off-the-shelf-edge shales. Horizontal crawling traces in these shales suggest that there was no return to the stratified water mass that characterized the Woodford environment. The principal evidence for the existence of a shelf to the north is the presence of the aforementioned marine limestone of shallow-shelf origin in the northernmost I-35 section. As noted, the age of this limestone is problematic. Whatever its precise age, it is clear that the carbonate shelf did not extend to the southern section, where calcareous shales and siliceous deposits are possible correlatives.

4. The Sycamore (sensu stricto) deposits that followed

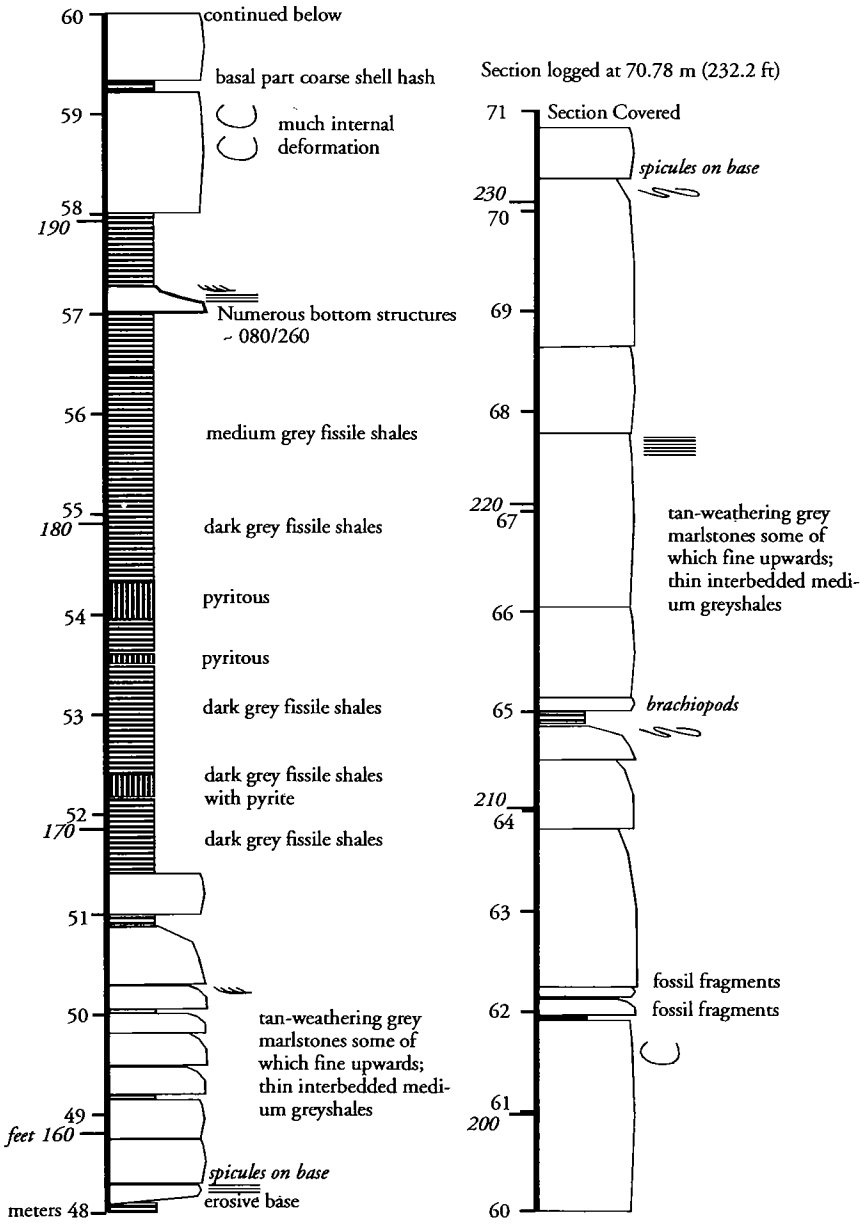

Figure 4 *(continued).*

comprise interbedded shales (visually similar to those of the underlying transition strata but richer in kaolinite) and marlstones in the form of laterally persistent beds of mixed silt-sized siliciclastic and carbonate grains. The marlstones are well cemented, of very limited porosity, highly fractured, and hard, forming positive relief in the section. They are interpreted as turbidites deposited as small submarine fans in a contemporaneous basin that deepened to the south and west (Fig. 12). Paleocurrent data, which are sparse but consistent, suggest transport from a shelf that lay to the east-northeast. Turbidites in the northern section display some features that suggest that this section was more proximal than the southern section. The siliciclastic grains (mostly quartz) suggest that contemporaneous uplift was taking place some distance to the east and north. The abundant carbonate grains attest to the existence of a carbonate shelf in the same area.

5. A period of tectonism followed cessation of fan activity, following which the overlying Caney shales were deposited unconformably atop the Sycamore in a basin that developed rapidly on the site of the old aulacogen. This basin filled with shales and siliciclastic sandstones: there was no return to the platform carbonates of earlier times.

ACKNOWLEDGMENTS

This study has benefited greatly from the encouragement, advice, and insights of Tim Denison, Barry Gouger, Jim Markello, and John Wickham; I thank them for their help.

REFERENCES CITED

Bouma, A. H., 1964, Ancient and Recent turbidites: Geol. Mijnbouw, v. 43e, p. 375–379.

Fay, R. O., 1989, Geology of the Arbuckle Mountains along Interstate 35, Carter and Murray Counties, Oklahoma [revised edition]: Oklahoma Geological Survey Guidebook 26, 50 p.

Gould, C. N., 1925, Index to the stratigraphy of Oklahoma: Oklahoma Geological Survey Bulletin 35, 115 p.

Ham, W. E. 1955, Geology of the Arbuckle Mountain region: Oklahoma Geological Survey Guidebook 3, 61 p.

_____1969, Regional geology of the Arbuckle Mountains, Oklahoma: Oklahoma Geological Survey Guidebook 17, 52 p.

_____1973, Regional geology of the Arbuckle Mountains, Oklahoma: Oklahoma Geological Survey Special Publication 73-3, 61 p.

Noble, P. J., 1995, Regional sedimentation patterns associated with the passive- to active-margin transition, Ouachita orogeny, southern Midcontinent, U.S.A., *in* Johnson, K. S. (ed.), Structural styles in the southern Midcontinent, 1992 symposium: Oklahoma Geological Survey Circular 97, p. 99–112.

Ormiston, A. R.; and Lane, H. R., 1976, A unique radiolarian fauna from the Sycamore Limestone (Mississippian) and its biostratigraphic significance: Palaeontographica, Abteilung, v. 154, p. 158–180.

Prestridge, J. D., 1959, Subdivisions of Sycamore Formation, *in* Petroleum geology of southern Oklahoma: American Association of Petroleum Geologists, Tulsa, v. 2, p. 156–164.

Schwartzapfel, J. A., 1990, Biostratigraphic investigations of late Paleozoic (Upper Devonian–Mississippian) Radiolaria within the Arbuckle Mountains and Ardmore basin of south central Oklahoma: University of Texas, Dallas, unpublished Ph.D. dissertation, 475 p.

Taff, J. A., 1903, Description of the Tishomingo quadrangle [Indian Territory]: U.S. Geological Survey Geologic Atlas, Folio 98, 8 p.

Table 1.—Composition of Five Marlstones from Sycamore Formation

Sample	1	2	3	4	5
Quartz	34	26	33	46	23
Feldspar	tr	tr	1	5	2
Muscovite	tr	tr	1	1	--
Fossils	8	28	7	1	2
Peloids	8	5	16	4	6
Micrite grains	10	11	20	7	12
"Cement"	39	31	20	35	55
Dolomite rhombs	--	--	tr	--	--
Phosphate	tr	--	1	--	--
Glauconite	tr	--	tr	1	--
Pyrite	tr	tr	tr	tr	--

Samples 1–3 are from the southern road cuts; samples 4 and 5 are from the northern road cuts. "Cement" includes all calcite not otherwise allotted. Analysis based on 200 point counts each.

Figure 5. Outcrop of the basal part of the southern exposure of the Sycamore Formation sensu stricto, illustrating the regular bedding character.

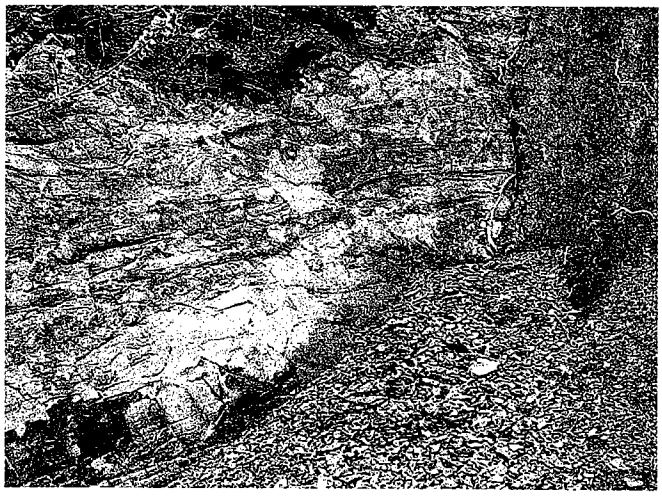

Figure 7. Base of a unit in the northern section of the Sycamore Formation sensu stricto, showing well-developed bottom structures (trending more or less horizontal in this view).

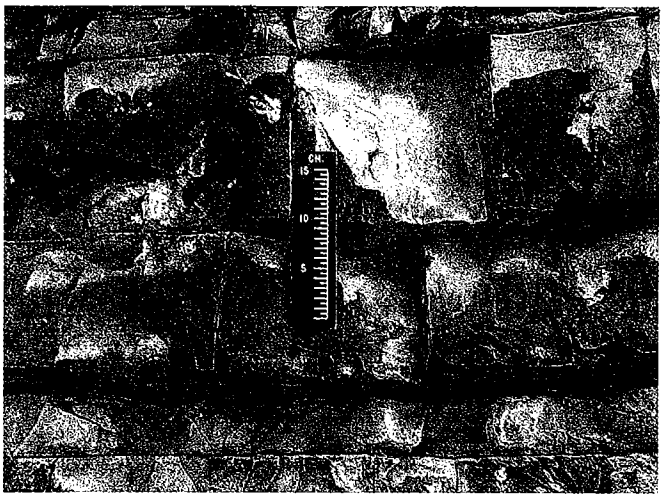

Figure 6. Part of the southern exposure of the Sycamore Formation sensu stricto, illustrating the regular bedding character. View downdip.

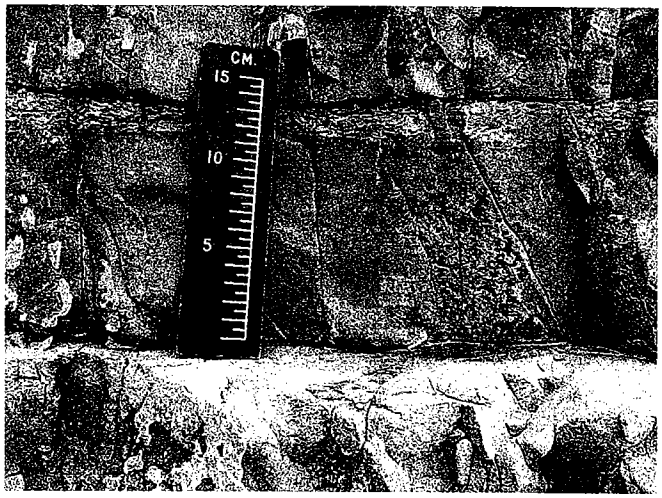

Figure 8. An individual stratum in the southern exposure, showing sharp bed contacts and horizontal burrowing at the top.

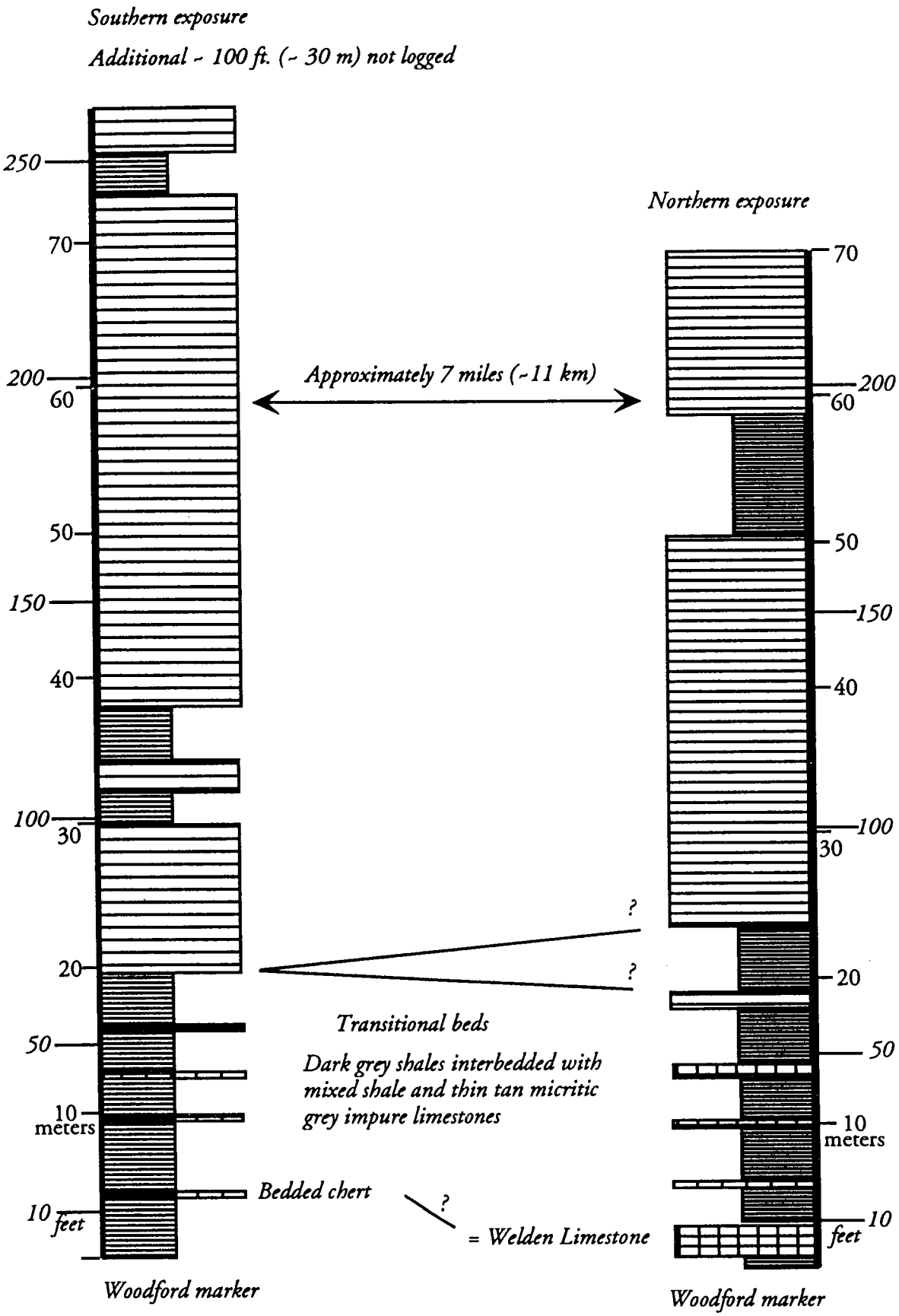

Figure 9. General correlation of the northern and southern sections of the Sycamore Formation on I-35.

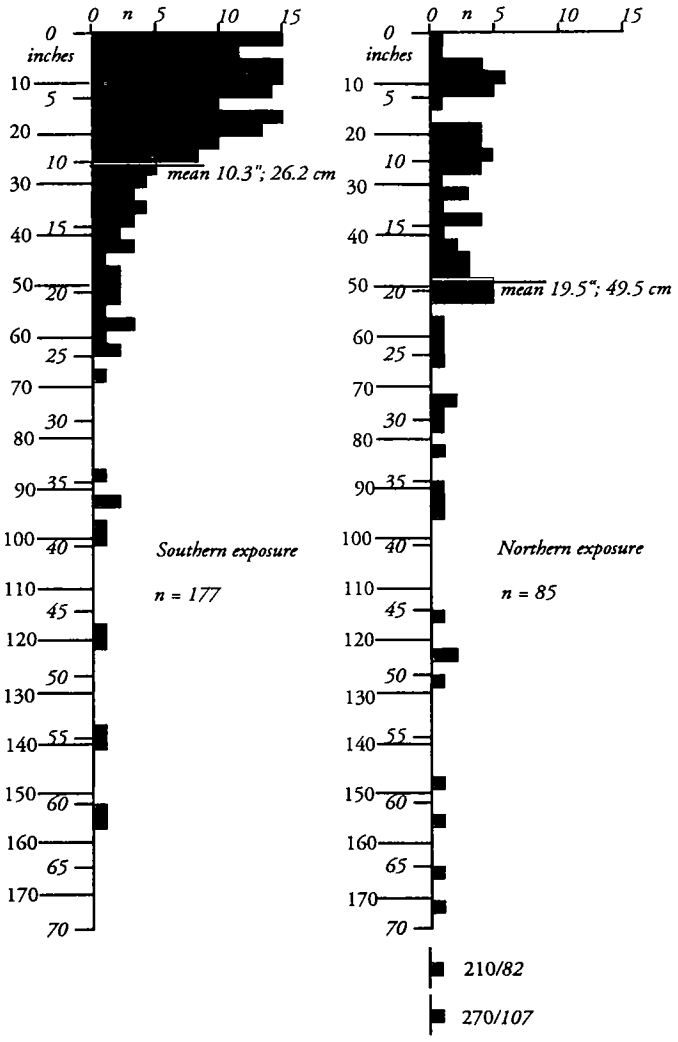

Figure 10. Individual-bed-thickness distribution in the northern and southern exposures. These data relate only to the Sycamore Formation sensu stricto. The data are interpreted to suggest that, on the whole, the northern strata are more proximal to source than the southern. Scale in centimeters is given at left.

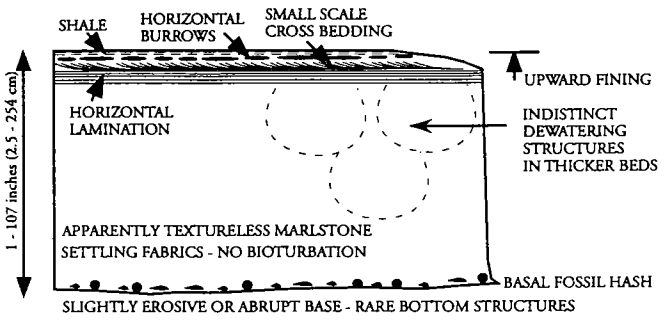

Figure 11. Synopsis of the features found in individual Sycamore beds; note that very few beds show all of these features.

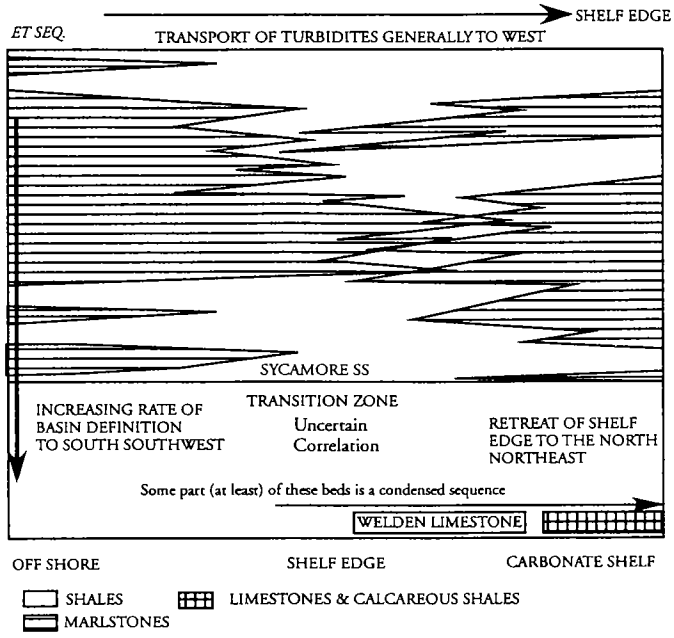

Figure 12. Summary of the development of the Sycamore basin. Note that correlation in the transition zone is uncertain and disputed.

Borehole-Image Applications in Silurian, Devonian, and Mississippian Midcontinent Reservoirs

Matthew G. Garber
Schlumberger Oilfield Services
Oklahoma City, Oklahoma

Formation imaging using microelectrical arrays has benefited the oil and gas industry since its introduction in the mid-1980s. The Formation Micro-Imager, or FMI, Schlumberger's latest generation electrical-imaging device, achieves 81% borehole coverage in a 7-7/8-in. borehole and delivers a vertical resolution of 2/10 in. This detail allows for the close examination of a reservoir downhole to gain a better understanding of the geologic processes concerning that reservoir. These processes are structural and stratigraphic and include secondary events that tend to increase or decrease porosity and permeability.

In the Midcontinent, the proper interpretation of borehole images yields structural and stratigraphic information that can help companies improve their offset-well placement and spacing. Frequently, FMI data are processed and interpreted on a rush basis to facilitate sidetracking, rather than offsetting, to improve a well's potential. In the right situations, this can save both time and money. Additionally, the identification of fracture and vug systems from borehole imaging enables log analysts to identify zones for completion, often with no other indication that a completion is warranted. Oil and gas companies have utilized this service on hundreds of Midcontinent wells, giving Schlumberger valuable experience in formations of all ages.

Successful image interpretations have been well documented in the numerous Midcontinent Paleozoic reservoirs. Image examples in Pennsylvanian strata are especially abundant, because they are rich in reservoir-quality rocks formed during sustained periods of deposition, uplift, and erosion. However, the Silurian, Devonian, and Mississippian Periods produced reservoirs of a different type. Many of these are carbonates and are the products of localized karstification, exposure, and weathering. Still others were deposited as carbonate grainstones in high-energy tidal and shallow-marine environments.

Various Silurian, Devonian, and Mississippian reservoirs, from the Hunton to the Chester, are displayed in this compilation of case studies (Figs. 1–5). In the cases cited, the Formation Micro-Imager was used for a variety of reasons specific to the particular reservoir being investigated. It is often used to analyze cross-bedding within shoaling or bar trends to determine the directions to thicker, more porous reservoir rock. Unconformity sand trends and thickening directions are uncovered from the examination of fill and compaction features as well as from the orientation of the unconformity itself. One example (Fig. 2) also demonstrates an equally important function of borehole imaging—to identify secondary porosity, its degree of connectivity, and its possible sources of development. This example directly compares the FMI data to those of full-bore core through a section of complex fractures and vugs.

This presentation explores a small sample of Silurian, Devonian, and Mississippian reservoirs through the eyes of microelectrical borehole imaging and its interpreters.

Garber, M. G., 2001, Borehole-image applications in Silurian, Devonian, and Mississippian Midcontinent reservoirs, *in* Johnson, K. S. (ed.), Silurian, Devonian, and Mississippian geology and petroleum in the southern Midcontinent, 1999 symposium: Oklahoma Geological Survey Circular 105, p. 151–161.

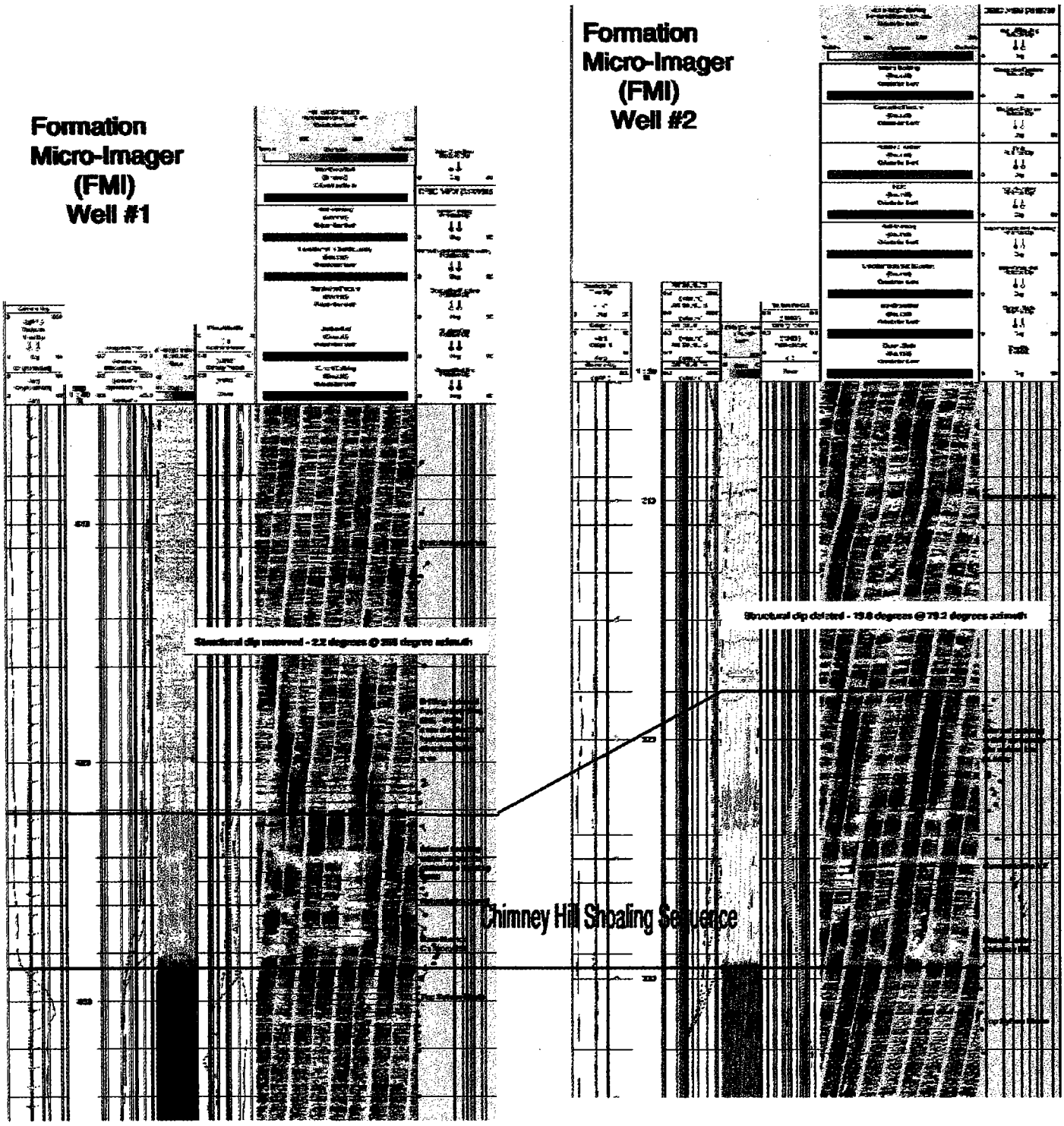

Figure 1 *(here and facing page)*. Formation Micro-Imager (FMI) data and block diagram, illustrating shoaling in the Chimneyhill Subgroup of the lower Hunton Group. Example from southern Oklahoma.

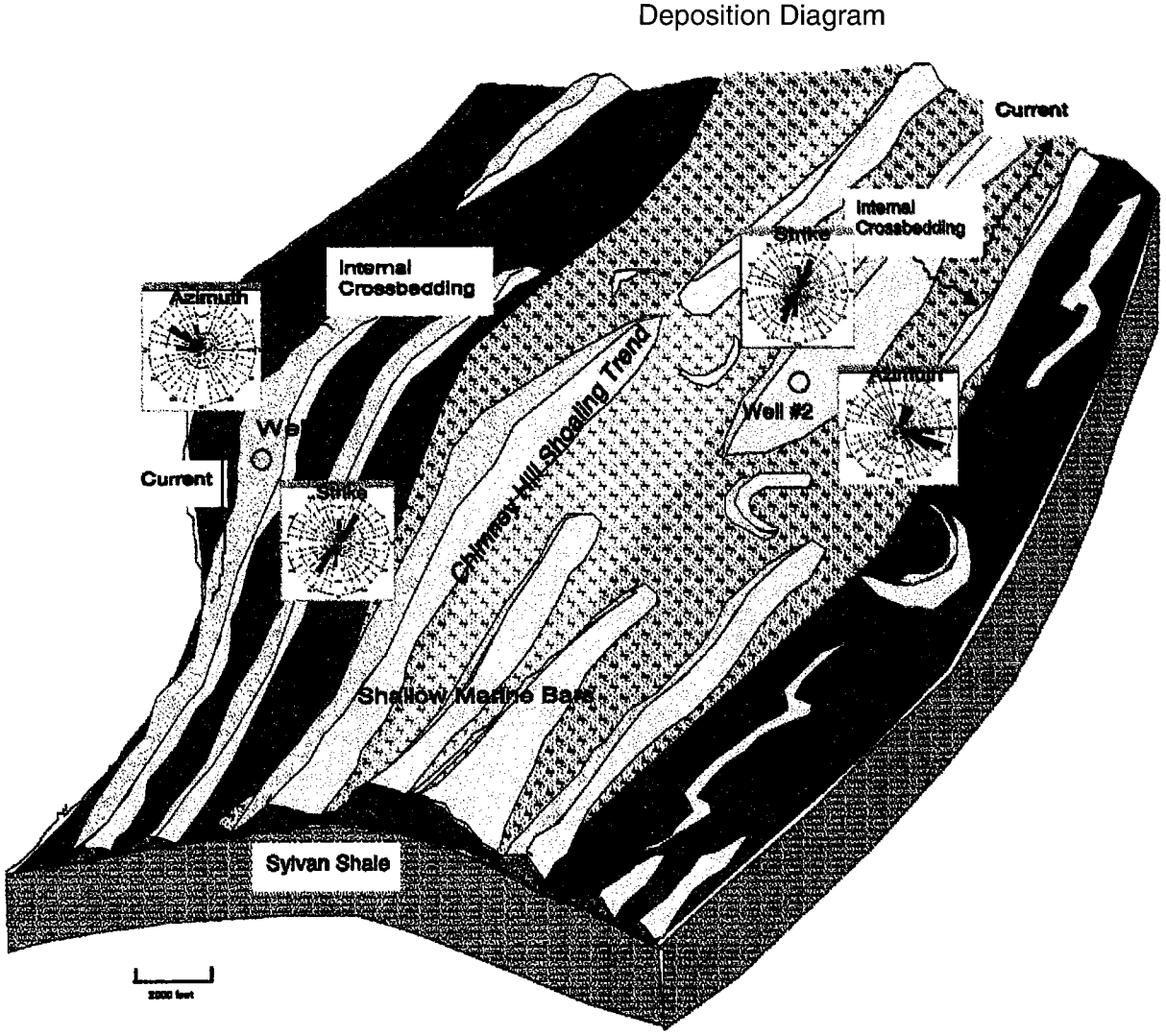

Chimney Hill Shoaling, Southern Oklahoma

Example Description

- Well 1 was drilled. Standard logs as well as the Formation Micro-Imager (FMI) were run.
- 6 ft of Chimneyhill porosity (9%) was penetrated.
- From the FMI, structural dip in the Hunton limestone was found to be 2.2°, dipping to the west (azimuth of 268°). This structural dip was rotated out before doing the stratigraphic analysis.
- The FMI stratigraphic interpretation found organized cross-bedding within the porous-lime interval, suggesting that the environment of deposition was shoaling.
  - —Internal cross-bedding (red plots) to the west-northwest were dominant. Commonly, these beds dip toward the bar pinchout and are perpendicular to the strike of the bar.
  - —A small current pattern (blue plot) to the north was interpreted as carbonate-sand-wave migration.
  - —Using this information, the shoaling trend for this area was determined to be north-northeast–south-southwest (N. 35° E., S. 35° W.) at well 1.
- Well 2 was drilled. Standard logs as well as the FMI were run.
- 11 ft of Chimneyhill porosity (11%) was penetrated.
- Structural dip in the Hunton limestone was found to be 19.8°, dipping to the east (azimuth of 79°). Because this structural dip was high, dip rotation was necessary before doing the stratigraphic analysis.
- The FMI stratigraphic interpretation confirmed the shoaling trend to be north-northeast–south-southwest (N. 25° E., S. 25° W.) at well 2.
  - —Internal cross-bedding (red plots) were dominant to the east-southeast, suggesting that the bar which contributed to the porous interval thins to the east-southeast.
  - —Carbonate-sand-wave migration (blue plot) was N. 25° E., exactly parallel to the strike of the bar, determined from the internal cross-bedding.
- It is not clear whether this structure existed during Hunton time, or if it contributed to the development of shoaling in this case.

Figure 1 *(continued)*.

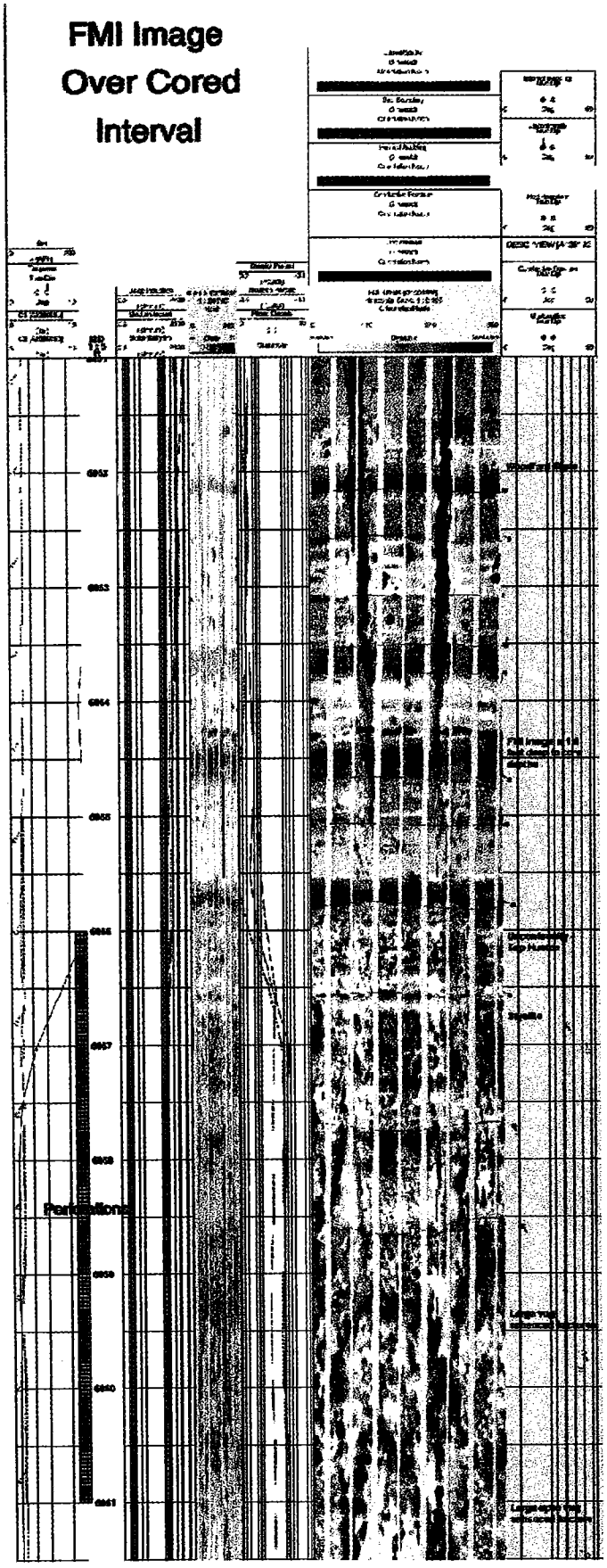

continued in next column

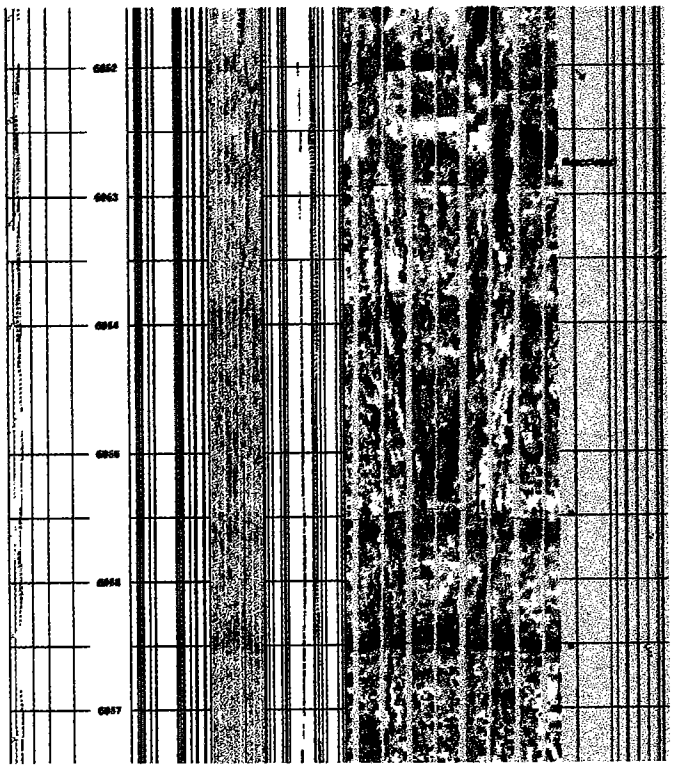

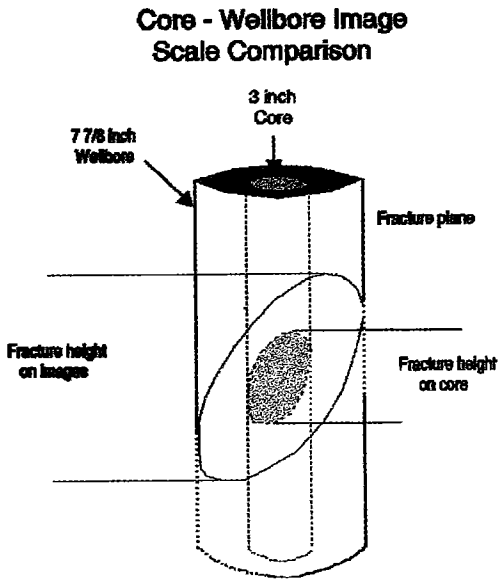

Figure 2 *(here and facing page).* FMI data compared to full-born core, resulting in identification of secondary porosity, permeability, and possible sources of development in Hunton limestone. Example from Logan County, Oklahoma.

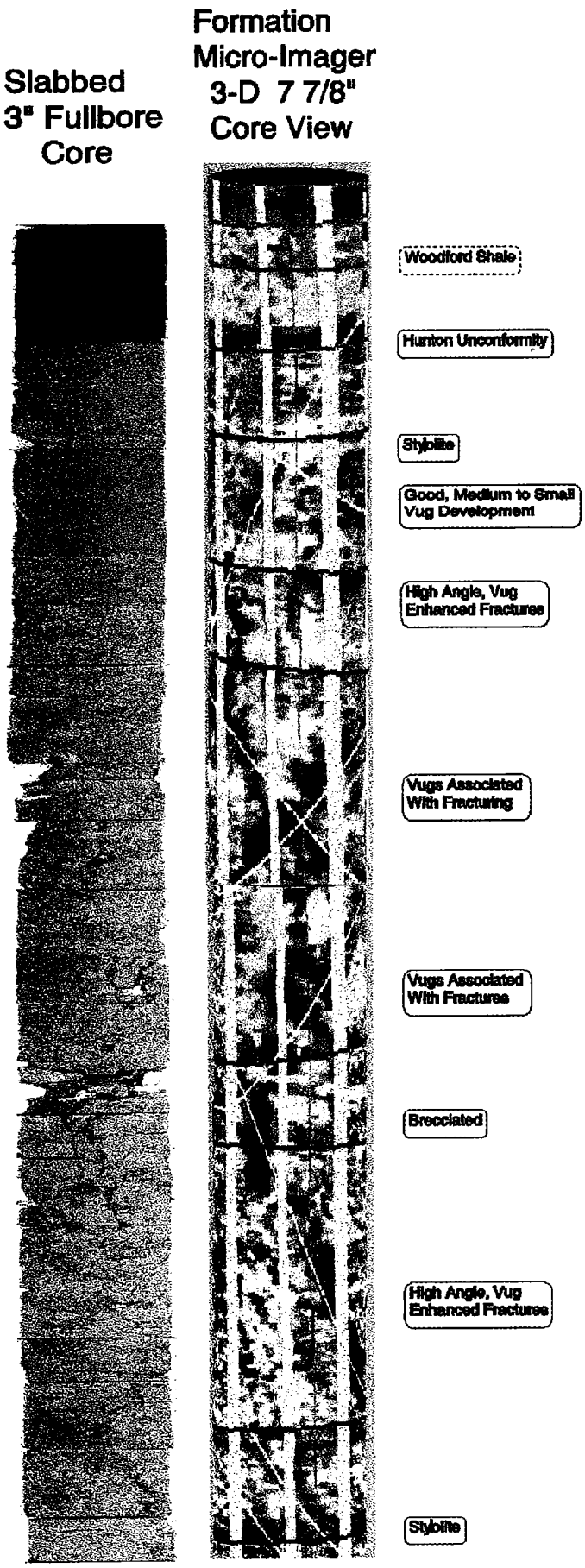

Hunton Limestone, Logan County, Oklahoma

Completion and Production Data

Perforation interval: 6,056–6,061 ft

Stimulation treatment: 500 gal of 15% HCl

Initially tested at: flowing: 185 BOPD (40° API gravity), 210 MCFG/D and 147 BWPD

Initial shut-in pressure: 300 psi

Hunton Fracture Strike Plot From FMI

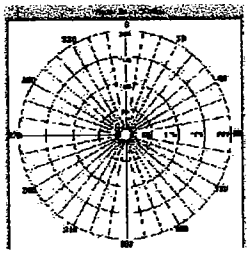

Figure 2 *(continued).*

Hunton Structure

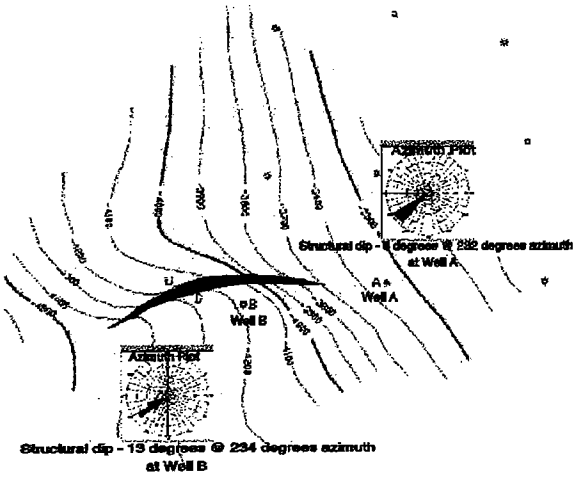

Hunton Structure Map
Scale: 1 in = 2000 ft
c.i. = 100 feet

Sycamore, Southern Oklahoma

Example Description

- Wells A and B were drilled 3,000 ft apart in an area of known Hunton faulting. Standard logs and the Formation Micro-Imager (FMI) were run on both wells.
- Well A encountered a decent Sycamore interval that included a 60-ft zone of clean, sandy limestone, averaging 8% porosity (X850–X910 ft).
- Well B penetrated no clean Sycamore, and a Woodford Shale section some 45 ft thicker than that in Well A.
- The FMI interpretation found:
  - —The Woodford Shale was dipping 8° southwest in well A and 13° southwest in well B.
  - —The Sycamore in well A was highly cross-bedded, indicating a relatively high-energy environment of deposition. Additionally, this Sycamore interval contained numerous fractures.
  - —The Sycamore interval in well B was highly laminated with shale, indicating a lower energy environment of deposition. This zone was only minimally fractured, the majority of fractures being healed.
  - —Burrow traces were common in the more shale-rich intervals in both wells.
- The difference in Sycamore reservoir quality between the two closely spaced wells is related to an abrupt lateral change in the environment of deposition. A depositional low during Sycamore and Woodford time likely caused this change, where faulting in the Hunton before (and/or during) Woodford and Sycamore time was the mechanism.

Production Data

Well A:

- Entire gross Sycamore interval was perforated
- Sycamore is producing gas but is commingled with Woodford and Hunton production
- Initial production: 230 MCFG/D

Well B:

- The Sycamore interval was deemed nonproductive and was not completed

Depositional Diagram

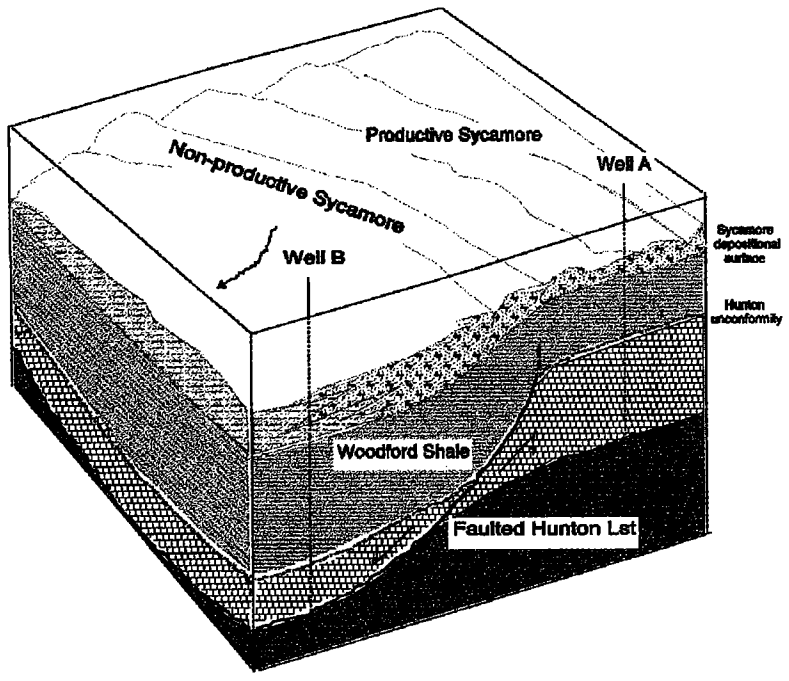

Figure 3 *(here and facing page)*. FMI data, structure map, and block diagram, illustrating structural and depositional patterns in Hunton limestone, Woodford Shale, and Sycamore Limestone. Example from southern Oklahoma.

Figure 3 *(continued)* — FMI images.

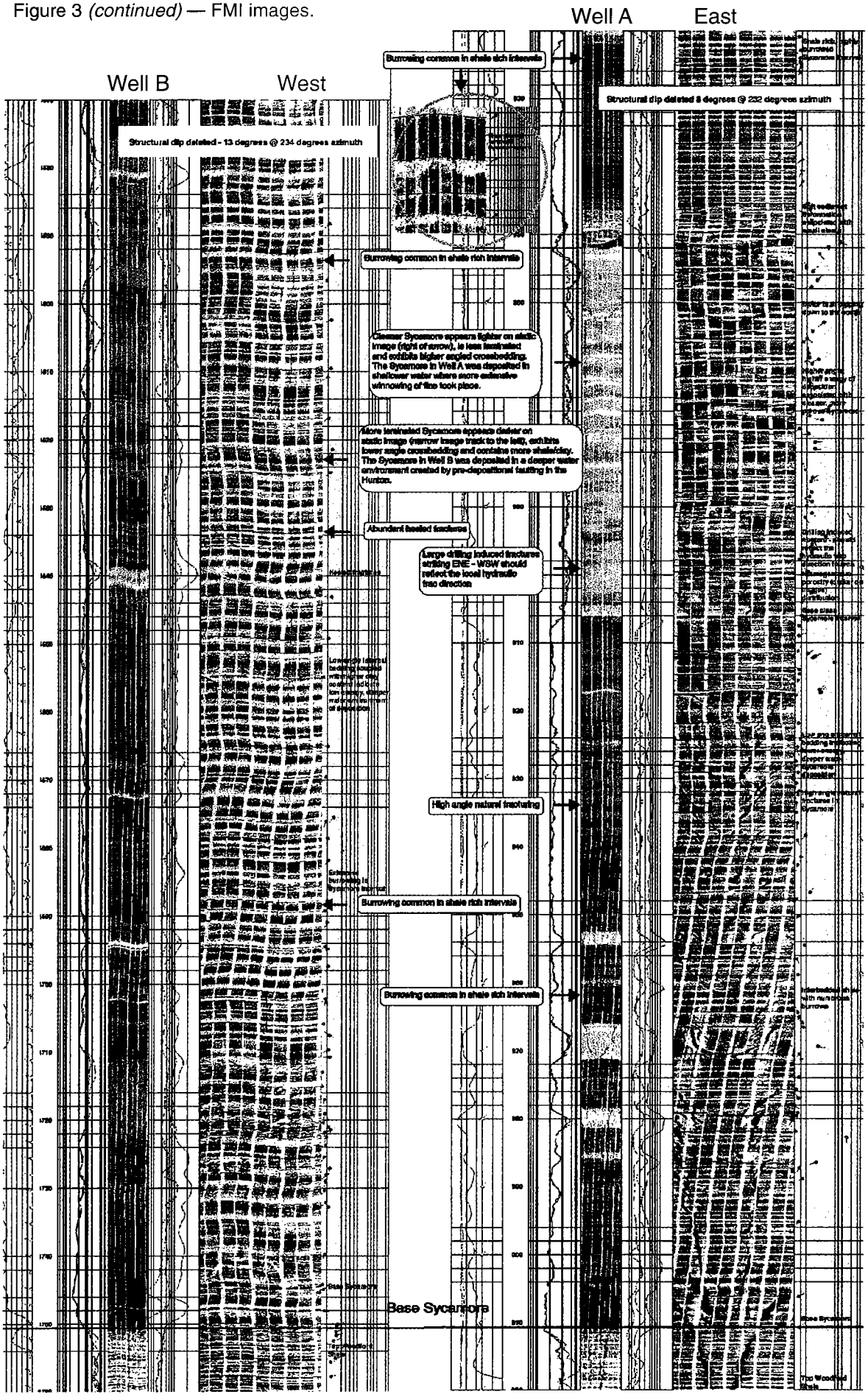

Explanation of colors

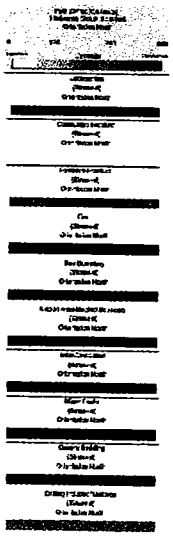

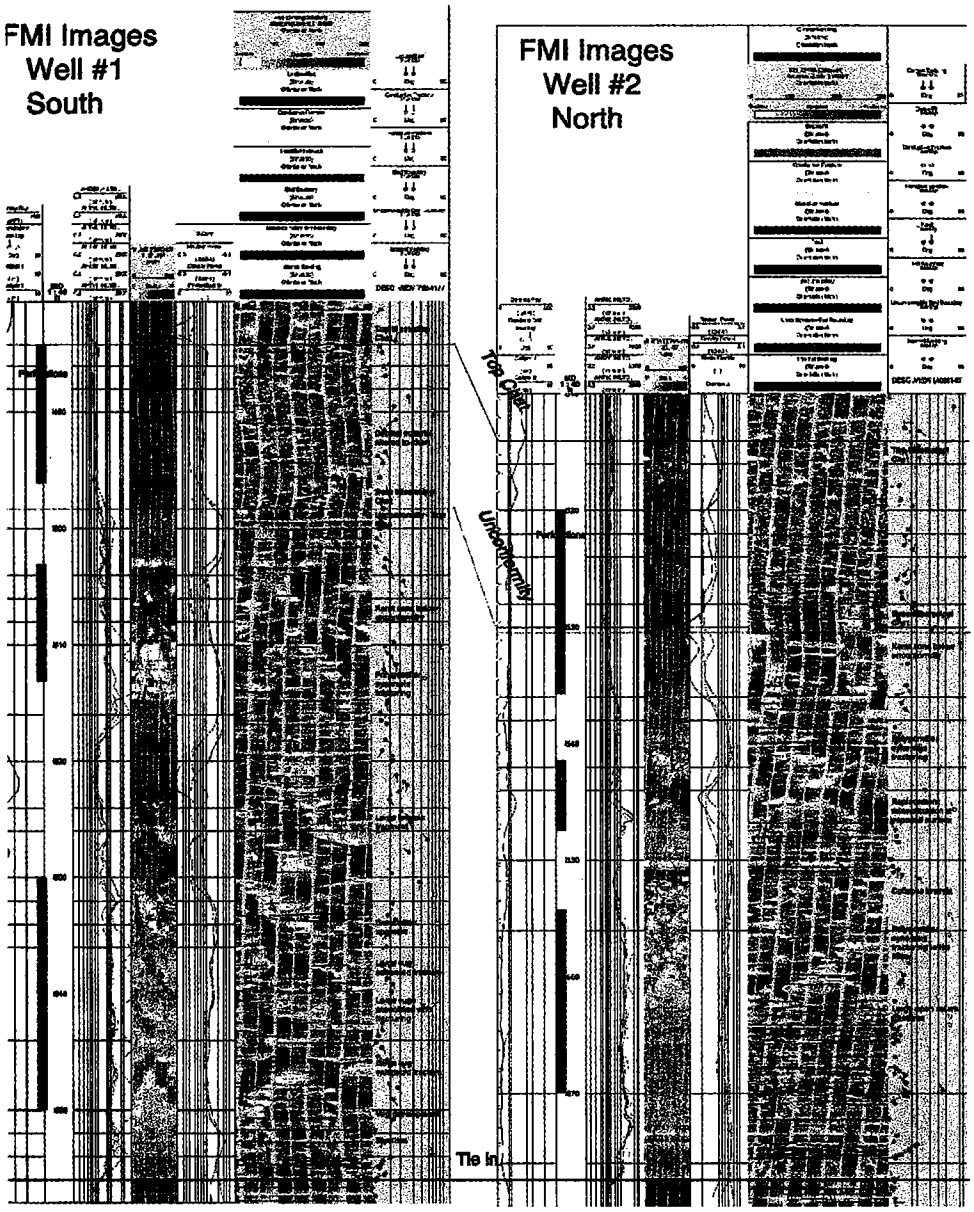

Figure 4 *(here and facing page).* FMI data, block diagram, and map, illustrating evolution and distribution of Mississippi chat in relation to Mississippian limestone. Example from northern Oklahoma.

Mississippi Chat, Northern Oklahoma

Example Description

- Mississippi chat deposition appeared coincident with Mississippian lime structural highs and pronounced karst breccia development.
- Well 1 was drilled. Standard logs as well as the FMI were run.
- The FMI interpretation found: structural dip down to the southwest in the lime, significant karst breccia directly below the Mississippian unconformity, and a 12-ft Mississippi chat porosity zone on the unconformity surface.
- It was determined that well 1 was positioned on the southwest side of a structural nose in the Mississippian lime dipping to the south.
- Internal bedding (red plots) within the chat was organized, bidirectional in nature, dipping north-northwest and south-southwest and resembling a bar.
- Well 2 offset selection was made by incorporating well 1 structural and stratigraphic information into existing subsurface control, placing it updip to the north.
- Well 2 was drilled. Standard logs as well as the FMI were run.
- The FMI interpretation found: structural dip in the lime to be due west, extensive karst breccia directly below the Mississippian unconformity, and a 15-ft Mississippi chat porosity zone on the unconformity surface.
- Well 2 penetrated the west flank of the Mississippian anticline.
- Internal bedding within the chat was again organized, barlike, and dominant to the north-northeast. The chat in well 2 also showed evidence of east-southeast sediment transport.

Acknowledgments:

Thanks to Cabot Oil and Gas Corporation for the release of these data and to Tom Belis for his cooperation and assistance.

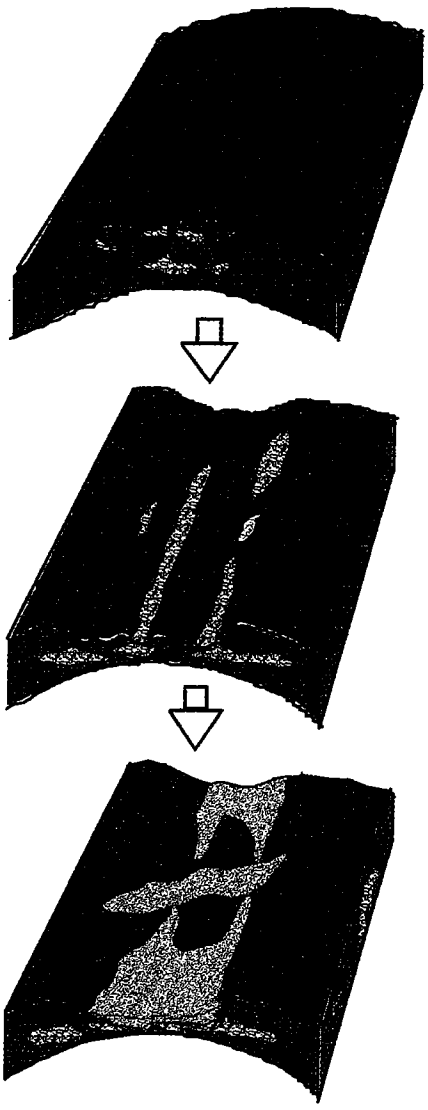

Suggested Evolution of Chat Deposition

- Anticlinal fold in the Mississippian limestone creates extensive fracturing and subsequent karst brecciation
- Continued cavern collapse and karst brecciation
- Anticlinal low created from karsting and collapse
- Water flow through karsted depression
- Dissolution of calcite works to concentrate preexisting chert incorporated within the limestone
- Secondary-chert percentages also increase by continued chertification
- Larger chert grains are then reworked and deposited locally, near source, by fluvial and/or shallow-marine processes

Production Data

Well 1 (chat and Mississippian limestone):

Perf. intervals: X484–X496 ft in chat; X503–X513 ft and X530–X550 ft in lime

Completion: chat and lime frac'ed separately

Current production: 100 MCFG/D, 6 BOPD, and 100 BWPD

Estimated cumulative production: 42,000 MCFG and 5,800 BO

Well 2 (chat and Mississippian limestone):

Perf. intervals: X520–X536 ft in chat; X542–X547 ft and X555–X570 ft in lime

Completion: chat completed naturally; lime acidized

Current production: 160 MCFG/D, 1 BOPD, and no water

Estimated cumulative production: 64,000 MCFG and 750 BO

Deposition Diagram

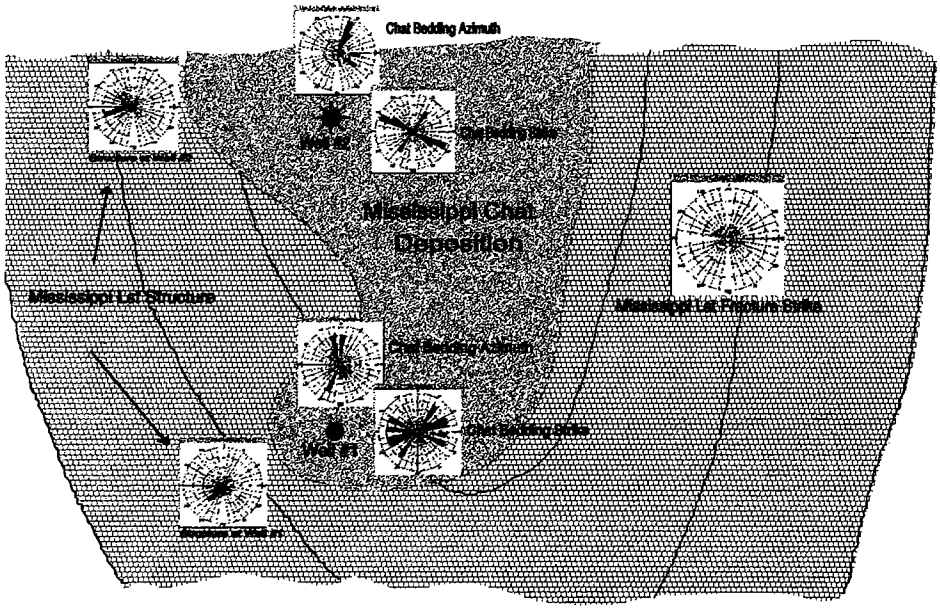

Figure 4 *(continued).*

Depositional Environment Diagram

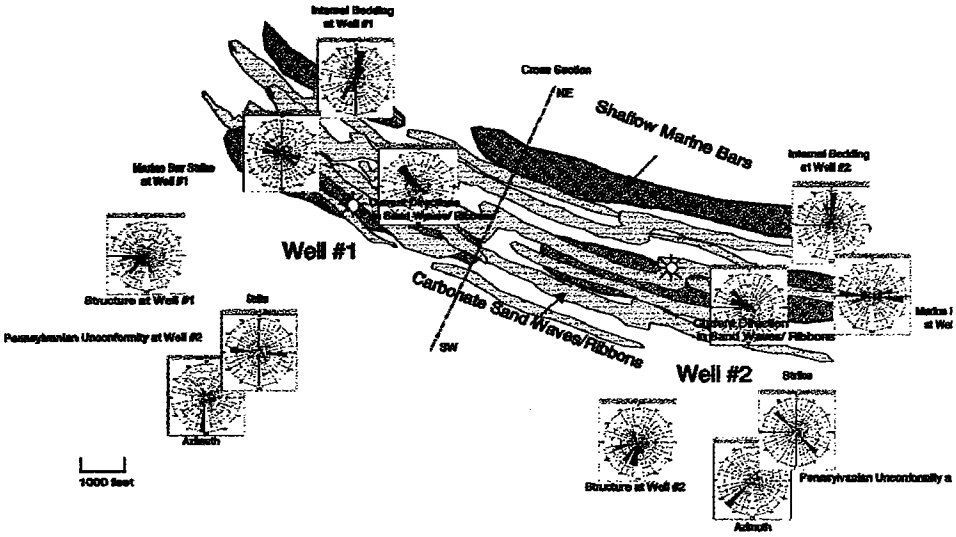

SW–NE Cross Sectional Diagram

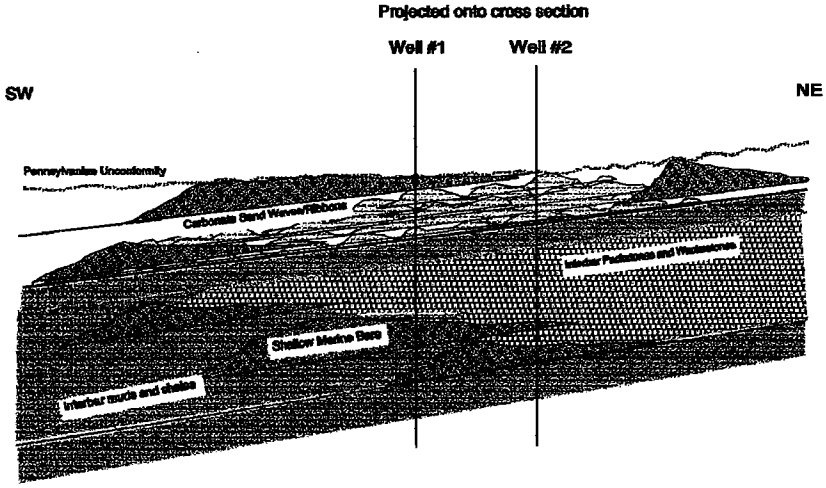

Figure 5 *(here and facing page)*. FMI data, diagram, and cross section, illustrating depositional environments and shoaling in the Chester limestone (Upper Mississippian). Example from northern Oklahoma shelf.

Chester Lime Shoaling, Northern Oklahoma Shelf

Example Description

- Well 1 was drilled. Standard logs as well as the FMI were run.
- FMI interpretation identified two productive facies.
- 1st facies: shallow-marine bar. Grainstone containing a bidirectional internal-bedding distribution (both north-northeast and south-southwest) within the Chester interval, suggesting that the bars are striking west-northwest and east-southeast. Internal-bedding (red plots) direction within marine bars commonly defines direction to pinch-out of the individual bar.
- 2nd facies: stacked carbonate sand wave and/or sand ribbon. Grainstone containing bidirectional current patterns (blue plots) parallel to bar strike. This facies was presumably reworked and redistributed by longshore currents or interbar tidal currents.
- The orientation of the Pennsylvanian unconformity and structural dip were determined. See depositional-environment diagram above.
- Well 2 offset location to the east-southeast of well 1 was selected by incorporating the FMI interpretation with other data to further evolve the subsurface model.
- Both facies were again identified in the correlative interval from the FMI. The internal cross-bedding within both grainstone facies suggests that the depositional strike becomes more east-west. See the diagrams above.

Production-Test Data

Well 1 (lower Chester only):
Perf. interval: X594–X605 ft
After frac and 9-hour flow test: 2.254 MMCFG/D
Shut-in pressure: 1,900 psi

Well 2 (lower Chester commingled with Oswego):
Perf. interval: X526–X538 ft
After frac and 18-hour flow test: 1.159 MMCFG/D
Shut-in pressure: 1,250 psi

Acknowledgments:
Thanks to Cabot Oil and Gas Corporation for the release of these data and to Tom Belis for his cooperation and assistance.

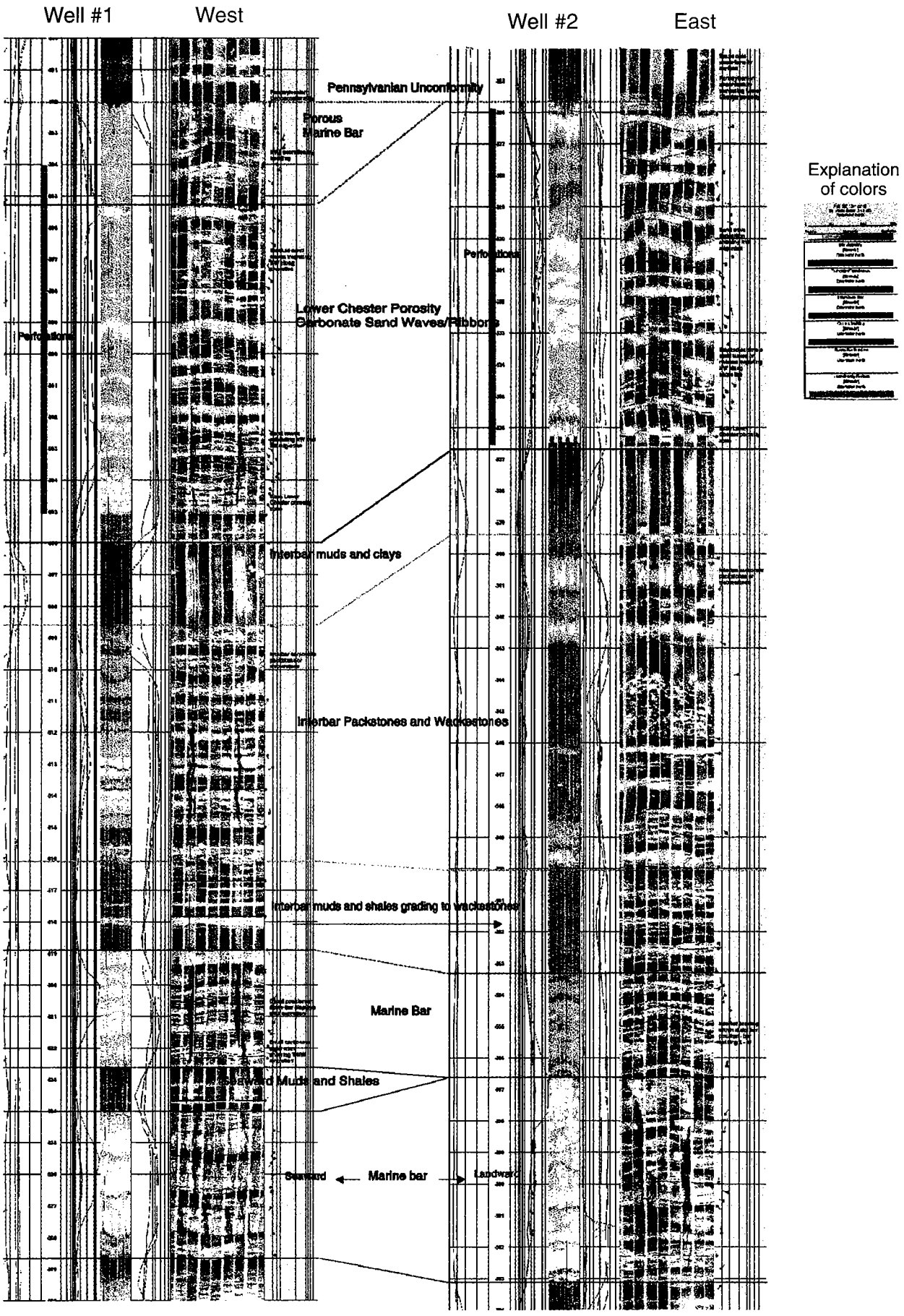

Figure 5 *(continued)* — FMI images.

Mississippian Stratigraphy of Southwestern Kansas: Resolving a Few of the Many Correlation Questions

Bob Slamal (deceased)
Consulting Geologist
Wichita, Kansas

INTRODUCTION

Joe Clair noted in a 1948 report of the Kansas Geological Society that the Mississippian was "for many years, to the majority of Kansas geologists . . . a top and base with varying thickness of very hard rock between." Ed Goebel's (1966) dissertation helped define Mississippian subdivisions in southwestern Kansas from the study of cores, samples, and microfossils. The Kansas Sample Log Service's lithologic strip logs, prepared primarily by geologist J. D. Davies, available from the Kansas Geological Society Library, also provide a wealth of rock descriptions and subdivisions of the Mississippian.

More than three decades have passed since Goebel's original overview study of the complete section of Mississippian rocks in southwestern Kansas was published. Many geologists and companies, adhering to Clair's 53-year-old remark above, often drill into only the top part of the section and report "Miss." with no reference to subdivisions.

Continued petroleum exploration has provided a wealth of new geophysical logs. Rotary-drilling samples regretfully are commonly of poor quality from severe caving of the overlying section (especially the basal Pennsylvanian) while drilling deeper into the Mississippian. This study presents up-to-date preliminary research, building upon earlier studies, of all wells that penetrated the complete section of Mississippian rocks in southwestern Kansas. Four well-log sections are presented that give a scattered sample of resolving some Mississippian correlation problems.

EXAMPLES OF CORRECTED CORRELATIONS

The first example (Fig. 1) shows the maximum thickness of Chesterian carbonates and interbedded thin shales in southwestern Kansas. This well is near the eastern zero-edge of the overlying Morrowan section in Kansas. The maximum thickness of the overlying Morrowan rocks is far to the west, in the southwest corner of Kansas. This discordance is due to regional tectonic tilting after Mississippian deposition. Suggestions are welcome concerning correlation with the more studied and resolved section in Oklahoma. Four stratigraphic notes are made concerning this section in Figure 1:

1. One direct stratigraphic-correlation "tie" has been made into Oklahoma; the nomenclature for the persistent shale marker bed from 6,406 to 6,422 ft is the Boatwright shale (personal communication at the workshop, 1999, Walter Hendrickson, IHS Energy Group, Oklahoma City).

2. The basal Chester limestone unit at 6,624–6,668 ft and the underlying Ste. Genevieve Limestone both are often described as "sandy limestone." This basal Chester unit often may be distinguished from the similar lithology of the Ste. Genevieve by simply using the caliper-log measurement. The basal Chester shale bed from 6,668 to 6,679 ft often washes out, whereas the shale units within the underlying Ste. Genevieve (6,704–6,718 ft) do not. This illustrates the regional disconformity between these units.

3. Related to item 2, above, a terra rosa zone also has developed in the basal Chester shale unit from 6,668 to 6,679 ft. This zone can be recognized from good samples—e.g., when drilling is halted to circulate up samples that actually represent the zone.

4. An added stratigraphic note: the Chesterian boundary has been moved in the last 15 years from the top of the Ste. Genevieve Limestone down to the top of the St. Louis Limestone by some Mississippian researchers in the upper Mississippi Valley area.

The second example (Fig. 2) illustrates J. D. Davies' sample descriptions: his subdivisions of the entire Kansas rock column are legendary. No other publicly available stratigraphic studies can compare with his Mississippian-subdivision research in Kansas, as his long-range correlations of Mississippian units across Kansas have not been duplicated. There are, however, some errors from early sparse well control and "bad" samples.

One such miscorrelation example shown in Figure 2 is the "false St. Louis" term that Davies often used in the western part of the Hugoton field area, and westward to the Colorado border. As Davies often noted, this zone has the characteristic orange chert and oolite development of the St. Louis. But he initially interpreted this zone to be part of the Ste. Genevieve because the underlying section is very sandy, similar to the Ste. Genevieve section above. He often used the phrase "back in typical Ste. Gen."

Slamal, Bob, 2001, Mississippian stratigraphy of southwestern Kansas: resolving a few of the many correlation questions, *in* Johnson, K. S. (ed.), Silurian, Devonian, and Mississippian geology and petroleum in the southern Midcontinent, 1999 symposium: Oklahoma Geological Survey Circular 105, p. 163–168.

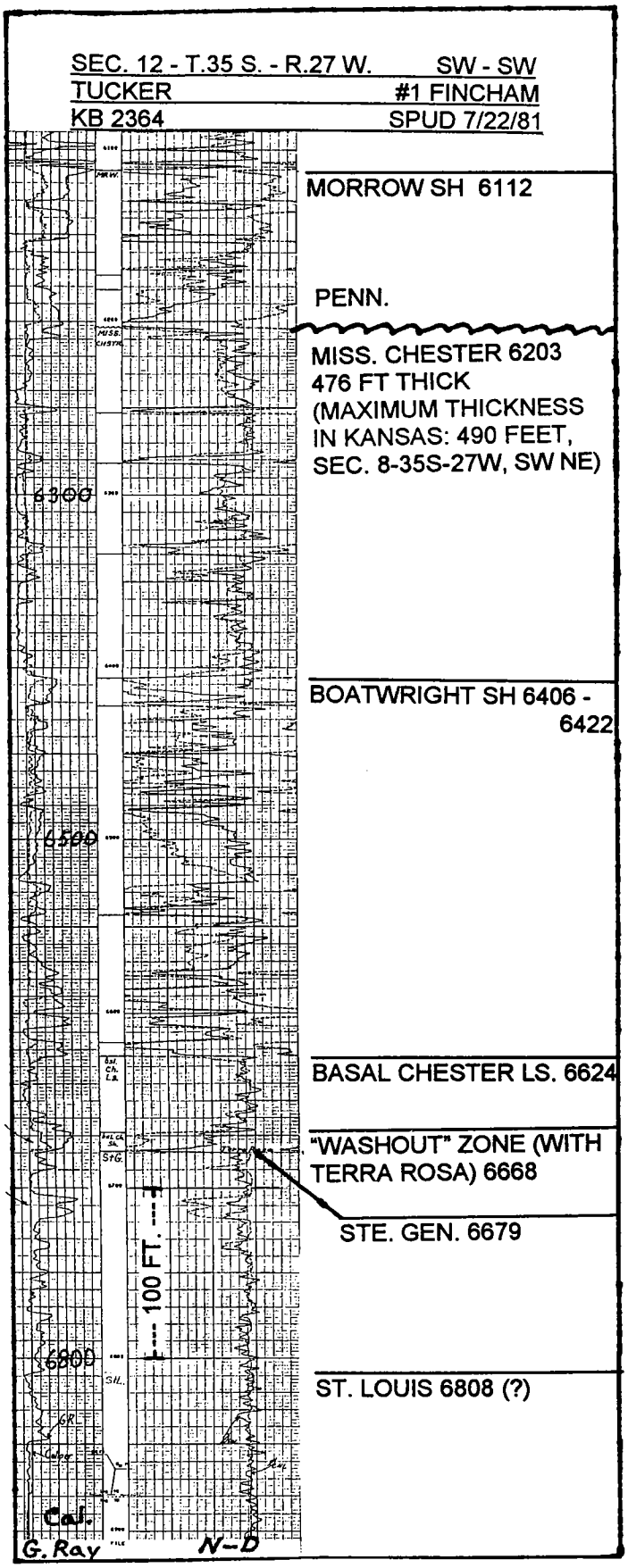

Figure 1. Thickest Chesterian carbonate section in Kansas, southeastern Meade County. *Cal.* = caliper; *G. Ray* = gamma ray; *N–D* = neutron density.

for this section. Therefore, Davies often picked the St. Louis lower, at a zone of typically well-developed, larger oolites. This is currently known as the informal St. Louis 'C' oolite zone. This downward miscorrelation also caused the Salem (Spergen) dolomite zone to be correlated too low in some wells. Additional well control provided the data to determine the existence of a westward facies change in the upper part of the St. Louis to more arenaceous limestone than was previously known in the eastern Hugoton field area. During later years, Davies, collaborating with other experts of his time, understood that this "false St. Louis" was actually the true top of the St. Louis (personal communication with Walt DeLozier, Davies' draftsman and business partner). The Kansas Sample Log Service never offered any redrafted strip logs to correct this early misconception.

The third example (Fig. 3) illustrates one of the best and most persistent correlation markers within the Mississippian in southwestern Kansas, the distinctive Gilmore City Formation. I am using Goebel's (1966) definition of the Gilmore City. Some more recent researchers, however, have discontinued this formational name after studying the outcrop belt in the Missouri area. The Gilmore City exhibits a massive, "clean" gamma-ray-log signature. Modern geophysical logs (especially the photoelectric, or *Pe*, log curves) clearly trace this pure-limestone marker unit from the overlying chert-rich section of the Mississippian Osage, and from the underlying cherty dolomite of the Ordovician Viola Formation. The Gilmore City samples characteristically are almost pure limestone, containing oolites and some minor dolomitic layers. Some wells are better key correlation wells because they have penetrated a section of Kinderhookian shale and sand below the Gilmore City Formation, which is related to the underlying unconformity developed at the top of the Ordovician.

Nevertheless, some operators still confused these units in "deep" wells (drilled to the Ordovician) in the area of this example during the infill-drilling and farmout period of Hugoton field development in the 1990s. They usually shifted their correlations too far upward by 100–200 ft at times, referring to the Gilmore City limestone as the Viola, the underlying Kinderhook clastic-detrital zone as the Simpson, and therefore the Viola cherty dolomite as the Arbuckle. Perhaps some geologists or operators are confused by the formal nomenclature of the Viola *Limestone:* this unit is cherty *dolomite* in southwestern Kansas. On one recent well log, the Mississippian Osage chert was identified as the Viola cherty dolomite, and the Gilmore City as the Arbuckle. These significant errors may be perplexing to geophysicists trying to tie the large three-dimensional (3-D) seismic surveys in this area to the geology provided by the operators.

The fourth and final example (Fig. 4) is from an area east of Hugoton field, where the typical shelf facies of the Gilmore City oolitic limestone exhibits a shelf-edge facies change: fewer oolites, grading to none,

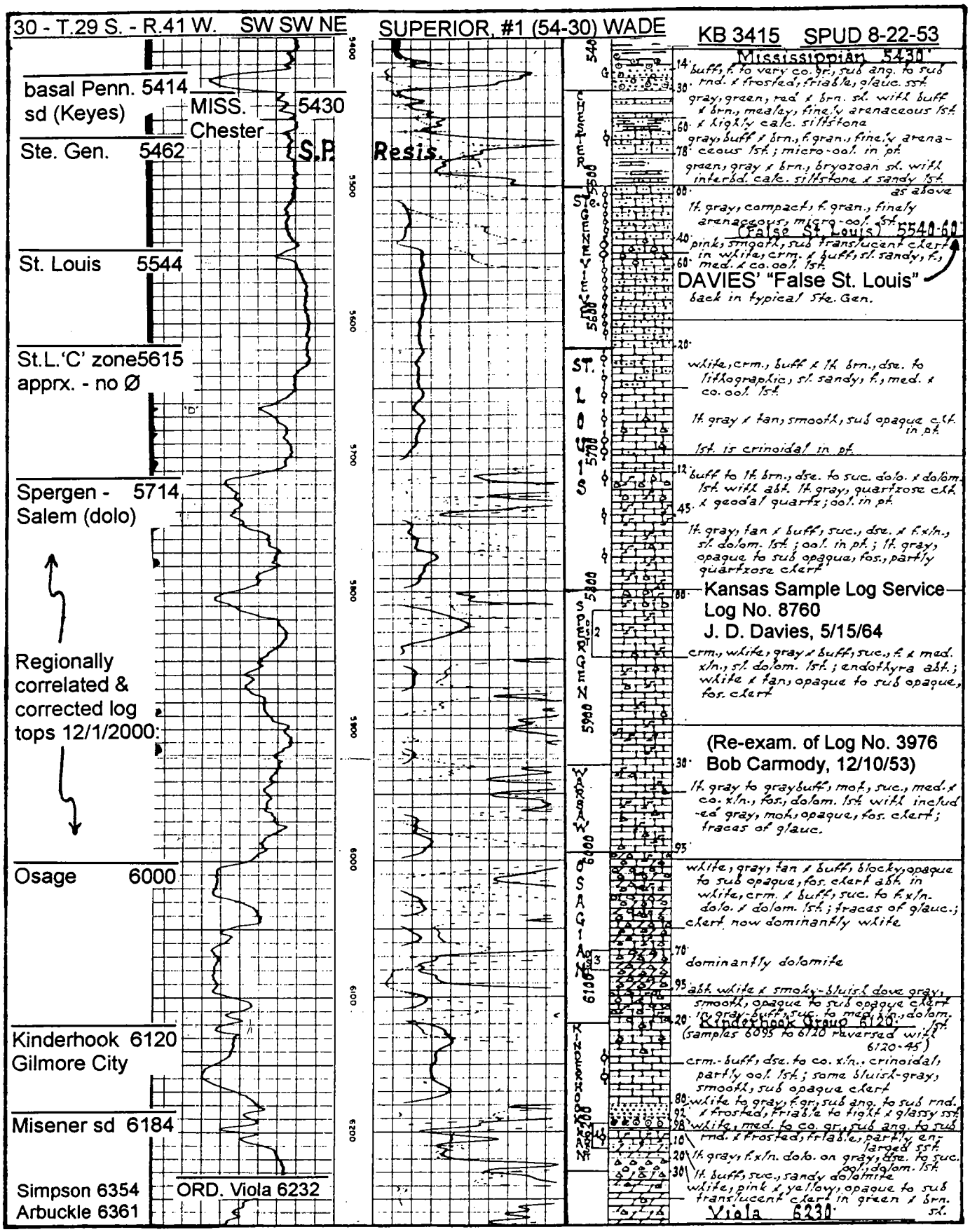

Figure 2. Clarification of the early "false St. Louis" miscorrelation. Acknowledgment to J. D. Davies (deceased), business partner, Kansas Sample Log Service. *S.P.* = spontaneous potential; *Resis.* = resistivity.

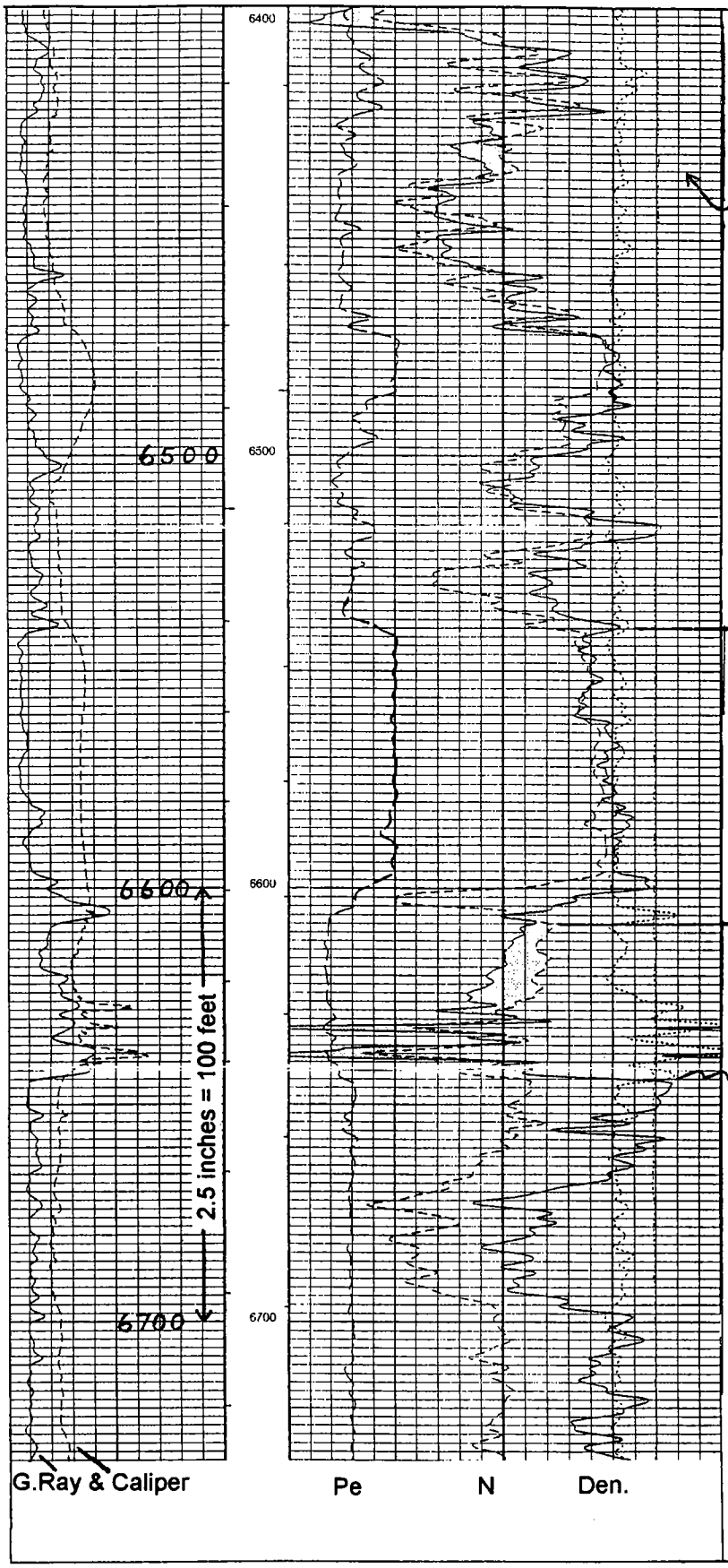

Sec. 19 - T.29 S. - R.37 W.
2140 FNL & 2140 FWL
ZINKE & TRUMBO, # 1-19 WINGER
KB 3133, SPUD 10/17/1997

(OSAGE 6332)

Characterized by predominance of chert in samples and from Pe log signature.

KINDERHOOK, GILMORE CITY 6540
(Reported as Viola in this well * and marked as Arbuckle in Sec. 20.)

Note the distinguishing massive, low ("clean") gamma ray log signature and "pure" limestone (cf. Pe log signature).

MISENER SD 6608
(Reported as Simpson sd)*

ORDOVICIAN, VIOLA 6643
(Reported as Arbuckle)*

Note "pure" dolomite from the Pe log signature. Viola is very difficult to distinguish from underlying Arbuckle dolo. on well logs in general area, except when remnant of Simpson clastics is locally present. (Arbuckle distinguished from Viola in samples by the presence of oolitic chert and quartz sand grains.)

* The source of this local miscorrelation in the 1990's may be two wells drilled to the Ordovician in the late 1980's in the NW/4 of Sec.30, T.29 S., R.39 W. ARCO reported (and heavily marked one log), the Gilmore City as Viola.

Figure 3. Kinderhookian-age Gilmore City limestone. *Pe* = photoelectric; *N* = neutron; *Den.* = density.

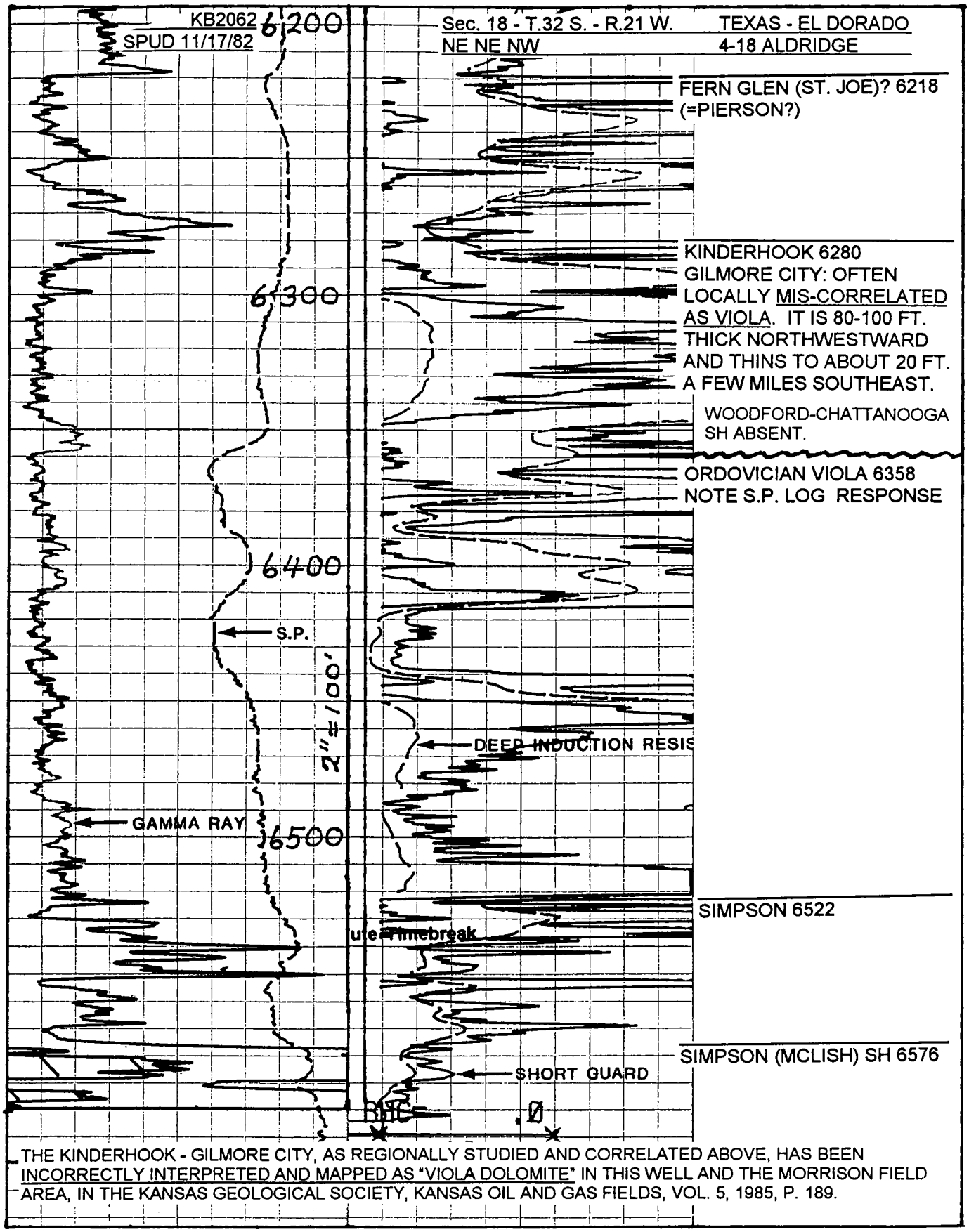

Figure 4. Gilmore City Formation shelf-edge facies change along the southern edge of Kansas.

with an increase in dolomite and chert. As previously noted, the Gilmore City limestone usually is easily distinguished from other Lower Mississippian units in southwestern Kansas by a clean, massive log signature and oolitic limestone. But some geologists have confused this different rock of the shelf-edge facies with the somewhat similar underlying Ordovician Viola Limestone. This is especially true in Meade and Clark Counties and the northwestern part of Comanche County, where the black, "hot" (high-gamma-ray-emission) Chattanooga–Woodford Shale is not present. The western limit of the distinctive Chattanooga–Woodford black shale is in T. 35 S., R. 20 W., southwestern Comanche County. The Gilmore City–Viola boundary (post-Ordovician unconformity) is similar carbonate on carbonate, so careful research is necessary to differentiate these units northwestward from this point, where their separation is easily recognized.

As a correlation guide in this area, the first unit with a clean gamma-ray signature below the Osage chert-rich section (or the shelf-edge facies-equivalent Cowley Formation) is invariably the Gilmore City Formation. The error of confusing the Gilmore City with the underlying Viola in many wells has resulted in many drillstem tests of the generally poor Gilmore City reservoir rock. Sometimes, therefore, the underlying true Viola section was not tested. Surprisingly, though, some marginal production has been established from the Gilmore City. Two examples are the Cash City field on the Meade–Clark county border in T. 33 S., and some of the development wells drilled during the 1980s that extended the field limits to the first Viola producing field in southwestern Kansas, the Morrison field, in T. 32 S., R. 21 W.

CONCLUSION

Finally, a positive observation can be made regarding future exploration. The maturely explored Mississippian subcrop plays flanking the central Kansas uplift are noted for "only near-the-top" production (directly below Pennsylvanian seals). In southwestern Kansas, Mississippian production can be obtained more widely spread "down-in" >500 ft below the post-Mississippian unconformity. As the exploration history of this area has shown, continued resolution of difficult Mississippian geology and correlations will result in new hydrocarbon discoveries for many more years.

DEDICATION AND ACKNOWLEDGMENT

This short stratigraphic note is dedicated to the memory of a generous geologist in Wichita, Kansas, with whom I enjoyed many Mississippian and other geological discussions: Rob Dietterich, who was killed in a car accident in August 1996.

I thank the donors and supporters of the Kansas Geological Society Library in Wichita for preserving and making available extensive well data at a reasonable cost.

SELECTED REFERENCES FOR MISSISSIPPIAN ROCKS IN SOUTHWESTERN KANSAS

Abegg, F. E., 1992, Lithostratigraphy, depositional environments, and sequence stratigraphy of the St. Louis and Ste. Genevieve Limestones (Upper Mississippian), southwestern Kansas: University of Kansas unpublished Ph.D. dissertation, 206 p. (Available as Kansas Geological Survey Open-File Report 92-72. Warning: this dissertation extrapolated a limited local study into many regional stratigraphic miscorrelations.)

Clair, J. R., 1948, Preliminary notes on lithologic criteria for identification and subdivision of the Mississippian rocks in western Kansas: Kansas Geological Society Guidebook, 14 p.

Dietterich, R. J., 1985, Porosity and permeability analysis in Mississippian System, St. Louis Limestone formation, Damme Field, Finney County, Kansas, utilizing petrographic image analysis: Wichita State University unpublished M.S. thesis, 223 p.

Goebel, E. D., 1966, Stratigraphy of Mississippian rocks in western Kansas: University of Kansas unpublished Ph.D. dissertation, 198 p. (Available as Kansas Geological Survey Open-File Report 66-10. The last comprehensive Mississippian research done in southwestern Kansas. I have used the old-nomenclature Gilmore City Formation as defined in this study.)

Handford, C. R.; and Francka, B. J., 1991, Mississippian carbonate–siliciclastic eolianites in southwestern Kansas, *in* Lomando, A. J.; and Harris, P. M. (eds.), Mixed carbonate–siliciclastic sequences: Society of Economic Paleontologists and Mineralogists Core Workshop 15, p. 205–243.

Kansas Geological Society Library, 212 N. Market Street, Suite 100, Wichita, KS 67202; telephone, 316-265-8676. (Geophysical well logs, geological reports, lithologic logs, etc.)

Kansas Sample Log Service, Lithologic strip logs: various geologists, primarily J. D. Davies. (Sample descriptions from wildcat wells in Kansas, available from Kansas Geological Society Library.)

Newell, K. D.; Watney, W. L.; Cheng, S. W. L.; and Brownrigg, R. L., 1987, Stratigraphic and spatial distribution of oil and gas production in Kansas: Kansas Geological Survey Subsurface Geology Series 9, 86 p. (Mississippian production, p. 33, fig. 20.)

Parham, K. D., 1989, Upper Mississippian oolite shoals of the St. Louis Formation in Gray County, Kansas—a guide for oil and gas exploration: Wichita State University unpublished M.S. thesis, 177 p.

Severy, C. L., 1975, Subsurface stratigraphy of the Chesterian Series, southwest Kansas: University of Colorado, Boulder, unpublished M.S. thesis, 61 p.

Conodont Biofacies and Biostratigraphy of Silurian Strata of the Hunton Group in Oklahoma, and Equivalent Units in West Texas and Eastern New Mexico

James E. Barrick
Texas Tech University
Lubbock, Texas

ABSTRACT.—During the Silurian Period, a broad carbonate shelf stretched across the southern Midcontinent region of North America from Arkansas southwestward into New Mexico. Major remnants of this shelf region occur in two areas: (1) the subsurface of the Anadarko–Arkoma basin region of Oklahoma, which is bordered by small outcrop belts in southern and northeastern Oklahoma; and (2) the subsurface of west Texas and eastern New Mexico, with outcrops only far to the west and southwest. Despite a long history of hydrocarbon production from Silurian carbonates in these two areas, the subdivision, correlation, and dating of Silurian units in the southern Midcontinent region developed only slowly. A combination of repetitive to monotonous lithofacies (Fusselman lithofacies, Hunton marlstones), overprinted by extensive dolomitization, allows little possibility of reliable subdivision and correlation of Silurian strata over large areas by physical means.

Studies of conodont faunas from Oklahoma and west Texas illustrate their potential for subdivision, correlation, and dating of Silurian strata in the southern Midcontinent region. Although the shallow-water lithofacies of Lower Silurian (Llandovery) strata have yielded only sparse conodonts, sufficient material has been obtained to distinguish these units (Fusselman in Texas, Cochrane in Oklahoma) from younger Silurian units, and to show that carbonate deposition occurred through most of Llandovery time. Neither biostratigraphic nor biofacies analysis has yet revealed evidence for sea-level events recognized for the Llandovery in other regions.

The abrupt shift to offshore conodont biofacies at the base of the Clarita (Oklahoma) and Wristen (Texas) Formations records a major regional rise in sea level that conodont faunas date as having occurred at the beginning of the Wenlock. This deepening event reset the pattern of depositional facies across the southern Midcontinent. In southern Oklahoma, deeper water lithofacies and conodont biofacies occur that grade northward into shallower water lithofacies and biofacies. A mid-Wenlock disconformity that lies within the Clarita Formation can be recognized using conodonts. Abundant and diverse conodont faunas show that the apparently homogeneous Late Silurian (Ludlow–Pridoli) Henryhouse marlstones in the outcrop area in southern Oklahoma comprise a mosaic of unconformity-bounded units (sequences?), of which only the youngest ones are widely distributed. Detailed analysis of conodont biofacies and subtle lithofacies variations permit comparison with Late Silurian oceanic episodes and events that have been proposed on the basis of conodonts and lithofacies patterns in the Baltic region. Conodont faunas confirm that the boundary between the Henryhouse and Haragan marlstones is unconformable.

In west Texas, the early Wenlock deepening event may have set up conditions that permitted the mid-Wenlock formation and subsequent progradation of the Fasken platform southward into the adjacent Frame basin. Conodont faunas record the persistence of the Fasken platform–Frame basin into the latest Silurian (Pridoli), but biostratigraphic subdivision of the platform carbonates has not been possible. In shelf-margin beds, conodont faunas record a brief hiatus at the Silurian–Devonian boundary, like that seen at the Henryhouse–Haragan contact in southern Oklahoma.

Barrick, J. E., 2001, Conodont biofacies and biostratigraphy of Silurian strata of the Hunton Group in Oklahoma, and equivalent units in west Texas and eastern New Mexico, *in* Johnson, K. S. (ed.), Silurian, Devonian, and Mississippian geology and petroleum in the southern Midcontinent, 1999 symposium: Oklahoma Geological Survey Circular 105, p. 169.

Thermal Maturation of the Woodford Shale in South-Central Oklahoma

Brian J. Cardott
Oklahoma Geological Survey
Norman, Oklahoma

ABSTRACT.—The study area includes the Ardmore and Marietta basins and the Criner uplift in south-central Oklahoma. The Woodford Shale (Upper Devonian–Lower Mississippian) is a major hydrocarbon source rock in Oklahoma. Thermal maturation (temperature-induced physicochemical changes in sedimentary organic matter) is an important aspect in the characterization of a hydrocarbon source rock. The Woodford Shale was deposited before the Pennsylvanian orogenies and therefore is a key bed used to track the effects of basinal heating on hydrocarbon generation, expulsion, and preservation.

The Woodford Shale is the oldest rock in Oklahoma that contains the vitrinite maceral, derived from the woody tissues of Devonian–Mississippian vascular tree-size plants such as *Archaeopteris* (a progymnosperm; woody parts are called *Callixylon*) and *Cordaitales* (a gymnosperm). Thermal maturation was determined by measuring vitrinite reflectance (random reflectance in nonpolarized light and oil immersion, R_o,r) from Woodford Shale outcrops, well cuttings, and core samples. The oil window (main zone of oil generation from hydrocarbon source rocks) is 0.5–1.3% R_o,r. The Woodford Shale is marginally mature (0.4–0.6% R_o,r) to early mature (0.6–0.9% R_o,r) in the Criner uplift (0.49–0.54% R_o,r from outcrop to a depth of 4,050 ft from four samples) and the Marietta basin (0.55–0.69% R_o,r from depths of 8,663–12,111 ft from six samples). The Woodford Shale is marginally mature to post-mature (>2% R_o,r; dry-gas preservation zone) in the Ardmore basin (0.49–2.45% R_o,r from outcrops on the south flank of the Arbuckle Mountains to depths of 900–18,540 ft in the basin from 25 samples). Woodford Shale samples were not available from depths of 11,061–17,250 ft and a vitrinite-reflectance range of 0.82–2.13% R_o,r in the Ardmore basin.

Qualitative fluorescence of *Tasmanites* alginite indicated that most of the Woodford Shale samples are at the early stage of oil generation (green to greenish yellow fluorescence). The vitrinite-reflectance equivalent (VRE), calculated from bitumen reflectance, indicated that vitrinite reflectance of the Woodford Shale in south-central Oklahoma is suppressed (lowered) by 0.04–0.28% R_o,r from the effect of bitumen and liptinite maceral content. The vitrinite reflectance of the Woodford Shale at the type locality increased from a measured value of 0.49 to 0.77% R_o,r VRE, shifting the interpretation from marginally mature to early mature.

The Woodford Shale is marginally mature to post-mature, with respect to the generation of liquid hydrocarbons, in south-central Oklahoma. The level of thermal maturation was attained from synorogenic and postorogenic maximum depth of burial.

Cardott, B. J., 2001, Thermal maturation of the Woodford Shale in south-central Oklahoma, *in* Johnson, K. S. (ed.), Silurian, Devonian, and Mississippian geology and petroleum in the southern Midcontinent, 1999 symposium: Oklahoma Geological Survey Circular 105, p. 170.

Sequence Stratigraphy of Chesterian Sandstones in the Black Warrior Basin, Northeastern Mississippi

Arthur W. Cleaves (deceased)
Oklahoma State University
Stillwater, Oklahoma

ABSTRACT.—Sequence stratigraphy is an important tool for interpreting sandstone provenance, source-rock accumulation, and depositional-systems distribution for Chesterian siliciclastic-rock units in northeastern Mississippi and adjacent parts of Alabama. Twelve major gas-producing sandstone units accumulated on the mixed carbonate–siliciclastic northern shelf of the Black Warrior basin in response to lowstand reciprocal sedimentation involving quartz-arenite detritus transported from a cratonic source area north of the Illinois basin. Highstand deltaic sedimentation for each major eustatic cycle took place in the Illinois basin at the same time that carbonate accretion constructed a carbonate shelf and ramp system along the northern margin of the Black Warrior basin. Productive lowstand deltas include both the wave-dominated variety such as the Evans and Hartselle units, as well as river-dominated systems like the Lewis, Rea, Abernathy, Sanders, Carter, and Gilmer units. Distributary-channel fill, bar fingers, and delta-fringe sheet sands constitute the principal reservoir facies elements. In contrast, the *"Millerella"* sandstone has an irregularly distributed net-sand map pattern that is more characteristic of a transgressive-marine rock body.

Evidence of at least five and perhaps even more cycles of eustatic sea-level change is preserved in the subsurface stratigraphic record of the two basins. At the southern end of the Illinois basin in central Kentucky, preservation of a 120-mi-long Bethel (Lewis) incised valley system that cut downward as much as 200 ft into underlying shelf carbonates demonstrates an effect of major sea-level lowering at the beginning of the Chesterian Epoch. Both the Lewis and Evans sandstones of the Black Warrior basin are overlain by sequence-bounding black-shale condensed zones. The Evans–Hartselle interval represents a single sequence and records a gradual marine transgression that resulted in the formation of >20 overlapping delta lobes distributed as far north as central Tennessee. Higher in the section, a large incised "gorge" cut into the lower Bangor carbonates of central Itawamba County, Mississippi, served as a conduit for the funneling of Sanders–Carter siliciclastics into the basin. Farther to the south, in the vicinity of the Corinne gas field, the Sanders formed an incised-valley system that removed subjacent Rea and Abernathy deltaic facies. Even the top of the Chester section is marked by an interregional disconformity surface, which is overlain by basal Pottsville braided-stream channels and incised valley-fill complexes.

Cleaves, A. W., 2001, Sequence stratigraphy of Chesterian sandstones in the Black Warrior basin, northeastern Mississippi, *in* Johnson, K. S. (ed.), Silurian, Devonian, and Mississippian geology and petroleum in the southern Midcontinent, 1999 symposium: Oklahoma Geological Survey Circular 105, p. 171.

Mississippian 3-D Case History—Porosity Prediction Using Seismic-Trace Inversion—A Prospector's Perspective

Jasha Cultreri
Independent Consultant
Midland, Texas

ABSTRACT.—Mississippian reservoirs in west-central Kansas produce prolifically from subtle structures. In the two townships surrounding the case-history project, per-field reserves average 1 MMBO, and per-well averages are 90 MBO at a depth of 4,700 ft. Many of these wells have initial potentials >100 BOPD. An average well produces 50 BOPD initially. However, close scrutiny indicates that although structure is critical, it is not the only criterion in determining well potential. Some wells in this area have made up to 250 MBO per well, with a two-well field making 500 MBO. And some wells structurally high to production are dry holes. The controlling factor is reservoir quality.

Seismic-trace inversion illustrates the rock-property differences between good and poor wells and is an excellent reservoir-quality indicator for carbonate rocks. Inversion involves converting the seismic trace to a pseudo-sonic log. Sonic logs yield significantly more lithologic information than seismic-amplitude traces and are useful for porosity detection.

A brief non-mathematical discussion and history of seismic-trace inversion was presented, followed by a 3-D case history. The post-drill 3-D inversion and analysis explained a dry hole and field-production anomalies in the Mississippian Warsaw Limestone, Lippold field, Hodgeman County, Kansas. Strengths, weaknesses, uses, and pitfalls were reviewed in the context of the case history.

Cultreri, Jasha, 2001, Mississippian 3-D case history—porosity prediction using seismic-trace inversion—a prospector's perspective, *in* Johnson, K. S. (ed.), Silurian, Devonian, and Mississippian geology and petroleum in the southern Midcontinent, 1999 symposium: Oklahoma Geological Survey Circular 105, p. 172.

Depositional Environment and Sequence Stratigraphy of Silurian through Mississippian Strata in the Midcontinent

Richard D. Fritz and Edward A. Beaumont
Masera Corporation
Tulsa, Oklahoma

ABSTRACT.—The Silurian to Mississippian interval is a key geologic and economic section in the Midcontinent. This interval contains the most important source rocks in the Midcontinent, encased by significant reservoirs that also provide migration pathways to overlying traps.

Tectonically, the Midcontinent can be divided into three stages of development: (1) rift, (2) subsidence, and (3) deformation. The Silurian to Mississippian interval straddles the latter two stages. The depositional environment and resulting stratigraphy were strongly influenced by the tectonic changes during this time period and can be better understood by integration of sequence analysis. L. L. Sloss related regional tectonic changes through unconformities to define the basic structure of sequence stratigraphy. The stratigraphy in the Midcontinent can be divided into four Sloss sequences: (1) Sauk—Cambrian to Early Ordovician, (2) Tippecanoe—Middle Ordovician to Early Devonian, (3) Kaskaskia—Late Devonian to Mississippian, and (4) Absaroka—Pennsylvanian to Upper Triassic.

The stratigraphy of the Silurian to Mississippian can be divided further into six groups that are genetically related: (1) Hunton Group, (2) Misener–Woodford siliciclastics, (3) pre-Chester carbonates, (4) Chester carbonates and siliciclastics, (5) Springer siliciclastics, and (6) Stanley siliciclastics.

Much of the Silurian-to-Mississippian rocks were deposited on a broad ramp, with carbonates dominant up-ramp and siliciclastics dominant down-ramp. Silurian to Early Devonian strata represent an overall regressive carbonate episode. The carbonate facies are fairly evenly represented by intertidal and subtidal wackestones to grainstones. Some supratidal rocks are present, but most were deposited north of Oklahoma and were later eroded. The Misener–Woodford interval represents an overall anoxic transgressional episode, when an influx of clastics came into this otherwise carbonate regime. The carbonate regime returned after Woodford time, although pre-Chester strata are more subtidally dominated and are represented by mudstones to grainstones. Clastics returned in the deeper parts of the Midcontinent basins during the end of pre-Chester deposition. These clastics were primarily silts and suspended clays, which were winnowed from or bypassed the carbonate banks around the rims of the basins. During Chester time, carbonates were deposited on the shelf during highstand, with siltstones and shales in the basins. During periods of lowstand in the Anadarko basin, Chester carbonates were bypassed, and roughly coeval Springer sands and shales were deposited. In the Arkoma basin, thick sequences of Stanley rocks were deposited primarily as turbidites derived from the east.

Sequence stratigraphy is best understood by an examination of its basic components—sequence boundaries and parasequences. The most easily recognized sequence boundaries are unconformities. Key unconformities in the Silurian to Mississippian strata include intra-Hunton, pre-Woodford, intra-Mississippi, and pre-Morrow. Carbonate parasequences in Silurian to Mississippian rocks are typically represented by upward-shoaling cycles. The facies are silty mudstones to grainstones that are encased in wackestones overlain by algal mudstones with some anhydrite. Bundles of these parasequences are correlatable over large areas of the Midcontinent.

Silurian to Mississippian carbonate-reservoir development is closely tied to facies and unconformities. Crinoidal wackestones and oolitic facies both are susceptible to dolomitization and dissolution associated with unconformities. Exceptions occur in carbonate mounds or build-ups where porosity is typically intergranular and moldic. Siliciclastic facies are typically nearshore to marine in origin. Reservoir development is closely tied to diagenesis, especially cementation percentages and dissolution of metastable grains.

As in the past, discoveries in Silurian to Mississippian rocks will provide significant future oil and gas reserves in the Midcontinent.

Fritz, R. D.; and Beaumont, E. A., 2001, Depositional environment and sequence stratigraphy of Silurian through Mississippian strata in the Midcontinent, *in* Johnson, K. S. (ed.), Silurian, Devonian, and Mississippian geology and petroleum in the southern Midcontinent, 1999 symposium: Oklahoma Geological Survey Circular 105, p. 173.

Exploration Potential of the Lower Mississippian Sycamore Limestone

Richard D. Fritz and Larry Gerken
Masera Corporation
Tulsa, Oklahoma

ABSTRACT.—The Sycamore Limestone is a mixed carbonate–siliciclastic reservoir primarily confined to central and southern Oklahoma. It is unique both geologically and economically in that it is surrounded by two of the best source rocks in Oklahoma, the Woodford Shale and the Caney Shale. Sycamore production was established in and around the Golden Trend field in south-central Oklahoma.

The Sycamore Limestone was deposited during a transitional period from dominantly subsidence to deformation in the Midcontinent. Stratigraphically, the Sycamore Limestone is Kinderhookian to Osagean and lies near the beginning of L. L. Sloss's Kaskaskia megasequence. The Sycamore has a well-defined log signature and is correlatable over large areas.

Sycamore strata were deposited during a relative lowstand as a carbonate-dominated inner shelf on the basinward flank of a broad, shallow ramp. This environment, with close proximity to both cratonic and marine siliciclastic sources, produced a mixed carbonate–clastic deposit.

Sycamore rocks are composed primarily of clastic-rich carbonate mudstones to packstones, with an abundance of pelloids and minor amounts of allochem debris. Sycamore carbonates are interbedded with siltstones and shales.

Diagenesis is relatively uncomplicated. Sparry calcite is the dominant diagenetic feature and is present as recrystallized matrix, replacement cement, and/or a subordinate fracture-filling mineral. Primary porosity is low, and secondary porosity consists of isolated, secondary dissolution pores. Both porosity and permeability are enhanced from fracturing of the rock.

The Sycamore is conformably overlain by the Caney Shale and is paraconformable with the underlying Woodford Shale. On the basis of parasequence boundaries, the Sycamore can be divided into four distinguishable parasequences: S1, S2, S3, and S4, in ascending order. Correlation is controlled by recognition of distinct marine shales between the parasequences. Correlation is difficult in areas where the Sycamore laps onto the Woodford as a result of syndepositional tectonic activity. Units S1 and S2 are not laterally consistent and appear to be developed primarily along a localized shelf edge or preserved around structural salients. Units S3 and S4 are more widespread and are absent only in the eastern part of the area, where they are truncated by the pre-Pennsylvanian unconformity.

Production within the area of interest comes from all of the subdivided zones of the Sycamore. Production in the Golden Trend area lies in a band trending from southeast to northwest. Any of the zones are potential targets; however, the best production is from within the fractured zones. The most intensely fractured interval is zone S3, which could be a good target for horizontal drilling. Owing to the northwest–southeast orientation of many of the faults and fracture systems, a drilling program trending southwest–northeast would probably intercept the most fractures and be most productive.

Fritz, R. D.; and Gerken, Larry, 2001, Exploration potential of the Lower Mississippian Sycamore Limestone, *in* Johnson, K. S. (ed.), Silurian, Devonian, and Mississippian geology and petroleum in the southern Midcontinent, 1999 symposium: Oklahoma Geological Survey Circular 105, p. 174.

3-D Seismic and Hydrocarbon-Microseepage Surveys: Exploration Adventures in Osage County, Oklahoma

Daniel C. Hitzman
Geo-Microbial Technologies, Inc.
Ochelata, Oklahoma

ABSTRACT.—In order to investigate new geophysical methodologies, as well as to encourage more aggressive domestic-exploration operations, the U.S. Department of Energy (DOE) commissioned a high-resolution 3-D seismic survey and a complementary surface geochemical survey in Osage County, Oklahoma. Except for Arbuckle fields, typical Osage County reservoirs are neither Silurian, Devonian, nor Mississippian in age. However, the exploration techniques tested here by the DOE are useful to all Oklahoma explorationists, regardless of the intended reservoir target.

In December 1996, an approximately 7-mi^2 3-D seismic survey was designed to test new ideas of high-resolution identification and observation of the subtle geologic features in Osage County. The seismic data were collected in 55-ft bins. For additional comparison, 922 surface-soil samples were collected every 440 ft to test for evidence of hydrocarbon microseepage. Specific light-hydrocarbon-oxidizing microbes that correspond to oil and gas seeps were measured. There is a direct and positive relationship between light-hydrocarbon concentrations in soils and these microbial populations—a relationship that is dynamic and reproducible. The mapped microbial signatures reveal a significant and dominant cluster of microbial values that correspond closely with a Pennsylvanian Layton channel feature identified by the high-resolution seismic survey. Additionally, a part of the survey area that contains a depleted Pennsylvanian Bartlesville reservoir is characterized by low microseepage. This expected phenomenon represents depressured reservoirs that are incapable of sustaining microseepage signatures. Seismic, microbial, and additional geochemical-survey results were presented.

Hydrocarbon-Microseepage Signatures of High-Resolution 3-D Seismic Area

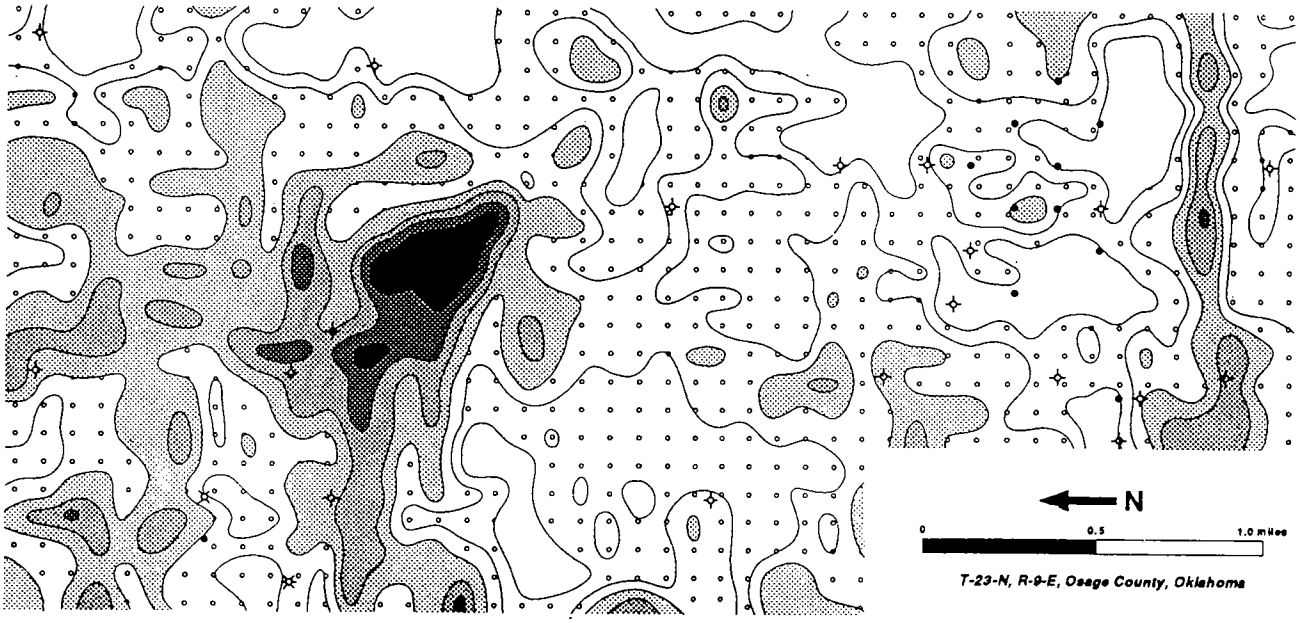

Hitzman, D. C., 2001, 3-D seismic and hydrocarbon-microseepage surveys: exploration adventures in Osage County, Oklahoma, *in* Johnson, K. S. (ed.), Silurian, Devonian, and Mississippian geology and petroleum in the southern Midcontinent, 1999 symposium: Oklahoma Geological Survey Circular 105, p. 175.

Advanced Reservoir Characterization of a Hunton Field, Kingfisher County, Oklahoma

Daniel C. Hitzman and Brooks A. Rountree
Geo-Microbial Technologies, Inc.
Ochelata, Oklahoma

Charles O'Donnell
Bristol Resources
Tulsa, Oklahoma

ABSTRACT.—The evaluation of hydrocarbon-microseepage signatures in a mature producing field helps identify prime drilling targets and exposes areas where additional drilling and exploitation are unwarranted. The objective of a microbial reservoir-characterization (MRC) survey completed in the Themer area of Kingfisher County, Oklahoma, was to identify the microseepage response of hydrocarbon-charged reservoir compartments or bypassed pay that could be exploited by additional drilling. Because hydrocarbon microseepage is nearly vertical, the extent of an anomaly at the surface can approximate the productive limits of the reservoir at depth. Futhermore, the pattern of microseepage over a field can reflect reservoir heterogeneity and distinguish hydrocarbon-charged compartments from drained or uncharged compartments. Since hydrocarbon microseepage is dynamic, seepage patterns can change rapidly in response to production-induced changes.

In March 1998, 323 soil samples collected every 330 ft (in a 17 × 19 grid pattern) were tested for specific light-hydrocarbon-oxidizing microbes. There is a direct positive relationship between the light-hydrocarbon concentrations in soils and these microbial populations—a relationship that is measurable and reproducible. The mapped Themer signatures revealed significant clusters of both elevated and depressed microbial values within the survey area and may represent contrasting pressure regimes within the Hunton reservoir target. Five main clusters of microbial highs were identified. One in-fill well was drilled on the smallest microbial anomaly and subsequently produced from the Hunton. Survey areas characterized by low microseepage may represent drained or uncharged parts of the reservoir.

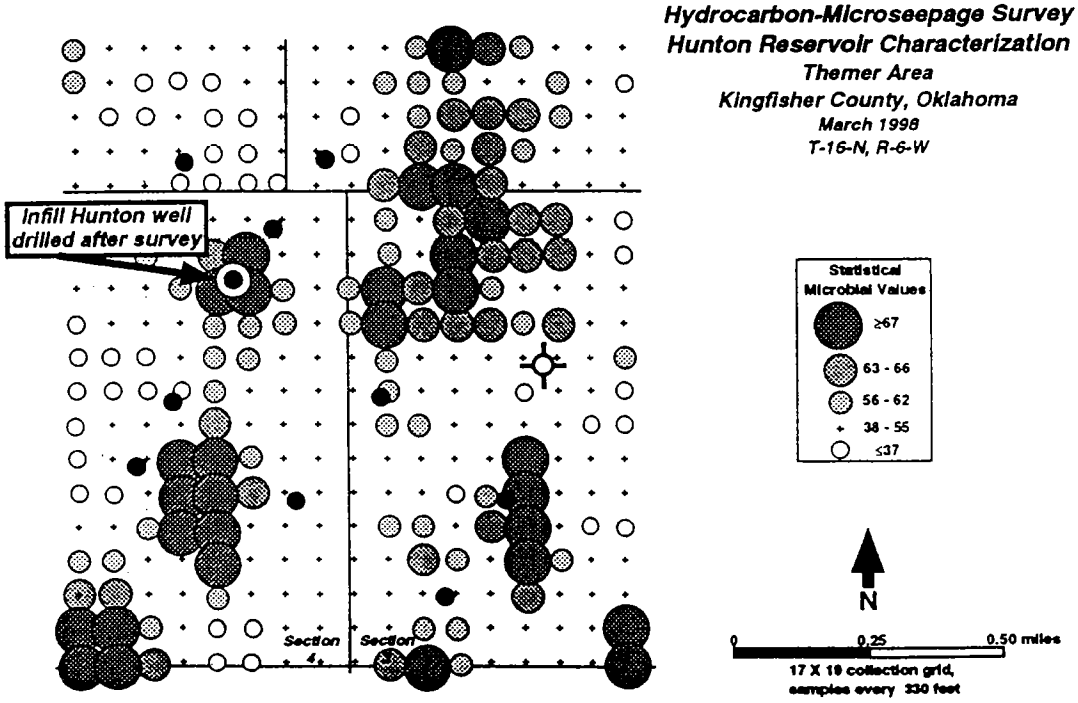

Hitzman, D. C.; Rountree, B. A.; and O'Donnell, Charles, 2001, Advanced reservoir characterization of a Hunton field, Kingfisher County, Oklahoma, *in* Johnson, K. S. (ed.), Silurian, Devonian, and Mississippian geology and petroleum in the southern Midcontinent, 1999 symposium: Oklahoma Geological Survey Circular 105, p. 176.

Discovery of Economic Fractured Source-Rock Reservoirs in the Devonian and Mississippian of Oklahoma

Fred S. Jensen (deceased)
Rio-Colorado Oil And Gas, Inc.
Denver, Colorado

Thomas L. Thompson and James R. Howe
Thompson's Geodiscovery, Inc.
Boulder, Colorado

ABSTRACT.—Naturally fractured source-rock reservoirs may represent the largest undeveloped oil resource in the world. Large quantities of oil, generated during the maturation of organic-rich shales, remain within the micro- and macrofractures of the source rocks.

Procedures for locating preferred drill sites should include integration of the following methods: (1) surface mapping and fracture analysis based on field work, air photography, and satellite images; (2) interpretation of crystalline-basement fracture trends based on residual aeromagnetic data; (3) structure contouring based on well control, surface mapping, and seismic data; (4) coordinated thermal maturation and paleostress analysis; (5) determination of the present state of maximum horizontal compressive stress based on well-bore breakouts; and (6) stratigraphic mapping of source-rock richness and zones of strong-ductility contrast as with interbedded shale and chert layers in the Woodford Formation.

Economic production of oil from fractured source-rock reservoirs in the Devonian–Mississippian Woodford Formation should result from drilling on wide spacing (320–640 acres per well) of horizontal, underbalanced wells at high angles to existing fractures where they parallel the present state of maximum horizontal compressive stress in thermally mature rocks. With the characteristic absence of moveable water in these types of reservoirs, moderate dips of 1,000 to 2,000 ft per mile would enhance ultimate recovery of petroleum by gas-segregation drive and by gravity drainage in downdip areas, particularly where the dip direction is parallel or subparallel to the present state of maximum horizontal compressive stress. Abnormally high formation pressure would further increase the cumulative production, which reasonably could range from 1 to 5 million barrels of oil per well.

Jensen, F. S.; Thompson, T. L.; and Howe, J. R., 2001, Discovery of economic fractured source-rock reservoirs in the Devonian and Mississippian of Oklahoma, *in* Johnson, K. S. (ed.), Silurian, Devonian, and Mississippian geology and petroleum in the southern Midcontinent, 1999 symposium: Oklahoma Geological Survey Circular 105, p. 177.

Mississippi Lime: Chert Occurrence Related to Productive Reservoirs, Blaine County, Oklahoma

Dan J. Towns (deceased)
Louis Dreyfus Natural Gas
Oklahoma City, Oklahoma

ABSTRACT.—The Mississippi lime produces extensively across the multi-pay Sooner Trend of northwestern Oklahoma, where Meramec and Osage rocks reach a thickness >600 ft. Although routinely referred to as an argillaceous to silty limestone, this unit is characterized by facies variations from claystone to siltstone to pure limestone. Carbonates are commonly siliceous, and chert is often reported in cores and drill cuttings. Although primary porosity is generally limited, fracturing occurs throughout the Mississippi lime.

The study area covers 12 sections in T. 17 N., Rs. 10–11 W., Blaine County, Oklahoma, where 29 Mississippi tests have been drilled since 1986. Of those completed from the Meramec and/or Osage, a bimodal distribution for production is obvious. Those tests with a well-developed 10–35-ft porosity zone approximately 350 ft into the Mississippi lime have typically resulted in strong producers (potential EUR >1.5 BCFG + 80 MBO), whereas those without are noneconomic (typically <75 MMCFG).

Detailed core analysis indicates that the productive facies consists primarily of calcareous, dolomitic siltstones that are interbedded with chert (sponge-spicule-rich spicularites). The siltstones have well-developed porosity formed through dissolution of sponge spicules and other siliceous materials; this porosity was then preserved by early migration of hydrocarbons. Later, both the chert and interbedded siltstones fractured, resulting in enhanced porosity through solution enlargement (vugs) along these fractures. The porosity zone described in the cored well is correlative with similar zones in all stronger Mississippi producers in this area. Abundant chert was observed in sample descriptions, and log analysis indicates that thin "shaly" interbeds are common to each. In contrast, offset wells that proved to be noneconomic drilled through less chert and predominantly limestone similar to that typical of the Mississippi lime above and below the zone of interest. Proficient recognition of these productive intervals through log analysis and sample evaluation will allow for selective testing of the Mississippi lime, which can significantly reduce completion expense.

Two north–south trends of porosity development are mapped in the study area. This porosity could be the result of the accumulation of sponge spicules, along with argillaceous muds and silts, in topographic lows on the sea floor adjacent to simultaneously developing Mississippian carbonates. Although neither chert nor siltstones alone have direct economic significance, favorable diagenetic processes can actively affect the two where interbedded, potentially creating an effective reservoir. Thorough evaluation of chert intervals, especially those exhibiting sample shows when drilled, may lead to the discovery of similar productive facies.

Towns, D. J., 2001, Mississippi lime: chert occurrence related to productive reservoirs, Blaine County, Oklahoma, *in* Johnson, K. S. (ed.), Silurian, Devonian, and Mississippian geology and petroleum in the southern Midcontinent, 1999 symposium: Oklahoma Geological Survey Circular 105, p. 178.

Reservoir Characterization and Comparison of the Hunton in the Texas–Oklahoma Anadarko Basin to Equivalent Devonian and Silurian (Fusselman) Rocks of the Texas Permian Basin

Ronald J. Woods, Charles E. Willey, Paul W. Smith, Walter J. Hendrickson, and John V. Hogan
IHS Energy Group[1]
Oklahoma City, Oklahoma

ABSTRACT.—Significant quantities of oil and gas have been produced from Silurian and Devonian reservoirs in both the Delaware basin and the Anadarko basin. Although the names are different for time-equivalent formations in the two basins, there are distinct similarities between the sections. In both regions the sections are thick, and the sequence is primarily carbonate. Reservoir traps in both basins were usually related to structure, with occasional stratigraphic implications.

Producing zones shown on electric logs were evaluated from 185 wells in 19 fields in the Delaware basin and from 368 wells in 42 fields in the Anadarko basin. Reservoir characteristics showed trends in thickness, porosity, water saturation, depth, production, and volumetric calculations.

In the Anadarko basin, the Hunton and the underlying Maquoketa dolomite and Viola are difficult to distinguish in some areas. Field-to-field correlations of the Silurian–Devonian section reported by operators in the Delaware basin suggest inconsistencies in the selection of formation boundaries. Reservoirs that are perforated and produced as Fusselman (Silurian) in the northern deep Delaware basin appear to be equivalent to the section correlated as Montoya (Ordovician) in the southern deep Delaware basin. In comparison, these miscorrelations would be similar to correlating Hunton with Viola in the Anadarko basin. Where problems in stratigraphic nomenclature occur, large opportunities usually exist.

[1]See Addendum on page 93.

Woods, R. J.; Willey, C. E.; Smith, P. W.; Hendrickson, W. J.; and Hogan, J. V., 2001, Reservoir characterization and comparison of the Hunton in the Texas–Oklahoma Anadarko basin to equivalent Devonian and Silurian (Fusselman) rocks of the Texas Permian basin, *in* Johnson, K. S. (ed.), Silurian, Devonian, and Mississippian geology and petroleum in the southern Midcontinent, 1999 symposium: Oklahoma Geological Survey Circular 105, p. 179.